THE UNIVERSITY OF CHICAGO

DEVELOPMENT OF PALLADIUM-CATALYZED ARENE DIFUNCTIONALIZATION REACTIONS ENABLED BY NORBORNENE

A DISSERTATION SUBMITTED TO

THE FACULTY OF THE DIVISION OF THE PHYSICAL SCIENCES

IN CANDIDACY FOR THE DEGREE OF

DOCTOR OF PHILOSOPHY

DEPARTMENT OF CHEMISTRY

BY

ALEXANDER J. RAGO

CHICAGO, ILLINOIS

JUNE 2021

To my family, friends, colleagues, and pets.

TABLE OF CONTENTS

LIST OF SCHEMES

LIST OF FIGURES

LIST OF TABLES

LIST OF ABBREVIATIONS

Ac	Acetyl
Ar	Aryl
Bn	Benzyl
Boc	*tert*-Butoxycarbonyl
Bu	Butyl
Bz	Benzoyl
BzCl	Benzoyl chloride
C–C	Carbon–carbon
C–H	Carbon–hydrogen
CMD	Concerted Metalation-Deprotonation
C–N	Carbon–nitrogen
COSY	Correlated Spectroscopy
δ	Delta – chemical shift
DCM	Dichloromethane
DMF	*N*,*N*-Dimethylformamide
DG	Directing group
ee	Enantiomeric excess
Et	Ethyl
Et_3N	triethylamine
Et_2O	Diethyl ether
EtOAc	Ethyl acetate
equiv.	Equivalent
HRMS	High-Resolution Mass Spectrometry

HSQC	Heteronuclear single quantum coherence spectroscopy
*i*Pr	Isopropyl
IR	Infrared
m	*Meta*
Me	Methyl
mol%	Mole percent
MOM	Methoxymethyl
MP	Melting Point
NBE	2-norbornene/[2.2.1]-bicyclohept-2-ene
NBS	*N*-Bromo Succinimide
NOESY	Nuclear Overhauser Effect Spectroscopy
NMR	Nuclear Magnetic Resonance
o	*Ortho*
p	*Para*
Ph	Phenyl
PhMe	Toluene
Piv	Pivaloyl
PMB	*para*-methoxybenzyl
*t*Bu	*tert*-Butyl
TFA	Trifluoroacetic acid; trifluoroacetyl
THF	Tetrahydrofuran
TLC	Thin-Layer Chromatography

ACKNOWLEDGMENTS

First and foremost, the completion of my Ph.D. would not have been possible without the leadership and mentorship of Prof. Guangbin Dong over the past five years. Prof. Dong's drive for new and interesting results pushed me to become a better researcher and organic chemist, and I will always appreciate that he saw potential in me and pushed me to realize this potential. Second, I would like to thank my undergraduate research advisor, Prof. Kami Hull, who sparked my interest in transition metal-catalyzed method development, which eventually lead to me joining Prof. Dong's lab. She was also my first organic chemistry professor, and her passion for teaching the class definitely influenced my choice to conduct research in the field.

I would also like to thank my committee members, Prof. Scott Snyder and Prof. John Anderson, for agreeing to serve on my committee, taking the time to read this thesis, offering feedback and advice, and being supportive of my future career goals. Prof. Snyder also served as the chair of my Ph.D. candidacy committee, and I am very grateful for his support and encouragement early on in my graduate career.

Next, I would like to thank those who I have worked closely with over the past several years. My undergraduate mentor, Dr. Seth Ensign, was instrumental in teaching me many of the skills that enabled me to be a successful organic chemist. Several members of the Dong group over the years have also been both great help during my studies and great friends, from my first mentor, Dr. Zhongxing Huang, to our current and former graduate students and post-doctoral researchers: Dr. Jianchun Wang, Dr. Zhe Dong, Dr. Zhao Wu, Mr. Jiaxin Xie, Mr. Renhe Li, Dr. Xin Liu, Dr. Sihua Hou, Dr. Serena Lee, Dr. Hairong Lyu, Dr. Ki-Young Yoon, Mr. Shusuke Ochi, Mr. Marcelo de la Mora, Dr. Tatsuhiro Tsukamoto, and many more. Dr. Brent Billett, in particular, helped me

to learn many new chemical techniques as I worked in his fume hood during my first year. Ms. Shin Young Choi could also be relied on for anything from supply ordering, to lending NMR tubes, and occasionally escaping the lab to grab coffee. Those from the Snyder lab who have lent advice and really helped during my search for a post-graduation position include Ms. Tessa Lynch-Colameta and Dr. Vlad Lisnyak.

Our dogs could always be relied on during the tough times, so my graduate studies would have been very different without four furry friends: Murphy (who will be greatly missed for many years to come), Mars, Atlas, and Luna. Finally, I would like to thank my family for their support during my graduate studies, including my father, stepmother Karen, brother Daniel, Aunt Gerry, my grandmother, and my late grandfather, who unfortunately did not have the opportunity to read this thesis. Last, but not least, I would like to thank my girlfriend, Phuong, who has made the latter half of my graduate studies much more bearable. I cannot thank her enough for putting up with the late nights, odd hours, and high stress that comes along with working in a field as competitive as the Catellani reaction. I dedicate this thesis to all of them, and I look forward to seeing what the future holds.

Alexander J. Rago

University of Chicago

May 2021

ABSTRACT

In this thesis, various approaches from the literature employing carbon–hydrogen bond activation for the synthesis of indoles and their close derivatives, indolines and carbazoles, have been discussed. Palladium/norbornene cooperative catalysis, in particular, presents an attractive platform for the preparation of indoles *via* the regioselective difunctionalization of an aryl halide and its unactivated *ortho*-carbon–hydrogen bond. The detailed development of a synthetic strategy for the preparation of indoles using this catalytic duo *via* an *ortho*-amination, *ipso*-Heck cyclization cascade is presented. Moreover, a synthesis of indolines *via* a modification of this strategy employing a reductive Heck cyclization is also presented, in addition to preliminary results for the enantioselective version of this transformation. Finally, an unexpected *ortho*-Heck reaction of aryl iodides is presented, whereupon an alkene was found to couple at the arene *ortho*-position, instead of the typical *ipso* position. An isotope labeling study was conducted, finding that the transformation was likely proceeding through an uncommon reaction pathway for palladium. The knowledge gained in these combined works is expected to help guide the development of new transformations employing palladium/norbornene cooperative catalysis.

CHAPTER 1

Synthesis of Indoles, Indolines, and Carbazoles *via* Palladium-Catalyzed C–H Bond Activation

1.1. Introduction

The construction of indole, indoline, and carbazole heterocycles has been of significant interest in the synthetic community over the last century due to their prevalence in natural products and other biologically active compounds. In particular for indoles, many conventional methods developed to date require highly pre-functionalized arene precursors, diminishing their attractiveness as "green" syntheses. Carbon–hydrogen bond activation, on the other hand, presents an elegant solution to this problem and can achieve the construction of indoles and their derivatives from comparatively simpler arene precursors. In this short review, we discuss various approaches for preparing indoles, indolines, and carbazoles *via* palladium-catalyzed C–H bond activation, highlighting their reaction mechanisms and synthetic applications (Figure 1.1).

Figure 1.1. C–H Bond Activation for the Synthesis of Indoles and their Close Derivatives

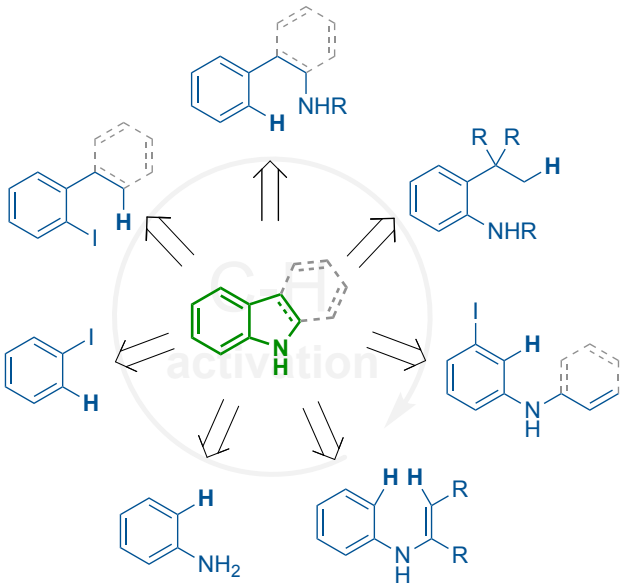

Indoles and their derivatives are among the most common heterocycles found in nature. As a result, a wide variety of compounds, including amino acids, natural products, and approved pharmaceutical drugs, contain such a structural motif (Figure 1.2), many of which exhibit rich biological activity.[1] As a consequence, significant efforts have been made to prepare substituted indoles[2-4] and their close derivatives, indolines[5] and carbazoles.[6] Traditional approaches often involve harsh reaction conditions, complex substrates, or potentially toxic byproducts, diminishing their attractiveness as "green" syntheses. An emerging tool to mitigate these concerns is carbon–hydrogen (C–H) bond activation, whereupon an inert C–H bond is directly transformed into the desired carbon–carbon (C–C) or carbon–heteroatom (C–X) bond by a transition metal catalyst.[7, 8] In this regard, substrate complexity can be decreased, as pre-functionalization would be unnecessary, allowing for the use of more readily available precursors for heterocycle syntheses. In addition, harsh conditions or toxic byproducts can often be avoided.

Figure 1.2. Natural Products and FDA-Approved Drug Molecules bearing Indoles and Carbazoles

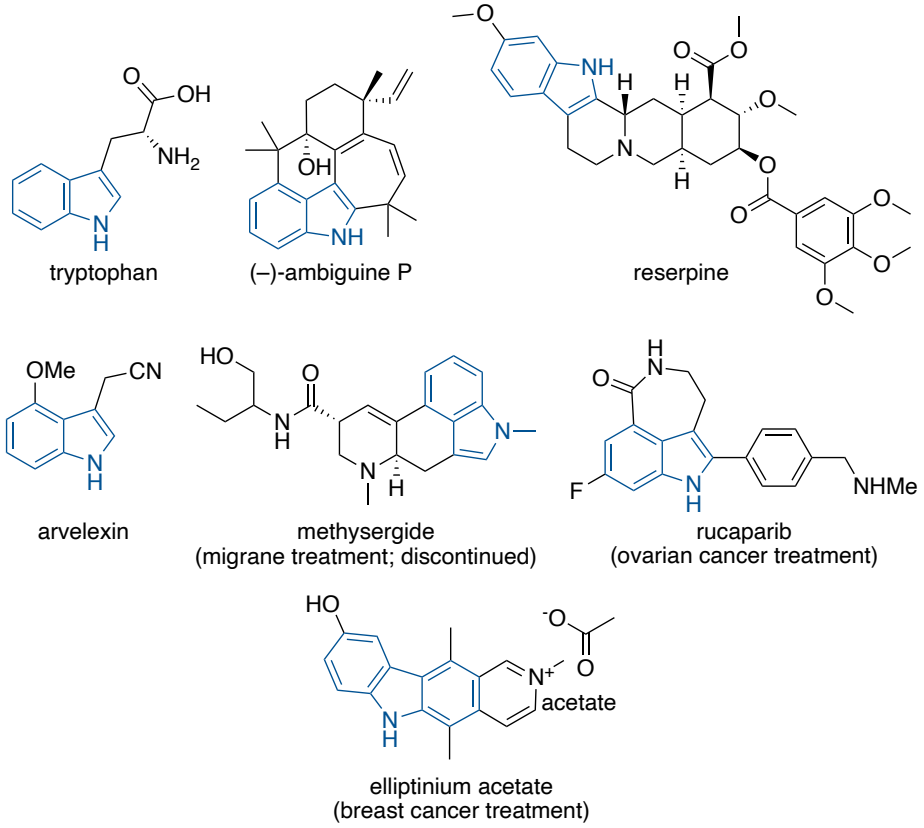

There have been excellent reviews on the topic of indole synthesis *via* C–H bond activation reported until 2017;[9-11] however, significant advances in the field have appeared in the literature since. In this short review, we will highlight different synthetic strategies that have been developed for the construction of indoles and their close derivatives, indolines and carbazoles, *via* palladium-catalyzed C–H bond activation. A particular focus is given to approaches developed after 2016. It is not our intent to comprehensively cover each transformation developed to date, but to emphasize the versatility of palladium catalysis for the construction of these heterocyclic rings from a variety of simple precursors. The content is divided based on whether the ring is formed through an intramolecular (unimolecular) or a multi-component (bi- or trimolecular) event. Besides reaction

development, mechanistic details and synthetic applications of the transformations are also discussed.

1.2. Synthesis of Indoles and their Derivatives *via* Palladium-Catalyzed C–H Bond Activation

To date, many methods have been developed for indole synthesis, in addition to indole functionalization.[12, 13] Among these synthetic approaches, the oldest and most well-known indole-forming reaction is likely the Fischer indole synthesis. Discovered in 1883, this transformation uses an aryl hydrazone, formed by condensation of an aryl hydrazine with a carbonyl, which is treated with acid at elevated temperatures in order to promote a [3,3]-sigmatropic rearrangement, eventually resulting in the formation of the indole ring with expulsion of gaseous ammonia (Scheme 1.1a).[14] In a related work reported over a century later in 1998, Buchwald and co-workers showed that the aryl C–N bond can be forged *via* a palladium-catalyzed coupling reaction between an aryl bromide and a hydrazone, which can then be treated under standard Fischer conditions to form the indole ring (Scheme 1.1b).[15] This advance allowed for a new disconnection to be made when considering how to prepare aryl hydrazones.

Scheme 1.1. Fischer Indole Synthesis and Buchwald's Modification

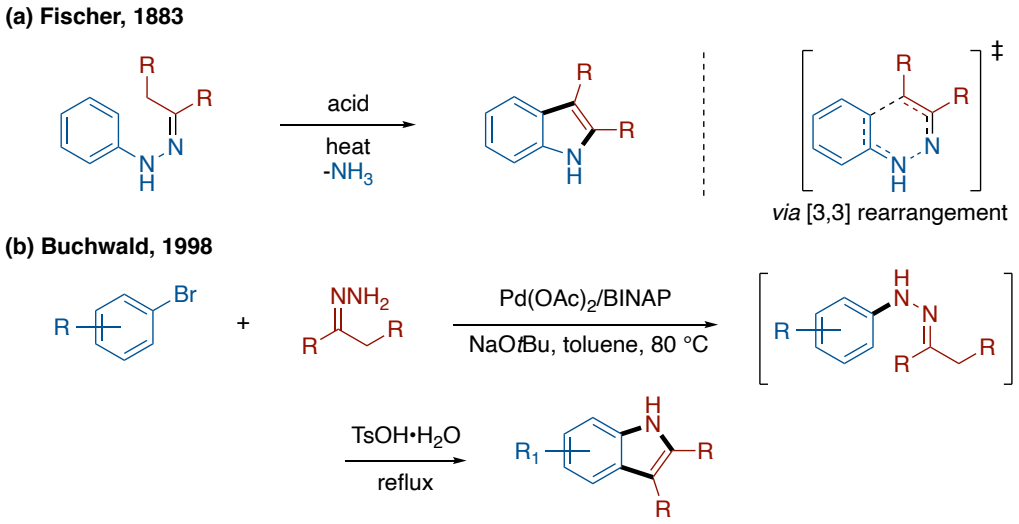

In these examples, however, relatively harsh acidic conditions are required in order to furnish the final products. Other strategies have since been developed, such as the Mori-Ban (Scheme 1.2a)[16] and Larock (Scheme 1.2b)[17] indole syntheses, which employ milder palladium-catalyzed conditions to construct the heterocycles; however, these examples suffer from the necessity of more complex pre-functionalized arene starting materials. More recently, Jørgensen and coworkers have found 1,2-dihaloarenes to be effective substrates for Pd-catalyzed indole synthesis *via* an amination/cyclization cascade with allyl amines, although this work exhibits the same drawback, resulting in a somewhat limited aryl substrate selection (Scheme 1.2c).[18] Additionally, this method was recently extended to nickel catalysis by Tian, allowing for the reaction to proceed from aryl dichloride starting materials.[19] Although all of these reactions efficiently deliver indole products, methods that can avoid using doubly functionalized arene precursors would further simply the syntheses.

Scheme 1.2. Pd-catalyzed Synthesis of Indoles from Pre-Functionalized Arenes

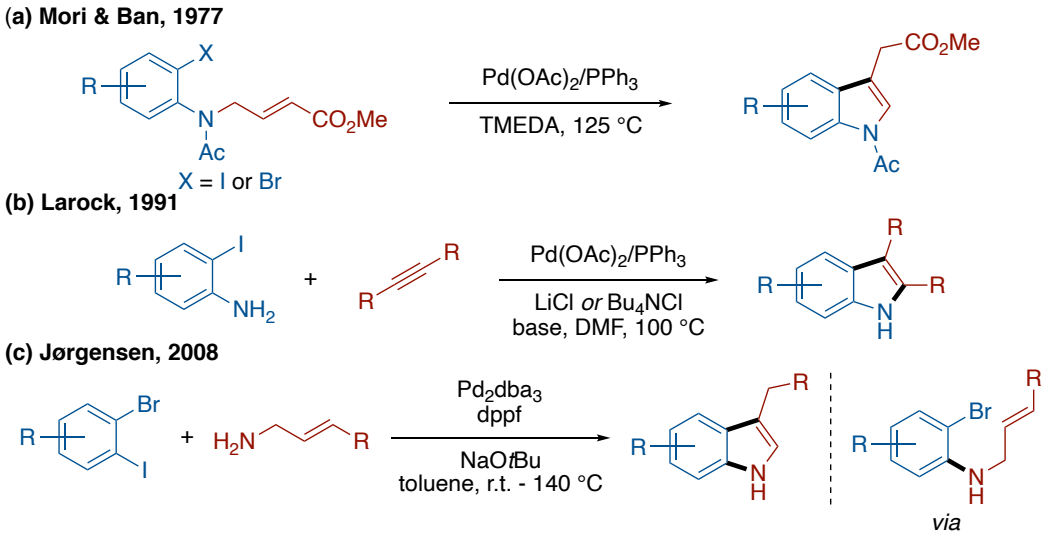

Clearly, substrate complexity is one factor that should be considered when designing a synthesis, and it could influent the "greenness" of the overall process. Over the past few decades, many innovative approaches have emerged, which directly transform an aryl C–H bond into the desired C–C or C–X bond, reducing overall chemical byproducts and enabling a rapid increase in molecular complexity from simple precursors.[7, 8] Consequently, these C–H bond activation methods are advantageous when compared to traditional aryl halide cross-coupling strategies, which often require the installation of the halogen atom (or (pseudo)halogen unit) prior to the coupling reaction if the desired substrate is not commercially available (Scheme 1.3).

Scheme 1.3. Traditional Cross-Coupling vs C–H Bond Activation Strategies

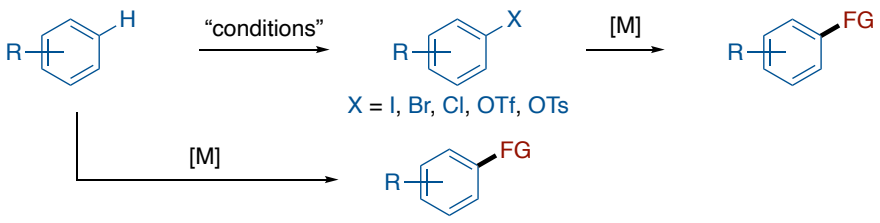

Palladium catalysis, in particular, offers a wide variety of scaffolds and approaches for the synthesis of indoles and their close derivatives *via* both traditional cross-coupling and C–H bond activation strategies. The aminating reagents have also been designed to fulfill a dual role as the oxidant in many examples, mitigating the necessity for potentially harmful external oxidants. By applying C–H bond activation towards the synthesis of these heterocycles, an inert C–H bond can be directly transformed into a C–C or a carbon–nitrogen (C–N) bond. Specifically, two major classifications can be designated with regard to indole synthesis: (**1**) intramolecular and (**2**) multi-component construction of the five-membered nitrogen heterocycles, both of which can be further defined depending on the bonds that are formed (*vide infra)*.

1.2.1. Intramolecular Cyclization Strategies for the Synthesis of Indoles and their Derivatives

Intramolecular construction of indoles and their close derivatives *via* palladium-catalyzed C–H bond activation can be achieved through a few possible disconnections: either of the C–N bonds, or of the C–C bond (Scheme 1.4). The latter can offer complementary bond disconnection strategies compared to the Heck cyclization method (Scheme 1.2a), with the added benefit of allowing less functionalized arene precursors to deliver the heterocyclic products. A recent review has covered this area quite thoroughly,[20] thus only a selection of significant examples are discussed

here. While many of these transformations can be carried out under mild conditions with relatively benign oxidants, some transformations required the addition of stronger oxidants to promote the formation of Pd(IV) intermediates, which could more readily undergo C–N bond reductive elimination to form the desired products than their Pd(II) counterparts.

Scheme 1.4. Strategies for the Intramolecular Construction of Indoles, Indolines, and Carbazoles

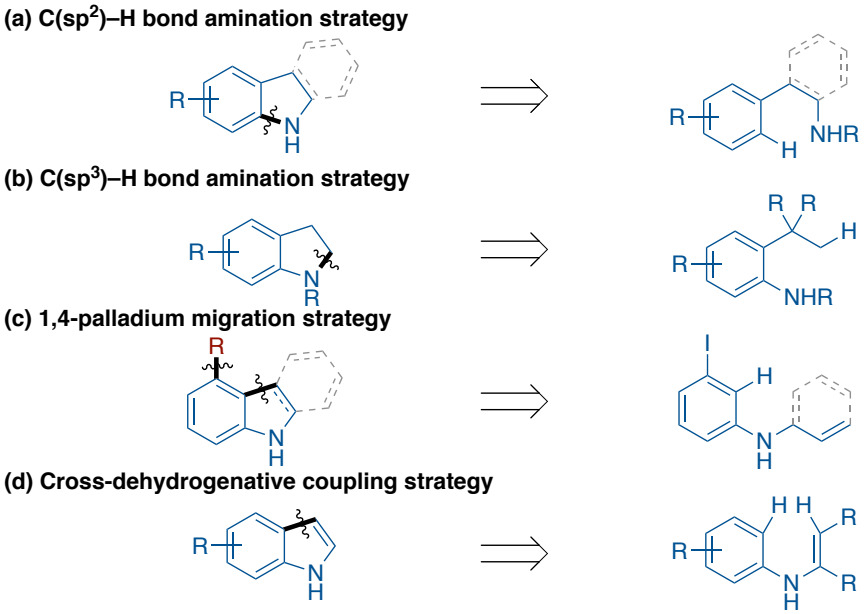

1.2.1.1. Synthesis of Indoles, Carbazoles, and Indolines via Intramolecular C–H Bond Amination

Carbazoles and indolines were the first indole derivatives synthesized *via* C–H bond amination. In 2005, Buchwald and co-workers first developed a palladium-catalyzed protocol for the intramolecular synthesis of carbazoles using *N*-acetyl 2-aminobiphenyl starting materials (Scheme 1.5a).[21, 22]

Scheme 1.5. Intramolecular Synthesis of Carbazoles *via* C–H Amination

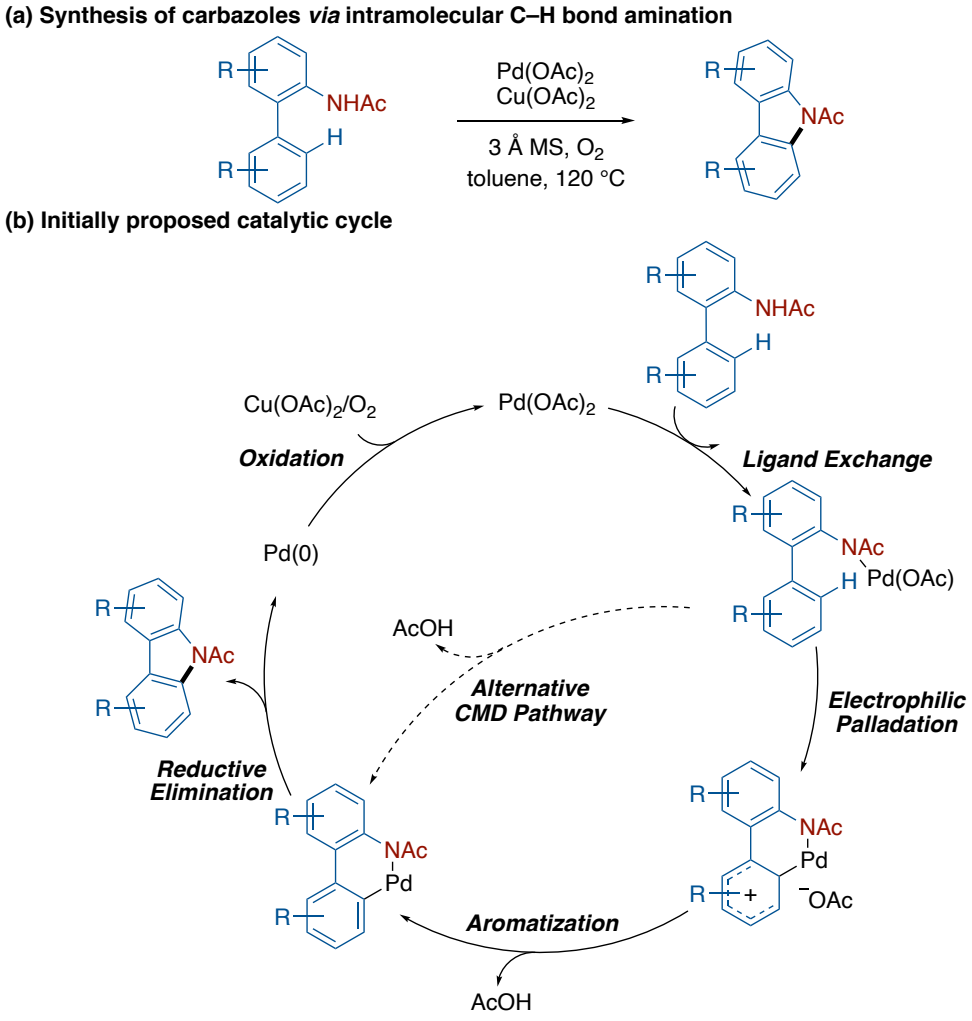

An electrophilic palladation pathway was initially proposed for the C–H bond activation (Scheme 1.5b); however, it was observed that substrates with electron-deficient substituents *para* to the C–N bond forming site performed better compared to those with electron-rich substituents, suggesting that some other C–H activation mechanism was operating (Scheme 1.6a). Moreover, the transformation was found to be inefficient if the temperature was reduced below 120 °C. From these results, two plausible alternative mechanisms were proposed: Heck- or Wacker-type cyclization pathways (Scheme 1.6b). Although these are the pathways proposed by the authors, it

should be noted that a mechanism involving a concerted metalation-deprotonation (CMD) pathway with the acetate ligand cannot be excluded (Scheme 1.5b).

Scheme 1.6. Substituent Effects and Revised Mechanisms

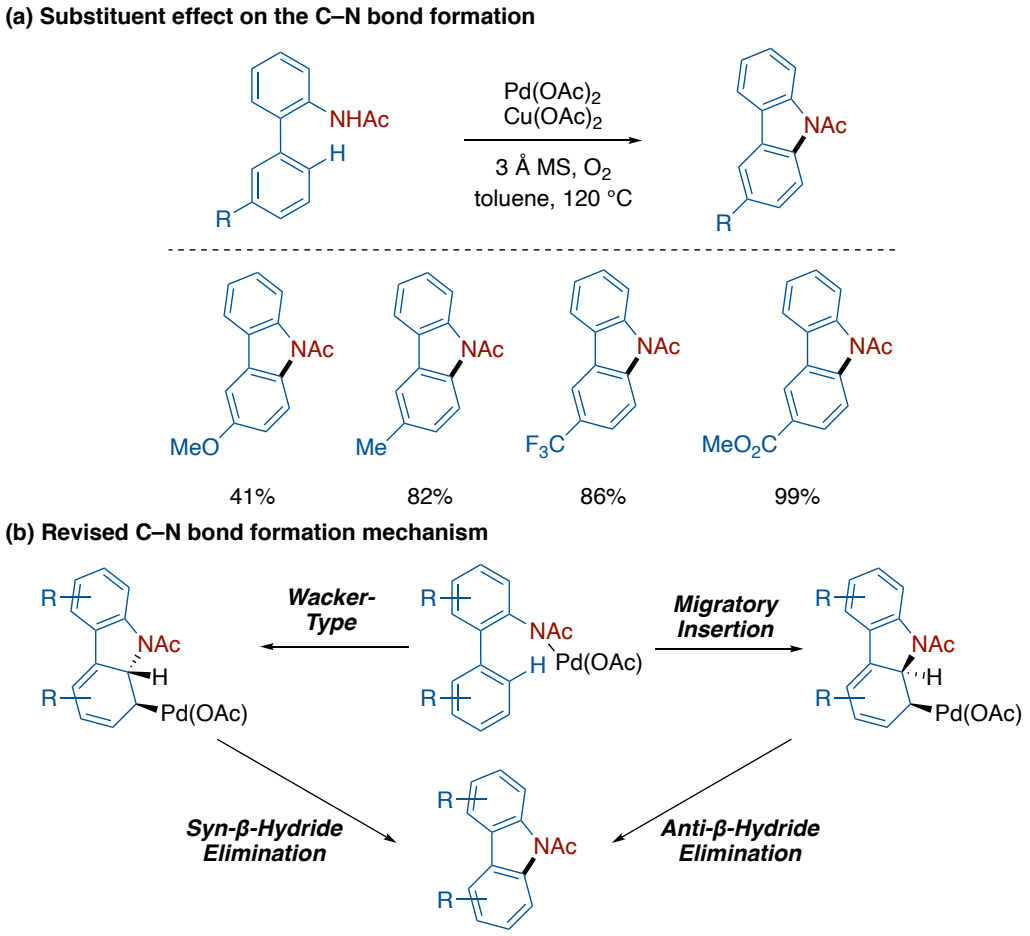

Shortly after, Yu and co-workers employed a similar aryl C–N bond disconnection for the synthesis of indolines, with the major difference being the role of the oxidant (Scheme 1.7a).[23] In this particular reaction, the oxidant was necessary in order to promote formation of a higher-valent palladium(IV) species, which could readily undergo the C–N reductive elimination; the oxidant was crucial for the transformation, as C–N bond formation was found to be quite challenging for the lower-valent Pd(II) species with these substrates (Scheme 1.7b). A wide

range of oxidants was surveyed, finding an F^+ reagent to be the best oxidant for the reaction, which could smoothly deliver the corresponding indoline products. This oxidant, in particular, minimized non-productive reductive elimination pathways (e.g. halogenation or acetoxylation side-products). The synthetic utility of the method was highlighted with a concise synthesis of 4-bromoindole, an important precursor in the synthesis of ergot alkaloids,[24] which was more efficient than previously developed routes (Scheme 1.7c). The same group later improved upon this transformation with the more readily removable $–SO_2$(2-py) protecting group, using $PhI(OAc)_2$ as the oxidant.[25]

Scheme 1.7. Synthesis of Indolines *via* C(sp^2)–H Amination

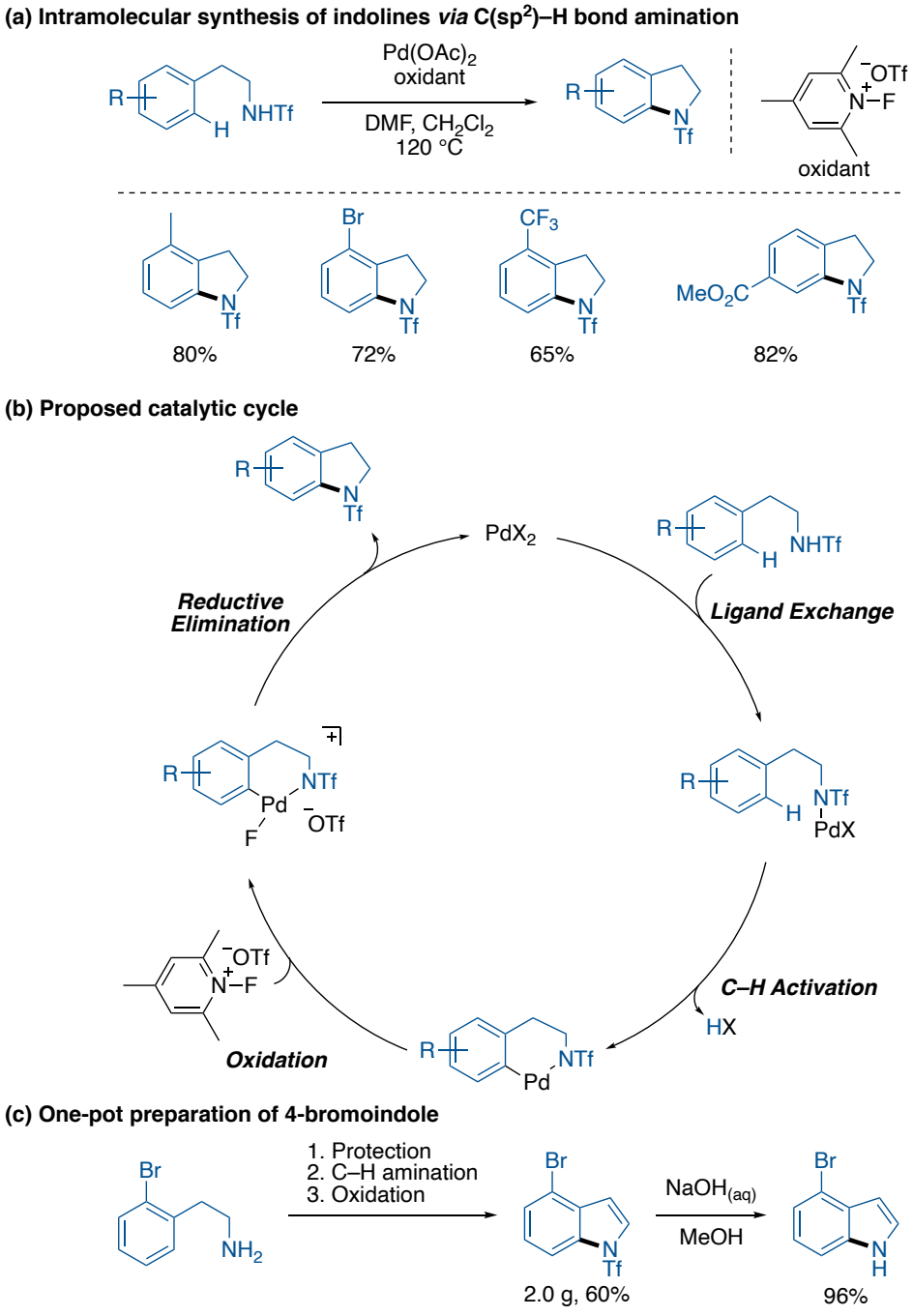

Concurrently, Glorius and co-workers developed a complementary C(sp^3)–H amidation strategy for the synthesis of indolines.[26] A wide-ranging substrate scope was demonstrated, using the

commercially available oxidant, AgOAc (Scheme 1.8a). In this transformation, an acetamide unit acts as an anionic directing group towards the palladium catalyst, facilitating the C(sp^3)–H bond activation. After ruling out a potential acetoxylation/nucleophilic substitution pathway, it was proposed that the Pd(II) intermediate could either undergo reductive amination to furnish the indoline product with a Pd(0) species, or be oxidized to a Pd(IV) intermediate, which could readily undergo C–N bond formation to regenerate the active Pd(II) catalyst (Scheme 1.8b).

Scheme 1.8. Synthesis of Indolines *via* C(sp^3)–H Amidation

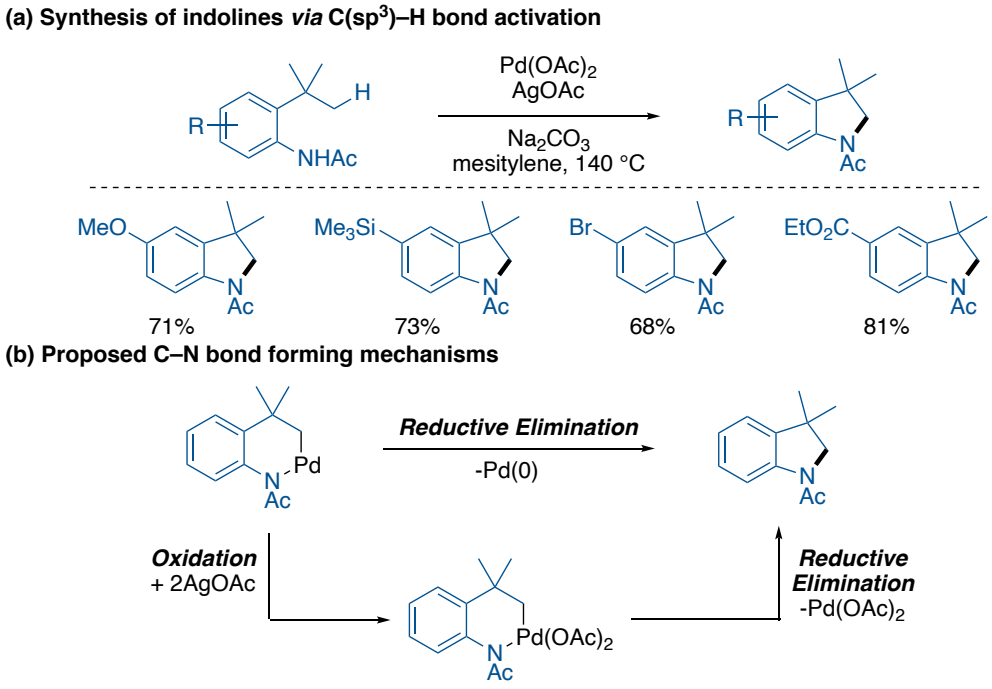

Hartwig and co-workers developed the first redox-neutral intramolecular synthesis of indoles using oxime esters as both the amine source and oxidant in 2010 (Scheme 1.9a).[27] The reaction was proposed to proceed through initial oxidative addition of Pd(0) into the oxime N–O bond, followed by tautomerization and subsequent C–H bond activation on the proximal phenyl ring. C–N reductive elimination could then smoothly deliver the desired indole product, with no need of

an external oxidant (Scheme 1.9b). At the time of publication, Pd(0) was merely proposed to undergo oxidative addition into the N–O bond of the oxime; this proposed intermediate was isolated and its structure was unambiguously elucidated *via* X-ray crystallography in this work, confirming the proposed mechanism (Scheme 1.9c). This transformation exemplifies a "green" synthesis, as the oxime starting materials can readily be prepared from ketones, and the reaction itself generates a benign acetate by-product, without the need for any potentially toxic or harmful oxidants.

Scheme 1.9. Redox-Neutral Intramolecular Synthesis of Indoles from Oxime Esters

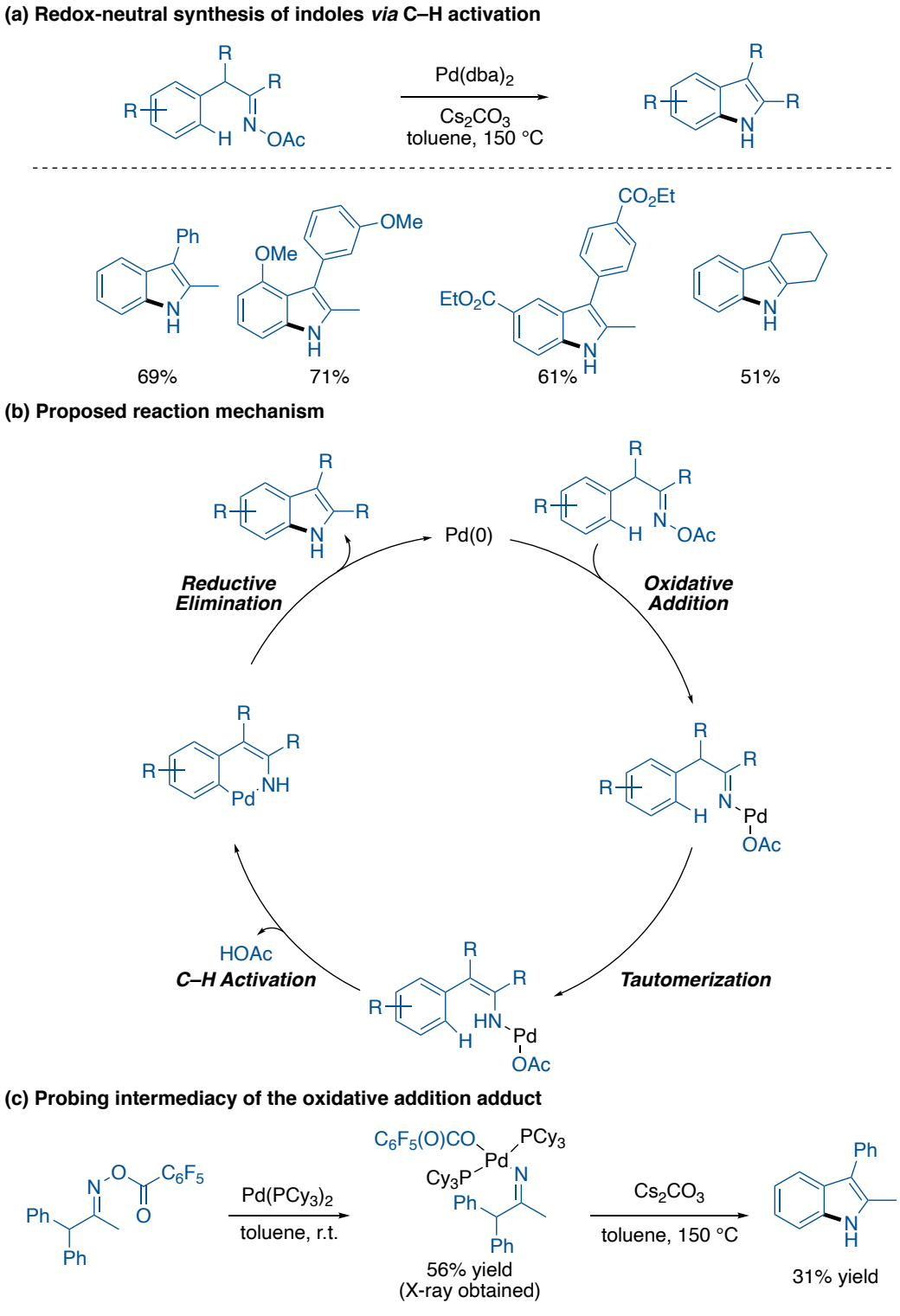

The analogous oxidative indole synthesis from amine substrates was later developed by Youn in 2014, using oxone as the terminal oxidant to prepare *N*-Ts indoles (Scheme 1.10a).[28] In a closely-related synthesis of carbazoles[29] from the same group, it was proposed that the strong oxidant could generate a high-valent Pd(IV) intermediate, which could readily undergo reductive elimination to forge the C–N bond. In this regard, the oxidant fulfills a similar role as the oxidant in Yu's indoline synthesis (Scheme 1.7).[23] This template was further expanded by Stahl and co-workers in 2016, using molecular oxygen as the terminal oxidant, for the preparation of *N*-acetyl indoles (Scheme 1.10b).[30] Mechanistically, this transformation was proposed to operate similarly to the intramolecular carbazole synthesis developed by Buchwald,[21] which was proposed to proceed through a Pd(II)/Pd(0) catalytic cycle (Scheme 1.5b).

Scheme 1.10. Intramolecular Synthesis of Indoles *via* Oxidative C–H Bond Amination

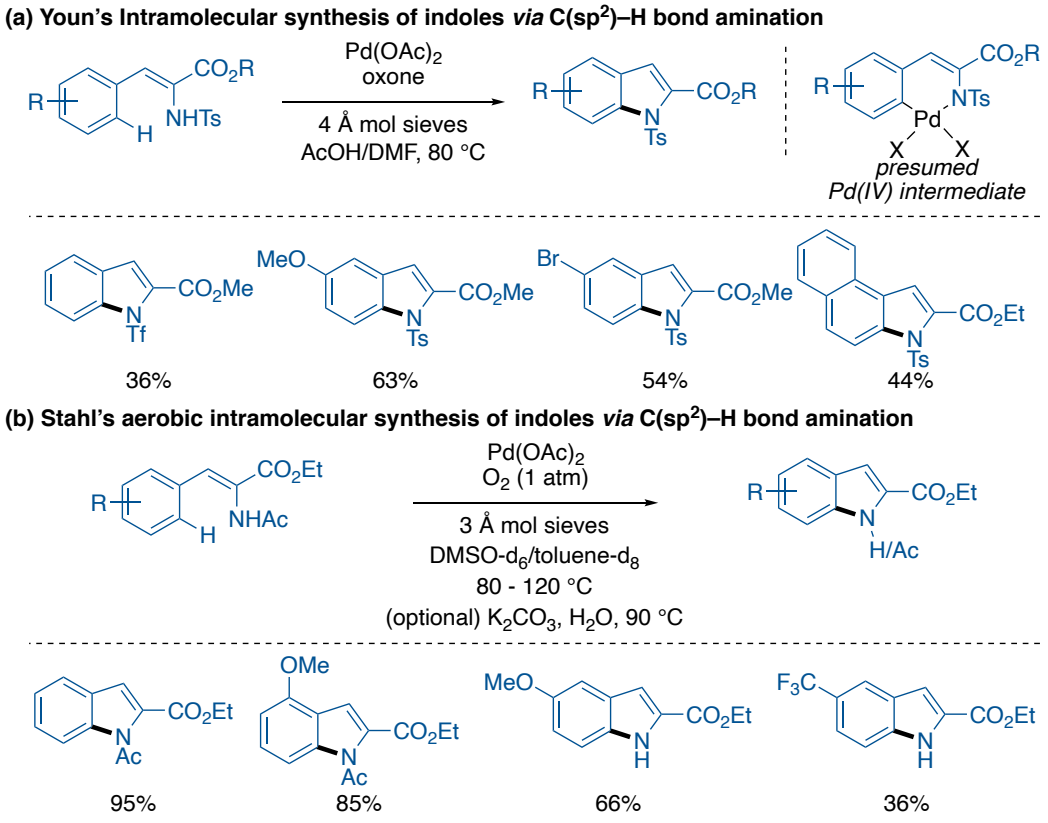

Other Pd-catalyzed C–H bond animation transformations have been developed for the synthesis of indoles from 2-nitrostyrene or β-nitrostyrene compounds.[31-33] However, the mechanisms of these transformations are not entirely understood, and likely do not involve a C–H activation step with the formation of a C–Pd bond; for example, a nitrene insertion pathway was initially proposed to be involved the C–N bond forming step.[31] As such, transformations of this type are not discussed.

1.2.1.2. Synthesis of Indoles *via* Intramolecular C–H Bond Carbonation

As reported by Mori and Ban,[16] a typical Heck cyclization strategy for indole synthesis begins with the formation of an arylpalladium(II) species from an aryl halide (Scheme 1.2a). Larock and co-workers hypothesized that this arylpalladium(II) species could instead be formed *via* a 1,4-palladium migration with an unactivated arene C–H bond, which could then undergo Heck cyclization with an allylic amine to afford indole products (Scheme 1.11a).[34, 35] In this regard, multi-substituted indoles can be prepared in a single step from simple 3-iodoaniline precursors. Alternatively, subsequent C–H bond activation on a nearby phenyl ring can deliver multi-substituted carbazole products (Scheme 1.11b).

Scheme 1.11. Synthesis of Indoles and Carbazoles *via* 1,4-Palladium Migration

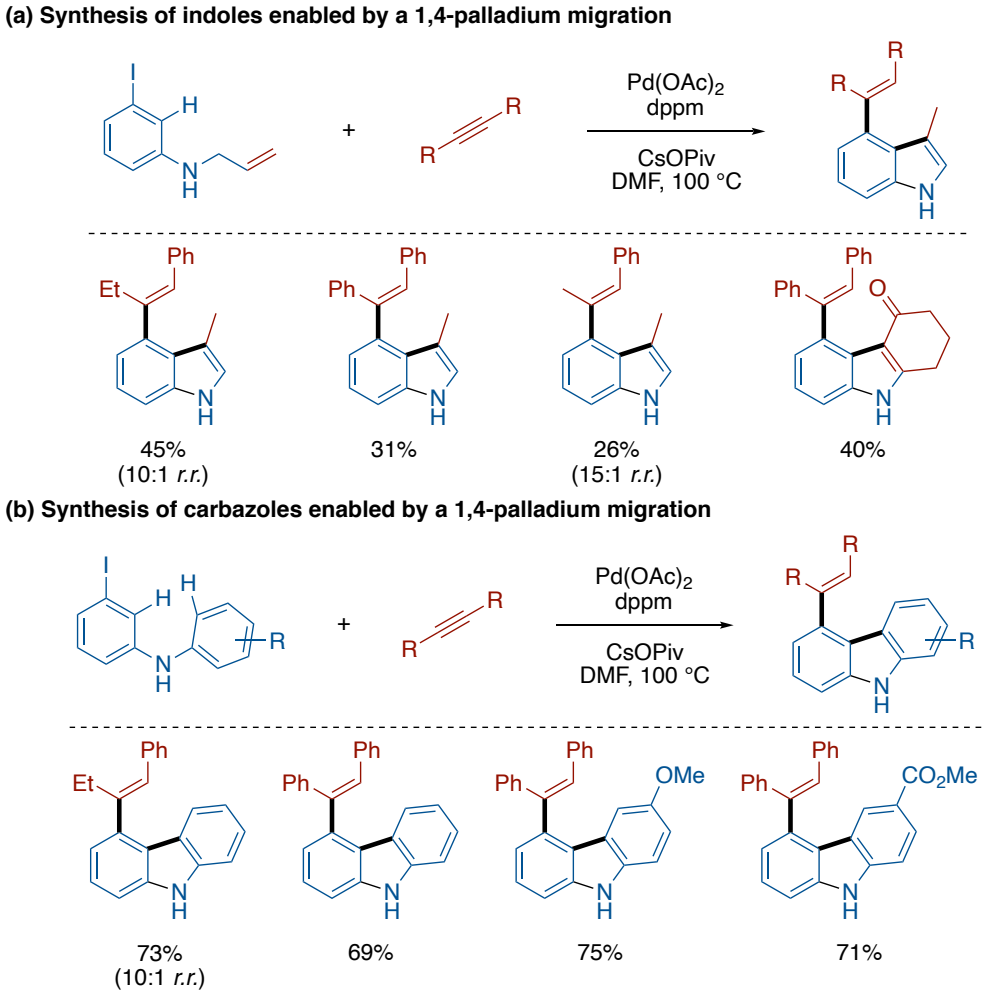

A deuterium labeling study was conducted in order to further elucidate the mechanism of the *ortho*-C–H bond migration. Using a deuterium labeled oxygen-tethered substrate, incorporation of 70% deuterium, or 85% deuterium with a large excess of D_2O, on the newly formed internal alkene was observed (Scheme 1.12a). Consequentially, it was proposed that the alkenylpalladium(II) intermediate likely oxidatively inserted into the *ortho*-C–H bond, resulting in the formation of a Pd(IV)-hydride species. This hydride intermediate was poised to undergo facile C–H reductive elimination with the alkenyl ligand to form the key arylpalladium(II) intermediate, which could go

on to cyclize with a proximal olefin to form indole products or undergo another C–H activation to prepare carbazoles or dibenzofurans (Scheme 1.12b). Since the deuterium incorporation was not 100%, H/D exchange was proposed to occur with this Pd(IV)-hydride intermediate by way of reductive elimination of an equivalent of acid, which is evident from the increase in deuterium incorporation with an excess of a deuteric additive. Although, a mechanism involving concerted sigma bond metathesis, with reversible C–H activation slightly eroding the deuterium incorporation at the ortho position prior to the metathesis, cannot be excluded. This work highlights the utility of metal migrations to prepare intermediates in typical aryl halide-initiated cross-coupling reactions, allowing for a rapid increase in molecular complexity from simple substrates.

Scheme 1.12. Probing the Mechanism of the 1,4-Palladium Migration

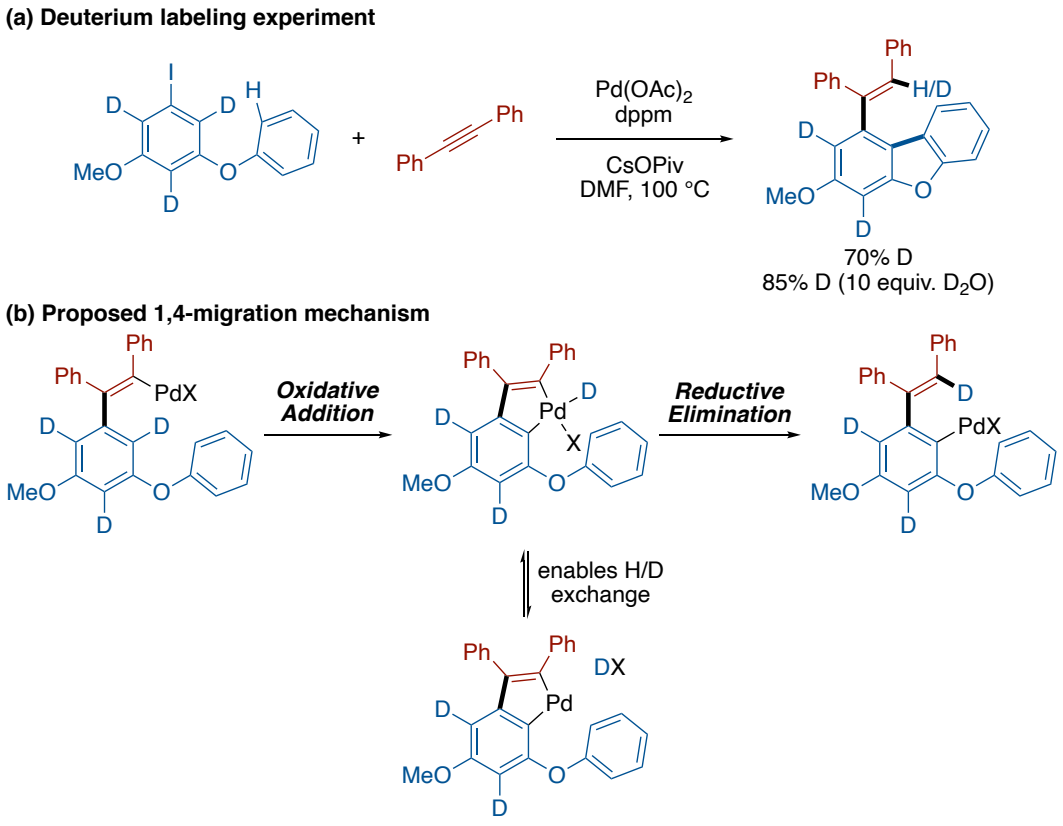

Glorius and co-workers later developed an intramolecular synthesis of indoles *via* construction of the C–C bond. Aryl enamine precursors were employed in a cross-dehydrogenative coupling (CDC), whereupon an annulation was achieved by the extrusion of two hydrogen atoms from the starting material (Scheme 1.13a).[36] Moreover, the substrates could be easily prepared from commercially available anilines. Mechanistically, after electrophilic palladation of the enamine moiety, an electrophilic palladation pathway was initially proposed for the subsequent aryl C–H bond activation. However, electron-donating substituents *para* to the amine resulted in a slower reaction rate, suggesting against this proposed electrophilic palladation pathway (Scheme 1.13b). Additionally, a large primary kinetic isotope effect (KIE) of 4.6 suggested some other mechanism was operating (Scheme 1.13c). With these results in hand, the mechanism was revised to involve one of two potential pathways: σ-bond metathesis or base-assisted deprotonation of the arene C–H bond (Scheme 1.13d).

Scheme 1.13. Cross-Dehydrogenative Coupling for the Synthesis of Indoles

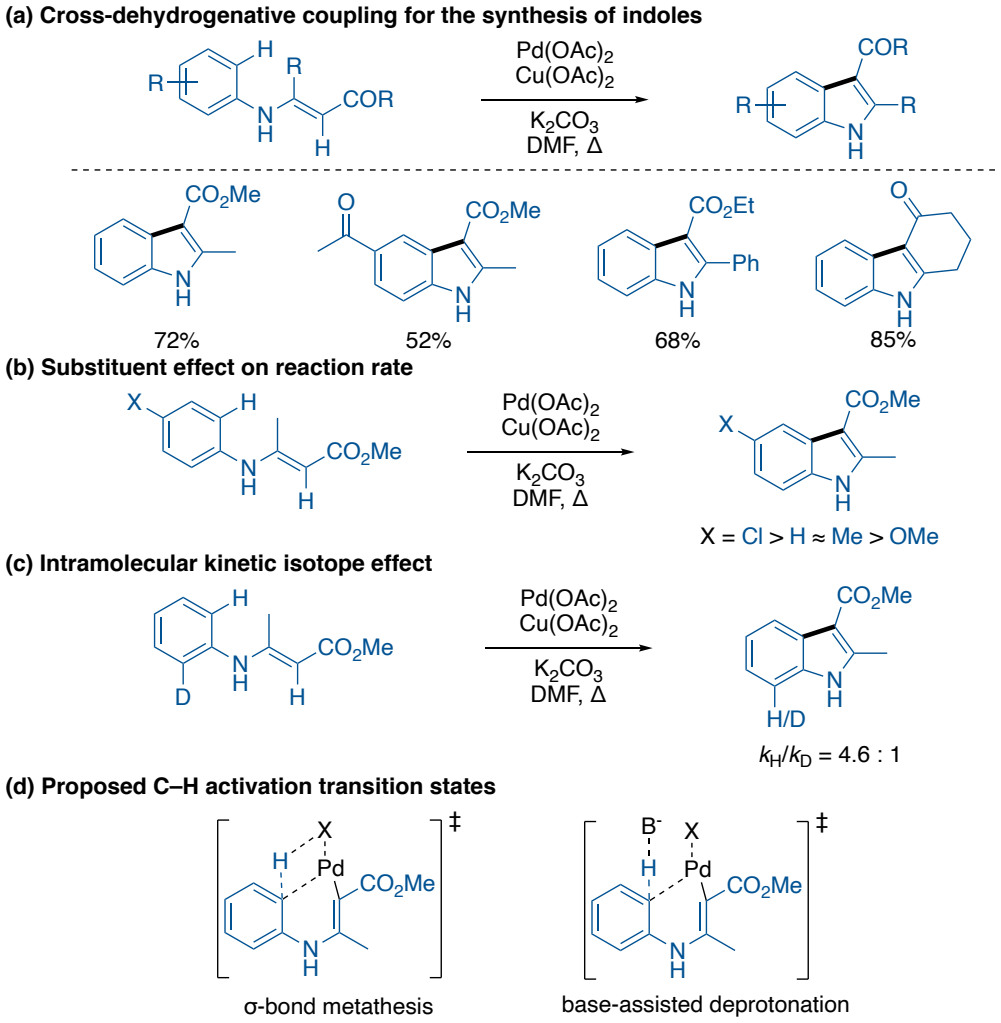

Clearly, indole synthesis is greatly simplified by the intramolecular C–H cyclization strategy, compared to conventional cross-coupling approaches with aryl halides. In these transformations, however, the substrates need to be carefully designed in order to facilitate the cyclization. Construction of the heterocyclic ring from two or three components, on the other hand, would allow for even simpler starting materials to afford the desired indole products.

1.2.2. Multi-Component Synthesis of Indoles

Multi-component construction of the pyrrole nucleus of indoles, along with their close derivatives, through C−H bond activation would simultaneously form two or three bonds; therefore, simpler building blocks have been employed as substrates. This section primarily focuses on various synthetic strategies that assemble the 5-membered nitrogen heterocycle through different bond disconnections (Scheme 1.14).

Scheme 1.14. Strategies for the Multi-Component Construction of Indoles, Indolines, and Carbazoles

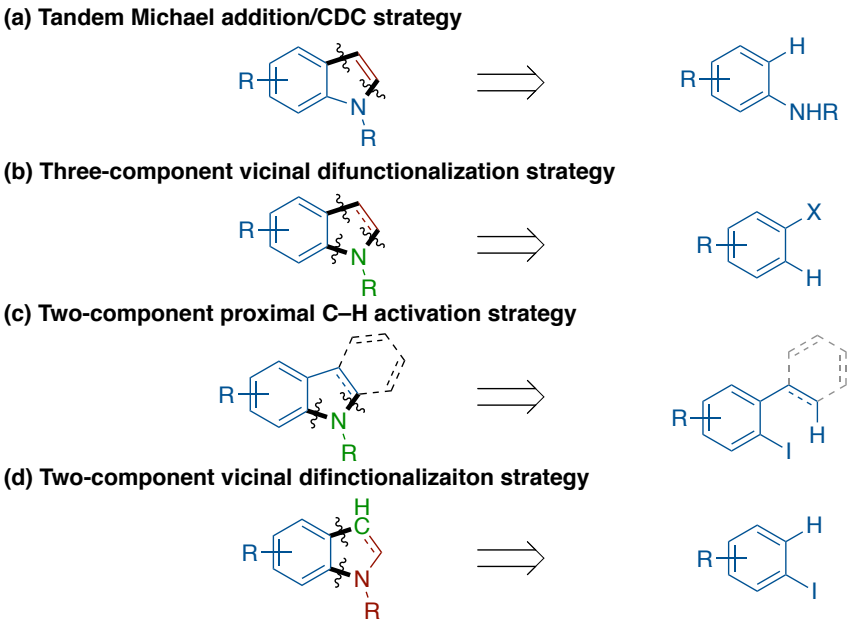

1.2.2.1. Bimolecular Synthesis of Indoles from Anilines

Jiao and co-workers have developed a modified indole synthesis based on the CDC strategy,[36] which involves a Michael addition to prepare the aryl enamines *in situ*, followed by the CDC reaction.[37] In this regard, simple, commercially available anilines and internal alkynes can be

directly transformed to indoles (Scheme 1.15a). Moreover, molecular oxygen is used as the sole oxidant in the reaction, avoiding the use of potentially toxic reagents in the reaction. While the authors proposed a tandem Michael addition/electrophilic palladation/CDC pathway, they could not rule out an initial aminopaladation of the alkyne to directly form the alkenylpalladium(II) species (Scheme 1.15b). Beyond this first C–N bond formation, the transformation also differs mechanistically from Glorius' report (Scheme 1.13a);[36] an electrophilic palladation pathway was proposed for the second C–H activation because of an observed intramolecular competition KIE of 1.2 (Scheme 1.15c). Finally, the synthetic utility of the transformation was highlighted by conducting a formal synthesis of a high-affinity 5-HT_3 receptor antagonist (Scheme 1.15d).[38]

Scheme 1.15. Synthesis of Indoles from Anilines and Alkynes

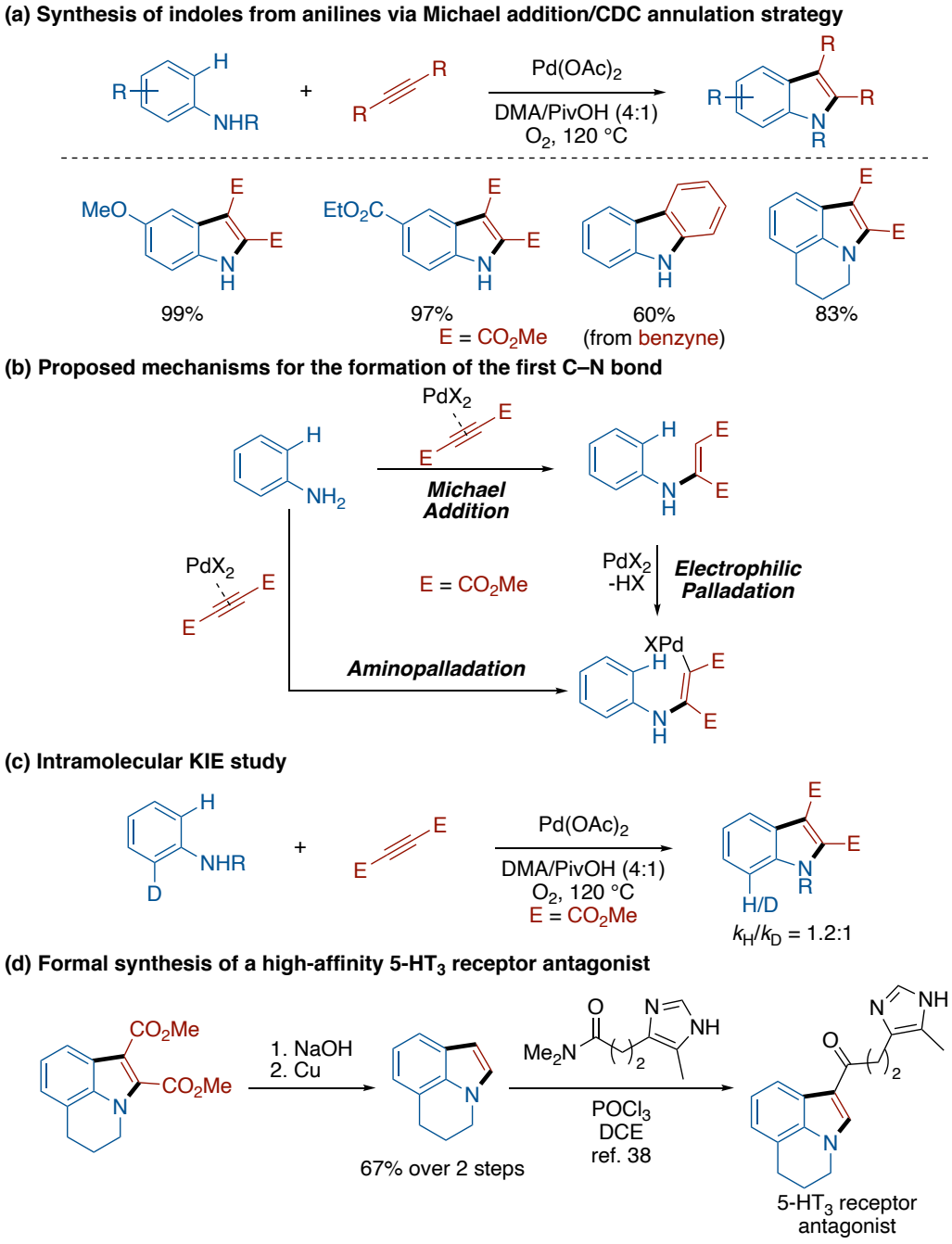

This template was later expanded to better accommodate unsymmetrical alkynes by Zhang, Cao, and co-workers for the synthesis of 2-perfluoroalkyl indoles.[39] Additionally, Yoshikai[40] and Xiao[41]

demonstrated that alkynes could be replaced with ketones for the one-pot synthesis of indoles from anilines.

1.2.2.2. Bi- and Tri-molecular Synthesis of Indoles, Indolines, and Carbazoles *via* Construction of Both C–N Bonds

A diaziridinone reagent, di-*tert*-butyldiaziridinone, has been employed extensively in the multi-component synthesis of *N*-*t*Bu indoles, although this reagent was first used in the synthesis of indolines. This reagent is also proposed to serve a dual role as an oxidant towards key pallada(II)cycle intermediates, promoting the formation of high-valent Pd(IV) intermediates, which can readily form the desired C–N bonds (*vide infra*). The resulting *N*-*t*Bu-protected products can be readily deprotected by treatment with strong acid, making them attractive substrates for nitrogen heterocycle synthesis (Scheme 1.16).

Scheme 1.16. Synthesis of Indoles and Indolines with a Diaziridinone Reagent

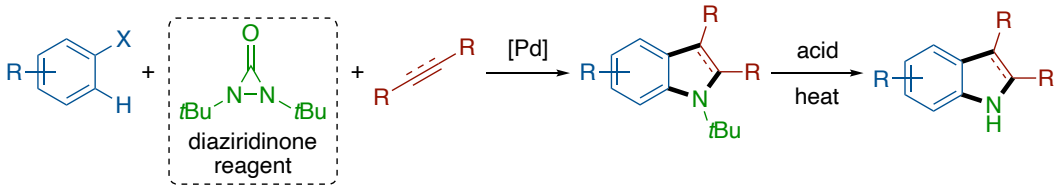

Inspired by their previous studies of the reactivity of di-*tert*-butyldiaziridinone with terminal olefins,[42] Shi and co-workers first used this diaziridinone reagent for the synthesis of spirocyclic indoline products from α-methylstyrenes (Scheme 1.17).[43] This transformation was proposed to

involve two catalytic processes – the formation of an allylic urea intermediate and subsequent transformation of this intermediate into the spirocyclic indoline product.

Scheme 1.17. Synthesis of Spirocyclic Indolines *via* Arene C–H Bond Activation

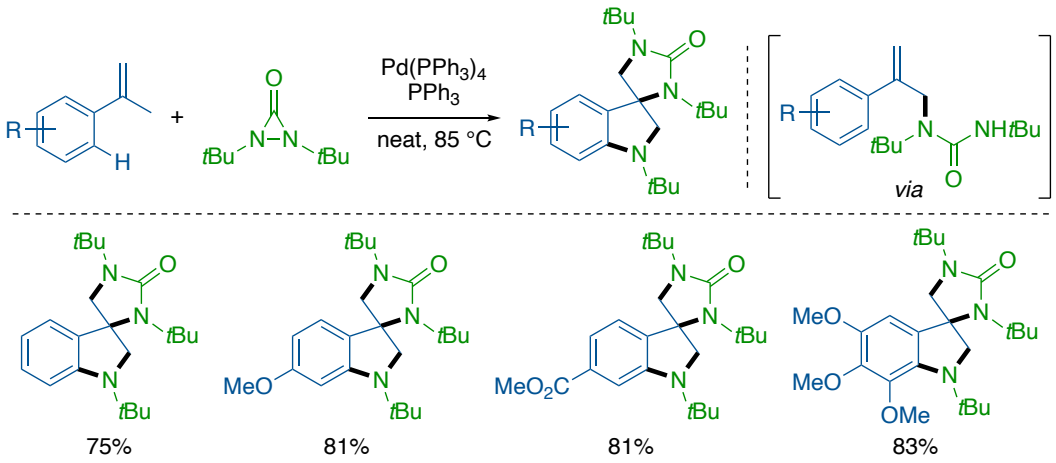

The reaction mechanism was proposed to begin with oxidative addition of Pd(0) into the N–N bond of the diaziridinone, which could form an allylic Pd(II) species upon reaction with the α-methylstyrene. This allylic species was proposed to form an allylic amine upon reductive elimination, which could coordinate with another Pd(II)-urea unit. Aminopalladation of the amine with the olefin could form the 5-membered cyclic urea motif and an alkylpalladium(II) intermediate, which was poised to undergo a C–H bond activation at the arene ortho position to form a 5-membered pallada(II)cycle. This palladacycle was proposed to undergo yet another round of oxidative addition into the N–N bond of the diaziridinone to form a higher-valent Pd(IV)-urea species, which could deliver the product through potentially two distinct pathways: pathway **(a)** could involve C–N reductive elimination to form potentially two 8-membered palladacycles, which then underwent β-nitrogen elimination and C–N reductive elimination to produce the same indoline product (Scheme 1.18a); pathway **(b)** could involve formation of a Pd(IV)-nitrene species,

which could furnish the indoline product *via* a sequence involving nitrene insertion and C–N reductive elimination (Scheme 1.18b).

Scheme 1.18. Proposed Mechanisms for the Pd-Catalyzed Spirocyclic Indoline Synthesis

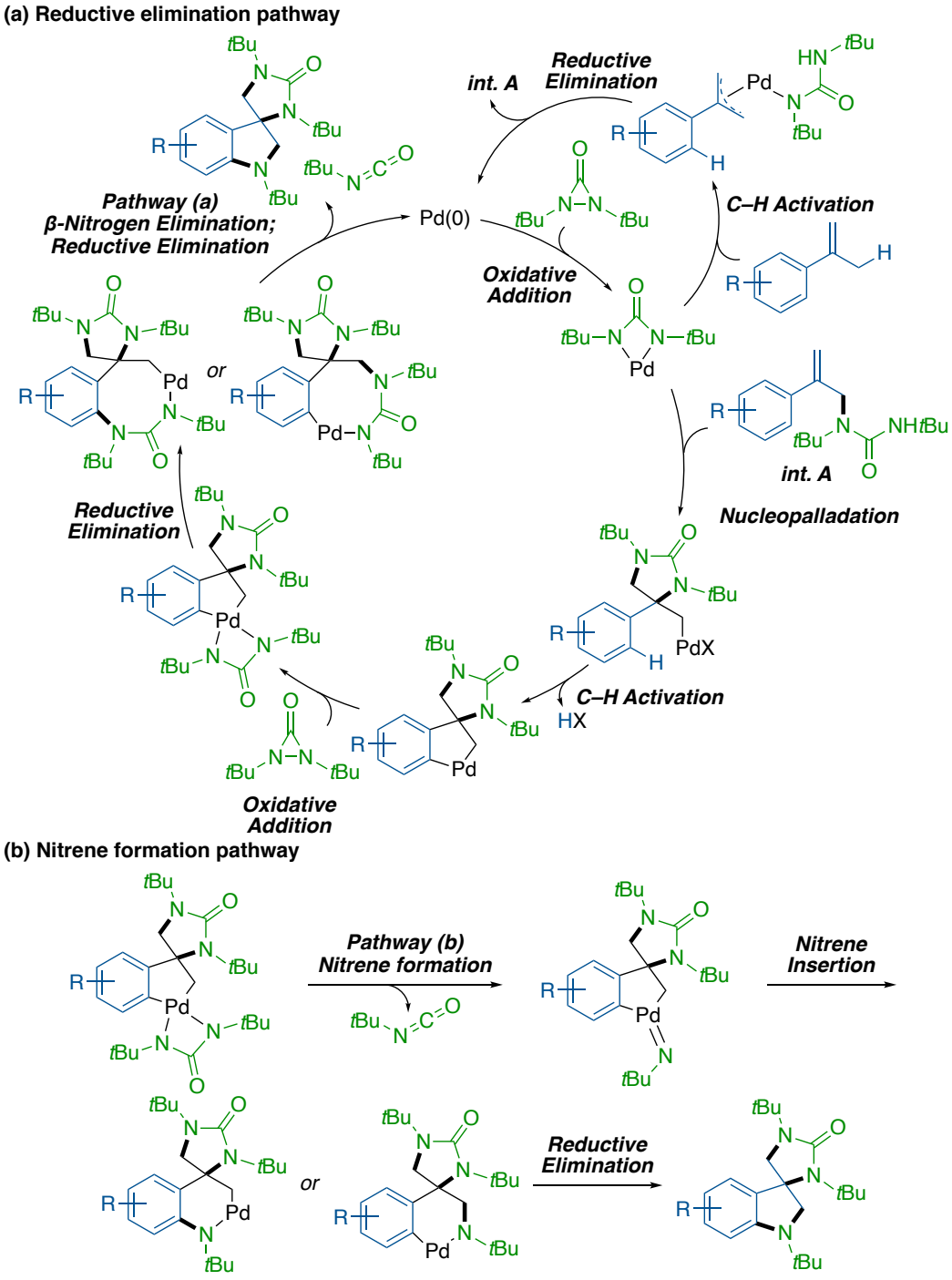

In an effort to confirm their proposed reaction mechanism, the intermediacy of the proposed allylic urea intermediate was probed by subjecting it to the standard reaction conditions, obtaining the corresponding indoline product in 35% yield (Scheme 1.19a), and an aryl pallada(II)cycle was found to be a competent catalyst for the transformation, even producing its corresponding indoline product when used in stoichiometric quantities (Scheme 1.19b). Together, these results support the proposed reaction mechanism.

Scheme 1.19. Mechanistic Probes for the Spirocyclic Indoline Formation

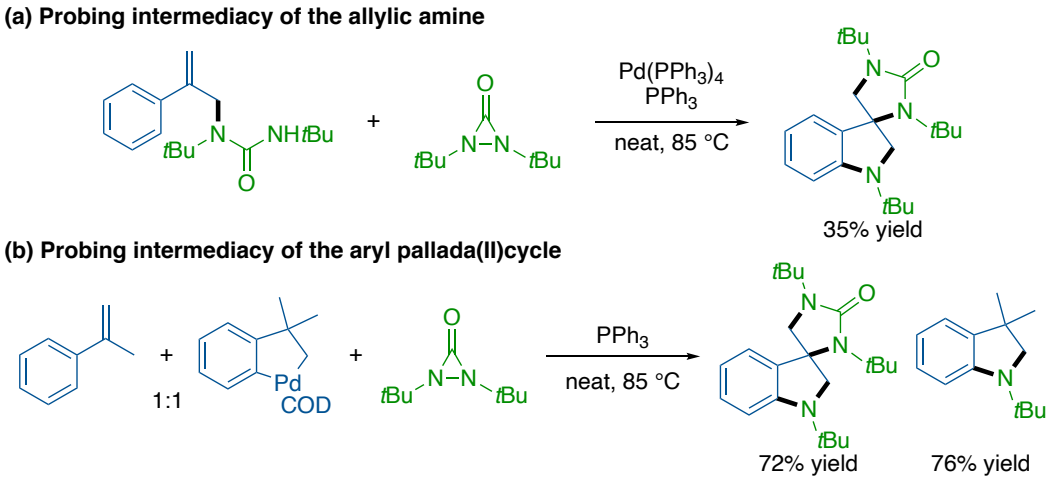

On the other hand, a strategy that can catalytically prepare the palladacycle without the spirocyclic moiety would further increase the synthetic potential of the diaziridinone reagent. Gratifyingly, the same group later modified their strategy to selectively install an *N*-*t*Bu amine moiety at the ortho position of aryl iodides, which furnished indolines upon reaction with norbornenes (Scheme 1.20a) or a tethered alkene (Scheme 1.20b).[44] Moreover, the product obtained from 2,5-norbornadiene allows for a retro Diels-Alder reaction to occur at an elevated temperature, affording the aromatic indole product (Scheme 1.20c).

Scheme 1.20. Synthesis of Indolines *via* a Three-Component Coupling

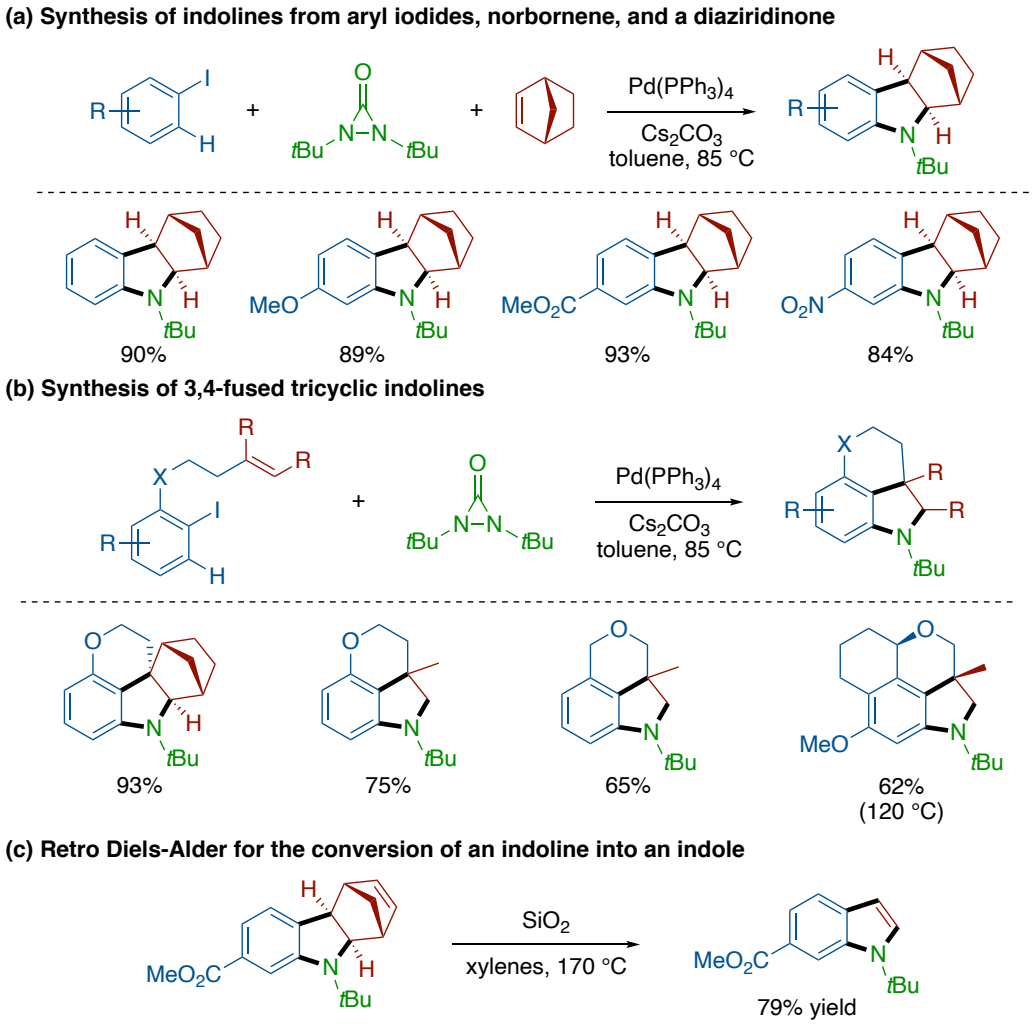

Interestingly, a bidentate ligand (such as BINAP) failed to deliver any of the desired product, possibly because it prevents coordination of the diaziridinone to the key pallada(II)cycle intermediate. Mechanistically, the transformation was proposed to begin with oxidative addition of Pd(0) into the aryl iodide, followed by migratory insertion of the alkene into the aryl–Pd bond to give an alkylpalladium(II) species, which could undergo a C–H activation with the *ortho*-C–H bond to form the key pallada(II)cycle with two carbon ligands. As shown in their previous study [43], Shi proposed that this electron-rich palladacycle could then react with the diaziridinone *via* an

oxidative addition pathway to furnish a Pd(IV) intermediate, eventually resulting in the formation of the desired indoline products through the previously proposed pathways (Scheme 1.21a). Gratifyingly, the potential side-reaction of the diaziridinone with Pd(0) was avoided, likely due to the high reactivity of aryl iodides towards Pd(0). Alternative reactivity was also observed when using a phenyl-substituted alkene. This led to C–H activation taking place on this phenyl substituent, instead of the starting aromatic ring, presumably to minimize the overall strain of the pallada(II)cycle intermediate. Consequentially, this less strained palladacycle furnishes a spirocyclic indoline product (Scheme 1.21b), the structure of which was unambiguously confirmed by X-ray crystallography of a related derivative.

Scheme 1.21. Proposed Mechanism for the Synthesis of Indolines from Aryl Iodides, Norbornene, and Di-*tert*-butyldiaziridinone and Spirocyclic Indoline Formation

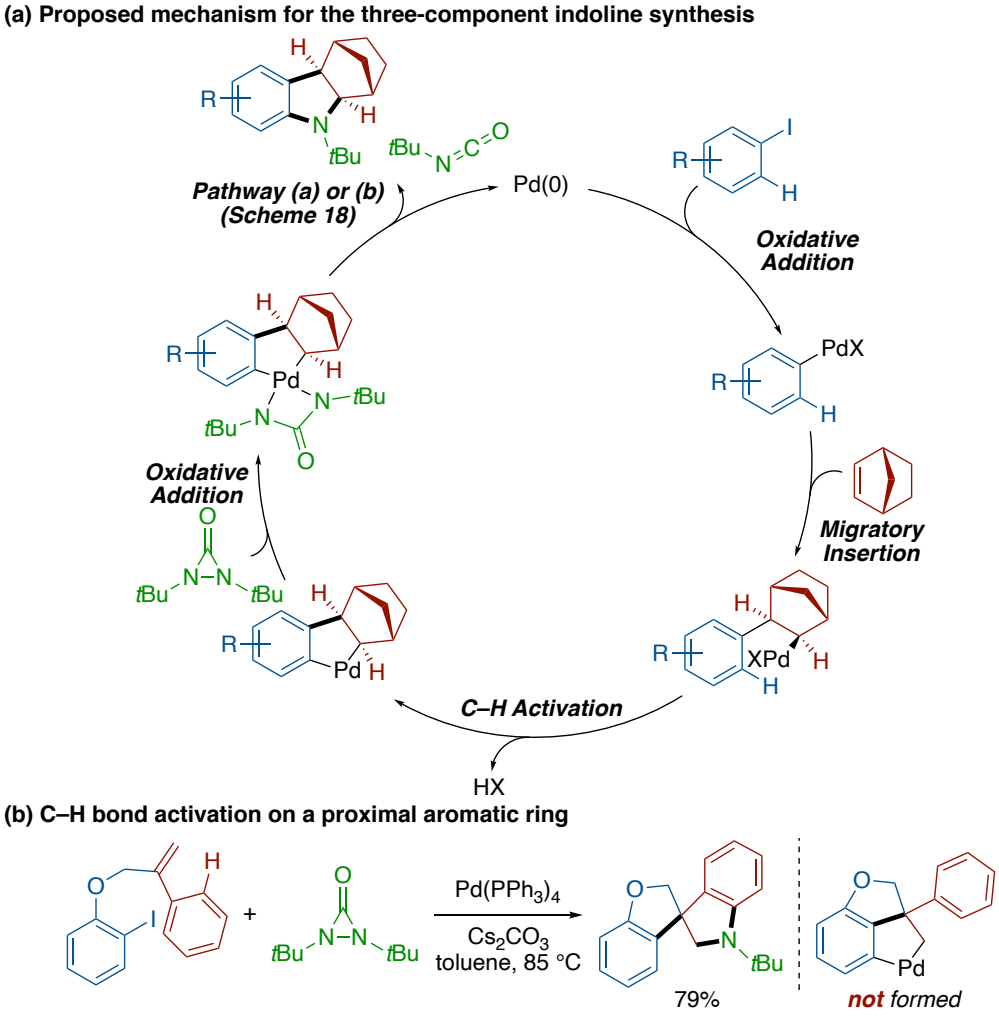

The diaziridinone reagent was also shown to be effective for the preparation of carbazoles and an indole by Zhang and co-workers (Scheme 1.22a).[45] In this work, C(sp^2)–H bond activation occurred on a proximal arene/olefin after oxidative addition of Pd(0) into the aryl iodide, resulting in the formation of a 5-membered pallada(II)cycle, which could further react with the diaziridinone

as in the previous examples (Scheme 1.22b). The intermediacy of this proposed palladacycle was proved in a stoichiometric study, albeit in a reduced yield, presumably because of the bipyridine ligand being a less efficient ligand than triphenylphosphine for the amination process (Scheme 1.22c). In particular, this transformation highlights the potential of the diaziridinone reagent to react with many pallada(II)cycles bearing two carbon ligands, regardless of the hybridization of those carbon ligands (e.g. aryl, alkyl, alkenyl).

Scheme 1.22. Palladium-Catalyzed Synthesis of Carbazoles or Indoles from 2-Iodobiphenyls or 2-Iodostyrenes and Di-*tert*-butyldiaziridinone

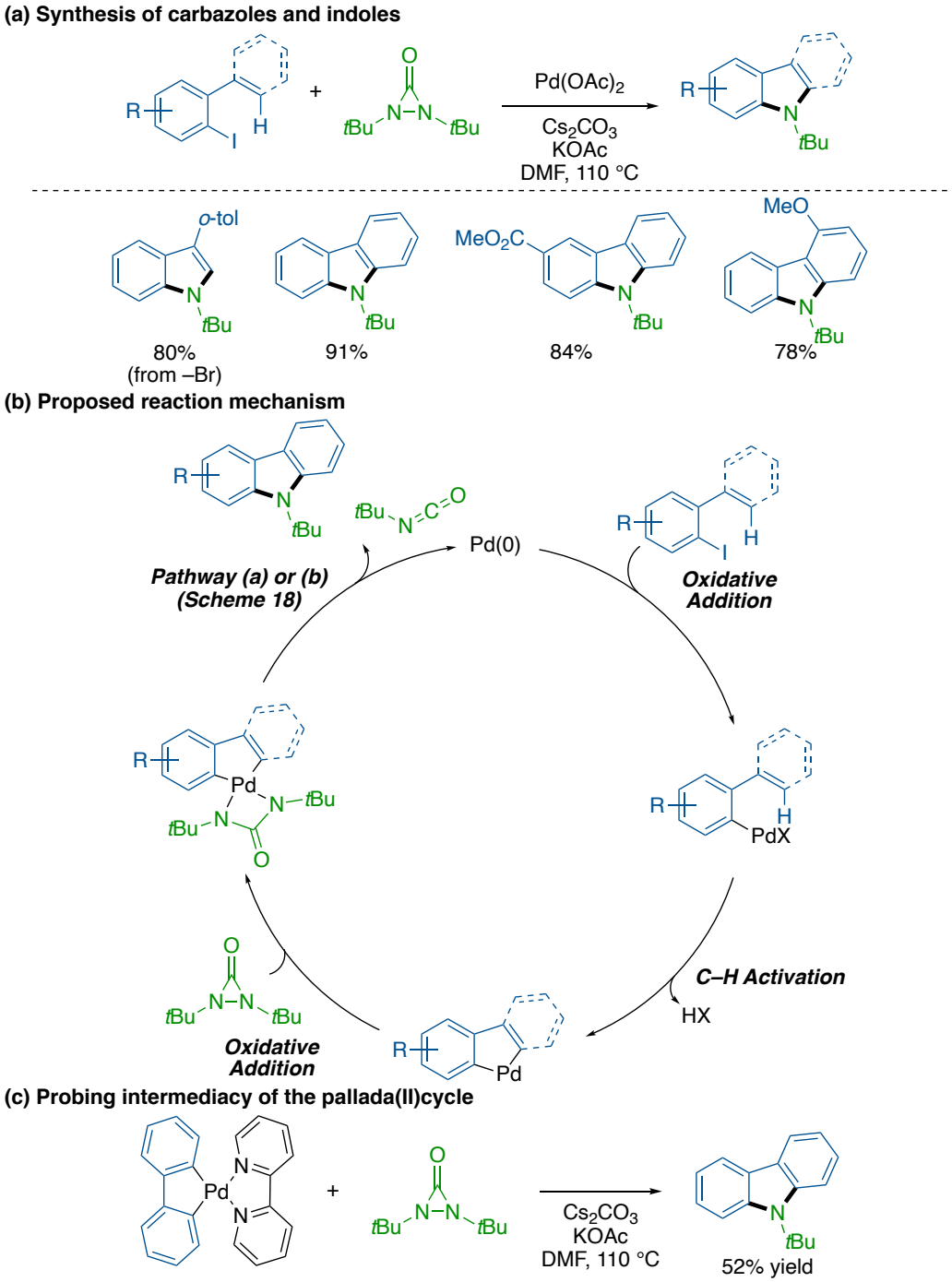

The same group later showed that the diaziridinone reagent can react with pallada(II)cycles generated from C(sp^3)–H activation with a proximal alkyl group (Scheme 1.23a).[46] Notably, 3,3-dimethylindoline structures are attractive scaffolds in the drug discovery process[47] and can easily be accessed by using this method. A study of the stoichiometric palladacycle showed that the phosphine ligand was necessary to promote the amination process, as the desired indoline product could not be obtained when 1,5-cyclooctadiene (COD) was used as the sole ligand (Scheme 1.23b). Additionally, a kinetic isotope effect of 7 was found in an intramolecular competition experiment (Scheme 1.23c) and a KIE of 2.1 was found in a parallel study, indicating that the C–H activation was likely involved in the rate-determining step of the transformation.

Scheme 1.23. Synthesis of Indolines *via* C(sp^3)–H Bond Activation

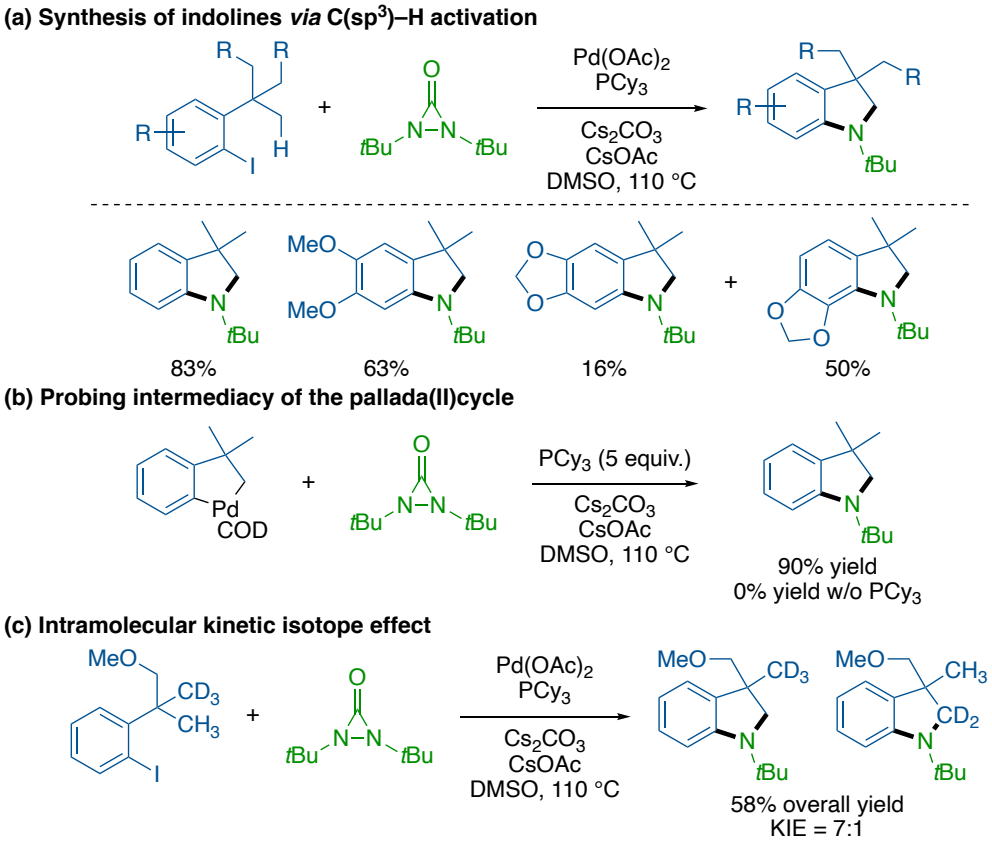

The same group also directly prepared indoles *via* a three-component reaction among aryl iodides, alkynes, and the diaziridinone (Scheme 1.24a).[48] This transformation was proposed to be mechanistically similar to Shi's prior work (Scheme 1.20),[44] with the alkyne fulfilling the role of the alkene. The versatility of this transformation was highlighted in the substrate scope study – a wide variety of electron-rich and -poor functional groups can be tolerated, along with several internal alkynes. Zhang later expanded this method to include tethered alkynes for the preparation of 3,4-fused tricyclic indoles (Scheme 1.24b),[49] which was also reported by Jiang, Yu, and co-workers shortly after.[50] Zhang further illustrated the utility of their intramolecular cyclization strategy by developing a short synthesis of the FDA-approved cancer drug, Rucaparib (Scheme 1.24c).

Scheme 1.24. Three-Component Synthesis of Indoles from Aryl Iodides

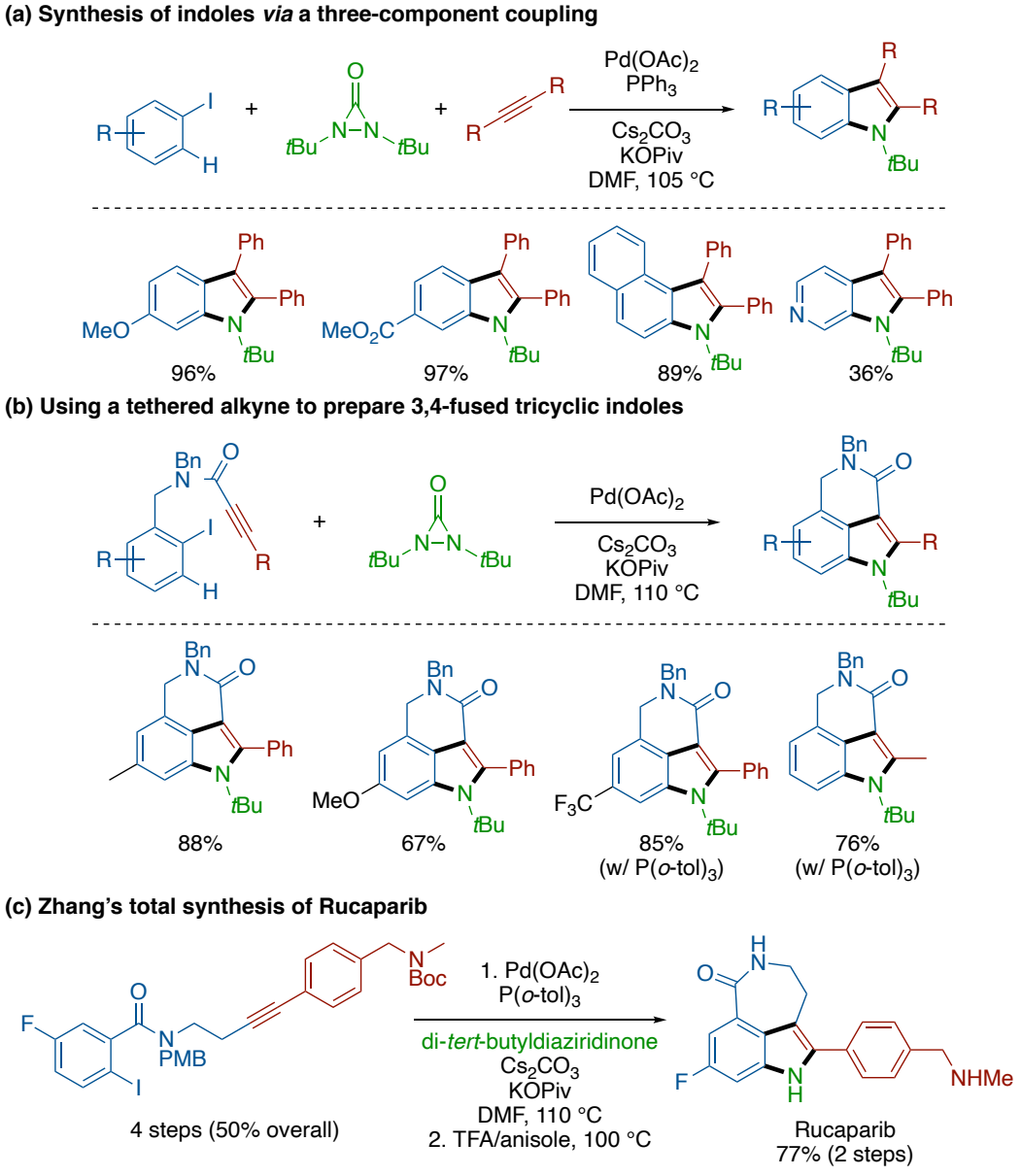

In a departure from using the diaziridinone reagent for C–H bond amination, Luan and co-workers recently showed that hydroxylamines can be effective reagents for the preparation of fused tricyclic *N*-Ts indoles (Scheme 1.25a).[51] Related to the work of Zhang (Scheme 1.24),[49] along with recent advances in *ortho*-amination in the palladium/norbornene cooperative catalysis (*vide*

infra),[52] hydroxylamines were chosen as the coupling partner due to their ease of preparation, derivatization, and precedence in *ortho*-amination reactions. By carefully tuning the electronics of the benzoyloxy leaving group, the desired 3,4-fused tricyclic indoles could be obtained in yields as high as 97% (Scheme 1.25b). In general, more electron-deficient leaving groups performed better under the reaction conditions, which indicates that better leaving group ability may be a key component in this reaction. Notably, various ring sizes and positions can be tolerated in this transformation, albeit typically resulting in lower overall yields for larger fused rings.

Scheme 1.25. Synthesis of Fused Tricyclic Indoles using Hydroxylamine Electrophiles

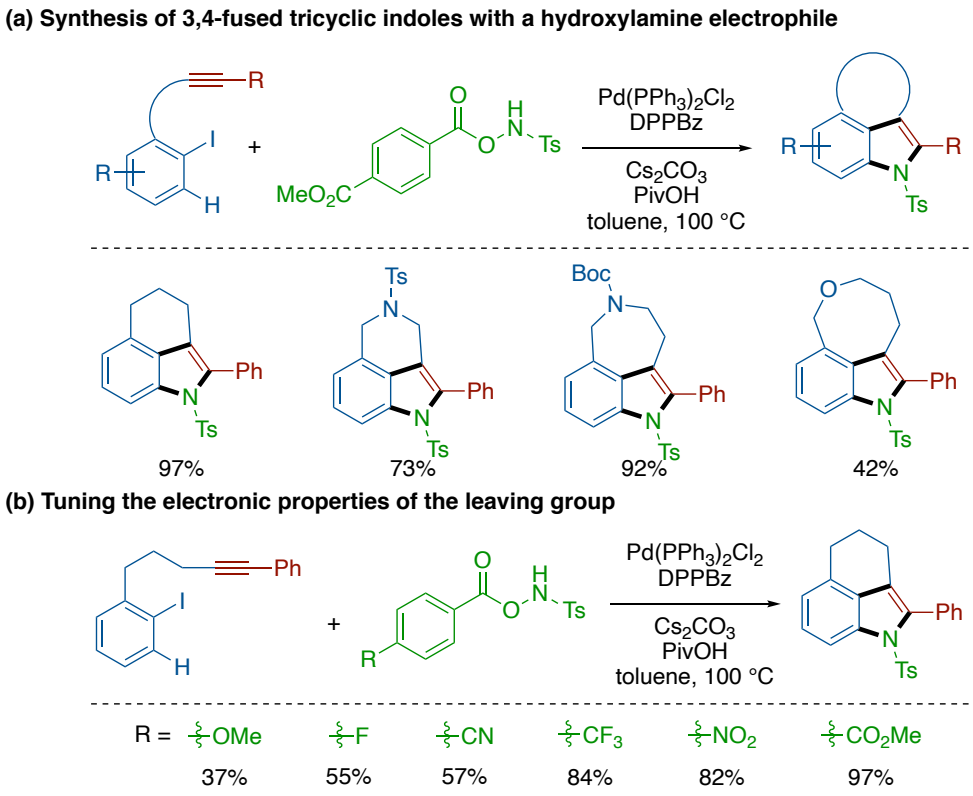

An oxidative addition pathway involving the hydroxylamine reagent was ruled out, since the more acidic N–H bond would likely be deprotonated under the reaction's basic conditions. Instead, two

pathways involving a concerted 1,2-migration or formation of a Pd(IV) nitrene species were proposed for the formation of the aryl C–N bond (Scheme 1.26).

Scheme 1.26. Proposed Mechanisms for C–N Bond Formation

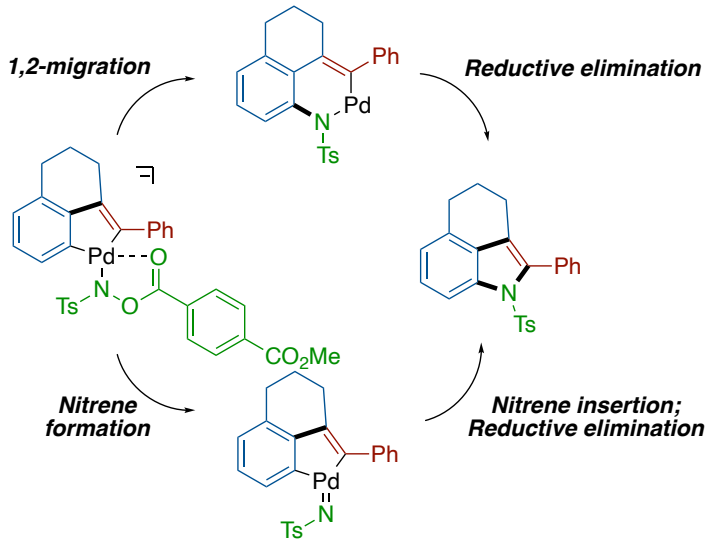

1.2.2.3. Indole Synthesis *via* the Palladium/Norbornene Cooperative Catalysis

The palladium/norbornene (Pd/NBE) cooperative catalysis, also known as Catellani-type reactions, has been established as an effective tool for the vicinal difunctionalization of an aryl halide and its *ortho*-C–H bond.[52-57] Consequentially, it has used to prepare indoles and their derivatives, among other heterocycles. In this dual catalyst system, norbornene acts as a catalytic directing group, enabling C–H activation to occur at the arene ortho position. This results in the formation of a key intermediate known as the aryl-norbornyl palladacycle, typically referred to as the ANP intermediate, which can then react with an electrophile to functionalize the arene ortho position. Subsequently, the norbornylpalladium species can undergo β-carbon elimination to

regenerate the norbornene co-catalyst; finally, the resulting arylpalladium species can participate in a typical cross-coupling reaction to close the catalytic cycle (Scheme 1.27).

Scheme 1.27. Mechanism of a Typical Pd/NBE-Catalyzed Aryl Iodide Difunctionalization

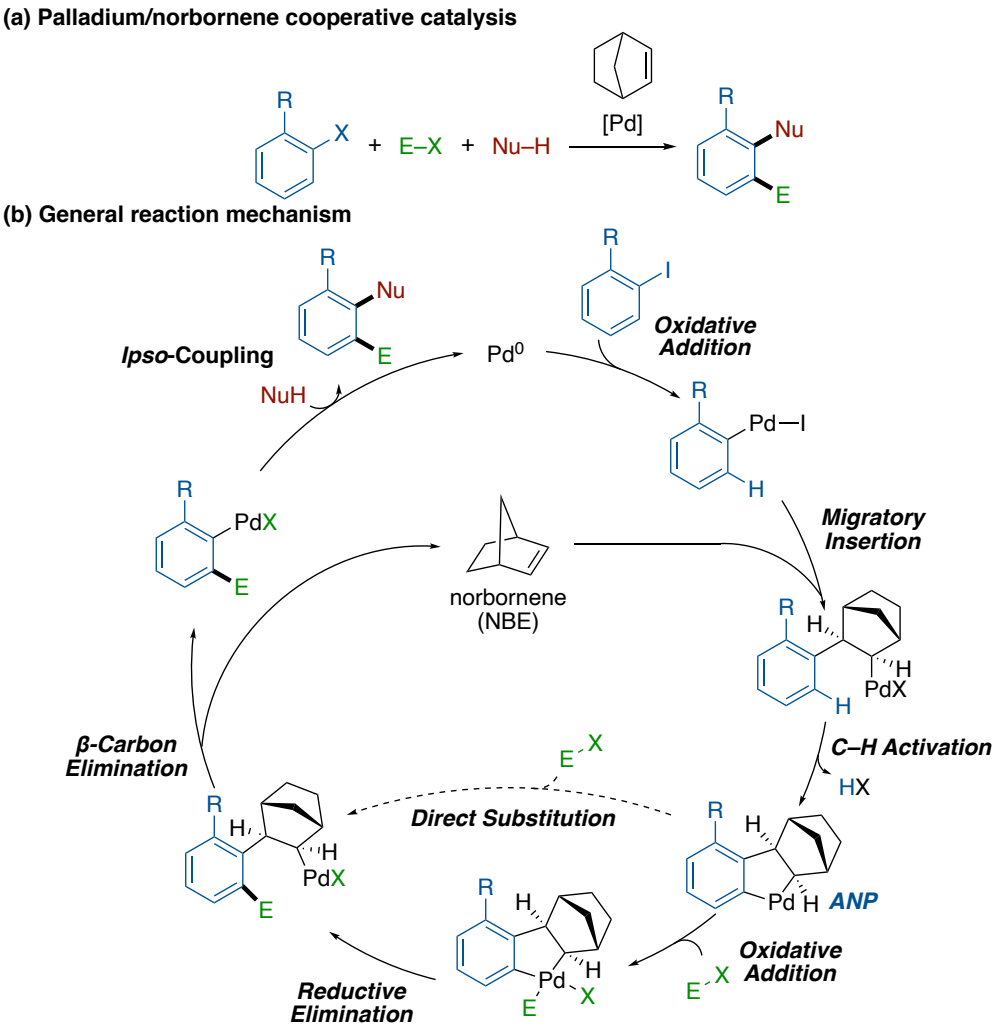

The first example of an indole synthesis using this dual catalyst system was reported by Lautens in 2010, where 2*H*-azirines were used to prepare indoles in a single step from aryl iodides (Scheme 1.28a).[58] It should be noted that, unlike the previously discussed multi-component heterocycle construction methods, no C–H bond amination takes place in this reaction, but rather a C–H

carbonation. Mechanistically, this reaction was proposed to occur by oxidative addition of the ANP intermediate into the azirine C–N single bond, followed by C–C reductive elimination at the arene ortho position. After norbornene extrusion, the ipso position was aminated *via* C–N reductive elimination to first form a 3*H*-indole, which isomerized to the aromatic 1*H*-indole (Scheme 1.28b). Notably, this method can produce unprotected indoles in a single step from aryl iodides.

Scheme 1.28. Synthesis of Indoles from Aryl Iodides and 2*H*-Azirines

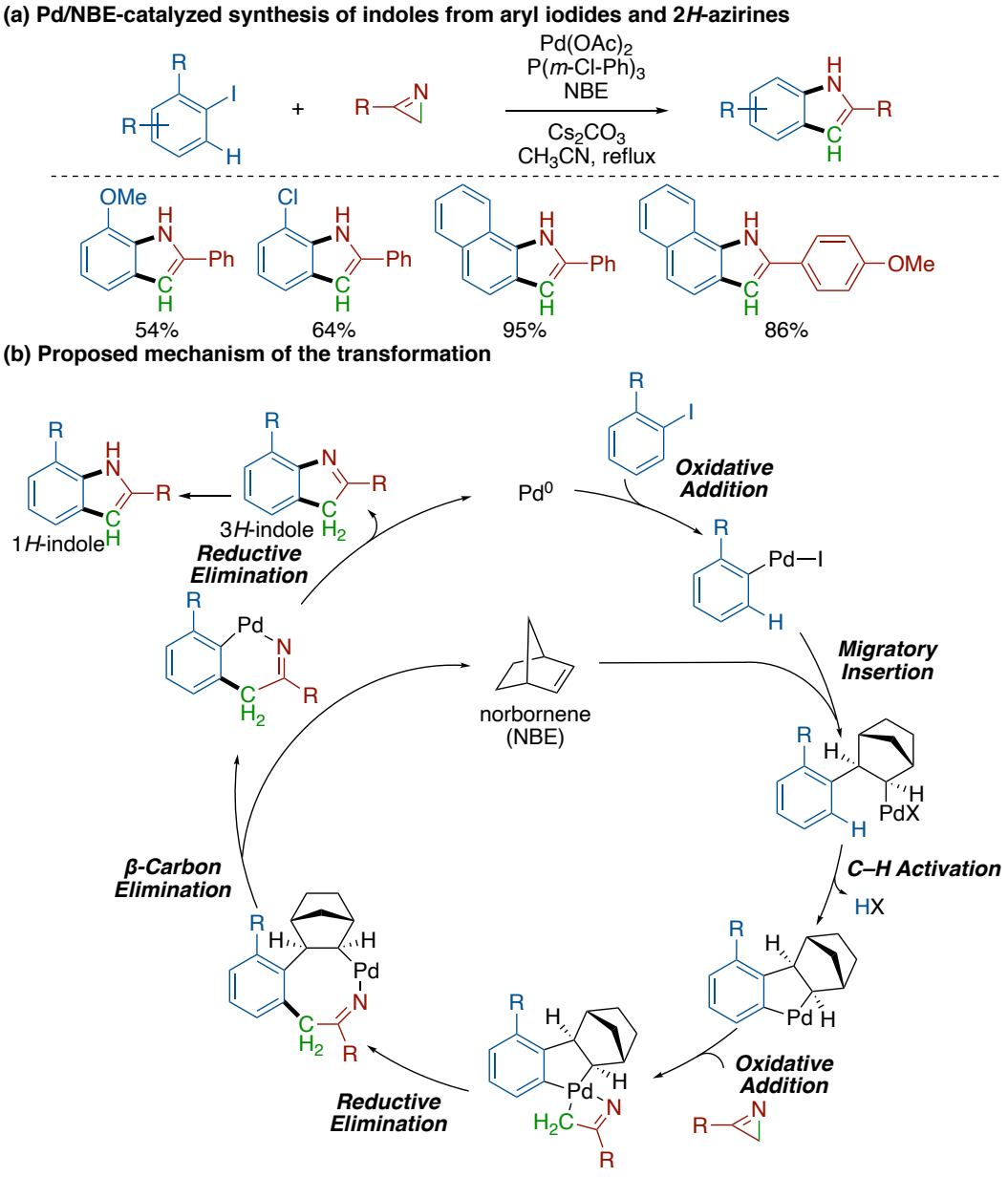

One drawback of using 2*H*-azirines, though, was their high reactivity under the reaction conditions – it was critical for them to be added slowly and under dilute conditions, as fast addition or a more concentrated reaction promoted the formation of undesired dihydroimidazoles. These dihydroimidazole side-products were proposed to be formed from a palladium-catalyzed formal

[3+2] cycloaddition of the 3*H*-indole with another 2*H*-azirine, supporting the importance of diluted conditions to favor the aromatization (Scheme 1.29).

Scheme 1.29. Conversion of the Indole Products into Dihydroimidazoles

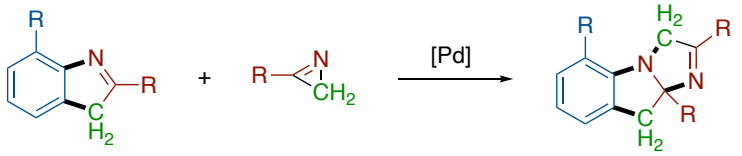

Liang and co-workers later showed that the saturated derivatives of 2*H*-azirines, aziridines, could efficiently undergo the difunctionalization reaction to deliver indoline products (Scheme 1.30a).[59] This transformation was proposed to proceed through a similar reaction mechanism as Lautens' indole synthesis (Scheme 1.28b).[58] The versatility of the transformation was demonstrated by forming a collection of 3-substituted and 2,3-disubstituted indoline products, although the selectivity between 2- and 3-substituted indoline isomers for the former was difficult to control if an aromatic ring was bound to the 2-position of the aziridine. Conversely, 2-alkyl aziridines dramatically favored formation of the 3-alkyl indoline products. Additionally, the use of an enantiopure chiral aziridine resulted in full transfer of chirality to the indoline products (Scheme 1.30b). Moreover, the inversion of configuration found with the 3-phenylindoline product isomer suggested that an S_N2-type oxidative addition with the ANP intermediate was operating, which is in agreement with a previously reported *ortho*-alkylation stereochemical investigation by Lautens.[60]

Scheme 1.30. Synthesis of Indolines from Aryl Iodides and Aziridines

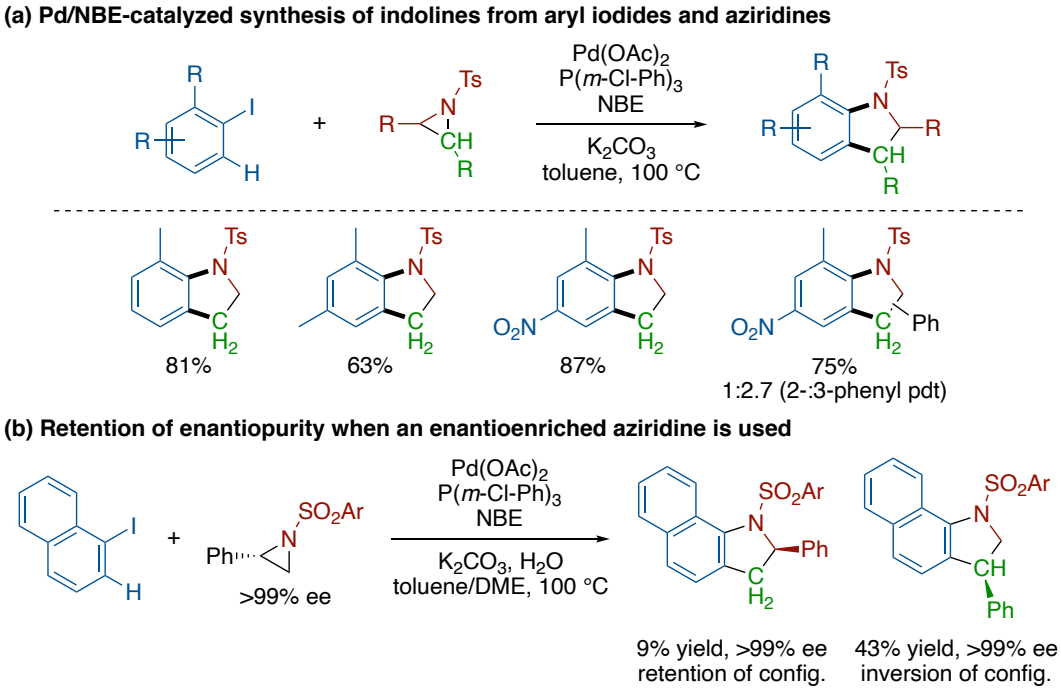

Pd/NBE cooperative catalysis has also been used to achieve indole synthesis though C–H bond amination. Liang and co-workers recently developed a three-component indole synthesis from aryl iodides, internal alkynes, and an *N,N*-dimethylhydroxylamine electrophile (Scheme 1.31a).[61] In principle, this transformation could conceivably occur in the absence of norbornene, as in Zhang's three-component indole synthesis;[48] however, no formation of the desired indole product was observed in the absence of the norbornene co-catalyst. Since it was not clear when the demethylation step occurred, density functional theory (DFT) calculations were employed to show that the skeleton of the indole was formed prior to the C–N bond cleavage, which is thermodynamically driven by aromatization of the indole heterocycle. The alternative pathway, termed "concerted metallization" by the authors, where the demethylation occurs prior to the cyclization, was found to have an incredibly high activation barrier of 75.4 kcal/mol. Conversely,

demethylation of a quaternary indolium species *after* the cyclization was found to have a much lower activation barrier of 27.9 kcal/mol (Scheme 1.31b-c). While this method is effective for the preparation of linear *N*-alkyl indoles, namely *N*-methyl, ethyl, or propyl indoles, *N*-benzyl or -aryl indoles were found to be challenging products to access using this transformation.

Scheme 1.31. Three-Component Synthesis of Indoles *via* the Pd/NBE Cooperative Catalysis

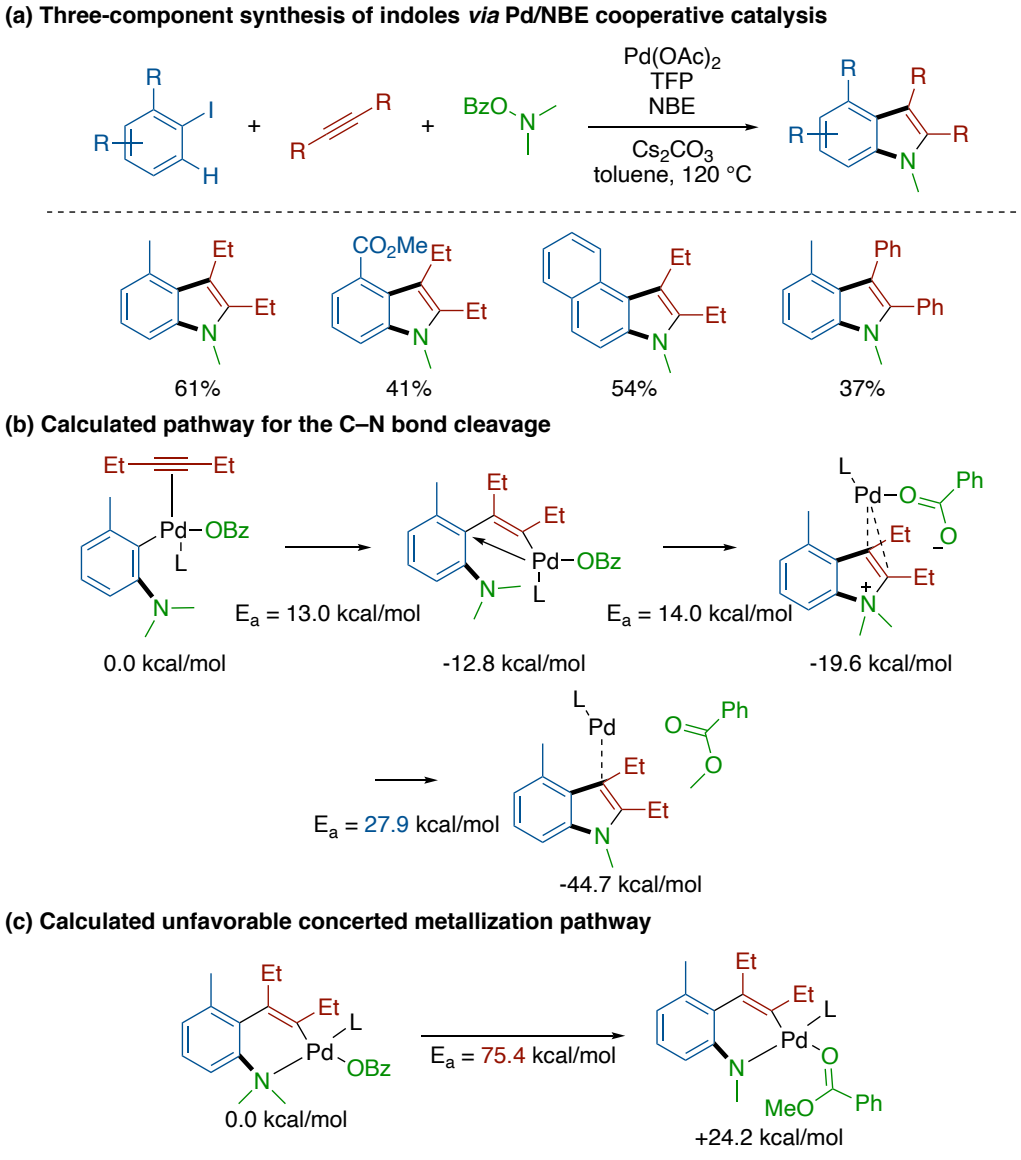

1.3. Conclusions and Outlook

In summary, recent strategies of constructing indoles and their close derivatives *via* Pd-catalyzed C–H bond activation are discussed in this short review article. Compared to conventional approaches, these palladium-catalyzed methods represent "greener" choices, as highly functionalized products could be accessed from simpler precursors under milder conditions. It is particularly attractive to directly use aryl halides or anilines as substrates, which greatly streamlined the synthesis of these heterocycles. Among the reported examples, the directed orthopalladation has been a powerful strategy for preparing indoles either intramolecularly or through multi-component couplings. In addition, the 1,4-palladium migration provides unique opportunities to transfer a reactive site to its adjacent position. Moreover, the palladium/norbornene cooperative catalysis offers a versatile platform to construct not only indoles and indolines, but also other heterocycles, due to the wide-range of *ipso*-terminating reagents and *ortho*-coupling partners that have been developed to date.[52]

As an outlook, the future development of indole, indoline, and carbazole syntheses would benefit from the use of more readily available reagents, lower catalyst loading, broader substrate scope, and milder reaction conditions. We anticipate that new C–H bond activation strategies will continue being developed for preparing indoles and other biologically important heterocycles, and eventually find their utilities in preparing pharmaceuticals. It is our hope that direct and regioselective double/vicinal C–H bond functionalization on the arene could be realized one day for multi-component indole synthesis, which would further reduce the complexity of the precursor molecules.

1.4. References

1. Kaushik, N. K.; Kaushik, N.; Attri, P.; Kumar, N.; Kim, C. H.; Verma, A. K.; Choi, E. H. *Molecules* **2013,** *18*, 6620-6662.

2. Gribble, G. W. *J. Chem. Soc. Perk. T. 1* **2000,** (7), 1045-1075.

3. Humphrey, G. R.; Kuethe, J. T. *Chem. Rev.* **2006,** *106* (7), 2875-2911.

4. Taber, D. F.; Tirunahari, P. K. *Tetrahedron* **2011,** *67* (38), 7195-7210.

5. Silva, T. S.; Rodrigues, M. T.; Santos, H.; Zeoly, L. A.; Almeida, W. P.; Barcelos, R. C.; Gomes, R. C.; Fernandes, F. S.; Coelho, F. *Tetrahedron* **2019,** *75* (14), 2063-2097.

6. Aggarwal, T.; Sushmita; Verma, A. K. *Org. Biomol. Chem.***2019,** *17* (36), 8330-8342.

7. Gensch, T.; Hopkinson, M. N.; Glorius, F.; Wencel-Delord, J. *Chem. Soc. Rev.* **2016,** *45* (10), 2900-2936.

8. He, J.; Wasa, M.; Chan, K. S. L.; Shao, Q.; Yu, J.-Q. *Chem. Rev.* **2017,** *117* (13), 8754-8786.

9. Yoshikai, N.; Wei, Y. *Asian J. Org. Chem.* **2013,** *2* (6), 466-478.

10. Guo, T.; Huang, F.; Yu, L.; Yu, Z. *Tetrahedron Lett.* **2015,** *56* (2), 296-302.

11. Agasti, S.; Dey, A.; Maiti, D. *Chem. Commun.* **2017,** *53* (49), 6544-6556.

12. Leitch, J. A.; Bhonoah, Y.; Frost, C. G. *ACS Catal.* **2017,** *7* (9), 5618-5627.

13. Cacchi, S.; Fabrizi, G. *Chem. Rev.* **2005,** *105* (7), 2873-2920.

14. Fischer, E.; Jourdan, F. *Ber. Dtsch. Chem. Ges.* **1883,** *16* (2), 2241-2245.

15. Wagaw, S.; Yang, B. H.; Buchwald, S. L. *J. Am. Chem. Soc.* **1998,** *120* (26), 6621-6622.

16. Mori, M.; Chiba, K.; Ban, Y., *Tetrahedron Lett.* **1977,** *18* (12), 1037-1040.

17. Larock, R. C.; Yum, E. K. *J. Am. Chem. Soc.* **1991,** *113* (17), 6689-6690.

18. Jensen, T.; Pedersen, H.; Bang-Andersen, B.; Madsen, R.; Jørgensen, M. *Angew. Chem. Int. Ed.* **2008,** *47* (5), 888-890.

19. Chen, X.; Lin, J.; Wang, B.; Tian, X. *Org. Lett.* **2020,** *22* (19), 7704-7708.

20. Romero, A. H. *Top. Curr. Chem.* **2019,** *377* (4), 21.

21. Tsang, W. C. P.; Zheng, N.; Buchwald, S. L. *J. Am. Chem. Soc.* **2005,** *127* (42), 14560-14561.

22. Tsang, W. C. P.; Munday, R. H.; Brasche, G.; Zheng, N.; Buchwald, S. L. *J. Org. Chem.* **2008,** *73* (19), 7603-7610.

23. Mei, T.-S.; Wang, X.; Yu, J.-Q. *J. Am. Chem. Soc.* **2009,** *131* (31), 10806-10807.

24. Liras, S.; Lynch, C. L.; Fryer, A. M.; Vu, B. T.; Martin, S. F. *J. Am. Chem. Soc.* **2001,** *123* (25), 5918-5924.

25. Mei, T.-S.; Leow, D.; Xiao, H.; Laforteza, B. N.; Yu, J.-Q. *Org. Lett.* **2013,** *15* (12), 3058-3061.

26. Neumann, J. J.; Rakshit, S.; Dröge, T.; Glorius, F. *Angew. Chem. Int. Ed.* **2009,** *48* (37), 6892-6895.

27. Tan, Y.; Hartwig, J. F. *J. Am. Chem. Soc.* **2010,** *132* (11), 3676-3677.

28. Jeong, E. J.; Youn, S. W. *B. Korean Chem. Soc.* **2014,** *35* (9), 2611-2612.

29. Youn, S. W.; Bihn, J. H.; Kim, B. S. *Org. Lett.* **2011,** *13* (14), 3738-3741.

30. Clagg, K.; Hou, H.; Weinstein, A. B.; Russell, D.; Stahl, S. S.; Koenig, S. G. *Org. Lett.* **2016,** *18* (15), 3586-3589.

31. Akazome, M.; Kondo, T.; Watanabe, Y. *J. Org. Chem.* **1994,** *59* (12), 3375-3380.

32. Ragaini, F.; Sportiello, P.; Cenini, S. *J. Organomet. Chem.* **1999,** *577* (2), 283-291.

33. Ferretti, F.; EL-Atawy, M. A.; Muto, S.; Hagar, M.; Gallo, E.; Ragaini, F. *Eur. J. Org. Chem.* **2015,** *2015* (26), 5712-5715.

34. Zhao, J.; Larock, R. C. *Org. Lett.* **2005,** *7* (4), 701-704.

35. Zhao, J.; Larock, R. C. *J. Org. Chem.* **2006,** *71* (14), 5340-5348.

36. Würtz, S.; Rakshit, S.; Neumann, J. J.; Dröge, T.; Glorius, F. *Angew. Chem. Int. Ed.* **2008,** *47* (38), 7230-7233.

37. Shi, Z.; Zhang, C.; Li, S.; Pan, D.; Ding, S.; Cui, Y.; Jiao, N. *Angew. Chem. Int. Ed.* **2009,** *48* (25), 4572-4576.

38. van Wijngaarden, I.; Hamminga, D.; van Hes, R.; Standaar, P. J.; Tipker, J.; Tulp, M. T. M.; Mol, F.; Olivier, B.; de Jonge, A.1. *J. Med. Chem.* **1993,** *36* (23), 3693-3699.

39. Shen, D.; Han, J.; Chen, J.; Deng, H.; Shao, M.; Zhang, H.; Cao, W. *Org. Lett.* **2015,** *17* (13), 3283-3285.

40. Wei, Y.; Deb, I.; Yoshikai, N. *J. Am. Chem. Soc.* **2012,** *134* (22), 9098-9101.

41. Ren, L.; Nan, G.; Wang, Y.; Xiao, Z. *J. Org. Chem.* **2018,** *83* (23), 14472-14488.

42. Du, H.; Yuan, W.; Zhao, B.; Shi, Y. *J. Am. Chem. Soc.* **2007,** *129* (24), 7496-7497.

43. Ramirez, T. A.; Wang, Q.; Zhu, Y.; Zheng, H.; Peng, X.; Cornwall, R. G.; Shi, Y. *Org. Lett.* **2013,** *15* (16), 4210-4213.

44. Zheng, H.; Zhu, Y.; Shi, Y. *Angew. Chem. Int. Ed.* **2014,** *53* (42), 11280-11284.

45. Shao, C.; Zhou, B.; Wu, Z.; Ji, X.; Zhang, Y. *Adv. Synth. Catal.* **2018,** *360* (5), 887-892.

46. Sun, X.; Wu, Z.; Qi, W.; Ji, X.; Cheng, C.; Zhang, Y. *Org. Lett.* **2019,** *21* (16), 6508-6512.

47. Wang, Y.-J.; Kathawala, R. J.; Zhang, Y.-K.; Patel, A.; Kumar, P.; Shukla, S.; Fung, K. L.; Ambudkar, S. V.; Talele, T. T.; Chen, Z.-S. *Biochem. Pharmacol.* **2014,** *90* (4), 367-378.

48. Zhou, B.; Wu, Z.; Ma, D.; Ji, X.; Zhang, Y. *Org. Lett.* **2018,** *20* (20), 6440-6443.

49. Cheng, C.; Zuo, X.; Tu, D.; Wan, B.; Zhang, Y. *Org. Lett.* **2020,** *22* (13), 4985-4989.

50. Zhang, L.; Chen, J.; Zhong, T.; Zheng, X.; Zhou, J.; Jiang, X.; Yu, C. *J. Org. Chem.* **2020,** *85* (16), 10823-10834.

51. Fan, L.; Hao, J.; Yu, J.; Ma, X.; Liu, J.; Luan, X. *J. Am. Chem. Soc.* **2020,** *142* (14), 6698-6707.

52. Wang, J.; Dong, G. *Chem. Rev.* **2019,** *119* (12), 7478-7528.

53. Ye, J.; Lautens, M. *Nat. Chem.* **2015,** *7* (11), 863-870.

54. Della Ca', N.; Fontana, M.; Motti, E.; Catellani, M. *Acc. Chem. Res.* **2016,** *49* (7), 1389-1400.

55. Wegmann, M.; Henkel, M.; Bach, T. *Org. Biomol. Chem.***2018,** *16* (30), 5376-5385.

56. Zhao, K. Ding, L.; Gu, Z. *Synlett* **2019,** *30* (02), 129-140.

57. Li, R.; Dong, G. *J. Am. Chem. Soc.* **2020,** *142* (42), 17859-17875.

58. Candito, D. A.; Lautens, M. *Org. Lett.* **2010,** *12* (15), 3312-3315.

59. Liu, C.; Liang, Y.; Zheng, N.; Zhang, B.-S.; Feng, Y.; Bi, S.; Liang, Y.-M. *Chem. Commun.* **2018,** *54* (27), 3407-3410.

60. Rudolph, A.; Rackelmann, N.; Lautens, M. *Angew. Chem. Int. Ed.* **2007,** *46* (9), 1485-1488.

61. Zhang, B.-S.; Wang, F.; Yang, Y.-H.; Gou, X.-Y.; Qiu, Y.-F.; Wang, X.-C.; Liang, Y.-M.; Li, Y.; Quan, Z.-J. *Org. Lett.* **2020,** *22* (21), 8267-8271.

(This chapter has previously been published in *Green Synthesis and Catalysis*: Rago, A. J.; Dong, G. *Green Synth. Catal.* **2021**, *In Press.* DOI: 10.1016/j.gresc.2021.02.001)

CHAPTER 2

Synthesis of C3,C4-Disubstituted Indoles *via* the Palladium/Norbornene-Catalyzed *Ortho*-Amination/*Ipso*-Heck Cyclization

2.1. Introduction

Indoles and their derivatives represent some of the most abundant heterocycles in nature and pharmaceutical drugs. Consequentially, their synthesis and functionalization have been of the utmost importance to synthetic organic chemists over the past century. Herein, we report the synthesis of C3,C4-disubstituted indoles via the palladium/norbornene cooperative catalysis. Utilizing *N*-benzoyloxy allylamines as the coupling partner, a cascade process involving *ortho*-amination and *ipso*-Heck cyclization takes place with *ortho*-substituted aryl iodides to afford diverse indole products. The reaction exhibits good functional group tolerance, in addition to tolerating a removable protecting group on the indole nitrogen. Divergent reactivity has been observed using the allylamine coupling partner containing more substituted olefins. Construction of the core framework of mitomycin has also been attempted with this strategy.

Figure 2.1. Synthesis of Indoles *via* Pd/NBE Cooperative Catalysis

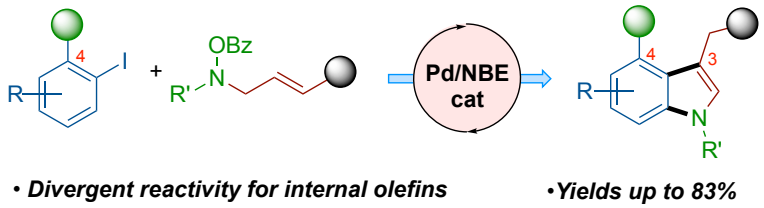

Indole and its closely related heterocycles are highly prevalent in natural products and drug molecules (Fig. 1).[1] Consequently, they have been attractive scaffolds for preparation and derivation.[2-7]

Figure 2.2. Indoles and their derivatives in Natural Products and Pharmaceuticals

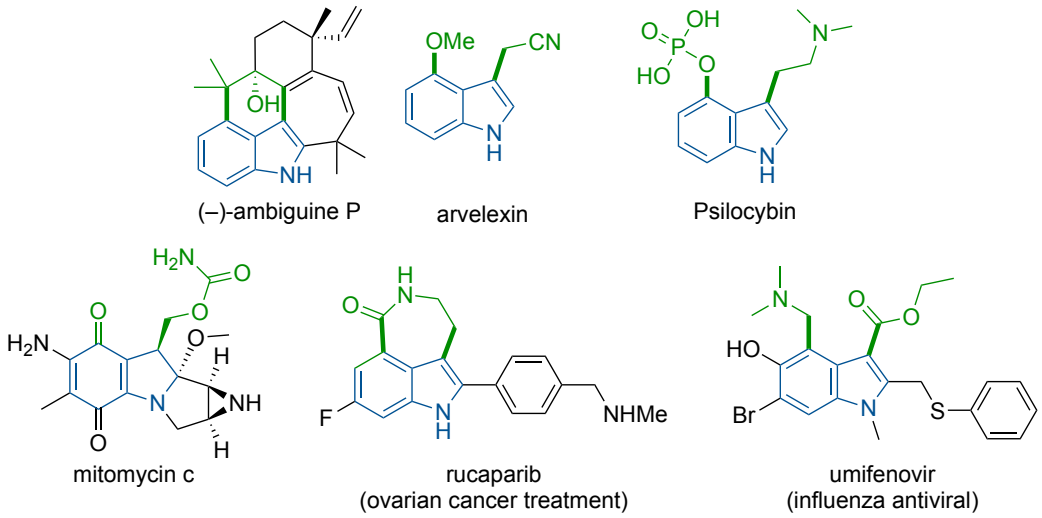

While numerous effective indole synthesis methods have been developed to date, it remains nontrivial to prepare C3,C4-disubstituted indoles in a modular manner.[8-12] On the other hand, the palladium/norbornene cooperative catalysis, first reported by Catellani,[13] represents an emerging useful tool for modular synthesis of polysubstituted arenes.[14-19] In this transformation, an electrophile and a nucleophile are coupled at the arene *ortho* and *ipso* positions, respectively

(**Scheme 1a**). Seminal work by Lautens in 2010 described a novel preparation of C2,C7-disubstituted indoles through an *ortho*-carbonation/*ipso*-amination through coupling with highly strained 2H-azirines (**Scheme 1b**).[20] In 2018, the Liang group devised an elegant approach to synthesize indolines using widely available aziridines as the reagent.[21] The development of coupling with *N*-benzoyloxy amines as electrophiles in 2013 allows convenient installation of various amine moieties at the arene *ortho* position via the Pd/NBE catalysis.[22-34] Recently, the Liang group disclosed an *ortho*-amination of 2-iodoanilines followed by *ipso*-cyclization with norbornadiene and then a retro-Diels−Alder reaction to access 4-aminoindoles.[35] More recently, an *ortho*-amination followed by demethylative annulation with internal alkynes was reported for indole synthesis with moderate efficiency (**Scheme 1c**).[36]

Scheme 2.1. Indole Synthesis via the Pd/NBE Catalysis

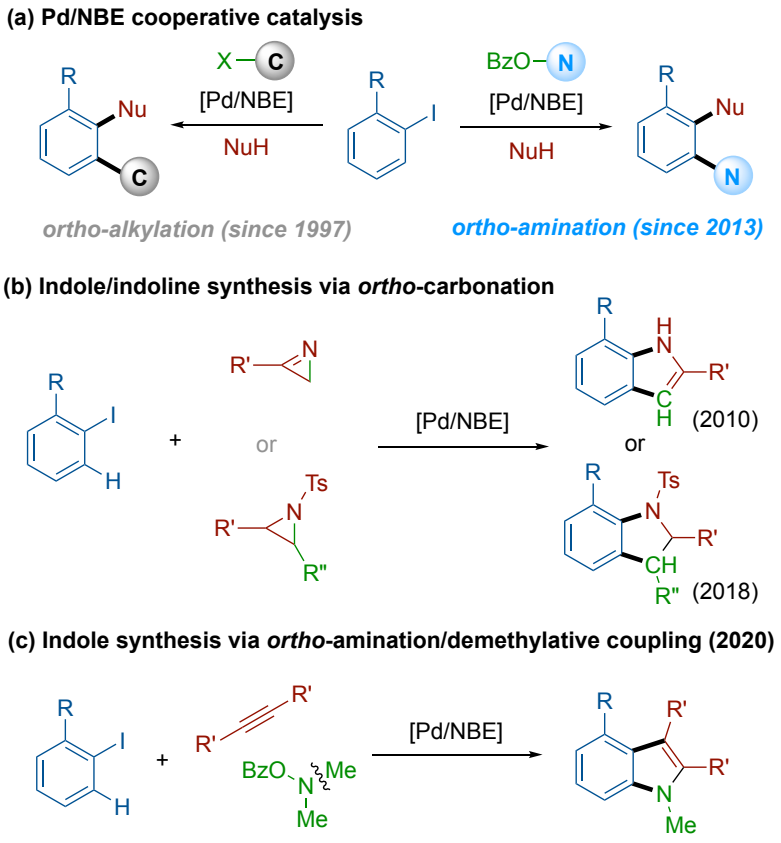

In this chapter, we describe a convenient method for preparing C3,C4-disubstituted indoles *via* an *ortho*-amination/Heck cyclization cascade[37] between common 2-substitttuted aryl iodides and readily prepared *N*-benzoyloxy allylamines (**Scheme 1d**). It can be envisioned that, upon forming the key aryl-norbornyl-palladacycle (ANP), the reaction with the electrophile should install an allylamine moiety at the *ortho* position of the arene. Upon NBE extrusion, an *ipso* Heck is expected to take place; the resulting exocyclic alkene then isomerizes to the more stable internal position to deliver the indole product.[38]

Scheme 2.2. This work – Indole Synthesis *via Ortho*-Amination/Intramolecular Heck Cascade

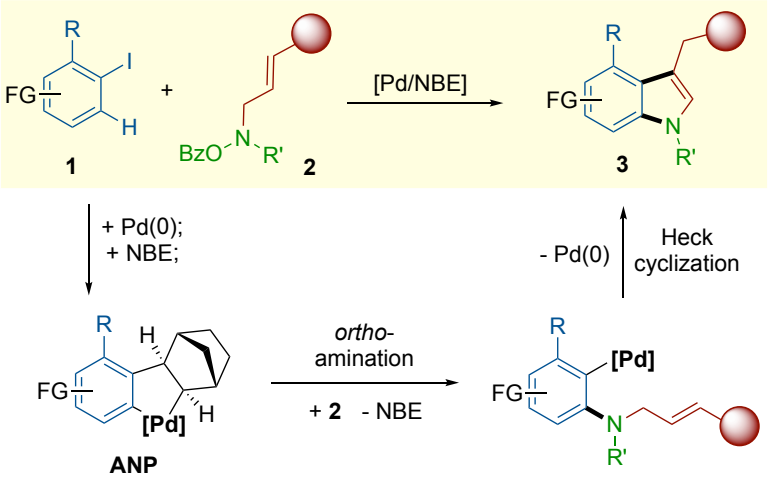

2.2. Results & Discussion

Our investigation began with 2-iodotoluene (**1k**) and an *N*-methyl-allylamine derived coupling partner (**2a)** as the model substrates (Scheme 2.1). Of three solvents previously found to efficiently facilitate *ortho*-amination reactions, toluene could give **3ka** in 47% yield. Moreover, 2-iodoanisole (**1a**) and a tertiary amine-substituted aryl iodide (**1l**) could also deliver their corresponding indole products in approximately 50% yield.

Scheme 2.1. Initial Reaction Discovery[a]

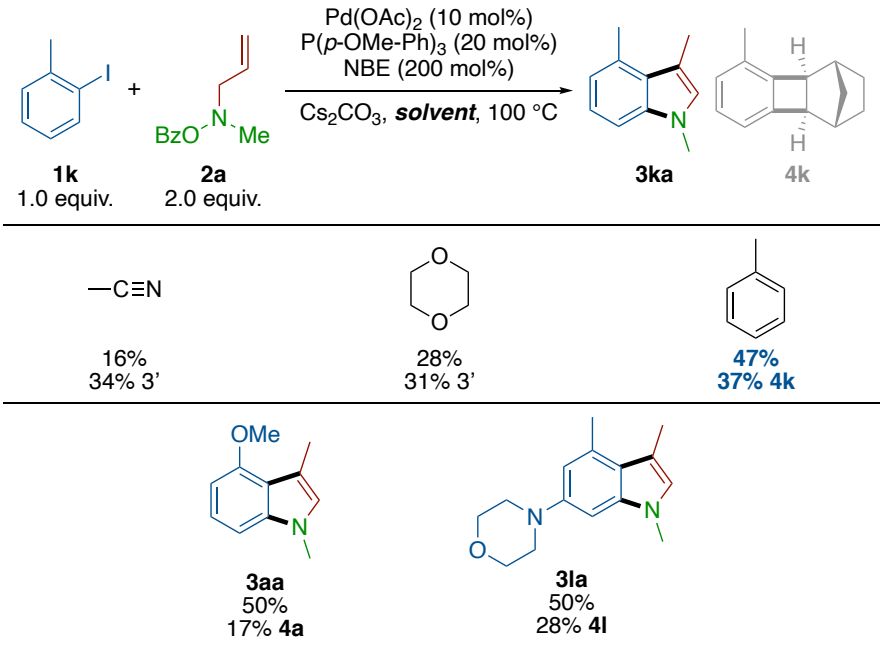

[a]Unless otherwise noted, all reactions were carried out with **1a** (0.1 mmol) and **2a** (0.2 mmol), in 1.0 mL of toluene for 18 h. NMR yields determined using 1,1,2,2-tetrachloroethane as the internal standard.

After extensive evaluation of the reaction conditions with both **1k** and **1l**, yields higher than 50% could still not be achieved. We hypothesized whether the size of the *ortho*-substituent could be important for the reaction efficiency, so we turned our attention to the smaller 2-iodoanisole (**1a**). We investigated the metal to ligand ratio, as we wondered if excess ligand could help to promote the initial formation of the active Pd(0) species. Gratifyingly, our results showed that the yield can be improved by increasing the amount of phosphine ligand used beyond 20 mol%. Additionally, the reproducibility of the reaction was drastically improved by using the higher loading of the monodentate phosphine ligand (Table 2.1). Moreover, cesium carbonate was found to be essential for the transformation, as potassium carbonate exhibited significantly reduced reaction efficacy,

and acetate salts exhibited little to no reactivity whatsoever. This is likely a consequence of using the highly nonpolar toluene as the solvent, as Cs_2CO_3 could be exhibiting better solubility at the elevated reaction temperature, along with increased basicity relative to K_2CO_3.

Table 2.1. Probing the base and Ligand:Metal Ratio[a]

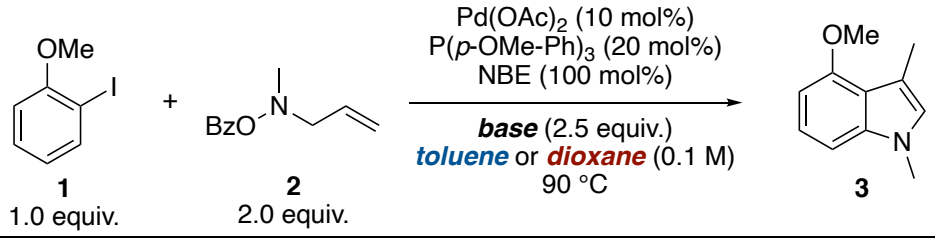

1 1.0 equiv. + **2** 2.0 equiv. → **3**

Base	% **1** remaining	% yield **3**
Cs_2CO_3	Not observed	41%
CsOAc	Not observed	1%
K_2CO_3	28%	11%
KOAc	Not observed	Not observed
Cs_2CO_3/CsOAc (1:1)	13%	33%
Phosphine loading	**% 1 remaining**	**% yield 3**
10 mol%	Not observed	23%
20 mol%	Not observed	35%
30 mol%	Not observed	65%
40 mol%	Not observed	67%

[a]Unless otherwise noted, all reactions were carried out with **1a** (0.1 mmol) and **2a** (0.2 mmol), in 1.0 mL of toluene for 18 h. NMR yields determined using 1,1,2,2-tetrachloroethane as the internal standard.

After careful evaluation of various reaction parameters, the desired indole product (**3aa**) was ultimately formed in 71% yield using $Pd(OAc)_2$ and *tris*(4-methoxyphenyl)phosphine as the optimal metal/ligand combination with Cs_2CO_3 as the base (**Table 2.2**, entry 1). The 1:4 ratio between Pd and the phosphine was still found to be necessary to promote higher yields and reproducibility of the reaction (**Table 2.2**, entries 2 and 3), though the exact reason is unclear. Other monodentate phosphine ligands that are less electron-rich than *tris*(4-

methoxyphenyl)phosphine or bidentate phosphine ligands proved to less efficient and, in some instances, generated more four-membered side-product **4a** (**Table 2.2**, entries **4-6**; *vide infra*).

Table 2.2. Selected Optimization of the Reaction Conditions[a]

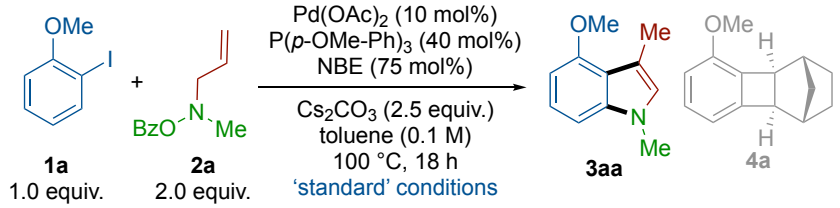

1a 1.0 equiv. **2a** 2.0 equiv. **3aa**

Entry	Change from the 'standard' condition	Yield of **3aa** (%)[b]	Yield of **4a** (%)[b]
1	none	71% (67%[c])	7%
2	25 mol% ligand	51%	14%
3	30 mol% ligand	65%	12%
4	PPh_3 as the ligand[d]	64%	15%
5	P(*p*-CF_3-Ph)$_3$ as the ligand[d]	56%	13%
6	P(2-furyl)$_3$ as the ligand[d]	38%	22%
7	**N2** instead of NBE	17%	—
8	**N3** instead of NBE	n.d.	—
9	**N4** instead of NBE	67%	—
10	50 mol% NBE	69%	9%
11	1:1 1,4-dioxane/toluene as solvent	62%	15%
12	1,4-dioxane as solvent	52%	19%
13	5 µL water added (0.5% *v*/*v* solvent)	27%	45%

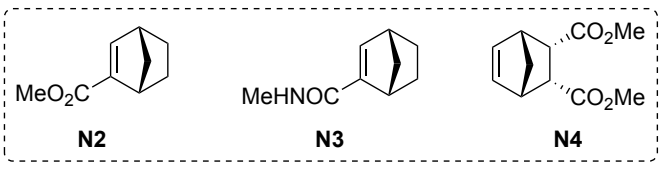

N2 **N3** **N4**

[a]Unless otherwise noted, all reactions were carried out with **1a** (0.1 mmol) and **2a** (0.2 mmol), in 1.0 mL of toluene for 18 h. [b]NMR yields determined using 1,1,2,2-tetrachloroethane as the internal standard; n.d. = not detected; – = not determined. [c]Isolated yield from **1a** (0.2 mmol) and **2a** (0.4 mmol) in 2.0 mL of toluene for 18 h. [d]NBE (100 mol%) was used.

It is likely that tri(4-methoxyphenyl)phosphine can suppress undesired off-cycle reactivity that cannot be traced when other ligands are used. Use of a 5,6-disubstituted norbornene (**N4**) was found to deliver similar results as simple NBE (**Table 2.2**, entry **9**).[39] Other structurally modified NBEs,[40] such as C2-ester-[41] and amide-substituted[42] NBEs, exhibited much lower reactivity, likely due to their steric hindrance when reacting with the relatively bulky amine electrophile **2a** (**Table 2.2**, entries **7** and **8**). Moreover, reducing the NBE loading to 50 mol% could result in similar yield and selectivity for the indole product, highlighting that it is indeed acting catalytically (**Table 2.2**, entry **10**). Toluene was found to be the best solvent, which is also consistent with our prior studies of the *ortho*-amination transformation.[22, 33] Increasing the polarity of the solvent by using a mixture of dioxane and toluene or 1,4-dioxane alone resulted in reduced yield and more side-product formation (**Table 2.2**, entries **11** and **12**). Notably, the reaction is very sensitive to the presence of water, with a sharp reversal in the selectivity between **3aa** and **4a** when just 5 μL is added to the reaction (**Table 2.2**, entry **13**).

Beyond these selected optimization examples, a wide-range of mono- and bidentate phosphine ligands were surveyed in this transformation (**Scheme 2.3**). In general, aryl groups bound to the phosphorus atom were found to be necessary, with the only exception being the electron-rich bidentate ligand dCypb. Substitution of one phenyl group of PPh_3 with a methyl group, for example, resulted in a drastic reduction in the amount of the indole product. Moreover, P(*n*-Bu)$_3$ failed to deliver any of the indole product, while tricyclopentylphosphine exhibited

drastically reduced efficiency compared to the triarylphosphines. Moreover, bidentate ligands generally performed with similar efficiency, although none exhibited reactivity comparable to that of *tris*(4-methoxyphenyl)phosphine. Additionally, increasing the loading of bidentate ligands was found to have little to no impact on the yield of the indole product. This could indicate that some ligand dissociation that is detrimental to the reaction is occurring, with a higher loading of the monodentate ligands helping to prevent this from occurring.

Scheme 2.3. Full phosphine ligand screen[a]

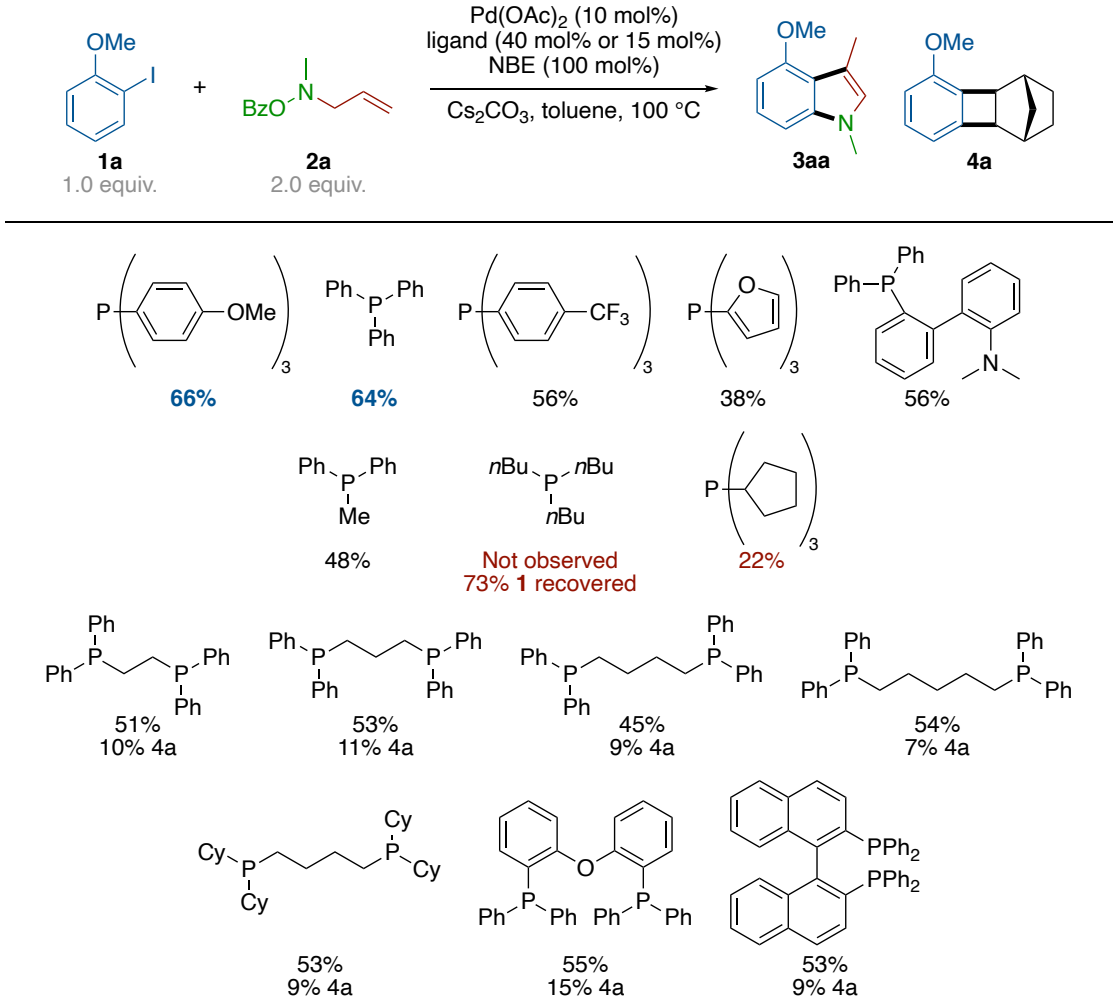

[a]Unless otherwise noted, all reactions were carried out with **1a** (0.1 mmol) and **2a** (0.2 mmol), in 1.0 mL of toluene for 18 h. NMR yields determined using 1,1,2,2-tetrachloroethane as the internal standard.

A comprehensive survey of palladium pre-catalysts identified several catalysts that could perform similar to $Pd(OAc)_2$ in this reaction (**Scheme 2.4**). Of the carboxylate Pd salts, the more hindered $Pd(OPiv)_2$ afforded a reduced yield. This is likely due to the added bulk of the *t*-Bu group preventing approach of the electrophile to the ANP intermediate, as evidenced with the shift in selectivity towards **4a**. The activated Pd(II) complexes, the Pd G3 dimer and PPh_3 Pd G3 (with added PPh_3 instead of the standard ligand), could also perform with similar efficiency. Finally, the Pd(0) dimer, Pd_2dba_3, could also perform well in the reaction. Interestingly, the heterogenous Pd/C could furnish 11% yield of the desired indole product. Somewhat counterintuitively, though, $Pd(PPh_3)_4$ could give significantly worse selectivity than using 40 mol% of PPh_3 with $Pd(OAc)_2$ – the exact reason for this difference is not so clear.

Scheme 2.4. Investigation of the Palladium Pre-Catalyst[a]

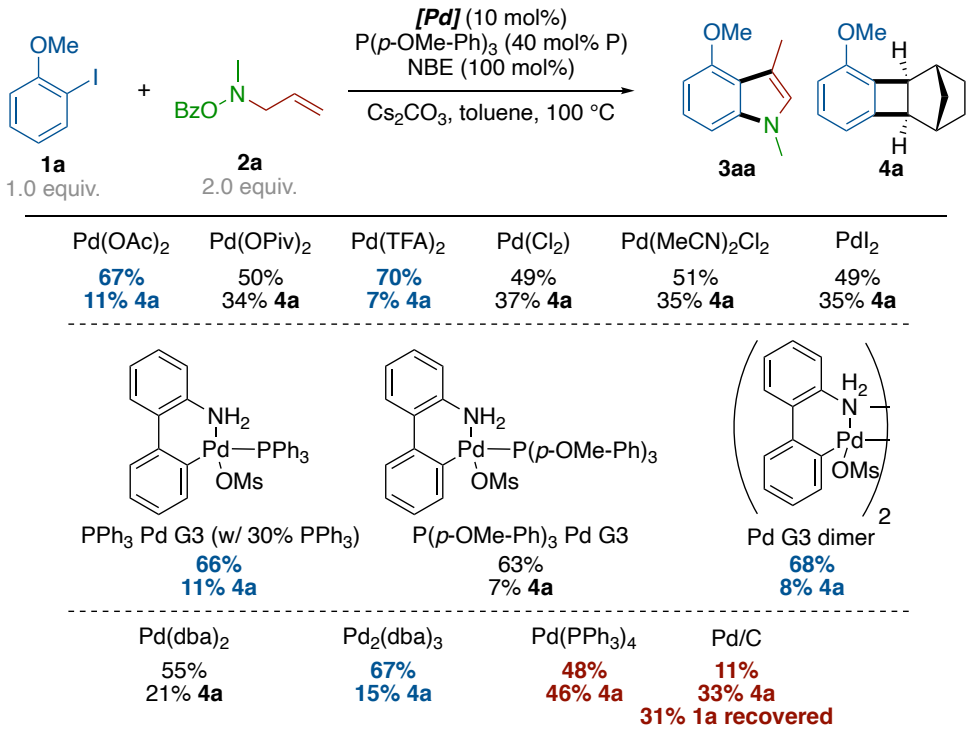

[a]Unless otherwise noted, all reactions were carried out with **1a** (0.1 mmol) and **2a** (0.2 mmol), in 1.0 mL of toluene for 18 h. NMR yields determined using 1,1,2,2-tetrachloroethane as the internal standard.

Moreover, the catalyst loading could be decreased to 7.5 mol% without significantly impacting the yield of the transformation (**Table 2.3**). This holds true for both the standard concentration of 0.1 M, in addition to slightly increasing the concentration to 0.13 M to keep the concentration of the palladium catalyst constant with the standard condition.

Table 2.3. Palladium Catalyst Loading – Constant Solvent Volume vs Constant [Pd][a]

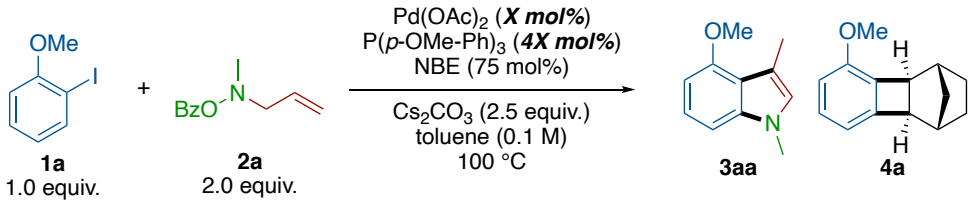

$Pd(OAc)_2$ loading	% **1a** remaining	% yield **3aa**	% yield **4a**
2.5 mol%	Not observed	39%	7%
5.0 mol%	Not observed	50%	21%
7.5 mol%	Not observed	70%	10%
10.0 mol%	Not observed	72%	11%
[Pd] = 10 mM			
2.5 mol%	Not observed	28%	9%
5.0 mol%	Not observed	54%	12%
7.5 mol%	Not observed	67%	8%
10.0 mol%	Not observed	70%	14%

[a]Unless otherwise noted, all reactions were carried out with **1a** (0.1 mmol) and **2a** (0.2 mmol), in 1.0 mL of toluene for 18 h. NMR yields determined using 1,1,2,2-tetrachloroethane as the internal standard.

To gain more insight on the reaction, the kinetic profile was measured (**Figure 2.3**). First, the reaction did not show an induction period, which is likely due in part from the excess phosphine ligand enabling rapid reduction of Pd(II) to Pd(0). The side-product **4a** was formed from the beginning of the reaction, alongside the desired product **3aa**, which suggests competing pathways with the ANP intermediate: oxidative addition with *N*-benzoyloxy amine **2a** versus direct reductive elimination to give **4a**. The reaction was nearly completed within one hour, indicating a rapid reaction rate. Afterwards, the coupling partner **2a** slowly decomposed, likely due to the basic reaction conditions and elevated reaction temperature.

Figure 2.3. Kinetic profile of the reaction; NBE (100 mol%) was used

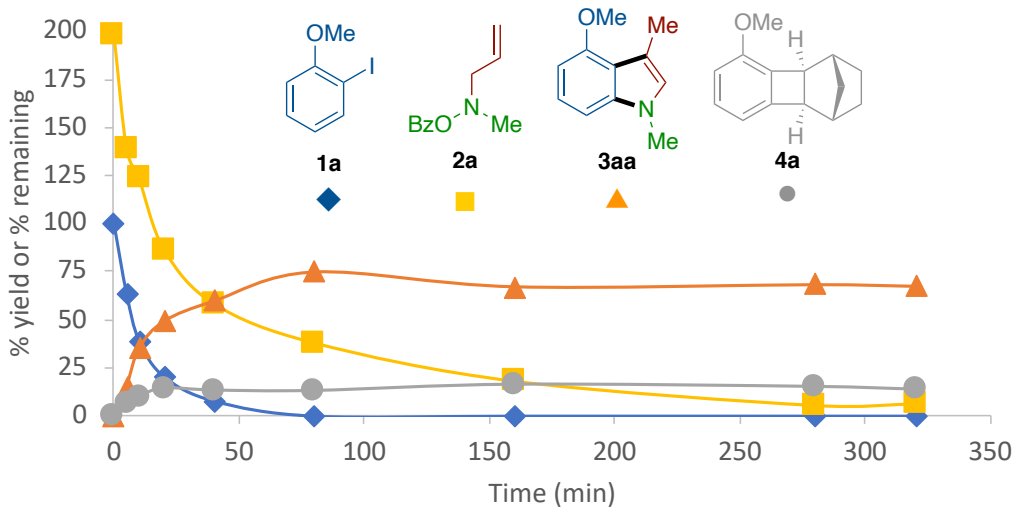

With these results in hand, we sought to explore the scope of the indole-forming reaction (**Scheme 2.5**). First, the isolated yield of the model product **3aa** can reach 72% on 1.0 mmol scale.[43] In addition, a diverse range of functional groups, such as methyl (**3ba**) and benzyl ethers (**3ia**), an unprotected tertiary alcohol (**3ca**), ester (**3ea**), bromide (**3da**), chloride (**3ma**), nitro (**3fa** and **3oa**), acetal (**3ha**) and tertiary amine (**3la**), were tolerated under the reaction conditions, affording various C3,C4-disubstituted indoles.

Scheme 2.5. Substrate Scope of the *Ortho*-Amination/Heck Cyclization Cascade[a]

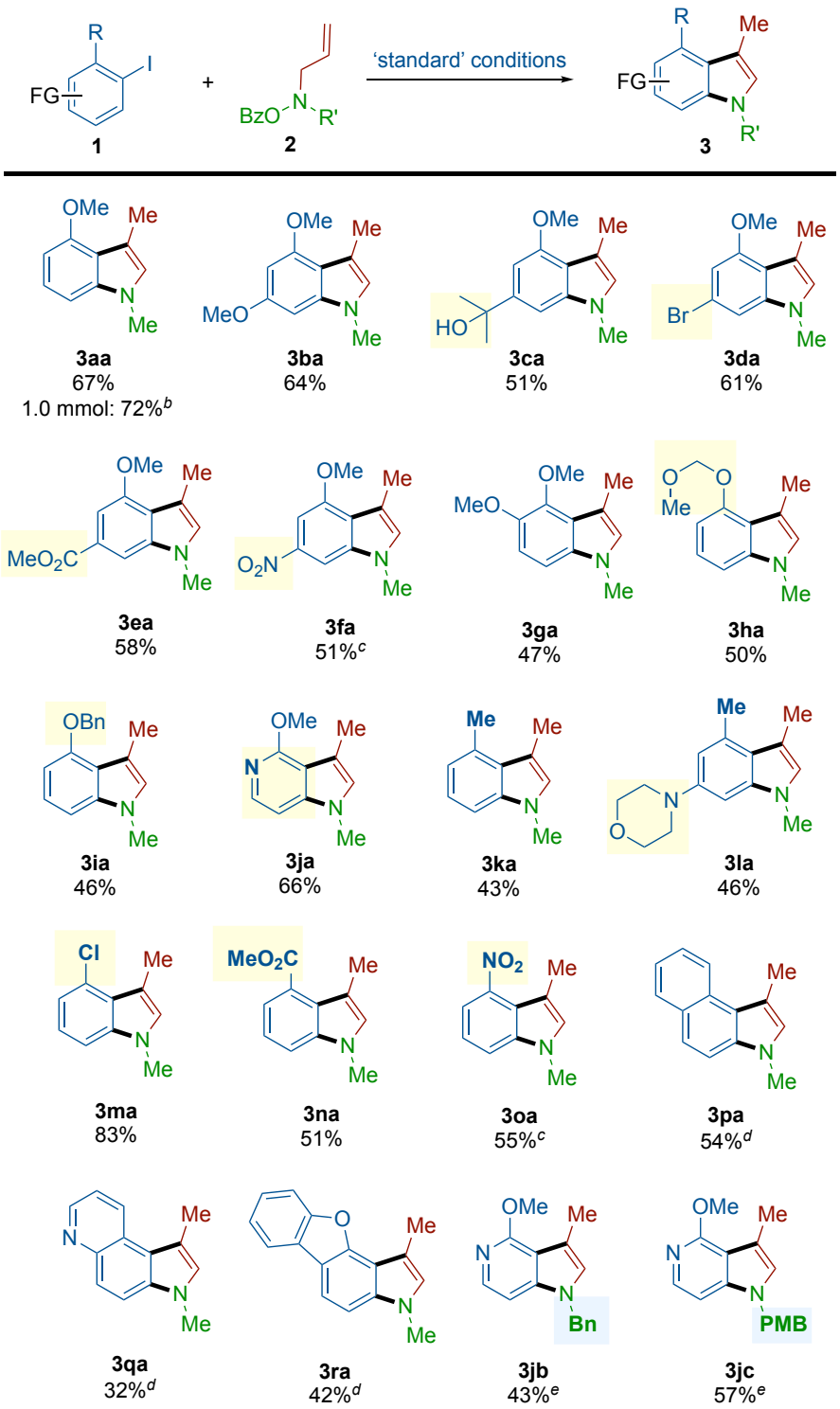

[a]Unless otherwise noted, all reactions were carried out with **1** (0.2 mmol) and **2** (0.4 mmol) in 2.0 mL of toluene for 18 h; all yields are isolated yields. [b]Carried out with $Pd(TFA)_2$ instead of $Pd(OAc)_2$, **1a** (1.0 mmol), and **2a** (2.0 mmol) in toluene (10.0 mL). [c]Carried out with 40 mol% of *tris*(4-trifluoromethylphenyl)phosphine as the ligand. [d]Carried out with **2a-2** (see the supporting information) instead of **2a** and with PPh_3 as the ligand at 120 °C. [e]Carried out at 80 °C.

Both electron-rich and -deficient substituents on the aromatic ring are compatible for this transformation. Notably, the yields for the highly electron-poor nitro-substituted aryl iodides (**3fa** and **3oa**) can be increased by changing the phosphine ligand to the electron-deficient *tris*-(4-trifluoromethylphenyl)phosphine (**Scheme 2.6**).

Scheme 2.6. Ligand Optimization of 2-Nitroiodobenzene[a]

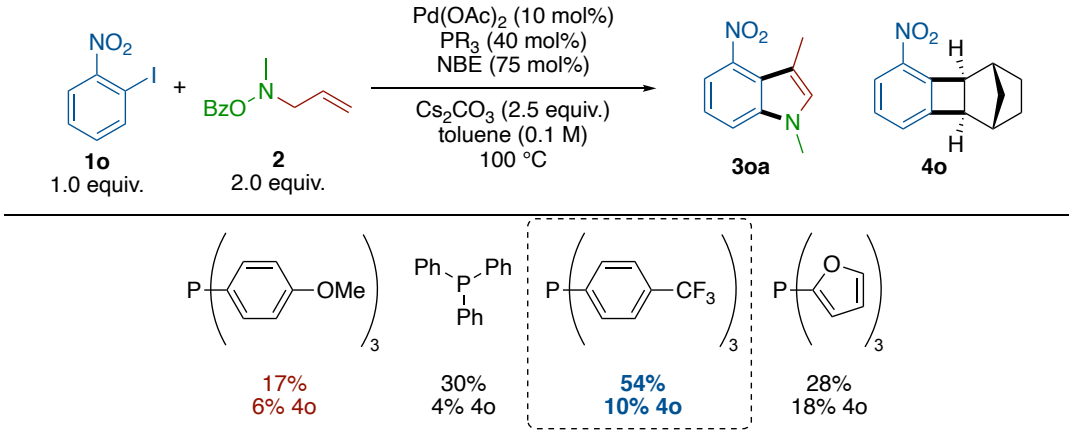

[a]Unless otherwise noted, all reactions were carried out with **1a** (0.1 mmol) and **2a** (0.2 mmol), in 1.0 mL of toluene for 18 h. NMR yields determined using 1,1,2,2-tetrachloroethane as the internal standard.

Interestingly, up to 83% yield can be obtained for the 4-chloroindole product (**3ma**). A clear trend can be observed: the yield of the indole product typically decreases if the *ortho*-substituent is larger

in size, indicating that the reaction is sensitive to the steric environment of the Heck cyclization and subsequent aromatization. Moreover, a number of heteroarene-derived iodides were competent substrates, including pyridines (**3ja-c**), quinoline (**3qa**) and dibenzofuran (**3ra**). In addition to accessing *N*-methyl indoles, by decreasing the reaction temperature to 80 °C, C3,C4-disubstituted indoles with removable protecting groups on the nitrogen, i.e. –Bn[44] (**3jb**) and –PMB[45, 46] (**3jc**), can be constructed with this method. At higher temperatures, worse selectivity for the indole product was observed. Of the other challenging substrates in this transformation, only **3fa** could benefit from the use of the electron-deficient ligand. Other functional groups at the *ortho* position, including –CN and $–CF_3$, proved to be ineffective in this reaction no matter the ligand chosen (**Scheme 2.7**). Additionally, $–OCF_3$ and a chloropyridine also resulted in somewhat low yields. In the case of the latter, coordination of Pd to the pyridine nitrogen (due to less steric repulson of the –Cl relative to the –OMe in **1j**) could possibly be the reason for the poor reactivity exhibited by the substrate.

Scheme 2.7. Investigating the Electron-Deficient Ligand with other Challenging Substrates[a]

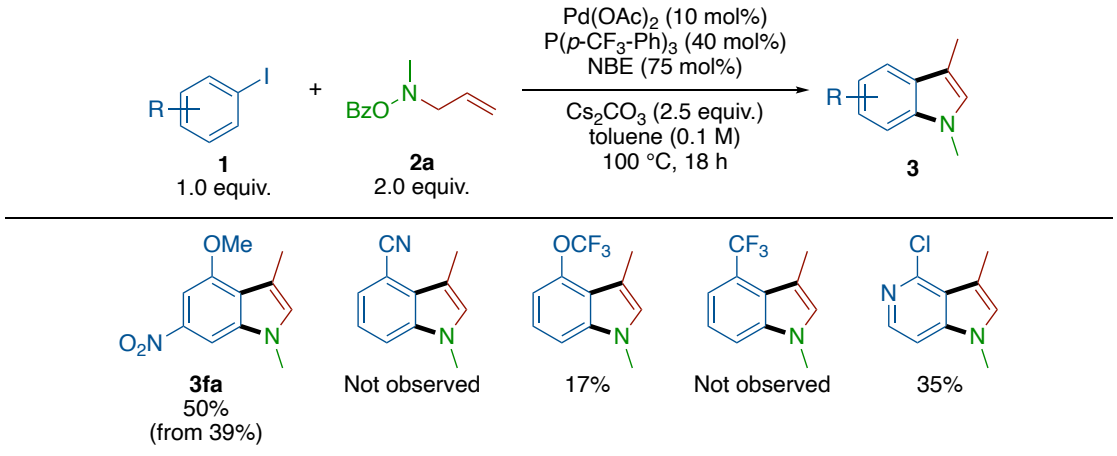

[a]Unless otherwise noted, all reactions were carried out with **1a** (0.1 mmol) and **2a** (0.2 mmol), in 1.0 mL of toluene for 18 h. NMR yields determined using 1,1,2,2-tetrachloroethane as the internal standard.

Apart from simple allylamine electrophiles, we questioned whether *N*-benzoyloxy amines with a more substituted internal olefin would react in the same manner. Consequently, the coupling reagents containing a 1,2-disubstituted alkene (**2d**) and a trisubstituted alkene (**2e**) were prepared. Interestingly, **2d** provided a separable mixture of the desired indole product (**3ad**) and an indoline isomer (**3ad'**), resulting in a combined yield of 65% (**Scheme 2.8**). In contrast, a sole indoline product (**3ae'**) was isolated in good yield when using the amine coupling partner with a trisubstituted olefin (**2e**).

Scheme 2.8. Aminating Reagents with Internal Olefins – Indole *vs* Indoline Competition[a]

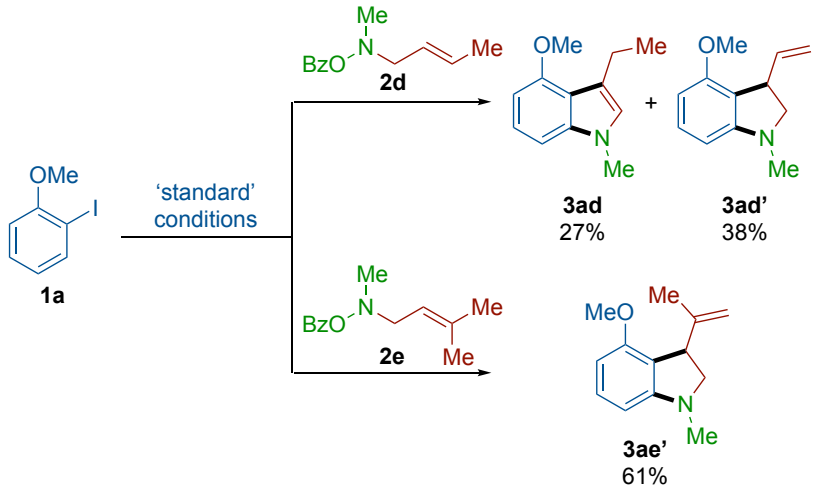

[a]All reactions were carried out with **1a** (0.2 mmol) and **2** (0.4 mmol) in 2.0 mL of toluene for 18 h; all yields are isolated yields.

The divergent reactivity observed with substituted allylamines provides useful insights into the reaction mechanism and selectivity, particularly regarding the *ipso*-Heck cyclization (**Scheme 2.9**). During the Heck coupling, the terminal mono-substituted alkene moiety undergoes kinetically favorable *5-exo-trig* cyclization, followed by β-hydride elimination, to give an exocyclic alkene intermediate, which leads to the desired indole products. When a 1,2-disubstiuted alkene is used, the moderate steric hindrance allows the β-hydride elimination to occur at either position (*inward* and *outward*), resulting in a mixture of indole and indoline products. In contrast, in the case of the trisubstituted alkene, the inward elimination would be largely inhibited due to the strong steric repulsion between the *ortho*-substituent (i.e. −OMe) and the nearly coplanar alkene substituent (i.e. −Me). Therefore, high selectivity towards the indoline formation through a less bulky outward β-hydride elimination is observed with the trisubstituted alkene.

Scheme 2.9. Divergent Reaction Pathways for Substituted Alkene Coupling Partners

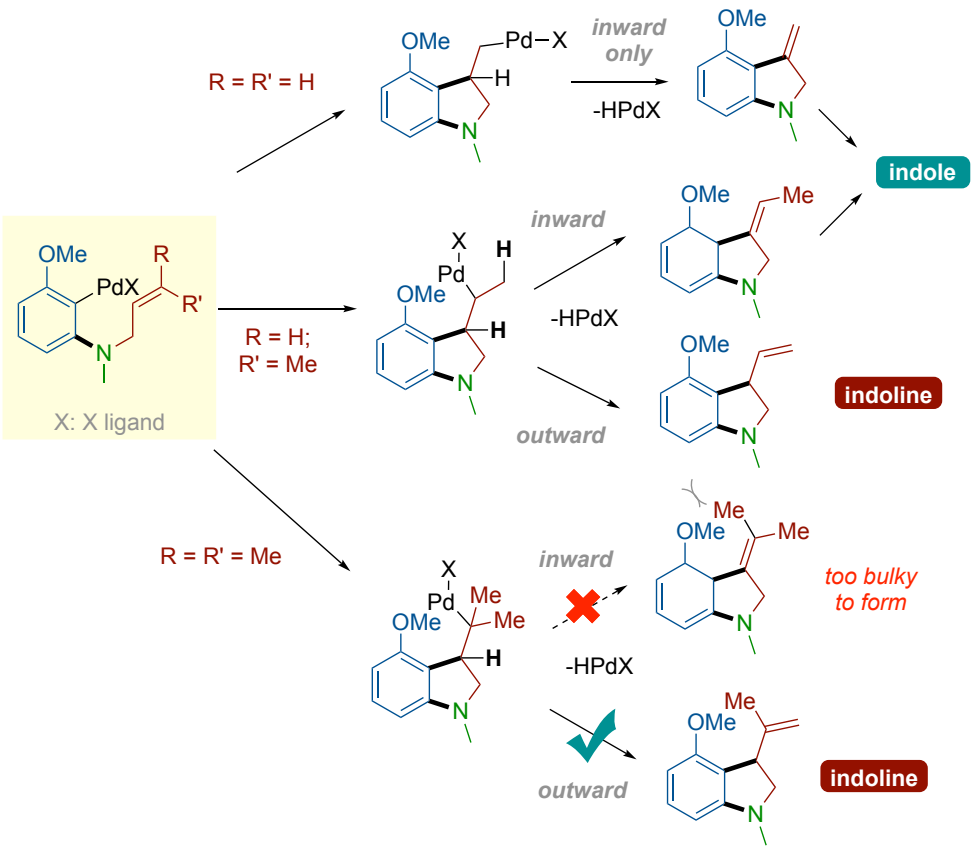

Finally, to explore the potential synthetic application of this method, construction of the core carbon skeleton of the mitomycin family of natural products has been demonstrated (**Scheme 2.10**).[47, 48] Utilizing a more complex 2-vinylpyrrolidine-derived coupling partner (**2f**), the desired *ortho*-amination/*ipso*-Heck cyclization can indeed take place under the standard conditions. Based on the analysis of the reaction's crude NMR, the non-aromatic indoline product with an exocyclic olefin was formed in 31% yield, with little to none of the indole isomer. Unsurprisingly, during the chromatography purification on silica gel, the exocyclic alkene was fully isomerized to deliver the more stable tricyclic indole isomer (**3af**). Efforts on systematically optimizing this transformation, trapping the indoline intermediate, and ultimately applying this method to mitomycin synthesis are ongoing in our laboratory.

Scheme 2.10. Attempt to Access the Carbon Skeleton of Mitomycin[a]

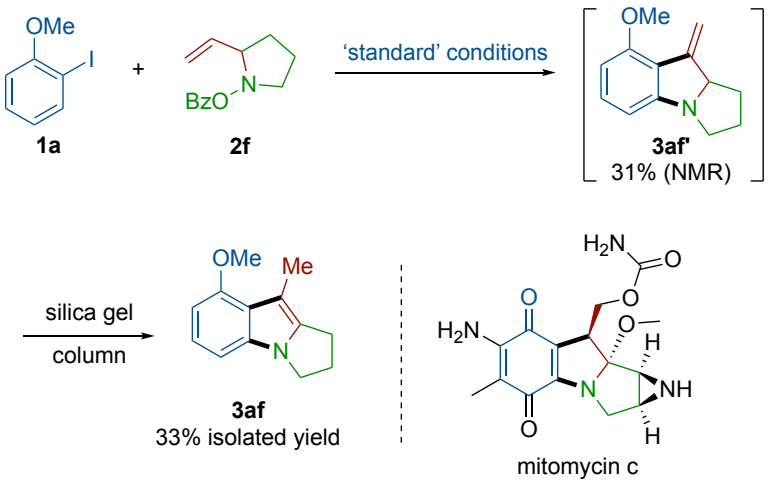

[a]Conducted with **1a** (0.1 mmol) and **2f** (0.15 mmol) in 1.0 mL of toluene.

We also attempted to demonstrate the versatility of this method to deliver unprotected indoles by subjecting the –PMB-protected product **3jc** to the debenzylation conditions developed by Davis and co-workers (**Scheme 2.11**).[46] Unsurprisingly, the highly acidic conditions only resulted in formation of the HTFA salt of **3jc** due to protonation of the basic pyridyl moiety. Analog **3ac**, however, could avoid this issue due to the absence of the pyridine ring. While no reaction was observed upon subjecting **3ac** to anisole/TFA at 0 °C, full conversion of the starting material was found at room temperature within 15 minutes. Unfortunately, though, while the N–PMB bond was cleaved, the indole C2 captured the benzylic cation to form **3ac-3** as the sole product of the reaction. This isn't necessarily a surprising result, as Miki observed this sort of –PMB group migration when attempting to remove the protecting group under acidic conditions.[45] Perhaps the DDQ conditions highlighted in their report could facilitate this deprotection, although this was not attempted. Alternatively, an additive that is more electron-rich than anisole could be used to capture the benzylic cation before the indole C2 position can intercept it.

Scheme 2.11. Attempted Indole *N*–PMB Deprotection

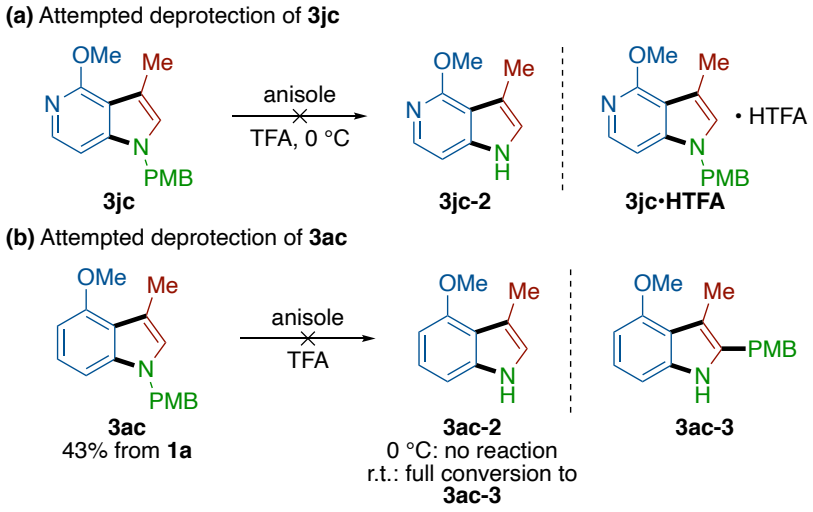

2.3. Conclusion

In summary, an *ortho*-amination, *ipso*-Heck cyclization cascade of aryl iodides for the synthesis of C3,C4-disubstituted indoles has been developed. The reaction appears to be general for a diverse range of aryl iodides, typically with smaller *ortho* substituents delivering the desired indole products in greater yields than larger substituents. A broad range of functional groups and heterocycles can be tolerated. Additionally, a steric effect has been found to be responsible for the divergent reactivity with more substituted alkene-derived coupling partners. Currently, expansion of this platform towards synthesis of other pharmaceutically relevant heterocycles, including indolines, is underway.

2.4. Experimental

General Considerations for key reactions: All reaction vials were flame-dried and allowed to cool to room temperature while capped in order to remove as much moisture as possible from the glass surface. $Pd(OAc)_2$, $Pd(TFA)_2$, and tris(*p*-methoxyphenyl)phosphine were purchased from

Sigma-Aldrich and used without further modification. Toluene used in the key reactions was distilled over Na/benzophenone, then degassed *via* freeze-pump-thaw. It was important that cesium carbonate was purchased from Strem, as other manufacturers' Cs_2CO_3 did not perform as well in the reaction. All commercially available substrates were used without further purification; however, if a liquid aryl iodide was used, it was first filtered through an alumina plug. All reactions were carried out in vials (test-scale reactions, 4 mL vials; isolation-scale reactions, 8 mL vials; 1.0 mmol-scale reaction, 40 mL vial) Thin layer chromatography (TLC) analysis was conducted on silica gel plates purchased from EMD Chemical (silica gel 60, F254). Infrared spectra were recorded on a Nicolet iS5 FT-IR Spectrometer using neat thin film technique. High-resolution mass spectra (HRMS) were obtained on an Agilent 6224 Tof-MS spectrometer and are reported as calculated/observed *m/z*. Nuclear magnetic resonance spectra (^{1}H NMR and ^{13}C NMR) were obtained using a Bruker Model DMX 400 (400 MHz, ^{1}H at 400 MHz, ^{13}C at 101 MHz); some NMR spectra (^{1}H, ^{13}C) were obtained using a Bruker Model DMX 500 (500 MHz, ^{1}H at 500 MHz, ^{13}C at 125 MHz). For $CDCl_3$ solutions, the chemical shifts were reported as parts per million (ppm) referenced to residual proton or carbon of the solvents: $CHCl_3$ δ H (7.26 ppm) and $CDCl_3$ δ C (77.16 ppm). Coupling constants were reported in Hertz (Hz). Data for ^{1}H NMR spectra were reported as following: chemical shift (δ, ppm), multiplicity (br = broad, s = singlet, d = doublet, t = triplet, q = quartet, dd = doublet of doublets, td = triplet of doublets, ddd = doublet of doublet of doublets, m = multiplet), coupling constant (Hz), and integration.

Compounds **1a**, **1b**, **1f**, **1j**, **1k**, and **1m**-**1p** are commercially available. Compounds **1d**,[49] **1e**,[50] and **1q**[51] have been previously reported and were prepared *via* a diazotization procedure[51] from the corresponding anilines. Compounds **1g**,[52] **1h**,[53] **1i**,[54] **1l**,[39] **1r**,[55] **2a**,[56] **2b**[57], **4a**,[58] **N2**,[59] **N3**,[42] and **N4**[60] have all been previously reported in the literature.

Figure 2.4. Commercially Available, Known, and New Compounds

Commercially available compounds:

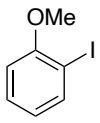

1a

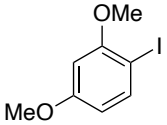

1b

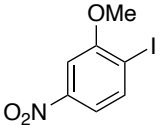

1f

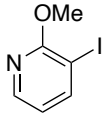

1j

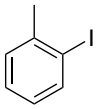

1k

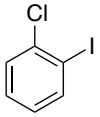

1m

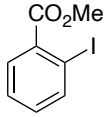

1n

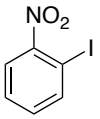

1o

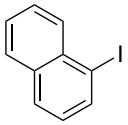

1p

Known compounds:

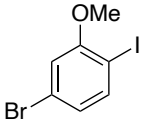

1d

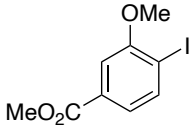

1e

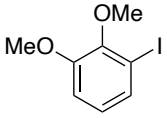

1g

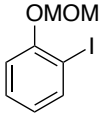

1h

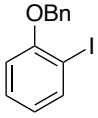

1i

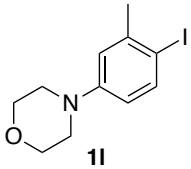

1l

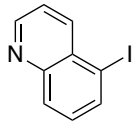

1q

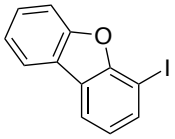

1r

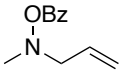

2a

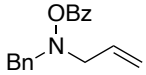

2b

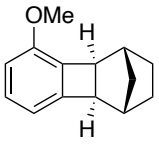

4a

Known compounds (continued):

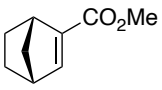

N2

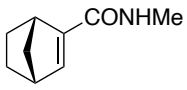

N3

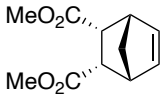

N4

New compounds:

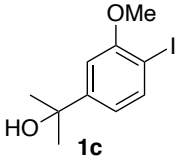

1c

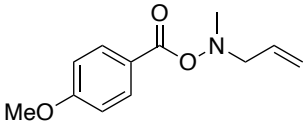

2a-2

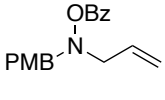

2c

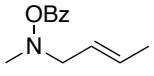

2d

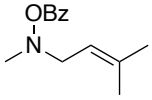

2e

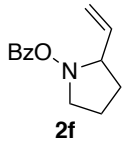

2f

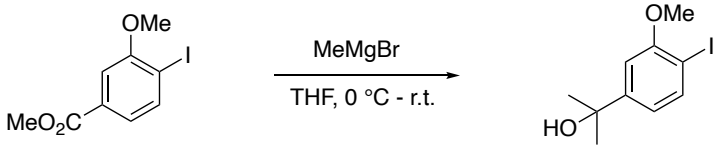

2-(4-iodo-3-methoxyphenyl)propan-2-ol (1c): Tetrahydrofuran (13.7 mL, 0.25 M) and methyl 4-iodo-3-methoxybenzoate (**1e**; 1.0 g, 3.42 mmol, 1.0 equiv.) were placed in a flame-dried Schlenk flask equipped with a stir bar under an N_2 atmosphere, then cooled to 0 °C. Methylmagnesium bromide solution (2.28 mL, 6.84 mmol, 2.0 equiv.) was added dropwise and the reaction was allowed to stir at room temperature overnight, after which the reaction was quenched with sat. NH_4Cl solution. The aqueous layer was extracted with EtOAc; the combined organics were washed with brine, dried over $MgSO_4$, and filtered. The solution was concentrated, and the crude oil was purified *via* silica gel chromatography (EtOAc/hexanes) to produce a viscous pale-yellow oil in 68% yield (637.6 mg). R_f = 0.34 (7:3 hexanes/EtOAc). **^{1}H NMR** (500 MHz, $CDCl_3$) δ 7.70 (d, *J* = 8.1 Hz, 1H), 7.05 (d, *J* = 2.0 Hz, 1H), 6.78 (dd, *J* = 8.1, 2.0 Hz, 1H), 3.90 (s, 3H), 1.72 (s, 1H), 1.57 (s, 6H). **^{13}C NMR** (126 MHz, $CDCl_3$) δ 158.1, 151.6, 139.1, 118.9, 107.7, 83.7, 72.6, 56.4, 31.9. **IR** (KBr, cm^{-1}) 3043, 2973, 2935, 2855, 1568, 1478, 1462, 1395, 1277, 1225, 1176, 1040, 1015, 961, 824, 693. **HRMS** (ESI) Calcd for $C_{10}H_{13}IO_2$ $[M+H-H_2O]^+$: 274.9933; Found: 274.9931.

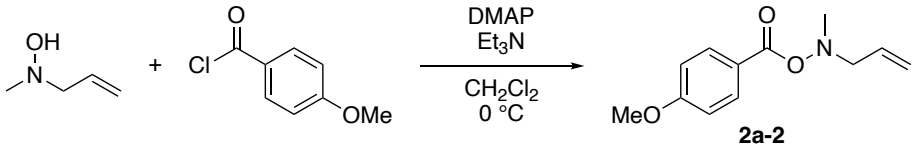

2a-2

***N*-allyl-*O*-(4-methoxybenzoyl)-*N*-methylhydroxylamine (2a-2):** *N*-allyl-*N*-methylhydroxylamine was prepared according to a known procedure.[61] CH_2Cl_2 (46 mL, 0.25 M), *N*-allyl-*N*-methylhydroxylamine (1.0 g, 11.49 mmol, 1.0 equiv.), DMAP (13.4 mg, 0.11 mmol, 1.0 mol%), and triethylamine (2.4 mL, 17.23 mmol, 1.5 equiv.) were placed in a flame-dried Schlenk flask under an N_2 atmosphere, which was then cooled to 0 °C. 4-methoxybenzoyl chloride (1.87 mL, 13.78 mmol, 1.2 equiv.) was added dropwise and the reaction was allowed to stir at 0 °C for

1 hour, after which the reaction was quenched with sat. NH_4Cl solution. The aqueous layer was extracted with EtOAc; the combined organics were washed with brine, dried over $MgSO_4$, and filtered. The solution was concentrated, and the crude oil was purified *via* silica gel chromatography (EtOAc/hexanes) to obtain a yellow liquid in 76% yield (1.93 g) with 10% of *p*-methoxybenzoic acid. **^{1}H NMR** (500 MHz, $CDCl_3$) δ 7.99 – 7.91 (m, 2H), 6.95 – 6.89 (m, 2H), 6.01 (ddt, *J* = 16.9, 10.3, 6.6 Hz, 1H), 5.29 (dq, *J* = 17.1, 1.5 Hz, 1H), 5.21 (dq, *J* = 10.2, 1.3 Hz, 1H), 3.87 (s, 3H), 3.64 (dt, *J* = 6.6, 1.3 Hz, 2H), 2.90 (s, 3H). **^{13}C NMR** (126 MHz, $CDCl_3$) δ 165.0, 163.5, 132.8, 131.6, 121.7, 119.4, 113.7, 64.0, 55.5, 46.3. **IR** (KBr, cm^{-1}) 3080, 2964, 2841, 1735, 1606, 1511, 1462, 1316, 1255, 1169, 1062, 1028, 847, 765, 695, 608. **HRMS** (ESI) Calcd for $C_{12}H_{15}NO_3$ $[M+H]^+$: 222.1130; Found: 222.1133.

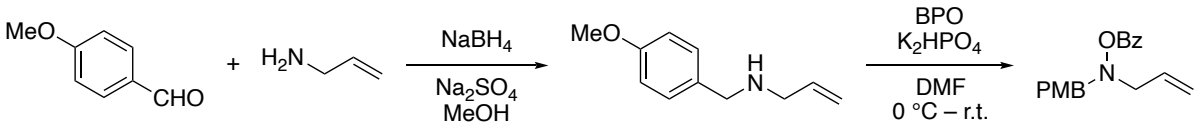

***N*-allyl-*O*-benzoyl-*N*-(4-methoxybenzyl)hydroxylamine (2c): (1)** Allylamine (1.28 mL, 17.1 mmol, 1.0 equiv.) was added to a methanolic solution of *p*-anisaldehyde (2.29 mL, 18.8 mmol, 1.1 equiv.) in a round-bottom flask with a small amount of Na_2SO_4 and stirred at room temperature until full formation of the imine was observed by TLC (about 1 hour). The flask was cooled to 0 °C, then $NaBH_4$ (775.5 mg, 20.5 mmol, 1.2 equiv.) was added slowly at 0 °C and the reaction was allowed to stir for one hour at room temperature. Once the starting material had been fully consumed (monitored by TLC), the reaction was quenched with sat. NH_4Cl solution. The aqueous layer was extracted with EtOAc; the combined organics were washed with brine, dried over $MgSO_4$, and filtered. The solution was concentrated, and the crude residue (3.04 g, quantitative) was directly used in the next step with no further purification.

(2) *N*-allyl-*N*-4-methoxybenzylamine (1.1 g, 6.2 mmol, 1.5 equiv.) was added dropwise to a solution of 75 wt% benzoyl peroxide (1.33 g, 4.1 mmol, 1.0 equiv.) and K_2HPO_4 (1.45 g, 8.3 mmol, 2.0 equiv.) in DMF (10.25 mL, 0.4 M) inside of a round-bottom flask at 0 °C. The reaction was allowed to stir overnight at room temperature, at which point it was diluted with water. The aqueous layer was extracted with EtOAc; the combined organics were washed with water and brine, dried over $MgSO_4$, and filtered. The solution was concentrated, and the crude oil was purified *via* silica gel chromatography (EtOAc/hexanes) to afford the title compound in 76% yield (925 mg). White solid with MP = 57 – 59 °C. R_f = 0.32 (4:1 hexanes:EtOAc). **^{1}H NMR** (500 MHz, $CDCl_3$) δ 7.93 – 7.89 (m, 2H), 7.55 – 7.50 (m, 1H), 7.40 (dd, *J* = 8.5, 7.1 Hz, 2H), 7.35 – 7.30 (m, 2H), 6.86 – 6.79 (m, 2H), 6.04 (ddt, *J* = 16.9, 10.2, 6.6 Hz, 1H), 5.25 (dq, *J* = 17.2, 1.5 Hz, 1H), 5.18 (dq, *J* = 10.3, 1.2 Hz, 1H), 4.13 (s, 2H), 3.77 (s, 3H), 3.68 – 3.63 (m, 2H). **^{13}C NMR** (126 MHz, $CDCl_3$) δ 165.2, 159.3, 133.0, 133.0, 131.0, 129.5, 128.5, 127.7, 119.5, 113.8, 62.1, 61.2, 55.3. **IR** (KBr, cm^{-1}) 3072, 2934, 2836, 1743, 1612, 1513, 1451, 1248, 1176, 1084, 1064, 1026, 812, 709. **HRMS** (ESI) Calcd for $C_{18}H_{19}NO_3$ $[M+H]^+$: 298.1443; Found: 298.1449.

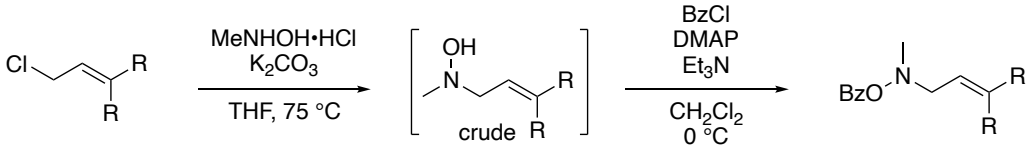

General Procedure for synthesis of allylamine electrophiles with an internal olefin: *N*-methylhydroxylamine hydrochloride (1.0 equiv.) and potassium carbonate (3.0 equiv.) were placed in a flame-dried vial, followed by tetrahydrofuran (1.0 M). The substituted allyl chloride (1.0 equiv.) was then added and allowed to stir at 75 °C overnight. The reaction was filtered to remove the solids and the filtrate was washed 3x with 10% HCl. The combined aqueous phases were then neutralized with solid KOH, and extracted 3x with Et_2O. The combined organics were

washed with brine, dried over $MgSO_4$, filtered, and concentrated to afford the crude, impure *N*-allyl-*N*-methylhydroxylamine derivative, which was directly used in the next step without further purification (caution: products are volatile). The impure hydroxylamine was placed in a flame-dried Schlenk flask under a N_2 atmosphere and cooled to 0 °C, at which point CH_2Cl_2 (0.25 M), Et_3N (1.5 equiv.), and DMAP (1.0 mol%) dissolved in minimal CH_2Cl_2. Benzoyl chloride (1.2 equiv.) was added dropwise, and the reaction was allowed to stir for 1 hour at 0 °C, during which it became cloudy in composition. The reaction was then quenched with sat. NH_4Cl solution and extracted with EtOAc. The combined organics were washed with brine, dried over $MgSO_4$, filtered, and concentrated to afford a crude residue, which was purified *via* silica gel chromatography to obtain the desired *O*-benzoylhydroxylamine.

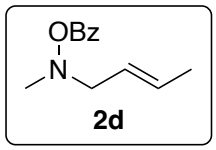

(*E*)-*O*-benzoyl-*N*-(but-2-en-1-yl)-*N*-methylhydroxylamine (2d): Synthesized from crotyl chloride according to the general procedure, obtaining the *N*-methyl-*N*-allylhydroxylamine derivative as a pale yellow oil (10 mmol scale; 513.0 mg, 51% crude yield), which was used in the next step without further purification. The crude hydroxylamine was further benzoylated to produce the title compound as a colorless oil in 78% yield (4.9 mmol scale; 785.2 mg) after purification *via* silica gel chromatography. R_f = 0.15 (hexane/EtOAc = 9:1). **^{1}H NMR** (400 MHz, $CDCl_3$) **^{13}C NMR** (101 MHz, $CDCl_3$) δ 165.3, 133.1, 131.1, 129.6, 129.6, 128.5, 125.3, 63.3, 46.1, 18.0. **IR** (KBr, cm^{-1}) 3063, 3006, 2966, 2918, 2856, 1742, 1601, 1451, 1262, 1059, 968, 709. **HRMS** (ESI) Calcd for $C_{12}H_{15}NO_2$ $[M+H]^+$: 206.1181; Found: 206.1173.

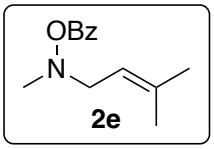

***O*-benzoyl-*N*-methyl-*N*-(3-methylbut-2-en-1-yl)hydroxylamine (2e):** Synthesized from 1-chloro-3-methylbut-2-ene according to the general procedure, obtaining the *N*-methyl-*N*-allylhydroxylamine derivative as a yellow oil (5.75 mmol scale; 372.6 mg, 56% crude yield), which was used in the next step without further purification. The crude hydroxylamine was further benzoylated to produce the title compound as a colorless oil in 52% yield (4.9 mmol scale; 554.7 mg) after purification *via* silica gel chromatography. Note: this compound darkens in color over a few days' time with a polar decomposition product appearing on the TLC. R_f = 0.15 (hexane/EtOAc = 9:1). **^{1}H NMR** (400 MHz, $CDCl_3$) δ 8.03 – 7.96 (m, 2H), 7.55 (ddt, *J* = 8.1, 6.9, 1.4 Hz, 1H), 7.48 – 7.39 (m, 2H), 5.36 (tt, *J* = 7.1, 1.5 Hz, 1H), 3.61 (s, 2H), 2.87 (s, 3H), 1.72 (s, 3H), 1.70 (s, 3H). **^{13}C NMR** (101 MHz, $CDCl_3$) ^{13}C NMR (101 MHz, $CDCl_3$) δ 165.3, 137.5, 133.1, 129.7, 129.6, 128.5, 118.5, 58.7, 46.0, 26.0, 18.3. **IR** (KBr, cm^{-1}) 3063, 2969, 2915, 2857, 1742, 1451, 1249, 1059, 709. **HRMS** (ESI) Calcd for $C_{13}H_{17}NO_2$ $[M+H]^+$: 220.1338; Found: 220.1344.

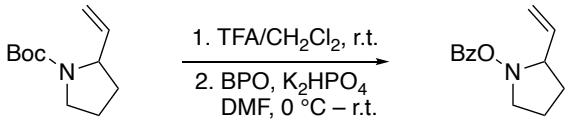

2-vinylpyrrolidin-1-yl benzoate (2f): *Tert*-butyl 2-vinylpyrrolidine-1-carboxylate was prepared according to a known procedure.[62] The Boc-protected amine (360.6 mg, 1.8 mmol, 1.0 equiv.) was placed in a 40 mL vial, followed by a 1:4 mixture of trifluoroacetic acid/CH_2Cl_2 (3.6 mL, 0.5 M) and stirred for 2 hours, with occasionally opening the vial to relieve pressure from CO_2 formation. The solvent was then removed and the crude amine•HTFA salt was directly used in the next step. The amine salt (1.8 mmol, 1.5 equiv.) was diluted with DMF (3.0 mL, 0.4 M) and cooled

to 0 °C, at which point K_2HPO_4 (627.0 mg, 3.6 mmol. 3.0 equiv.) and 75 wt% benzoyl peroxide (387.6 mg, 1.2 mmol, 1.0 equiv.) were added. The reaction was allowed to stir overnight at room temperature, at which point it was diluted with water and extracted with EtOAc. The combined organics were washed with brine, dried over $MgSO_4$, filtered, and concentrated to afford a brown crude residue, which was purified *via* silica gel chromatography to deliver a yellow oil (104.2 mg, 40% over 2 steps). R_f = 0.18 (hexane/EtOAc = 17:3). **^{1}H NMR** (500 MHz, $CDCl_3$) δ 8.01 – 7.95 (m, 2H), 7.58 – 7.52 (m, 1H), 7.42 (ddt, *J* = 7.9, 6.7, 1.1 Hz, 2H), 5.97 (ddd, *J* = 17.4, 10.3, 7.3 Hz, 1H), 5.25 (ddd, *J* = 17.2, 1.6, 1.1 Hz, 1H), 5.13 (ddd, *J* = 10.3, 1.6, 1.0 Hz, 1H), 3.75 – 3.59 (m, 2H), 3.04 (d, *J* = 9.7 Hz, 1H), 2.16 – 2.03 (m, 1H), 2.03 – 1.90 (m, 2H), 1.81 (q, *J* = 9.9 Hz, 1H). **^{13}C NMR** (126 MHz, $CDCl_3$) δ 165.6, 137.5, 133.1, 129.6, 128.5, 117.7, 70.7, 56.1, 27.1, 20.4. **IR** (KBr, cm^{-1}) 3073, 2979, 2857, 1740, 1451, 1261, 1085, 1065, 1026, 923, 709. **HRMS** (ESI) Calcd for $C_{13}H_{15}NO_2$ $[M+H]^+$: 218.1181; Found: 218.1177.

General Procedure for Pd/NBE reactions: $Pd(OAc)_2$ and P(*p*-OMe-Ph)$_3$ were placed into a flame-dried vial with a stir bar. Solid aryl iodide (**1**; 0.1 mmol) was also added at this stage. The vial was sealed and brought into a nitrogen-filled glovebox, and NBE, Cs_2CO_3, toluene, aryl halide (**1**; if liquid), and hydroxylamine electrophile (**2**) were added successively. The reaction vial was sealed, removed from the glove box, and heated at 100 °C for 18 h (note: the temperature was monitored *via* an alcohol thermometer submerged in a vial filled with silicone oil, not the hot plate's internal thermometer).

For test-scale reactions (0.1 mmol): Upon completion, the reactions were allowed to cool to room temperature, were filtered through a silica plug, concentrated, and placed under vacuum on a Schlenk line to remove residual solvent. The internal standard, 1,1,2,2-tetrachloroethane (16.8 mg, 0.1 mmol), was added to the crude residue, which was then diluted with $CDCl_3$ and analyzed *via*

^{1}H NMR analysis to determine yield and composition. If multiple reactions were conducted at a single time, a stock solution of palladium, ligand, and NBE in toluene was prepared.

For isolation-scale reactions (0.2 mmol): Upon completion, the reactions were allowed to cool to room temperature, were filtered through a silica plug, concentrated, and purified *via* silica gel chromatography (EtOAc/hexanes). Some compounds were further purified *via* preparatory TLC, and any impurities found have already been accounted for in the isolated yields. If multiple reactions were conducted at a single time, a stock solution of palladium, ligand, and NBE in toluene was prepared.

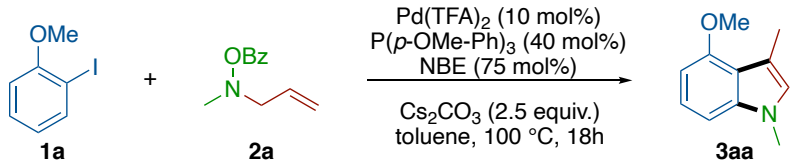

Procedure for 1.0 mmol-scale reaction: $Pd(TFA)_2$ (33.2 mg, 10 mol%) and *tris*(4-methoxyphenyl)phosphine (140.9 mg, 40 mol%) were placed in a flame-dried 40 mL vial, which was sealed and brought into a nitrogen-filled glove box. Norbornene (70.6 mg, 75 mol%) and Cs_2CO_3 (814.6 mg, 2.5 equiv.) were placed in the vial, followed by toluene (10.0 mL, 0.1 M), 2-iodoanisole (**1a**, 234.0 mg, 1.0 equiv.), and amine **2a** (382.5 mg, 2.0 equiv.). The vial was sealed, removed from the glove box, and heated at 100 °C (monitored by a thermometer submerged in silicone oil) for 18 hours. The reaction was then allowed to cool to room temperature, was filtered through a silica plug and eluted with Et_2O, and concentrated. The resulting crude solid was purified *via* silica gel chromatography (1-2% EtOAc/hexanes) to deliver the desired indole product as a white solid in 72% yield (126.5 mg).

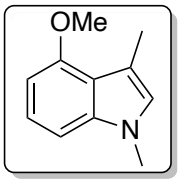

4-methoxy-1,3-dimethyl-1*H*-indole (3aa): Synthesized from **1a** and **2a** according to the general procedure. 0.2 mmol scale: 68% yield (26.2 mg); 1.0 mmol scale: 72% yield (126.5 mg). White solid with MP = 73-75 °C. R_f = 0.52 (hexane/EtOAc = 9:1). **^{1}H NMR** (400 MHz, $CDCl_3$) δ 7.09 (t, *J* = 8.0 Hz, 1H), 6.87 (d, *J* = 8.2 Hz, 1H), 6.66 (d, *J* = 1.2 Hz, 1H), 6.46 (d, *J* = 7.8 Hz, 1H), 3.91 (s, 3H), 3.68 (s, 3H), 2.46 (t, *J* = 0.9 Hz, 3H). **^{13}C NMR** (101 MHz, $CDCl_3$) δ 155.4, 138.9, 125.4, 122.4, 118.4, 110.8, 102.6, 99.0, 55.4, 32.8, 12.1. **IR** (KBr, cm^{-1}) 3112, 3077, 2944, 1611, 1501, 1419, 1261, 1095, 773, 730. **HRMS** (ESI) Calcd for $C_{11}H_{13}NO$ $[M+H]^+$: 176.1075; Found: 176.1075.

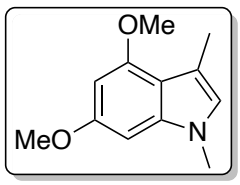

4,6-dimethoxy-1,3-dimethyl-1*H*-indole (3ba): Synthesized from **1b** and **2a** according to the general procedure. 0.2 mmol scale: 64% yield (26.4 mg). White solid with MP = 103 – 105 °C. R_f = 0.27 (hexane/EtOAc = 9:1). **^{1}H NMR** (400 MHz, $CDCl_3$) δ 6.55 (d, *J* = 1.3 Hz, 1H), 6.31 (d, *J* = 1.9 Hz, 1H), 6.16 (d, *J* = 1.9 Hz, 1H), 3.87 (s, 3H), 3.86 (s, 3H), 3.62 (s, 3H), 2.41 (d, *J* = 1.1 Hz, 3H). **^{13}C NMR** (101 MHz, $CDCl_3$) ^{13}C NMR (101 MHz, $CDCl_3$) δ 157.4, 155.7, 138.8, 124.0, 113.0, 110.8, 90.9, 85.1, 55.8, 55.3, 32.8, 12.0. **IR** (KBr, cm^{-1}) 2996, 2963, 2937, 1619, 1588, 1458, 1315, 1264, 1214, 1146, 1105, 795. **HRMS** (ESI) Calcd for $C_{12}H_{15}NO_2$ $[M+H]^+$: 206.1181; Found: 206.1183.

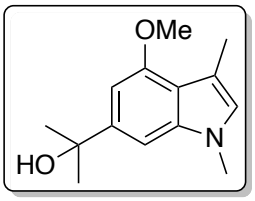

2-(4-methoxy-1,3-dimethyl-1*H*-indol-6-yl)propan-2-ol (3ca): Synthesized from **1X** and **2a** according to the general procedure. 0.2 mmol scale: 51% yield (23.8 mg). White solid with MP = 79 - 81 °C. R_f = 0.11 (hexane/EtOAc = 7:3). **^{1}H NMR** (400 MHz, $CDCl_3$) δ 6.99 (d, *J* = 1.3 Hz, 1H), 6.65 (q, *J* = 1.1 Hz, 1H), 6.60 (d, *J* = 1.3 Hz, 1H), 3.93 (s, 3H), 3.68 (s, 3H), 2.43 (d, *J* = 1.1 Hz, 3H), 1.80 (s, 1H), 1.66 (s, 6H). **^{13}C NMR** (101 MHz, $CDCl_3$) ^{13}C NMR (101 MHz, $CDCl_3$) δ 155.1, 144.4, 138.6, 125.7, 117.2, 110.6, 98.2, 96.6, 73.3, 55.4, 32.8, 32.2, 12.0. **IR** (KBr, cm^{-1}) 3405, 2971, 2933, 1618, 1577, 1553, 1467, 1416, 1321, 1262, 1179, 1093, 814, 665, 585. **HRMS** (ESI) Calcd for $C_{14}H_{19}NO_2$ $[M-H_2O+H]^+$: 216.1388; Found: 216.1386.

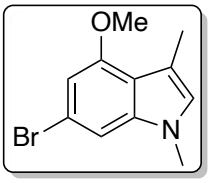

6-bromo-4-methoxy-1,3-dimethyl-1*H*-indole (3da): Synthesized from **1d** and **2a** according to the general procedure. 0.2 mmol scale: 61% yield (31.1 mg). White solid with MP = 81-82 °C. R_f = 0.45 (hexane/EtOAc = 9:1). **^{1}H NMR** (400 MHz, $CDCl_3$) δ 7.03 (d, *J* = 1.4 Hz, 1H), 6.62 (t, *J* = 1.1 Hz, 1H), 6.55 (d, *J* = 1.4 Hz, 1H), 3.88 (s, 3H), 3.63 (s, 3H), 2.41 (t, *J* = 0.9 Hz, 3H). **^{13}C NMR** (101 MHz, $CDCl_3$) δ 155.5, 139.1, 125.7, 117.3, 115.4, 111.2, 105.9, 103.1, 55.6, 32.9, 11.9. **IR** (KBr, cm^{-1}) 2933, 1603, 1545, 1483, 1467, 1416, 1318, 1247, 1202, 1104, 1022, 815. **HRMS** (ESI) Calcd for $C_{11}H_{12}BrNO$ $[M+H]^+$: 254.0181; Found: 254.0182.

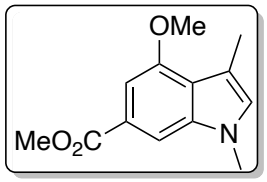

methyl 4-methoxy-1,3-dimethyl-1*H*-indole-6-carboxylate (3ea): Synthesized from **1e** and **2a** according to the general procedure. 0.2 mmol scale: 58% yield (27.0 mg). White solid with MP = 99-101 °C. R_f = 0.18 (hexane/EtOAc = 9:1). **^{1}H NMR** (400 MHz, $CDCl_3$) δ 7.69 (d, *J* = 1.2 Hz, 1H), 7.12 (d, *J* = 1.2 Hz, 1H), 6.82 (d, *J* = 1.1 Hz, 1H), 3.95 (s, 3H), 3.94 (s, 3H), 3.74 (s, 3H), 2.45 (d, *J* = 1.1 Hz, 3H). **^{13}C NMR** (101 MHz, $CDCl_3$) δ 168.4, 154.8, 137.9, 128.7, 124.0, 122.0, 111.4, 105.9, 99.4, 55.5, 52.1, 33.0, 11.9. **IR** (KBr, cm^{-1}) 2948, 1709, 1576, 1468, 1320, 1265, 1231, 1098, 767. **HRMS** (ESI) Calcd for $C_{13}H_{15}NO_3$ $[M+H]^+$: 234.1130; Found: 234.1140.

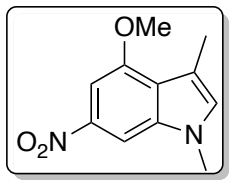

4-methoxy-1,3-dimethyl-6-nitro-1*H*-indole (3fa): Synthesized from **1f** and **2a** according to the general procedure, except using 40 mol% of *tris*(4-trifluoromethylphenyl) phosphine as the ligand. 0.2 mmol scale: 51% yield (22.5 mg). Orange solid with MP = 131 - 133 °C. R_f = 0.26 (hexane/EtOAc = 9:1). **^{1}H NMR** (400 MHz, $CDCl_3$) δ 7.92 (d, *J* = 1.8 Hz, 1H), 7.32 (d, *J* = 1.8 Hz, 1H), 6.94 (t, *J* = 1.1 Hz, 1H), 3.98 (s, 3H), 3.78 (d, *J* = 1.1 Hz, 3H), 2.44 (d, *J* = 1.0 Hz, 3H). **^{13}C NMR** (101 MHz, $CDCl_3$) δ 154.7, 143.7, 136.5, 131.1, 123.0, 112.3, 100.8, 94.4, 55.8, 33.2, 11.7. **IR** (KBr, cm^{-1}) 3103, 2924, 1512, 1468, 1320, 1246, 1202, 1103, 1063, 847, 737, 681. **HRMS** (ESI) Calcd for $C_{11}H_{12}N_2O_3$ $[M+H]^+$: 221.0926; Found: 221.0921.

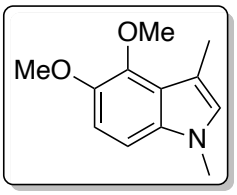

4,5-dimethoxy-1,3-dimethyl-1*H*-indole (3ga): Synthesized from **1g** and **2a** according to the general procedure. 0.2 mmol scale: 47% yield (19.4 mg). Colorless oil. Isolated with 20% of side product **4g** (accounted for in isolated yield). R_f = 0.29 (hexane/EtOAc = 9:1). **^{1}H NMR** (400 MHz, $CDCl_3$) δ 6.93 (d, *J* = 2.0 Hz, 2H), 6.71 (q, *J* = 1.1 Hz, 1H), 3.95 (s, 3H), 3.91 (s, 3H), 3.66 (s, 3H), 2.45 (d, *J* = 1.1 Hz, 3H). **^{13}C NMR** (101 MHz, $CDCl_3$) δ 145.1, 143.5, 134.9, 127.4, 122.6, 114.3, 111.9, 111.7, 109.4, 104.4, 61.6, 58.5, 32.7, 11.3. **IR** (KBr, cm^{-1}) 2942, 2830, 1497, 1419, 1299, 1257, 1119, 1063, 1019, 776. **HRMS** (ESI) Calcd for $C_{12}H_{15}NO_2$ $[M+Na]^+$: 228.1000; Found: 228.0995.

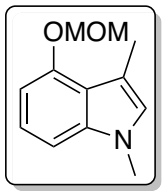

4-(methoxymethoxy)-1,3-dimethyl-1*H*-indole (3ha): Synthesized from **1h** and **2a** according to the general procedure. 0.2 mmol scale: 50% yield (20.4 mg). Colorless oil. R_f = 0.38 (hexane/EtOAc = 9:1). **^{1}H NMR** (500 MHz, $CDCl_3$) δ 7.08 (t, *J* = 8.0 Hz, 1H), 6.92 (dd, *J* = 8.2, 0.7 Hz, 1H), 6.69 (d, *J* = 1.2 Hz, 1H), 6.66 (dd, *J* = 7.7, 0.6 Hz, 1H), 5.31 (s, 2H), 3.69 (s, 3H), 3.54 (s, 3H), 2.49 (d, *J* = 1.2 Hz, 3H). **^{13}C NMR** (126 MHz, $CDCl_3$) δ 152.4, 139.2, 125.8, 122.3, 118.9, 110.5, 103.5, 102.4, 94.5, 56.2, 32.8, 12.1. **IR** (KBr, cm^{-1}) 3074, 2942, 2824, 1614, 1580, 1500, 1457, 1421, 1318, 1248, 1152, 1100, 1076, 1011, 923, 774, 730. **HRMS** (ESI) Calcd for $C_{12}H_{15}NO_2$ $[M+H]^+$: 206.1181; Found: 206.1183.

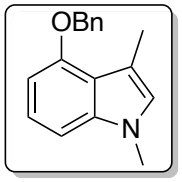

4-(benzyloxy)-1,3-dimethyl-1*H*-indole (3ia): Synthesized from **1i** and **2a** according to the general procedure. 0.2 mmol scale: 46% yield (23.2 mg). White solid with MP = 53-55 °C. R_f = 0.45 (hexane/EtOAc = 9:1). **^{1}H NMR** (400 MHz, $CDCl_3$) δ 7.52 (ddt, *J* = 7.5, 1.4, 0.7 Hz, 2H), 7.44 – 7.36 (m, 2H), 7.36 – 7.28 (m, 1H), 7.09 (t, *J* = 8.0 Hz, 1H), 6.89 (dd, *J* = 8.2, 0.7 Hz, 1H), 6.69 (d, *J* = 1.2 Hz, 1H), 6.53 (d, *J* = 7.7 Hz, 1H), 5.19 (s, 2H), 3.69 (s, 3H), 2.50 (d, *J* = 1.2 Hz, 3H). δ **^{13}C NMR** (101 MHz, $CDCl_3$) ^{13}C NMR (101 MHz, $CDCl_3$) δ 154.3, 139.1, 137.9, 128.6, 127.7, 127.2, 125.5, 122.4, 118.6, 110.8, 102.9, 100.2, 69.9, 32.8, 12.4. **IR** (KBr, cm^{-1}) 3063, 3032, 2924, 2867, 1614, 1581, 1551, 1500, 1453, 1319, 1259, 1180, 1096, 1024, 771, 727. **HRMS** (ESI) Calcd for $C_{10}H_{10}ClN$ $[M+H]^+$: 252.1388; Found: 252.1388.

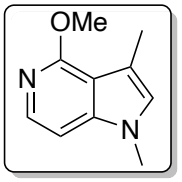

4-methoxy-1,3-dimethyl-1*H*-pyrrolo[3,2-*c*]pyridine (3ja): Synthesized from **1j** and **2a** according to the general procedure. 0.2 mmol scale: 66% yield (23.1 mg). Tan solid with MP = 80-81 °C. R_f = 0.26 (hexane/EtOAc = 4:1). **^{1}H NMR** (400 MHz, $CDCl_3$) δ 7.80 (d, *J* = 6.0 Hz, 1H), 6.81 (d, *J* = 5.9 Hz, 1H), 6.69 – 6.64 (m, 1H), 4.05 (s, 3H), 3.68 (s, 3H), 2.42 (d, *J* = 1.1 Hz, 3H). **^{13}C NMR** (101 MHz, $CDCl_3$) δ 159.6, 142.5, 137.8, 125.3, 112.4, 112.0, 100.5, 53.0, 32.8, 11.6. **IR** (KBr, cm^{-1}) 3007, 2950, 2927, 1605, 1573, 1482, 1468, 1307, 1186, 1103, 789, 638. **HRMS** (ESI) Calcd for $C_{10}H_{12}N_2O$ $[M+H]^+$: 177.1028; Found: 177.1028.

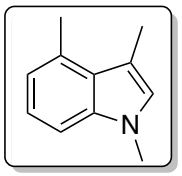

1,3,4-trimethyl-1*H*-indole (3ka): Synthesized from **1k** and **2a** according to the general procedure. 0.2 mmol scale: 43% yield (13.8 mg). R_f = 0.52 (hexane/EtOAc = 9:1). **^{1}H NMR** (400 MHz, $CDCl_3$) δ 7.13 – 7.03 (m, 2H), 6.80 (ddt, *J* = 6.4, 1.7, 0.9 Hz, 1H), 6.76 (q, *J* = 1.1 Hz, 1H), 3.69 (s, 3H), 2.72 (d, *J* = 0.9 Hz, 3H), 2.50 (d, *J* = 1.1 Hz, 3H). **^{13}C NMR** (101 MHz, $CDCl_3$) δ 137.6, 131.6, 127.1, 126.9, 121.7, 120.1, 111.1, 107.1, 77.5, 77.2, 76.8, 32.6, 20.1, 13.0. The NMR data are in agreement with previously reported spectra.[63]

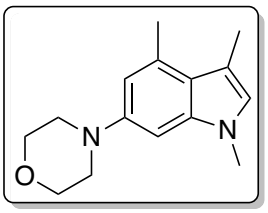

4-(1,3,4-trimethyl-1*H*-indol-6-yl)morpholine (3la): Synthesized from **1l** and **2a** according to the general procedure. 0.2 mmol scale: 46% yield (22.6 mg). White solid with MP = 135 - 137 °C. R_f = 0.15 (hexane/EtOAc = 4:1). **^{1}H NMR** (400 MHz, $CDCl_3$) δ 6.65 (d, *J* = 1.2 Hz, 1H), 6.56 (dd, *J* = 2.1, 1.0 Hz, 1H), 6.54 (d, *J* = 2.1 Hz, 1H), 3.93 – 3.87 (m, 4H), 3.63 (s, 3H), 3.20 – 3.13 (m, 4H), 2.66 (s, 3H), 2.44 (d, *J* = 1.1 Hz, 3H). **^{13}C NMR** (101 MHz, $CDCl_3$) δ 147.9, 138.4, 132.1, 125.9, 122.0, 112.8, 111.0, 94.2, 51.6, 32.6, 20.3, 12.9. **IR** (KBr, cm^{-1}) 2960, 2908, 2848, 2808, 1618, 1450, 1395, 1312, 1223, 1119, 1012, 875, 807, 775. **HRMS** (ESI) Calcd for $C_{15}H_{20}N_2O$ $[M+H]^+$: 245.1654; Found: 245.1648.

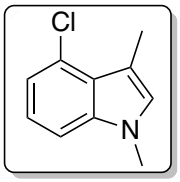

4-chloro-1,3-dimethyl-1*H*-indole (3ma): Synthesized from **1m** and **2a** according to the general procedure. 0.2 mmol scale: 83% yield (29.9 mg). Yellow oily solid. R_f = 0.43

(hexane/EtOAc = 9:1). **^{1}H NMR** (500 MHz, $CDCl_3$) δ 7.15 (dd, *J* = 8.0, 1.1 Hz, 1H), 7.07 (t, *J* = 7.8 Hz, 1H), 7.02 (dd, *J* = 7.5, 1.1 Hz, 1H), 6.81 (q, *J* = 1.2 Hz, 1H), 3.70 (s, 3H), 2.54 (d, *J* = 1.1 Hz, 3H). **^{13}C NMR** (101 MHz, $CDCl_3$) δ 138.6, 128.1, 127.1, 125.3, 122.0, 119.6, 111.0, 108.0, 32.9, 12.2. **IR** (KBr, cm^{-1}) 3059, 2923, 1612, 1456, 1307, 1206, 1070, 864, 769, 733. **HRMS** (ESI) Calcd for $C_{10}H_{10}ClN$ $[M+H]^+$: 180.0580; Found: 180.0584.

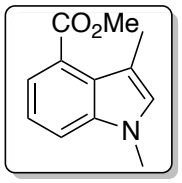

methyl 1,3-dimethyl-1*H*-indole-4-carboxylate (3na): Synthesized from **1n** and **2a** according to the general procedure. 0.2 mmol scale: 51% yield (20.8 mg). Yellow solid with MP = 80-82 °C. R_f = 0.30 (hexane/EtOAc = 9:1). **^{1}H NMR** (400 MHz, $CDCl_3$) δ 7.62 (dd, *J* = 7.4, 1.0 Hz, 1H), 7.44 (dt, *J* = 8.2, 0.9 Hz, 1H), 7.21 (t, *J* = 7.8 Hz, 1H), 6.94 (t, *J* = 1.0 Hz, 1H), 3.96 (d, *J* = 0.7 Hz, 3H), 3.75 (d, *J* = 0.9 Hz, 3H), 2.39 (d, *J* = 1.0 Hz, 3H). **^{13}C NMR** (101 MHz, $CDCl_3$) δ 169.1, 138.5, 130.1, 125.7, 124.2, 122.0, 120.5, 113.2, 110.9, 32.8, 13.2. **IR** (KBr, cm^{-1}) 3108, 3067, 2953, 2923, 1717, 1452, 1368, 1265, 1203, 1139, 1089, 1057, 743. **HRMS** (ESI) Calcd for $C_{12}H_{13}NO_2$ $[M+H]^+$: 204.1025; Found: 204.1026.

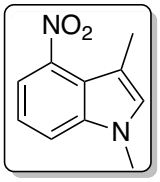

1,3-dimethyl-4-nitro-1H-indole (3oa): Synthesized from **1o** and **2a** according to the general procedure, except using 40 mol% of *tris*(4-trifluoromethylphenyl)phosphine as the ligand. 0.2 mmol scale: 55% yield (21.0 mg). Yellow/orange solid with MP = 101 - 103 °C. R_f = 0.39 (hexane/EtOAc = 7:3). **^{1}H NMR** (400 MHz, $CDCl_3$) δ 7.81 (dd, *J* = 7.9, 0.9 Hz, 1H), 7.53 (dd, *J* = 8.2, 0.9 Hz, 1H), 7.22 (t, *J* = 8.0 Hz, 1H), 7.04 (d, *J* = 1.1 Hz, 1H), 3.80 (s, 3H), 2.39 (d, *J* = 1.0

Hz, 3H). **^{13}C NMR** (101 MHz, $CDCl_3$) δ 143.2, 139.8, 132.0, 120.3, 120.1, 116.8, 115.0, 110.1, 33.1, 13.0. **IR** (KBr, cm^{-1}) 3116, 2963, 2922, 1542, 1517, 1351, 1329, 1304, 1061, 793, 725, 598. **HRMS** (ESI) Calcd for $C_{10}H_{10}N_2O_2$ $[M+H]^+$: 191.0821; Found: 191.0825.

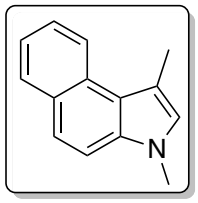

1,3-dimethyl-3*H*-benzo[*e*]indole (3pa): Synthesized from **1p** and **2a-2** according to the general procedure, except with with **2a-2**, triphenylphosphine as the ligand, and heating at 120 °C. 0.2 mmol scale: 54% yield (21.0 mg). Colorless oil that changed to a brown oil under vacuum. R_f = 0.38 (hexane/EtOAc = 9:1). **^{1}H NMR** (400 MHz, $CDCl_3$) δ 8.49 (dd, *J* = 8.3, 1.2 Hz, 1H), 7.93 (dd, *J* = 8.2, 1.4 Hz, 1H), 7.61 (d, *J* = 8.9 Hz, 1H), 7.56 (ddd, *J* = 8.4, 6.9, 1.4 Hz, 1H), 7.48 (d, *J* = 8.8 Hz, 1H), 7.41 (ddd, *J* = 8.1, 6.9, 1.3 Hz, 1H), 6.91 (d, *J* = 1.1 Hz, 1H), 3.85 (s, 3H), 2.72 (d, *J* = 1.0 Hz, 3H). **^{13}C NMR** (101 MHz, $CDCl_3$) ^{13}C NMR (101 MHz, $CDCl_3$) δ 134.0, 129.9, 129.4, 128.8, 125.7, 125.7, 123.3, 122.8, 122.7, 121.3, 112.9, 111.2, 32.9, 13.9. **IR** (KBr, cm^{-1}) 3044, 2933, 2860, 1597, 1402, 1292, 1124, 799, 743, 688. **HRMS** (ESI) Calcd for $C_{14}H_{13}N$ $[M+H]^+$: 196.1126; Found: 196.1128.

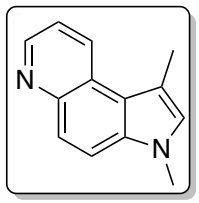

1,3-dimethyl-3*H*-pyrrolo[3,2-*f*]quinoline (3qa): Synthesized from **1q** and **2a-2** according to the general procedure, except with **2a-2**, triphenylphosphine as the ligand, and at 120 °C. 0.2 mmol scale: 32% yield (12.5 mg). Light yellow solid with MP = 104 - 107 °C. R_f = 0.12 (hexane/EtOAc = 7:3). **^{1}H NMR** (400 MHz, $CDCl_3$) δ 8.82 (dd, *J* = 4.3, 1.7 Hz, 1H), 8.77 – 8.71 (m, 1H), 7.87 (d, *J* = 9.1 Hz, 1H), 7.70 (d, *J* = 9.1 Hz, 1H), 7.44 (dd, *J* = 8.4, 4.3 Hz, 1H), 6.97 (d,

J = 1.1 Hz, 1H), 3.88 (s, 3H), 2.67 (d, J = 1.0 Hz, 3H). **^{13}C NMR** (101 MHz, $CDCl_3$) δ 146.5, 145.6, 133.5, 131.3, 126.7, 124.8, 123.7, 120.6, 120.4, 114.6, 113.4, 33.1, 13.6. **IR** (KBr, cm^{-1}) 3052, 2926, 2859, 1590, 1535, 1523, 1462, 1388, 1368, 1292, 1120, 990, 807, 622, 605. **HRMS** (ESI) Calcd for $C_{13}H_{12}N_2$ $[M+H]^+$: 197.1079; Found: 197.1081.

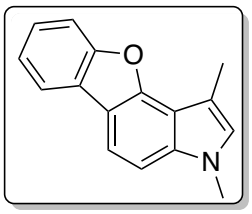

1,3-dimethyl-3*H*-benzofuro[2,3-*e*]indole (3ra): Synthesized from **1r** and **2a-2** according to the general procedure, except with with **2a-2**, triphenylphosphine as the ligand, and heating at 120 °C. 0.2 mmol scale: 42% yield (19.6 mg). Colorless oil. R_f = 0.42 (hexane/EtOAc = 9:1). **^{1}H NMR** (500 MHz, $CDCl_3$) δ 7.95 – 7.91 (m, 1H), 7.73 (d, J = 8.5 Hz, 1H), 7.64 (dt, J = 8.1, 0.8 Hz, 1H), 7.39 – 7.31 (m, 2H), 7.25 (d, J = 8.5 Hz, 1H), 6.87 (d, J = 1.2 Hz, 1H), 3.82 (s, 3H), 2.68 (d, J = 1.1 Hz, 3H). **^{13}C NMR** (126 MHz, $CDCl_3$) δ 155.9, 151.0, 137.9, 126.5, 125.7, 124.6, 122.5, 119.5, 114.8, 114.8, 113.8, 111.6, 109.4, 105.3, 33.3, 11.5. **IR** (KBr, cm^{-1}) 3053, 2291, 1642, 1482, 1464, 1420, 1323, 1291, 1195, 1170, 1118, 1054, 950, 770, 785, 736. **HRMS** (ESI) Calcd for $C_{16}H_{13}NO$ $[M+H]^+$: 236.1075; Found: 236.1073.

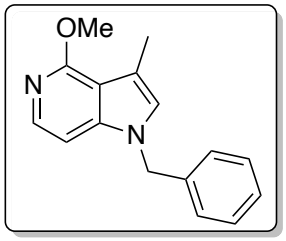

1-benzyl-4-methoxy-3-methyl-1*H*-pyrrolo[3,2-*c*]pyridine (3jb): Synthesized from **1c** and **2b** according to the general procedure, except with heating at 80 °C. 0.2 mmol scale: 43% yield (21.4 mg). Pale yellow oil. R_f = 0.31 (hexane/EtOAc = 4:1). **^{1}H NMR** (400 MHz, $CDCl_3$) δ 7.77 (d, J = 6.0 Hz, 1H), 7.34 – 7.23 (m, 3H), 7.12 – 7.05 (m, 2H), 6.79 (d, J = 6.0

Hz, 1H), 6.73 (d, J = 1.3 Hz, 1H), 5.19 (s, 2H), 4.07 (s, 3H), 2.44 (d, J = 1.1 Hz, 3H). **^{13}C NMR** (126 MHz, $CDCl_3$) δ 159.7, 142.3, 138.1, 137.3, 128.9, 127.9, 126.9, 124.6, 112.7, 112.7, 100.8, 53.1, 50.1, 11.7. **IR** (KBr, cm^{-1}) 3063, 3030, 2948, 2863, 1604, 1574, 1476, 1309, 1185, 1103, 1029, 784, 699. **HRMS** (ESI) Calcd for $C_{16}H_{16}N_2O$ $[M+H]^+$: 253.1341; Found: 253.1346.

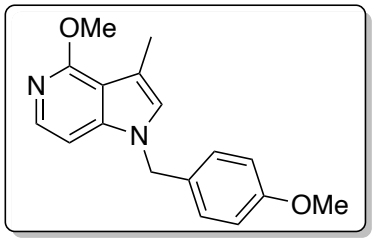

4-methoxy-1-(4-methoxybenzyl)-3-methyl-1*H*-pyrrolo[3,2-*c*]pyridine (3jc): Synthesized from **1c** and **2c** according to the general procedure, except with heating at 80 °C. 0.2 mmol scale: 57% yield (32.2 mg). Tan solid with MP = 74 - 76 °C. R_f = 0.19 (hexane/EtOAc = 4:1). **^{1}H NMR** (400 MHz, $CDCl_3$) δ 7.76 (d, J = 6.0 Hz, 1H), 7.07 – 7.01 (m, 2H), 6.86 – 6.81 (m, 2H), 6.80 (d, J = 6.0 Hz, 1H), 6.70 (q, J = 1.1 Hz, 1H), 5.12 (s, 2H), 4.05 (s, 3H), 3.77 (s, 3H), 2.42 (d, J = 1.1 Hz, 3H). **^{13}C NMR** (101 MHz, $CDCl_3$) δ 159.6, 159.3, 142.2, 138.0, 129.3, 128.4, 124.5, 114.3, 112.7, 112.6, 100.9, 55.4, 53.1, 49.6, 11.8. **IR** (KBr, cm^{-1}) 2950, 2835, 1604, 1573, 1546, 1514, 1476, 1305, 1250, 1177, 1102, 1075, 1034, 785, 614. **HRMS** (ESI) Calcd for $C_{17}H_{18}N_2O_2$ $[M+H]^+$: 283.1447; Found: 283.1445.

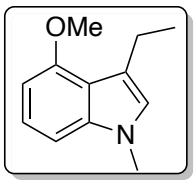

3-ethyl-4-methoxy-1-methyl-1*H*-indole (3ad): Synthesized from **1a** and **2d** according to the general procedure. 0.2 mmol scale: 27% yield (10.4 mg); isolated with 38% yield (14.5 mg) of **3ad'** for a total of 65% yield. Colorless oil. R_f = 0.56 (hexane/Et_2O = 9:1). **^{1}H NMR** (400 MHz, $CDCl_3$) δ 7.11 (t, J = 8.0 Hz, 1H), 6.88 (dd, J = 8.2, 0.7 Hz, 1H), 6.69 (d, J = 1.1 Hz,

1H), 6.47 (dd, *J* = 7.8, 0.7 Hz, 1H), 3.92 (s, 3H), 3.70 (s, 3H), 2.91 (qd, *J* = 7.4, 1.0 Hz, 2H), 1.28 (t, *J* = 7.4 Hz, 3H). **^{13}C NMR** (101 MHz, $CDCl_3$) δ 155.2, 139.0, 124.2, 122.3, 118.2, 117.7, 102.6, 99.0, 55.3, 32.9, 20.3, 15.9. **IR** (KBr, cm^{-1}) 3071, 2958, 1870, 2836, 1611, 1500, 1467, 1336, 1257, 1178, 1104, 1029, 779, 727. **HRMS** (ESI) Calcd for $C_{12}H_{15}NO$ $[M+H]^+$: 190.1232; Found: 190.1229.

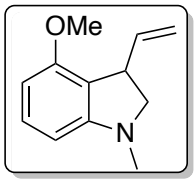

4-methoxy-1-methyl-3-vinylindoline (3ad'): Synthesized from **1a** and **2d** according to the general procedure. 0.2 mmol scale: 38% yield (14.5 mg); isolated with 27% yield (10.4 mg) of **3ad** for a total of 65% yield. Colorless oil. R_f = 0.39 (hexane/Et_2O = 9:1). **^{1}H NMR** (400 MHz, $CDCl_3$) δ 7.10 (t, *J* = 8.0 Hz, 1H), 6.31 (d, *J* = 8.2 Hz, 1H), 6.21 (d, *J* = 7.8 Hz, 1H), 6.02 (ddd, *J* = 17.1, 10.1, 7.0 Hz, 1H), 5.08 (dt, *J* = 17.2, 1.6 Hz, 1H), 5.03 (dt, *J* = 10.1, 1.4 Hz, 1H), 3.91 (ddd, *J* = 11.7, 7.0, 3.4 Hz, 1H), 3.80 (s, 3H), 3.36 (t, *J* = 8.8 Hz, 1H), 3.25 (dd, *J* = 8.9, 4.3 Hz, 1H), 2.74 (s, 3H). **^{13}C NMR** (101 MHz, $CDCl_3$) δ 156.8, 154.8, 138.8, 129.5, 117.9, 114.0, 101.9, 101.6, 62.2, 55.5, 42.6, 36.5. **IR** (KBr, cm^{-1}) 3077, 2999, 2949, 2835, 2806, 1612, 1484, 1334, 1262, 1228, 1065, 912, 767, 726. **HRMS** (ESI) Calcd for $C_{12}H_{15}NO$ $[M+H]^+$: 190.1232; Found: 190.1239.

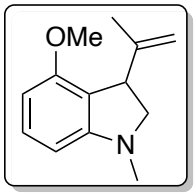

4-methoxy-1-methyl-3-(prop-1-en-2-yl)indoline (3ae): Synthesized from **1a** and **2e** according to the general procedure. 0.2 mmol scale: 61% yield (24.6 mg). Pale yellow oil. R_f = 0.39 (hexane/Et_2O = 9:1). **^{1}H NMR** (400 MHz, $CDCl_3$) δ 7.10 (t, *J* = 8.0 Hz, 1H), 6.30 (d, *J*

= 8.2 Hz, 1H), 6.20 (d, *J* = 7.8 Hz, 1H), 4.77 (p, *J* = 1.6 Hz, 1H), 4.70 (dd, *J* = 2.1, 1.0 Hz, 1H), 3.92 (dd, *J* = 9.3, 4.3 Hz, 1H), 3.78 (s, 3H), 3.36 (t, *J* = 9.2 Hz, 1H), 3.27 (dd, *J* = 9.0, 4.3 Hz, 1H), 2.73 (s, 3H), 1.75 (dd, *J* = 1.5, 0.8 Hz, 3H). **^{13}C NMR** (101 MHz, $CDCl_3$) δ 156.8, 155.3, 146.0, 129.5, 117.8, 110.7, 101.7, 101.5, 61.9, 55.5, 46.3, 36.4, 20.3. **IR** (KBr, cm^{-1}) 3072, 2965, 2835, 2807, 1646, 1610, 1484, 1373, 1334, 1262, 1224, 1066, 889, 786, 756, 721. **HRMS** (ESI) Calcd for $C_{13}H_{17}NO$ $[M+H]^+$: 204.1388; Found: 204.1387.

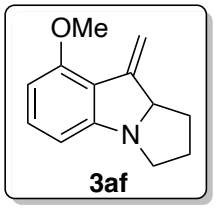

8-methoxy-9-methylene-2,3,9,9a-tetrahydro-1*H*-pyrrolo[1,2-*a*]indole (3af'): Synthesized from **1a** and **2f** according to the general procedure, except with 1.5 equiv. of **2f**. **3af'** was observed by crude NMR analysis, but isomerized to **3af** upon purification. 31 μmol scale: NMR yield = 31%. **^{1}H NMR** (500 MHz, $CDCl_3$) δ 7.11 (t, *J* = 8.1 Hz, 1H), 6.34 (dd, *J* = 8.3, 0.7 Hz, 1H), 6.31 (dd, *J* = 7.9, 0.7 Hz, 1H), 5.74 (dd, *J* = 2.6, 1.2 Hz, 1H), 5.06 (dd, *J* = 2.2, 1.2 Hz, 1H), 4.42 (ddt, *J* = 9.2, 7.0, 2.4 Hz, 1H), 3.87 (s, 3H), 3.43 (ddd, *J* = 10.2, 6.3, 5.5 Hz, 1H), 2.14 – 2.07 (m, 1H), 1.94 – 1.85 (m, 2H), 1.63 – 1.58 (m, 1H), 1.54 – 1.48 (m, 1H) (note: peaks are estimated to the best of our ability based on the crude NMR spectrum). **HRMS** (ESI) Calcd for $C_{13}H_{15}NO$ $[M+H]^+$: 202.1232; Found: 202.1237.

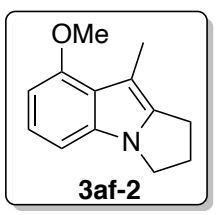

8-methoxy-9-methyl-2,3-dihydro-1*H*-pyrrolo[1,2-*a*]indole (3af): Synthesized from **1a** and **2f** according to the general procedure, except with 1.5 equiv. of **2f**. Obtained upon subjecting **3af'**, the product observed *via* crude NMR analysis, to purification *via*

silica gel chromatography; the indoline isomerized to the aromatic indole. 0.1 mmol scale: 33% yield (6.7 mg). Tan solid with MP = 109 – 111 °C. R_f = 0.25 (hexane/Et_2O = 9:1). **^{1}H NMR** (500 MHz, $CDCl_3$) δ 6.98 (t, *J* = 7.9 Hz, 1H), 6.81 (d, *J* = 8.0 Hz, 1H), 6.44 (d, *J* = 7.8 Hz, 1H), 3.99 (t, *J* = 7.0 Hz, 2H), 3.90 (s, 3H), 2.89 (t, *J* = 7.4 Hz, 2H), 2.56 (p, *J* = 7.2 Hz, 2H), 2.40 (s, 3H). **^{13}C NMR** (126 MHz, $CDCl_3$) δ 154.9, 139.8, 134.2, 122.4, 120.8, 103.0, 101.2, 99.2, 55.4, 43.9, 27.9, 22.9, 11.5. **IR** (KBr, cm^{-1}) 3083, 2925, 2854, 1615, 1566, 1498, 1447, 1254, 1127, 1034, 770, 725. **HRMS** (ESI) Calcd for $C_{13}H_{15}NO$ $[M+H]^+$: 202.1232; Found: 202.1227.

2.5. ^{1}H-NMR and ^{13}C-NMR Spectra

Figure 2.5. ^{1}H NMR Spectrum of **1c**

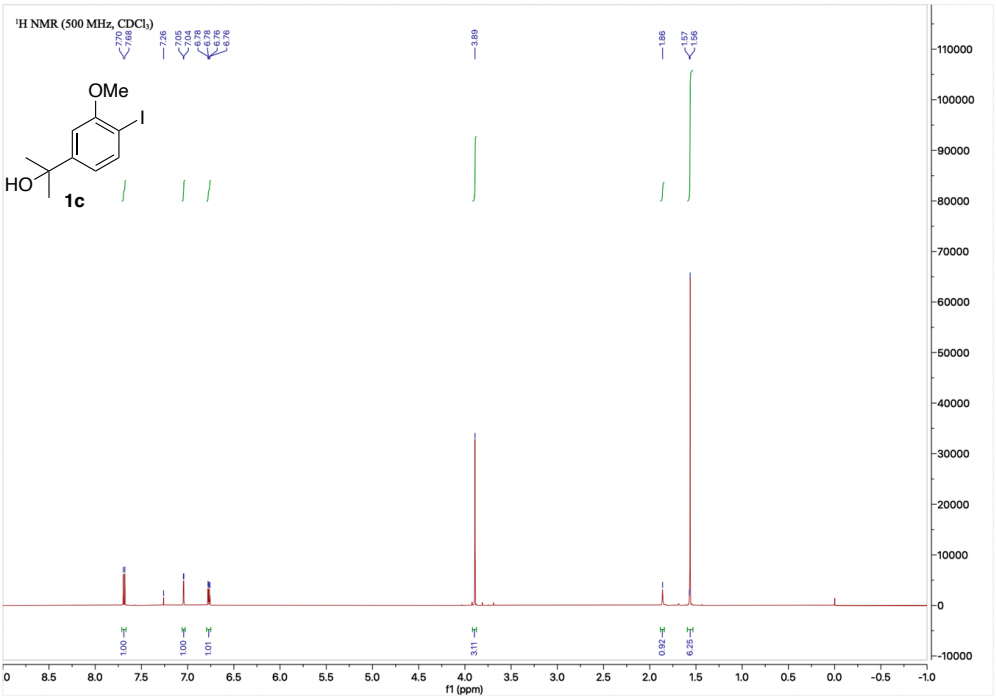

Figure 2.6. ^{13}C NMR Spectrum of **1c**

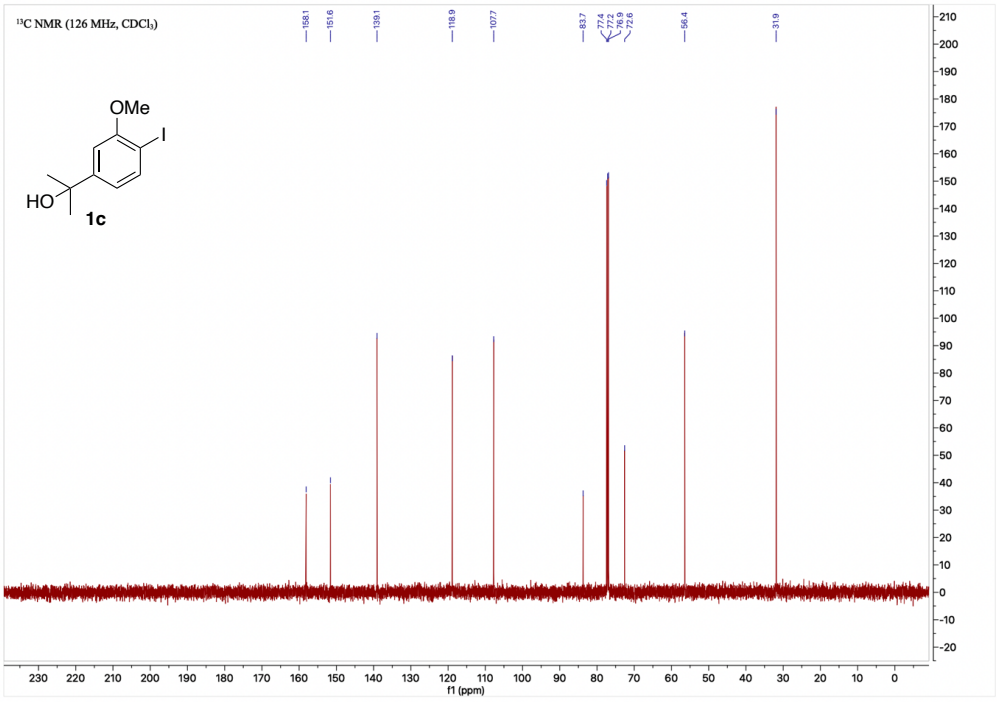

Figure 2.7. ^{1}H NMR Spectrum of **2a-2**

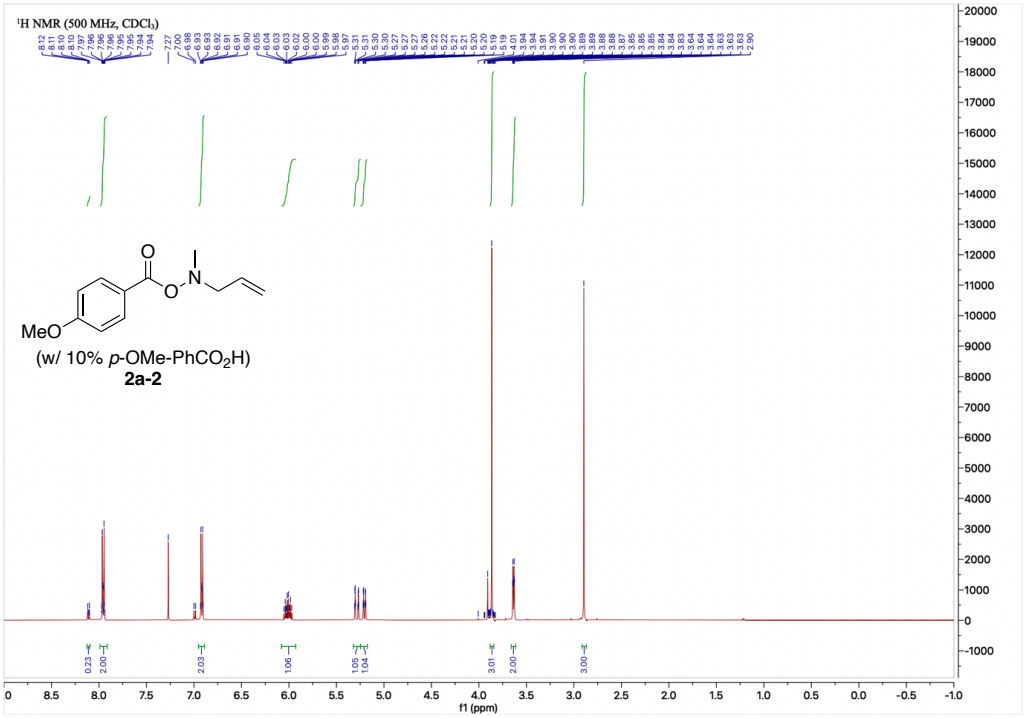

Figure 2.8. ^{13}C NMR Spectrum of **2a-2**

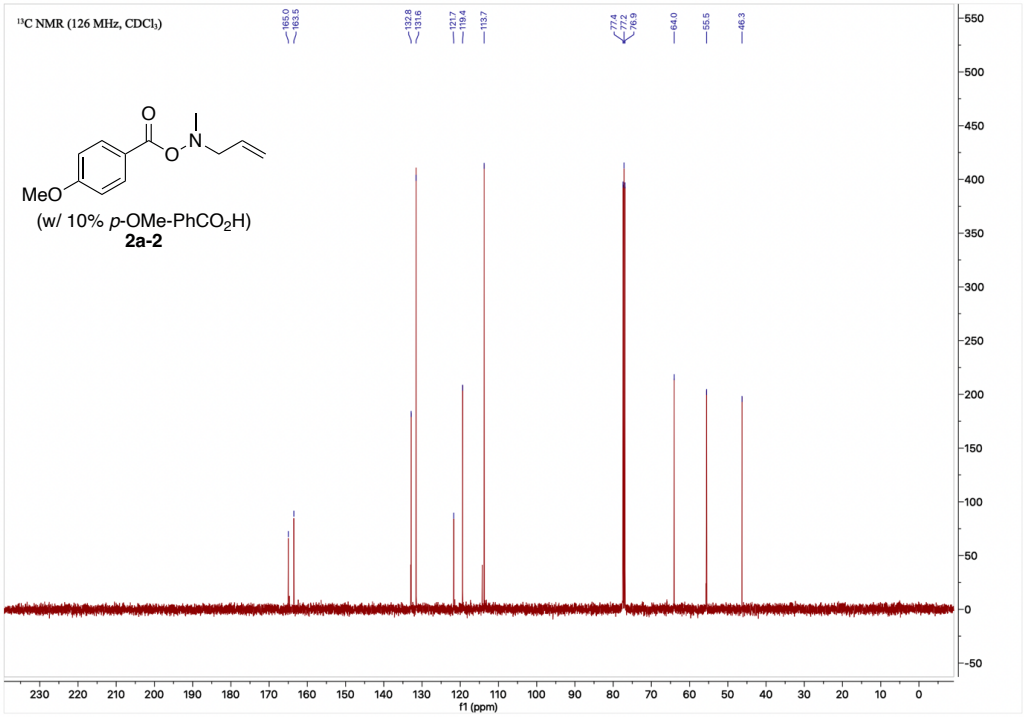

Figure 2.9. ^{1}H NMR Spectrum of **2c**

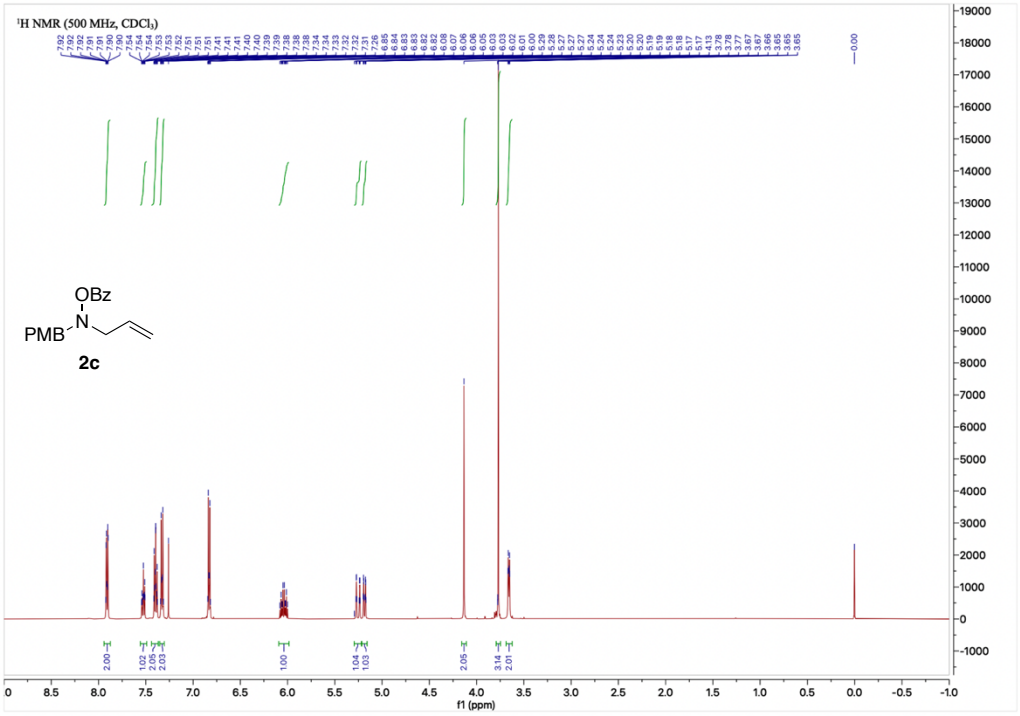

Figure 2.10. ^{13}C NMR Spectrum of **2c**

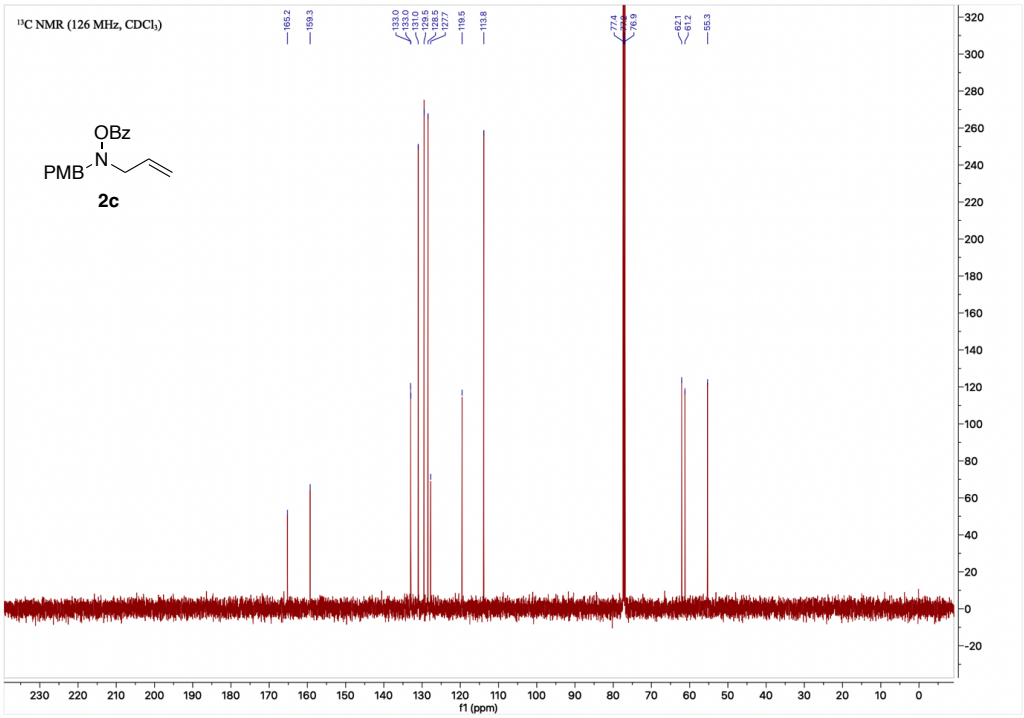

Figure 2.11. ^{1}H NMR Spectrum of **2d**

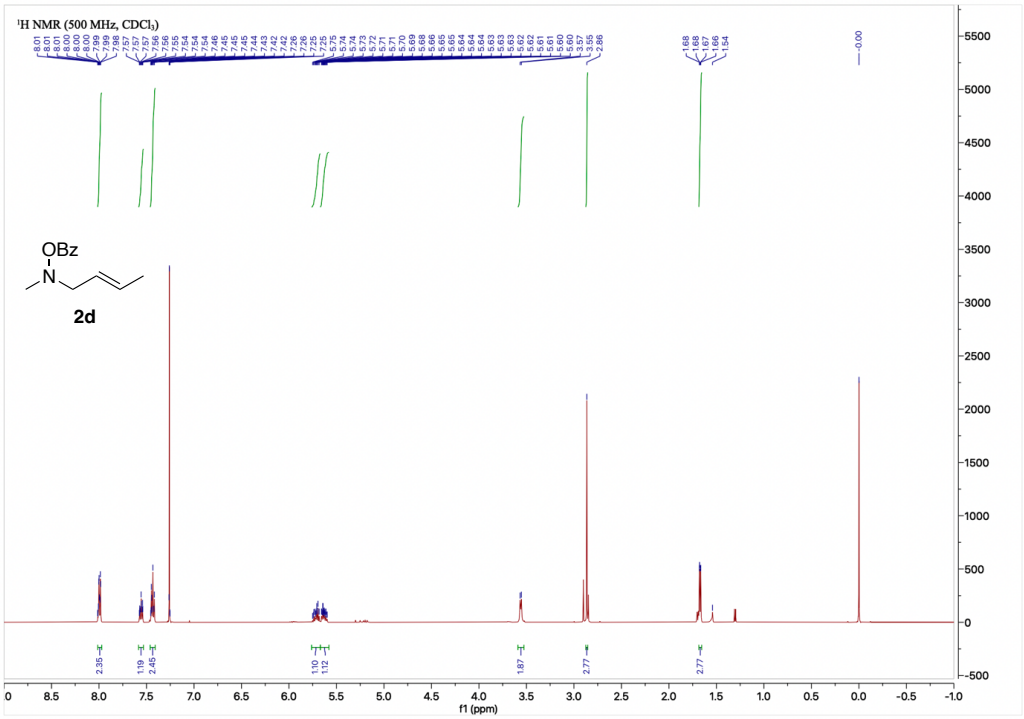

Figure 2.12. ^{13}C NMR Spectrum of **2d**

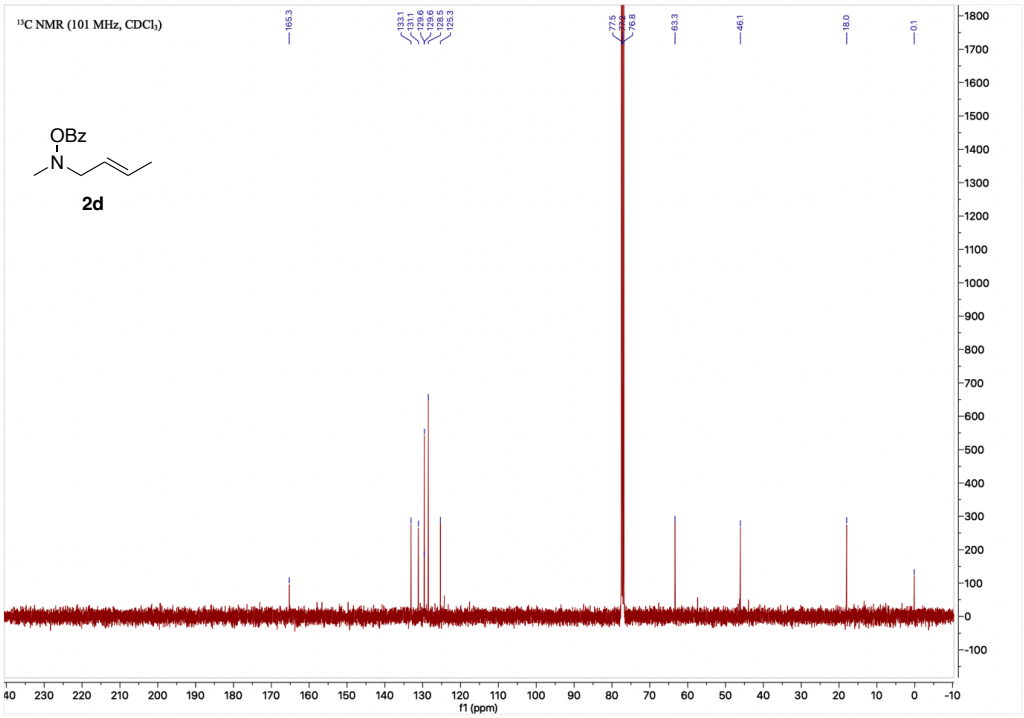

Figure 2.13. ^{1}H NMR Spectrum of **2e**

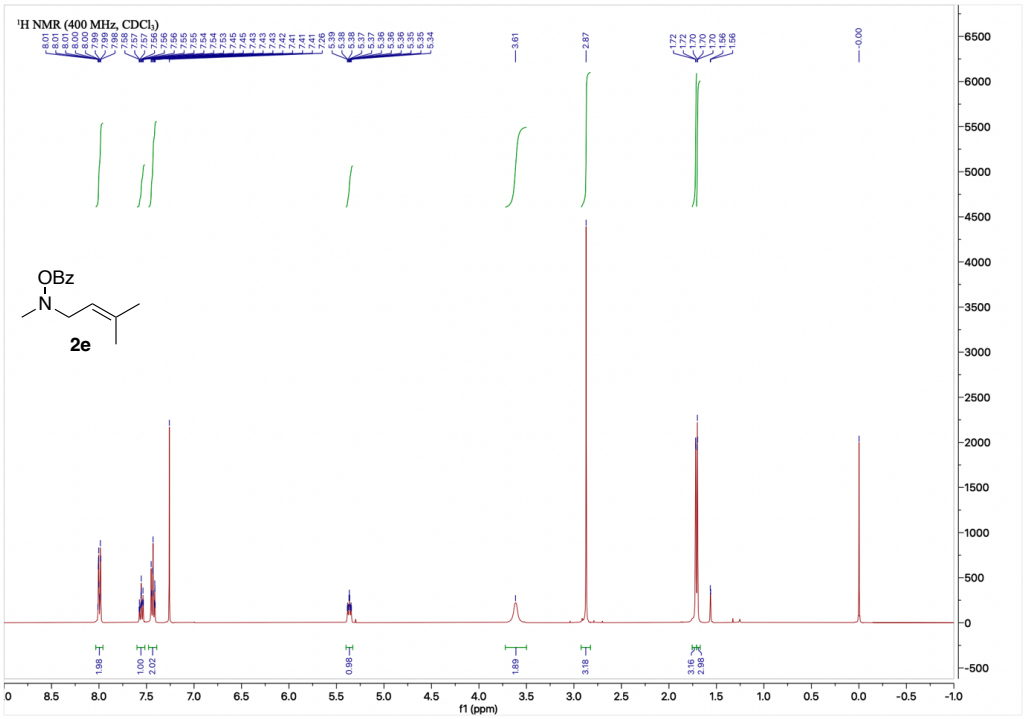

Figure 2.14. ^{13}C NMR Spectrum of **2e**

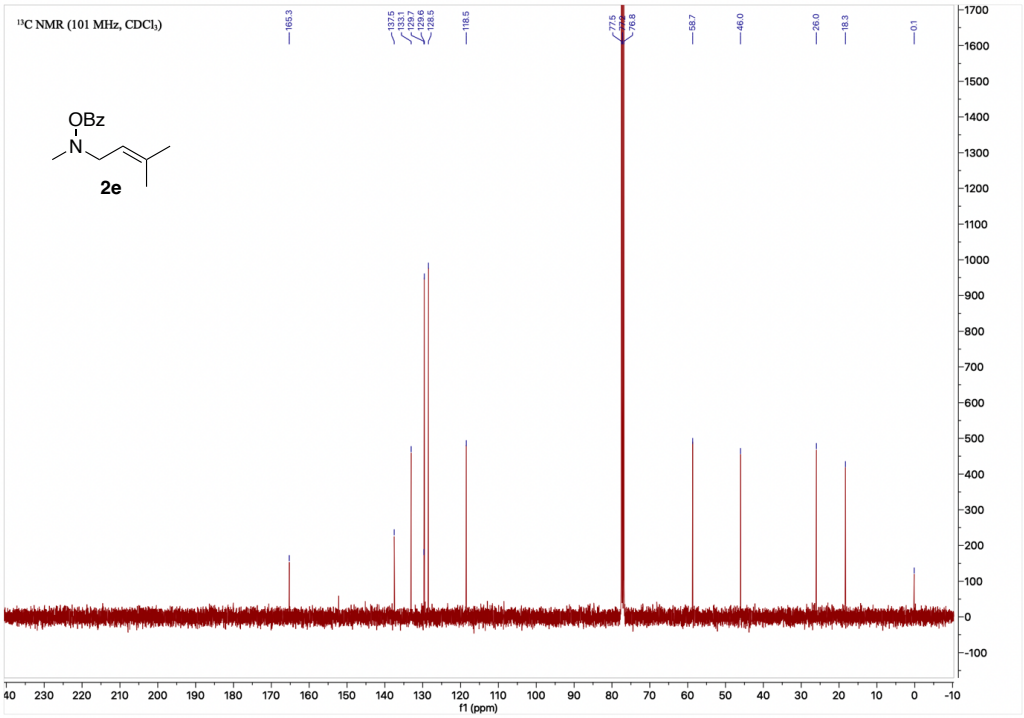

Figure 2.15. ^{1}H NMR Spectrum of **2f**

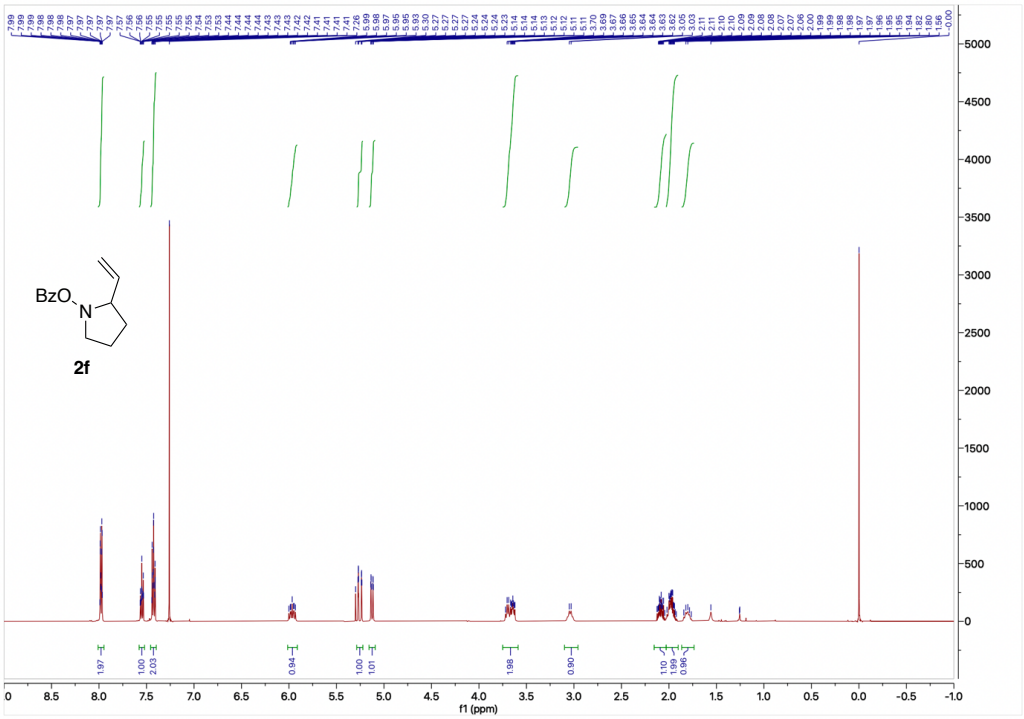

Figure 2.16. ^{13}C NMR Spectrum of **2f**

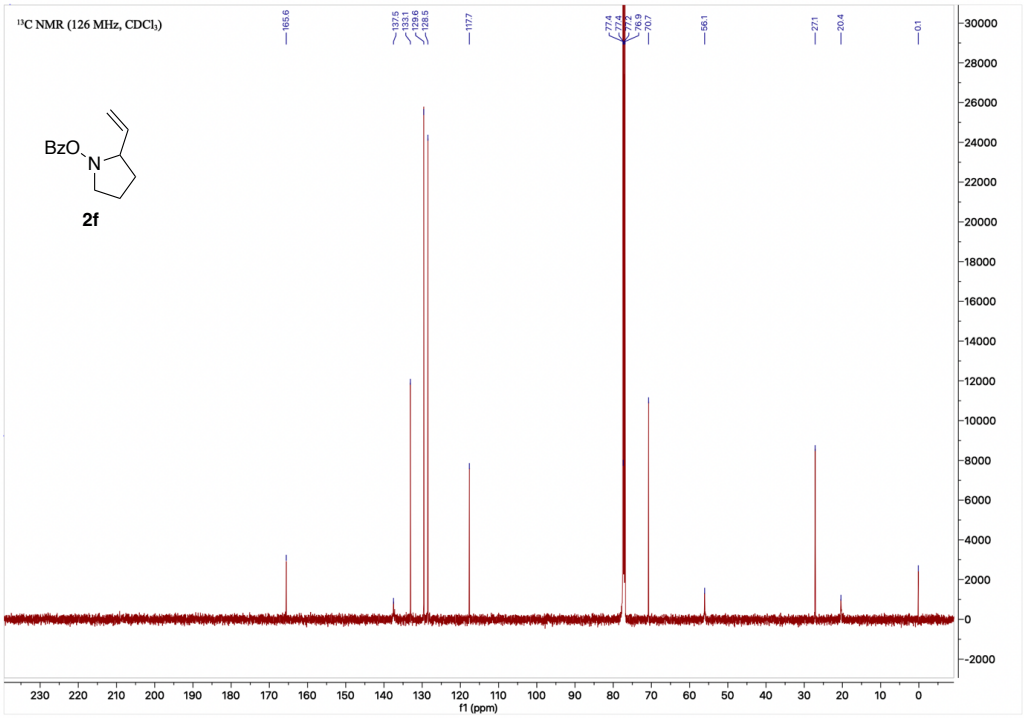

Figure 2.17. ^{1}H NMR Spectrum of **3aa**

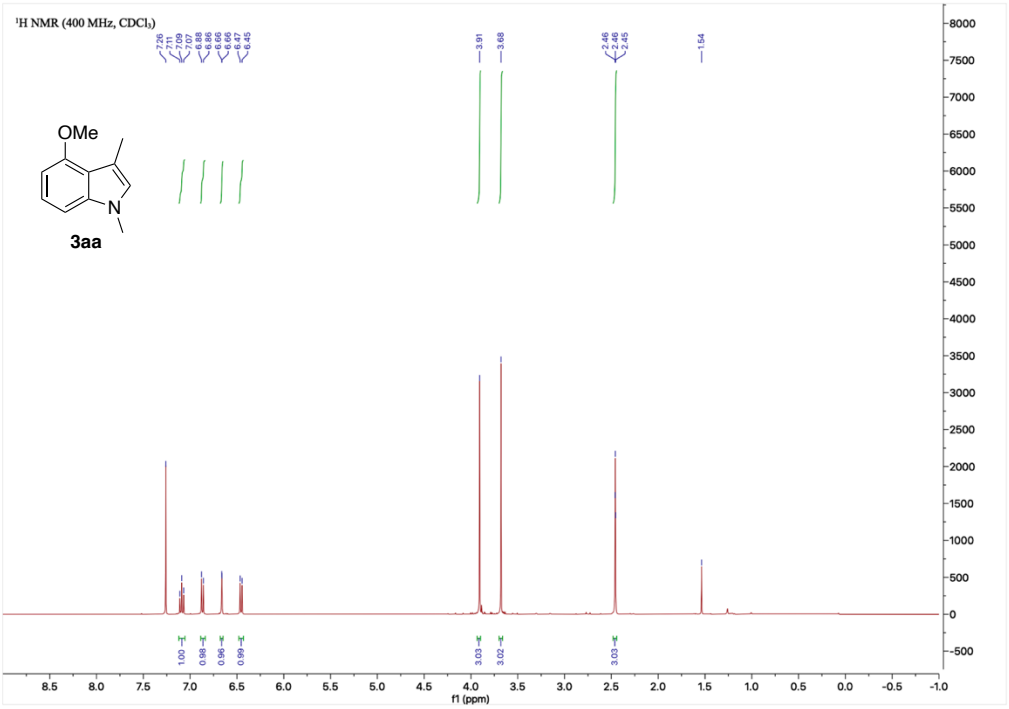

Figure 2.18. ^{13}C NMR Spectrum of **3aa**

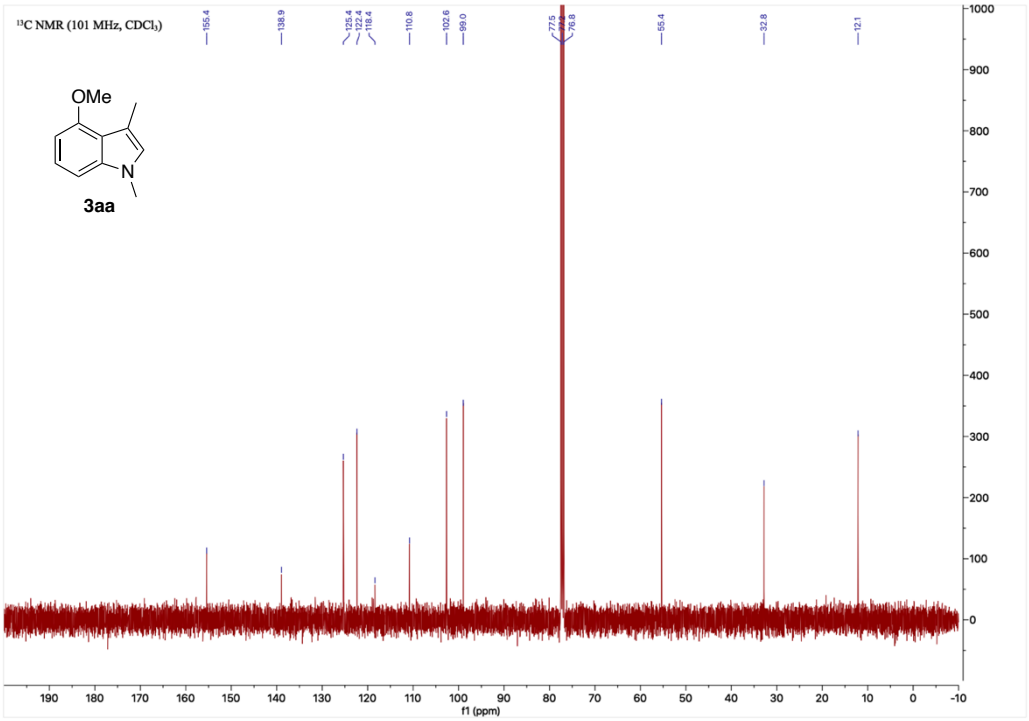

Figure 2.19. ^{1}H NMR Spectrum of **3ba**

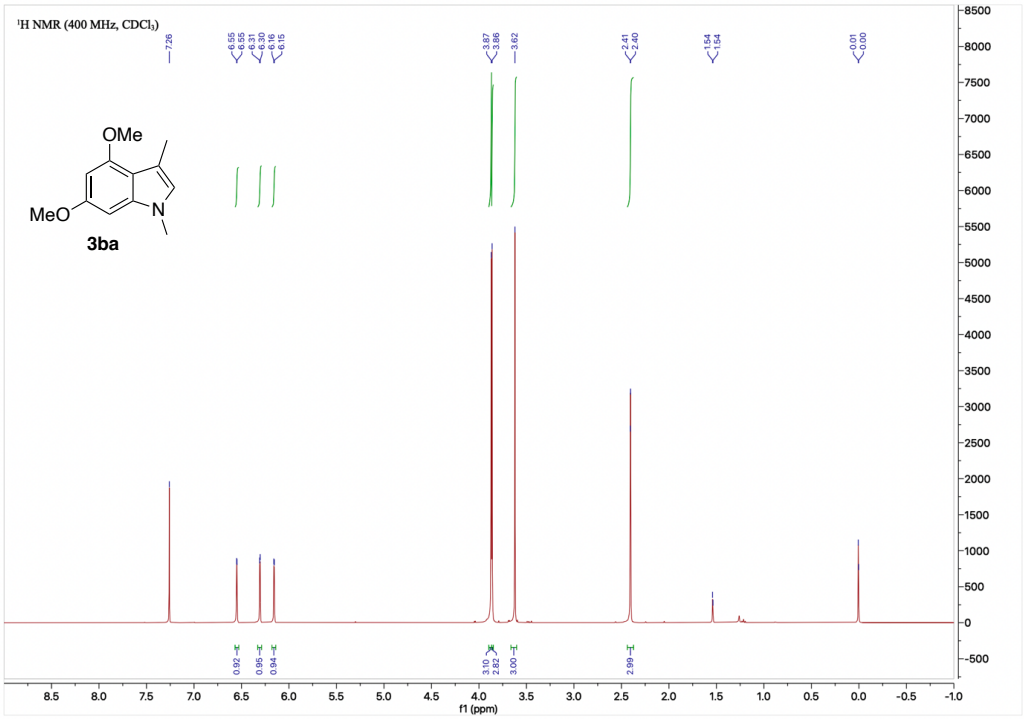

Figure 2.20. ^{13}C NMR Spectrum of **3ba**

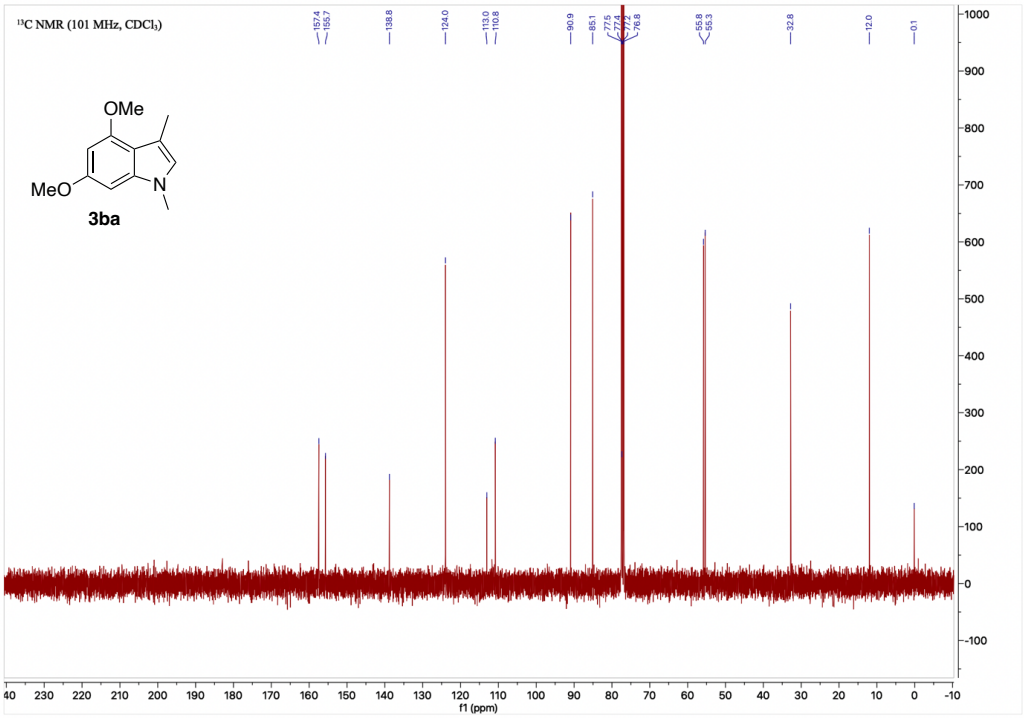

Figure 2.21. ^{1}H NMR Spectrum of **3ca**

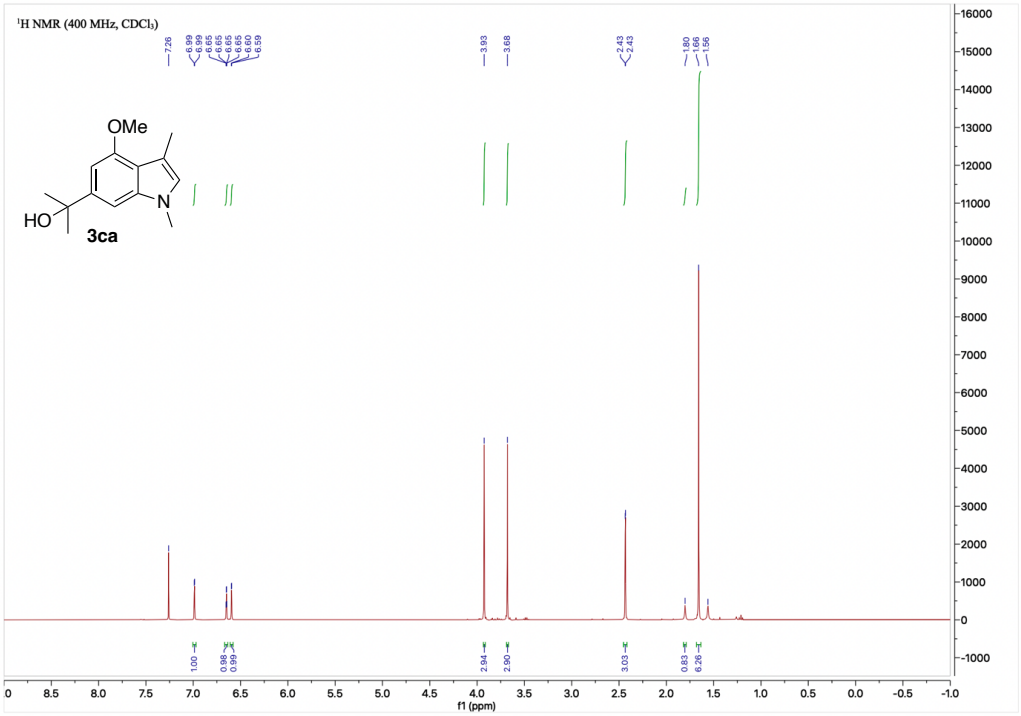

Figure 2.22. ^{13}C NMR Spectrum of **3ca**

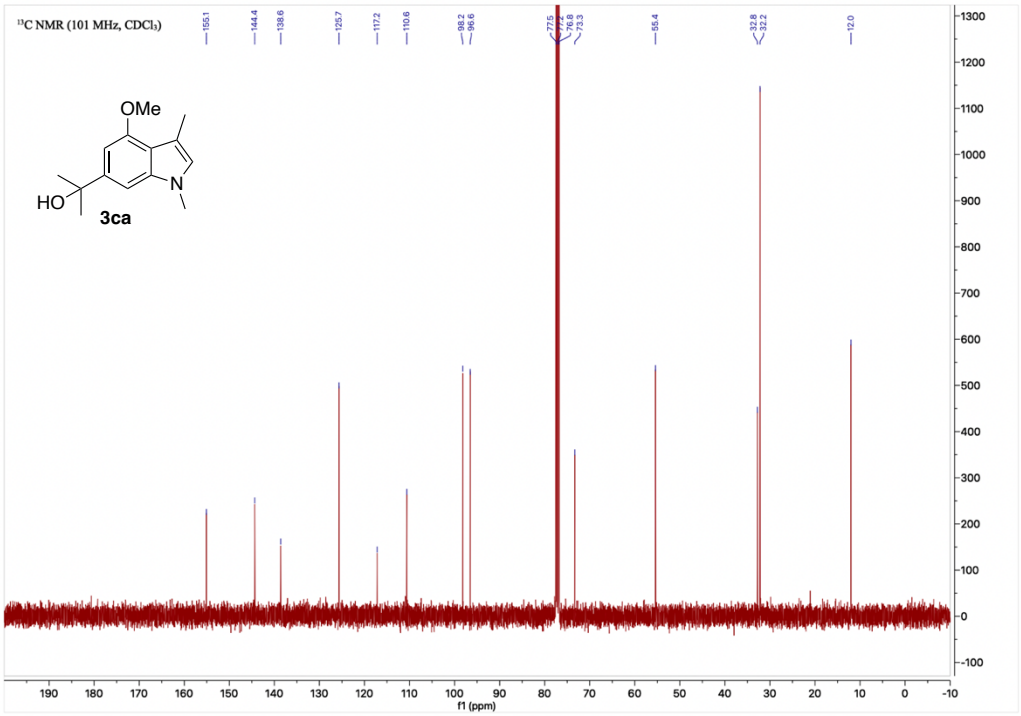

Figure 2.23. ^{1}H NMR Spectrum of **3da**

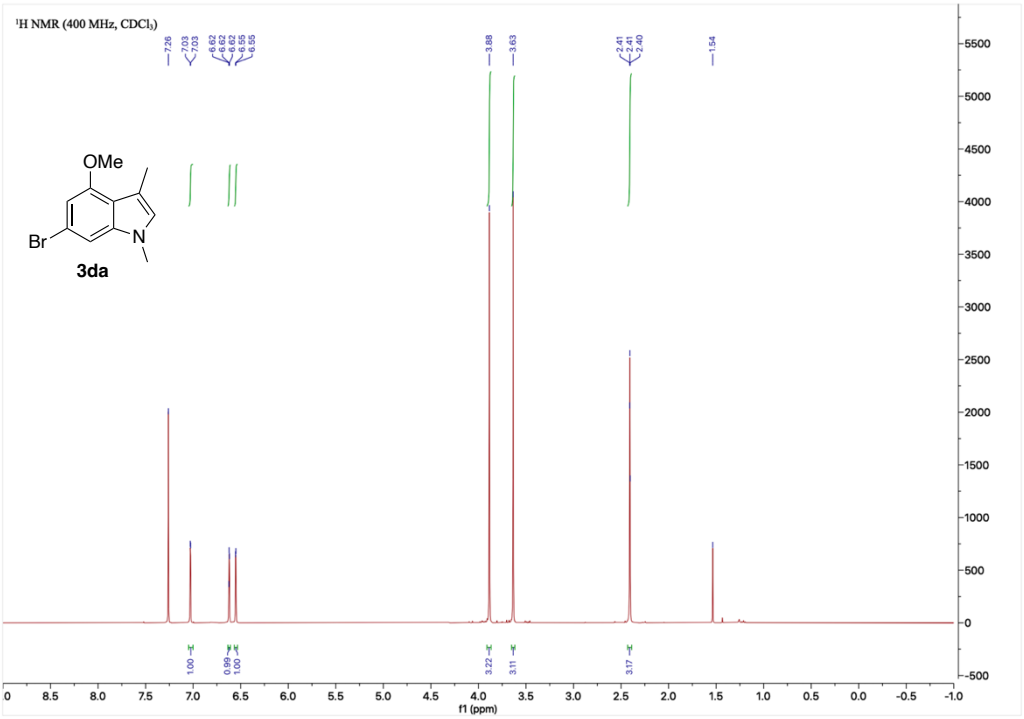

Figure 2.24. ^{13}C NMR Spectrum of **3da**

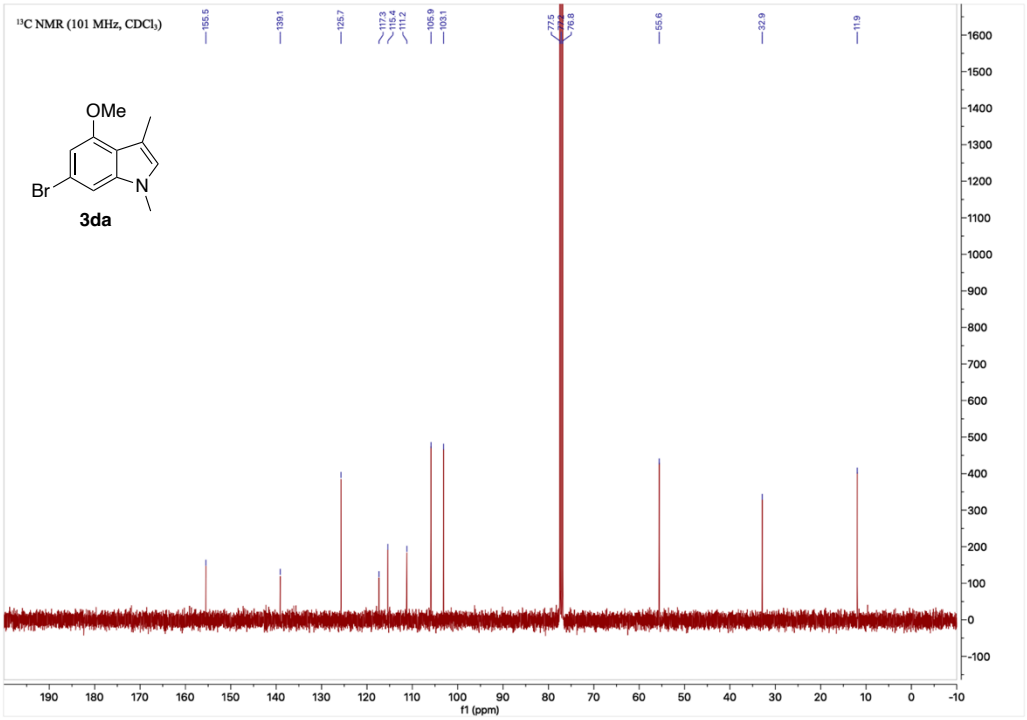

Figure 2.25. ^{1}H NMR Spectrum of **3ea**

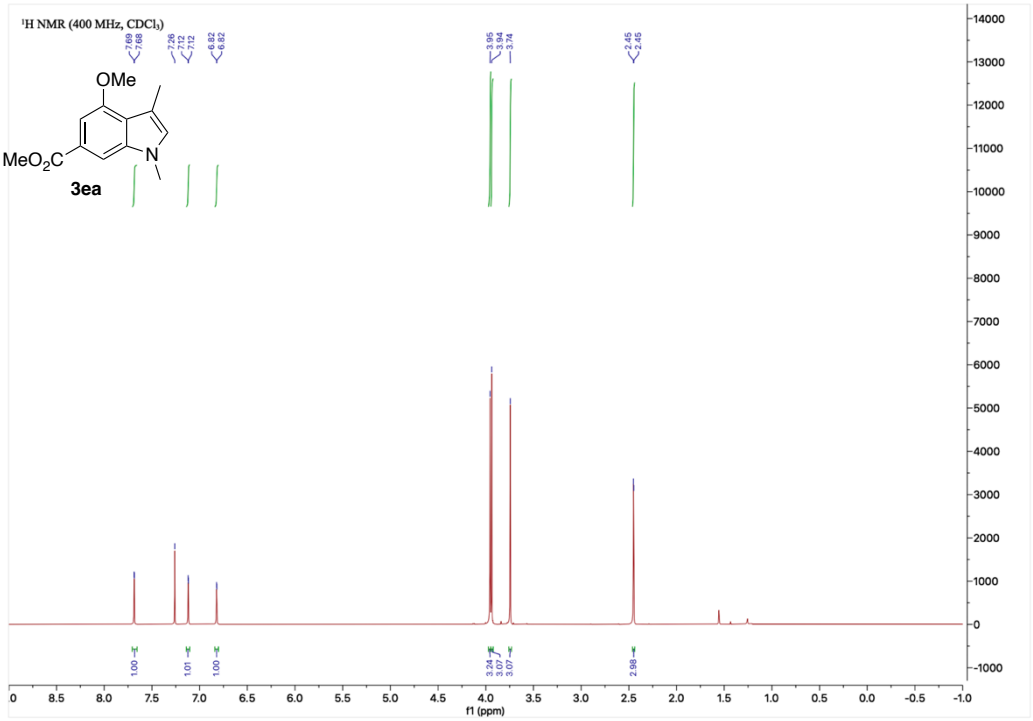

Figure 2.26. ^{13}C NMR Spectrum of **3ea**

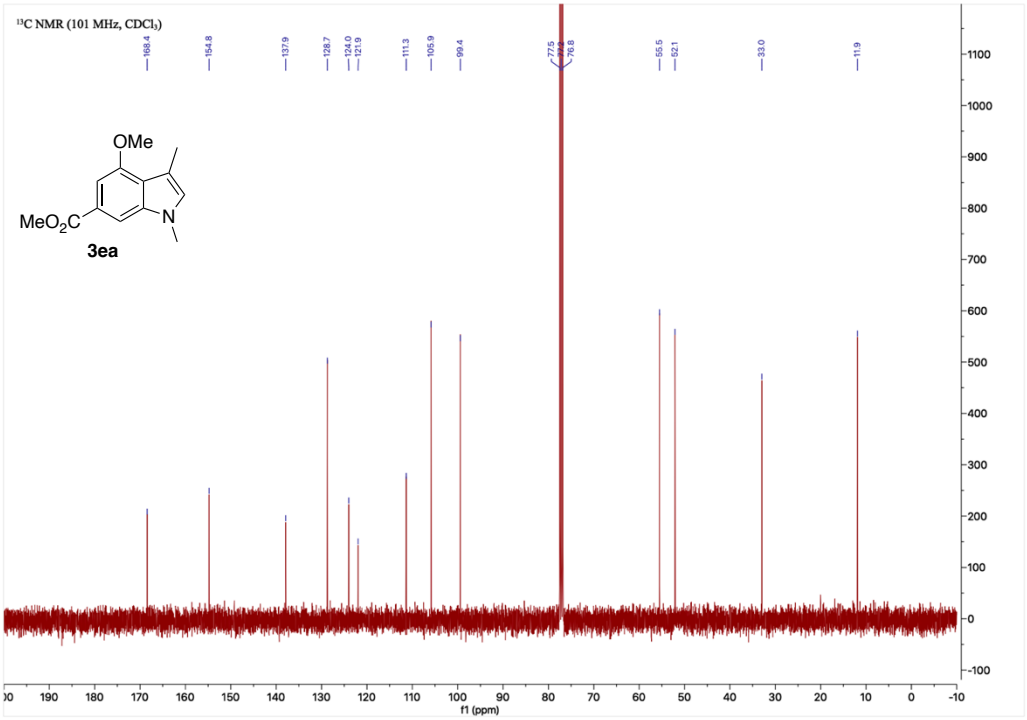

Figure 2.27. ^{1}H NMR Spectrum of **3fa**

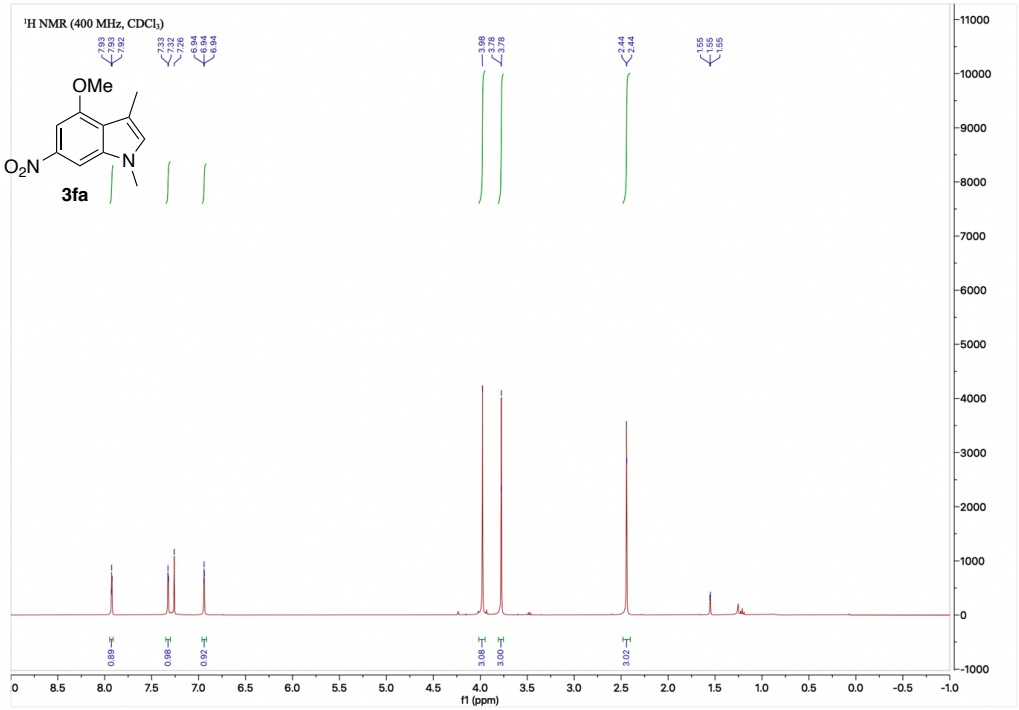

Figure 2.28. ^{13}C NMR Spectrum of **3fa**

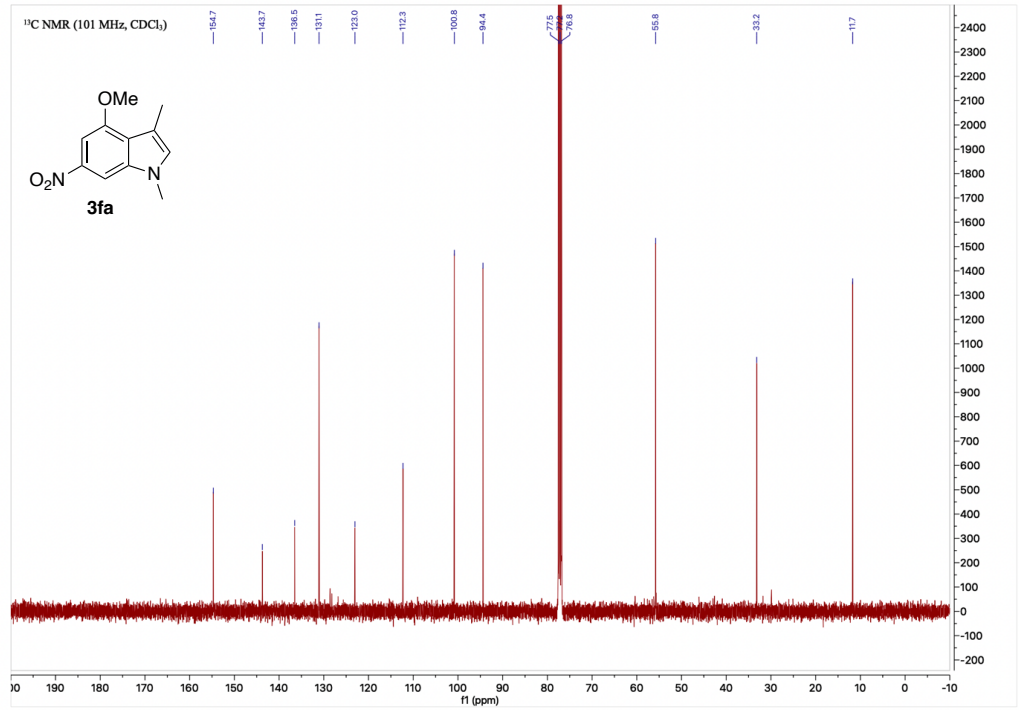

Figure 2.29. ^{1}H NMR Spectrum of **3ga**

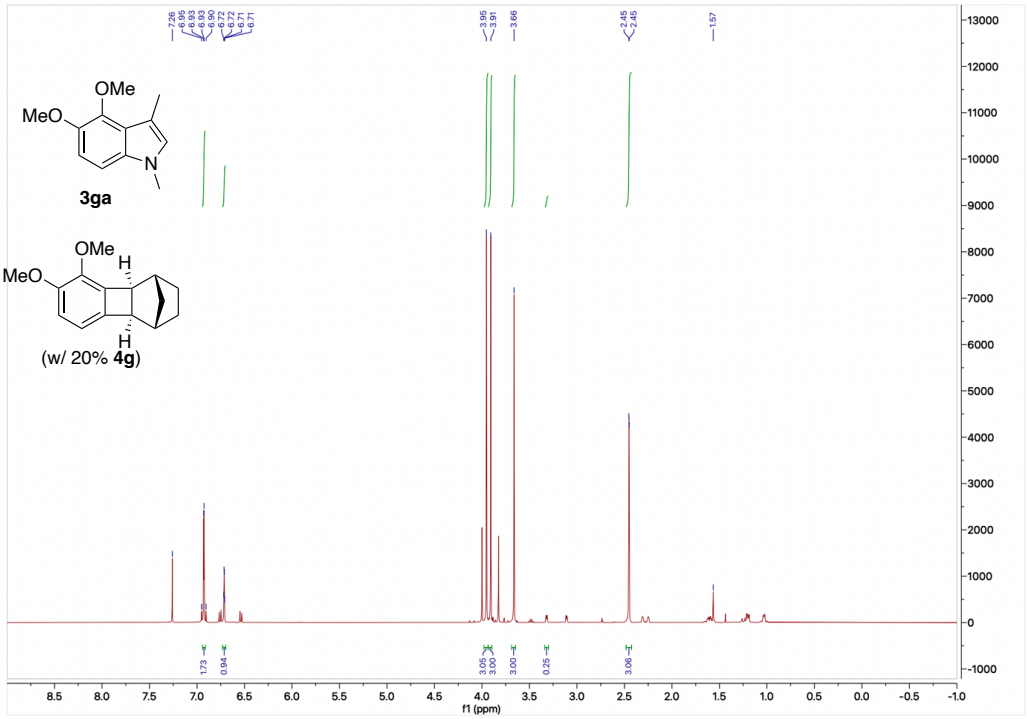

Figure 2.30. ^{13}C NMR Spectrum of **3ga**

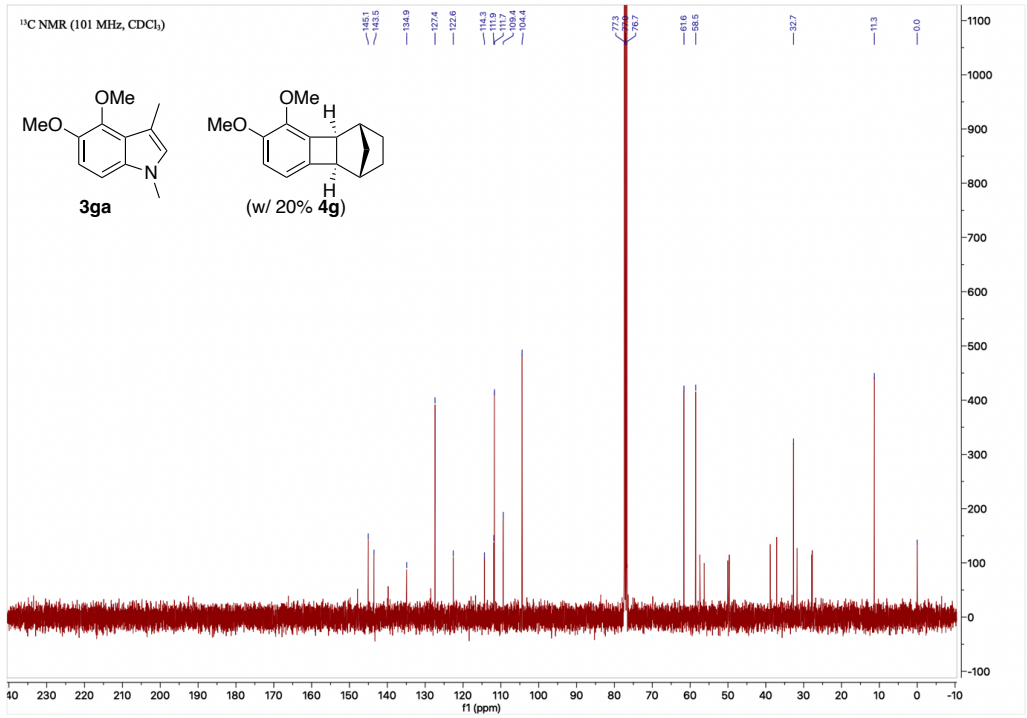

Figure 2.31. ^{1}H NMR Spectrum of **3ha**

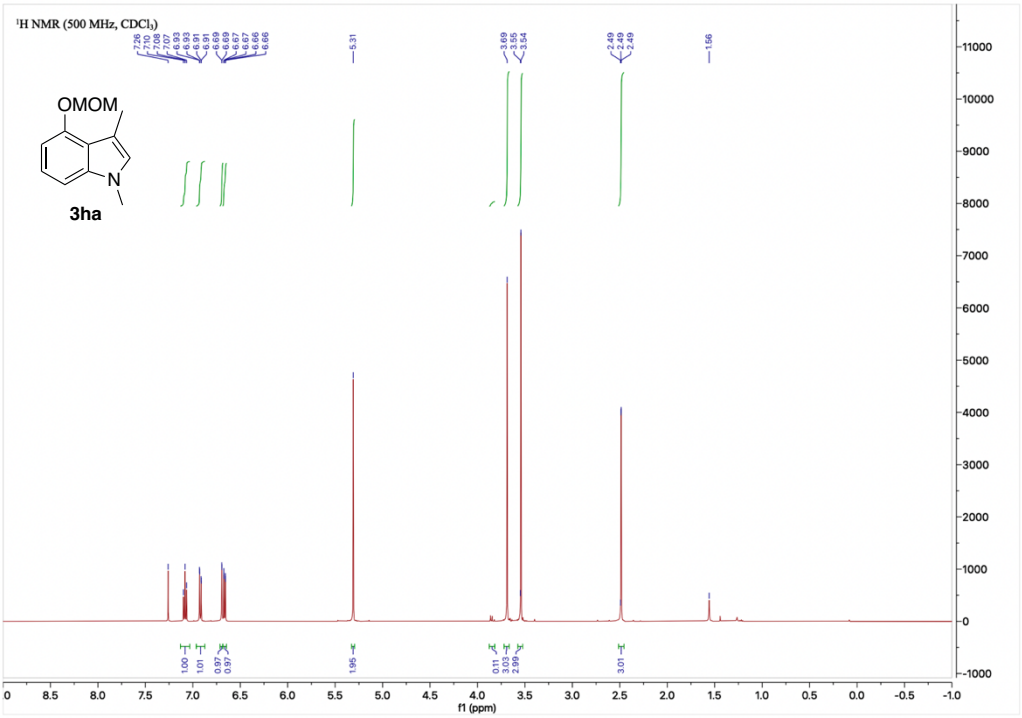

Figure 2.32. ^{13}C NMR Spectrum of **3ha**

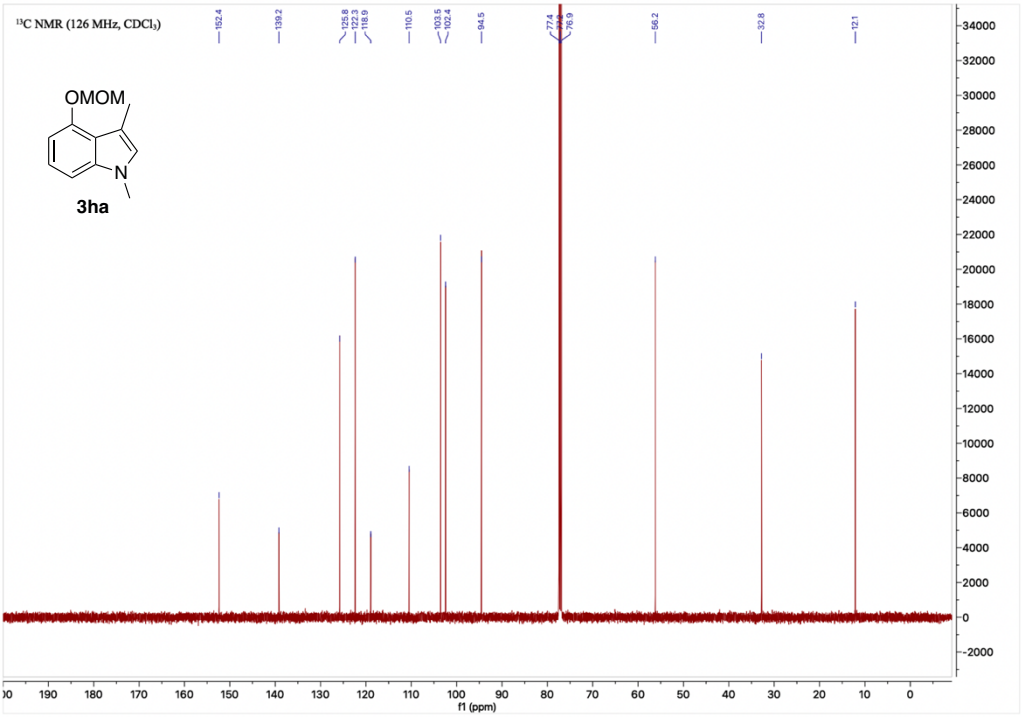

Figure 2.33. ^{1}H NMR Spectrum of **3ia**

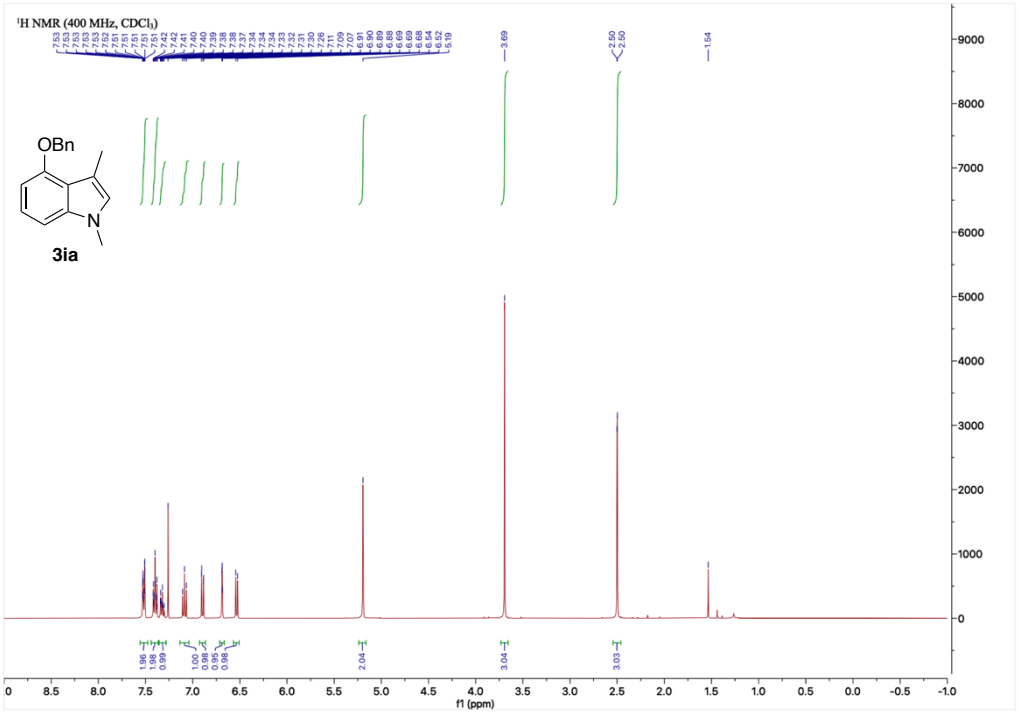

Figure 2.34. ^{13}C NMR Spectrum of **3ia**

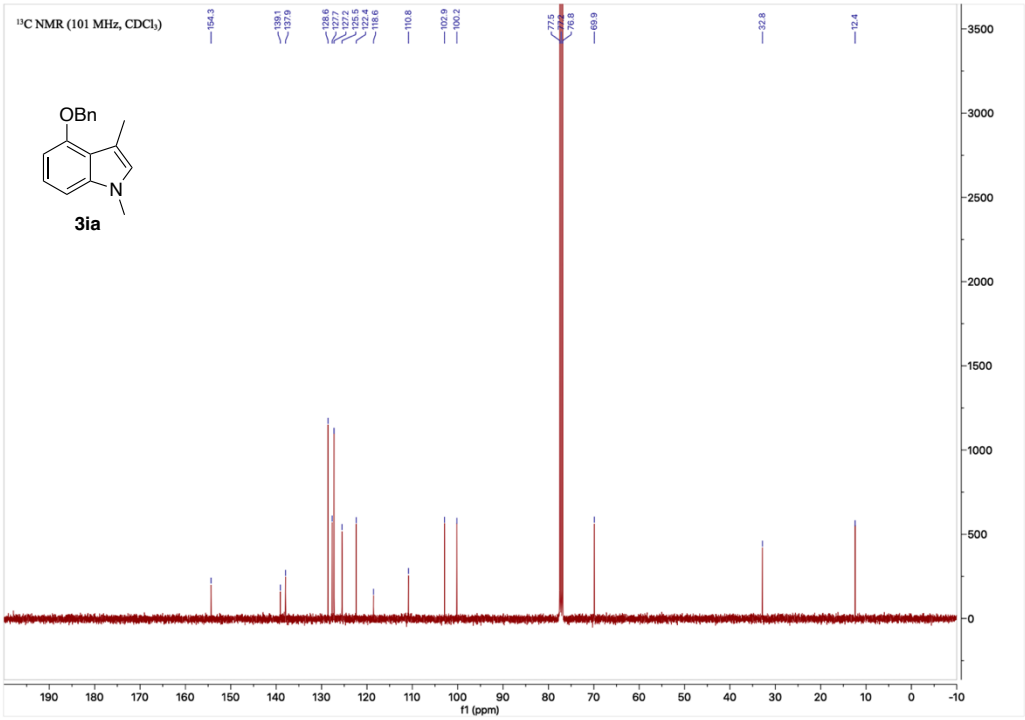

Figure 2.35. ^{1}H NMR Spectrum of **3ja**

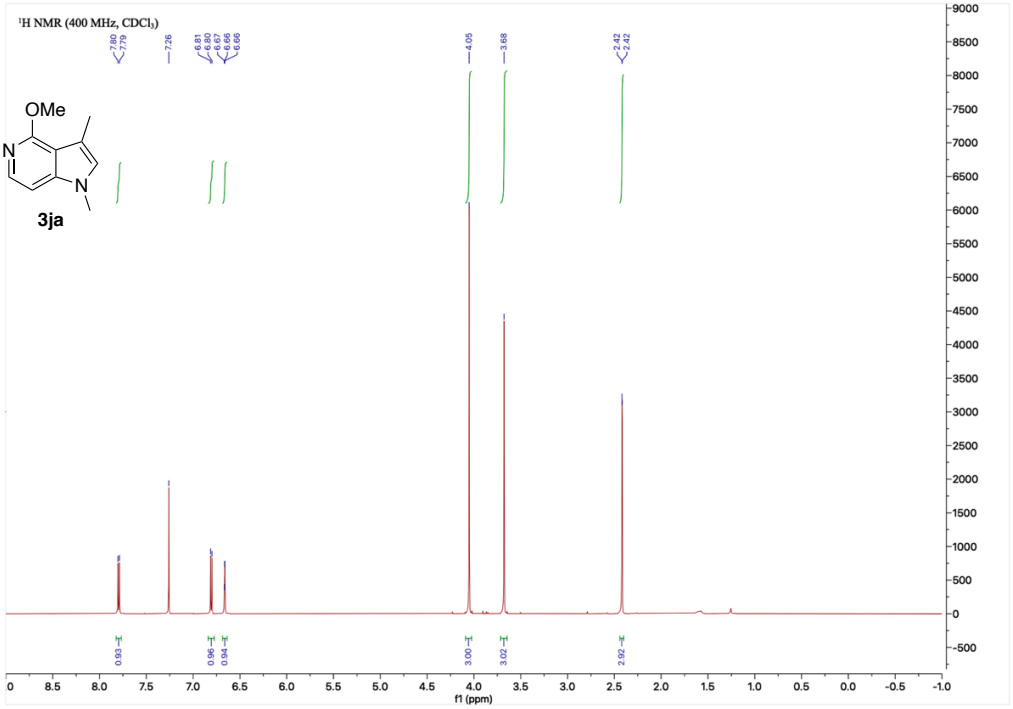

Figure 2.36. ^{13}C NMR Spectrum of **3ja**

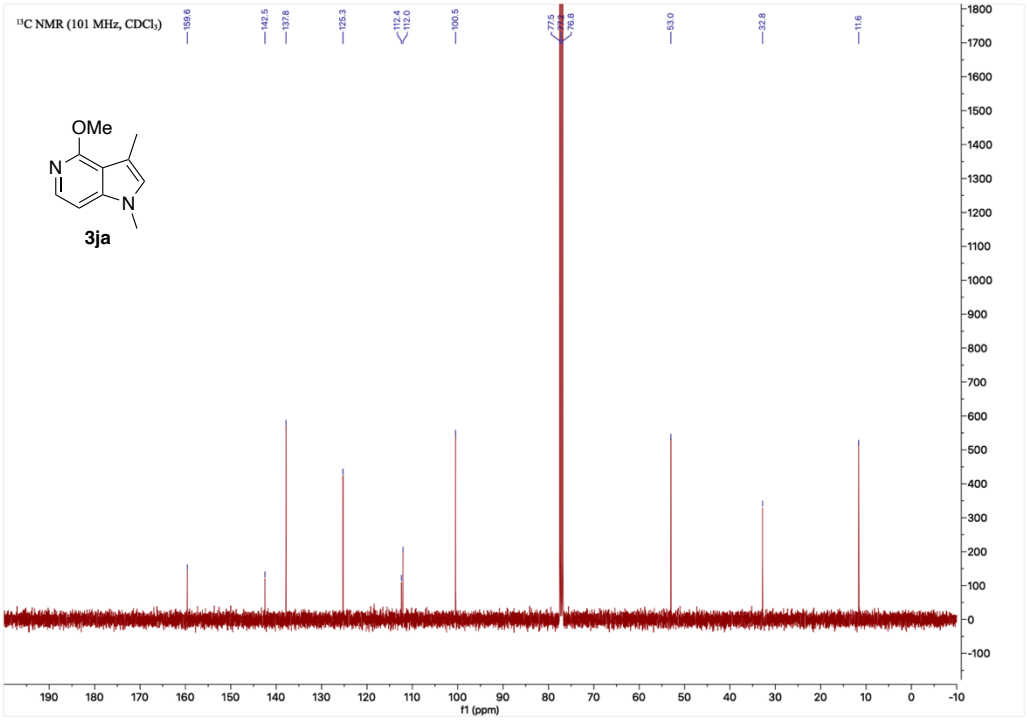

Figure 2.37. ^{1}H NMR Spectrum of **3ka**

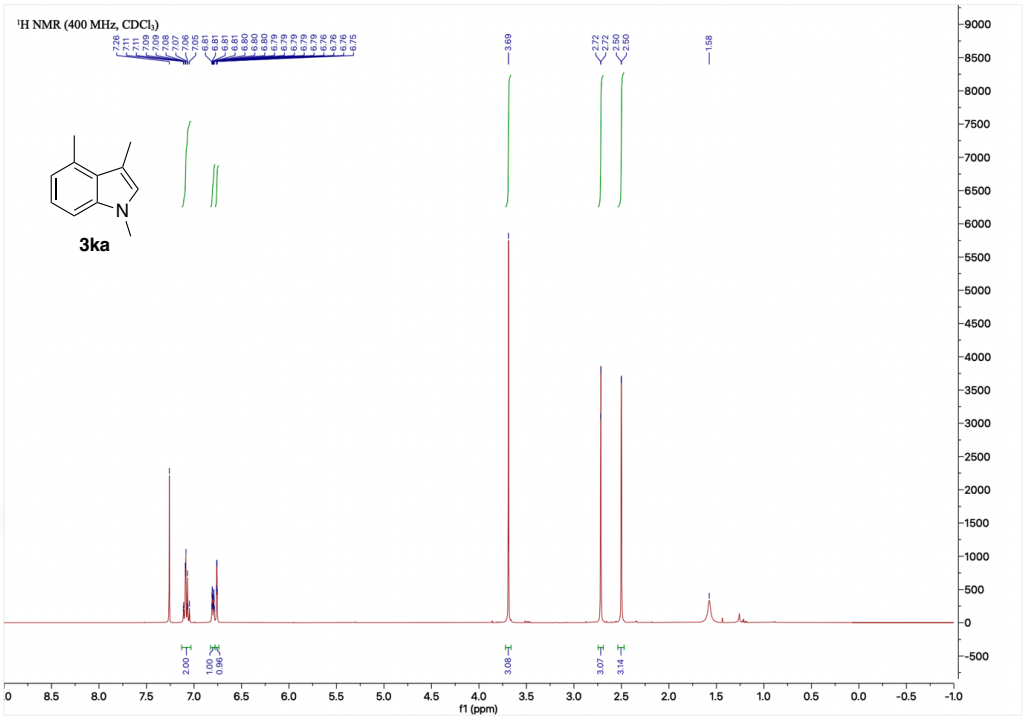

Figure 2.38. ^{13}C NMR Spectrum of **3ka**

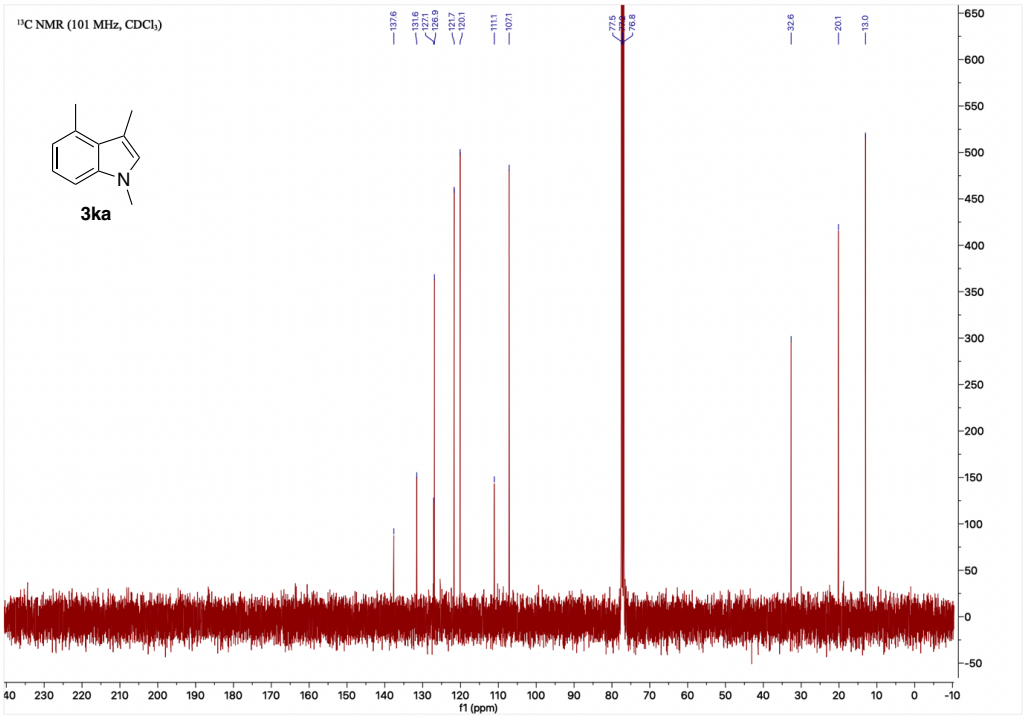

Figure 2.39. ^{1}H NMR Spectrum of **3la**

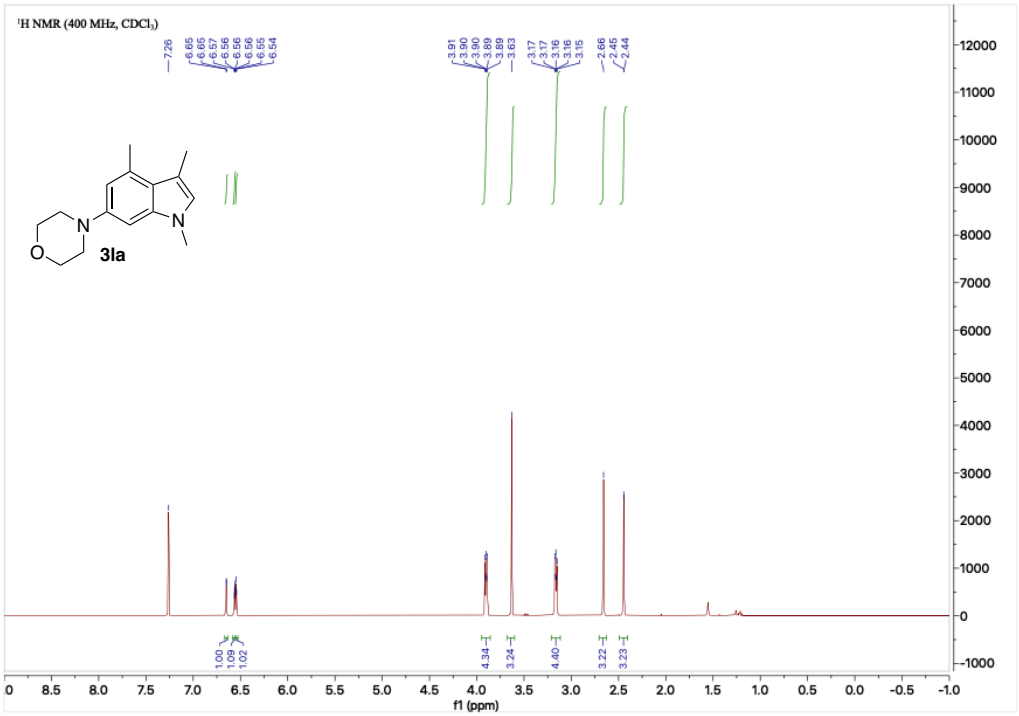

Figure 2.40. ^{13}C NMR Spectrum of **3la**

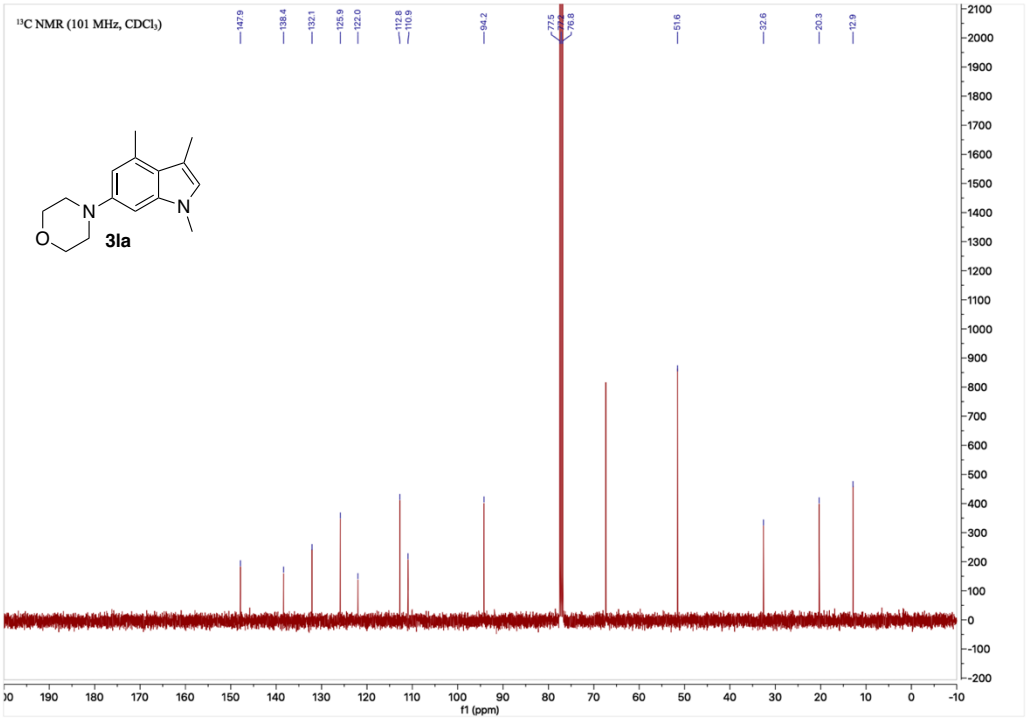

Figure 2.41. ^{1}H NMR Spectrum of **3ma**

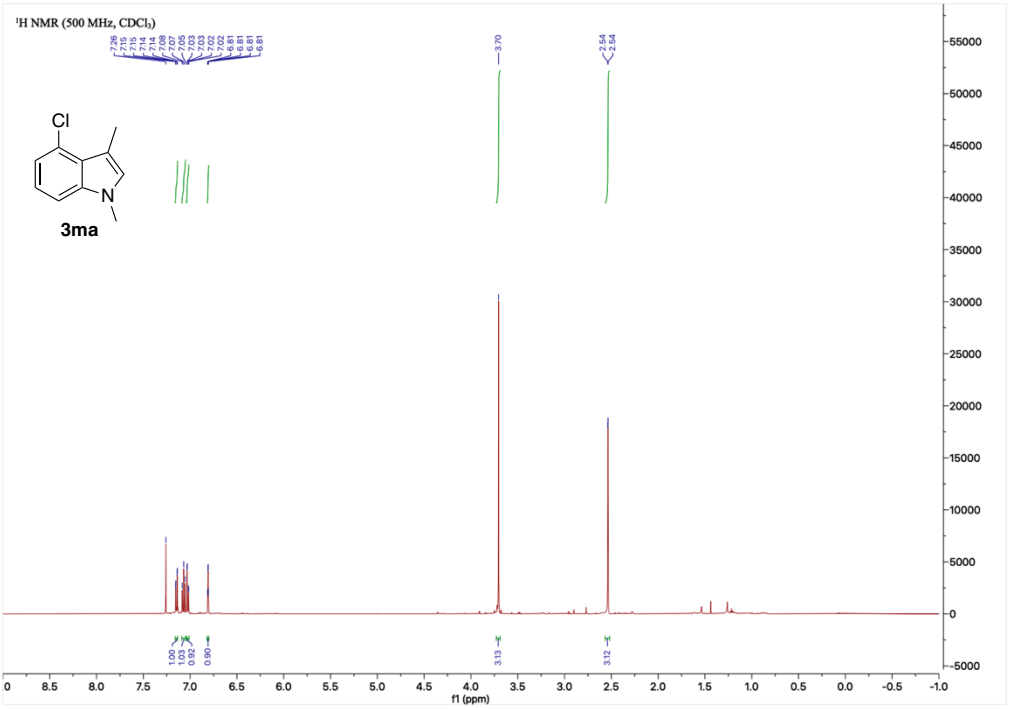

Figure 2.42. ^{13}C NMR Spectrum of **3ma**

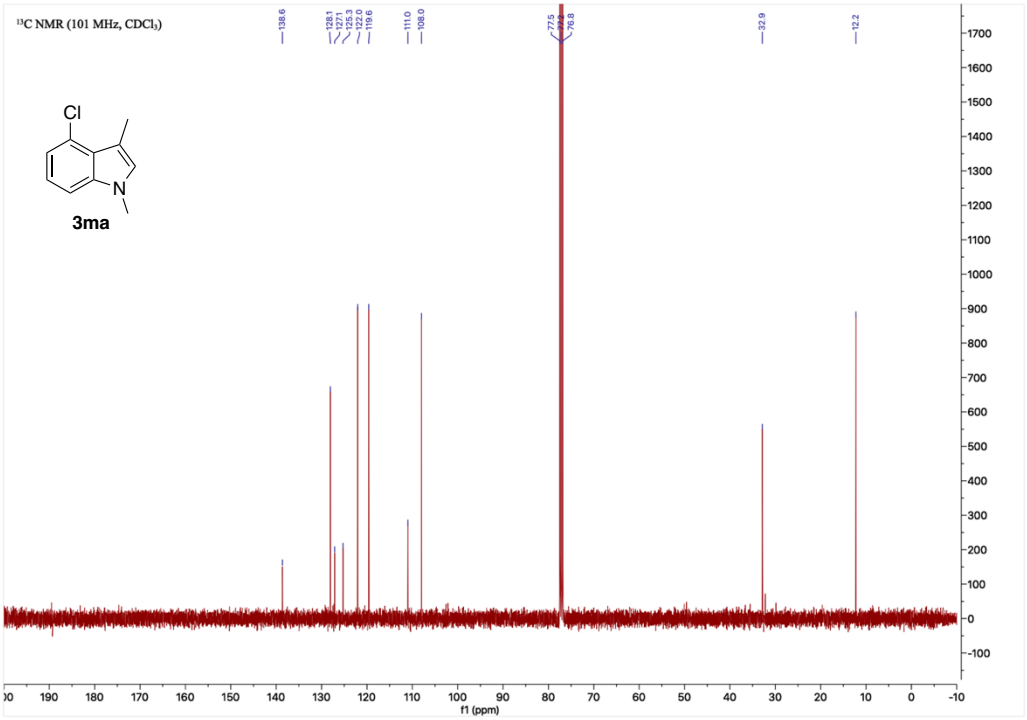

Figure 2.43. ^{1}H NMR Spectrum of **3na**

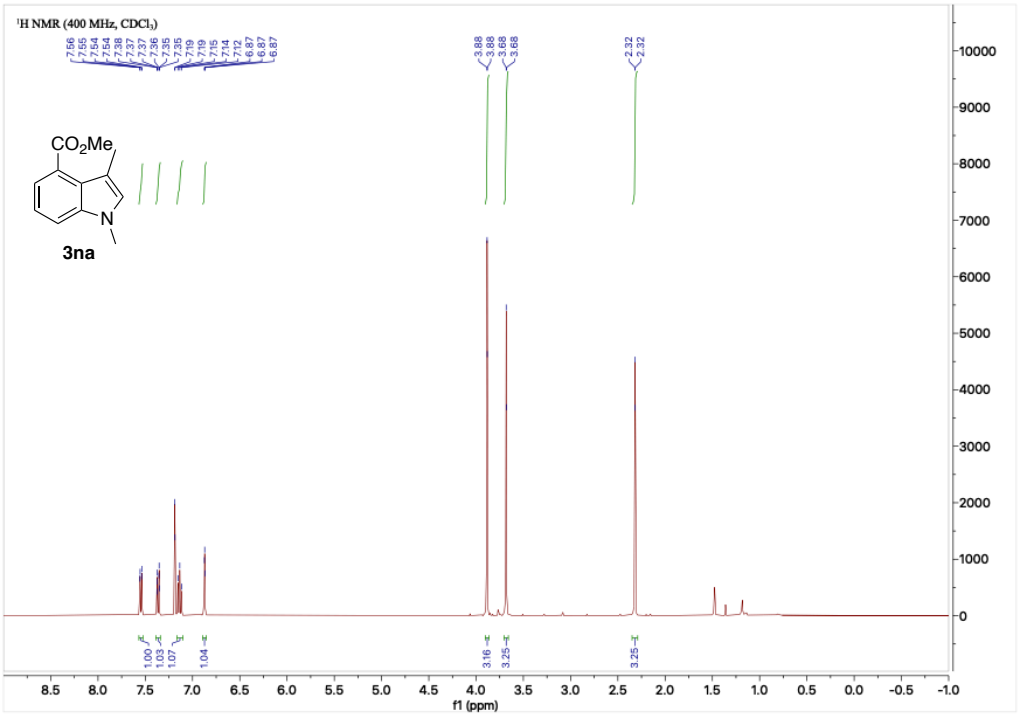

Figure 2.44. ^{13}C NMR Spectrum of **3na**

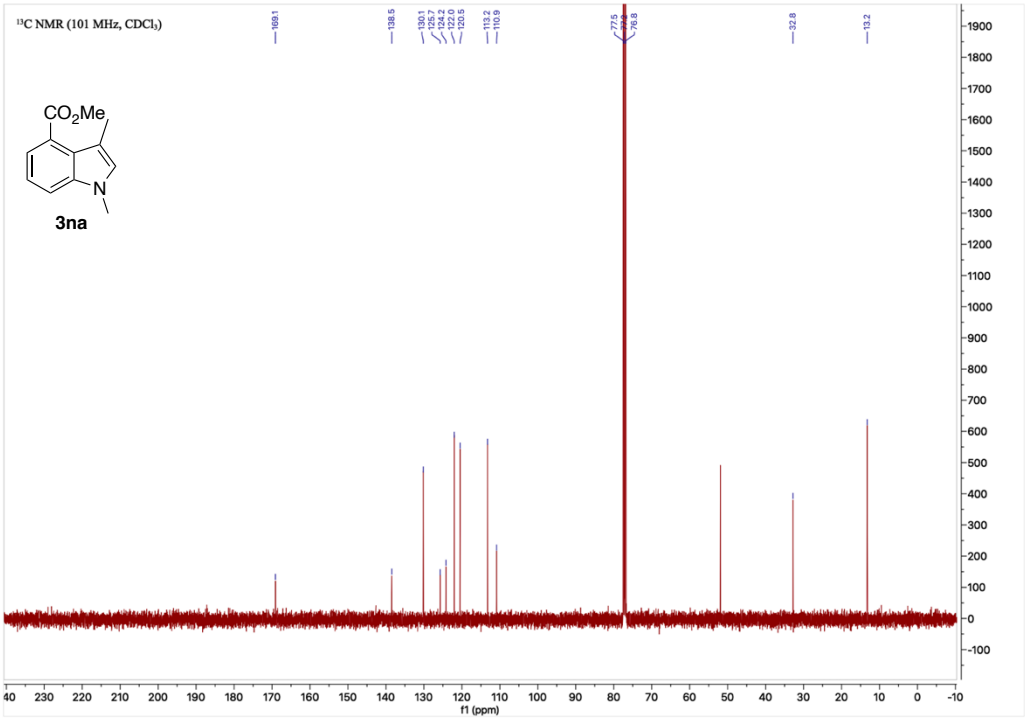

Figure 2.45. ^{1}H NMR Spectrum of **3oa**

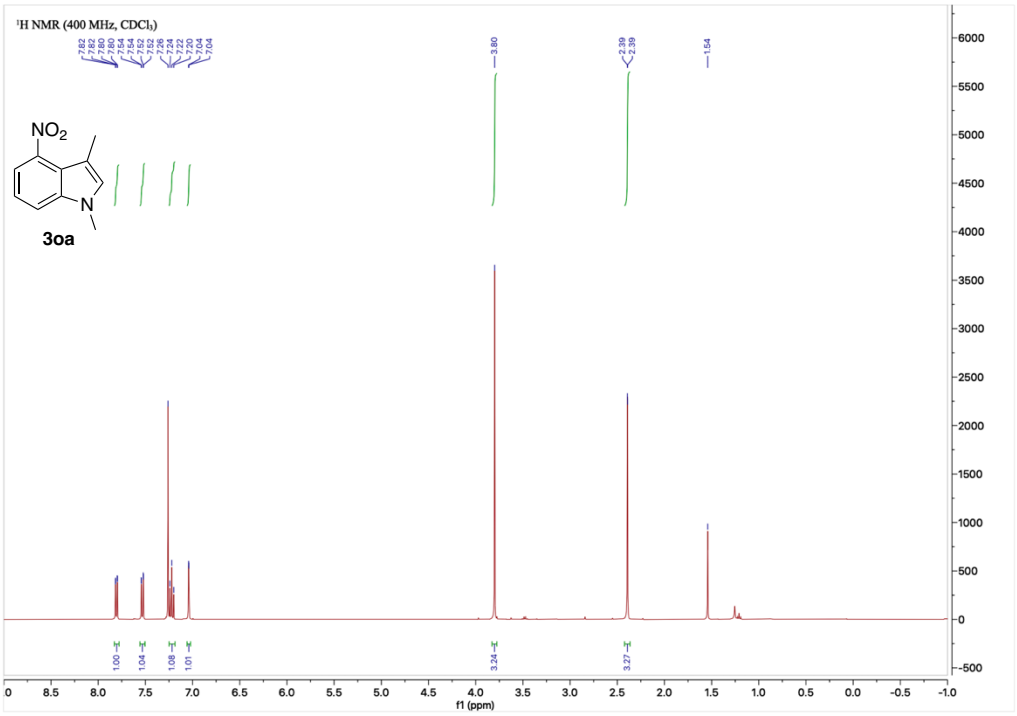

Figure 2.46. ^{13}C NMR Spectrum of **3oa**

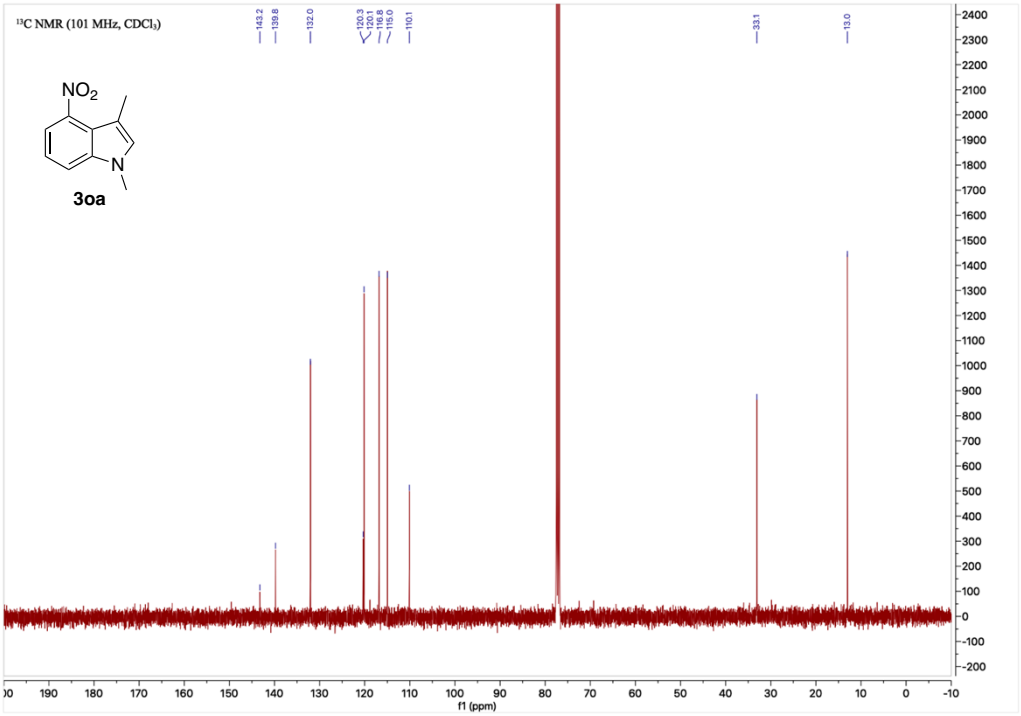

Figure 2.47. ^{1}H NMR Spectrum of **3pa**

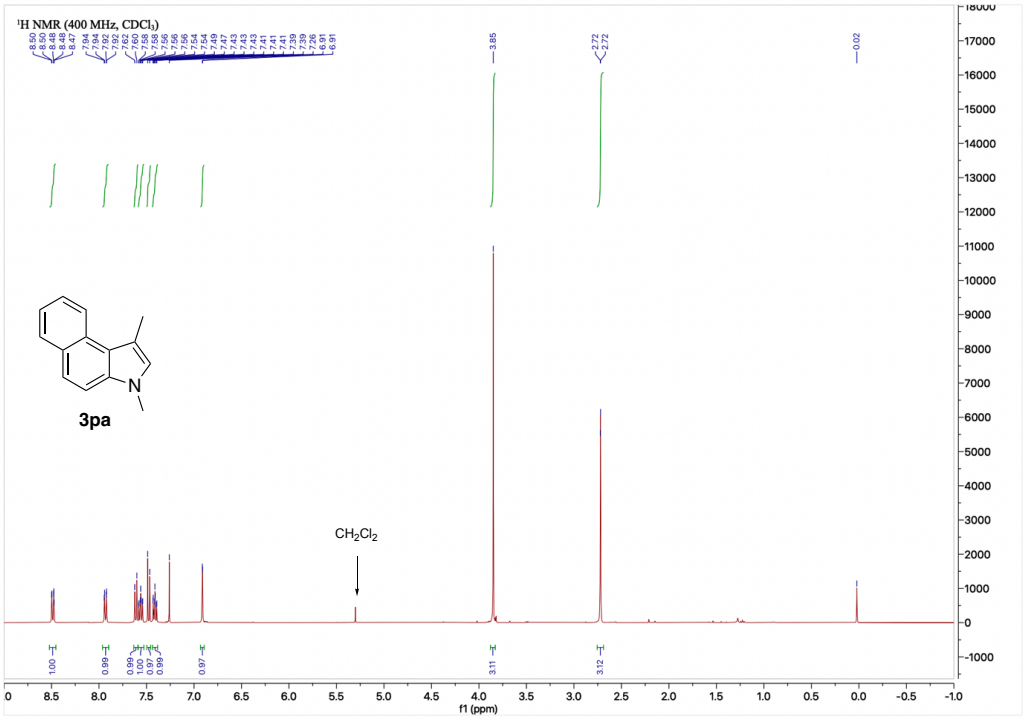

Figure 2.48. ^{13}C NMR Spectrum of **3pa**

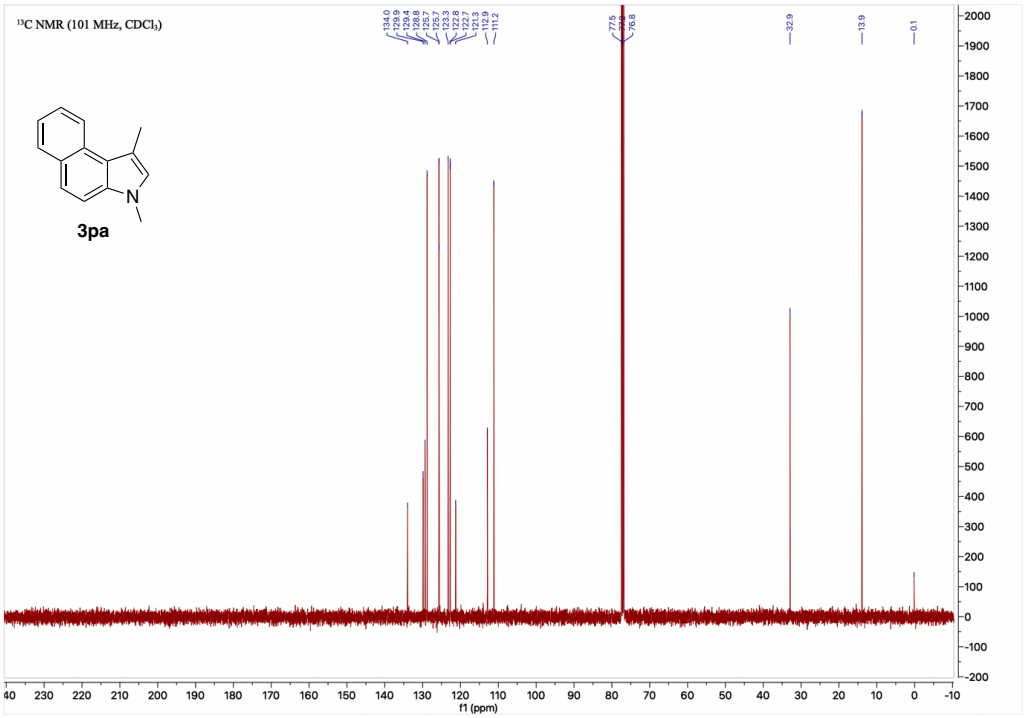

Figure 2.49. ^{1}H NMR Spectrum of **3qa**

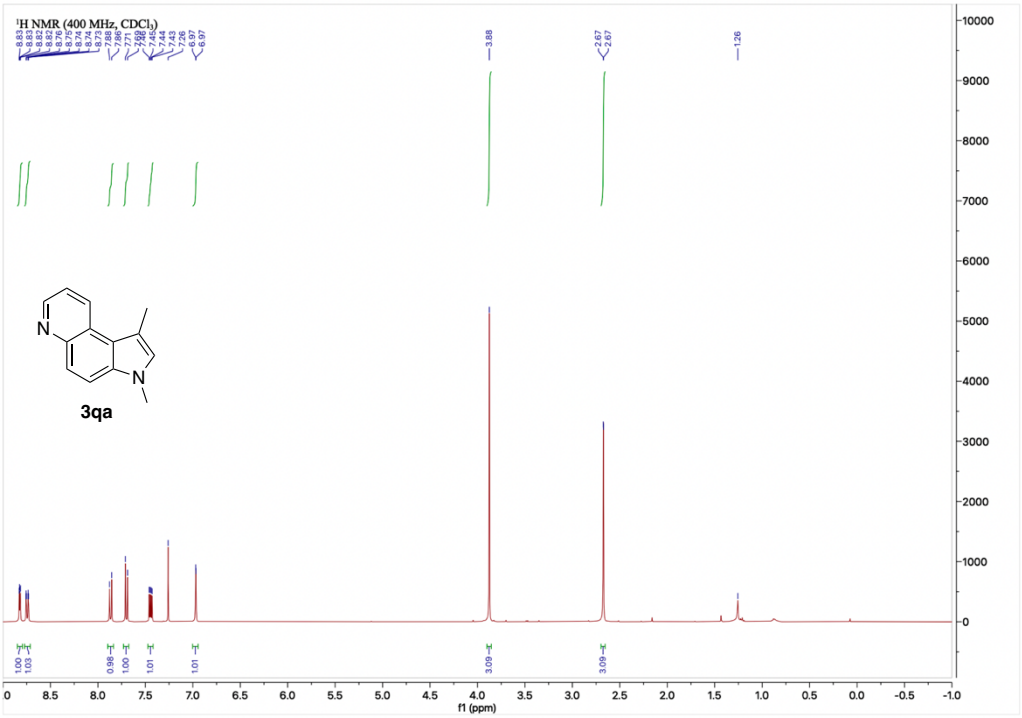

Figure 2.50. ^{13}C NMR Spectrum of **3qa**

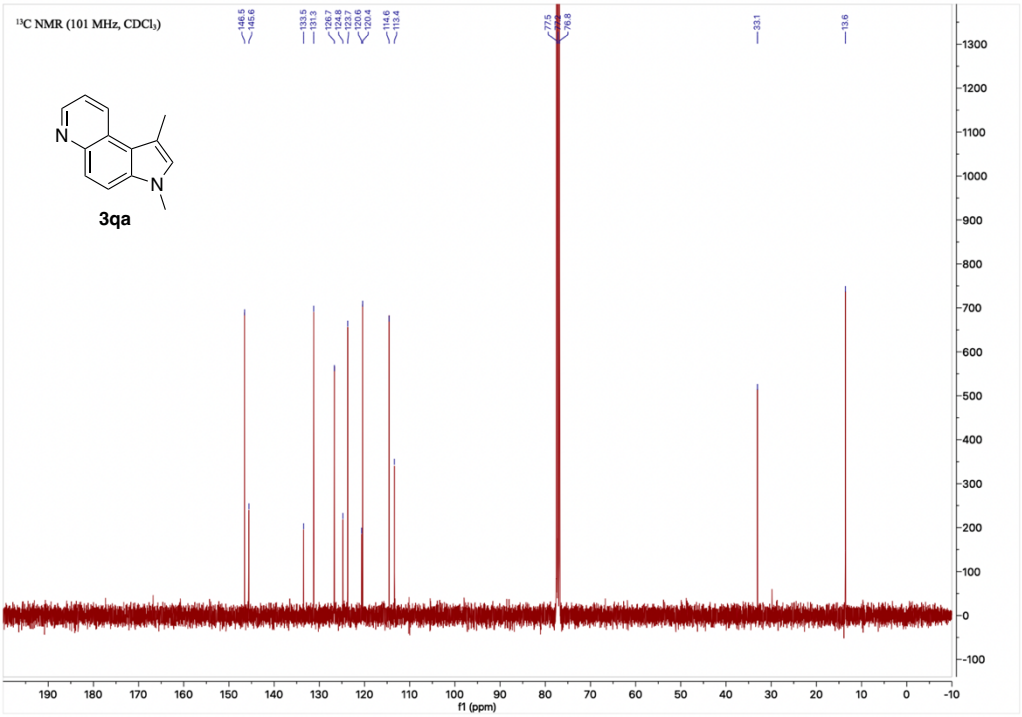

Figure 2.51. ^{1}H NMR Spectrum of **3ra**

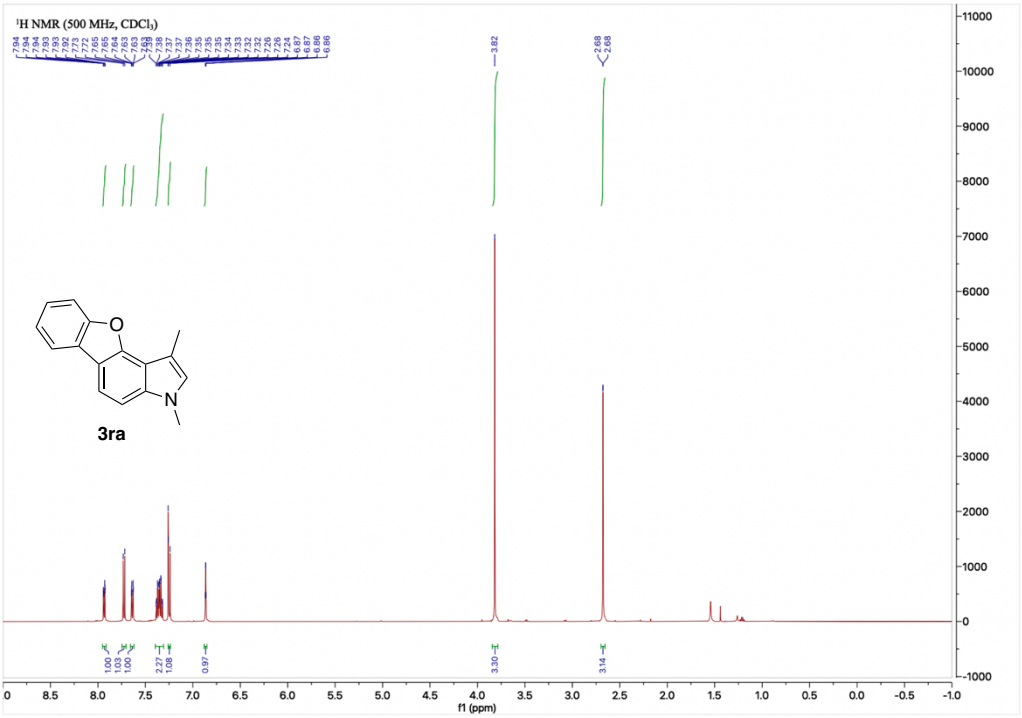

Figure 2.52. ^{13}C NMR Spectrum of **3ra**

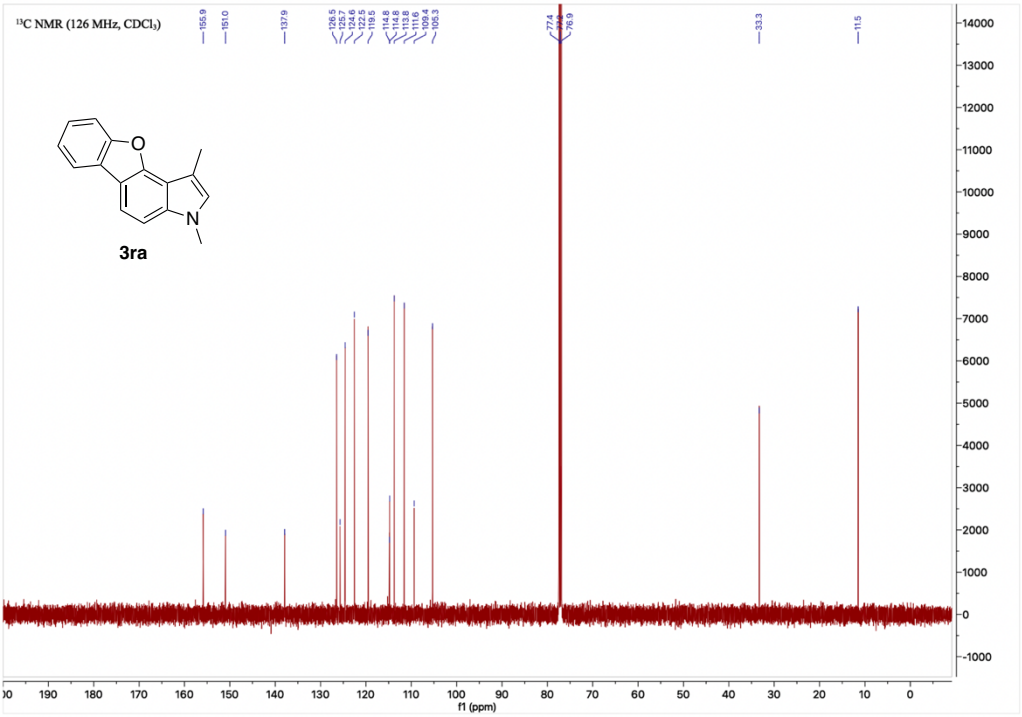

Figure 2.53. ^{1}H NMR Spectrum of **3jb**

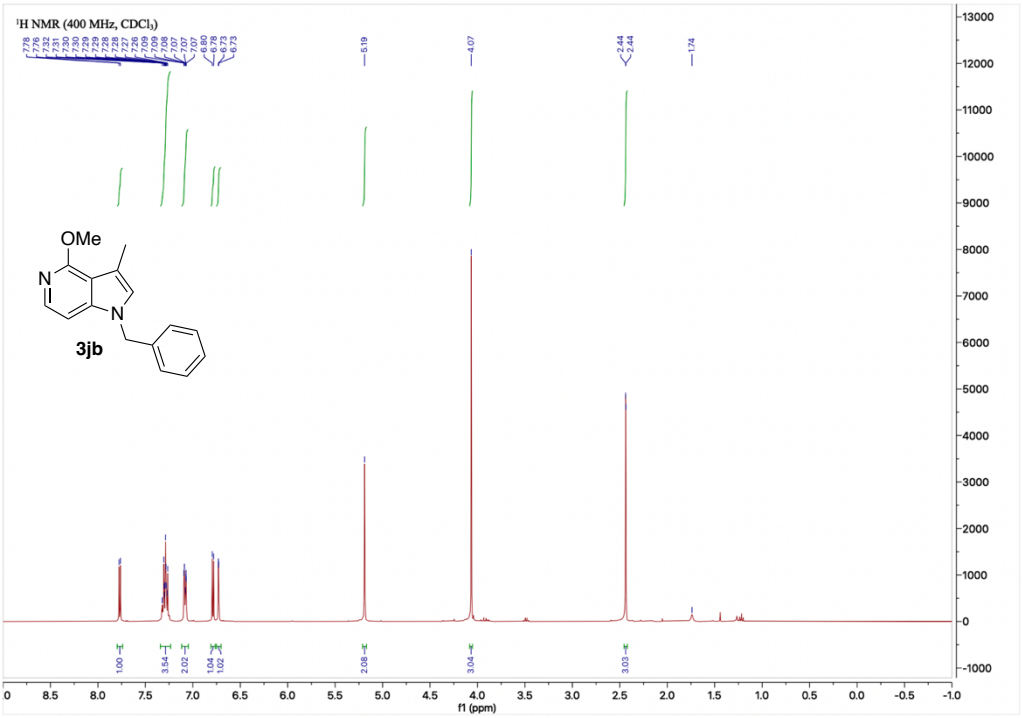

Figure 2.54. ^{13}C NMR Spectrum of **3jb**

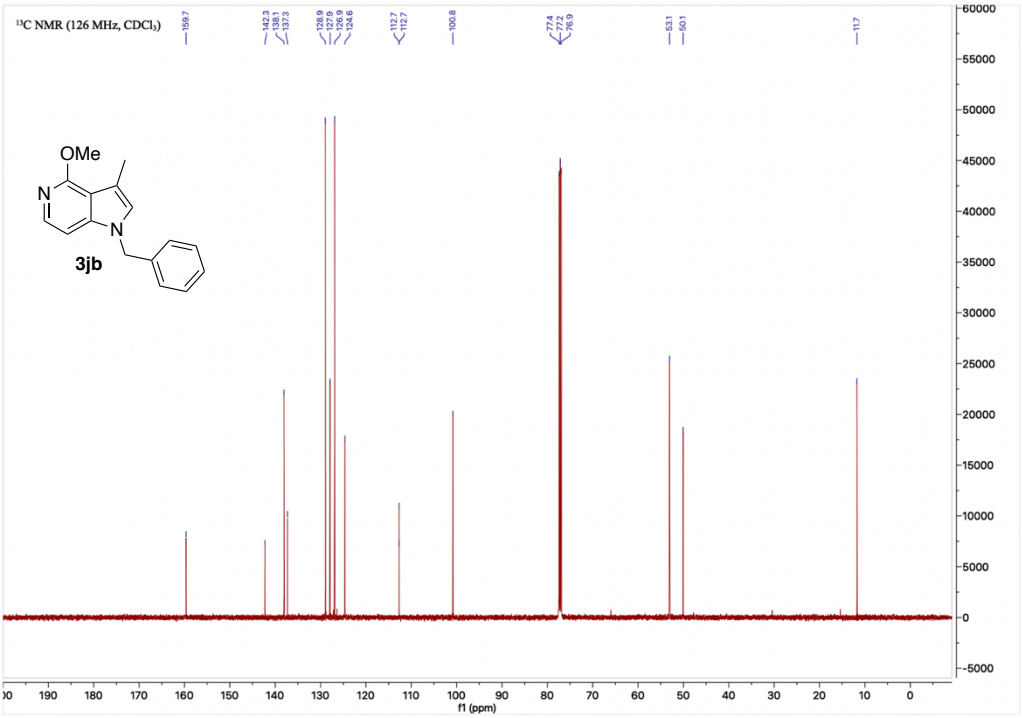

Figure 2.55. ^{1}H NMR Spectrum of **3jc**

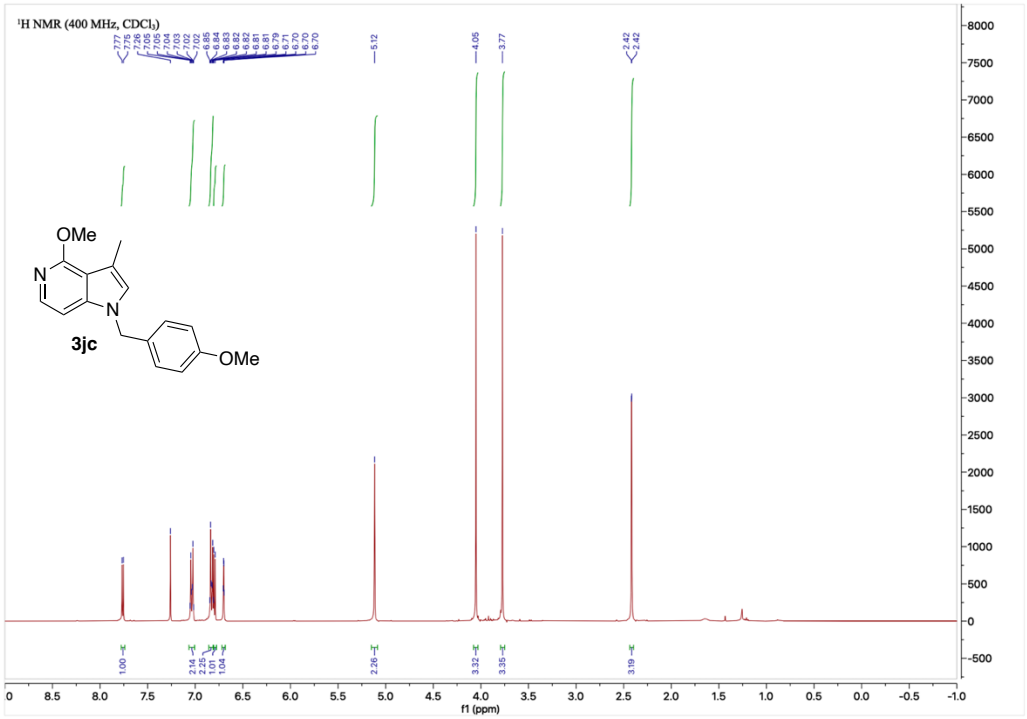

Figure 2.56. ^{13}C NMR Spectrum of **3jc**

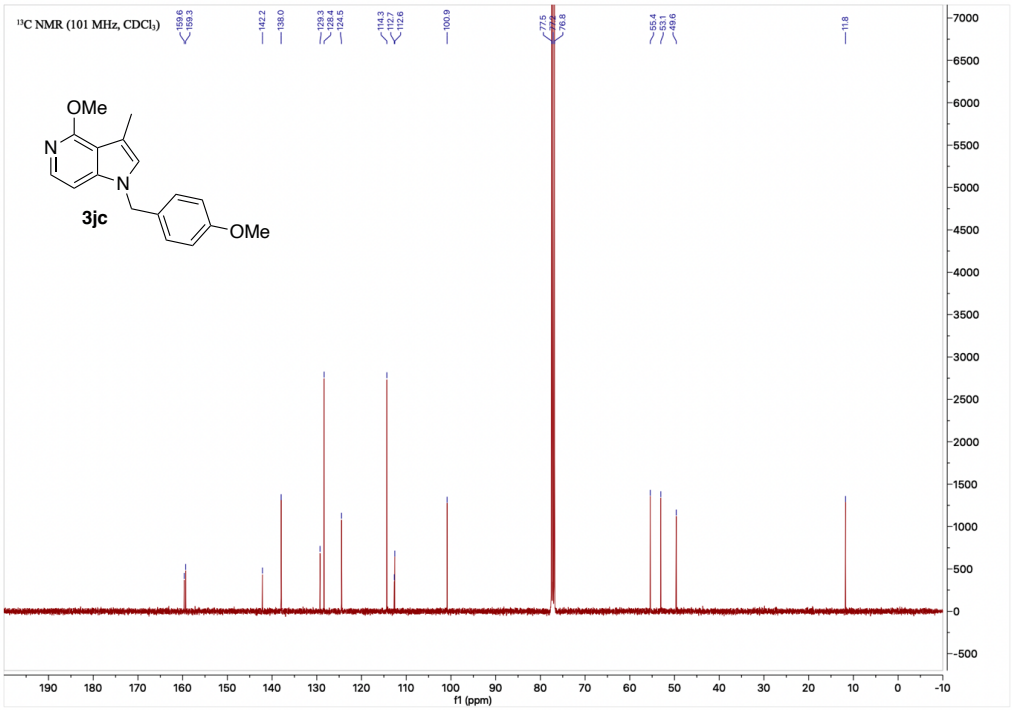

Figure 2.57. ^{1}H NMR Spectrum of **3ad**

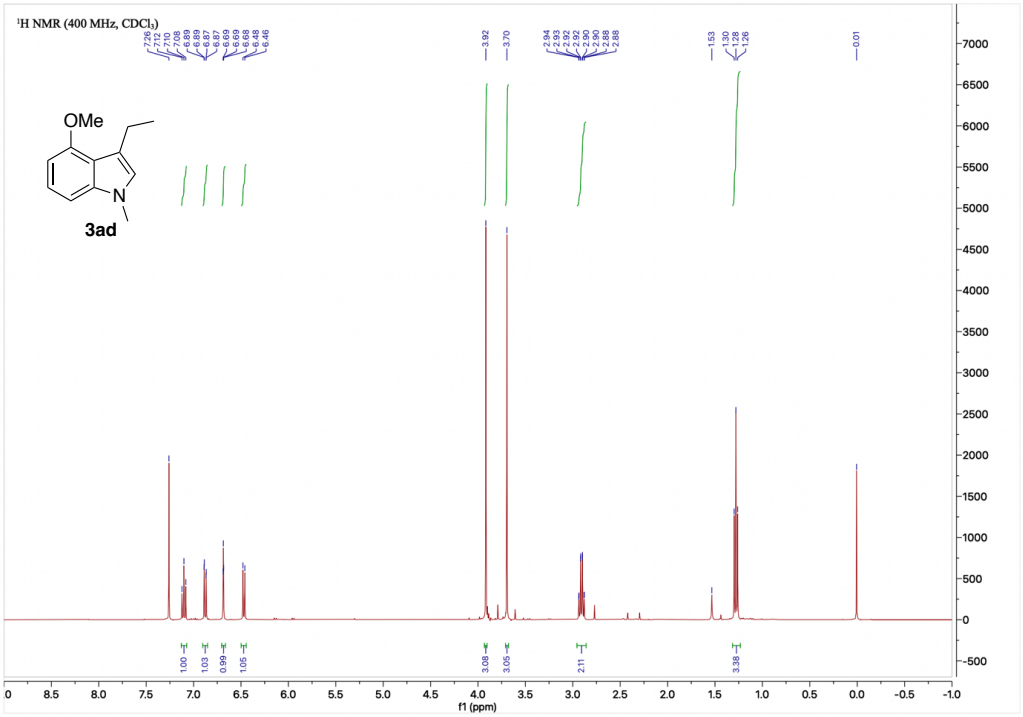

Figure 2.58. ^{13}C NMR Spectrum of **3ad**

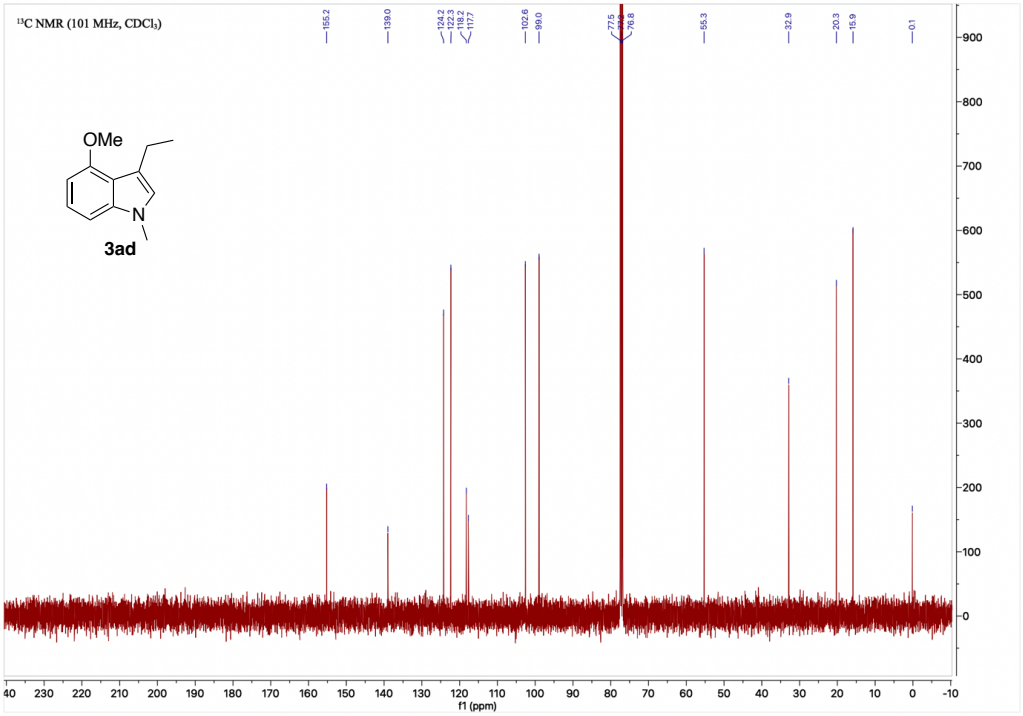

Figure 2.59. ^{1}H NMR Spectrum of **3ad'**

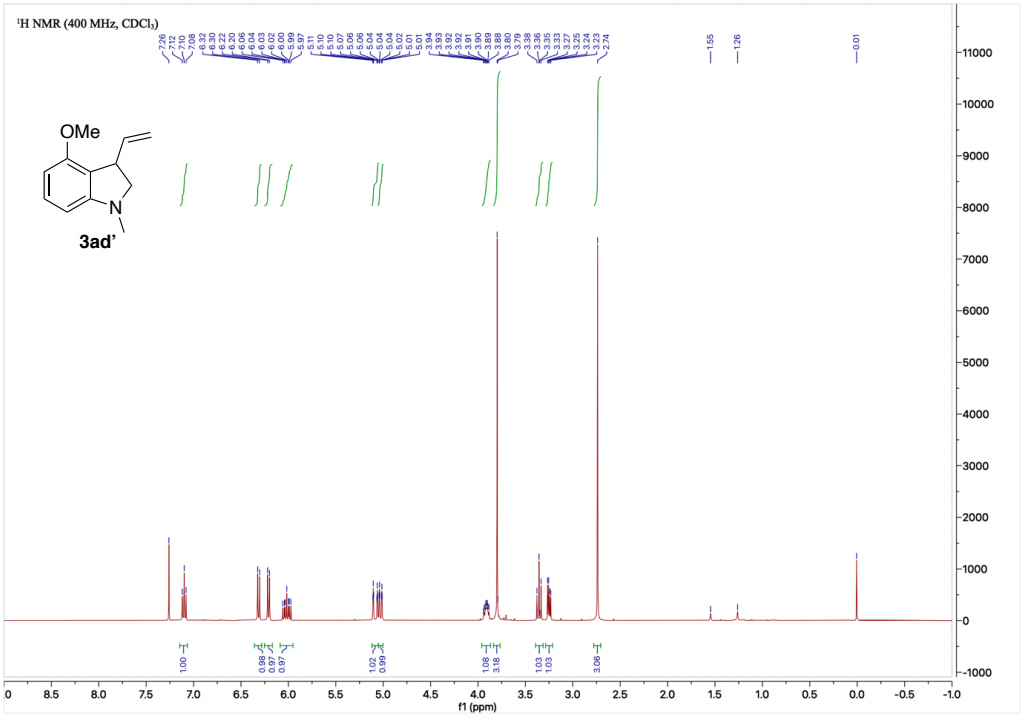

Figure 2.60. ^{13}C NMR Spectrum of **3ad'**

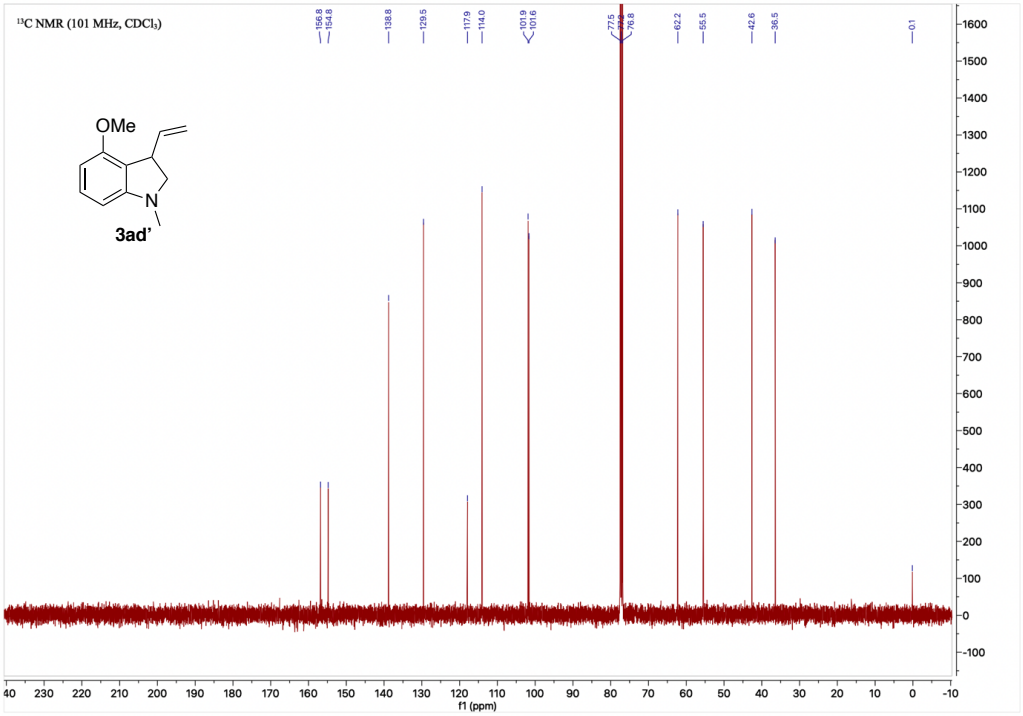

Figure 2.61. ^{1}H NMR Spectrum of **3ae'**

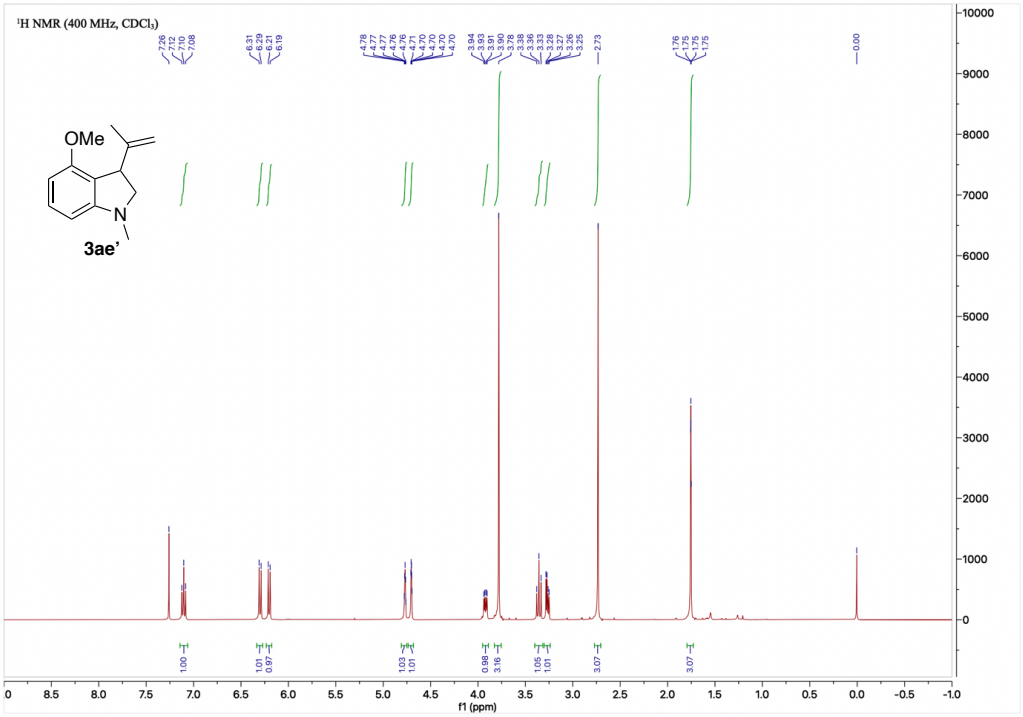

Figure 2.62. ^{13}C NMR Spectrum of **3ae'**

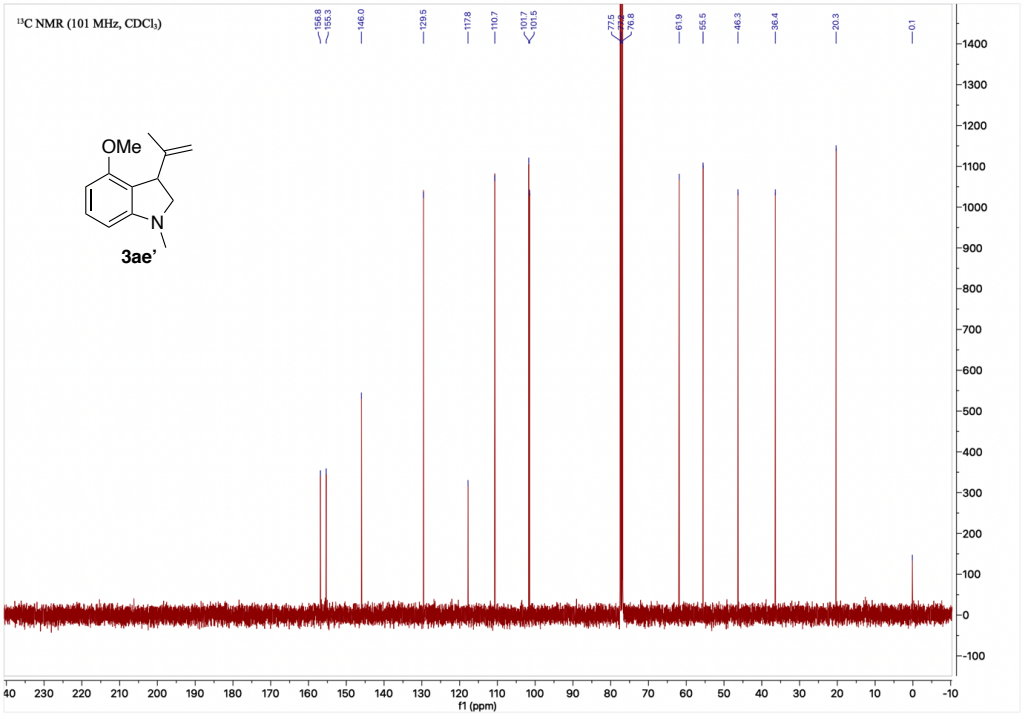

Figure 2.63. Crude ^{1}H NMR Spectrum of **3af'**

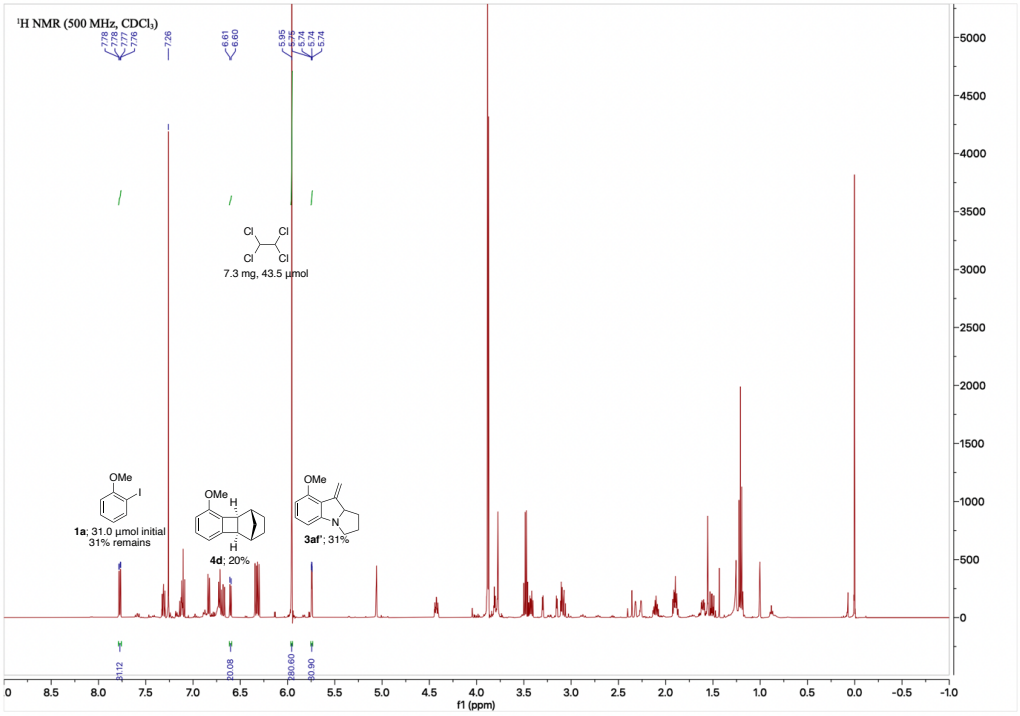

Figure 2.64. ^{1}H NMR Spectrum of **3af'** (best approximations)

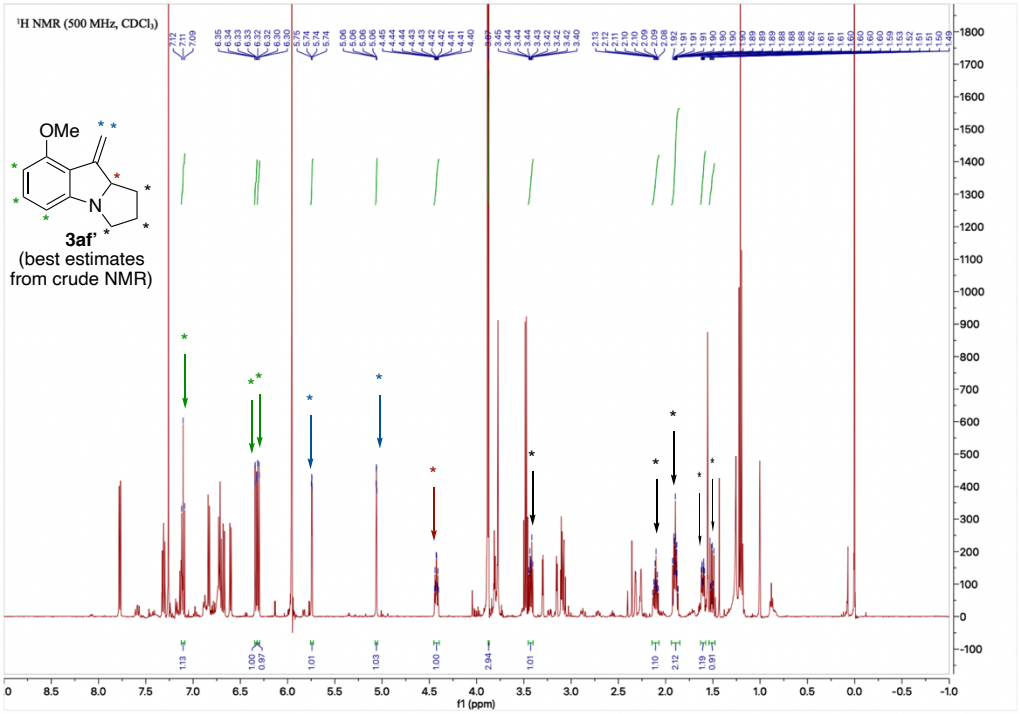

Figure 2.65. ^{1}H NMR Spectrum of **3af**

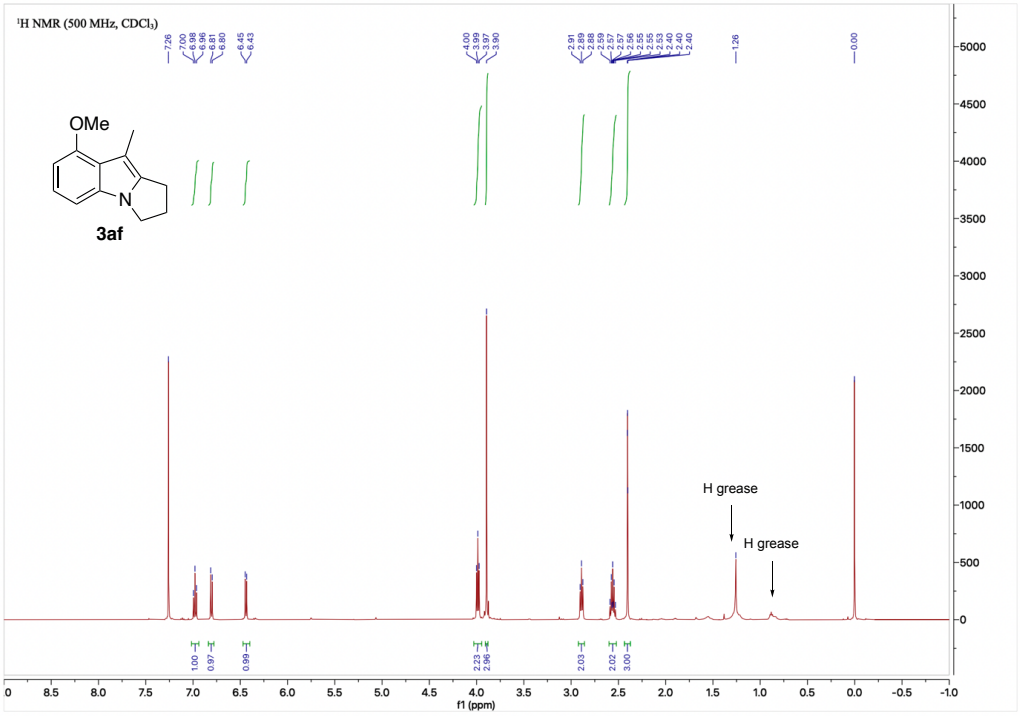

Figure 2.66. ^{13}C NMR Spectrum of **3af**

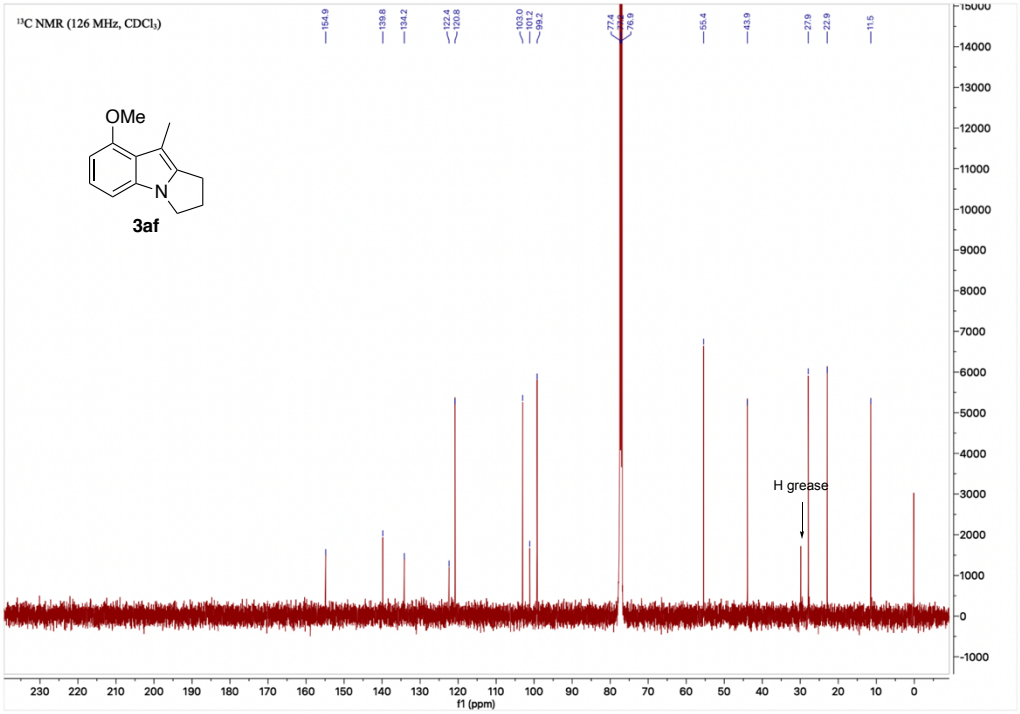

2.6. References

1. Kaushik, N. K.; Kaushik, N.; Attri, P.; Kumar, N.; Kim, C. H.; Verma, A. K.; Choi, E. H. *Molecules* **2013,** *18*, 6620-6662.

2. Gribble, G. W. *J. Chem. Soc. Perk. T. 1* **2000,** (7), 1045-1075.

3. Humphrey, G. R.; Kuethe, J. T. *Chem. Rev.* **2006,** *106* (7), 2875-2911.

4. Taber, D. F.; Tirunahari, P. K. *Tetrahedron* **2011,** *67* (38), 7195-7210.

5. Yoshikai, N.; Wei, Y. *Asian J. Org. Chem.* **2013,** *2* (6), 466-478.

6. Guo, T.; Huang, F.; Yu, L.; Yu, Z. *Tetrahedron Lett.* **2015,** *56* (2), 296-302.

7. Rago, A. J.; Dong, G. *Green Synth. Catal.* **2021**. *In Press.* DOI: 10.1016/j.gresc.2021.02.001.

8. Kogan, T. P.; Somers, T. C.; Venuti, M. C. *Tetrahedron* **1990,** *46* (19), 6623-6632.

9. Tidwell, J. H.; Senn, D. R.; Buchwald, S. L. *J. Am. Chem. Soc.* **1991,** *113* (12), 4685-4686.

10. Iwao, M.; Motoi, O. *Tetrahedron Lett.* **1995,** *36* (33), 5929-5932.

11. Zhou, N.; Zeller, W.; Krohn, M.; Anderson, H.; Zhang, J.; Onua, E.; Kiselyov, A. S.; Ramirez, J.; Halldorsdottir, G.; Andrésson, Þ.; Gurney, M. E.; Singh, J. *Bioorg. Med. Chem. Lett.* **2009,** *19* (1), 123-126.

12. Zhang, M.-Z.; Chen, Q.; Yang, G.-F. *Eur. J. Med. Chem.* **2015,** *89*, 421-441.

13. Catellani, M.; Frignani, F.; Rangoni, A. *Angew. Chem., Int. Ed.* **1997,** *36* (1-2), 119-122.

14. Ye, J.; Lautens, M. *Nat. Chem.* **2015,** *7* (11), 863-870.

15. Della Ca', N.; Fontana, M.; Motti, E.; Catellani, M. *Accounts of Chemical Research* **2016,** *49* (7), 1389-1400.

16. Zhao, K.; Ding, L.; Gu, Z. *Synlett* **2019,** *30* (02), 129-140.

17. Wegmann, M.; Henkel, M.; Bach, T. *Organic & Biomolecular Chemistry* **2018,** *16* (30), 5376-5385.

18. Cheng, H.-G.; Chen, S.; Chen, R.; Zhou, Q. *Angew. Chem., Int. Ed.* **2019,** *58* (18), 5832-5844.

19. Wang, J.; Dong, G. *Chem. Rev.* **2019,** *119* (12), 7478-7528.

20. Candito, D. A.; Lautens, M. *Org. Lett.* **2010,** *12* (15), 3312-3315.

21. Liu, C.; Liang, Y.; Zheng, N.; Zhang, B.-S.; Feng, Y.; Bi, S.; Liang, Y.-M. *Chem. Commun.* **2018,** *54* (27), 3407-3410.

22. Dong, Z.; Dong, G. *J. Am. Chem. Soc.* **2013,** *135* (49), 18350-18353.

23. Chen, Z.-Y.; Ye, C.-Q.; Zhu, H.; Zeng, X.-P.; Yuan, J.-J. *Chem. - Eur. J.* **2014,** *20* (15), 4237-4241.

24. Gao, Q.; Liu, Z.-S.; Hua, Y.; Li, L.; Cheng, H.-G.; Cong, H.; Zhou, Q. *Chem. Commun.* **2019,** *55* (60), 8816-8819.

25. Ye, C.; Zhu, H.; Chen, Z. *J. Org. Chem.* **2014,** *79* (18), 8900-8905.

26. Zhou, P.-X.; Ye, Y.-Y.; Ma, J.-W.; Zheng, L.; Tang, Q.; Qiu, Y.-F.; Song, B.; Qiu, Z.-H.; Xu, P.-F.; Liang, Y.-M. *J. Org. Chem.* **2014,** *79* (14), 6627-6633.

27. Sun, F.; Gu, Z. *Org. Lett.* **2015,** *17* (9), 2222-2225.

28. Pan, S.; Ma, X.; Zhong, D.; Chen, W.; Liu, M.; Wu, H. *Adv. Synth. Catal.* **2015,** *357* (14-15), 3052-3056.

29. Shi, H.; Babinski, D. J.; Ritter, T. *J. Am. Chem. Soc.* **2015,** *137* (11), 3775-3778.

30. Luo, B.; Gao, J.-M.; Lautens, M. *Org. Lett.* **2016,** *18* (17), 4166-4169.

31. Majhi, B.; Ranu, B. C. *Org. Lett.* **2016,** *18* (17), 4162-4165.

32. Fu, W. C.; Zheng, B.; Zhao, Q.; Chan, W. T. K.; Kwong, F. Y. *Org. Lett.* **2017,** *19* (16), 4335-4338.

33. Dong, Z.; Lu, G.; Wang, J.; Liu, P.; Dong, G. *J. Am. Chem. Soc.* **2018,** *140* (27), 8551-8562.

34. Whyte, A.; Olson, M. E.; Lautens, M. *Org. Lett.* **2018,** *20* (2), 345-348.

35. Zhang, B.-S.; Li, Y.; Zhang, Z.; An, Y.; Wen, Y.-H.; Gou, X.-Y.; Quan, S.-Q.; Wang, X.-G.; Liang, Y.-M. *J. Am. Chem. Soc.* **2019,** *141* (24), 9731-9738.

36. Zhang, B.-S.; Wang, F.; Yang, Y.-H.; Gou, X.-Y.; Qiu, Y.-F.; Wang, X.-C.; Liang, Y.-M.; Li, Y.; Quan, Z.-J. *Org. Lett.* **2020,** *22* (21), 8267-8271.

37. Lautens, M.; Piguel, S. *Angew. Chem., Int. Ed.* **2000,** *39* (6), 1045-1046.

38. Li, J.; Yang, Y.; Liu, Y.; Liu, Q.; Zhang, L.; Li, X.; Dong, Y.; Liu, H. *Org. Lett.* **2021**, *23* (8), 2988-2993.

39. Dong, Z.; Wang, J.; Ren, Z.; Dong, G. *Angew. Chem., Int. Ed.* **2015,** *54* (43), 12664-12668.

40. Li, R.; Dong, G. *J. Am. Chem. Soc.* **2020,** *142* (42), 17859-17875.

41. Shen, P.-X.; Wang, X.-C.; Wang, P.; Zhu, R.-Y.; Yu, J.-Q. *J. Am. Chem. Soc.* **2015,** *137* (36), 11574-11577.

42. Wang, J.; Dong, Z.; Yang, C.; Dong, G. *Nat. Chem.* **2019,** *11* (12), 1106-1112.

43. Substituting aryl iodides with aryl bromides proved to be a more challenging transformation. Our preliminary result showed that the desired product 3aa can be obtained in 38% yield (NMR) with 21% yield of 4a under the modified reaction conditions:

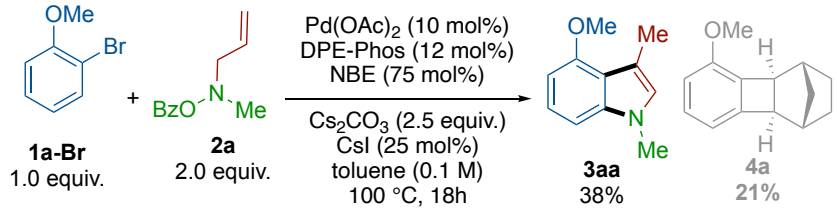

44. Haddach, A. A.; Kelleman, A.; Deaton-Rewolinski, M. V. *Tetrahedron Lett.* **2002,** *43* (3), 399-402.

45. Miki, Y.; Hachiken, H.; Kashima, Y.; Sugimura, W.; Yanase, N. *Heterocycles* **1998,** *48* (1), 1-4.

46. Davis, F. A.; Melamed, J. Y.; Sharik, S. S. *J. Org. Chem.* **2006,** *71* (23), 8761-8766.

47. Takahashi, K.; Kametani, T. *Heterocycles* **1979,** *13* (1), 411-467.

48. Andrez, J.-C. *Beilstein J. Org. Chem.* **2009,** *5*.

49. Lin, D. W.; Masuda, T.; Biskup, M. B.; Nelson, J. D.; Baran, P. S. *J. Org. Chem.* **2011,** *76* (4), 1013-1030.

50. Mok, N. Y.; Chadwick, J.; Kellett, K. A. B.; Casas-Arce, E.; Hooper, N. M.; Johnson, A. P.; Fishwick, C. W. G. *J. Med. Chem.* **2013,** *56* (5), 1843-1852.

51. Lautens, M.; Paquin, J.-F.; Piguel, S. *J. Org. Chem.* **2002,** *67* (11), 3972-3974.

52. Ho Park, K.; Chen, R.; Chen, D. Y. K. *Chem. Sci* **2017,** *8* (10), 7031-7037.

53. Liang, H.; He, X.; Zhang, Y.; Chen, B.; Ouyang, J.-s.; Li, Y.; Pan, B.; Subba Reddy, C. V.; Chan, W. T. K.; Qiu, L. *Chem. Commun.* **2020,** *56* (77), 11429-11432.

54. An, Y.; Zhang, B.-S.; Zhang, Z.; Liu, C.; Gou, X.-Y.; Ding, Y.-N.; Liang, Y.-M. *Chem. Commun.* **2020,** *56* (44), 5933-5936.

55. Amara, R.; Bentabed-Ababsa, G.; Hedidi, M.; Khoury, J.; Awad, H.; Nassar, E.; Roisnel, T.; Dorcet, V.; Chevallier, F.; Fajloun, Z.; Mongin, F. *Synthesis* **2017,** *49* (19), 4500-4516.

56. Chen, Y.-H.; Graßl, S.; Knochel, P. *Angew. Chem., Int. Ed.* **2018,** *57* (4), 1108-1111.

57. Li, Y.; Zhang, R.; Bi, X.; Fu, J. *Org. Lett.* **2018,** *20* (4), 1207-1211.

58. Wu, X.; Zhou, J. *Chem. Commun.* **2013,** *49* (94), 11035-11037.

59. Verkruijsse, H. D.; Brandsma, L. *Recl. Trav. Chim. Pays-Bas* **1986,** *105* (2), 66-68.

60. Wang, Y.; Hu, X.; Morales-Rivera, C. A.; Li, G.-X.; Huang, X.; He, G.; Liu, P.; Chen, G. *J. Am. Chem. Soc.* **2018,** *140* (30), 9678-9684.

61. Bourgeois, J.; Dion, I.; Cebrowski, P. H.; Loiseau, F.; Bédard, A.-C.; Beauchemin, A. M. *J. Am. Chem. Soc.* **2009,** *131* (3), 874-875.

62. Liang, S.; Zhao, X.; Yang, T.; Yu, W. *Org. Lett.* **2020,** *22* (5), 1961-1965.

63. Basak, S.; Alvarez-Montoya, A.; Winfrey, L.; Melen, R. L.; Morrill, L. C.; Pulis, A. P. *ACS Catal.* **2020,** *10* (8), 4835-4840.

(Portions of this chapter have previously been published in *Organic Letters*: Rago, A. J; Dong, G. *Org. Lett.* **2021**, *23*, 3755-3760).

CHAPTER 3

Studies Toward the Synthesis of C3,C3,C4-Trisubstituted Indolines *via* the Palladium/Norbornene-Catalyzed *Ortho*-Amination/*Ipso*-Reductive Heck Cyclization

3.1. Introduction

As an extension of our previously developed indole synthesis, we report the synthesis of C3,C3,C4-trisubstituted indolines via the palladium/norbornene cooperative catalysis. The transformation is realized by utilizing *N*-benzoyloxy allylamines to regioselectively aminate at the arene *ortho*-position, which is followed by a reductive Heck cyclization to afford the desired indoline products. A wide variety of functional groups have been demonstrated in this reaction, and the size of the *ortho*-substituent seems to have a significantly reduced impact reaction yield compared to our previously reported indole synthesis. Moreover, chiral all-carbon quaternary centers have been accessed using this method and a preliminary result of 46% *ee* has been obtained.

Figure 3.1. Synthesis of Indolines *via* Pd/NBE Cooperative Catalysis

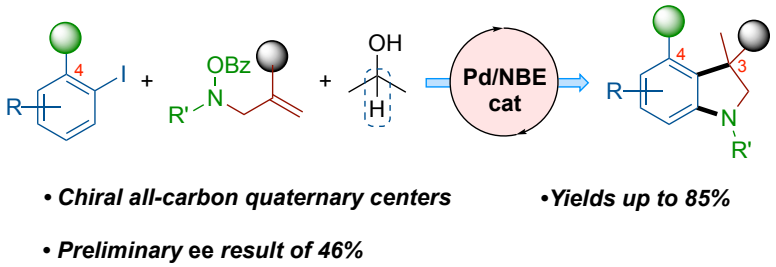

The synthesis of indole heterocycles has been of great interest to synthetic chemists due to their prevalence in natural products and bioactive molecules.[1-6] Indolines, their saturated derivative, have also received such interest,[7, 8] in part due to their prevalence in naturally occurring alkaloids.[9] While indole synthesis has been thoroughly explored in the literature, the synthesis of multi-substituted indolines in a modular manner still remains to be challenging. Many methods have been developed to date that can directly convert an indole into a multi-functionalized indoline;[7] however, direct assembly of the heterocyclic ring is less common. Carbon–hydrogen (C–H) bond activation has been used to achieve this, with examples from the literature including intramolecular C–H bond amination (**Scheme 3.1a**)[10, 11] and multi-component coupling with a diaziridinone reagent (**Scheme 3.1b**).[12-14]

Scheme 3.1. Synthesis of Indolines *via* C–H Bond Amination

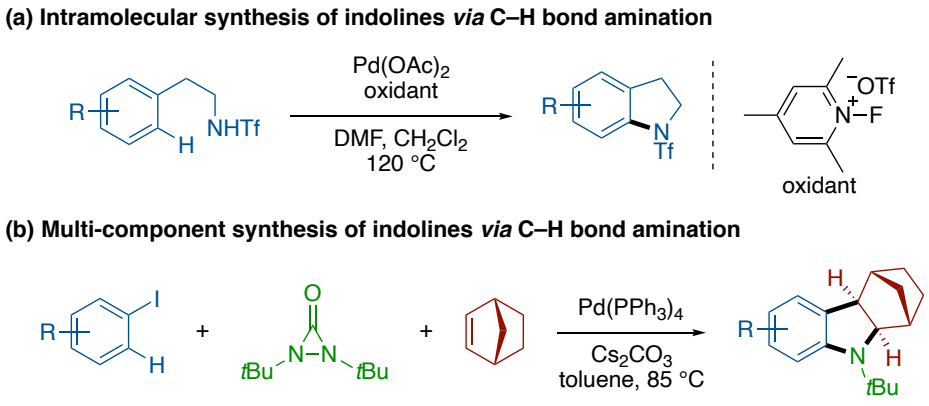

Palladium/norbornene (Pd/NBE) cooperative catalysis, on the other hand, presents a unique opportunity for the construction of these heterocycles through the regioselective difunctionalization of an aryl halide and its unactivated *ortho*-C–H bond.[15-20] First reported by Catellani in 1997 with the *ortho*-alkylation of aryl halides with alkyl halides,[21] this catalytic duo allows for the regioselective installation of an electrophile at the arene *ortho* position and a nucleophile at the arene *ipso* position. Naturally, the nucleophile and electrophile can be tethered in one molecule, allowing for annulative transformations to take place.[22] In particular for indole derivatives, in a seminal work, Lautens showed that strained 2*H*-azirines could deliver indole products through an *ortho*-alkylation, *ipso* amination cascade.[23] Later, Liang reported the first use of Pd/NBE cooperative catalysis to prepare indolines by using aziridines for the *ortho*-alkylation, *ipso*-amination cascade (**Scheme 3.2b**).[24] While both of these transformations are elegant examples of the heterocycle synthesis, an annulation reaction that could employ an *ortho*-amination to "switch" the regioselectivity of these transformations would be conceptually novel and could provide access to different substitution patterns on the heterocycles. In 2013, the first *ortho*-amination transformation was reported by our group, which allowed for a wide variety of tertiary amines to be prepared using Pd/NBE cooperative catalysis (**Scheme 3.2a**).[25] Recently, our group expanded upon this chemistry, with a two-component synthesis of indoles using bifunctional *N*-benzoyloxy allylamine reagents to regioselectively construct the heterocycles through an *ortho*-amination, *ipso*-Heck cyclization cascade (**Scheme 3.2c**).[26]

Scheme 3.2. Synthesis of Indoles and Indoles *via* Pd/NBE Cooperative Catalysis

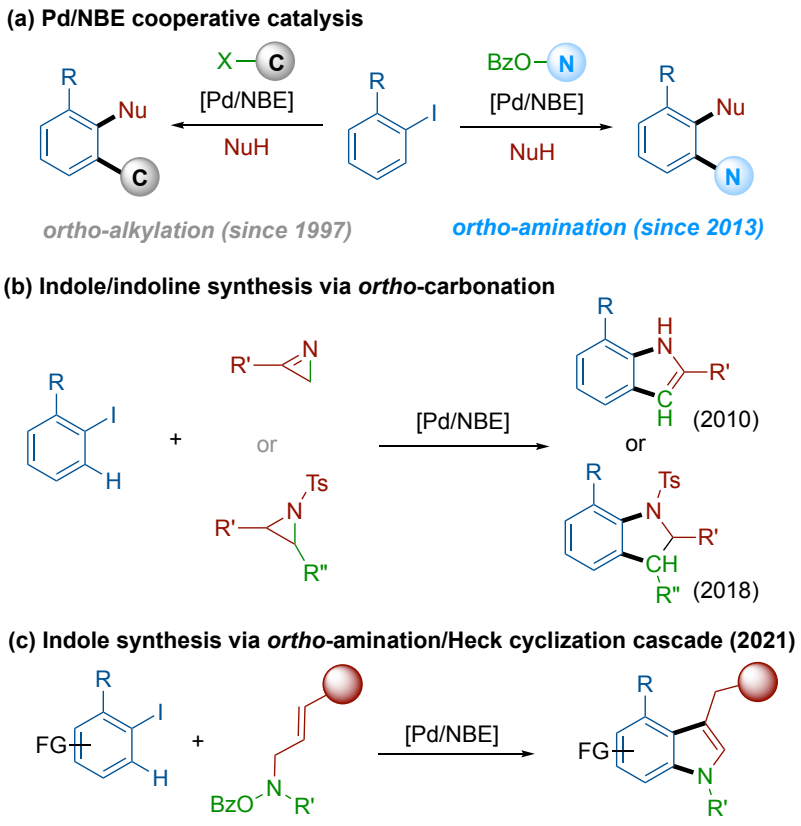

In this work, we report an evolution of this indole synthesis, whereupon a reductive Heck cyclization takes place instead of a typical Heck cyclization to deliver indoline products bearing an all-carbon quaternary center. Moreover, this transformation has the potential to prepare both achiral and chiral quaternary centers, depending on the substituent bound to the olefin in the amine electrophile (**Scheme 3.3**).

Scheme 3.3. This work – Indoline Synthesis *via* an *Otho*-Amination/Reductive Heck Cyclization Cascade

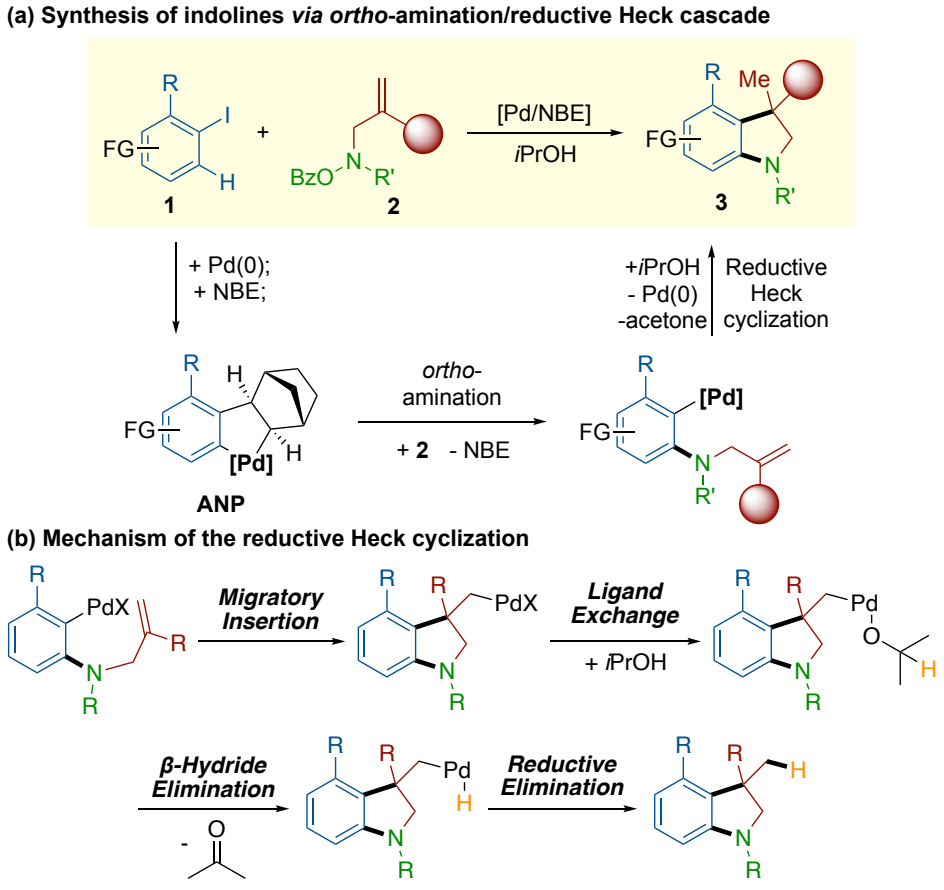

3.2. Results & Discussion

Our study began by using **1a** with disubstituted benzoyloxy allylamine **2a** as the aminating reagent and isopropyl alcohol as the hydride source. Gratifyingly, we could obtain 83% yield under the standard conditions, which used $Pd(TFA)_2$ and PPh_3 as the pre-catalyst/ligand combination (**Table 3.1**, entry 1). In another study (not shown), it was found that the 1:4 metal:ligand ratio was still important for the reproducibility of this transformation; however, the exact reason for this is still unknown. Moreover, other phosphine ligands were found to be less efficient in this reaction (entries 2-4). Moreover, the catalyst choice was also found to be important, with other Pd(II) or

Pd(0) precatalysts performing less efficiently in the reaction (entries 5-7). Similar to our indole-forming reaction, increasing the polarity of the solvent by using a 1:1 mixture of toluene and dioxane resulted in a reduced yield, with dioxane alone further reducing the yield (entries 8 and 9).

Table 3.1. Selected Reaction Optimization[a,b]

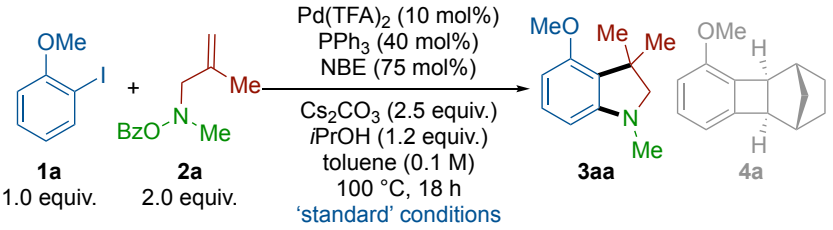

Entry	Change from the 'standard' condition	Yield of **3aa** (%)[b]	Yield of **4a** (%)[b]
1	none	83% (73%[c])	10%
2	P(*p*-OMe-Ph)$_3$ as the ligand	73%	7%
3	P(*p*-CF$_3$-Ph)$_3$ as the ligand	65%	12%
4	P(2-furyl)$_3$ as the ligand	64%	15%
5	Pd(OAc)$_2$ as the pre-catalyst	71%	10%
6	Pd G3 dimer as the pre-catalyst	61%	n.d.
7	Pd$_2$dba$_3$ as the pre-catalyst	71%	n.d.
8	1:1 1,4-dioxane/toluene as solvent	58%	8%
9	1,4-dioxane as solvent	39%	18%

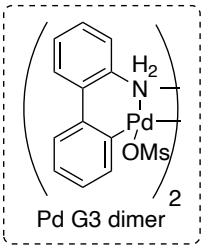

[a]Unless otherwise noted, all reactions were carried out with **1a** (0.1 mmol) and **2a** (0.2 mmol), in 1.0 mL of toluene for 18 h. [b]NMR yields determined using 1,1,2,2-tetrachloroethane as the internal standard. [c]Isolated yield from **1a** (0.2 mmol) and **2a** (0.4 mmol) in 2.0 mL of toluene for 18 h.

With the optimal conditions in hand, we set forth to explore the functional group tolerance of the indoline-forming reaction (**Scheme 3.4**). Gratifyingly, we found that model compound **3aa** could be isolated in 73% yield. Moreover, electron-rich (**3ba**, **3ca**) and -deficient (**3da**) substituents can be well-tolerated on the aromatic ring with very little perturbation of the indoline yield. Moreover, the electron-deficient phosphine ligand, *tris*(4-trifluoromethylphenyl) phosphine can allow for the severely electron-deficient nitro substituents to perform well in this reaction (**3ea, 3oa**). Labile functional groups, such as acetals (**3ga**) and the removable benzyl-protected alcohol (**3ha**) can also perform well in the reaction. Several functional groups that can serve as a handle can also be tolerated at the *ortho* position, including –Cl (**3ma**), $–CO_2Me$ (**3na**), and $–NO_2$ (**3oa**). Gratifyingly, indolines with fluorinated groups at the *ortho* position, such as $–CF_3$ (**3pa**) and –F (**3qa**), can also be prepared in moderate yields. A naphthyl-derived indoline (**3ta**) can be prepared in moderate yield, although this compound appears to be silica unstable since the crude NMR yield was nearly 20% higher. Heterocyclic rings were also investigated in this transformation, obtaining indolines with pyridine (**3ia**), quinoline (**3ua**), and dibenzofuran (**3va**) rings.

Scheme 3.4. Aryl Halide Scope of the *Ortho*-Amination/Reductive Heck Cyclization Cascade[a]

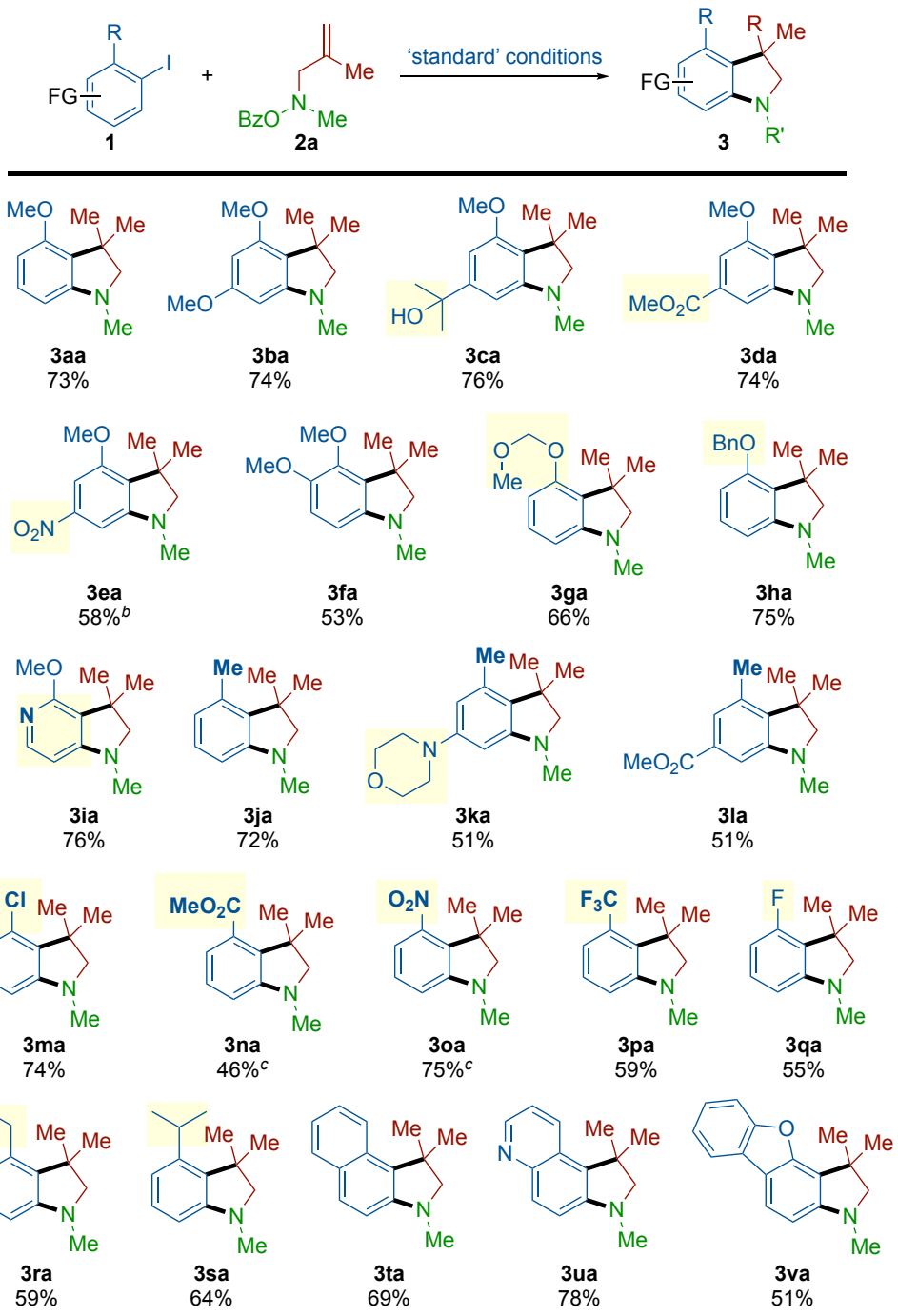

[a]Unless otherwise noted, all reactions were carried out with **1** (0.2 mmol) and **2** (0.4 mmol) in 2.0 mL of toluene for 18 h; all yields are isolated yields.

Alkyl groups, such as –Me (**3ja**), –Et (**3ra**), and –*i*Pr (**3sa**) can also deliver their corresponding indoline products in moderate to good yields. These substrates represent a large departure from the limitations of our prior indole synthesis, as the –Et- and –*i*Pr-substituted aryl iodides did not perform well in that reaction. This is likely due to the absence of a near co-planaer intermediate in the reductive cyclization, allowing for more sterically bulky substituents to be tolerated at the *ortho* position in this work (**Scheme 3.5**).

Scheme 3.5. Possible Explanation for Difference in Bulky Substituent Tolerability

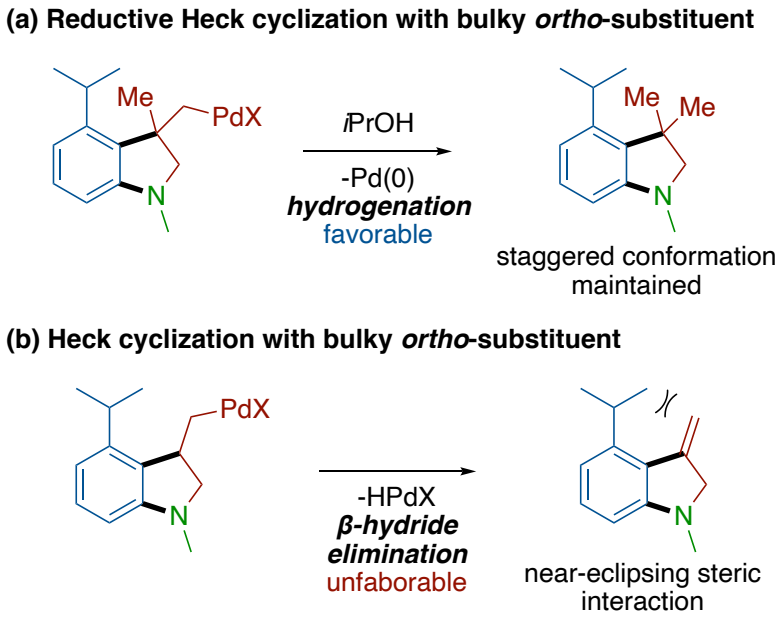

The scope of the amine coupling partner was also investigated. By changing the R group bound to the alkene moiety, indolines bearing all-carbon chiral quaternary centers can be obtained. In this regard, we can efficiently access quaternary centers with –Ph (**3ab**), –*n*Bu (**3ac**), and –*t*Bu (**3ad**) substituents (**Scheme 3.6**). Moreover, the drastic increase in steric bulk of the *t*Bu group does not drastically reduce the yield of the indoline product. Finally, the removable protecting groups –Bn (**3ae**) and –PMB (**3af**) were investigated, although these indolines could only prepared

in relatively low amounts. Efforts towards improving the efficiency of these bulkier amine electrophiles are ongoing.

Scheme 3.6. Amine Scope of the *Ortho*-Amination/Reductive Heck Cyclization Cascade[a]

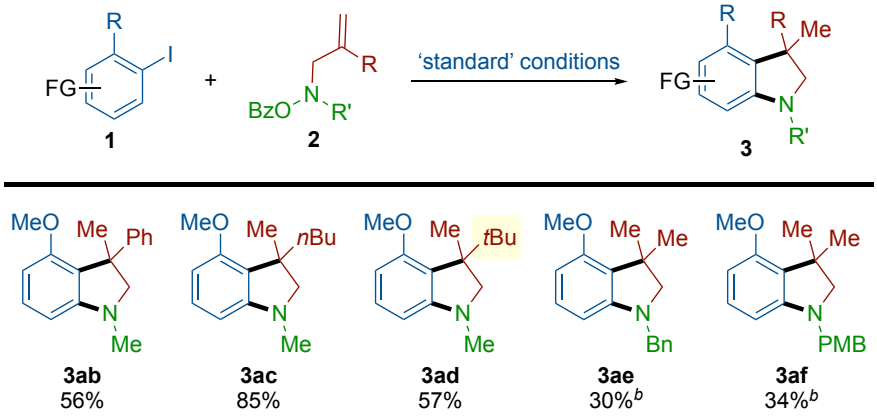

[a]Unless otherwise noted, all reactions were carried out with **1** (0.2 mmol) and **2** (0.4 mmol) in 2.0 mL of toluene for 18 h; all yields are isolated yields. [b]Carried out with **1** (0.1 mmol) and **2** (0.2 mmol) in 1.0 mL of toluene for 18 h; NMR yields determined using 1,1,2,2-tetrachloroethane as the internal standard.

With having investigated the formation of chiral quaternary centers, we wondered whether or not this transformation could be achieved enantioselectively. Taking inspiration from previously reported enantioselective Heck cyclization transformations[27] and enantioselective *ipso*-Heck cyclization reports in Pd/NBE catalysis,[28, 29] a handful of chiral monodentate ligands and (*S*)-BINAP were surveyed (**Scheme 3.7**).

Scheme 3.7. Preliminary Studies towards the Enantioselective Indoline Synthesis[a]

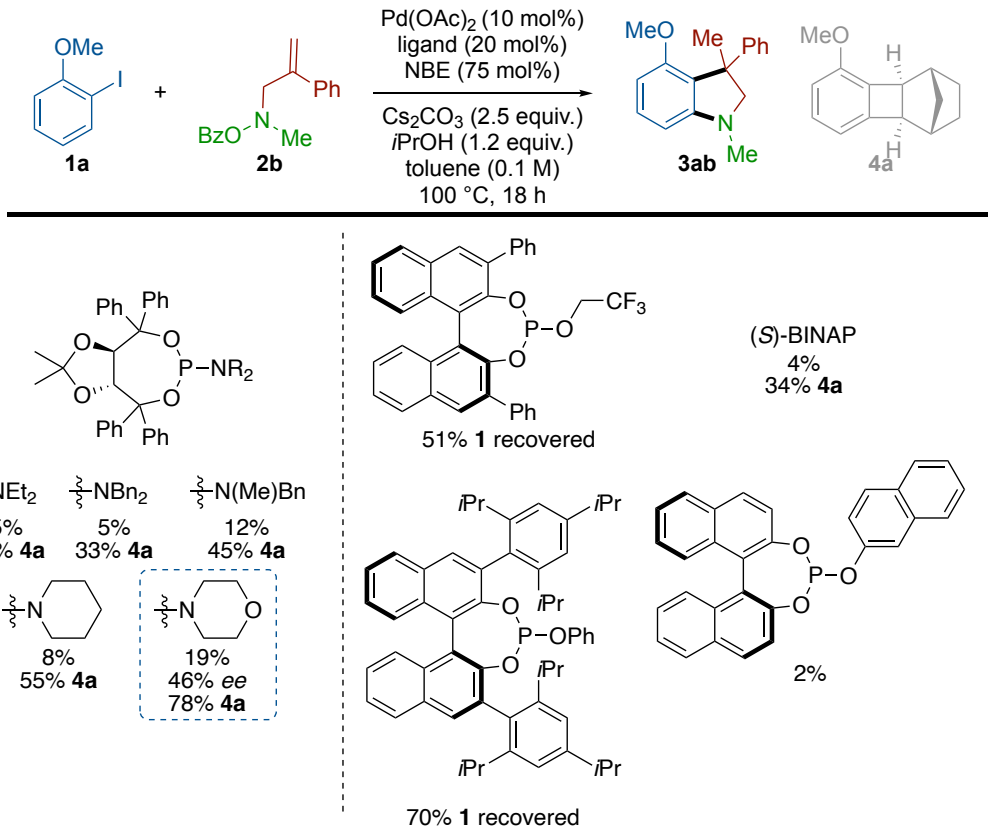

[a]Unless otherwise noted, all reactions were carried out with **1a** (0.1 mmol) and **2b** (0.2 mmol), in 1.0 mL of toluene for 18 h; NMR yields determined using 1,1,2,2-tetrachloroethane as the internal standard. Enantiomeric excess was determined by using chiral-phase HPLC analysis.

Unfortunately, phosphite ligands were found to be very inefficient for this transformation. Moreover, the reaction is evidently very sensitive to the steric bulk of the ligand, with two bulky phosphite ligands returning more than 50% unreacted **1a**. While many of the phosphoramidite ligands that were surveyed failed to afford the desired product in amounts higher than 15% yield, a morpholine-substituted ligand was found to deliver the indoline product in 19% yield. We were pleased to find an enantiomeric excess of 46% when using this ligand, which marks a promising

preliminary result. Efforts towards improving the *ee* of this transformation are ongoing. One possible avenue of investigation lies with the norbornene mediator – prior work in an asymmetric Pd/NBE Heck cyclization found that changing the substituents bound to the 5- and 6-positions of the norbornene mediator can help to further improve the *ee* of the transformation.[29]

3.3. Conclusion

In summary, an *ortho*-amination, *ipso*-reductive Heck cyclization cascade of aryl iodides has been explored. Results show a significantly better reaction scope and functional group tolerance than our previous work on the synthesis of indoles using this *ortho*-amination, *ipso*-cyclization strategy, suggesting that the reductive cyclization can occur more smoothly than the simple Heck cyclization. This may be attributed to the absence of a near coplanar intermediate, which likely limits the steric bulk of the *ortho*-substituent to a large degree in the former work. Moreover, chiral all-carbon quaternary centers have been prepared with this transformation, with a preliminary result of 46% *ee* for the asymmetric transformation being achieved. Currently, further exploration of the asymmetric version of this reaction is underway, along with optimizing the reaction to better accommodate the removable –Bn and –PMB protecting groups. Another direction we are pursuing involves trapping the neopentyl palladium species with a different coupling partner aside from hydride for an even larger increase in molecular complexity of the indoline products.

3.4. Experimental

General Considerations for key reactions: All reaction vials were flame-dried and allowed to cool to room temperature while capped in order to remove as much moisture as possible from the glass surface. $Pd(OAc)_2$, $Pd(TFA)_2$, and tris(*p*-methoxyphenyl)phosphine were purchased from Sigma-

Aldrich and used without further modification. Toluene used in the key reactions was distilled over Na/benzophenone, then degassed *via* feeze-pump-thaw. It was important that cesium carbonate was purchased from Strem, as other manufacturers' Cs_2CO_3 did not perform as well in the reaction. All commercially available substrates were used without further purification; however, if a liquid aryl iodide was used, it was first filtered through an alumina plug. All reactions were carried out in vials (test-scale reactions, 4 mL vials; isolation-scale reactions, 8 mL vials; 1.0 mmol-scale reaction, 40 mL vial) Thin layer chromatography (TLC) analysis was conducted on silica gel plates purchased from EMD Chemical (silica gel 60, F254). Infrared spectra were recorded on a Nicolet iS5 FT-IR Spectrometer using neat thin film technique. High-resolution mass spectra (HRMS) were obtained on an Agilent 6224 Tof-MS spectrometer and are reported as calculated/observed *m/z*. Nuclear magnetic resonance spectra (^{1}H NMR, ^{13}C NMR and ^{19}F NMR) were obtained using a Bruker Model DMX 400 (400 MHz, ^{1}H at 400 MHz, ^{13}C at 101 MHz, ^{19}F at 376 MHz); some NMR spectra (^{1}H, ^{13}C) were obtained using a Bruker Model DMX 500 (500 MHz, ^{1}H at 500 MHz, ^{13}C at 125 MHz). For $CDCl_3$ solutions, the chemical shifts were reported as parts per million (ppm) referenced to residual proton or carbon of the solvents: $CHCl_3$ δ H (7.26 ppm) and $CDCl_3$ δ C (77.16 ppm). Coupling constants were reported in Hertz (Hz). Data for ^{1}H NMR spectra were reported as following: chemical shift (δ, ppm), multiplicity (br = broad, s = singlet, d = doublet, t = triplet, q = quartet, dd = doublet of doublets, td = triplet of doublets, ddd = doublet of doublet of doublets, m = multiplet), coupling constant (Hz), and integration.

Compounds **1a**, **1b**, **1e**, **1i**, **1j**, **1l**, and **1m-1t** are commercially available. Compounds **1c**,[26] **1d**,[30] and **1u**[31] have been previously reported and were prepared *via* a diazotization procedure[31] from the corresponding anilines. Compounds **1f**,[32] **1g**,[33] **1h**,[34] **1k**,[35] **1v**,[36] and **4a**,[37] have all been previously reported in the literature.

Figure 3.2. Commercially Available, Known, and New Compounds

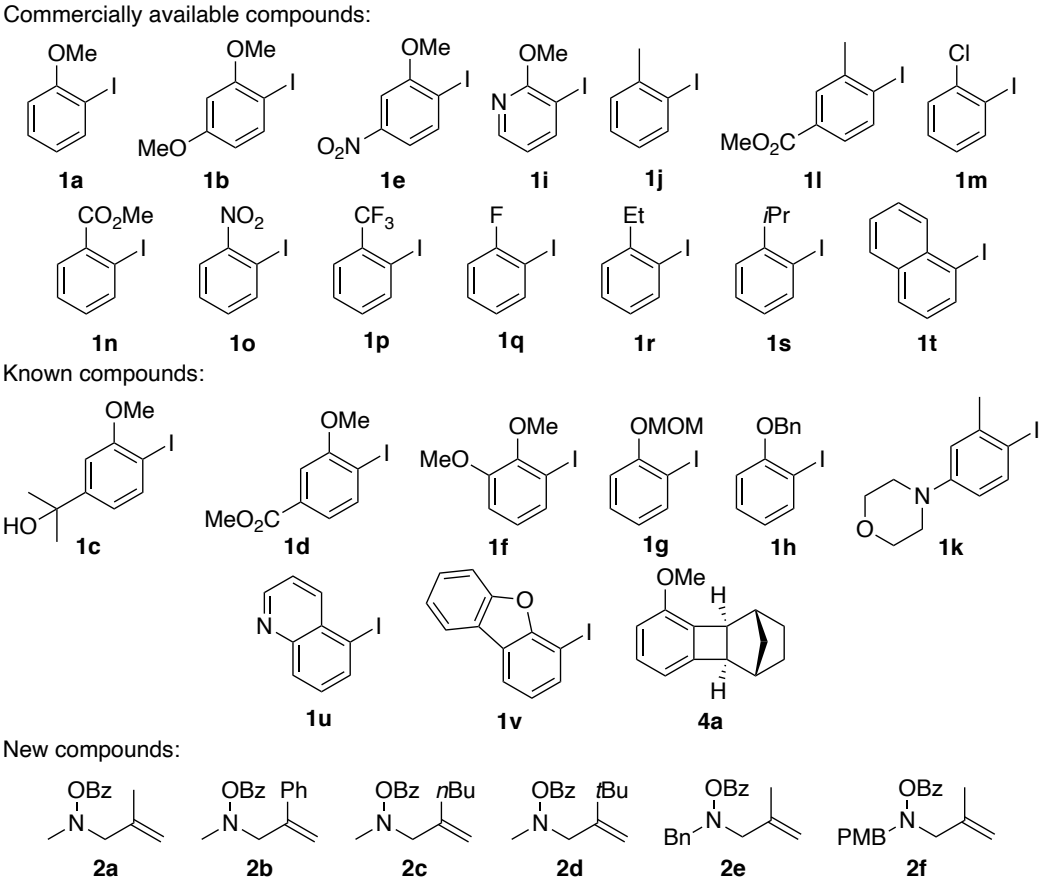

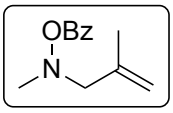

***O*-benzoyl-*N*-methyl-*N*-(2-methylallyl)hydroxylamine (2a):** *N*-methyl-*N*-(2-methylallyl)hydroxylamine was prepared according to a known procedure.[38] CH_2Cl_2 (102 mL, 0.25 M), *N*-methyl-*N*-(2-methylallyl)hydroxylamine (2.58 g, 25.5 mmol, 1.0 equiv.), DMAP (31.7 mg, 0.26 mmol, 0.01 equiv.), and triethylamine (5.33 mL, 38.25 mmol, 1.5 equiv.) were placed in

a flame-dried Schlenk flask under an N_2 atmosphere, which was then cooled to 0 °C. Benzoyl chloride (3.55 mL, 30.6 mmol, 1.2 equiv.) was added dropwise and the reaction was allowed to stir at 0 °C for 1 hour, after which the reaction was quenched with sat. NH_4Cl solution. The aqueous layer was extracted with EtOAc; the combined organics were washed with brine, dried over $MgSO_4$, and filtered. The solution was concentrated, and the crude oil was purified *via* silica gel chromatography (EtOAc/hexanes) to obtain a pale-yellow liquid in 87% yield (4.55 g). **^{1}H NMR** (400 MHz, $CDCl_3$) δ 8.00 – 7.95 (m, 2H), 7.58 – 7.52 (m, 1H), 7.46 – 7.39 (m, 2H), 4.96 (dq, J = 2.1, 1.1 Hz, 1H), 4.89 (p, J = 1.6 Hz, 1H), 3.53 (s, 2H), 2.90 (s, 3H), 1.86 (t, J = 1.2 Hz, 3H). **^{13}C NMR** (126 MHz, $CDCl_3$) δ 165.2, 141.1, 133.1, 129.6, 128.5, 114.9, 67.9, 46.8, 21.1. **HRMS** (ESI) Calcd for $C_{12}H_{15}NO_2$ $[M+H]^+$: 206.1181; Found: 206.1189.

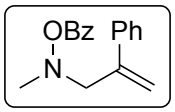

***O*-benzoyl-*N*-methyl-*N*-(2-phenylallyl)hydroxylamine (2b):** (3-bromoprop-1-en-2-yl)benzene was prepared according to a known procedure.[39] *N*-methylhydroxylamine hydrochloride (2.79 g, 33.39 mmol, 1.0 equiv.), K_2CO_3 (13.8 g, 100.17 mmol, 3.0 eqiuv.), Et_2O (33.4 mL, 1.0 M), and (3-bromoprop-1-en-2-yl)benzene (6.58 g, 33.39 mmol, 1.0 equiv.) were placed in a flame-dried vial and stirred overnight at room temperature. The solids were then removed by filtration and the organic solution was washed 3x with 10% HCl. The combined aqueous washes were neutralized with solid KOH, then extracted 3x with diethyl ether. The combined organics were washed with brine, dried over $MgSO_4$, filtered, and concentrated to afford crude *N*-methyl-*N*-(2-phenylallyl)hydroxylamine as a solid in 69% yield (3.78 g), which was used directly with no further purification. CH_2Cl_2 (46 mL, 0.25 M), *N*-methyl-*N*-(2-phenylallyl)hydroxylamine (2.0 g, 12.26 mmol, 1.0 equiv.), DMAP (14.7 mg, 0.12 mmol, 0.01 equiv.), and triethylamine (2.6 mL, 18.39 mmol, 1.5 equiv.) were placed in a flame-dried Schlenk

flask under an N_2 atmosphere, which was then cooled to 0 °C. Benzoyl chloride (1.71 mL, 14.71 mmol, 1.2 equiv.) was added dropwise and the reaction was allowed to stir at 0 °C for 1 hour, after which the reaction was quenched with sat. NH_4Cl solution. The aqueous layer was extracted with EtOAc; the combined organics were washed with brine, dried over $MgSO_4$, and filtered. The solution was concentrated, and the crude oil was purified *via* silica gel chromatography (EtOAc/hexanes) to obtain a pale-yellow liquid in 98% yield (3.22 g). **^{1}H NMR** (500 MHz, $CDCl_3$) δ 7.93 – 7.87 (m, 2H), 7.61 – 7.56 (m, 2H), 7.56 – 7.51 (m, 1H), 7.40 (t, J = 7.8 Hz, 2H), 7.34 (td, J = 6.9, 1.5 Hz, 2H), 7.28 (dt, J = 8.3, 1.6 Hz, 1H), 5.53 (d, J = 1.1 Hz, 1H), 5.41 – 5.36 (m, 1H), 4.04 (s, 2H), 2.93 (s, 3H). **^{13}C NMR** (126 MHz, $CDCl_3$) δ 165.0, 142.9, 139.8, 133.0, 129.5, 129.4, 128.5, 128.4, 127.9, 126.5, 117.3, 65.1, 46.2. **HRMS** (ESI) Calcd for $C_{17}H_{17}NO_2$ $[M+H]^+$: 268.1338; Found: 268.1348.

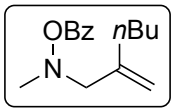

***O*-benzoyl-*N*-methyl-*N*-(2-methylenehexyl)hydroxylamine (2c):** 2-(bromomethyl)hex-1-ene was prepared according to a known procedure,[39] and was used without prior purification. *N*-methylhydroxylamine hydrochloride (459 mg, 5.5 mmol, 1.0 equiv.), K_2CO_3 (2.28 g, 16.5 mmol, 3.0 eqiuv.), Et_2O (7.6 mL, 0.72 M), and crude 2-(bromomethyl)hex-1-ene (459 mg, 5.5 mmol, 1.0 equiv.) were placed in a flame-dried vial and stirred overnight at room temperature. The solids were then removed by filtration and the organic solution was washed 3x with 10% HCl. The combined aqueous washes were neutralized with solid KOH, then extracted 3x with diethyl ether. The combined organics were washed with brine, dried over $MgSO_4$, filtered, and concentrated to afford crude *N*-methyl-*N*-(2-methylenehexyl)hydroxylamine as a yellow oil in 45% yield (356.7 mg), which was used directly with no further purification. CH_2Cl_2 (10.0 mL, 0.25 M), *N*-methyl-*N*-(2-methylenehexyl)hydroxylamine (356.7 mg, 2.50 mmol, 1.0 equiv.),

DMAP (2.4 mg, 0.02 mmol, 0.01 equiv.), and triethylamine (0.52 mL, 3.74 mmol, 1.5 equiv.) were placed in a flame-dried Schlenk flask under an N_2 atmosphere, which was then cooled to 0 °C. Benzoyl chloride (0.35 mL, 2.99 mmol, 1.2 equiv.) was added dropwise and the reaction was allowed to stir at 0 °C for 1 hour, after which the reaction was quenched with sat. NH_4Cl solution. The aqueous layer was extracted with EtOAc; the combined organics were washed with brine, dried over $MgSO_4$, and filtered. The solution was concentrated, and the crude oil was purified *via* silica gel chromatography (EtOAc/hexanes) to obtain a pale-yellow liquid in 57% yield (352.6 mg). **^{1}H NMR** (500 MHz, $CDCl_3$) δ 8.00 – 7.95 (m, 2H), 7.57 – 7.51 (m, 1H), 7.42 (t, *J* = 7.7 Hz, 2H), 5.01 (s, 1H), 4.90 – 4.87 (m, 1H), 3.54 (s, 2H), 2.89 (s, 3H), 2.22 – 2.15 (m, 2H), 1.44 (p, *J* = 7.8, 7.3 Hz, 2H), 1.32 (dq, *J* = 14.4, 7.3 Hz, 2H), 0.89 (t, *J* = 7.3 Hz, 3H). **^{13}C NMR** (126 MHz, $CDCl_3$) δ 165.2, 145.1, 133.0, 129.6, 129.6, 128.5, 113.8, 66.6, 46.8, 34.0, 29.9, 22.5, 14.1. **IR** (KBr, cm^{-1}) **HRMS** (ESI) Calcd for $C_{15}H_{21}NO_2$ $[M+H]^+$: 248.1651; Found: 248.1660.

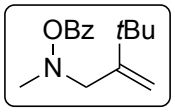

***O*-benzoyl-*N*-methyl-*N*-(2-methylenehexyl)hydroxylamine (2d):** 2-(bromomethyl)-3,3-dimethylbut-1-ene was prepared according to a known procedure.[40] *N*-methylhydroxylamine hydrochloride (835.2 g, 10.0 mmol, 1.0 equiv.), K_2CO_3 (4.15 g, 30.0 mmol, 3.0 eqiuv.), Et_2O (10.0 mL, 1.0 M), and crude 2-(bromomethyl)-3,3-dimethylbut-1-ene (~10.0 mmol, 1.0 equiv.) were placed in a flame-dried vial and stirred overnight at room temperature. The solids were then removed by filtration and the organic solution was washed 3x with 10% HCl. The combined aqueous washes were neutralized with solid KOH, then extracted 3x with diethyl ether. The combined organics were washed with brine, dried over $MgSO_4$, filtered, and concentrated to afford crude *N*-(3,3-dimethyl-2-methylenebutyl)-*N*-methylhydroxylamine as a yellow liquid in 15% yield (212.4 mg), which was used directly with no further purification. CH_2Cl_2 (5.9 mL, 0.25

M), *N*-(3,3-dimethyl-2-methylenebutyl)-*N*-methylhydroxylamine (212.4 mg, 1.48 mmol, 1.0 equiv.), DMAP (1.8 mg, 0.015 mmol, 0.01 equiv.), and triethylamine (0.31 mL, 2.22 mmol, 1.5 equiv.) were placed in a flame-dried Schlenk flask under an N_2 atmosphere, which was then cooled to 0 °C. Benzoyl chloride (0.21 mL, 1.78 mmol, 1.2 equiv.) was added dropwise and the reaction was allowed to stir at 0 °C for 1 hour, after which the reaction was quenched with sat. NH_4Cl solution. The aqueous layer was extracted with EtOAc; the combined organics were washed with brine, dried over $MgSO_4$, and filtered. The solution was concentrated, and the crude oil was purified *via* silica gel chromatography (EtOAc/hexanes) to obtain a pale-yellow liquid in 85% yield (312.9 mg).**^{1}H NMR** (400 MHz, $CDCl_3$) ^{1}H NMR (500 MHz, $CDCl_3$) δ 8.01 – 7.94 (m, 2H), 7.55 (tt, *J* = 7.0, 1.3 Hz, 1H), 7.46 – 7.41 (m, 2H), 5.19 (d, *J* = 1.3 Hz, 1H), 5.05 – 4.99 (m, 1H), 3.62 (s, 2H), 2.93 (s, 3H), 1.13 (s, 9H). **^{13}C NMR** (126 MHz, $CDCl_3$) δ 165.2, 151.8, 133.0, 129.7, 129.5, 128.5, 110.9, 62.8, 46.8, 35.5, 29.4. **IR** (KBr, cm^{-1}) **HRMS** (ESI) Calcd for $C_{15}H_{21}NO_2$ $[M+H]^+$: 248.1651; Found: 248.1658.

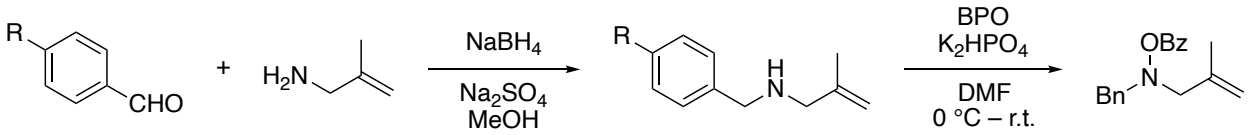

General procedure for *N*-benzyl benzoyloxy allylamine synthesis: (1) 3-methylallylamine (1.0 equiv.) was added to a methanolic solution (0.85 M) of benzaldehyde (1.0 equiv.) with a spatula scoop's worth of Na_2SO_4 and stirred at room temperature until full formation of the imine was observed by TLC (typically 1 hour). $NaBH_4$ (1.2 equiv.) was added slowly at 0 °C and the reaction was allowed to stir for an hour at room temperature, at which point it was quenched with sat. NH_4Cl solution. The aqueous layer was extracted with EtOAc; the combined organics were washed with brine, dried over $MgSO_4$, and filtered. The solution was concentrated, and the crude

residue was directly used in the next step with no further purification. **(2)** The *N*-benzyl-*N*-allylamine (1.5 equiv.) was added dropwise to a solution of wet benzoyl peroxide (1.0 equiv.) and K_2HPO_4 (2.0 equiv.) in DMF (0.4 M) at 0 °C. The reaction was then allowed to stir overnight at room temperature, at which point it was diluted with water. The aqueous layer was extracted with EtOAc; the combined organics were washed with water and brine, dried over $MgSO_4$, and filtered. The solution was concentrated, and the crude oil was purified *via* silica gel chromatography (EtOAc/hexanes) to afford the desired product.

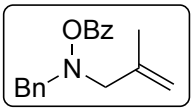

***O*-benzoyl-*N*-benzyl-*N*-(2-methylallyl)hydroxylamine (2e):** Synthesized from benzaldehyde according to the general procedure, obtaining *N*-benzyl-2-methylprop-2-en-1-amine as a yellow oil (10.0 mmol scale: 1.42 g, 88% crude yield), which was used in the next step without further purification. The crude amine was further oxidized to produce the title compound as a paleyellow solid in 77% yield (5.37 mmol scale: 1.17 g) after purification *via* silica gel chromatography (EtOAc/hexanes). **^{1}H NMR** (400 MHz, $CDCl_3$) δ 7.89 (d, J = 7.2 Hz, 2H), 7.51 (t, J = 7.4 Hz, 1H), 7.44 (d, J = 7.1 Hz, 2H), 7.38 (t, J = 7.7 Hz, 2H), 7.30 (t, J = 7.2 Hz, 2H), 7.25 (d, J = 7.0 Hz, 1H), 4.95 (s, 1H), 4.87 (s, 1H), 4.18 (s, 2H), 3.54 (s, 2H), 1.88 (s, 3H). **^{13}C NMR** (101 MHz, $CDCl_3$) δ 165.1, 141.5, 136.2, 132.9, 129.6, 129.5, 129.5, 128.4, 127.7, 114.8, 64.9, 62.8, 21.1. **IR** (KBr, cm^{-1}) **HRMS** (ESI) Calcd for $C_{18}H_{19}NO_2$ $[M+H]^+$: 282.1494; Found:282.1503.

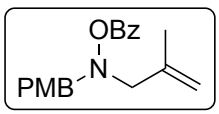

***O*-benzoyl-*N*-(4-methoxybenzyl)-*N*-(2-methylallyl)hydroxylamine (2f):** Synthesized from *p*-methoxybenzaldehyde according to the general procedure, obtaining *N*-(4-methoxybenzyl)-2-methylprop-2-en-1-amine as a yellow oil (20 mmol scale: 3.77 g, 99% crude

yield), which was used in the next step without further purification. The crude amine was further oxidized to produce the title compound as a white solid in 81% yield (10.0 mmol scale; 2.51 g) after purification *via* silica gel chromatography (EtOAc/hexanes). **^{1}H NMR** (400 MHz, $CDCl_3$) δ 7.96 – 7.86 (m, 2H), 7.55 – 7.48 (m, 1H), 7.40 (t, *J* = 7.7 Hz, 2H), 7.35 (d, *J* = 8.7 Hz, 2H), 6.89 – 6.80 (m, 2H), 4.98 – 4.91 (m, 1H), 4.86 (s, 1H), 4.13 (s, 2H), 3.78 (s, 3H), 3.51 (s, 2H). **^{13}C NMR** (101 MHz, $CDCl_3$) δ 165.1, 159.2, 141.5, 132.9, 130.8, 129.7, 129.5, 128.5, 128.2, 114.7, 113.8, 64.6, 62.3, 55.3, 21.1. **IR** (KBr, cm^{-1}) **HRMS** (ESI) Calcd for $C_{19}H_{21}NO_3$ $[M+H]^+$: 312.1600; Found: 312.1600.

General Procedure for Pd/NBE reactions: $Pd(TFA)_2$ and PPh_3 were placed into a flame-dried vial with a stir bar. Solid aryl iodides (**1**; 0.1 mmol) were also added at this stage. The vial was sealed and brought into a nitrogen-filled glovebox, where NBE, Cs_2CO_3, toluene, aryl halide (**1**; if liquid), hydroxylamine electrophile (**2**), and *i*PrOH were added successively. The reaction vial was sealed, removed from the glove box, and heated at 100 °C for 18 h (note: the temperature was monitored *via* an alcohol thermometer submerged in a vial filled with silicone oil, not the hot plate's internal thermometer).

For test-scale reactions (0.1 mmol): Upon completion, the reactions were allowed to cool to room temperature, were filtered through a silica plug with Et_2O, concentrated, and placed under vacuum on a Schlenk line to remove residual solvent. The internal standard, 1,1,2,2-tetrachloroethane (16.8 mg, 0.1 mmol), was added to the crude residue, which was then diluted with $CDCl_3$ and analyzed *via* ^{1}H NMR analysis to determine yield and composition. If multiple reactions were conducted at a single time, a stock solution of palladium, ligand, and NBE in toluene was prepared.

For isolation-scale reactions (0.2 mmol): Upon completion, the reactions were allowed to cool to room temperature, were filtered through a silica plug with Et_2O, concentrated, and purified *via*

silica gel chromatography (EtOAc or Et_2O/hexanes). Some compounds were further purified *via* preparatory TLC, and any impurities found have been accounted for in the isolated yields. If multiple reactions were conducted at a single time, a stock solution of palladium, ligand, and NBE in toluene was prepared.

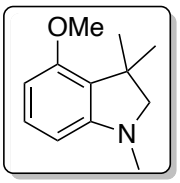

4-methoxy-1,3,3-trimethylindoline (3aa): Synthesized from **1a** and **2a** according to the general procedure. 0.2 mmol scale: 73% yield (28.0 mg). Pale yellow oil. R_f = 0.46 (hexane/Et_2O = 9:1). **^{1}H NMR** (400 MHz, $CDCl_3$) δ 7.06 (t, *J* = 8.0 Hz, 1H), 6.29 (dd, *J* = 8.2, 0.7 Hz, 1H), 6.17 (dd, *J* = 7.8, 0.7 Hz, 1H), 3.79 (s, 3H), 3.04 (s, 2H), 2.73 (s, 3H), 1.38 (s, 6H). **^{13}C NMR** (101 MHz, $CDCl_3$) δ 156.9, 154.0, 128.9, 123.8, 101.9, 101.4, 70.9, 55.3, 40.9, 36.2, 26.3. **IR** (KBr, cm^{-1}) 3067, 2952, 2864, 2835, 2805, 1603, 1484, 1465, 1422, 1333, 1231, 1199, 1778, 1102, 1068, 1001, 890, 777, 723. **HRMS** (ESI) Calcd for $C_{12}H_{17}NO$ $[M+H]^+$: 192.1388; Found: 192.1389.

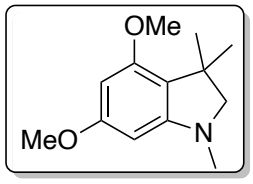

4,6-dimethoxy-1,3,3-trimethylindoline (3ba): Synthesized from **1b** and **2a** according to the general procedure. 0.2 mmol scale: 74% yield (32.8 mg). Colorless oil. R_f = 0.24 (hexane/Et_2O = 9:1). **^{1}H NMR** (400 MHz, $CDCl_3$) δ 5.87 (d, *J* = 2.0 Hz, 1H), 5.76 (d, *J* = 2.0 Hz, 1H), 3.78 (s, 3H), 3.77 (s, 3H), 3.04 (s, 2H), 2.72 (s, 3H), 1.34 (s, 6H). **^{13}C NMR** (101 MHz, $CDCl_3$) δ 161.6, 157.1, 154.4, 116.4, 88.9, 87.4, 71.2, 55.5, 55.3, 40.4, 36.0, 26.5. **IR** (KBr, cm^{-1})

2953, 2863, 2838, 2805, 1607, 1460, 1247, 1218, 1202, 1149, 1068, 800. **HRMS** (ESI) Calcd for $C_{13}H_{19}NO_2$ $[M+H]^+$: 222.1494; Found: 222.1500.

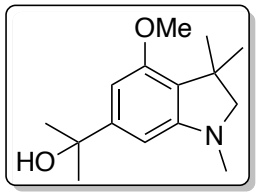

2-(4-methoxy-1,3,3-trimethylindolin-6-yl)propan-2-ol (3ca): Synthesized from **1c** and **2a** according to the general procedure. 0.2 mmol scale: 76% yield (37.7 mg). Thick brown oil, which later turned to a tan/brown solid. R_f = 0.20 (hexane/EtOAc = 7:3). **^{1}H NMR** (400 MHz, $CDCl_3$) δ 6.44 (d, *J* = 1.4 Hz, 1H), 6.27 (d, *J* = 1.4 Hz, 1H), 3.81 (s, 3H), 3.05 (s, 2H), 2.74 (s, 3H), 1.72 (br s, 1H), 1.58 (s, 6H), 1.36 (s, 6H). **^{13}C NMR** (101 MHz, $CDCl_3$) δ 156.5, 153.8, 150.9, 122.4, 98.6, 97.8, 73.1, 71.1, 55.3, 40.7, 36.2, 31.9, 26.3. **IR** (KBr, cm^{-1}) 3405, 2956, 2863, 2804, 1610, 1593, 1461, 1412, 1362, 1306, 1247, 1221, 1171, 1116, 1082, 829, 806, 669. **HRMS** (ESI) Calcd for $C_{15}H_{23}NO_2$ $[M+H]^+$: 250.1807; Found: 250.1805.

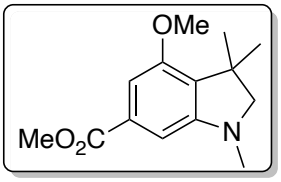

methyl 4-methoxy-1,3,3-trimethylindoline-6-carboxylate (3da): Synthesized from **1d** and **2a** according to the general procedure. 0.2 mmol scale: 74% yield (36.7 mg). Colorless oil. R_f = 0.14 (hexane/Et_2O = 9:1). **^{1}H NMR** (400 MHz, $CDCl_3$) ^{1}H NMR (400 MHz, $CDCl_3$) δ 6.99 (d, *J* = 1.3 Hz, 1H), 6.81 (d, *J* = 1.2 Hz, 1H), 3.88 (s, 3H), 3.84 (s, 3H), 3.08 (s, 2H), 2.76 (s, 3H), 1.37 (s, 6H). **^{13}C NMR** (101 MHz, $CDCl_3$) δ 167.7, 156.3, 153.8, 131.0, 129.0, 103.7, 102.3, 70.7, 55.5, 52.1, 41.1, 35.9, 26.0. **IR** (KBr, cm^{-1}) 2953, 2866, 2808, 1720, 1592, 1437, 1414, 1372, 1315, 1227, 1113, 1086, 1012, 854, 769. **HRMS** (ESI) Calcd for $C_{14}H_{19}NO_3$ $[M+H]^+$: 250.1443; Found: 250.1442.

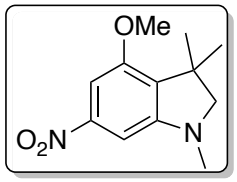

4-methoxy-1,3,3-trimethyl-6-nitroindoline (3ea): Synthesized from **1e** and **2a** according to the general procedure. 0.2 mmol scale: 58% yield (27.3 mg). Orange solid. R_f = 0.44 (hexane/Et_2O = 9:1). **^{1}H NMR** (400 MHz, $CDCl_3$) δ 7.16 (d, *J* = 1.9 Hz, 1H), 6.93 (d, *J* = 1.9 Hz, 1H), 3.86 (s, 3H), 3.16 (s, 2H), 2.79 (s, 3H), 1.37 (s, 6H). **^{13}C NMR** (101 MHz, $CDCl_3$) δ 156.0, 153.8, 149.7, 130.5, 97.9, 96.0, 70.5, 55.7, 41.2, 35.3, 25.9. **IR** (KBr, cm^{-1}) 3127, 2959, 2868, 1617, 1523, 1412, 1356, 1332, 1238, 1082, 830, 775, 728. **HRMS** (ESI) Calcd for $C_{12}H_{16}N_2O_3$ $[M+H]^+$: 237.1239; Found: 237.1238.

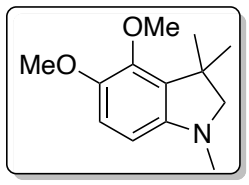

4,5-dimethoxy-1,3,3-trimethylindoline (3fa) Synthesized from **1f** and **2a** according to the general procedure. 0.2 mmol scale: 53% yield (23.6 mg); isolated with 11% ANP reductive elimination side-pdt (yield adjusted accordingly). Yellow oil. R_f = 0.14 (hexane/Et_2O = 9:1). **^{1}H NMR** (400 MHz, $CDCl_3$) δ 6.68 (d, *J* = 8.3 Hz, 1H), 6.15 (d, *J* = 8.3 Hz, 1H), 3.87 (s, 3H), 3.79 (s, 3H), 2.99 (s, 2H), 2.68 (s, 3H), 1.40 (s, 6H). **^{13}C NMR** (101 MHz, $CDCl_3$) ^{13}C NMR (101 MHz, $CDCl_3$) δ 148.0, 146.8, 146.2, 131.0, 112.7, 102.3, 71.4, 60.8, 56.9, 41.2, 36.9, 26.7. **IR** (KBr, cm^{-1}) 2953, 2863, 2829, 2797, 1615, 1486, 1464, 1258, 1063, 1045, 788, 681. **HRMS** (ESI) Calcd for $C_{13}H_{19}NO_2$ $[M+H]^+$: 222.1494; Found: 222.1495.

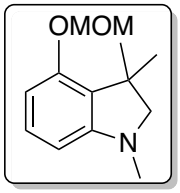

4-(methoxymethoxy)-1,3,3-trimethylindoline (3ga): Synthesized from **1g** and **2a** according to the general procedure. 0.2 mmol scale: 66% yield (29.3 mg). Pale yellow oil. R_f = 0.25 (hexane/Et_2O = 9:1). **^{1}H NMR** (400 MHz, $CDCl_3$) δ 7.02 (t, *J* = 8.0 Hz, 1H), 6.43 (dd, *J* = 8.3, 0.8 Hz, 1H), 6.19 (dd, *J* = 7.8, 0.8 Hz, 1H), 5.18 (s, 2H), 3.48 (s, 3H), 3.05 (s, 2H), 2.73 (s, 3H), 1.40 (s, 6H). **^{13}C NMR** (101 MHz, $CDCl_3$) δ 154.1, 128.9, 124.5, 104.2, 102.0, 93.8, 70.8, 56.2, 41.0, 36.1, 26.3. **IR** (KBr, cm^{-1}) 3066, 2954, 2861, 2803, 1607, 1482, 1451, 1404, 1331, 1296, 1227, 1192, 1154, 1083, 1036, 924, 778, 727, 631. **HRMS** (ESI) Calcd for $C_{13}H_{19}NO_2$ $[M+H]^+$: 222.1494; Found: 222.1492.

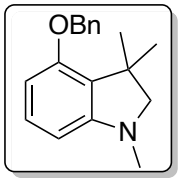

4-(benzyloxy)-1,3,3-trimethylindoline (3ha): Synthesized from **1h** and **2a** according to the general procedure. 0.2 mmol scale: 75% yield (40.2 mg). Colorless oil. R_f = 0.43 (hexane/Et_2O = 9:1). **^{1}H NMR** (400 MHz, $CDCl_3$) δ 7.44 (d, *J* = 7.3 Hz, 2H), 7.42 – 7.35 (m, 2H), 7.32 (td, *J* = 7.2, 6.0, 3.1 Hz, 1H), 7.05 (t, *J* = 8.0 Hz, 1H), 6.35 (d, *J* = 8.2 Hz, 1H), 6.19 (d, *J* = 7.7 Hz, 1H), 5.08 (s, 2H), 3.07 (s, 2H), 2.75 (s, 3H), 1.42 (s, 6H). **^{13}C NMR** (101 MHz, $CDCl_3$) δ 155.9, 154.1, 137.9, 128.9, 128.6, 127.7, 127.3, 124.0, 102.7, 101.6, 70.9, 69.7, 41.0, 36.2, 26.4 **IR** (KBr, cm^{-1}) 3065, 3031, 2953, 2860, 2803, 1609, 1483, 1451, 1298, 1266, 1227, 1195, 1101, 1057, 775, 723, 701. **HRMS** (ESI) Calcd for $C_{18}H_{21}NO$ $[M+H]^+$: 268.1701; Found: 268.1702.

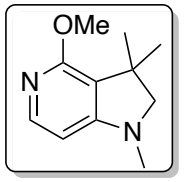

4-methoxy-1,3,3-trimethyl-2,3-dihydro-1*H*-pyrrolo[3,2-*c*]pyridine (3ia): Synthesized from **1i** and **2a** according to the general procedure. 0.2 mmol scale: 76% yield (29.1 mg). Yellow oil. R_f = 0.35 (hexane/EtOAc = 4:1). **^{1}H NMR** (400 MHz, $CDCl_3$) δ 7.81 (d, *J* = 5.6 Hz, 1H), 6.10 (d, *J* = 5.6 Hz, 1H), 3.91 (s, 3H), 3.15 (s, 2H), 2.78 (s, 3H), 1.34 (s, 6H). **^{13}C NMR** (101 MHz, $CDCl_3$) δ 160.8, 159.8, 146.8, 115.2, 98.9, 69.8, 52.9, 40.1, 34.3, 26.3. **IR** (KBr, cm^{-1}) 2950, 2865, 2821, 1605, 1503, 1453, 1412, 1312, 1236, 1110, 1073, 1053, 999, 797, 687, 614. **HRMS** (ESI) Calcd for $C_{11}H_{16}N_2O$ $[M+H]^+$: 193.1341; Found: 193.1349.

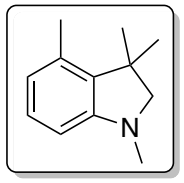

1,3,3,4-tetramethylindoline (3ja): Synthesized from **1j** and **2a** according to the general procedure. 0.2 mmol scale: 72% yield (25.1 mg). Colorless oil. R_f = 0.52 (hexane/Et_2O = 9:1). **^{1}H NMR** (400 MHz, $CDCl_3$) δ 7.00 (t, *J* = 7.7 Hz, 1H), 6.47 (d, *J* = 7.6 Hz, 1H), 6.36 (d, *J* = 7.8 Hz, 1H), 3.02 (s, 2H), 2.73 (s, 3H), 2.32 (s, 3H), 1.37 (s, 6H). **^{13}C NMR** (101 MHz, $CDCl_3$) δ 152.7, 135.4, 133.7, 127.7, 121.1, 105.6, 71.1, 41.3, 36.2, 26.2, 18.7. **IR** (KBr, cm^{-1}) 3045, 2954, 2862, 2800, 1597, 1482, 1463, 1290, 1215, 1160, 1067, 773, 739. **HRMS** (ESI) Calcd for $C_{12}H_{17}N$ $[M+H]^+$: 176.1439; Found: 176.1439.

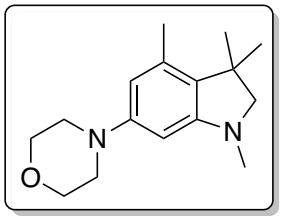

4-(1,3,3,4-tetramethylindolin-6-yl)morpholine (3ka): Synthesized from **1k** and **2a** according to the general procedure. 0.2 mmol scale: 51% yield (26.4 mg). Pale yellow oil. R_f = 0.11 (hexane/EtOAc = 4:1). **^{1}H NMR** (400 MHz, $CDCl_3$) δ 6.05 – 5.98 (m, 1H), 5.95 (d, *J* = 2.1 Hz, 1H), 3.83 (dd, *J* = 5.8, 3.8 Hz, 4H), 3.13 (dd, *J* = 5.7, 3.8 Hz, 4H), 3.02 (s, 2H), 2.72 (s, 3H), 2.28 (s, 3H), 1.34 (s, 6H). **^{13}C NMR** (101 MHz, $CDCl_3$) δ 153.7, 151.9, 134.0, 128.0, 108.2, 94.4, 71.4, 67.3, 50.1, 40.6, 36.1, 26.4, 19.0. **IR** (KBr, cm^{-1}) 2954, 2855, 2811, 1608, 1450, 1263, 1235, 1186, 1122, 1030, 986, 911, 815. **HRMS** (ESI) Calcd for $C_{16}H_{24}N_2O$ $[M+H]^+$: 261.1967; Found: 261.1972.

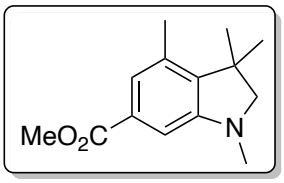

methyl 1,3,3,4-tetramethylindoline-6-carboxylate (3la): Synthesized from **1l** and **2a** according to the general procedure. 0.2 mmol scale: 68% yield (31.7 mg). Pale yellow oil. R_f = 0.36 (hexane/EtOAc = 9:1). **^{1}H NMR** (400 MHz, $CDCl_3$) δ 7.19 (dd, *J* = 1.5, 0.8 Hz, 1H), 6.95 (d, *J* = 1.5 Hz, 1H), 3.87 (s, 3H), 3.06 (s, 2H), 2.76 (s, 3H), 2.34 (s, 3H), 1.37 (s, 6H). **^{13}C NMR** (101 MHz, $CDCl_3$) δ 167.9, 152.8, 140.7, 133.5, 129.7, 123.1, 105.9, 70.9, 52.0, 41.4, 35.9, 25.9, 18.6. **IR** (KBr, cm^{-1}) 2954, 2866, 2805, 1717, 1589, 1484 1435, 1412, 1299, 1244, 1210, 1170, 1114, 1035, 995, 875, 769. **HRMS** (ESI) Calcd for $C_{14}H_{19}NO_2$ $[M+H]^+$: 234.1494; Found: 234.1501.

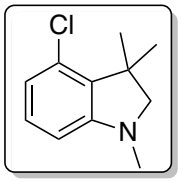

4-chloro-1,3,3-trimethylindoline (3ma): Synthesized from **1m** and **2a** according to the general procedure. 0.2 mmol scale: 74% yield (29.0 mg). Pale yellow oil. R_f = 0.53 (hexane/Et_2O = 9:1). **^{1}H NMR** (400 MHz, $CDCl_3$) δ 6.99 (t, *J* = 7.9 Hz, 1H), 6.59 (d, *J* = 8.0 Hz, 1H), 6.33 (d, *J* = 7.8 Hz, 1H), 3.10 (s, 2H), 2.74 (s, 3H), 1.44 (s, 6H). **^{13}C NMR** (101 MHz, $CDCl_3$δ 154.0, 133.9, 130.4, 129.0, 119.1, 105.6, 70.5, 42.1, 35.6, 25.8. **IR** (KBr, cm^{-1}) 3061, 2957, 2865, 2811, 1599, 1485, 1448, 1421, 1291, 1202, 1131, 1087, 1002, 961, 840, 771, 731. **HRMS** (ESI) Calcd for $C_{11}H_{14}ClN$ $[M+H]^+$: 196.0893; Found: 196.0891.

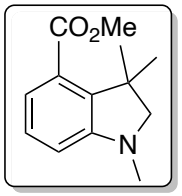

methyl 1,3,3-trimethylindoline-4-carboxylate (**3na**): Synthesized from **1n** and **2a** according to the general procedure, except with using *tris*(4-trifluoromethylphenyl)phosphine as the ligand. 0.2 mmol scale: 46% yield (20.2 mg). Tan solid. R_f = 0.28 (hexane/Et_2O = 9:1). **^{1}H NMR** (400 MHz, $CDCl_3$) δ 7.16 – 7.06 (m, 2H), 6.59 (dd, *J* = 7.6, 1.4 Hz, 1H), 3.88 (s, 3H), 3.06 (s, 2H), 2.75 (s, 3H), 1.42 (s, 6H). **^{13}C NMR** (101 MHz, $CDCl_3$) δ 168.6, 153.6, 138.4, 127.7, 127.7, 119.4, 110.7, 71.7, 51.9, 41.8, 36.1, 25.6. **IR** (KBr, cm^{-1}) 2952, 2865, 2804, 1724, 1595, 1446, 1328, 1267, 1127, 1099, 1058, 868, 777, 754. **HRMS** (ESI) Calcd for $C_{13}H_{17}NO_2$ $[M+H]^+$: 220.1338; Found: 220.1341.

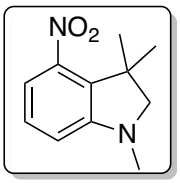

1,3,3-trimethyl-4-nitroindoline (3oa): Synthesized from **1o** and **2a** according to the general procedure. 0.2 mmol scale: 74% yield (30.9 mg). Reddish-orange oil. R_f = 0.39 (hexane/EtOAc = 9:1). **^{1}H NMR** (400 MHz, $CDCl_3$) δ 7.21 – 7.11 (m, 2H), 6.62 (dd, *J* = 7.4, 1.4 Hz, 1H), 3.13 (s, 2H), 2.78 (s, 3H), 1.43 (s, 6H). **^{13}C NMR** (101 MHz, $CDCl_3$) δ 154.8, 147.2, 131.4, 128.8, 113.2, 111.4, 85.4, 71.5, 42.2, 35.7, 24.9. **IR** (KBr, cm^{-1}) 3068, 2958, 2870, 2814, 1612, 1526, 1457, 1356, 1297, 1132, 1059, 1008, 902, 801, 787, 730. **HRMS** (ESI) Calcd for $C_{11}H_{14}N_2O_2$ $[M+H]^+$: 207.1134; Found: 207.1133.

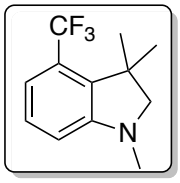

1,3,3-trimethyl-4-(trifluoromethyl)indoline (3pa): Synthesized from **1p** and **2a** according to the general procedure, except with using *tris*(4-trifluoromethylphenyl)phosphine as the ligand. 0.2 mmol scale: 59% yield (27.2 mg). Pale yellow oil. Product was found to be somewhat volatile, so clean spectra could not be obtained. R_f = 0.50 (hexane/Et_2O = 9:1). **^{1}H NMR** (400 MHz, $CDCl_3$) δ 7.20 – 7.14 (m, 1H), 6.95 (dd, *J* = 7.9, 1.0 Hz, 1H), 6.63 (d, *J* = 7.9 Hz, 1H), 3.07 (s, 2H), 2.77 (s, 3H), 1.38 (q, *J* = 1.1 Hz, 6H). **^{13}C NMR** (101 MHz, $CDCl_3$) δ 154.2, 135.6, 135.5, 128.0, 126.3, 126.1, 126.0, 123.4, 119.0, 115.5, 115.4, 115.3, 115.3, 111.0, 71.5, 42.0, 35.9, 26.1, 26.1, 26.0, 26.0. **IR** (KBr, cm^{-1}) 3073, 2960, 2871, 2809, 1602, 1482, 1451, 1328, 1309, 1161, 1122, 1082, 1058, 861, 795, 740, 714. **HRMS** (ESI) Calcd for $C_{12}H_{14}F_3N$ $[M+H]^+$: 230.1157; Found: 230.1154.

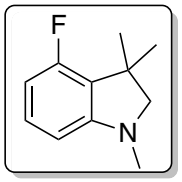

4-fluoro-1,3,3-trimethylindoline (3qa): Synthesized from **1q** and **2a** according to the general procedure. 0.2 mmol scale: 55% yield (19.8 mg). Pale yellow oil. R_f = 0.54 (hexane/Et_2O = 9:1). **^{1}H NMR** (400 MHz, $CDCl_3$) δ 7.02 (td, *J* = 8.0, 5.6 Hz, 1H), 6.34 (ddd, *J* = 9.3, 8.3, 0.8 Hz, 1H), 6.23 (d, *J* = 7.8 Hz, 1H), 3.10 (s, 2H), 2.75 (s, 3H), 1.41 (s, 6H). **^{13}C NMR** (101 MHz, $CDCl_3$) δ 161.2, 158.7, 154.8, 154.7, 129.4, 129.3, 123.3, 123.1, 105.6, 105.4, 103.2, 103.2, 70.5, 40.7, 40.7, 35.8, 26.7, 26.7. **IR** (KBr, cm^{-1}) 3067, 2953, 2869, 2809, 1625, 1592, 1489, 1453, 1220, 1008, 775, 726. **HRMS** (ESI) Calcd for $C_{11}H_{14}FN$ $[M+H]^+$: 180.1189; Found: 180.1184.

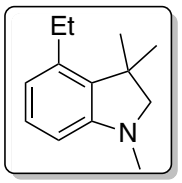

4-ethyl-1,3,3-trimethylindoline (3ra): Synthesized from **1r** and **2a** according to the general procedure. 0.2 mmol scale: 59% yield (22.3 mg). Pale yellow oil. R_f = 0.45 (hexane/Et_2O = 9:1). **^{1}H NMR** (400 MHz, $CDCl_3$) δ 7.06 (t, *J* = 7.7 Hz, 1H), 6.55 (dd, *J* = 7.7, 0.9 Hz, 1H), 6.35 (dd, *J* = 7.8, 1.0 Hz, 1H), 3.01 (s, 2H), 2.73 (s, 3H), 2.68 (q, *J* = 7.5 Hz, 2H), 1.39 (s, 6H), 1.26 (t, *J* = 7.6 Hz, 3H). **^{13}C NMR** (101 MHz, $CDCl_3$) δ 152.7, 140.3, 134.8, 127.9, 119.0, 105.3, 71.1, 41.4, 36.2, 27.1, 24.6, 15.9. **IR** (KBr, cm^{-1}) 3044, 2959, 2870, 2799, 1590, 1480, 1448, 1290, 1007, 789, 740. **HRMS** (ESI) Calcd for $C_{13}H_{19}N$ $[M+H]^+$: 190.1596; Found: 190.1594.

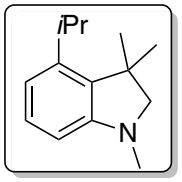

4-isopropyl-1,3,3-trimethylindoline (3sa): Synthesized from **1s** and **2a** according to the general procedure. 0.2 mmol scale: 64% yield (26.2 mg). Pale yellow oil. R_f = 0.45 (hexane/Et_2O = 9:1). **^{1}H NMR** (400 MHz, $CDCl_3$) δ 7.09 (t, *J* = 7.8 Hz, 1H), 6.65 (d, *J* = 7.8 Hz, 1H), 6.32 (d, *J* = 7.7 Hz, 1H), 3.23 (p, *J* = 6.8 Hz, 1H), 3.03 (s, 2H), 2.73 (s, 3H), 1.41 (s, 6H), 1.25 (d, *J* = 6.9 Hz, 6H). **^{13}C NMR** (101 MHz, $CDCl_3$) δ 152.50, 145.59, 134.04, 128.04, 115.83, 104.96, 71.14, 41.24, 36.08, 28.57, 27.55, 24.37. **IR** (KBr, cm^{-1}) 3051, 2959, 2867, 2800, 1593, 1482, 1446, 1420, 1363, 1287, 1263, 1164, 1131, 1072, 1030, 1007, 791, 740, 633. **HRMS** (ESI) Calcd for $C_{14}H_{21}N$ $[M+H]^+$: 204.1752; Found: 204.1752.

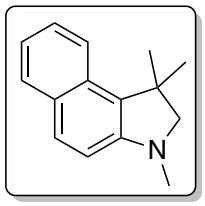

1,1,3-trimethyl-2,3-dihydro-1*H*-benzo[*e*]indole (3ta): Synthesized from **1t** and **2a** according to the general procedure. 0.2 mmol scale: 69% yield (29.1 mg). Yellow oil. R_f = 0.39 (hexane/Et_2O = 9:1). **^{1}H NMR** (400 MHz, $CDCl_3$) δ 7.91 (d, *J* = 8.6 Hz, 1H), 7.74 (d, *J* = 8.2 Hz, 1H), 7.65 (d, *J* = 8.6 Hz, 1H), 7.37 (ddd, *J* = 8.4, 6.8, 1.3 Hz, 1H), 7.18 (ddd, *J* = 8.0, 6.8, 1.0 Hz, 1H), 6.94 (d, *J* = 8.6 Hz, 1H), 3.18 (s, 2H), 2.85 (s, 3H), 1.58 (s, 6H). **^{13}C NMR** (101 MHz, $CDCl_3$) δ 150.1, 130.6, 129.5, 129.1, 128.9, 128.2, 126.2, 121.7, 121.4, 111.3, 42.0, 36.8, 27.3. **IR** (KBr, cm^{-1}) 3057, 2953, 2860, 2802, 1621, 1592, 1520, 1459, 1367, 1300, 1214, 1143, 1001, 806, 743, 665. **HRMS** (ESI) Calcd for $C_{15}H_{17}N$ $[M+H]^+$: 212.1439; Found: 212.1438.

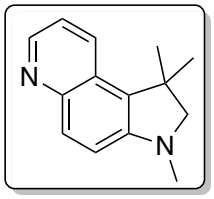

1,1,3-trimethyl-2,3-dihydro-1*H*-pyrrolo[3,2-*f*]quinoline (3ua): Synthesized from **1u** and **2a** according to the general procedure. 0.2 mmol scale: 78% yield (33.0 mg). Yellow/orange oil. R_f = 0.14 (hexane/EtOAc = 7:3). **^{1}H NMR** (400 MHz, $CDCl_3$) δ 8.61 (dd, *J* = 4.2, 1.7 Hz, 1H), 8.21 (ddd, *J* = 8.6, 1.7, 0.9 Hz, 1H), 7.90 (dd, *J* = 8.9, 0.9 Hz, 1H), 7.24 (dd, *J* = 8.6, 4.1 Hz, 1H), 7.11 (d, *J* = 8.9 Hz, 1H), 3.22 (s, 2H), 2.86 (s, 3H), 1.55 (s, 6H). **^{13}C NMR** (101 MHz, $CDCl_3$) δ 150.2, 145.8, 144.1, 130.3, 129.6, 127.6, 125.8, 120.9, 114.2, 71.7, 41.8, 36.3, 27.5. **IR** (KBr, cm^{-1}) 2955, 2865, 2807, 1610, 1513, 1463, 1410, 1361, 1319, 1294, 1211, 1180, 1125, 998, 825, 807, 667. **HRMS** (ESI) Calcd for $C_{14}H_{16}N_2$ $[M+H]^+$: 213.1392; Found: 213.1392.

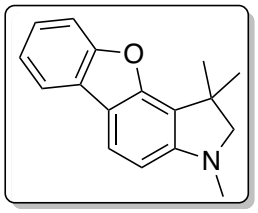

1,1,3-trimethyl-2,3-dihydro-1*H*-benzofuro[2,3-*e*]indole (3va): Synthesized from **1v** and **2a** according to the general procedure. 0.2 mmol scale: 51% yield (25.7 mg). Colorless oil. R_f = 0.46 (hexane/EtOAc = 9:1). **^{1}H NMR** (400 MHz, $CDCl_3$) δ 7.81 – 7.77 (m, 1H), 7.66 (d, *J* = 8.1 Hz, 1H), 7.51 – 7.47 (m, 1H), 7.31 (td, *J* = 7.7, 1.5 Hz, 1H), 7.26 (td, *J* = 7.6, 1.2 Hz, 1H), 6.54 (d, *J* = 8.1 Hz, 1H), 3.22 (s, 2H), 2.86 (s, 3H), 1.58 (s, 6H). **^{13}C NMR** (101 MHz, $CDCl_3$) δ 156.3, 153.1, 153.1, 125.3, 125.0, 122.5, 119.9, 119.8, 119.2, 116.7, 111.3, 103.8, 71.0, 40.6, 36.4, 26.7. **IR** (KBr, cm^{-1}) 3057, 2957, 2864, 2813, 164**5**, 1611, 1497, 1454, 1378, 1328, 1297, 1255, 1172, 1142, 1117, 1011, 921, 799, 775, 747, 736, 559. **HRMS** (ESI) Calcd for $C_{17}H_{17}NO$ $[M+H]^+$: 252.1388; Found: 252.1388.

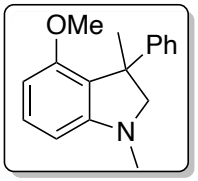

4-methoxy-1,3-dimethyl-3-phenylindoline (3ab): Synthesized from **1a** and **2b** according to the general procedure. 0.2 mmol scale: 56% yield (28.4 mg). Colorless oil. R_f = 0.34 (hexane/Et_2O = 9:1). **^{1}H NMR** (400 MHz, $CDCl_3$) ^{1}H NMR (400 MHz, $CDCl_3$) δ 7.31 – 7.23 (m, 4H), 7.19 – 7.12 (m, 2H), 6.34 (dd, *J* = 8.3, 0.8 Hz, 1H), 6.25 (dd, *J* = 7.9, 0.7 Hz, 1H), 3.66 (s, 3H), 3.50 (d, *J* = 8.8 Hz, 1H), 3.26 (d, *J* = 8.7 Hz, 1H), 2.74 (s, 3H), 1.81 (s, 3H). **^{13}C NMR** (101 MHz, $CDCl_3$) δ 157.1, 154.6, 147.7, 129.6, 128.1, 126.3, 126.0, 122.5, 102.2, 101.7, 72.8, 55.3, 48.5, 36.2, 25.3. **IR** (KBr, cm^{-1}) 3059, 3022, 2954, 2835, 2806, 1602, 1483, 1462, 1331, 1292, 1263, 1224, 1160, 1065, 778, 763, 699. **HRMS** (ESI) Calcd for $C_{17}H_{19}NO$ $[M+H]^+$: 254.1545; Found: 254.1550.

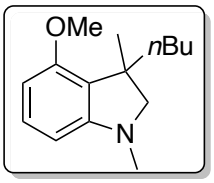

3-*n*-butyl-4-methoxy-1,3-dimethylindoline (3ac): Synthesized from **1a** and **2c** according to the general procedure. 0.2 mmol scale: 85% yield (39.8 mg). Pale yellow oil. R_f = 0.47 (hexane/Et_2O = 9:1). **^{1}H NMR** (400 MHz, $CDCl_3$) δ 7.05 (t, *J* = 8.0 Hz, 1H), 6.27 (dd, *J* = 8.3, 0.7 Hz, 1H), 6.15 (dd, *J* = 7.8, 0.7 Hz, 1H), 3.78 (s, 3H), 3.18 (d, *J* = 8.7 Hz, 1H), 2.94 (d, *J* = 8.7 Hz, 1H), 2.72 (s, 3H), 1.81 – 1.63 (m, 2H), 1.34 (s, 3H), 1.29 (qd, *J* = 7.2, 4.0 Hz, 3H), 1.17 – 1.06 (m, 1H), 0.87 (t, *J* = 7.2 Hz, 3H). **^{13}C NMR** (101 MHz, $CDCl_3$) ^{13}C NMR (101 MHz, $CDCl_3$) δ 156.9, 154.2, 128.8, 123.1, 101.7, 101.3, 67.9, 55.2, 44.6, 38.6, 36.2, 27.5, 24.9, 23.5, 14.3. **IR** (KBr, cm^{-1}) 3067, 2954, 2858, 2806, 1602, 1484, 1465, 1261, 1231, 1068, 776, 723. **HRMS** (ESI) Calcd for $C_{15}H_{23}NO$ $[M+H]^+$: 234.1858; Found: 234.1852.

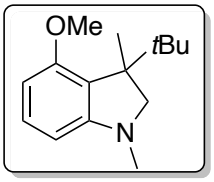

3-*tert*-butyl-4-methoxy-1,3-dimethylindoline (3ad): Synthesized from **1a** and **2d** according to the general procedure. 0.2 mmol scale: 57% yield (26.6 mg). Isolated with 9% of **4a**, which could not be separated by preparative TLC (yield has been adjusted). Pale yellow oil. R_f = 0.59 (hexane/Et_2O = 9:1). **^{1}H NMR** (400 MHz, $CDCl_3$) ^{1}H NMR (400 MHz, $CDCl_3$) δ 7.06 (t, *J* = 8.0 Hz, 1H), 6.27 (d, *J* = 8.2 Hz, 1H), 6.11 (d, *J* = 7.8 Hz, 1H), 3.75 (s, 3H), 3.49 (d, *J* = 9.2 Hz, 1H), 2.75 (d, *J* = 9.2 Hz, 1H), 2.67 (s, 3H), 1.38 (s, 3H), 0.95 (s, 9H). **^{13}C NMR** (101 MHz, $CDCl_3$) ^{13}C NMR (101 MHz, $CDCl_3$) δ 157.5, 155.8, 129.0, 121.6, 101.7, 100.8, 66.9, 54.9, 51.0, 37.9, 36.1, 26.7, 21.8. **IR** (KBr, cm^{-1}) 3067, 2954, 2869, 2805, 1598, 1484, 1364, 1295, 1263, 1221, 1068, 775, 728. **HRMS** (ESI) Calcd for $C_{15}H_{23}NO$ $[M+H]^+$: 234.1858; Found: 234.1856.

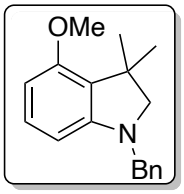

1-benzyl-4-methoxy-3,3-dimethylindoline (3ae): Synthesized from **1a** and **2e** according to the general procedure. 0.1 mmol scale: 30% yield (NMR yield).

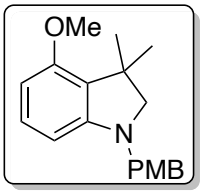

4-methoxy-1-(4-methoxybenzyl)-3,3-dimethylindoline (3af): Synthesized from **1a** and **2f** according to the general procedure. 0.1 mmol scale: 34% yield (NMR yield).

3.5. ^{1}H-NMR, ^{13}C-NMR, and ^{19}F-NMR Spectra

Figure 3.3. ^{1}H NMR Spectrum of **2a**

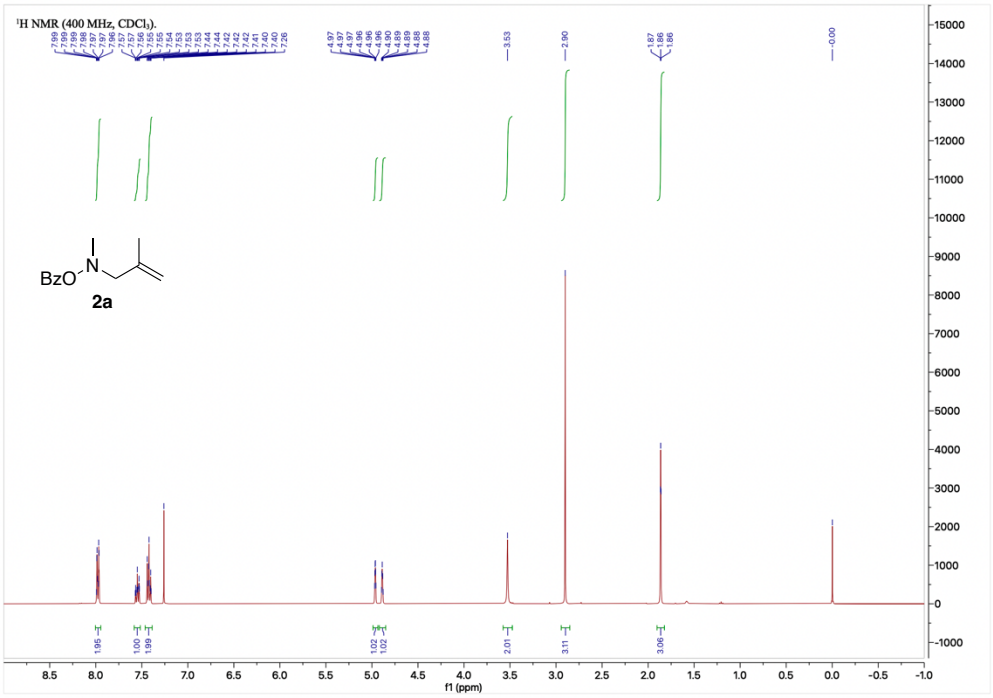

Figure 3.4. ^{13}C NMR Spectrum of **2a**

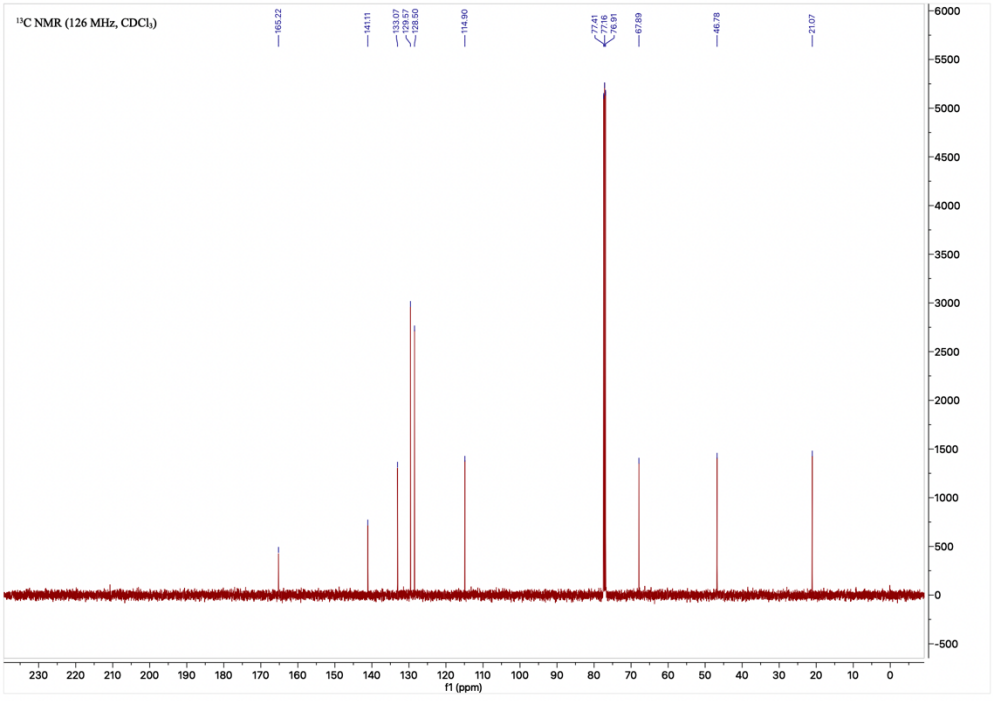

Figure 3.5. ^{1}H NMR Spectrum of **2b**

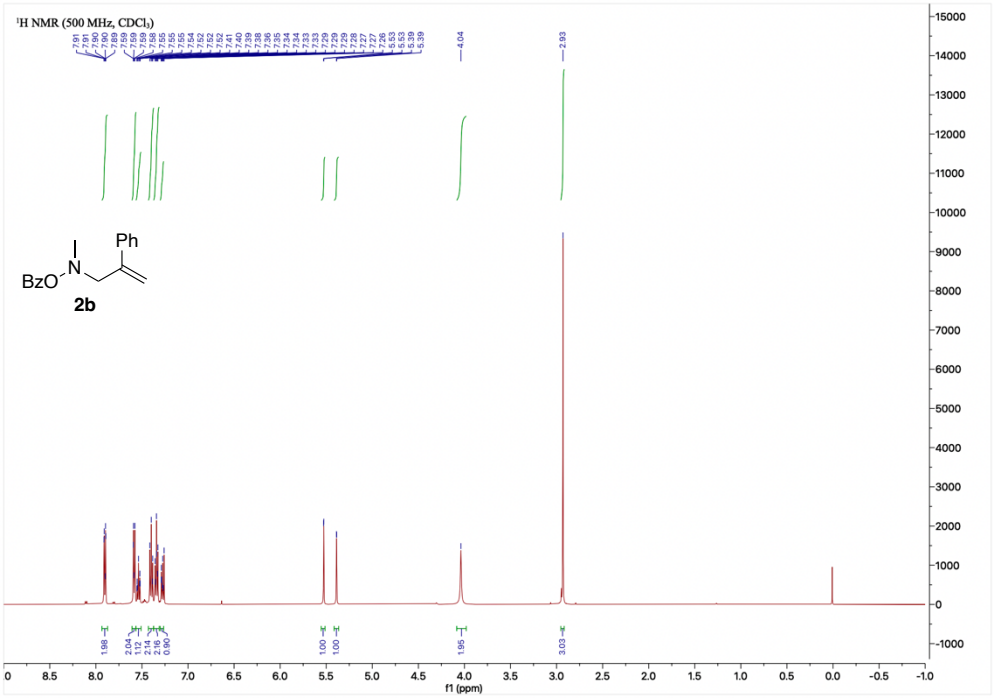

Figure 3.6. ^{13}C NMR Spectrum of **2b**

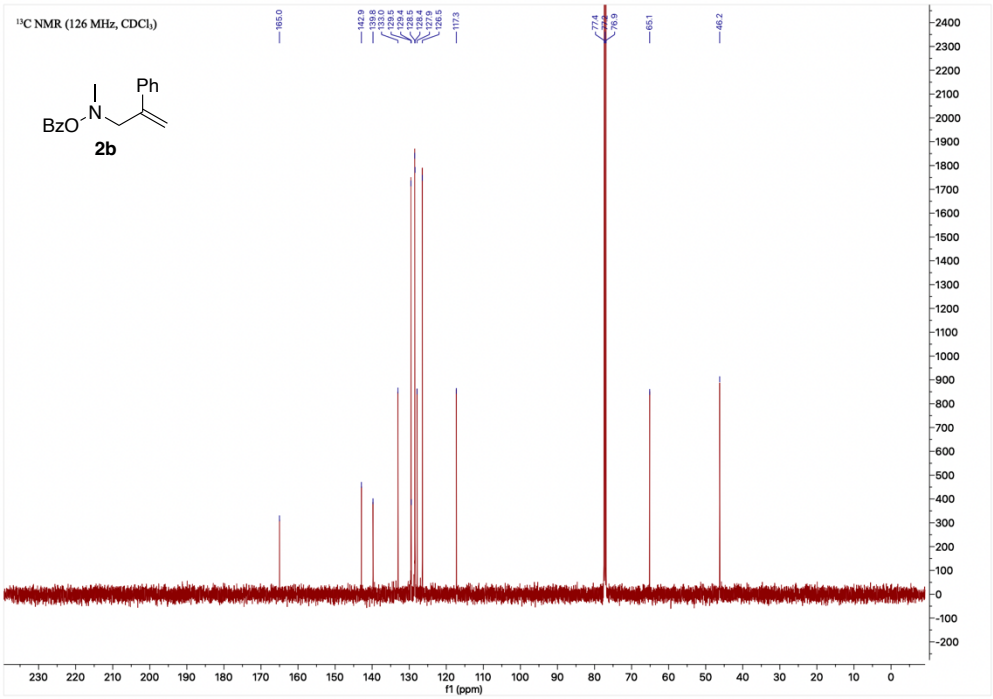

Figure 3.7. ^{1}H NMR Spectrum of **2c**

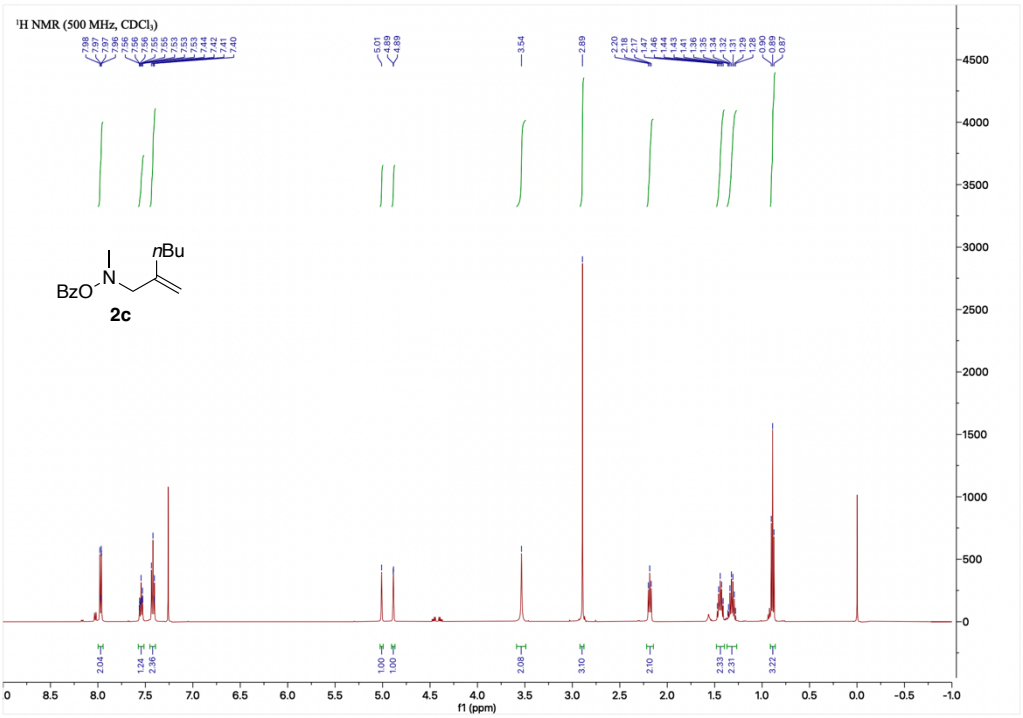

Figure 3.8. ^{13}C NMR Spectrum of **2c**

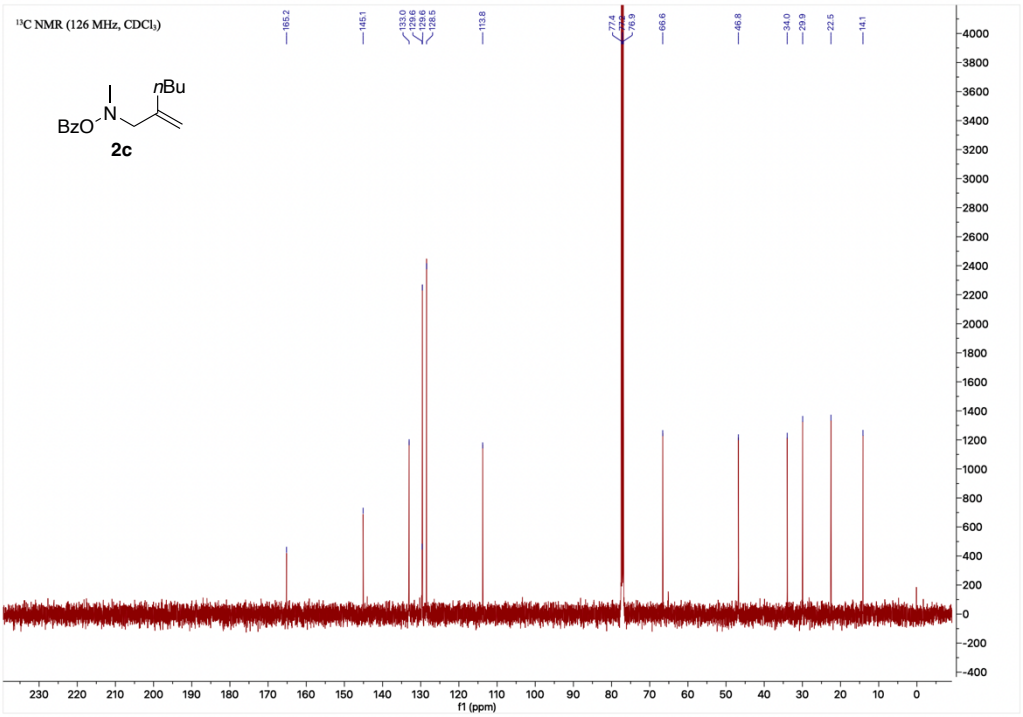

Figure 3.9. ^{1}H NMR Spectrum of **2d**

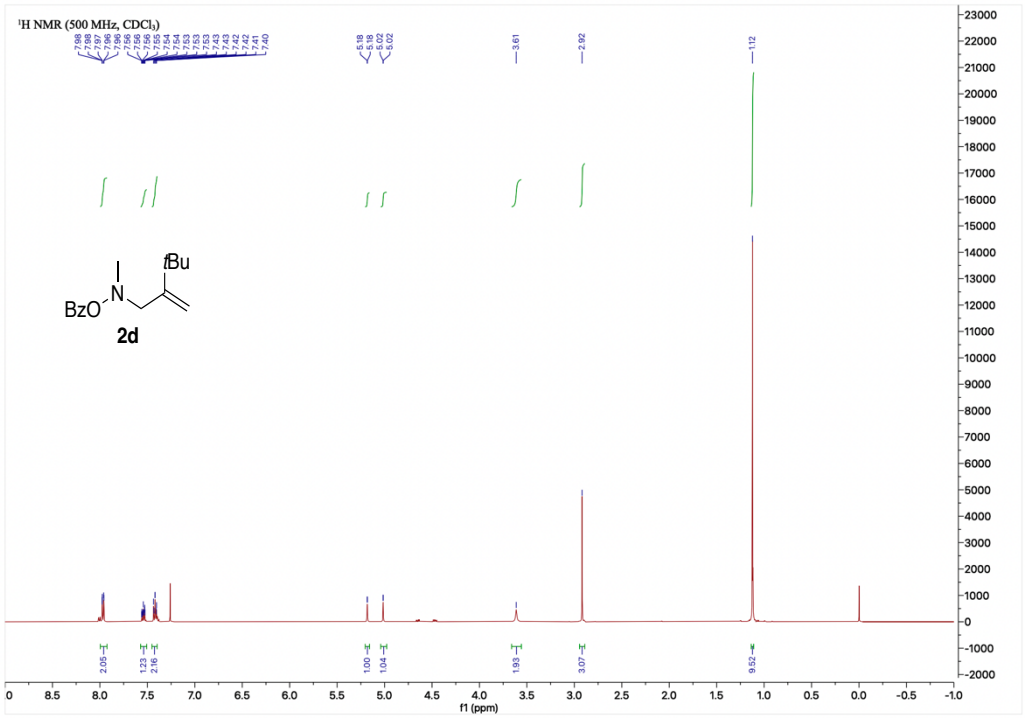

Figure 3.10. ^{13}C NMR Spectrum of **2d**

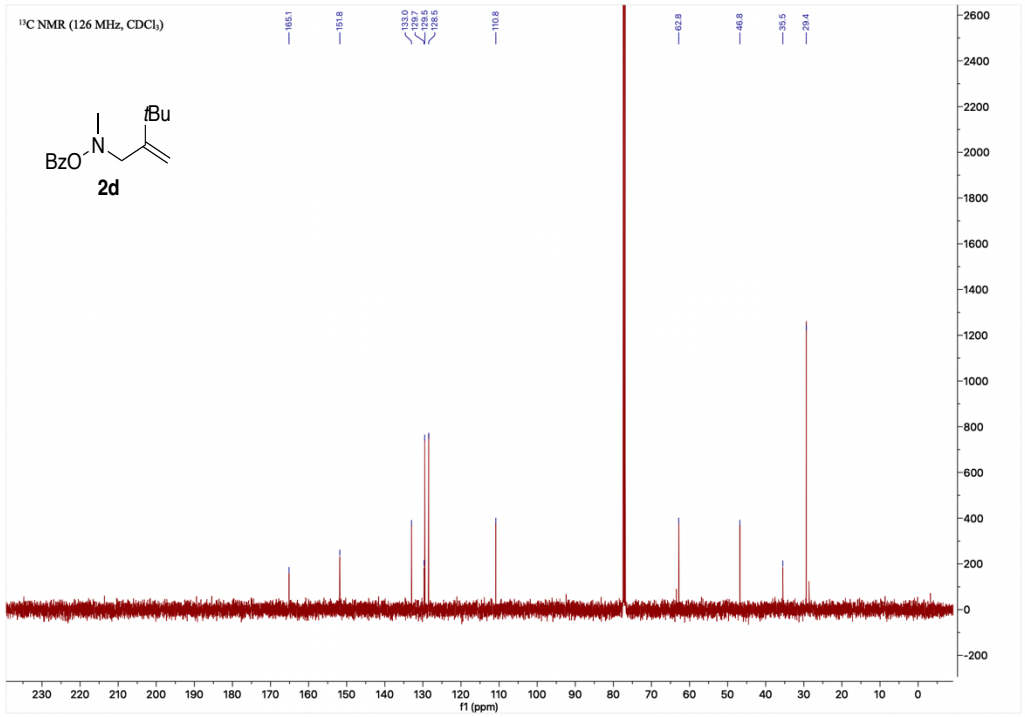

Figure 3.11. ^{1}H NMR Spectrum of **2e**

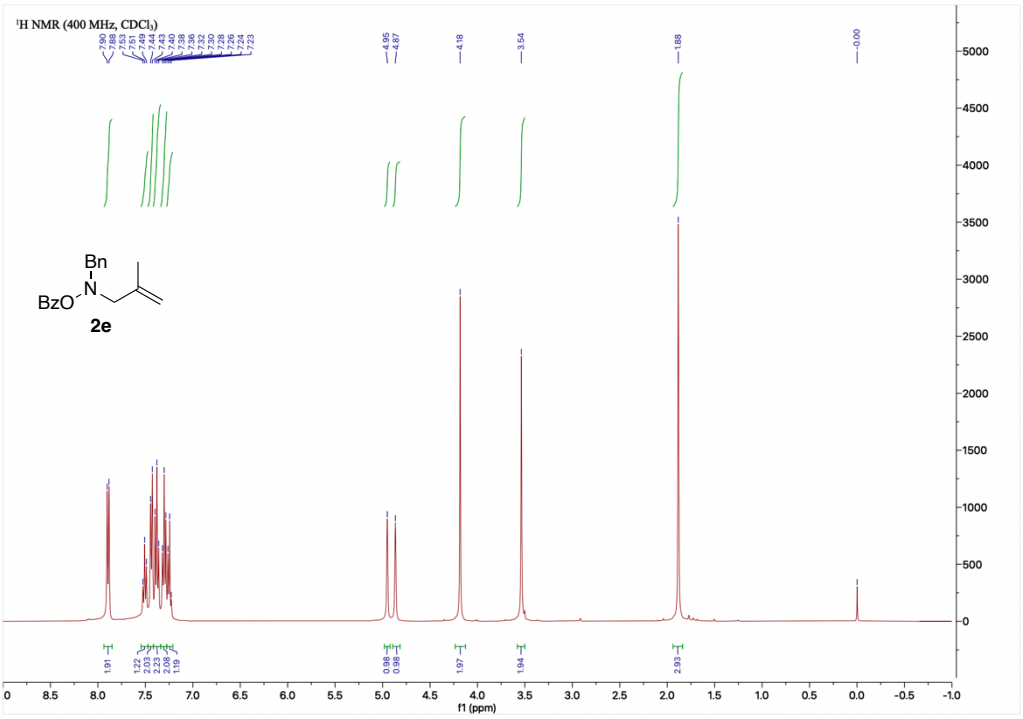

Figure 3.12. ^{13}C NMR Spectrum of **2e**

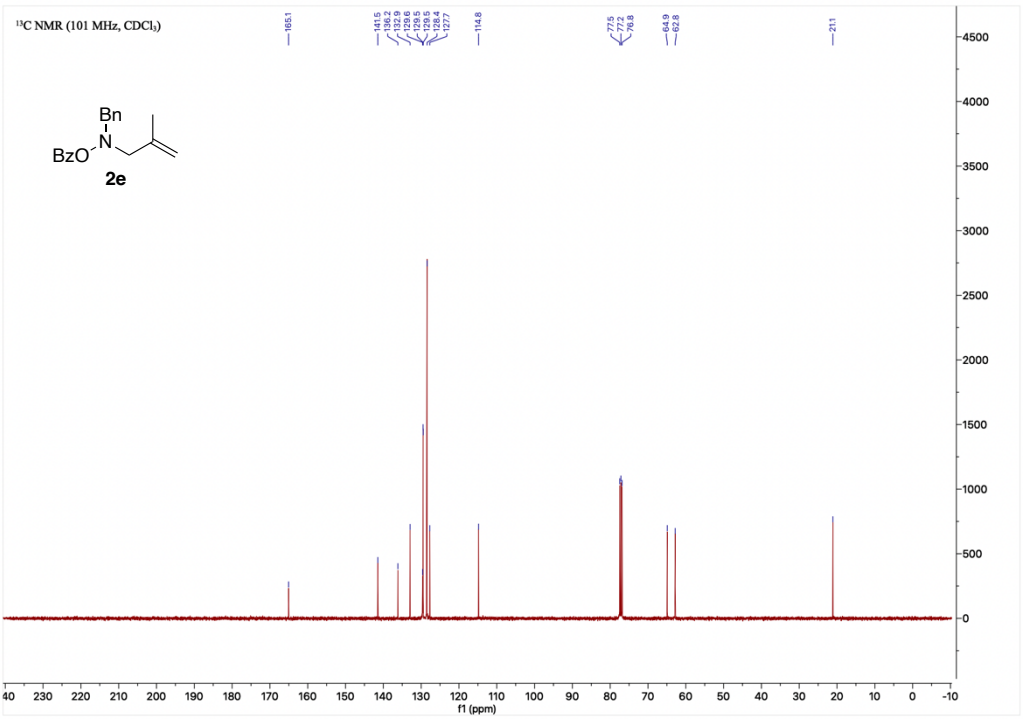

Figure 3.13. ^{1}H NMR Spectrum of **2f**

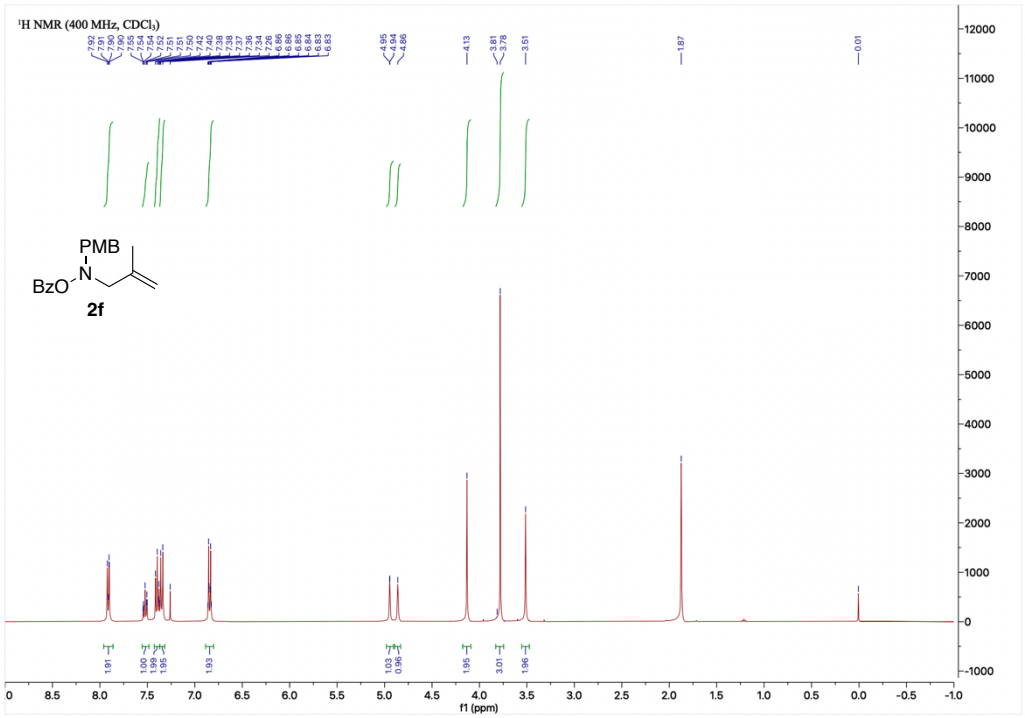

Figure 3.14. ^{13}C NMR Spectrum of **2f**

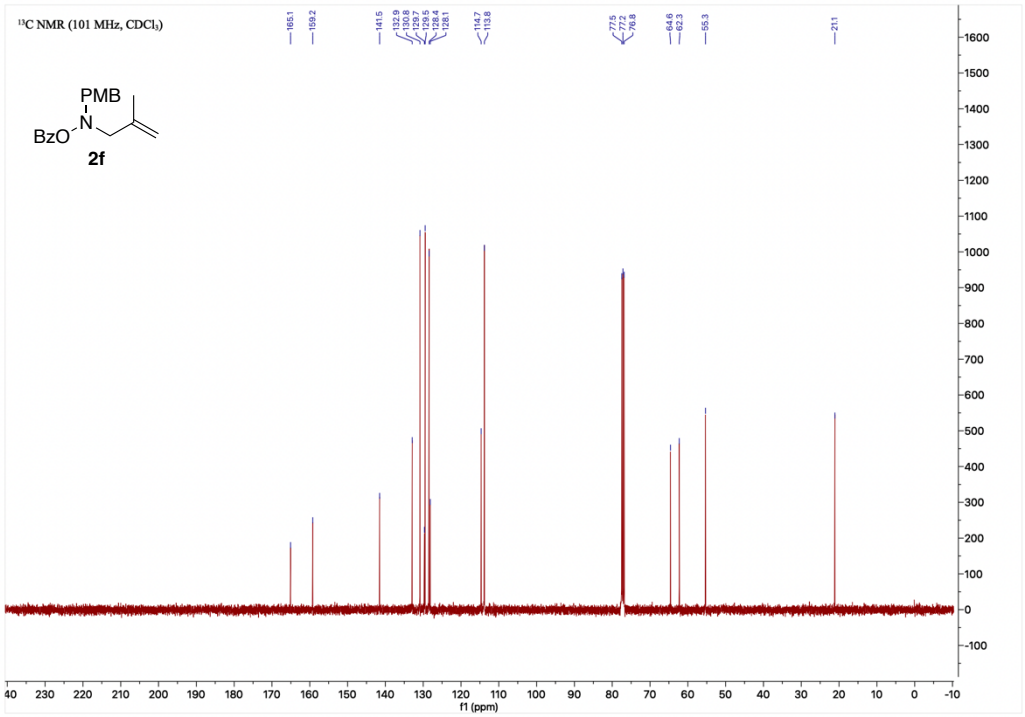

Figure 3.15. ^{1}H NMR Spectrum of **3aa**

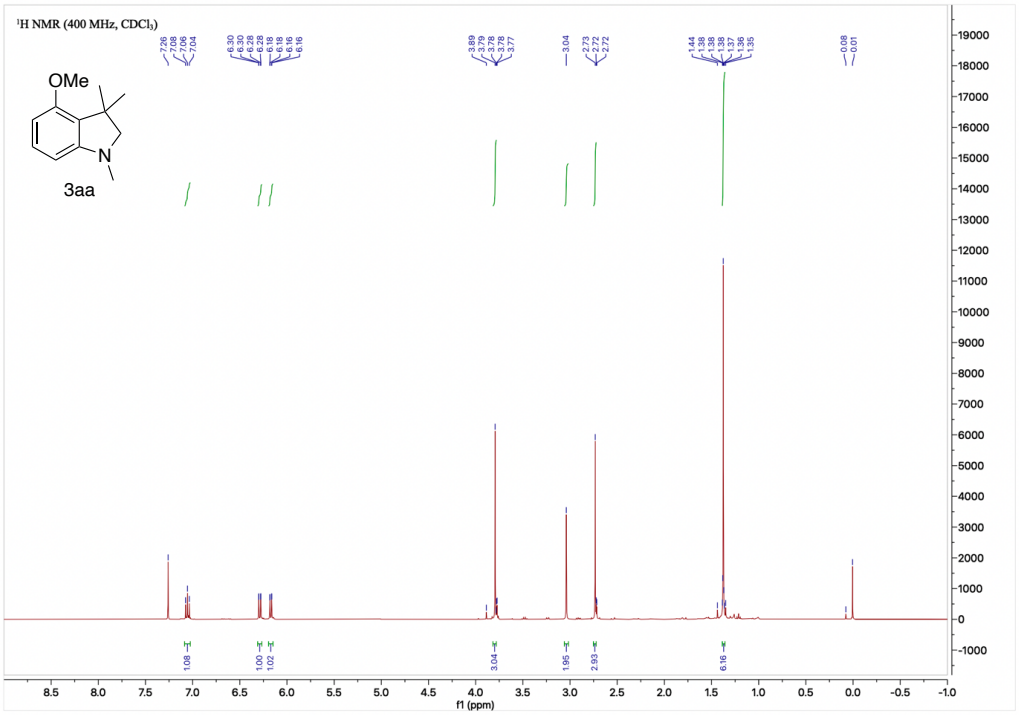

Figure 3.16. ^{13}C NMR Spectrum of **3aa**

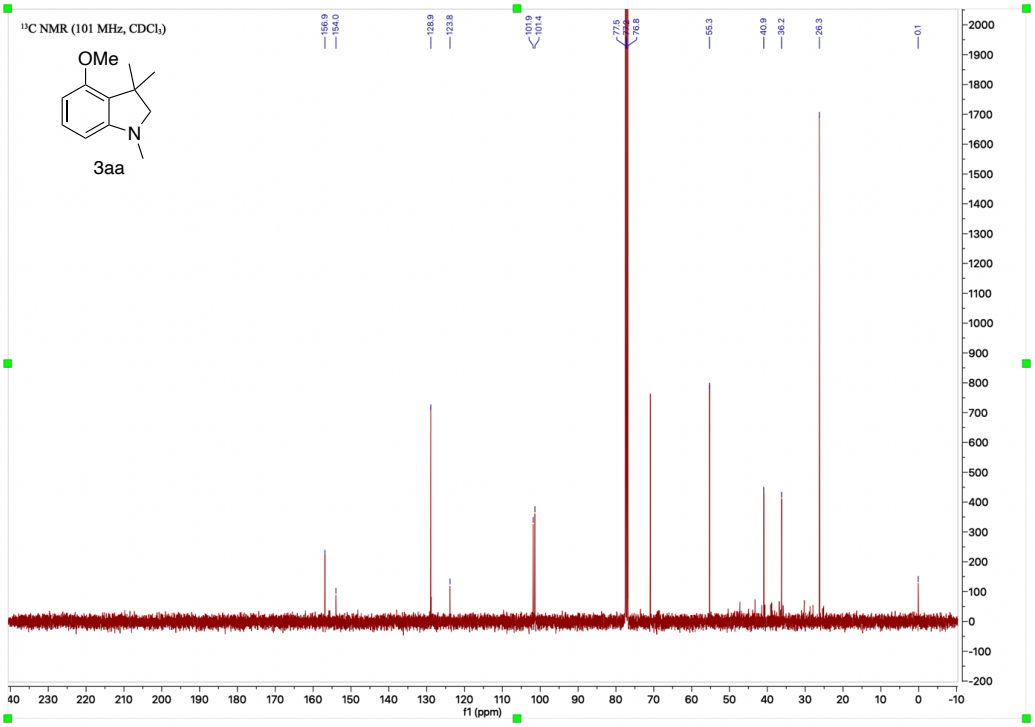

Figure 3.17. ^{1}H NMR Spectrum of **3ba**

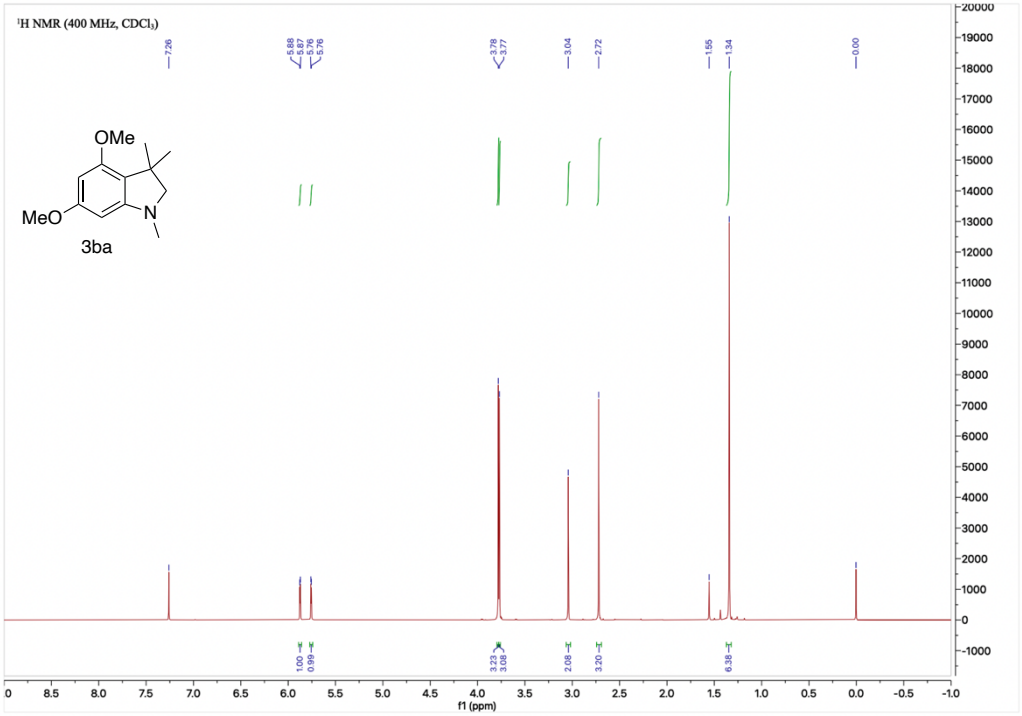

Figure 3.18. ^{13}C NMR Spectrum of **3ba**

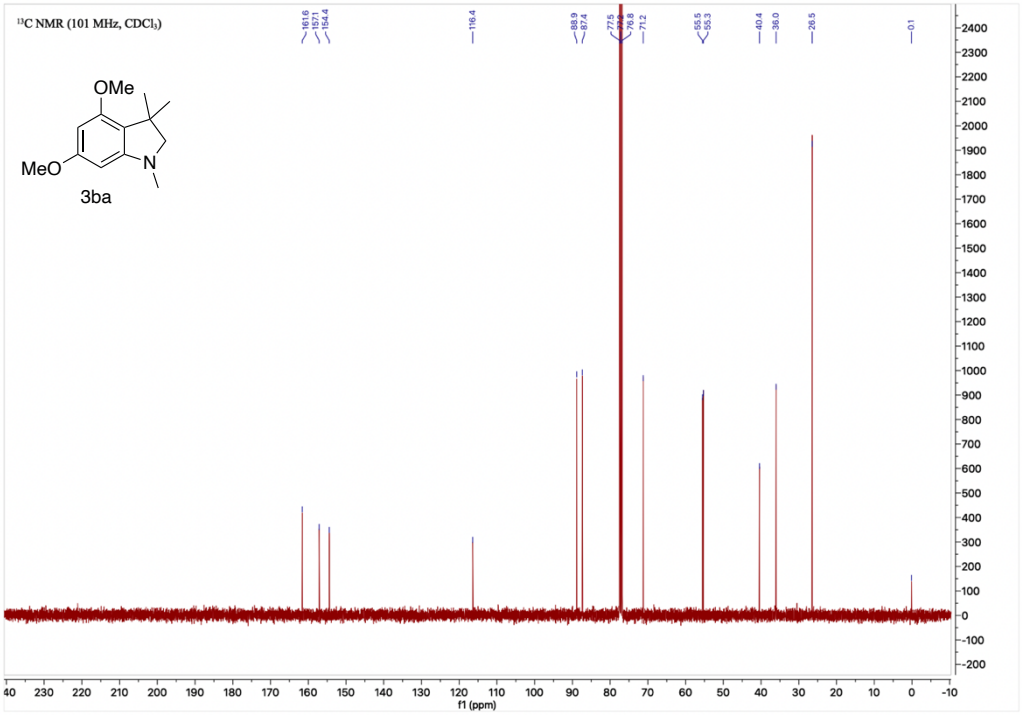

Figure 3.19. ^{1}H NMR Spectrum of **3ca**

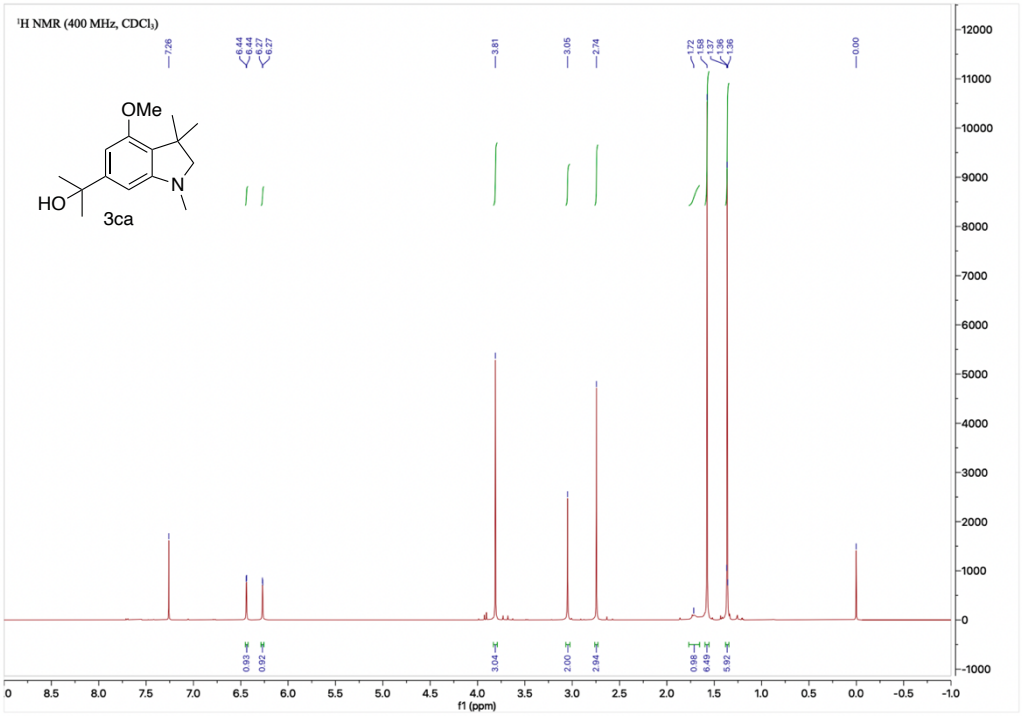

Figure 3.20. ^{13}C NMR Spectrum of **3ca**

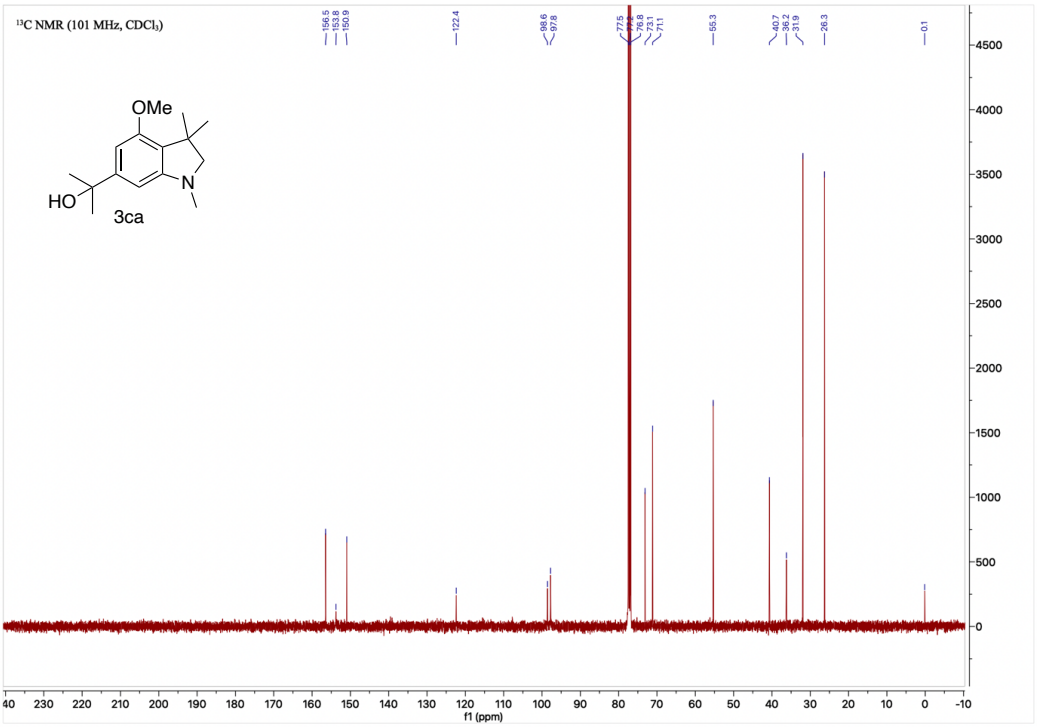

Figure 3.21. ^{1}H NMR Spectrum of **3da**

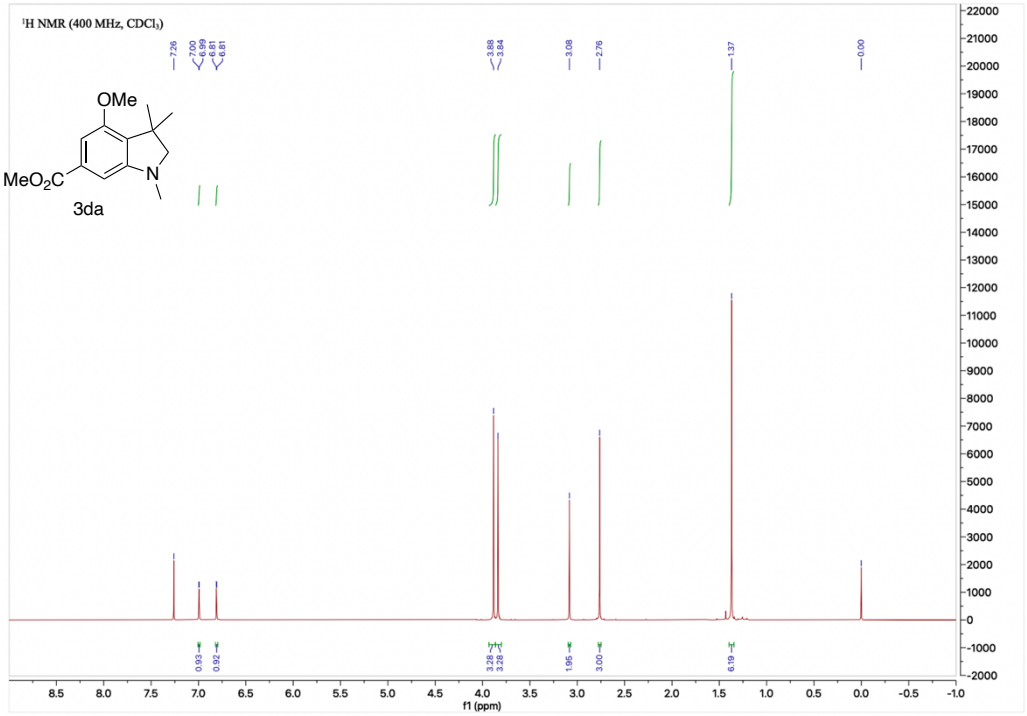

Figure 3.22. ^{13}C NMR Spectrum of **3da**

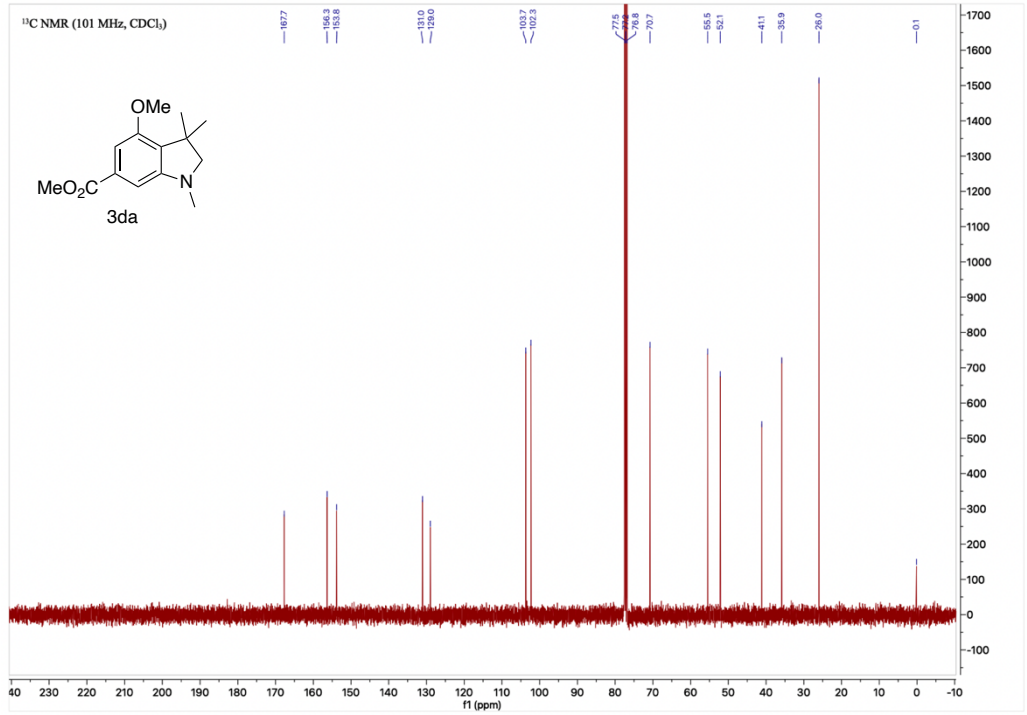

Figure 3.23. ^{1}H NMR Spectrum of **3ea**

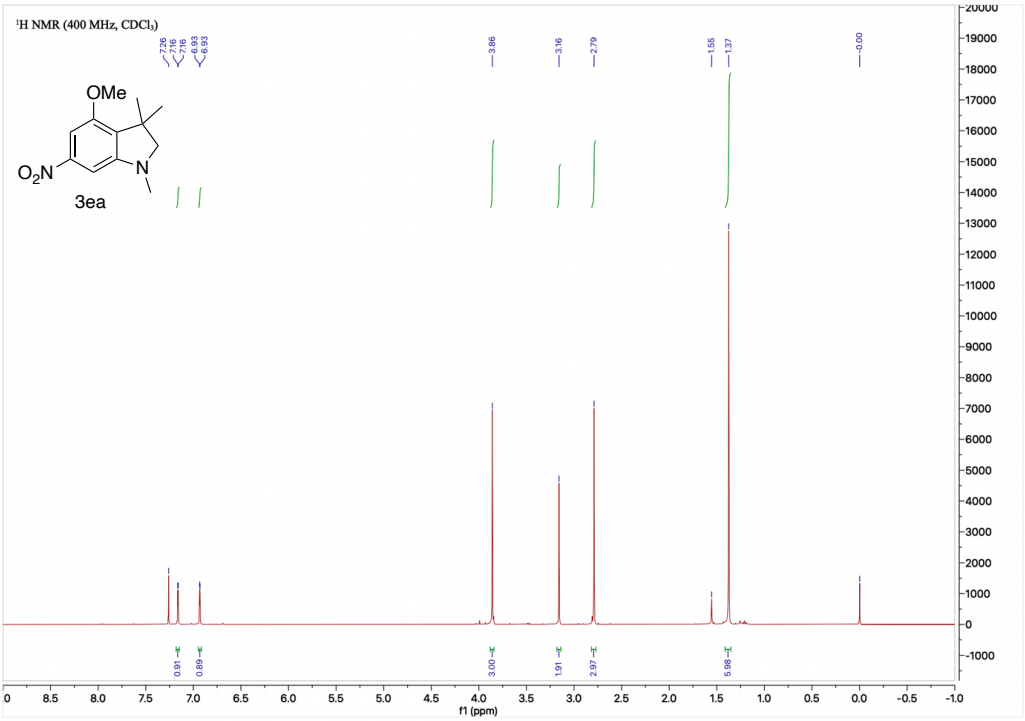

Figure 3.24. ^{13}C NMR Spectrum of **3ea**

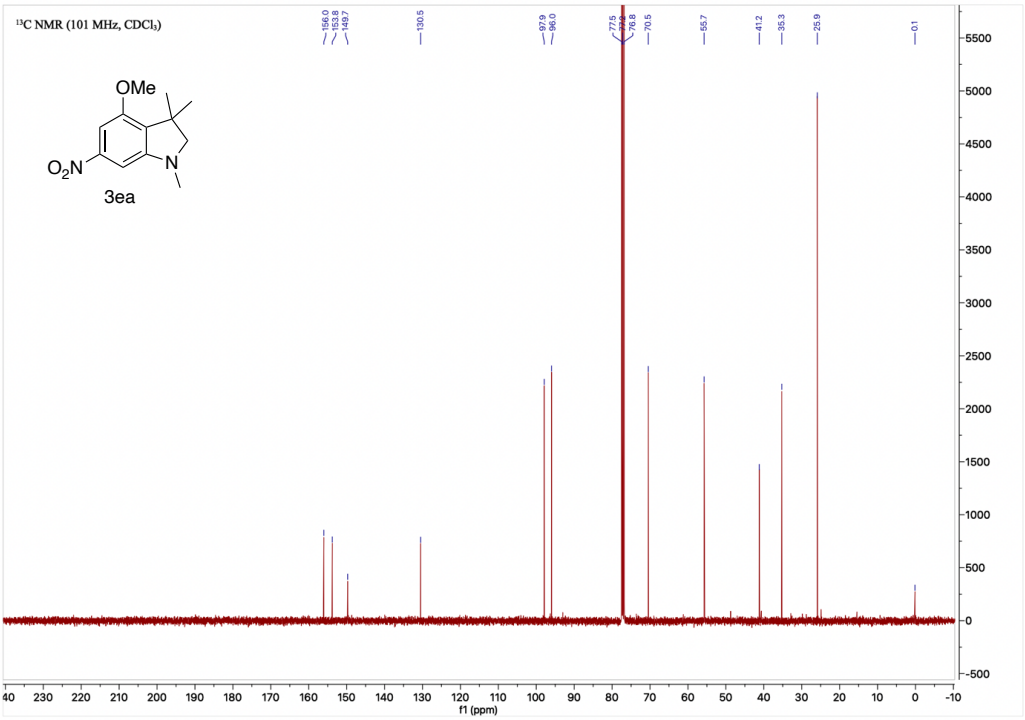

Figure 3.25. ^{1}H NMR Spectrum of **3fa**

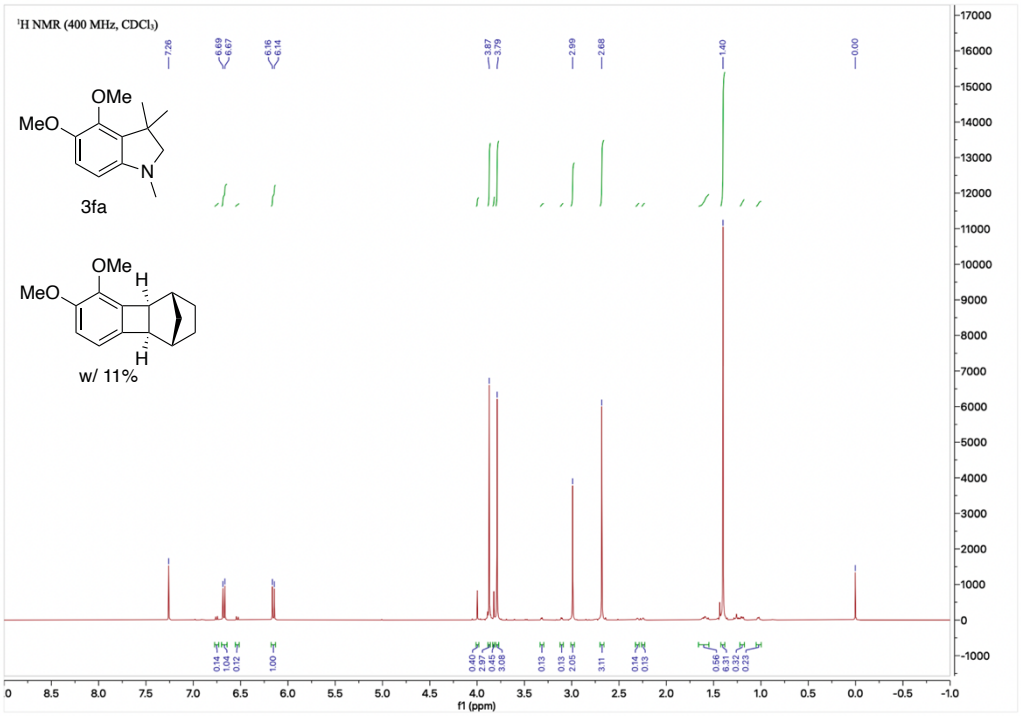

Figure 3.26. ^{13}C NMR Spectrum of **3fa**

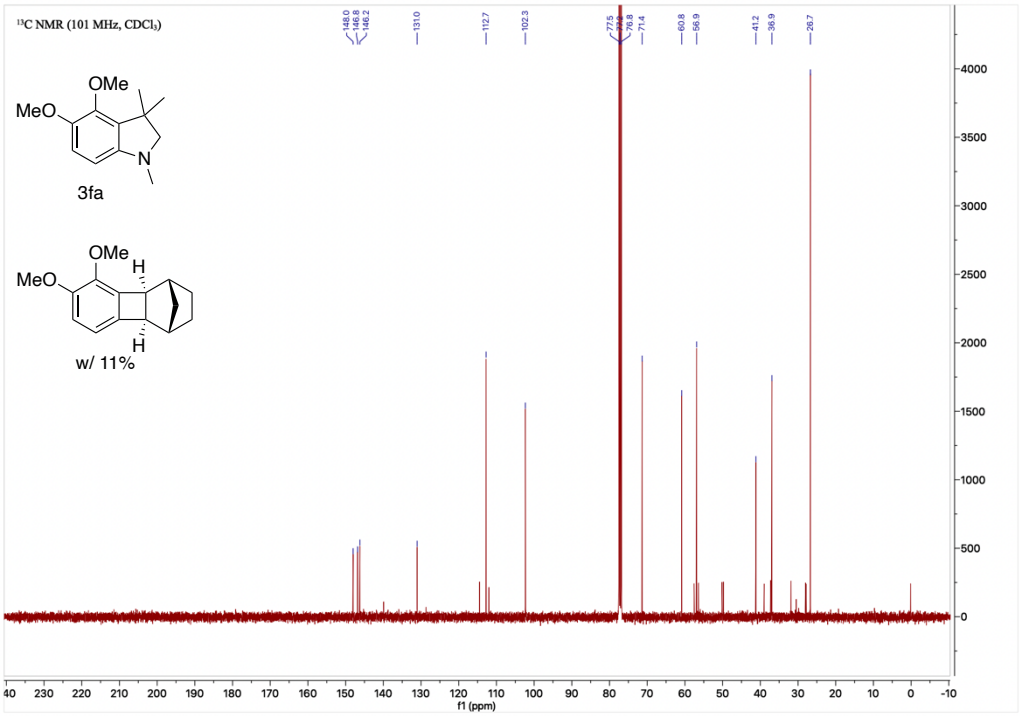

Figure 3.27. ^{1}H NMR Spectrum of **3ga**

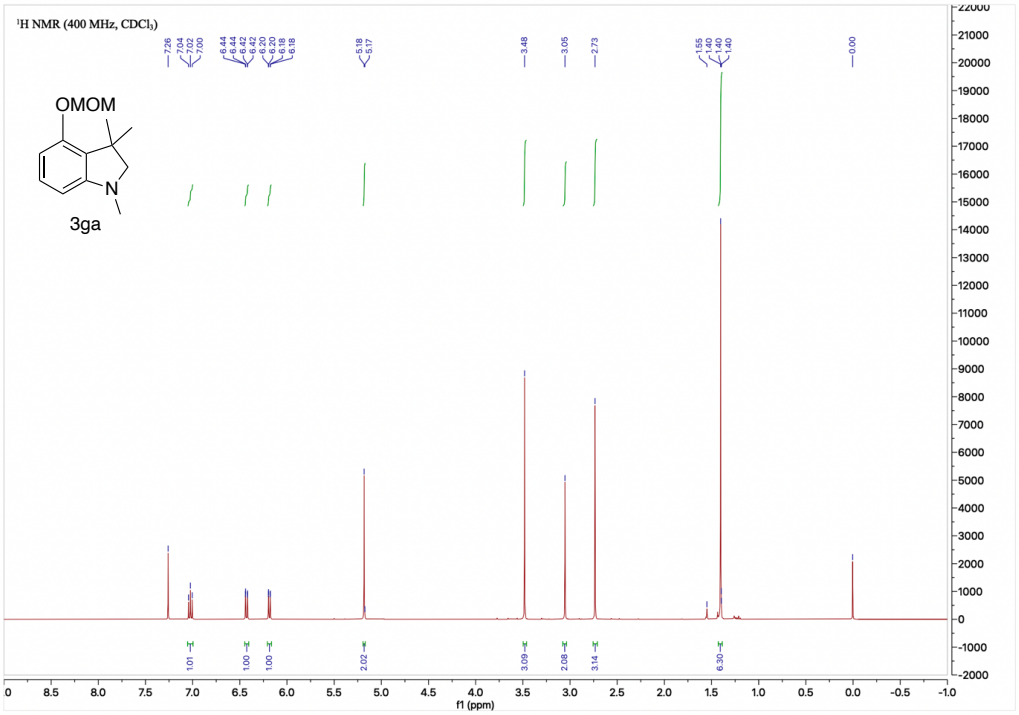

Figure 3.28. ^{13}C NMR Spectrum of **3ga**

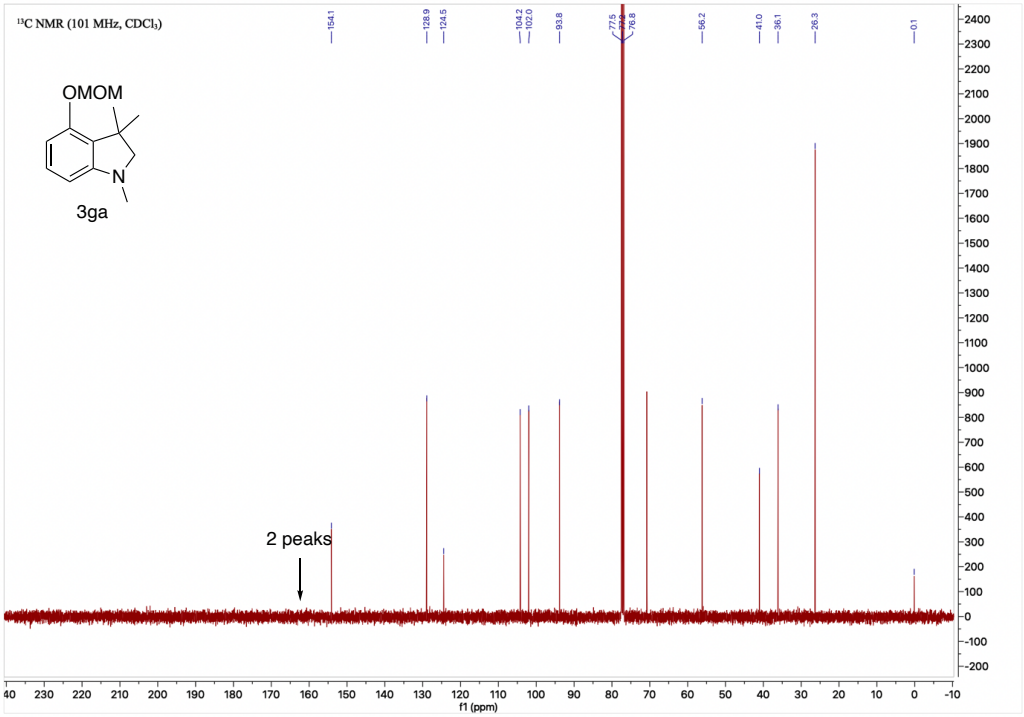

Figure 3.29. ^{1}H NMR Spectrum of **3ha**

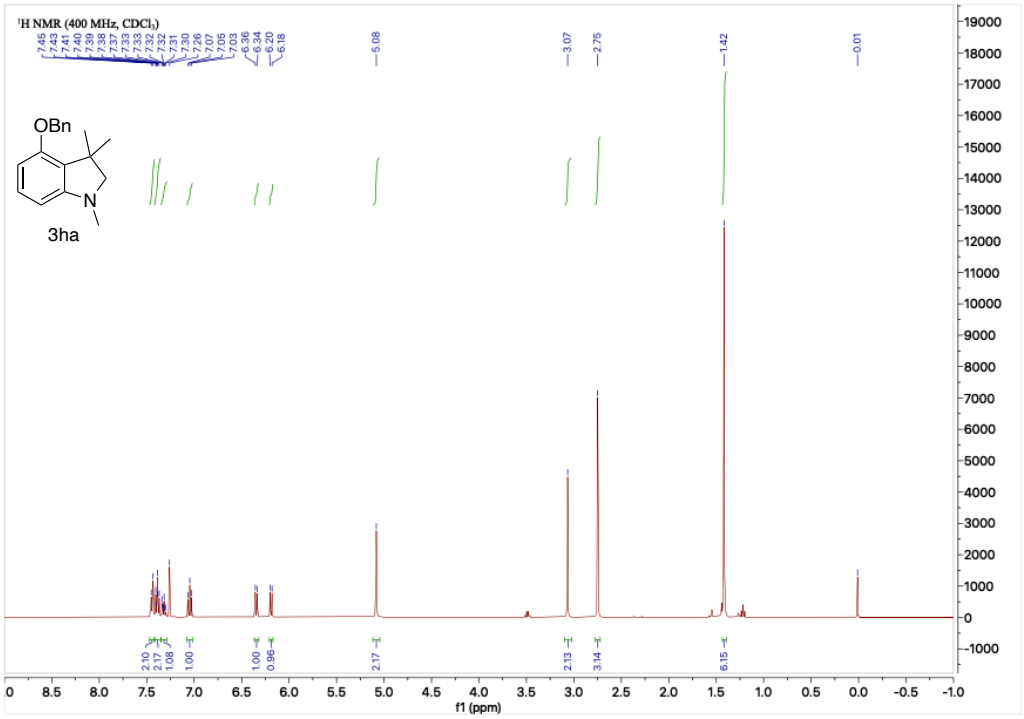

Figure 3.30. ^{13}C NMR Spectrum of **3ha**

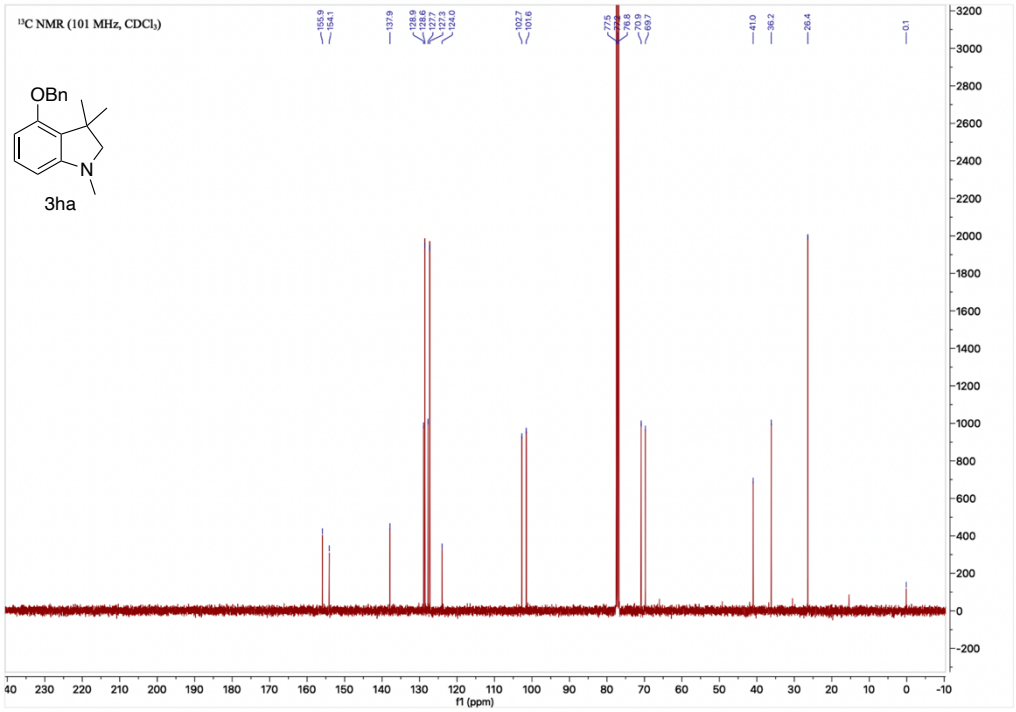

Figure 3.31. ^{1}H NMR Spectrum of **3ia**

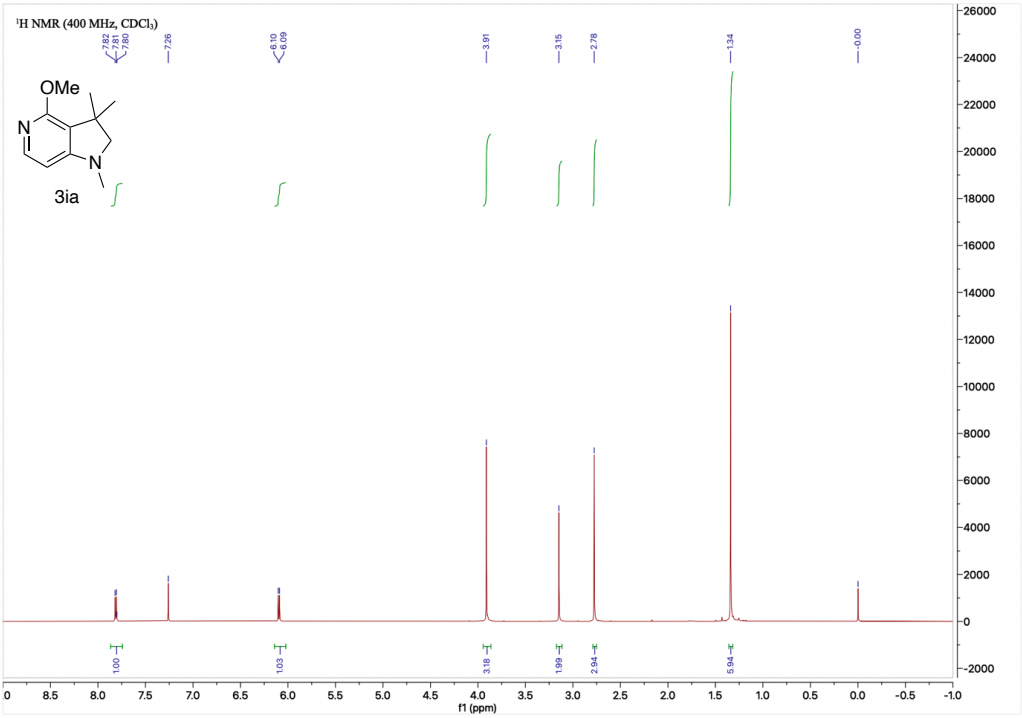

Figure 3.32. ^{13}C NMR Spectrum of **3ia**

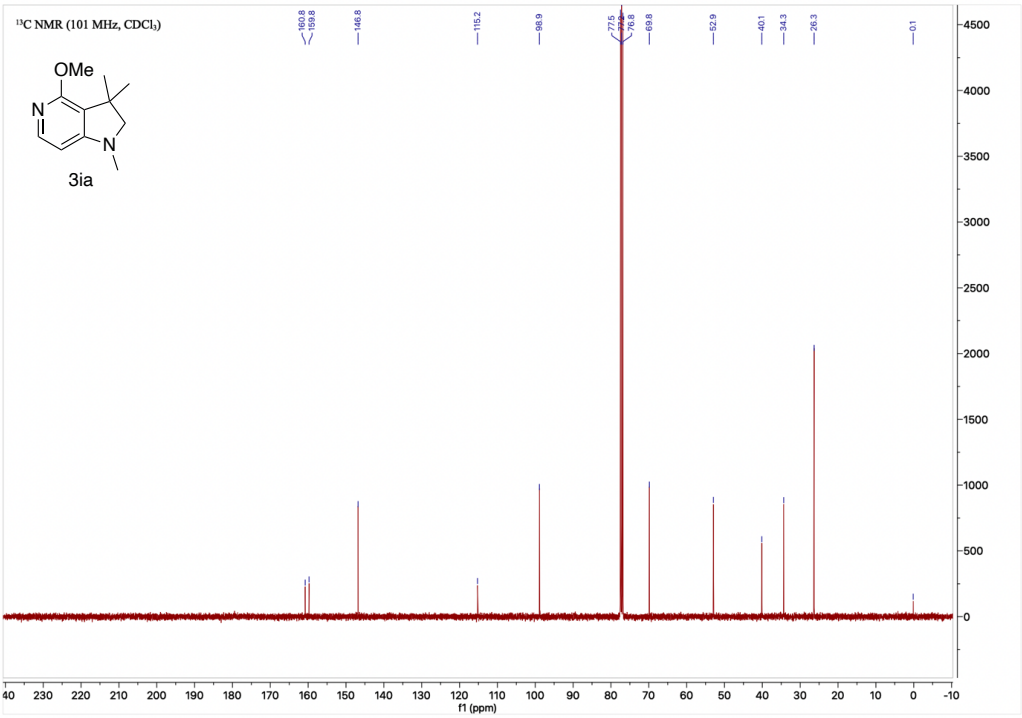

Figure 3.33. ^{1}H NMR Spectrum of **3ja**

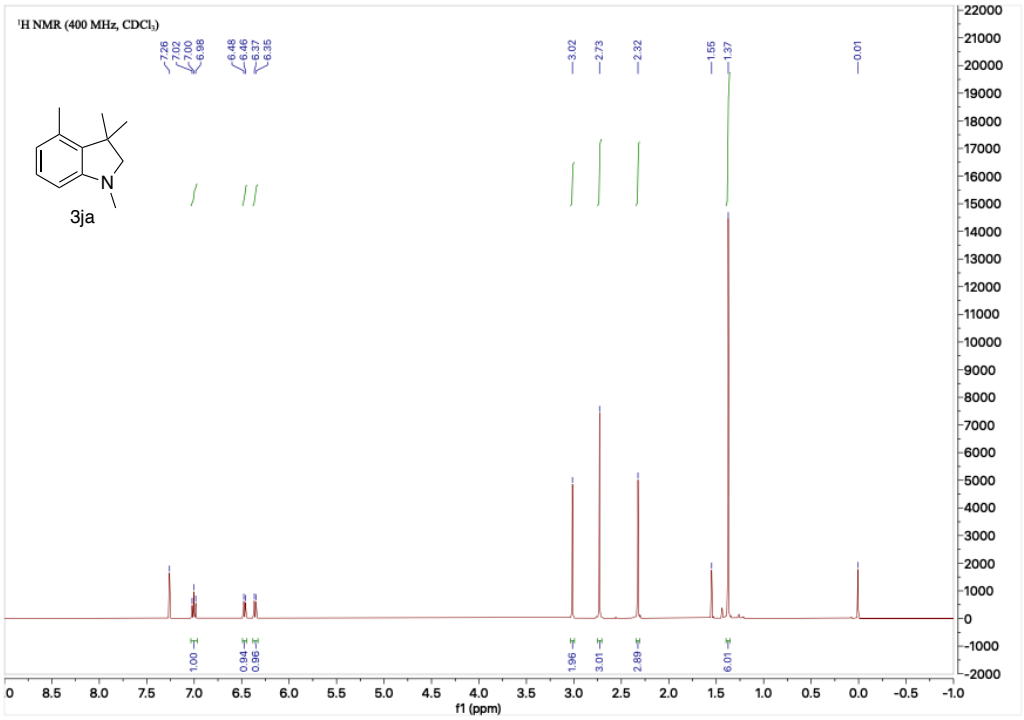

Figure 3.34. ^{13}C NMR Spectrum of **3ja**

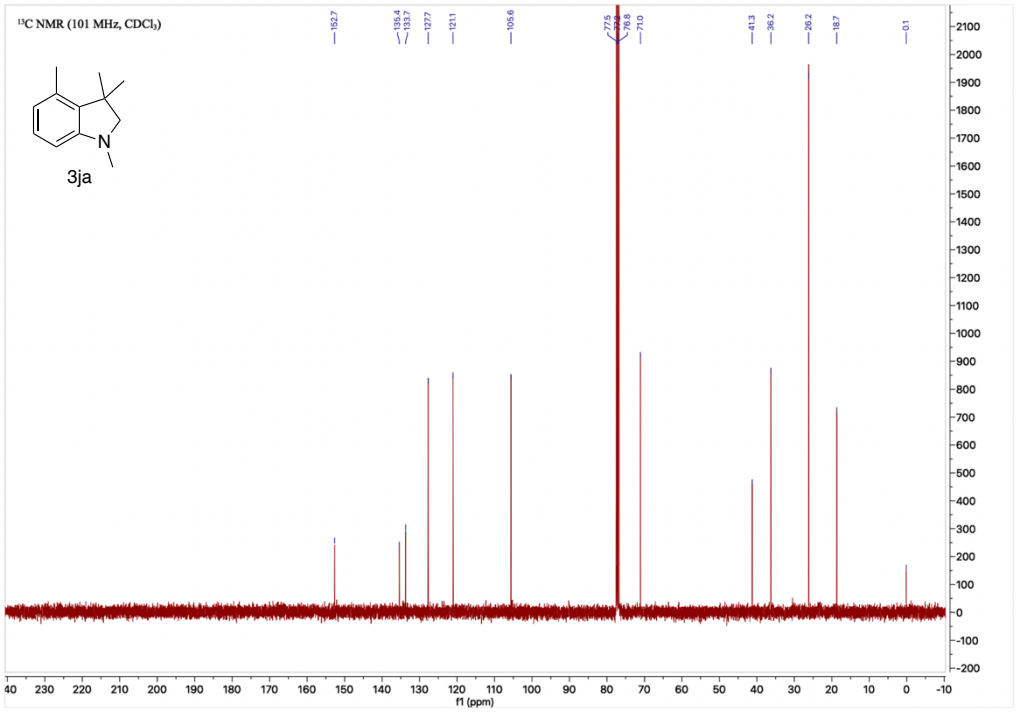

Figure 3.35. ^{1}H NMR Spectrum of **3ka**

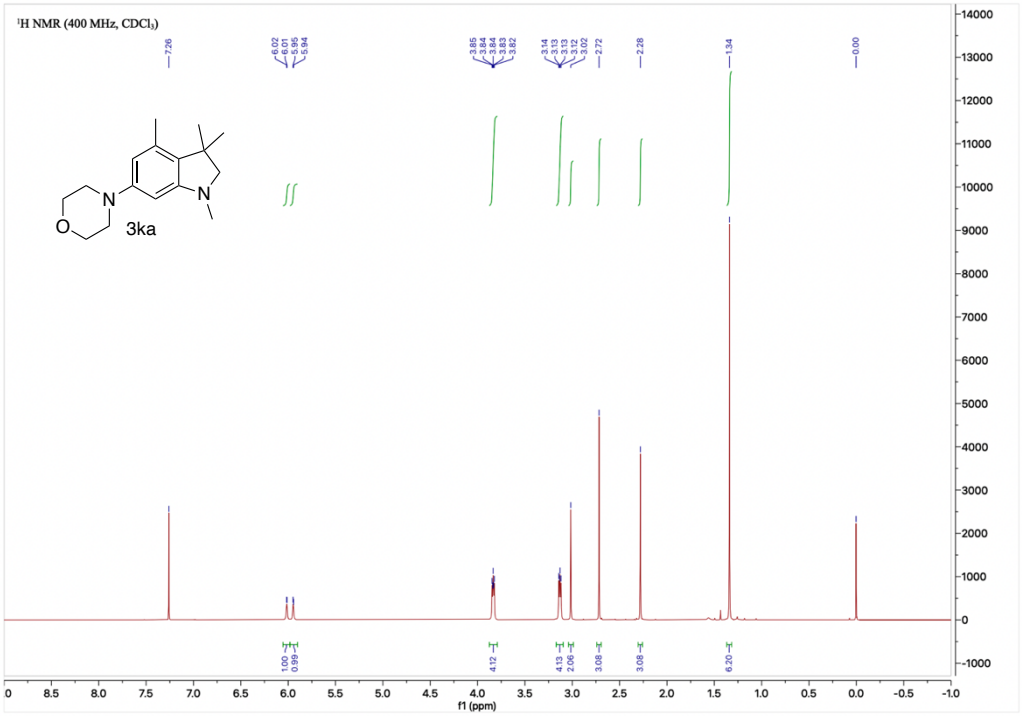

Figure 3.36. ^{13}C NMR Spectrum of **3ka**

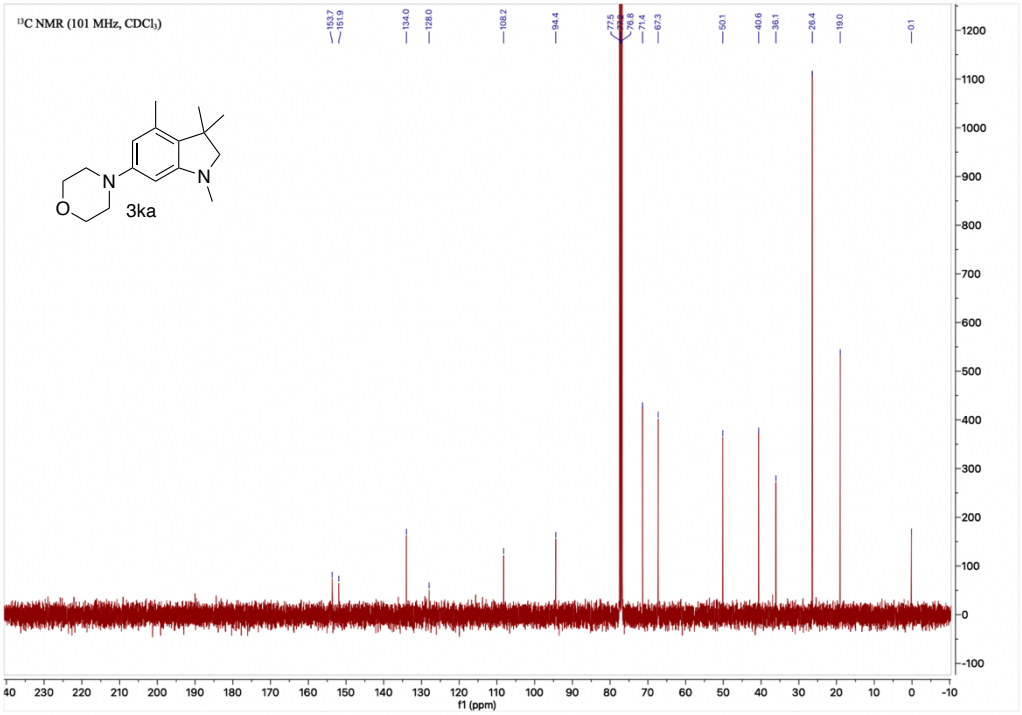

Figure 3.37. ^{1}H NMR Spectrum of **3la**

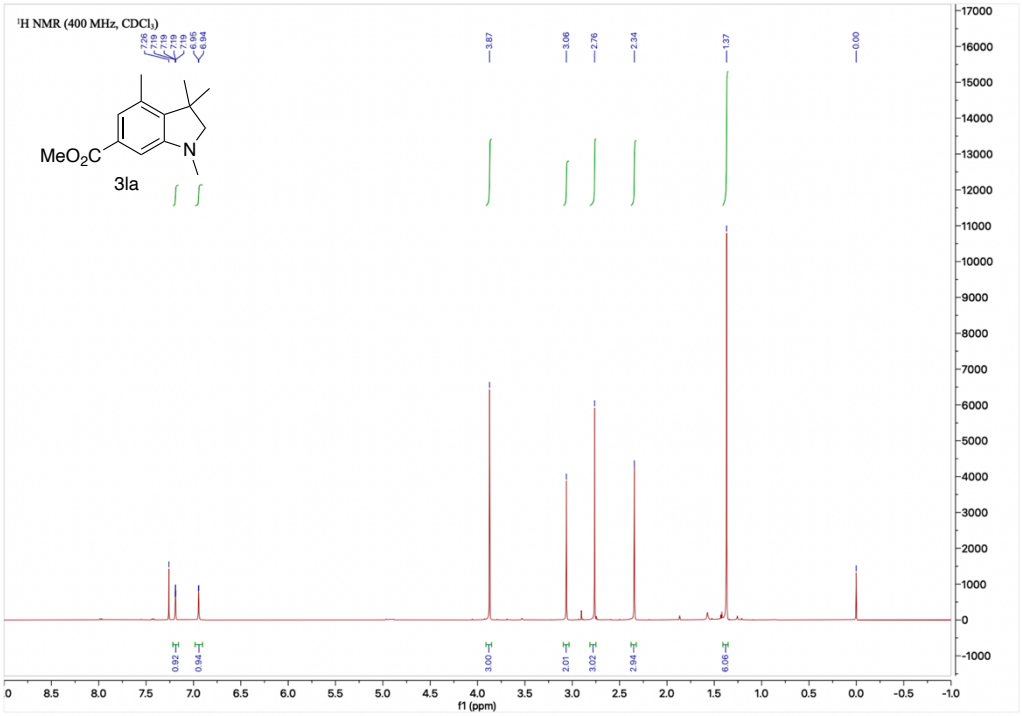

Figure 3.38. ^{13}C NMR Spectrum of **3la**

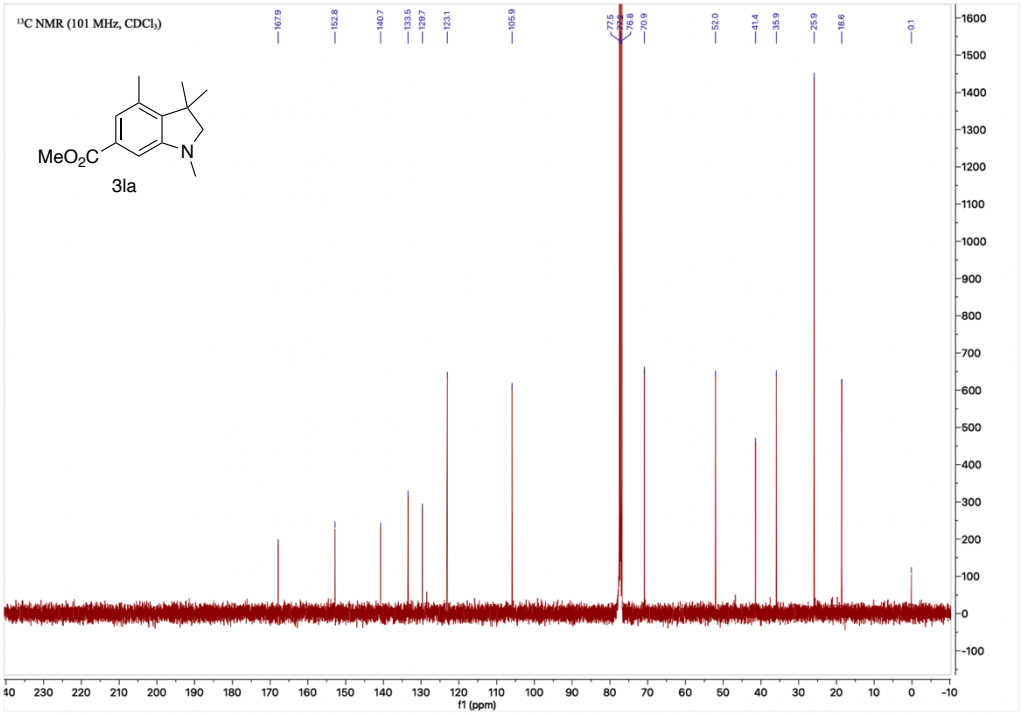

Figure 3.39. ^{1}H NMR Spectrum of **3ma**

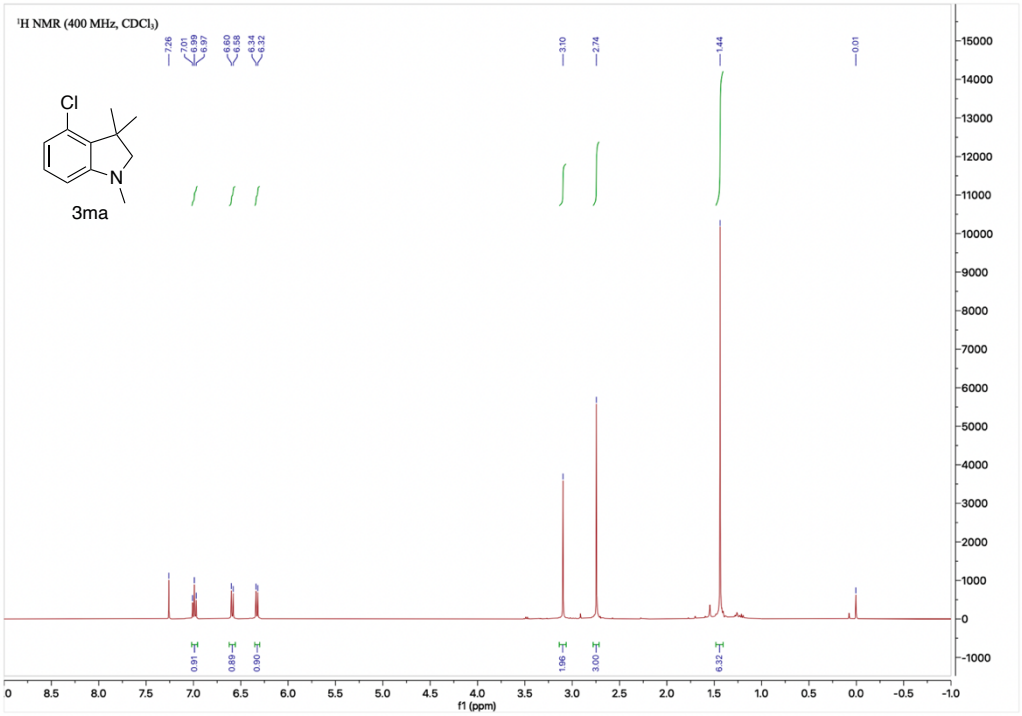

Figure 3.40. ^{13}C NMR Spectrum of **3ma**

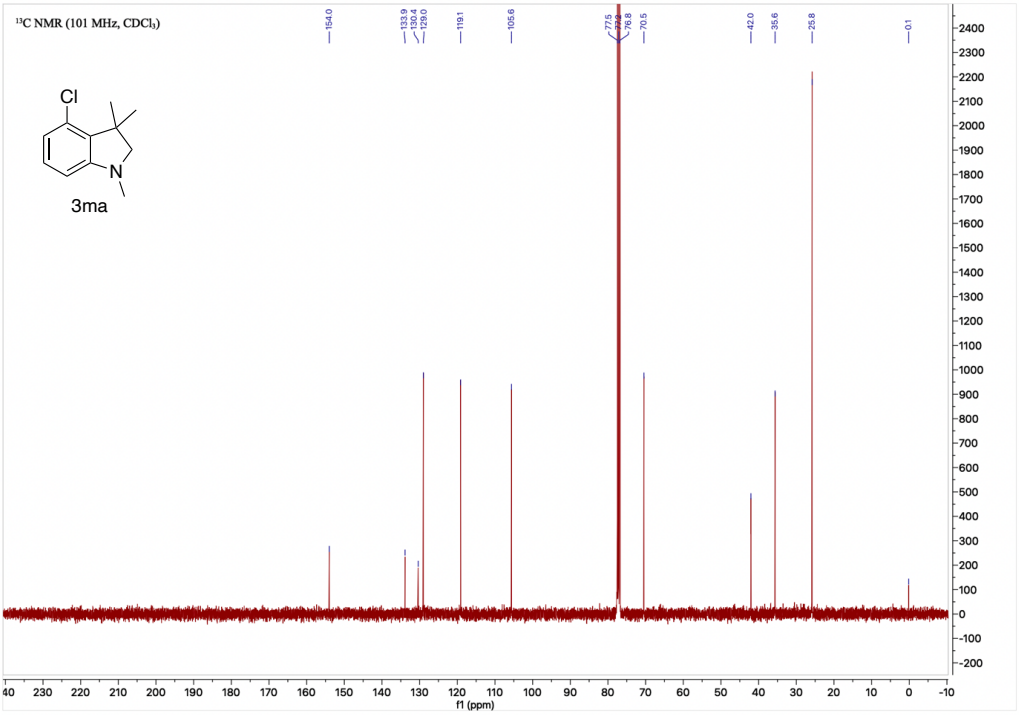

Figure 3.41. ^{1}H NMR Spectrum of **3na**

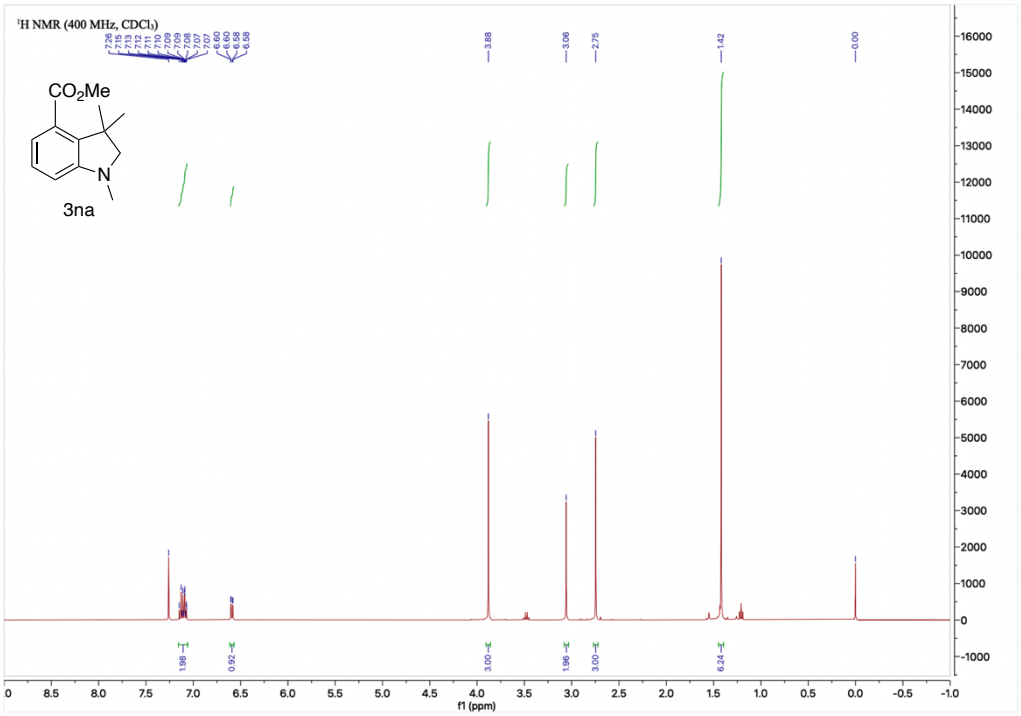

Figure 3.42. ^{13}C NMR Spectrum of **3na**

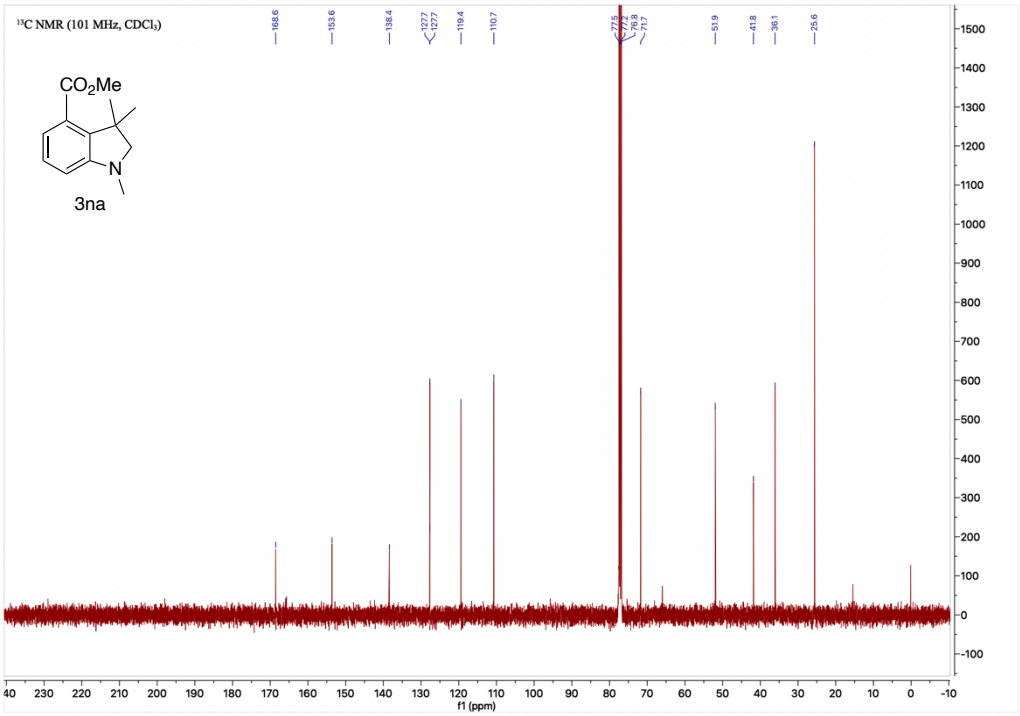

Figure 3.43. ^{1}H NMR Spectrum of **3oa**

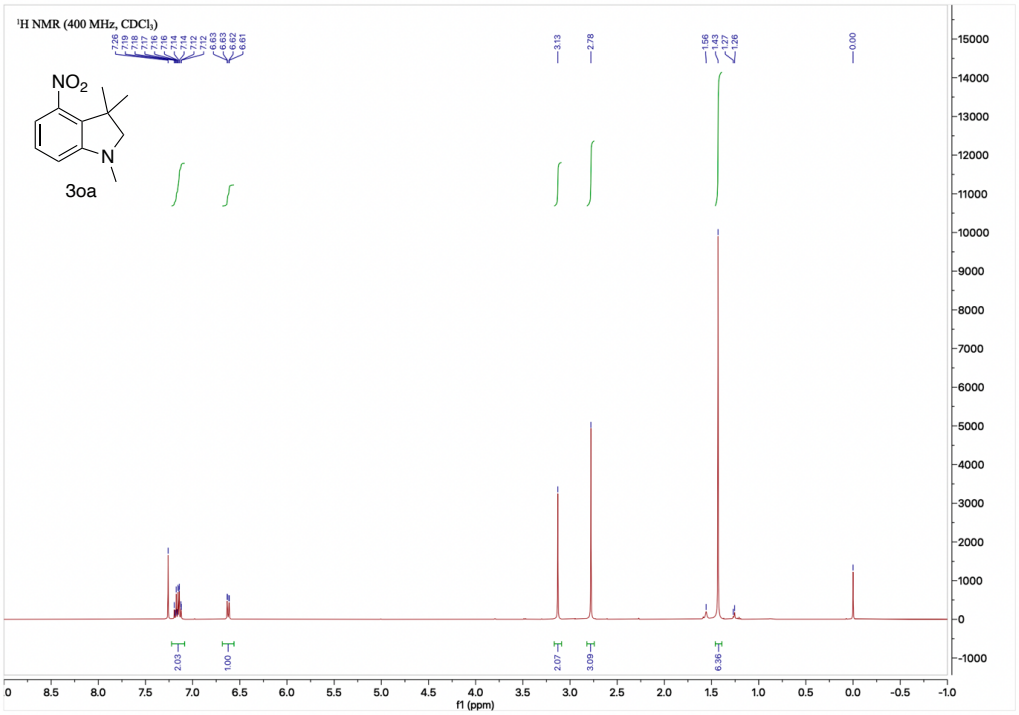

Figure 3.44. ^{13}C NMR Spectrum of **3oa**

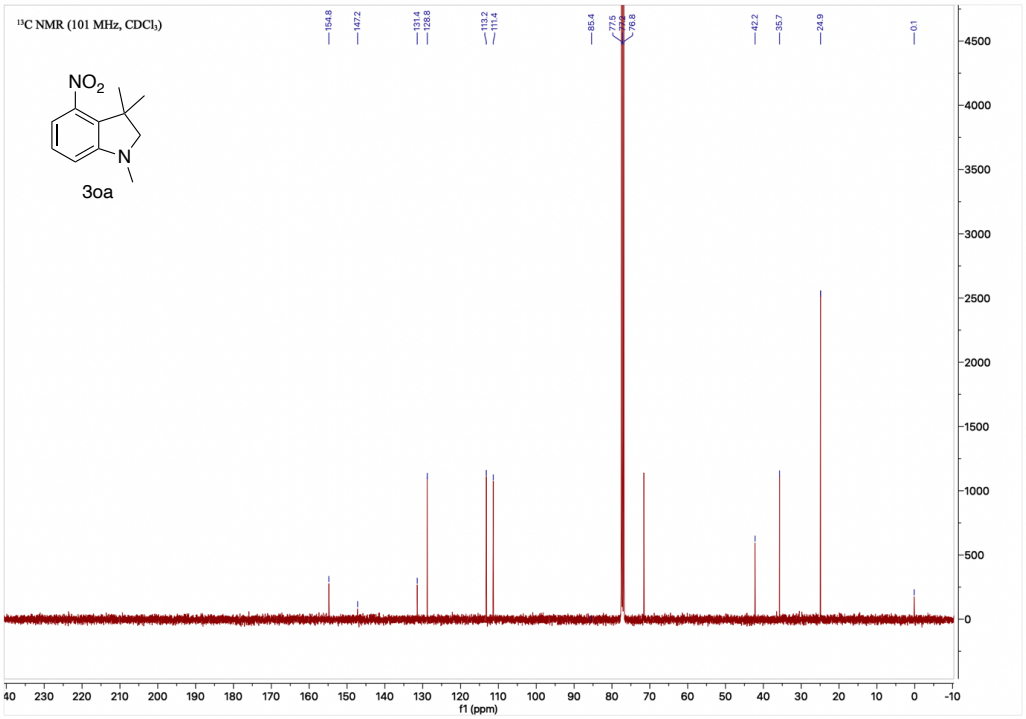

Figure 3.45. ^{1}H NMR Spectrum of **3pa**

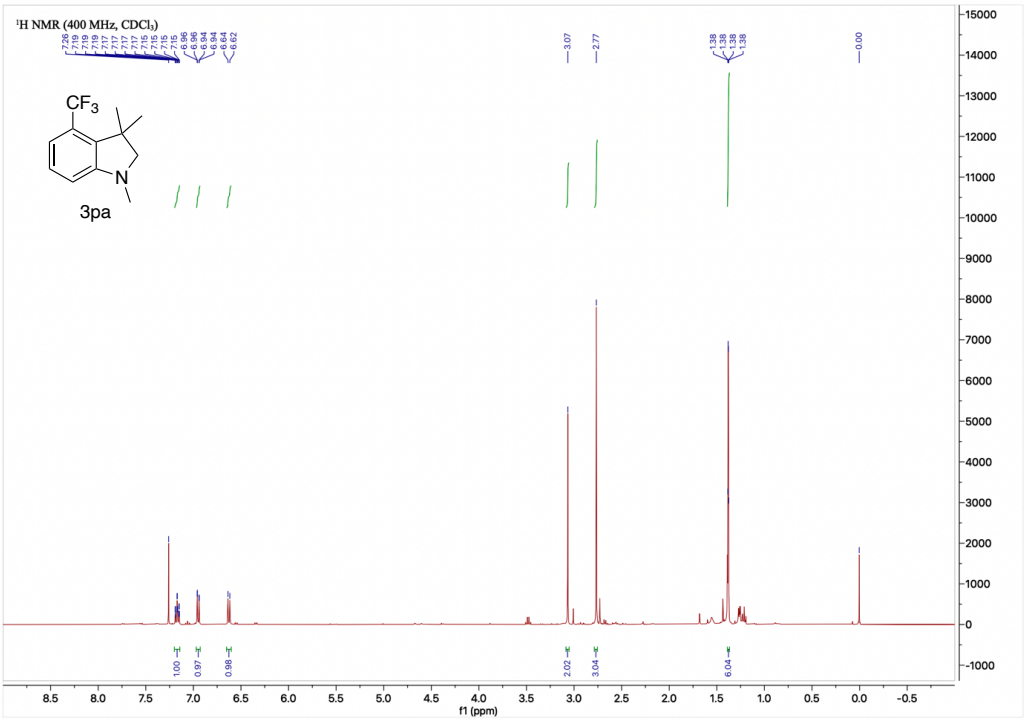

Figure 3.46. ^{13}C NMR Spectrum of **3pa**

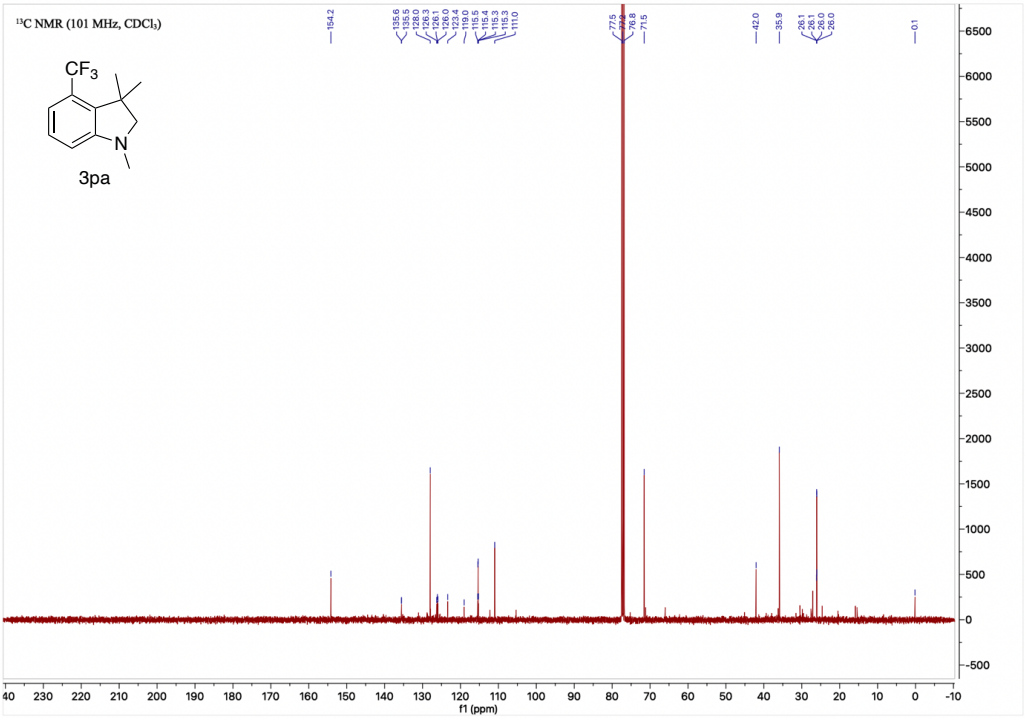

Figure 3.47. ^{19}F NMR Spectrum of **3pa**

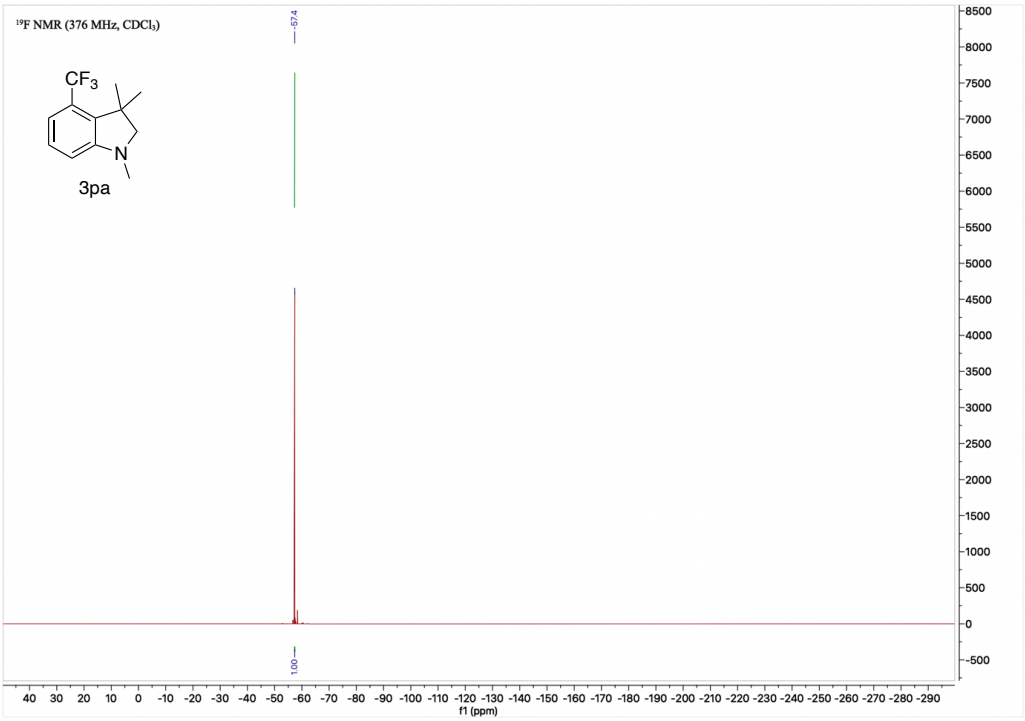

Figure 3.48. ^{1}H NMR Spectrum of **3qa**

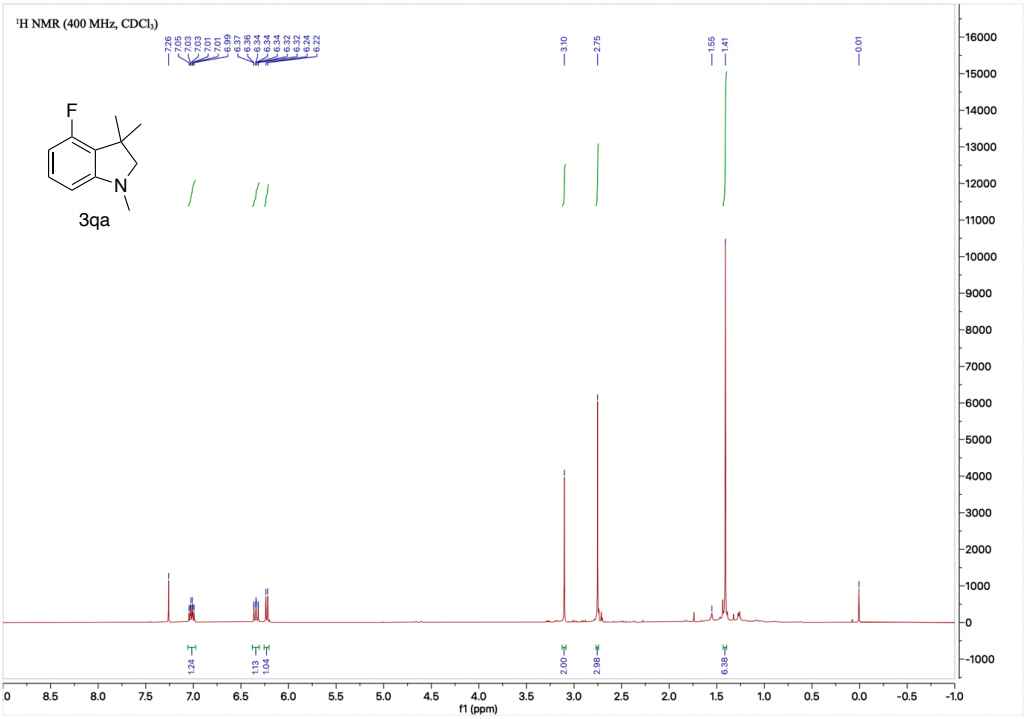

Figure 3.49. ^{13}C NMR Spectrum of **3qa**

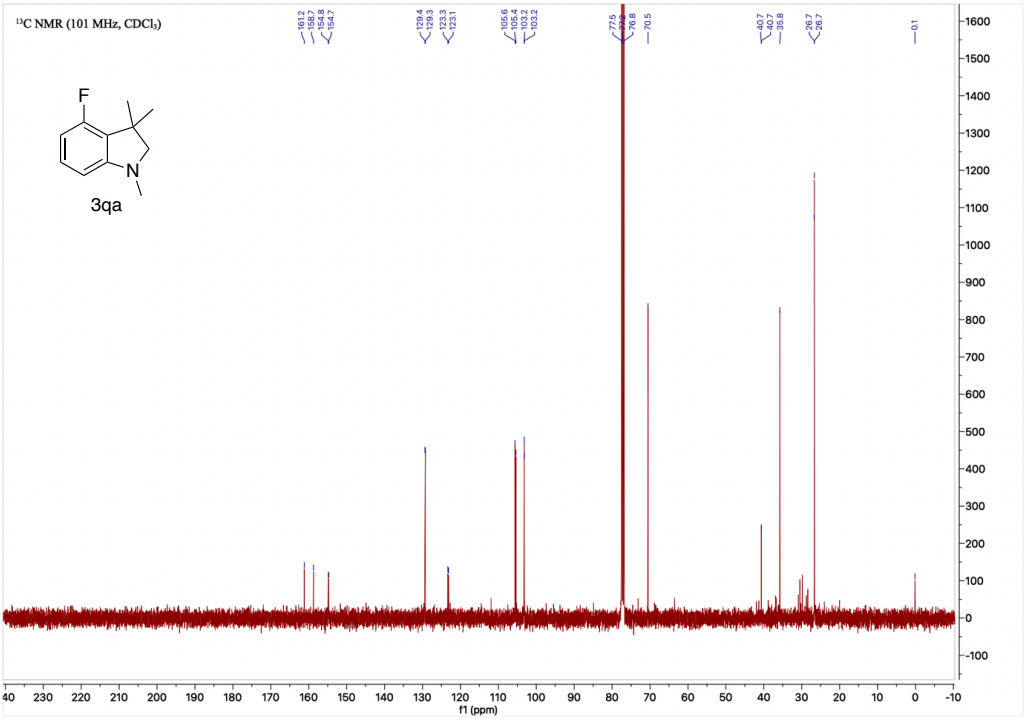

Figure 3.50. ^{19}F NMR Spectrum of **3qa**

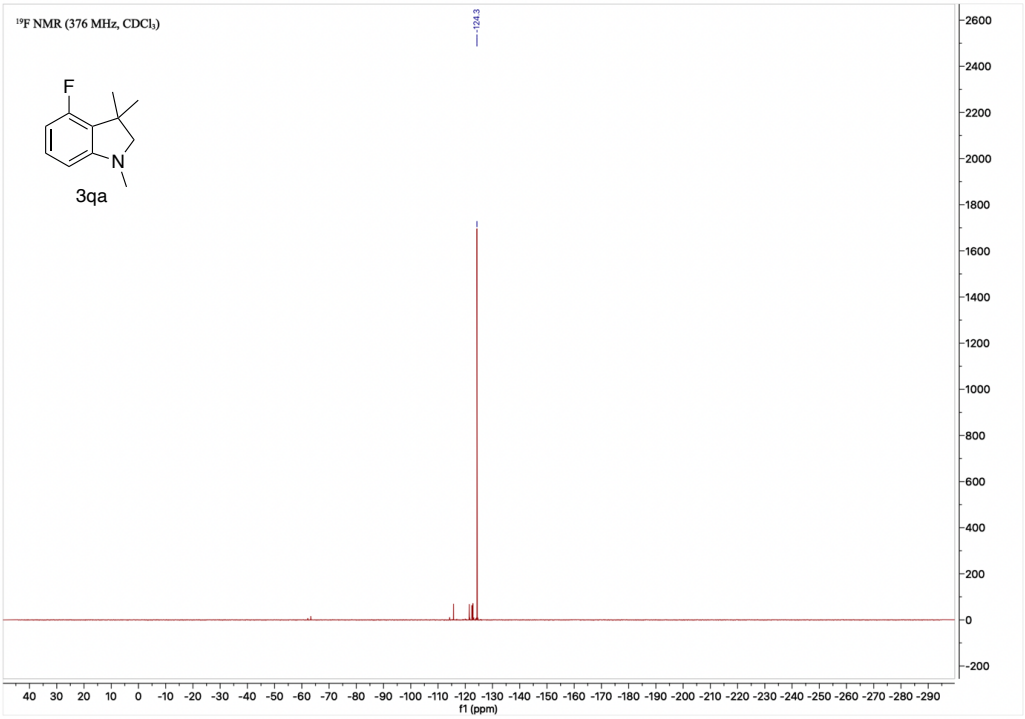

Figure 3.51. ^{1}H NMR Spectrum of **3ra**

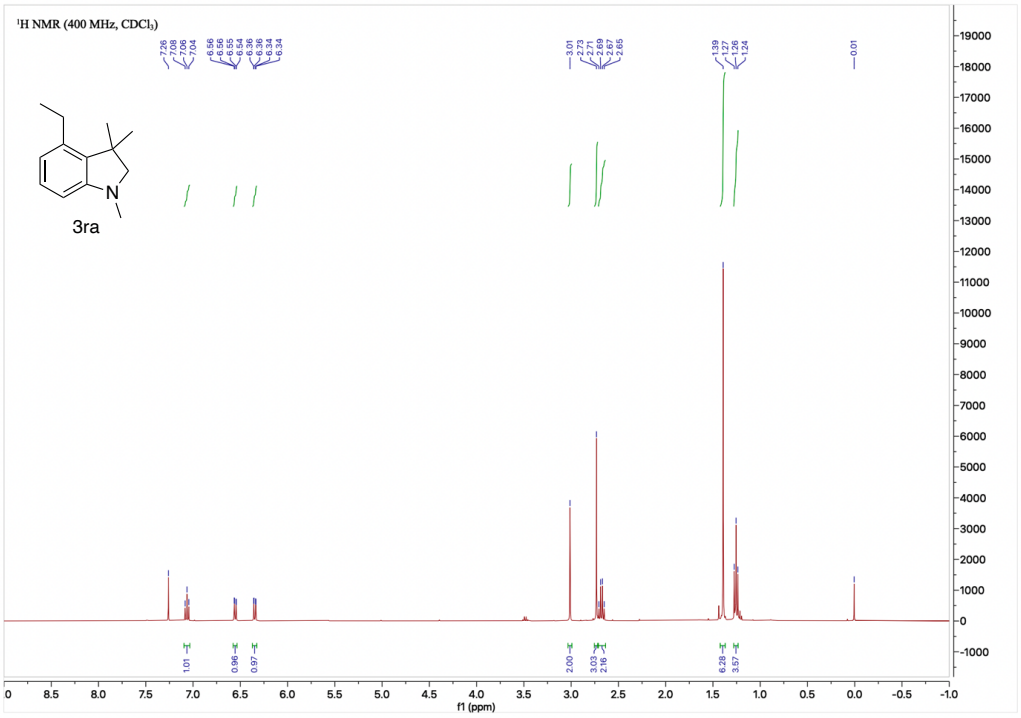

Figure 3.52. ^{13}C NMR Spectrum of **3ra**

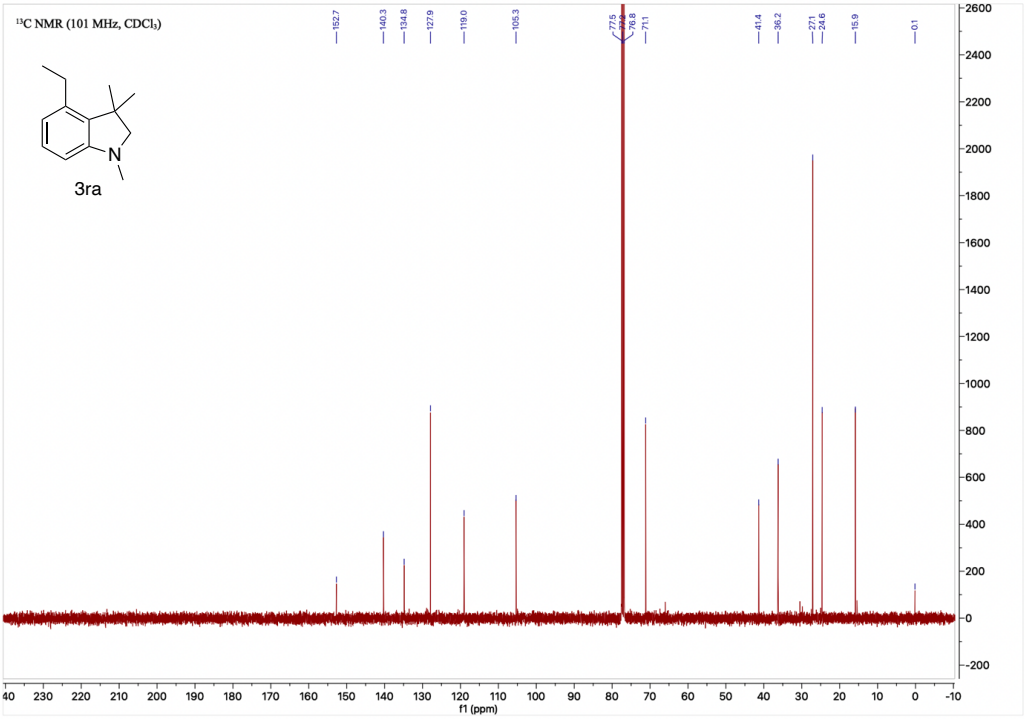

Figure 3.53. ^{1}H NMR Spectrum of **3sa**

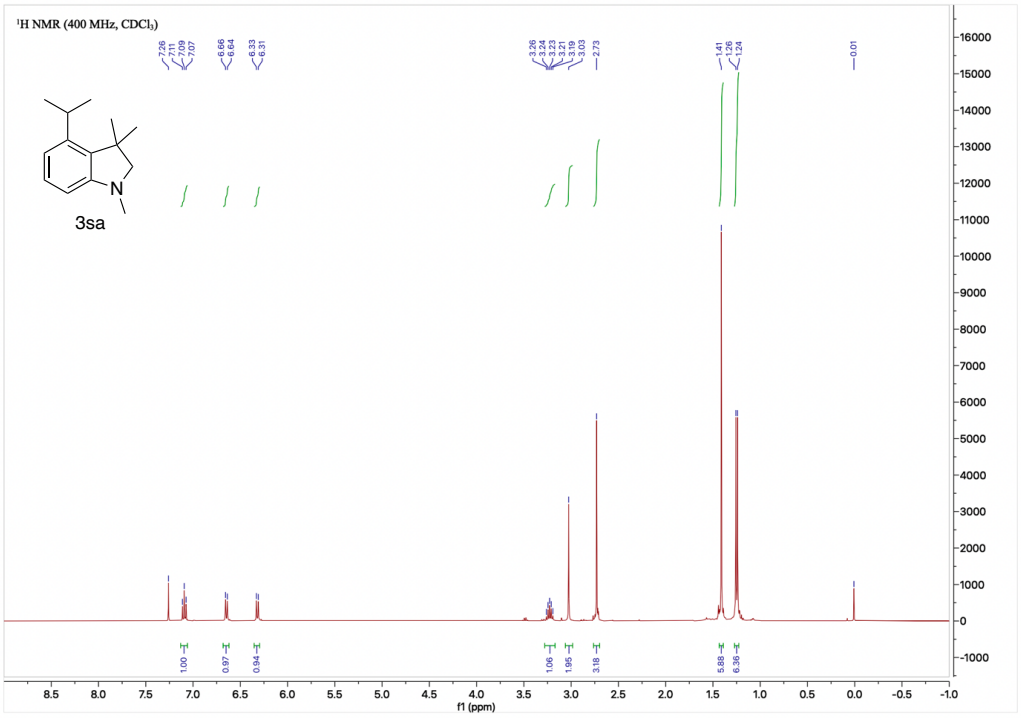

Figure 3.54. ^{13}C NMR Spectrum of **3sa**

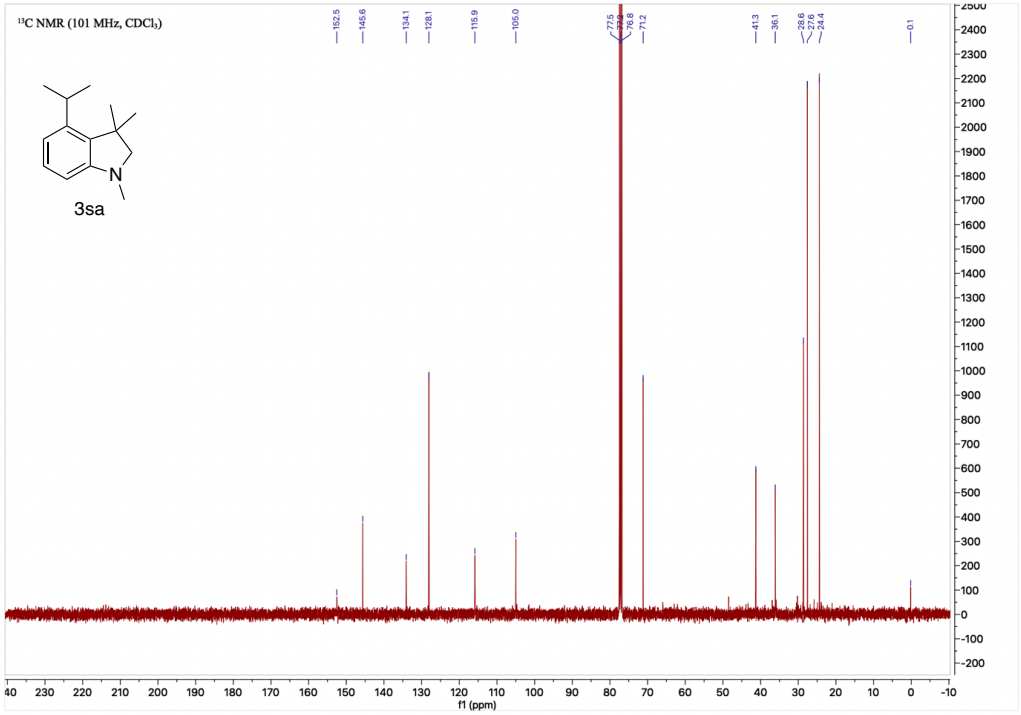

Figure 3.55. ^{1}H NMR Spectrum of **3ta**

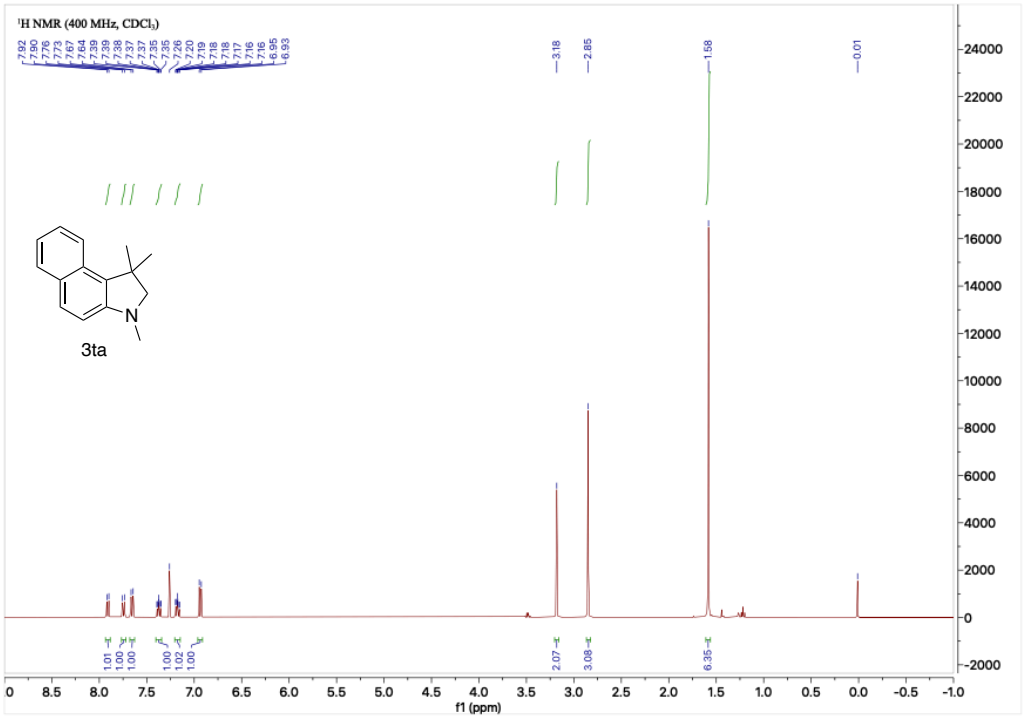

Figure 3.56. ^{13}C NMR Spectrum of **3ta**

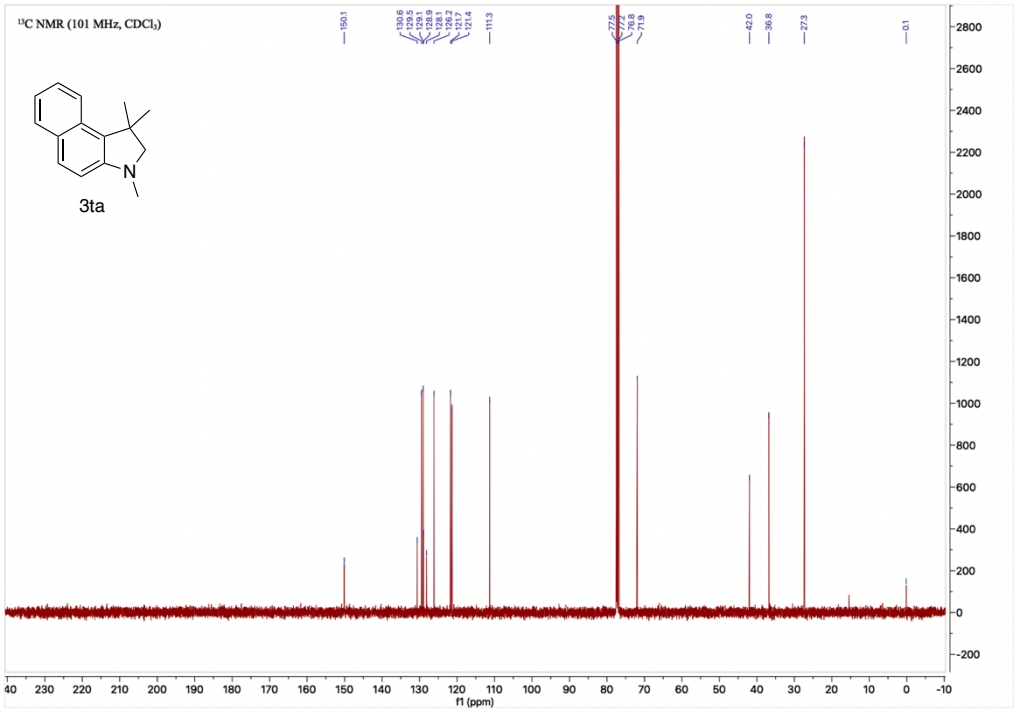

Figure 3.57. ^{1}H NMR Spectrum of **3ua**

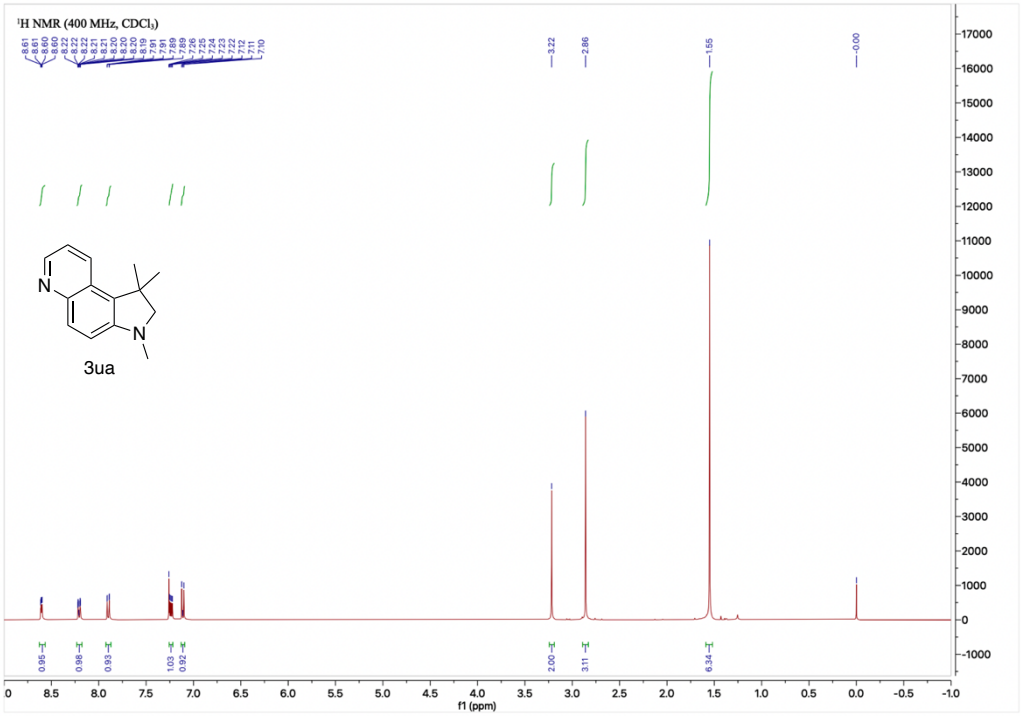

Figure 3.58. ^{13}C NMR Spectrum of **3ua**

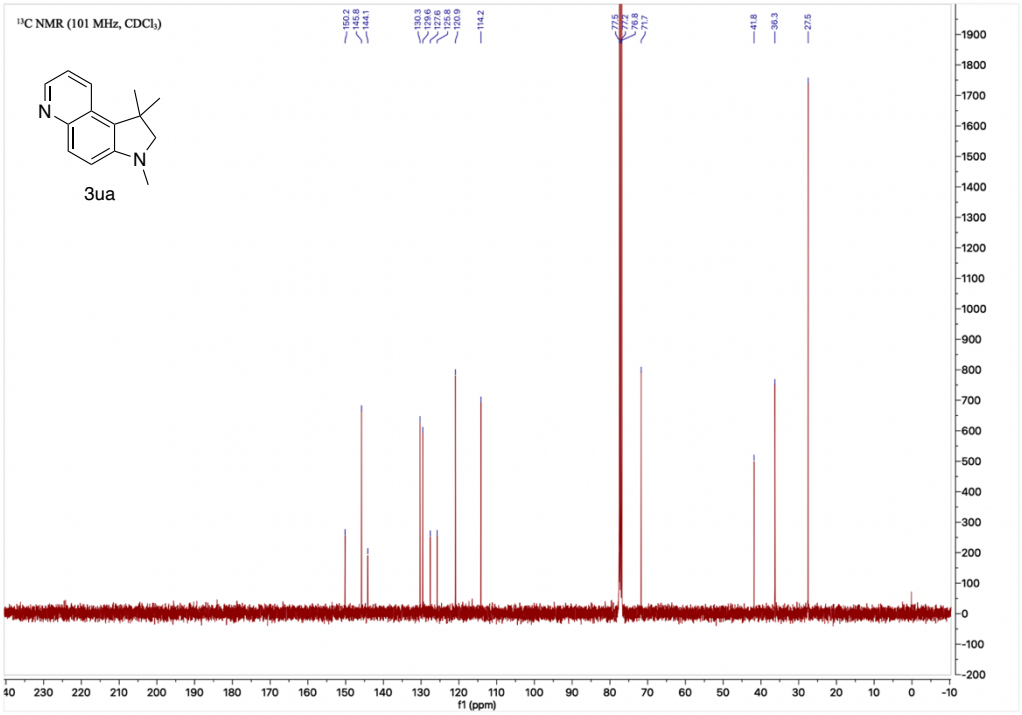

Figure 3.59. ^{1}H NMR Spectrum of **3va**

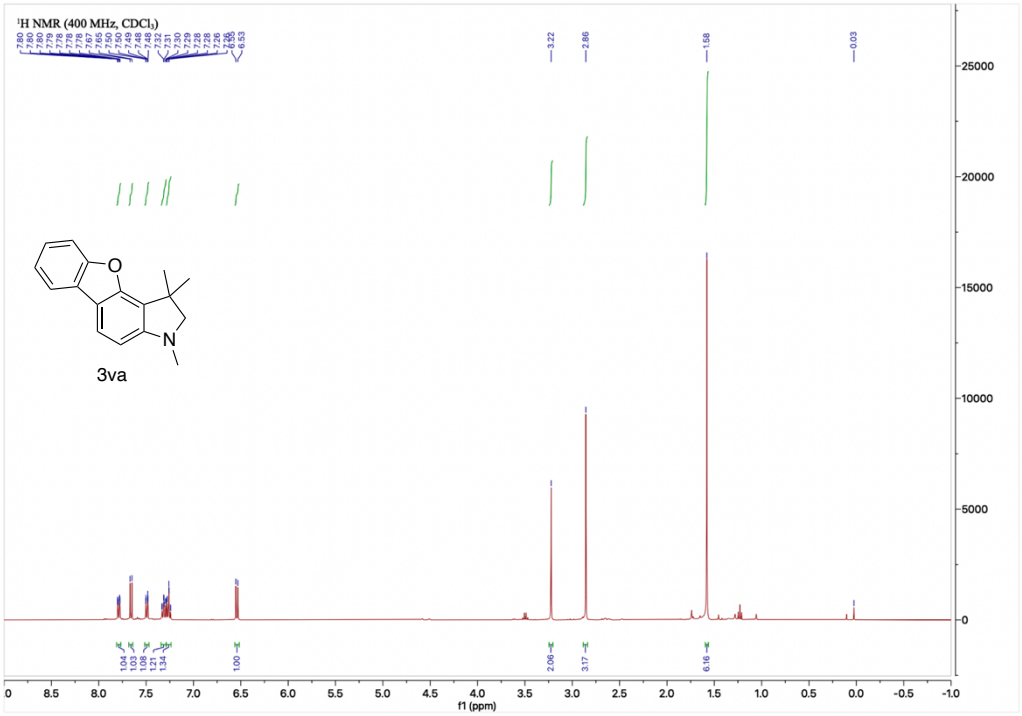

Figure 3.60. ^{13}C NMR Spectrum of **3va**

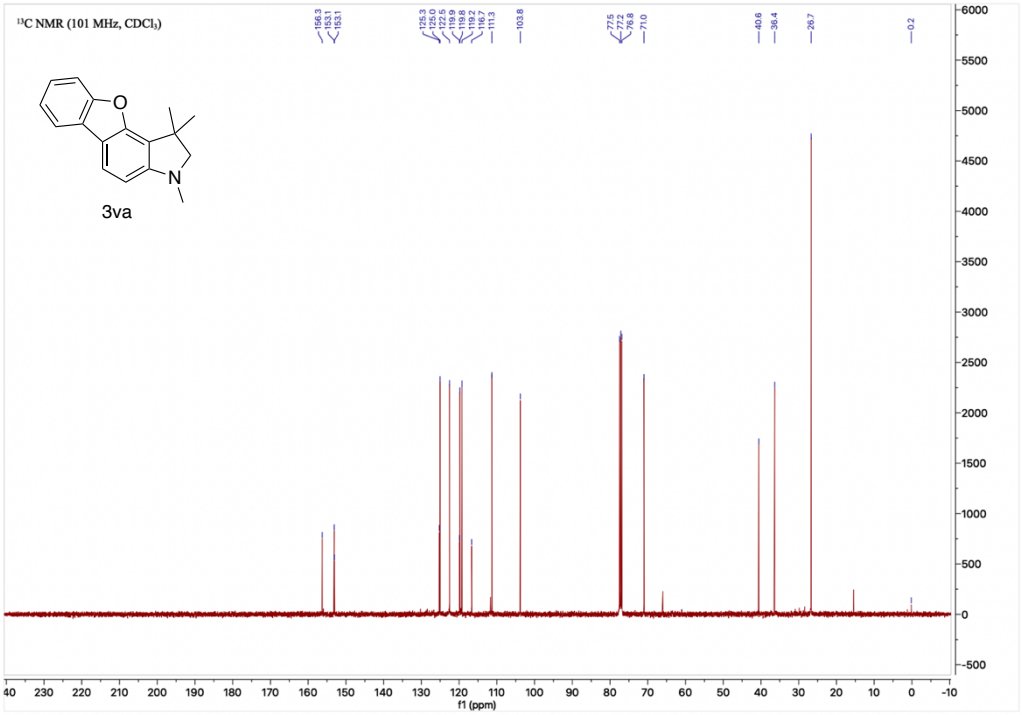

Figure 3.61. ^{1}H NMR Spectrum of **3ab**

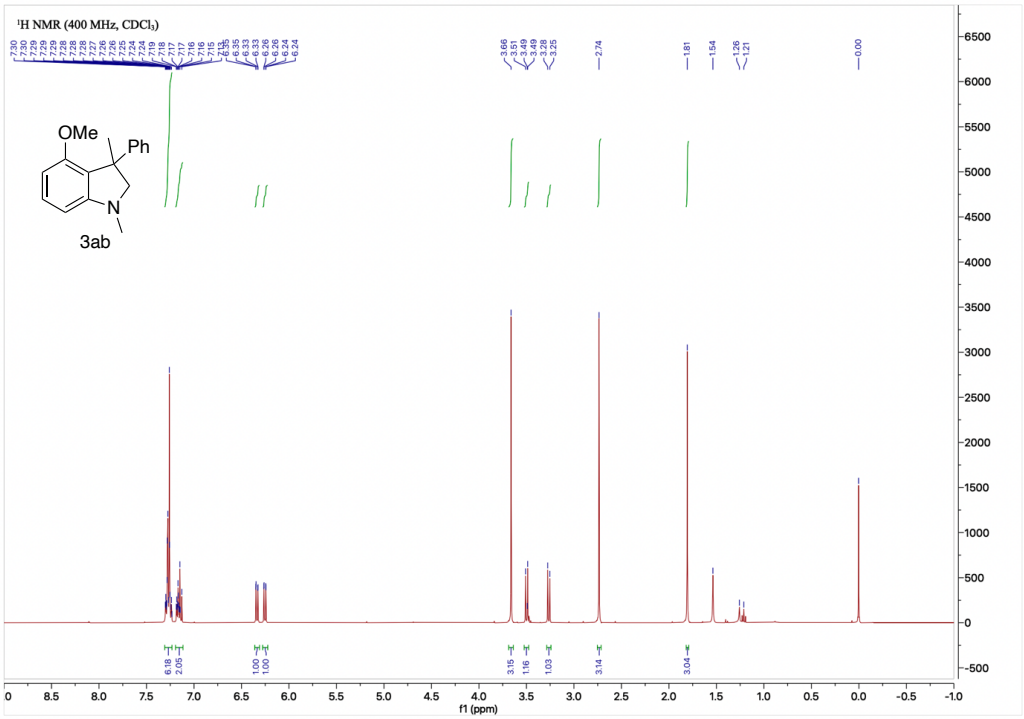

Figure 3.62. ^{13}C NMR Spectrum of **3ab**

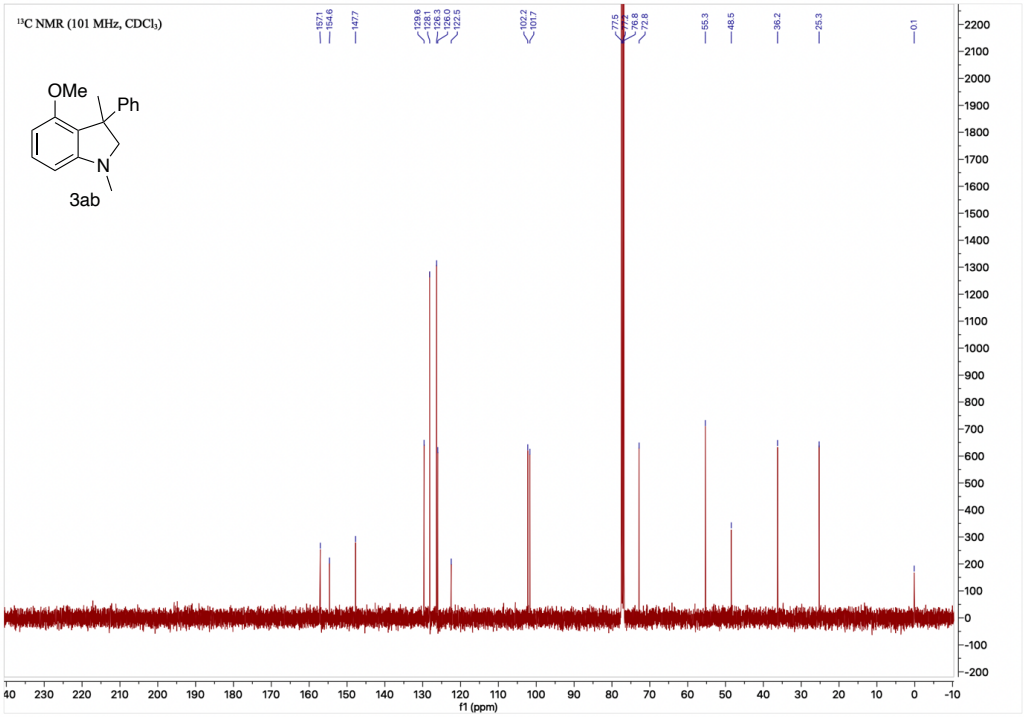

Figure 3.63. ^{1}H NMR Spectrum of **3ac**

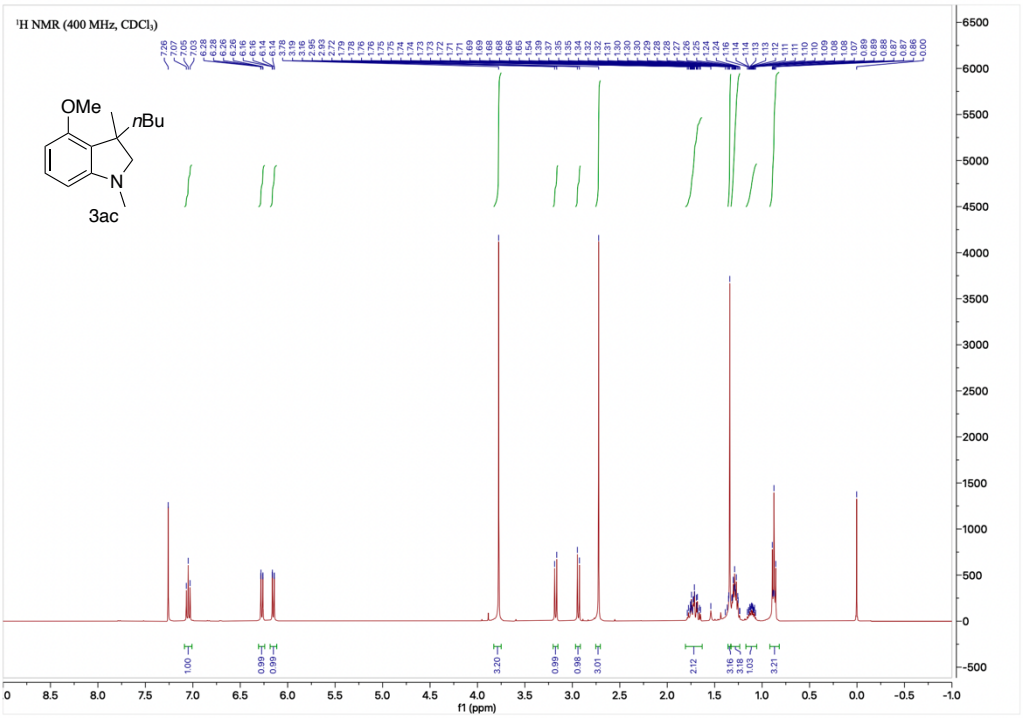

Figure 3.64. ^{13}C NMR Spectrum of **3ac**

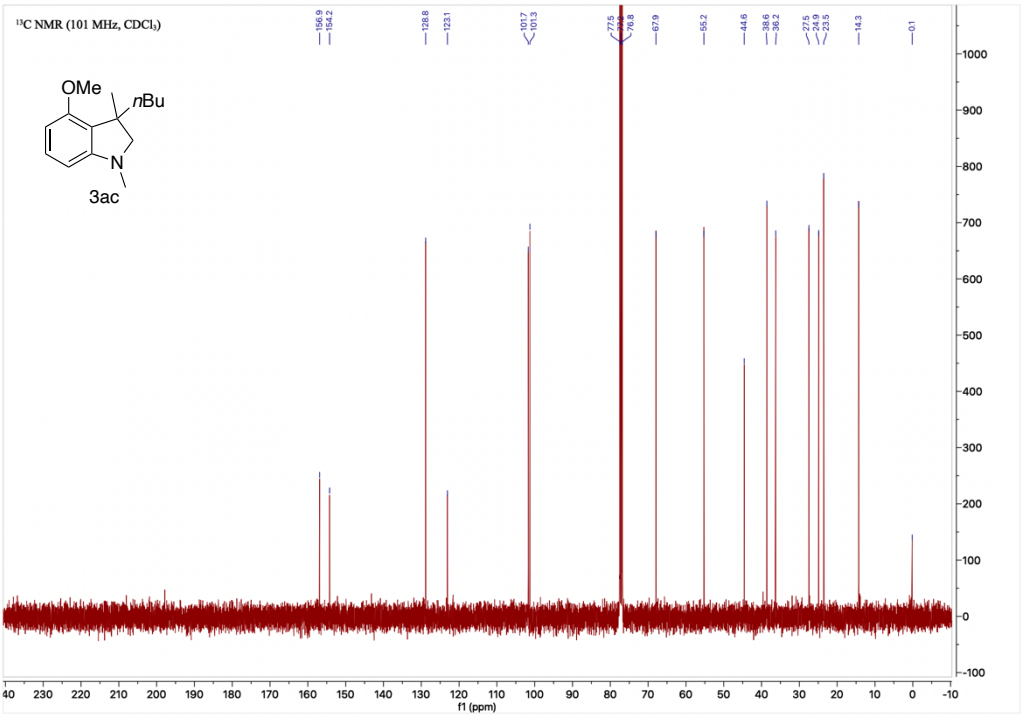

Figure 3.65. ^{1}H NMR Spectrum of **3ad**

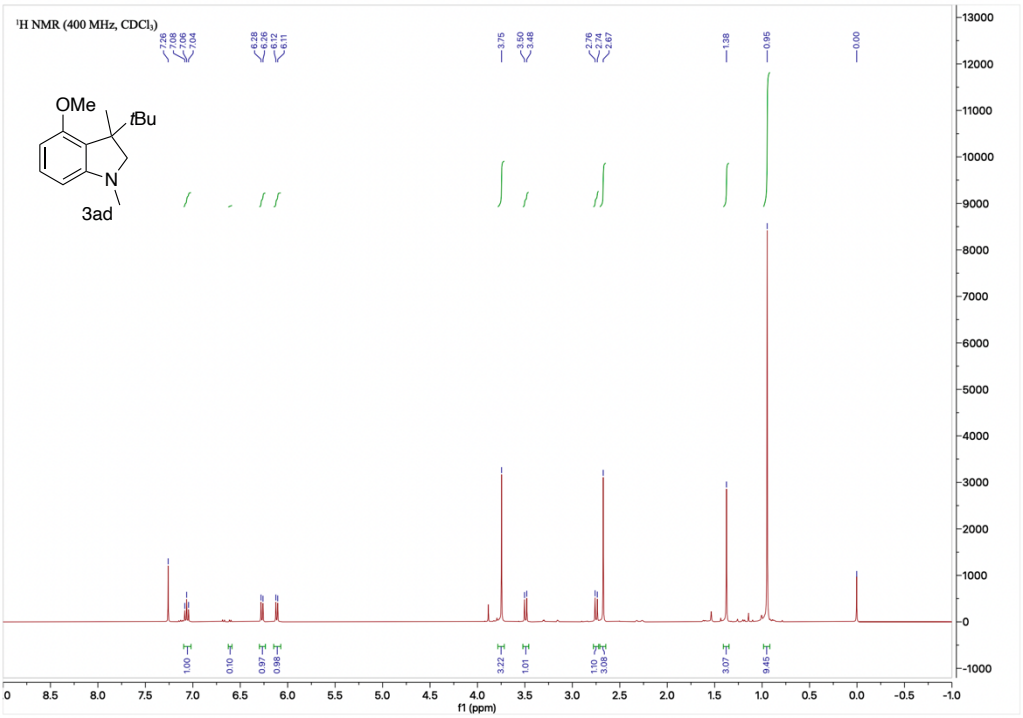

Figure 3.66. ^{13}C NMR Spectrum of **3ad**

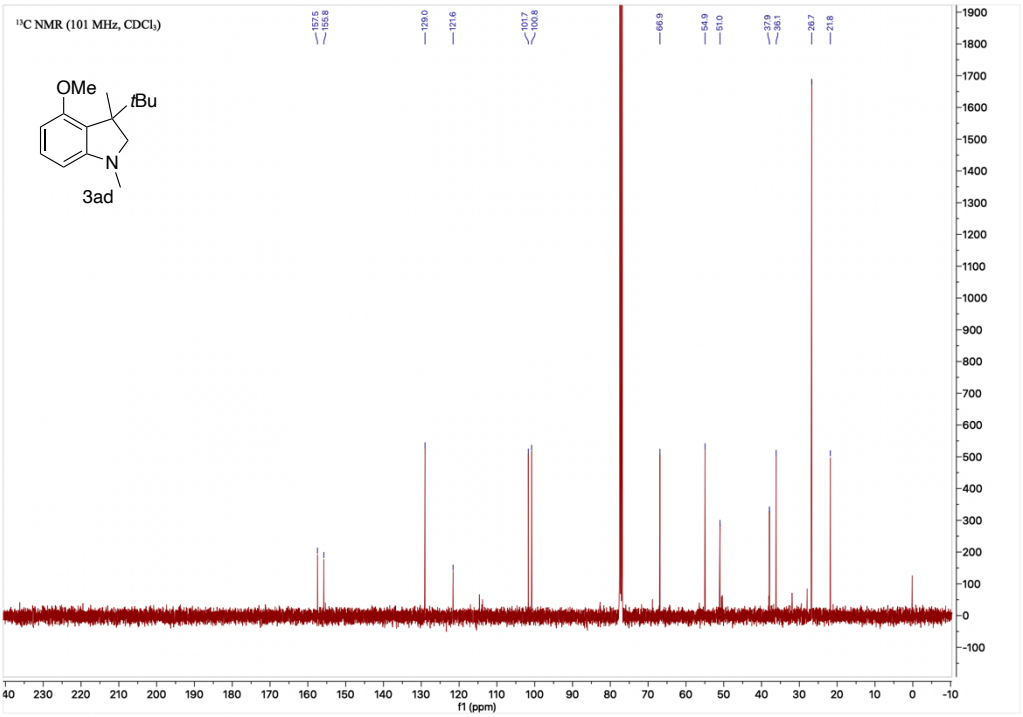

3.6. Chiral-Phase HPLC Traces

Figure 3.67. HPLC trace of racemic **3ab**

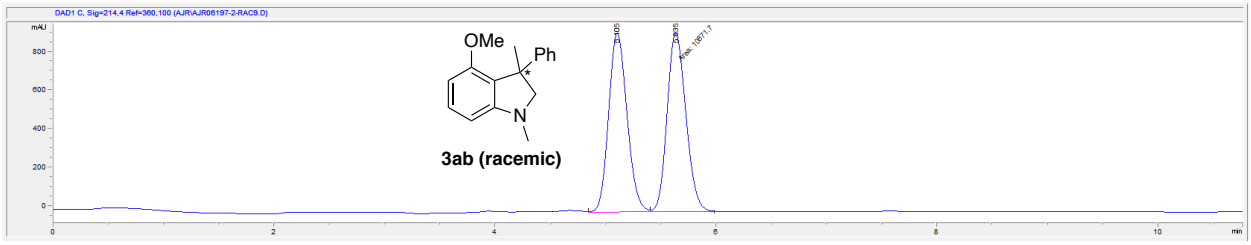

#	Time	Area	Height	Width	Area%	Symmetry
1	5.105	10668.4	928.5	0.178	49.528	0.835
2	5.635	10871.7	931.1	0.1946	50.472	0.815

Conditions: CHIRALPAK IB; 3% *i*PrOH/hexanes; 1.0 mL/min; 4 µL injection volume

Figure 3.68. HPLC trace of enantioenriched **3ab** (46% *ee*)

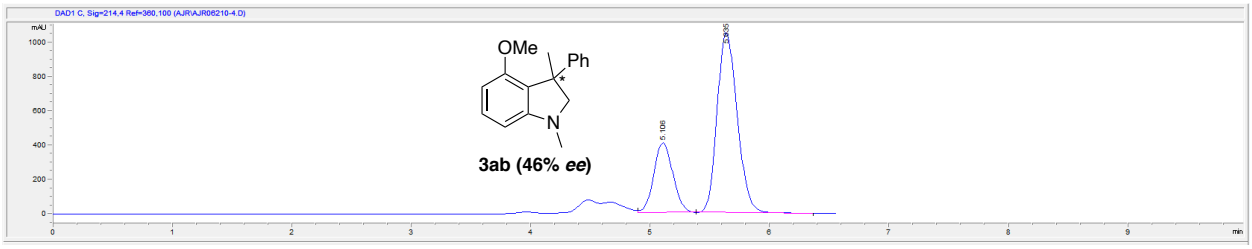

#	Time	Area	Height	Width	Area%	Symmetry
1	5.106	4539.4	407.3	0.174	26.943	0.888
2	5.635	12309.1	1050.1	0.1808	73.057	0.779

Conditions: CHIRALPAK IB; 3% *i*PrOH/hexanes; 1.0 mL/min; 4 µL injection volume

3.7. References

1. Gribble, G. W. *J. Chem. Soc. Perk. Trans. 1* **2000,** (7), 1045-1075.
2. Humphrey, G. R.; Kuethe, J. T. *Chem. Rev.* **2006,** *106* (7), 2875-2911.
3. Taber, D. F.; Tirunahari, P. K. *Tetrahedron* **2011,** *67* (38), 7195-7210.

4. Yoshikai, N.; Wei, Y. *Asian J. Org. Chem.* **2013,** *2* (6), 466-478.

5. Guo, T.; Huang, F.; Yu, L.; Yu, Z. *Tetrahedron Lett.* **2015,** *56* (2), 296-302.

6. Rago, A. J.; Dong, G. *Green Synth. Catal.* **2021**.

7. Silva, T. S.; Rodrigues, M. T.; Santos, H.; Zeoly, L. A.; Almeida, W. P.; Barcelos, R. C.; Gomes, R. C.; Fernandes, F. S.; Coelho, F. *Tetrahedron* **2019,** *75* (14), 2063-2097.

8. Hua, T.-B.; Xiao, C.; Yang, Q.-Q.; Chen, J.-R. *Chinese Chem. Lett.* **2020,** *31* (2), 311-323.

9. Zhang, D.; Song, H.; Qin, Y. *Acc. Chem. Res.* **2011,** *44* (6), 447-457.

10. Mei, T.-S.; Wang, X.; Yu, J.-Q. *J. Am. Chem. Soc.* **2009,** *131* (31), 10806-10807.

11. Neumann, J. J.; Rakshit, S.; Dröge, T.; Glorius, F. *Angew. Chem., Int. Ed.* **2009,** *48* (37), 6892-6895.

12. Ramirez, T. A.; Wang, Q.; Zhu, Y.; Zheng, H.; Peng, X.; Cornwall, R. G.; Shi, Y. *Org. Lett.* **2013,** *15* (16), 4210-4213.

13. Zheng, H.; Zhu, Y.; Shi, Y. *Angew. Chem., Int. Ed.* **2014,** *53* (42), 11280-11284.

14. Sun, X.; Wu, Z.; Qi, W.; Ji, X.; Cheng, C.; Zhang, Y. *Org. Lett.* **2019,** *21* (16), 6508-6512.

15. Ye, J.; Lautens, M. *Nat. Chem.* **2015,** *7* (11), 863-870.

16. Della Ca', N.; Fontana, M.; Motti, E.; Catellani, M. *Acc. Chem. Res.* **2016,** *49* (7), 1389-1400.

17. Zhao, K.; Ding, L.; Gu, Z. *Synlett* **2019,** *30* (02), 129-140.

18. Wegmann, M.; Henkel, M.; Bach, T. *Org. Biomol. Chem.* **2018,** *16* (30), 5376-5385.

19. Cheng, H.-G.; Chen, S.; Chen, R.; Zhou, Q. *Angew. Chem., Int. Ed.* **2019,** *58* (18), 5832-5844.

20. Wang, J.; Dong, G. *Chem. Rev.* **2019,** *119* (12), 7478-7528.

21. Catellani, M.; Frignani, F.; Rangoni, A. *Angew. Chem., Int. Ed.* **1997,** *36* (1-2), 119-122.

22. Lautens, M.; Piguel, S. *Angew. Chem., Int. Ed.* **2000,** *39* (6), 1045-1046.

23. Candito, D. A.; Lautens, M. *Org. Lett.* **2010,** *12* (15), 3312-3315.

24. Liu, C.; Liang, Y.; Zheng, N.; Zhang, B.-S.; Feng, Y.; Bi, S.; Liang, Y.-M. *Chem. Commun.* **2018,** *54* (27), 3407-3410.

25. Dong, Z.; Dong, G. *J. Am. Chem. Soc.* **2013,** *135* (49), 18350-18353.

26. Rago, A. J.; Dong, G. *Org. Lett.* **2021,** *23*, 3755-3760.

27. Busacca, C. A.; Senanayake, C. H. In *Comprehensive Chirality*, Carreira, E. M.; Yamamoto, H., Eds. Elsevier: Amsterdam, 2012; pp 167-216.

28. Zhao, K.; Xu, S.; Pan, C.; Sui, X.; Gu, Z. *Org. Lett.* **2016,** *18* (15), 3782-3785.

29. Liu, Z.-S.; Qian, G.; Gao, Q.; Wang, P.; Cheng, H.-G.; Wei, Q.; Liu, Q.; Zhou, Q. *ACS Catal.* **2018,** *8* (6), 4783-4788.

30. Mok, N. Y.; Chadwick, J.; Kellett, K. A. B.; Casas-Arce, E.; Hooper, N. M.; Johnson, A. P.; Fishwick, C. W. G. *J. Med. Chem.* **2013,** *56* (5), 1843-1852.

31. Lautens, M.; Paquin, J.-F.; Piguel, S. *J. Org. Chem.* **2002,** *67* (11), 3972-3974.

32. Ho Park, K.; Chen, R.; Chen, D. Y. K. *Chem. Sci.* **2017,** *8* (10), 7031-7037.

33. Liang, H.; He, X.; Zhang, Y.; Chen, B.; Ouyang, J.-s.; Li, Y.; Pan, B.; Subba Reddy, C. V.; Chan, W. T. K.; Qiu, L. *Chem. Commun.* **2020,** *56* (77), 11429-11432.

34. An, Y.; Zhang, B.-S.; Zhang, Z.; Liu, C.; Gou, X.-Y.; Ding, Y.-N.; Liang, Y.-M. *Chem. Commun.* **2020,** *56* (44), 5933-5936.

35. Dong, Z.; Wang, J.; Ren, Z.; Dong, G. *Angew. Chem., Int. Ed.* **2015,** *54* (43), 12664-12668.

36. Amara, R.; Bentabed-Ababsa, G.; Hedidi, M.; Khoury, J.; Awad, H.; Nassar, E.; Roisnel, T.; Dorcet, V.; Chevallier, F.; Fajloun, Z.; Mongin, F. *Synthesis* **2017,** *49* (19), 4500-4516.

37. Wu, X.; Zhou, J. *Chem. Commun.* **2013,** *49* (94), 11035-11037.

38. Bourgeois, J.; Dion, I.; Cebrowski, P. H.; Loiseau, F.; Bédard, A.-C.; Beauchemin, A. M. *J. Am. Chem. Soc.* **2009,** *131* (3), 874-875.

39. Ma, W.; Fang, J.; Ren, J.; Wang, Z. *Org. Lett.* **2015,** *17* (17), 4180-4183.

40. He, J.; Xue, Y.; Han, B.; Zhang, C.; Wang, Y.; Zhu, S. *Angew. Chem., Int. Ed.* **2020,** *59* (6), 2328-2332.

(This chapter has not been previously published at the time of writing.)

CHAPTER 4

Unexpected *Ortho*-Heck Reaction of Aryl Iodides under the Catellani Conditions

4.1. Introduction

An unexpected *ortho*-Heck reaction has been discovered during the study of the palladium/norbornene (Pd/NBE) catalysis. Under the Catellani reaction conditions in the presence of lithium salts and olefins, the Heck coupling takes place at the *ortho* position instead of the commonly observed *ipso* position; meanwhile, a norbornyl group is introduced at the arene *ipso* position. Systematic deuterium labelling and crossover experiments suggest an unusual 1,4-palladium migration/intramolecular hydrogen transfer pathway. The knowledge gained in this study could provide insights for future development of the Pd/NBE catalysis.

Figure 4.1. *Ortho*-Heck Reaction of Aryl Iodides

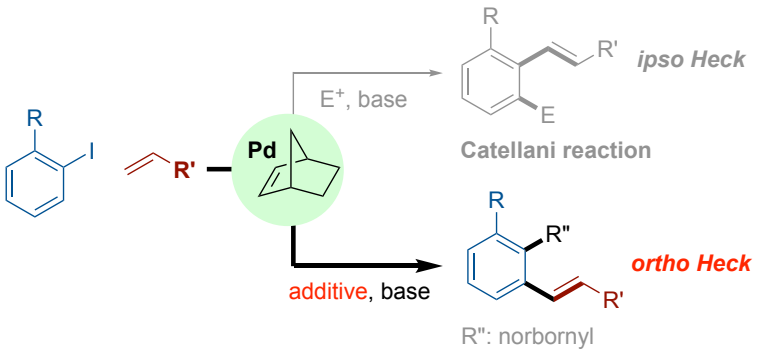

Palladium/norbornene (Pd/NBE) cooperative catalysis,[1-6] originally discovered by Catellani,[7] has emerged as a versatile and useful means to achieve vicinal difunctionalization of arenes over the past two decades. In a typical Catellani reaction, through forming an aryl-norbornyl-palladacycle (ANP) intermediate, an electrophile is coupled at the arene *ortho* position and a nucleophile or an olefin reacts at the *ipso* position.[8-26] In particular, the use of a Heck reaction, the coupling with an olefin, for *ipso* functionalization is among one of the most extensively studied reaction modes in the Pd/NBE catalysis (**Scheme 4.2a**). However, during our recent exploration of a potential *ortho* borylation reaction, an unexpected *ortho* (instead of *ipso*) Heck product was observed as the major product under typical Catellani conditions, except using catecholboryl chloride as the electrophile and cesium acetate as the base (**Scheme 4.1**).

Scheme 4.1. Initial Reaction Design and Unexpected Product

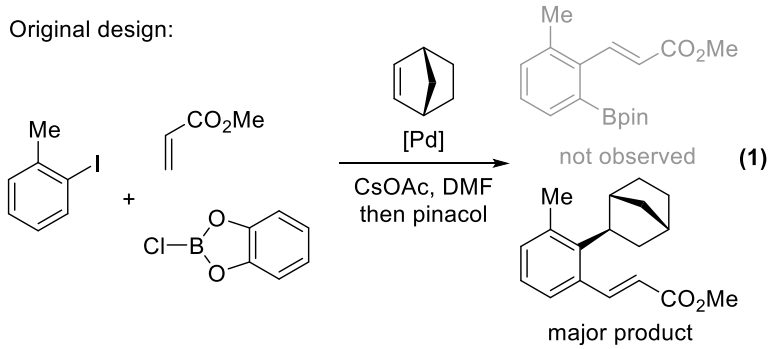

This result is unusual because olefins, such as acrylates, have not been known as electrophiles in the Pd/NBE catalysis.[1-6] In addition, careful analysis of other Catellani-type reactions also revealed formation of similar side-products, though in small quantities (*vide infra*, **Scheme 4.8b**).[27] The intriguing reactivity and site-selectivity "switch" motivated us to better understand this unusual reaction, which is anticipated to benefit future development of the Pd/NBE catalysis. Herein, we describe the discovery, mechanistic study, and reaction scope of the Pd-catalyzed, NBE-mediated, *ortho*-Heck reaction (**Scheme 4.2b**).

Scheme 4.2. *Ortho*-Heck *vs* a Typical Catellani Reaction

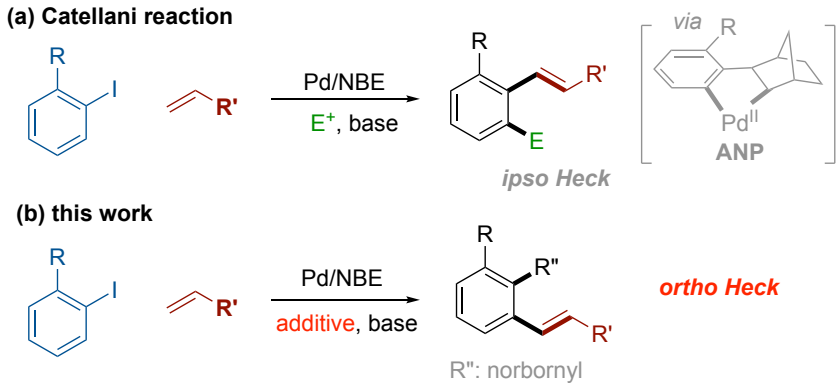

4.2. Results & Discussion

Our study began with optimizing the reaction conditions using aryl iodide **1a** as a model substrate (**Table 4.1**). A high yield of the *ortho*-Heck product (4a) was obtained using $Pd(dba)_2$ and trifurylphosphine as the metal/ligand combination (entry 1) and Li_2CO_3 as the base. The use of Bu_2BOTf and LiBr as additives significantly increased the yield of the reaction, though their roles are not essential for product formation (entries 1-4). LiBr as the sole additive (entry 2) was found to substantially increase the yield of the reaction relative to no additives (entry 4). This could be due to the bromide anions acting as ligands towards palladium, preventing the carbonate anions, which can facilitate formation of the ANP intermediate,[1] from coordinating to palladium. As expected, in the absence of the Pd catalyst, no *ortho*-Heck product was observed (entry 5). Using $Pd(OAc)_2$ instead of $Pd(dba)_2$ decreased the yield (entry 6). Li_2CO_3 was found to be essential for this transformation, since using K_2CO_3 or Cs_2CO_3 instead resulted in significantly diminished yields under the current conditions (entries 7-9). The potassium and sodium bases were, however, found to perform somewhat better without Bu_2BOTf present in the reaction (*vide infra*). DMF proved to be a better solvent, whereas using other solvents, such as the less polar 1,4-dioxane or toluene, gave poor results (entries 10 and 11). Finally, addition of *n*BuI as an electrophile could still afford 42% of the *ortho*-Heck product without furnishing the regular Catellani product (entry 12).

Table 4.1. Selected Optimization of the Reaction Conditions[a] (change to chemdraw???)

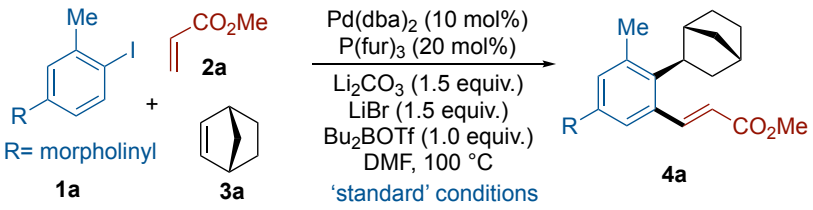

entry	changes from the 'standard' conditions	yield of 4a (%)[b]	yield of 4aa (%)[b]
1	None	80 (69)[c]	10
2	Without Bu_2BOTf	70	10
3	Without LiBr	57	21
4	Without Bu_2BOTf or LiBr	28	21
5	Without catalyst	n.d.	n.d.
6	$Pd(OAc)_2$ instead of $Pd(dba)_2$	55	11
7	Without Li_2CO_3	n.d.	n.d.
8	K_2CO_3 instead of Li_2CO_3	3	1
9	Cs_2CO_3 instead of Li_2CO_3	16	5
10	1,4-dioxane instead of DMF	4	n.d.
11	Toluene instead of DMF	n.d.	n.d.
12	With 1.0 equiv. *n*BuI[d]	42	4

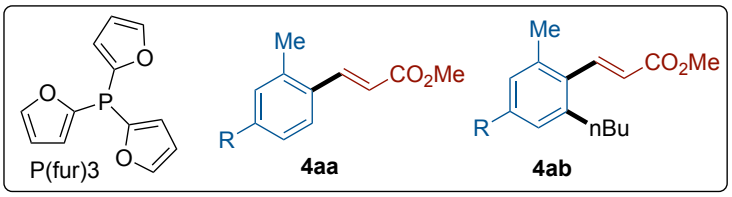

[a]Unless otherwise noted, all reactions were carried out with **1a** (0.1 mmol), **2a** (0.12 mmol), and **3a** (0.1 mmol) in 1.0 mL of DMF for 18 h. [b]NMR yields determined using 1,1,2,2-tetrachloroethane as the internal standard. [c]Conducted with **1a** (0.2 mmol), **2a** (0.24 mmol), and

3a (0.1 mmol) in 2.0 mL of DMF for 18h; isolated yield is reported. [d]Catellani product **4ab** was not observed and 25% 1a was recovered. n.d.= not detected.

The reaction without the boron additive was also investigated (**Table 4.2**). In this regard, we now observe that other carbonate salts can deliver larger quantities of the desired product **4a**. It is possible that some interaction between the cations and boron, perhaps formation of a boronate complex, caused the reaction to significantly lose efficiency in the presence of the additive. Based on these results, LiBr is clearly a critical additive for improving the efficiency of the reaction. For example, Cs_2CO_3 alone essentially did not produce the desired *ortho*-Heck product. However, the addition of LiBr allowed for the reaction to reach a modest 44% yield.

Table 4.2. Investigating the Base *without* the Boron Additive[a]

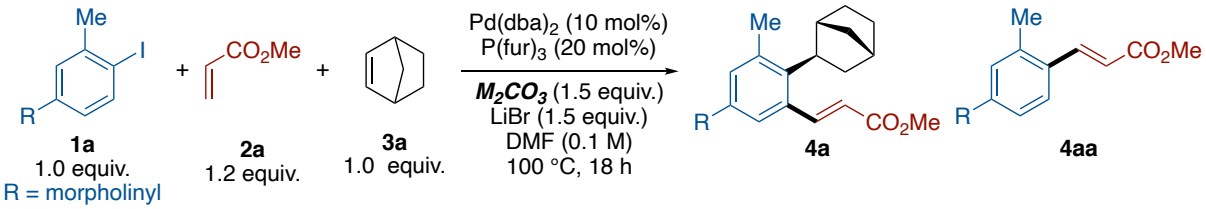

	Carbonate salt	% **1a** recovered	% yield **4a**	% yield **4aa**
w/o LiBr	Na_2CO_3	Not observed	15%	10%
	K_2CO_3	Not observed	23%	16%
	Cs_2CO_3	Not observed	1%	2%
w/ LiBr	Na_2CO_3	Not observed	49%	13%
	K_2CO_3	Not observed	61%	8%
	Cs_2CO_3	Not observed	44%	13%

[a]All reactions were carried out with **1a** (0.1 mmol), **2a** (0.12 mmol), and **3a** (0.1 mmol) in 1.0 mL of DMF for 18 h. NMR yields determined using 1,1,2,2-tetrachloroethane as the internal standard.

Regarding the reaction mechanism, two pathways could be proposed for the formation of the *ortho*-Heck product (**Scheme 4.3**). Path (**a**) involves first forming the ANP intermediate via

ortho C−H palladation,[28, 29] followed by migratory insertion (or conjugate addition) of the aryl group to the olefin. The following β-hydride elimination and C−H reductive elimination steps could give the *ortho*-Heck product. Alternatively, in path (**b**), a 1,4-palladiuim shift[30, 31] could take place instead of forming the ANP intermediate, and the resulting aryl-palladium species could then undergo a typical Heck reaction pathway to afford the product.

Scheme 4.3. Possible Reaction Pathways

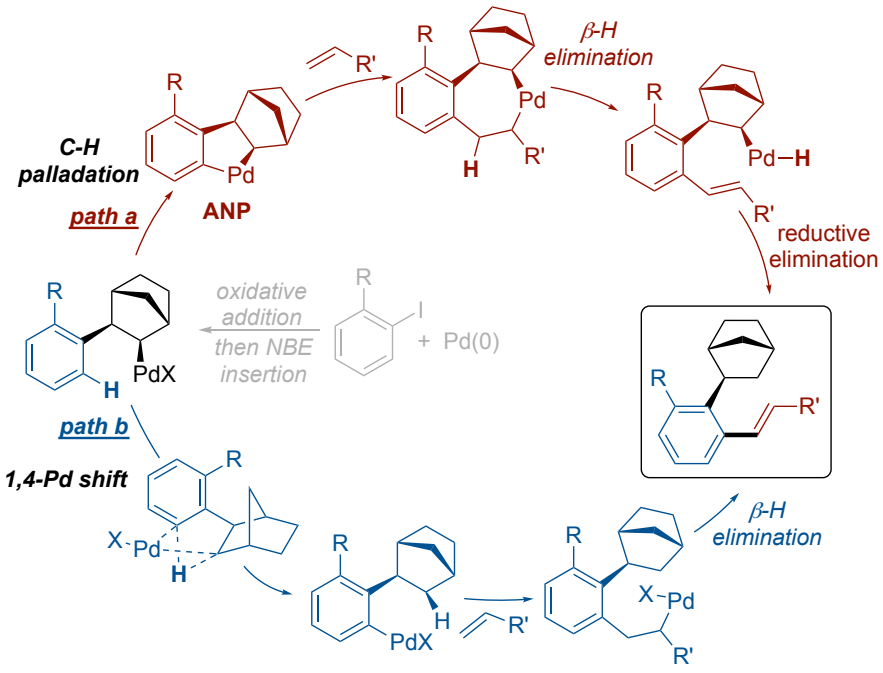

To differentiate the two mechanisms, a systematic deuterium labeling study was carried out (**Scheme 4.4**). First, we employed a method recently developed by Ackermann and Bechtoldt to transform **2a** into deuterium labeled **2a-d$_3$**.[32] When this labeled acrylate was used in place of **2a**, no deuterium incorporation was observed at the C3 position of the norbornyl group (**Scheme 4.4a**). This result strongly disfavors path (**a**), in which a hydride would be anticipated to transfer from the acrylate *beta*-position to the norbornyl C3 position. In addition, the C3 hydrogen was found to be not originating from a proton source, as the addition of deuterated methanol or acetic acid led

to no observable deuteration on the norbornyl moiety (**Scheme 4.4b**). This result alone *excludes* a pathway involving ANP formation, followed by protonation of the norbornyl group. On the other hand, using fully deuterated 1-iodonaphthalene (**1i-d$_7$**) resulted in complete deuteration at the C3 position, even in the presence of various proton sources (**Scheme 4.4c**). Additionally, both the deuterium and the aryl group were found to be located at the norbornyl *exo* positions, as characterized by various 2D-NMR experiments. These results indicate that the C3 hydrogen originally comes from the arene substrate and could migrate through a 1,4-metal shift.[33-35]

Scheme 4.4. Deuterium Labeling Studies[a,b]

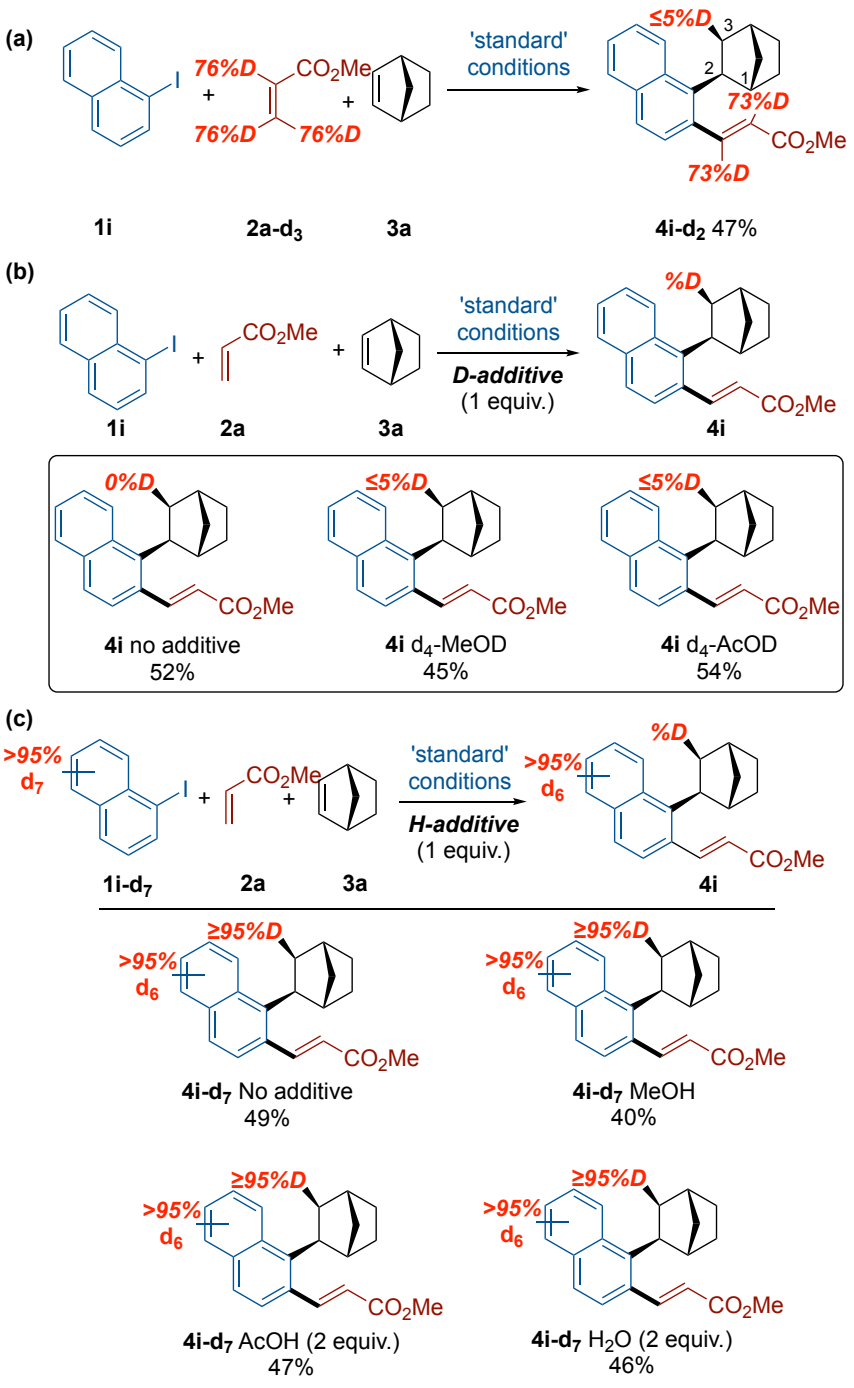

[a]Unless otherwise noted, all reactions were carried out with **1i** or **1i-d**$_7$ (0.1 mmol), **2a** (0.12 mmol), and **3a** (0.1 mmol) in 1.0 mL of DMF for 18 h. NMR yields determined using 1,1,2,2-

tetrachloroethane as the internal standard. [b]NMR (^{1}H or ^{2}H) analysis was used to determine deuterium incorporation on the norbornyl ring.

Moreover, an isotope crossover experiment was conducted with a 1:1 ratio of deuterated **1i-d$_7$** and non-deuterated substrate **1a** (**Scheme 4.5**). The absence of deuterium crossover supports an *intramolecular* hydrogen transfer from the aryl *ortho* position to the norbornyl C3 position. Taken together, all of the mechanistic data obtained are consistent with the 1,4-palladium shift pathway (**b**).[36, 37] The readily available **1i-d$_7$** also prompted us to investigate whether or not a strong KIE could be observed between **1i** and **1i-d$_7$**. Within 15 minutes of beginning the reaction, 19% yield of the product could be obtained with 40% of the deuterated product, suggesting that a KIE of ~1.5 was being observed. While more data between t = 0 and t = 15 minutes was not obtained, it is likely that the *ortho*-C–H bond is not involved in the rate-determining step of this transformation.

Scheme 4.5. Isotope Crossover Experiment and Preliminary KIE Result[a,b]

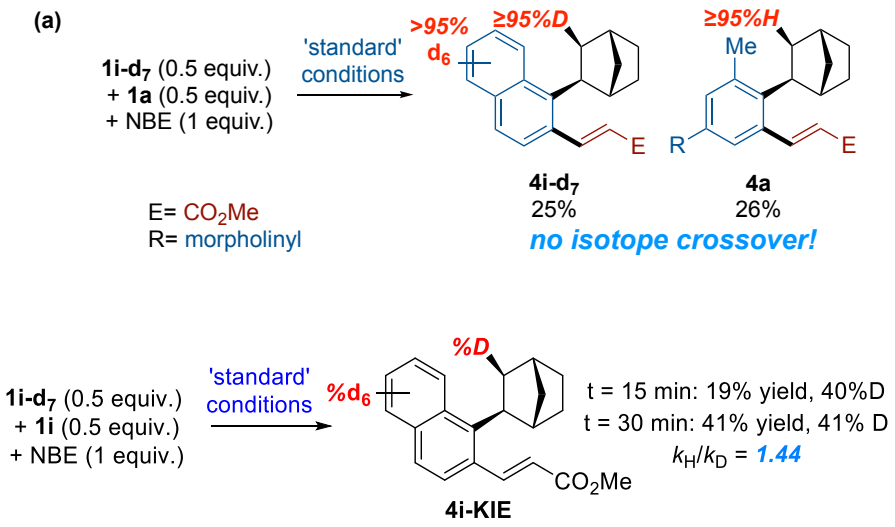

[a]Unless otherwise noted, all reactions were carried out with **1i** or **1i-d$_7$** (0.1 mmol), **2a** (0.12 mmol), and **3a** (0.1 mmol) in 1.0 mL of DMF for 18 h. NMR yields determined using 1,1,2,2-

tetrachloroethane as the internal standard. ^{b}NMR (^{1}H or ^{2}H) analysis was used to determine deuterium incorporation on the norbornyl ring.

Next, the scope and functional group tolerance of the transformation were investigated next (**Scheme 4.6**). First, olefins with a strongly electron-withdrawing group, such as an ester, amide, ketone, nitrile, or sulfone, can all be coupled in good yields (**4a**-**4g**).[38] The reaction is also scalable; on a 1 mmol scale, product **4a** was isolated in 75% yield. Interestingly, less electron-deficient styrene also provided the desired product (**4h**), albeit in 20% yield. Additionally, the structure of product **4d** was unambiguously elucidated by X-ray crystallography. Both naphthalene- (**4i**) and quinoline-based (**4j**) substrates delivered the desired product smoothly. In general, electron-donating substituents *para* to the iodide (**4a**, **4k**, **4l**) gave higher yields, though electron-neutral (**4m**, **4n**) and -poor (**4o**, **4p**) arenes also delivered their corresponding *ortho*-Heck products. Small *ortho* substituents, such as –OMe (**4q**) and –F (**4r**), can also be tolerated. Interestingly, having fluoride as the *ortho*-substituent (**4r**) resulted in a sequential double 1,4-migration side-product (**4ra**), in which two NBE insertions took place before the reaction with acrylate. Note that a similar multiple sequential NBE insertion has been previously observed in a Rh-catalyzed system.[39] In the absence of an *ortho* substituent, the *ortho*-Heck product (**4s**) can still form. Additionally, an alkenyl iodide (**4t**) was shown to be a competent substrate, producing a satisfying 59% yield of the desired product. Moreover, NBEs with substitutions at the 5- and 6-positions are suitable coupling partners (**4u**-**4v**). Unsurprisingly, unsymmetrical dicyclopentadiene (**4u**) gave an inseparable mixture of alkene regio-isomers. Under the current reaction conditions, 2,5-norbornadiene was unable to deliver the corresponding product, only producing the *ipso*-Heck side product for some unknown reason (**4w**).

Scheme 4.6. Substrate Scope of the Transformation[a]

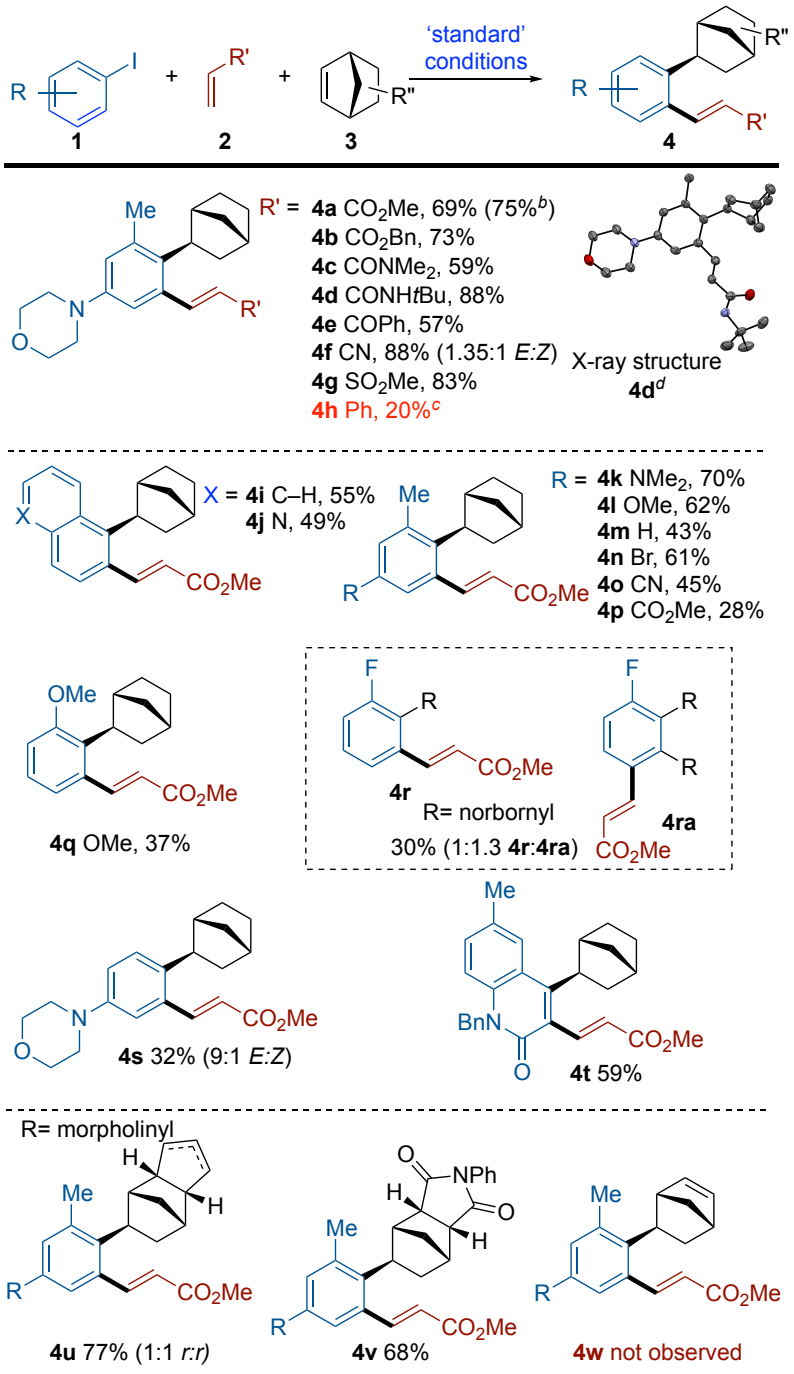

[a]Unless otherwise noted, all reactions were carried out with **1** (0.2 mmol), **2** (0.24 mmol), and **3** (0.2 mmol) in 2.0 mL of DMF for 18 h; all yields are isolated yields. [b]Carried out with **1a** (1.0

mmol), **2a** (1.2 mmol), and **3a** (1.0 mmol) in 10.0 mL of DMF for 18 h. [c]Carried out with **1a** (0.1 mmol), **2h** (0.12 mmol), and **3a** (0.1 mmol) in 1.0 mL of DMF for 18 h; NMR yield is reported. [d]Solid state structure of **4d** with thermal ellipsoids drawn at 50% probability. For clarity, the norbornyl enantiomer and hydrogen atoms have been removed.

Other unsuccessful substrates include iodobenzene, 2-bromoiodobenzene, the *ortho*-ester substituted aryl halide, and vinyl acetate (**Scheme 4.7**). In the case of iodobenzene, a complex reaction mixture was obtained. It is likely that multiple NBE insertion/1,4-migrations occurred to generate this complex mixture.

Scheme 4.7. Unsuccessful Substrates

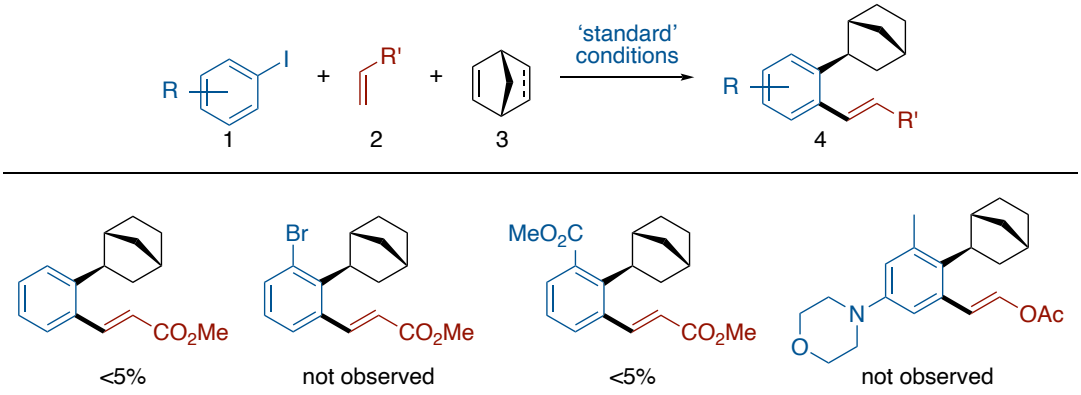

Finally, the competition between the *ortho*-Heck and a typical Catellani *ortho*-alkylation reaction was studied (**Scheme 4.8**). In the absence of LiBr and Bu_2BOTf, but with the addition of *n*-butyl iodide as an electrophile, carbonate bases with different metal cations were surveyed (**Scheme 4.8a**). While similar yields of the *ortho*-Heck product were obtained in all cases, the use of Cs_2CO_3 resulted in a significantly higher yield of the Catellani product (**4ab**). This result indicates that Cs_2CO_3 is indeed a better base to promote formation of the ANP intermediate, which is consistent with the fact that a majority of Catellani reactions published to date prefer using the

cesium salt.[1] On the other hand, running the reaction with substrate **1a** under similar conditions reported by Catellani and Cugini,[8] the *ortho*-Heck product (**4a**) was still observed and, particularly, formed in a higher yield at a higher reaction temperature (**Scheme 4.8b**).

Scheme 4.8. Investigating Competition between *Ortho*-Heck and a Catellani Reaction[a]

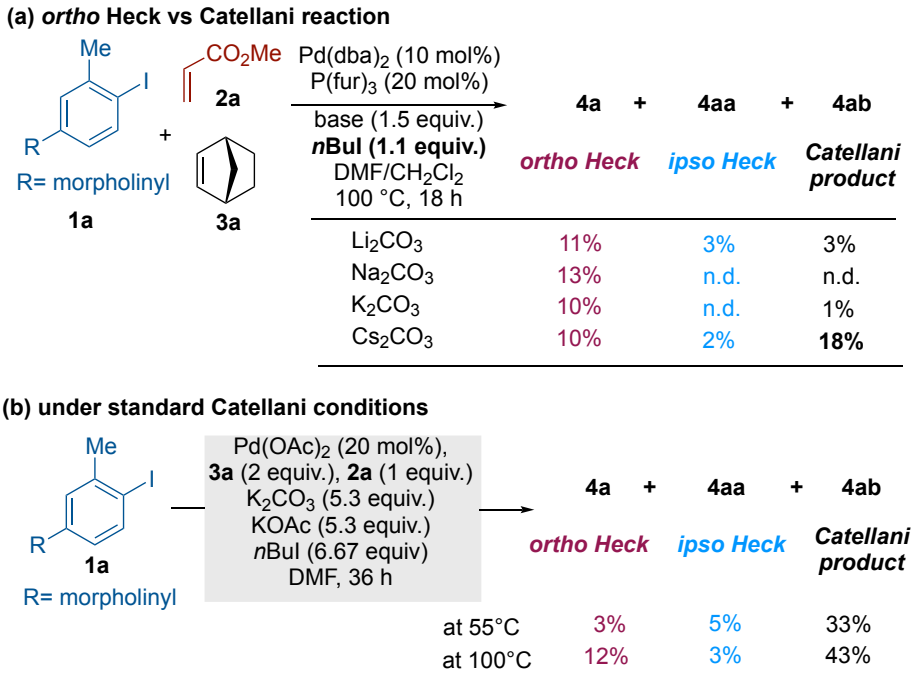

[a]All reactions were carried out with 1a (0.1 mmol), 2a (0.12 mmol), and 3a (0.1 mmol) in 1.0 mL of DMF for 18 h. NMR yields determined using 1,1,2,2-tetrachloroethane as the internal standard.

4.3. Conclusion

In summary, a non-canonical Pd-catalyzed, NBE-mediated, *ortho*-Heck reaction has been identified and explored during a study of the Catellani reaction. Deuterium labeling studies suggest a 1,4-Pd migration reaction pathway, leading to olefin coupling at the arene *ortho* position instead of the commonly observed *ipso* position. Such a reaction mode appears to be quite general for diverse aryl iodides, olefins, and NBEs. The knowledge gained here should have implications on

developing more efficient Pd/NBE catalytic systems or new remote C−H functionalization methods[40, 41] by minimizing or promoting such a 1,4-metal migration process.

4.4. Experimental

All reaction vials were flame-dried and allowed to cool to room temperature while capped in order to remove as much moisture as possible from the glass surface. $Pd(dba)_2$ was purchased from Chem Impex Intl. Inc. and Sigma-Aldrich. Extra-dry dimethylformamide (DMF) used in the key reactions was purchased from Acros Organics. All commercially available substrates were used without further purification. All reactions were carried out in vials (test-scale reactions, 4 mL vials; isolation-scale reactions, 8 mL vials; 1.0 mmol-scale reaction, 20 mL vial) unless otherwise noted. All reactions that required heating were conducted on hot plates using appropriately sized heating blocks for vials and the temperature was monitored *via* a thermometer submerged in a vial filled with silicone oil (instead of the hot plate's temperature probe reading). Thin layer chromatography (TLC) analysis was run on silica gel plates purchased from EMD Chemical (silica gel 60, F254). Infrared spectra were recorded on a Nicolet iS5 FT-IR Spectrometer using neat thin film technique. High-resolution mass spectra (HRMS) were obtained using an Agilent 6224 Tof-MS spectrometer (ESI) and an Agilent 7200B QTof GC-MS spectrometer (EI) and are reported as calculated/observed *m/z* for $[M]^+$, $[M+H]^+$, or $[M+Na]^+$ ions. Nuclear magnetic resonance spectra (^{1}H NMR, ^{13}C NMR and ^{19}F NMR) were obtained using a Bruker Model DMX 400 (400 MHz: ^{1}H at 400 MHz, ^{13}C at 101 MHz, ^{19}F at 376 MHz); some NMR spectra (^{1}H, ^{2}H, ^{13}C) were obtained using a Bruker Model DMX 500 (500 MHz: ^{1}H at 500 MHz, ^{2}H at 77 MHz, ^{13}C at 126 MHz). For $CDCl_3$ solutions, the chemical shifts were reported as parts per million (ppm) referenced to residual protium or carbon of the solvents: $CDCl_3$ δ H (7.26 ppm) and $CDCl_3$ δ C (77.16 ppm). Coupling constants were reported in Hertz (Hz). Data for ^{1}H NMR spectra were reported as following:

chemical shift (δ, ppm), multiplicity (br = broad, s = singlet, d = doublet, t = triplet, q = quartet, dd = doublet of doublets, td = triplet of doublets, ddd = doublet of doublet of doublets, m = multiplet), coupling constant (Hz), and integration. Deuterium incorporation was assigned by ^{1}H or ^{2}H NMR analysis of the reaction products. The X-ray structure of **4d** was obtained using a Bruker D8 VENTURE Single Crystal Dual-Source Diffractometer. All *ortho*-Heck products obtained were racemic; stereochemistry was shown to highlight that the products were single diastereomers.

Compounds **1a**,[42] **1k**,[43] **1s**,[42,44] **1t**,[45] **2e**,[46] and **3v**[47] were prepared according to literature procedures. A diazotization procedure[7] was used to prepare compounds **1j**,[48] **1l**,[49] and **1o**,[50] which all matched previously reported spectra. Isotopically labeled compound **1i-d$_7$** is new and was prepared *via* a bromination[51] procedure, and then converted to the aryl iodide *via* lithium-halogen exchange; labeled acrylate **2a-d$_3$**[32] is known. Compounds **1i**, **1m**, **1n**, **1p**, **1q**, **1r**, **2a**, **2b**, **2c**, **2d**, **2f**, **2g**, **2h**, and **3u** are all commercially available.

Figure 4.2. Known, Commercially Available, and New Compounds

Known compounds:

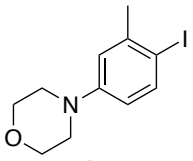

1a

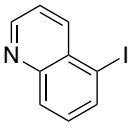

1j

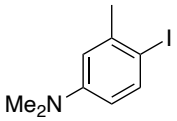

1k

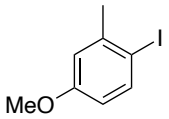

1l

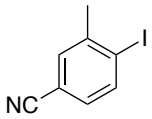

1o

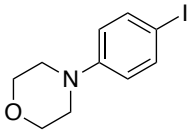

1s

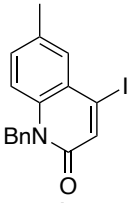

1t

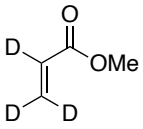

2a-d_3

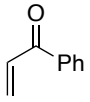

2e

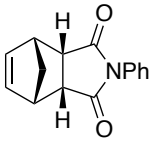

3v

Commercial compounds:

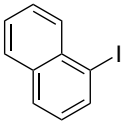

1i

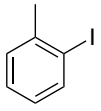

1m

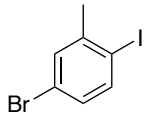

1n

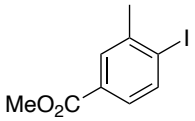

1p

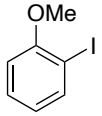

1q

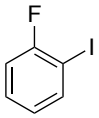

1r

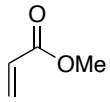

2a

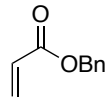

2b

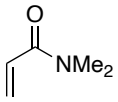

2c

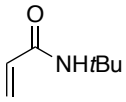

2d

2f

2g

2h

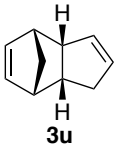

3u

3w

New compound:

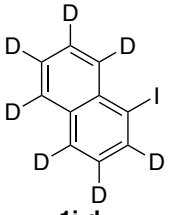

1i-d_7

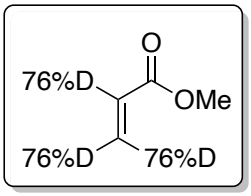

Methyl acrylate-76%*d*$_3$ (2a-d$_3$): Prepared from **2a** *via* a known procedure in a Schlenk flask sealed with a rubber septum.[52] After distillation, the labeled acrylate was found to contain 76% deuterium at all three acrylic positions. **^{1}H NMR** (500 MHz, Chloroform-*d*) δ 6.44 – 6.35 (m, 0.24H), 6.16 – 6.08 (m, 0.23H), 5.85 – 5.78 (m, 0.25H), 3.76 (s, 3H). **^{2}H NMR** (77 MHz, $CDCl_3$) δ 6.42 (s, 1H), 6.15 (s, 1H), 5.85 (s, 1H). Note: on smaller scale, the high D-incorporations reported by Ackermann and co-workers[52] could be reproduced. On the larger scale used for material isolation, however, we obtained a partially deuterated acrylate. This is most likely due to unfamiliarity with the reaction setup and may have been mitigated by changing the reaction vessel to a sealed reaction tube or using a glass stopper. For our purposes, though, 76% deuteration of the acrylic protons was sufficient enough to rule out one of the proposed reaction pathways, thus we did not attempt the reaction again.

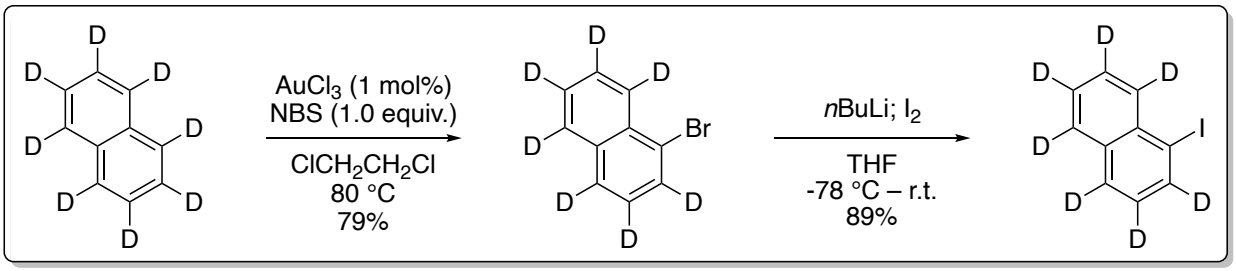

1-iodonaphthalene-*d*$_7$ (1i-d7): Naphthalene-*d*$_8$ (1.0 equiv., 5.0 mmol, 681.1 mg), $AuCl_3$ (0.01 equiv., 0.05 mmol, 15.2 mg), 1,2-dichloroethane (0.5 M, 10.0 mL), and *N*-bromosuccinimide (1.0 equiv., 5.0 mmol, 889.9 mg) were added successively to a flame-dried 40 mL vial inside a nitrogen-filled glove box. The vial was sealed, brought outside the glove box, and heated at 80 °C

overnight. The reaction was allowed to cool, was concentrated, and purified *via* silica gel chromatography to obtain 848.7 mg (79%) as a yellow oil, which matched the previously reported spectra.[52] The aryl bromide (1.0 equiv., 3.74 mmol, 800 mg) was then dissolved in dry THF (0.1 M, 37.4 mL) inside a nitrogen-filled Schlenk flask and then cooled to -78 °C. *n*BuLi (1.1 equiv., 4.11 mmol, 1.64 mL; 2.5 M in hexanes) was added dropwise and allowed to stir at -78 °C for 30 min. Iodine (1.2 equiv., 4.48 mmol, 1.14 g) was then dissolved in minimal THF and added dropwise to the solution. The reaction was allowed to stir at room temperature for 6 hours, then quenched with sat. NH_4Cl, extracted with diethyl ether, washed with 10% $Na_2S_2O_3$, dried over $MgSO_4$, filtered, and concentrated. Pale yellow oil. 89% yield (869 mg). R_f = 0.7 (hexanes). **^{2}H NMR** (77 MHz, $CDCl_3$) δ 8.15, 7.91, 7.84, 7.64, 7.58, 7.54. **^{13}C NMR** (101 MHz, $CDCl_3$) δ 137.3, 137.1, 136.8, 134.4, 134.1, 133.4, 132.0, 131.7, 131.5, 128.9, 128.6, 128.4, 128.2, 127.9, 127.7, 127.5, 127.3, 127.1, 126.7, 126.5, 126.4, 126.3, 126.2, 126.1, 125.6, 125.4, 125.2, 99.4. **IR** (KBr, cm^{-1}) 2289, 2270, 1536, 1437, 1250, 902, 624. **HRMS** (EI) m/z: $[M]^+$ Calcd for $C_{10}D_7I$: 261.0032; Found: 261.0033.

General Procedure for Pd/NBE reactions: $Pd(dba)_2$, $P(fur)_3$, and base (if not moisture sensitive) were placed into a flame-dried vial with a stir bar. Solid aryl iodide (0.1 mmol) was also added at this stage. The vial was sealed and brought into a nitrogen-filled glovebox, and NBE, LiBr, DMF, acrylate, and Bu_2BOTf (1.0 M in CH_2Cl_2) were added successively. If Cs_2CO_3 or a liquid aryl halide was used, it was added inside the glove box prior to the addition of DMF. The reaction vial was sealed, removed from the glove box, and heated at 100 °C for 18 h (note: the temperature was monitored *via* an alcohol thermometer submerged in a vial filled with silicone oil, not the hot plate's temperature probe).

For test-scale reactions (0.1 mmol): Upon completion, the reactions were allowed to cool to room temperature, were quenched by pouring onto water in a 13x100mm test tube, and extracted 4x with diethyl ether. The organic fractions were dried by filtering through an $MgSO_4$ plug, concentrated, and placed under vacuum on a Schlenk line to remove residual solvent. The internal standard, 1,1,2,2-tetrachloroethane (16.8 mg, 0.1 mmol), was added to the crude residue, which was then diluted with $CDCl_3$ and analyzed *via* crude ^1H NMR analysis to determine yield and composition.

For isolation-scale reactions (0.2 mmol): Upon completion, the reactions were allowed to cool to room temperature, and diluted with ethyl acetate. The reactions were quenched by pouring onto water, then extracted with diethyl ether. The organic fractions were dried by filtering through an $MgSO_4$ plug, concentrated, and purified *via* silica gel chromatography (EtOAc/hexanes). Some compounds were further purified *via* preparatory TLC, and any impurities found have been accounted for in the isolated yields.

For the large-scale reaction (1.0 mmol): Upon completion, the reaction was allowed to cool to room temperature, diluted with ethyl acetate, quenched by pouring onto water in a separatory funnel, and extracted with diethyl ether. The organics were dried over $MgSO_4$, filtered, concentrated, and purified *via* silica gel chromatography (EtOAc/hexanes).

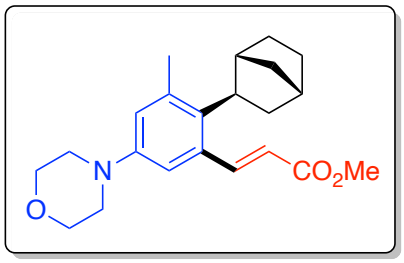

methyl (*E*)-3-(2-(bicyclo[2.2.1]heptan-2-yl)-3-methyl-5-morpholinophenyl)acrylate (4a): Synthesized from **1a**, **2a**, and **3a** according to the general procedure. 0.2 mmol scale: 69% yield (48.8 mg); 1.0 mmol scale: 75% yield (266.1 mg). Yellow

oil. R_f = 0.36 (hexane/EtOAc = 4:1). **^{1}H NMR** (400 MHz, Chloroform-*d*) δ 8.42 (d, *J* = 15.5 Hz, 1H), 6.77 (d, *J* = 2.8 Hz, 1H), 6.71 (d, *J* = 2.8 Hz, 1H), 6.09 (d, *J* = 15.5 Hz, 1H), 3.88 – 3.82 (m, 4H), 3.81 (s, 3H), 3.16 – 3.09 (m, 4H), 2.96 (t, *J* = 8.3 Hz, 1H), 2.57 – 2.53 (m, 1H), 2.38 (s, 3H), 2.36 (s, 1H), 1.83 (m, 2H), 1.66 – 1.58 (m, 2H), 1.54 (dddd, *J* = 11.9, 7.5, 3.7, 2.2 Hz, 1H), 1.45 – 1.35 (m, 1H), 1.35 – 1.17 (m, 2H). **^{13}C NMR** (101 MHz, $CDCl_3$) δ 167.6, 148.8, 148.6, 138.4, 135.8, 135.0, 120.4, 119.5, 114.1, 67.0, 51.8, 49.4, 45.4, 41.8, 40.88, 38.7, 36.7, 32.8, 28.6, 22.7. **IR** (KBr, cm^{-1}) 2952, 2868, 1718, 1598, 1251, 1169, 1123, 992. **HRMS** (ESI) m/z: $[M+Na]^+$ Calcd for $C_{22}H_{29}NO_3Na$: 378.2045; Found: 378.2047.

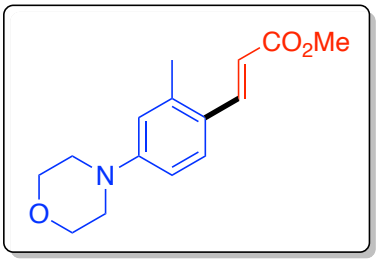

methyl (*E*)-3-(2-methyl-4-morpholinophenyl)acrylate (4aa): Palladium(II) acetate (0.05 equiv., 0.05 mmol, 11.2 mg), triphenylphosphine (0.1 equiv., 0.1 mmol, 26.2 mg), and aryl iodide **1a** (1.0 equiv., 1.0 mmol, 303 mg) were placed in a flame-dried 20 mL vial and transferred into a nitrogen-filled glovebox. Triethylamine (0.2 M, 5.0 mL) and acrylate **2a** (1.3 equiv., 1.3 mmol, 120 µL) were added successively, then the vial was sealed and heated at 90 °C overnight. The reaction was then allowed to cool to room temperature, concentrated, and purified *via* silica gel chromatography. 88% (229.8 mg). Tan solid. Melting point: 103 – 105 °C. R_f = 0.29 (hexane/EtOAc = 4:1). **^{1}H NMR** (400 MHz, Chloroform-*d*) δ 7.91 (d, *J* = 15.8 Hz, 1H), 7.52 (d, *J* = 8.7 Hz, 1H), 6.74 (dd, *J* = 8.7, 2.7 Hz, 1H), 6.69 (d, *J* = 2.7 Hz, 1H), 6.25 (d, *J* = 15.8 Hz, 1H), 3.88 – 3.83 (m, 4H), 3.79 (s, 3H), 3.26 – 3.18 (m, 4H). **^{13}C NMR** (101 MHz, $CDCl_3$) δ 167.7, 148.3, 143.9, 137.4, 134.3, 132.7, 127.4, 125.8, 119.6, 51.8, 46.3, 41.7, 40.7, 38.9, 36.7, 32.9, 28.7, 22.3. **IR** (KBr, cm^{-1}) 2952, 2851, 1709, 1598, 1240, 1165.

HRMS (ESI) m/z: $[M+Na]^+$ Calcd for $C_{15}H_{19}NO_3Na$: 284.1263; Found: 284.1265. The ^1H NMR spectrum matches the spectrum obtained from the proposed *ipso*-Heck side product isolated from the reaction mixtures in **Table 1.**

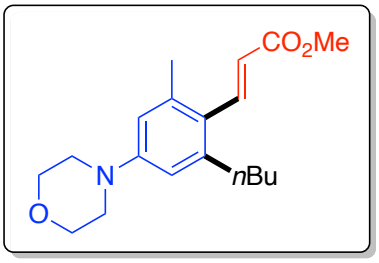

methyl (*E*)-3-(2-butyl-6-methyl-4-morpholinophenyl)acrylate (4ab): Synthesized according to similar conditions reported by Catellani & co-workers.[53] $Pd(OAc)_2$ (20 mol%, 4.5 mg), K_2CO_3 (5.3 equiv., 73.3 mg), KOAc (5.3 equiv., 52.0 mg), and aryl iodide **1a** (1.0 equiv., 30.3 mg) were placed in a flame-dried vial equipped with a magnetic stir-bar, which was then loosely capped and transferred to a nitrogen-filled glove box. Norbornene (2.0 equiv., 18.8 mg) and DMF (0.075 M, 1.33 mL), followed by methyl acrylate (1.0 equiv., 8.6 mg), and *n*BuI (6.67 equiv., 122.7 mg) in that order. The vial was sealed and heated at 55 °C or 100 °C for 18 h. The general procedure for test-scale reactions was then followed. 31% yield (55 °C) and 41% yield (100 °C). Note: NMR yields were obtained because while **4ab** is unreported, it is not the focus of this manuscript. R_f = 0.38 (hexane/EtOAc = 17:3). **^{1}H NMR** (400 MHz, Chloroform-*d*) δ 7.88 (d, *J* = 16.3 Hz, 1H), 6.60 (s, 2H), 6.02 (d, *J* = 16.3 Hz, 1H), 3.89 – 3.82 (m, 4H), 3.80 (s, 3H), 3.26 – 3.12 (m, 4H), 2.71 – 2.60 (m, 2H), 2.36 (s, 3H), 1.56 – 1.49 (m, 2H), 1.37 (q, *J* = 7.4 Hz, 2H), 0.92 (t, *J* = 7.3 Hz, 3H). **^{13}C NMR** (101 MHz, $CDCl_3$) δ 167.7, 148.3, 143.9, 137.4, 134.3, 132.7, 127.4, 125.8, 119.6, 51.8, 46.3, 41.7, 40.7, 38.9, 36.7, 32.9, 28.7, 22.3. **IR** (KBr, cm^{-1}) 2955, 2926, 2856, 1716, 1598, 1310, 1259, 1161, 1123, 989, 881. **HRMS** (ESI) m/z: $[M+Na]^+$ Calcd for $C_{19}H_{27}NO_3Na$: 340.1889; Found: 340.1882. This product was not observed in entry **12** of **Table 1**.

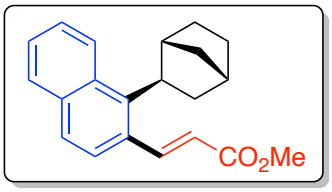

methyl (*E*)-3-(1-(bicyclo[2.2.1]heptan-2-yl)naphthalen-2-yl)acrylate (4i): Synthesized from **1i**, **2a**, and **3a** according to the general procedure. 0.2 mmol scale: 55% yield (42.7 mg). Colorless oil. R_f = 0.25 (hexane/EtOAc = 19:1). **^{1}H NMR** (400 MHz, Chloroform-*d*) δ 8.73 (d, *J* = 15.7 Hz, 1H), 8.34 – 8.28 (m, 1H), 7.80 (dd, *J* = 7.9, 1.7 Hz, 1H), 7.66 (d, *J* = 8.5 Hz, 1H), 7.56 – 7.45 (m, 2H), 7.43 (d, *J* = 8.6 Hz, 1H), 6.24 (d, *J* = 15.7 Hz, 1H), 3.84 (s, 3H), 3.67 (t, *J* = 8.5 Hz, 1H), 2.90 – 2.85 (m, 1H), 2.44 (s, 1H), 2.19 – 2.10 (m, 1H), 1.95 (dp, *J* = 10.0, 2.0 Hz, 1H), 1.74 (dtt, *J* = 9.1, 3.9, 2.4 Hz, 2H), 1.71 – 1.65 (m, 1H), 1.56 (ddq, *J* = 10.0, 3.0, 1.5 Hz, 1H), 1.51 – 1.44 (m, 2H). **^{13}C NMR** (101 MHz, $CDCl_3$) δ 167.7, 147.9, 142.1, 134.6, 132.8, 129.8, 128.9, 127.0, 126.6, 126.4, 126.2, 125.9, 120.1, 51.8, 46.0, 42.8, 42.1, 39.2, 36.9, 32.8, 29.0. **IR** (KBr, cm^{-1}) 3055, 2950, 2869, 1718, 1627, 1192, 1173, 814. **HRMS** (ESI) m/z: $[M+H]^+$ Calcd for $C_{21}H_{22}O_2H$: 307.1698; Found: 307.1693.

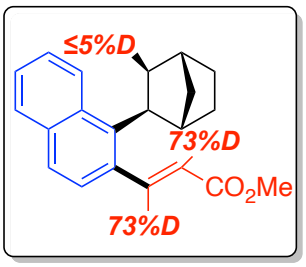

methyl (*E*)-3-(1-((1*S*,2*S*,4*R*)-bicyclo[2.2.1]heptan-2-yl)naphthalen-2-yl)acrylate-*d*$_2$ (4i-d$_2$): Synthesized from **1i**, **2a-d$_3$**, and **3a** according to the general procedure. 0.1 mmol scale: 47% yield (NMR). Colorless oil. R_f = 0.25 (hexane/EtOAc = 19:1).**^{1}H NMR** (400 MHz, Chloroform-*d*) δ 8.76 – 8.69 (m, 0.27H), 8.30 (d, *J* = 8.4 Hz, 1H), 7.80 (dd, *J* = 7.8, 1.8 Hz, 1H), 7.66 (d, *J* = 8.6 Hz, 1H), 7.56 – 7.41 (m, 4H), 6.28 – 6.18 (m, 0.27H), 3.84 (s, 3H), 3.66 (t, *J* = 8.4 Hz, 1H), 2.87 (d, *J* = 2.4 Hz, 1H), 2.44 (s, 1H), 2.14 (ddd, *J* = 12.0, 9.3, 2.3 Hz,

1H), 1.95 (dp, J = 10.1, 2.0 Hz, 1H), 1.80 – 1.71 (m, 2H), 1.71 – 1.64 (m, 1H), 1.55 (dt, J = 2.9, 1.3 Hz, 1H), 1.51 – 1.45 (m, 2H). **^{2}H NMR** (77 MHz, Chloroform-*d*) δ 8.77 (s, 1H), 6.27 (s, 1H).

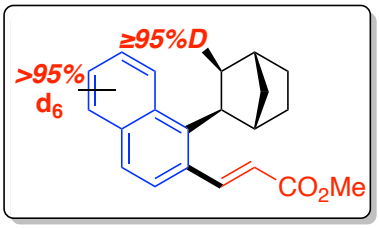

methyl (*E*)-3-(1-((1*S*,2*S*,3*S*,4*R*)-bicyclo[2.2.1]heptan-2-yl-3-*d*)naphthalen-2-yl-3,4,5,6,7,8-d_6)acrylate (4i-d_7): Synthesized from **1i-d_7**, **2a**, and **3a** according to the general procedure. 0.1 mmol scale: See **Scheme 3** for yields (NMR). Colorless oil. R_f = 0.25 (hexane/EtOAc = 19:1). **^{1}H NMR** (400 MHz, Chloroform-*d*) δ 8.72 (d, J = 15.6 Hz, 1H), 6.23 (d, J = 15.7 Hz, 1H), 3.84 (s, 4H), 3.65 (d, J = 9.3 Hz, 1H), 2.87 (d, J = 3.5 Hz, 1H), 2.43 (s, 1H), 2.15 – 2.07 (m, 1H), 1.94 (dt, J = 10.0, 2.1 Hz, 1H), 1.77 – 1.70 (m, 2H), 1.59 – 1.53 (m, 1H), 1.47 (dq, J = 9.3, 2.5 Hz, 2H). **^{2}H NMR** (77 MHz, Chloroform-*d*) δ 8.36 (s, 1H), 7.97 – 7.42 (m, 5H), 1.70 (s, 1H). **HRMS** (ESI) m/z: $[M+Na]^+$ Calcd for $C_{21}H_{15}D_7O_2Na$: 336.1957; Found: 336.1955.

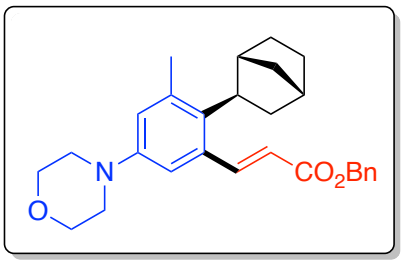

(*E*)-3-(2- benzyl (*E*)- 3-(2-(bicyclo[2.2.1]heptan-2-yl)-3-methyl-5-morpholinophenyl)acrylate (4b): Synthesized from **1a**, **2b**, and **3a** according to the general procedure. 0.2 mmol scale: 73% yield (62.9 mg). Yellow oil. R_f = 0.38 (hexane/EtOAc = 4:1). **^{1}H NMR** (400 MHz, Chloroform-*d*) δ 8.48 (d, J = 15.5 Hz, 1H), 7.46 – 7.32 (m, 5H), 6.77 (d, J = 2.8 Hz, 1H), 6.72 (d, J = 2.7 Hz, 1H), 6.15 (d, J = 15.5 Hz, 1H), 5.26 (s, 2H), 3.90 – 3.83 (m, 4H), 3.17 – 3.09 (m, 3H), 2.96 (t, J = 8.3 Hz, 1H), 2.55 (s, 1H), 2.38 (s, 3H), 2.34 (s, 1H),

1.90 – 1.73 (m, 2H), 1.71 – 1.50 (m, 2H), 1.40 – 1.26 (m, 3H). **^{13}C NMR** (101 MHz, $CDCl_3$) δ 166.9, 149.1, 148.6, 138.5, 136.3, 135.9, 134.8, 128.7, 128.4, 128.4, 120.4, 119.5, 114.0, 67.0, 66.4, 49.4, 45.5, 41.8, 40.9, 38.8, 36.7, 32.9, 28.7, 22.8. **IR** (KBr, cm^{-1}) 3032, 2954, 2867, 1713, 1598, 1160. **HRMS** (ESI) m/z: $[M+H]^+$ Calcd for $C_{28}H_{33}NO_3H$; 432.2539. Found: 432.2542.

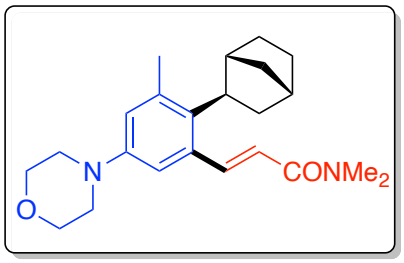

(*E*)-*O*-(3-(2-(bicyclo[2.2.1]heptan-2-yl)-3-methyl-5-morpholinophenyl)acryloyl)-*N*,*N*-dimethylhydroxylamine (4c): Synthesized from **1a**, **2c**, and **3a** according to the general procedure. 0.2 mmol scale: 59% yield (43.4 mg). Viscous dark red oil. R_f = 0.22 (hexane/EtOAc = 2:3). **^{1}H NMR** (400 MHz, Chloroform-*d*) δ 8.32 (dd, *J* = 15.1, 1.8 Hz, 1H), 6.73 (d, *J* = 2.9 Hz, 1H), 6.67 (d, *J* = 2.7 Hz, 1H), 6.47 (dd, *J* = 15.1, 1.4 Hz, 1H), 3.84 (dq, *J* = 5.1, 2.2 Hz, 4H), 3.18 – 3.09 (m, 7H), 3.07 (s, 3H), 2.95 (m, 1H), 2.55 (s, 1H), 2.38 (d, *J* = 1.8 Hz, 3H), 2.33 (s, 1H), 1.82 (ddd, *J* = 12.0, 9.6, 2.4 Hz, 2H), 1.63 – 1.53 (m, 3H), 1.45 – 1.23 (m, 5H). **^{13}C NMR** (101 MHz, $CDCl_3$) δ 166.8, 148.5, 146.6, 138.2, 136.4, 135.7, 119.8, 119.5, 114.6, 67.0, 49.6, 45.5, 41.8, 40.7, 38.7, 37.5, 36.6, 36.0, 32.7, 28.7, 22.8. **IR** (KBr, cm^{-1}) 3380, 2953, 2868, 2241, 1647, 1600, 1394, 1122, 731. **HRMS** (ESI) m/z: $[M+Na]^+$ Calcd for $C_{23}H_{32}N_2O_2Na$: 391.2361; Found: 391.2356.

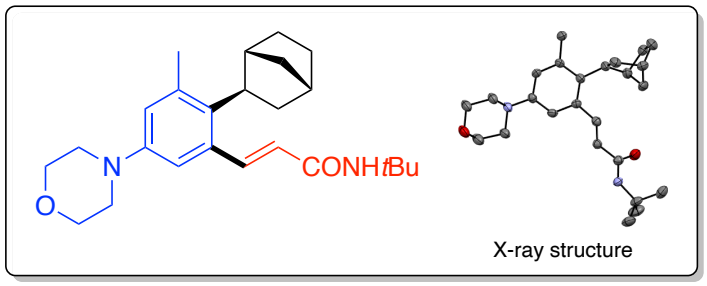

(bicyclo[2.2.1]heptan-2-yl)-3-methyl-5-morpholinophenyl)-*N*-(*tert*-butyl)acryl-amide (4d): Synthesized from **1a**, **2d**, and **3a** according to the general procedure. 0.2 mmol scale: 88% yield (69.5 mg). Pale-yellow solid. Decomposition point: 183 – 188 °C. R_f = 0.28 (hexane/EtOAc = 4:1). A single crystal was obtained by vapor diffusion of pentane into a solution of **4d** dissolved in ethyl acetate, which was analyzed *via* X-ray crystallography. **^{1}H NMR** (400 MHz, Chloroform-*d*) δ 8.20 (d, *J* = 15.0 Hz, 1H), 6.72 (d, *J* = 2.8 Hz, 1H), 6.66 (d, *J* = 2.8 Hz, 1H), 5.92 (d, *J* = 15.1 Hz, 1H), 5.36 (s, 1H), 3.88 – 3.79 (m, 4H), 3.16 – 3.08 (m, 4H), 2.95 (t, *J* = 8.3 Hz, 1H), 2.58 – 2.54 (m, 1H), 2.38 (s, 3H), 2.34 (s, 1H), 1.83 (tdt, *J* = 7.2, 5.4, 2.3 Hz, 2H), 1.63 – 1.50 (m, 4H), 1.43 (s, 9H), 1.33 – 1.25 (m, 2H). **^{13}C NMR** (101 MHz, $CDCl_3$) δ 165.3, 148.5, 143.9, 138.1, 135.9, 135.7, 124.1, 119.8, 114.4, 67.1, 51.5, 49.5, 45.5, 41.7, 40.8, 38.8, 36.7, 32.8, 29.1, 28.7, 22.8. **HRMS** (ESI) m/z: $[M+H]^+$ Calcd for $C_{25}H_{36}N_2O_2H$: 397.2855; Found: 397.2857.

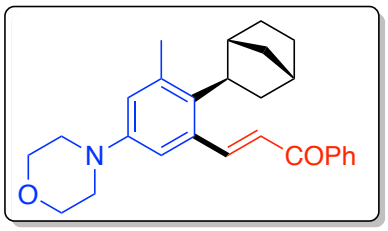

(*E*)-3-(2-(bicyclo[2.2.1]heptan-2-yl)-3-methyl-5-morpholinophenyl)-1-phenylprop-2-en-1-one (4e): Synthesized from **1a**, **2e**, and **3a** according to the general procedure. 0.2 mmol scale: 57% yield (46.1 mg). Yellow oil. R_f = 0.32 (hexane/EtOAc = 4:1). **^{1}H NMR** (400 MHz, Chloroform-*d*) δ 8.52 (d, *J* = 15.2 Hz, 1H), 8.04 – 7.98 (m, 2H), 7.61 – 7.55 (m, 1H), 7.53 – 7.48 (m, 2H), 7.16 (d, *J* = 15.2 Hz, 1H), 6.82 (d, *J* =

2.8 Hz, 1H), 6.80 (d, J = 2.8 Hz, 1H), 3.90 – 3.82 (m, 4H), 3.18 – 3.13 (m, 4H), 2.99 (t, J = 8.4 Hz, 1H), 2.56 (s, 1H), 2.40 (s, 3H), 2.33 (s, 2H), 1.88 – 1.81 (m, 1H), 1.78 (d, J = 10.5 Hz, 1H), 1.64 – 1.57 (m, 3H), 1.38 – 1.28 (m, 3H). **^{13}C NMR** (101 MHz, $CDCl_3$) δ 190.8, 149.1, 148.7, 138.5, 138.3, 136.5, 135.7, 132.8, 128.8, 128.6, 128.4, 124.2, 120.6, 114.2, 67.1, 49.5, 45.6, 41.9, 40.9, 38.7, 36.7, 32.8, 28.7, 22.8. **IR** (KBr, cm^{-1}) 2953, 2866, 1662, 1600, 1448, 1253, 1122, 1016, 694. **HRMS** (ESI) m/z: $[M+Na]^+$ Calcd for $C_{27}H_{31}NO_2Na$: 424.2252; Found: 424.2253.

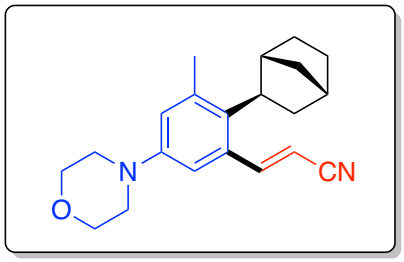

(*E*)-3-(2-(bicyclo[2.2.1]heptan-2-yl)-3-methyl-5-morpholinophenyl)acrylonitrile (4f): Synthesized from **1a**, **2f**, and **3a** according to the general procedure. 0.2 mmol scale: 88% yield (56.5 mg; *E:Z* = 1.35:1). Yellow oil. R_f = 0.4 (hexane/EtOAc = 4:1). **^{1}H NMR** (500 MHz, Chloroform-*d*) δ 8.15 (d, J = 16.2 Hz, 0.56H), 7.85 (d, J = 11.6 Hz, 0.43H), 6.86 (d, J = 2.8 Hz, 0.48H), 6.78 (dd, J = 6.0, 2.8 Hz, 1H), 6.57 (d, J = 2.8 Hz, 0.56H), 5.55 (d, J = 16.2 Hz, 0.52H), 5.47 (d, J = 11.5 Hz, 0.39H), 3.85 (t, J = 5.1 Hz, 4H), 3.14 (m, 4H), 2.91 (m, 1H), 2.55 – 2.49 (m, 1H), 2.37 (s, 3H), 2.33 (s, 0.69H), 1.86 (dtd, J = 11.3, 8.9, 2.3 Hz, 1H), 1.72 – 1.57 (m, 3H), 1.50 – 1.39 (m, 1H), 1.37 – 1.23 (m, 3H). **^{13}C NMR** (101 MHz, $CDCl_3$) δ 154.7, 154.0, 148.7, 138.7, 138.5, 135.4, 134.1, 133.3, 121.1, 120.8, 118.4, 117.3, 115.7, 113.6, 98.1, 97.6, 67.0, 66.9, 49.5, 49.3, 45.5, 41.6, 41.5, 41.0, 40.7, 38.8, 36.6, 36.5, 32.7, 32.6, 28.5, 22.8, 22.7. **IR** (KBr, cm^{-1}) 2955, 2868, 2216, 1597, 1450, 1258, 1122. **HRMS** (ESI) m/z: $[M+Na]^+$ Calcd for $C_{21}H_{26}N_2ONa$: 345.1943: Found: 345.1944.

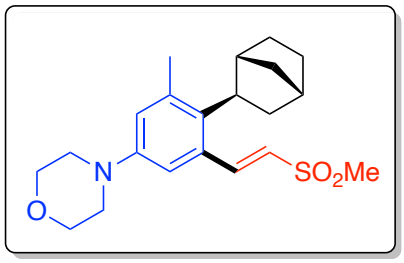

(*E*)-4-(4-(bicyclo[2.2.1]heptan-2-yl)-3-methyl-5-(2-(methylsulfonyl)vinyl)phenyl)morpholine (4g): Synthesized from **1a**, **2g**, and **3a** according to the general procedure. 0.2 mmol scale: 83% yield (62.0 mg). Dark yellow solid. Decomposition point: 179 – 183 °C. R_f = 0.12 (hexane/EtOAc = 1:1). **^{1}H NMR** (400 MHz, Chloroform-*d*) δ 8.40 (d, *J* = 15.1 Hz, 1H), 6.80 (d, *J* = 2.8 Hz, 1H), 6.63 (d, *J* = 2.8 Hz, 1H), 6.58 (d, *J* = 15.0 Hz, 1H), 3.87 – 3.82 (m, 4H), 3.15 – 3.10 (m, 4H), 3.02 (s, 3H), 2.99 – 2.91 (m, 1H), 2.54 (s, 1H), 2.38 (s, 3H), 2.37 (s, 1H), 2.17 (s, 3H), 1.88 (td, *J* = 10.3, 9.1, 2.2 Hz, 1H), 1.73 (d, *J* = 10.1 Hz, 1H), 1.63 (d, *J* = 9.4 Hz, 2H), 1.35 – 1.27 (m, 2H). **^{13}C NMR** (101 MHz, $CDCl_3$) δ 148.8, 148.1, 138.9, 136.2, 132.3, 127.5, 121.1, 114.0, 67.0, 49.4, 45.6, 43.2, 41.7, 41.0, 38.8, 36.7, 32.7, 28.7, 22.7. **IR** (KBr, cm^{-1}) 2955, 2867, 1596, 1451, 1305, 1131, 964, 834, 506. **HRMS** (ESI) m/z: $[M+H]^+$ Calcd for $C_{21}H_{29}NO_3SH$: 376.1946; Found: 376.1942.

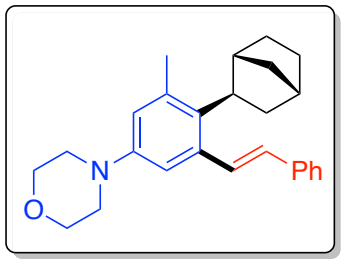

(*E*)-4-(4-(bicyclo[2.2.1]heptan-2-yl)-3-methyl-5-styrylphenyl)morpholine (4h): Synthesized from **1a**, **2h**, and **3a** according to the general procedure. 0.1 mmol scale: 20% yield (NMR). An NMR yield was obtained for **4h** because separation from unreacted **1a** *via* silica gel chromatography proved to be quite challenging. Colorless oil. R_f = 0.25 (hexane/EtOAc = 9:1). **^{1}H NMR** (400 MHz, Chloroform-*d*) δ 7.72 (d, *J* = 15.9 Hz, 1H), 7.51 – 7.44 (m, 2H), 7.36 (dd, *J* = 8.4, 6.7 Hz, 2H), 6.80 (d, *J* = 2.8 Hz, 1H), 6.71

(d, J = 2.8 Hz, 1H), 6.65 (d, J = 15.9 Hz, 1H), 3.92 – 3.70 (m, 4H), 3.27 – 3.01 (m, 4H), 3.00 (t, J = 8.3 Hz, 1H), 2.63 (s, 1H), 2.39 (s, 3H), 2.33 (s, 1H), 1.91 – 1.79 (m, 2H), 1.71 – 1.59 (m, 4H), 1.37 – 1.27 (m, 3H). **^{13}C NMR** (126 MHz, $CDCl_3$) δ 148.7, 138.1, 138.0, 138.0, 134.8, 132.1, 130.2, 128.9, 127.5, 126.5, 118.7, 114.6, 67.2, 49.7, 45.6, 41.8, 40.5, 38.8, 36.7, 32.8, 28.8, 22.9. **IR** (KBr, cm^{-1}) 3023, 2953, 2853, 1597, 1449, 1261, 1123, 692. **HRMS** (ESI) m/z: $[M+H]^+$ Calcd for $C_{26}H_{31}NOH$: 374.2484; Found: 374.2481.

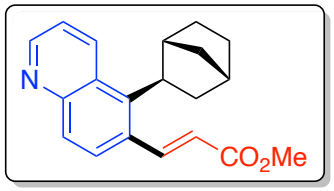

methyl (*E*)-3-(5-(bicyclo[2.2.1]heptan-2-yl)quinolin-6-yl)acrylate (4j): Synthesized from **1j**, **2a**, and **3a** according to the general procedure. 0.2 mmol scale: 49% yield (29.8 mg). Viscous yellow oil. R_f = 0.15 (hexane/EtOAc = 4:1). **^{1}H NMR** (400 MHz, Chloroform-*d*) δ 8.88 (dt, J = 3.9, 1.9 Hz, 1H), 8.69 – 8.65 (m, 1H), 8.64 (s, 1H), 7.92 (dd, J = 8.9, 2.3 Hz, 1H), 7.65 (dd, J = 8.8, 2.0 Hz, 1H), 7.43 (ddd, J = 9.1, 4.1, 1.9 Hz, 1H), 6.25 (dd, J = 15.7, 2.1 Hz, 1H), 3.84 (s, 3H), 3.58 (t, J = 8.4 Hz, 1H), 2.87 (d, J = 3.0 Hz, 1H), 2.44 (s, 1H), 2.08 (ddd, J = 12.0, 9.3, 2.3 Hz, 1H), 1.90 (dp, J = 10.0, 2.0 Hz, 1H), 1.75 – 1.71 (m, 2H), 1.71 – 1.61 (m, 1H), 1.56 (dq, J = 10.1, 1.7 Hz, 1H), 1.48 – 1.24 (m, 2H). **^{13}C NMR** (101 MHz, $CDCl_3$) δ 167.5, 150.2, 149.4, 146.8, 142.3, 134.2, 130.5, 130.4, 128.3, 127.9, 121.1, 121.1, 51.9, 45.8, 42.9, 41.9, 39.1, 36.9, 32.6, 28.9. **HRMS** (ESI) m/z: $[M+Na]^+$ Calcd for $C_{20}H_{21}NO_2Na$: 330.1470; Found: 330.1469.

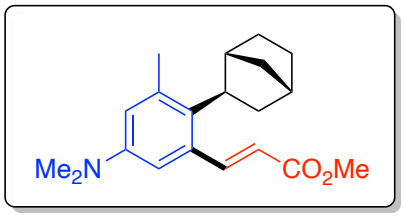

methyl (*E*)-3-(2-(bicyclo[2.2.1]heptan-2-yl)-5-(dimethylamino)-3-methylphenyl)acrylate (4k): Synthesized from **1k**, **2a**, and **3a** according to the general procedure. 0.2 mmol scale: 70% yield (44.1 mg). Yellow oil. R_f = 0.47 (hexane/EtOAc = 9:1). **^{1}H NMR** (400 MHz, Chloroform-*d*) δ 8.43 (d, *J* = 15.5 Hz, 1H), 6.62 (d, *J* = 2.9 Hz, 1H), 6.54 (d, *J* = 2.9 Hz, 1H), 6.12 (d, *J* = 15.5 Hz, 1H), 3.81 (s, 3H), 2.95 (t, *J* = 8.3 Hz, 1H), 2.91 (s, 6H), 2.56 – 2.51 (m, 1H), 2.38 (s, 3H), 2.35 (q, *J* = 3.1, 2.2 Hz, 1H), 1.83 (tdd, *J* = 9.0, 5.7, 2.3 Hz, 2H), 1.65 – 1.58 (m, 3H), 1.37 – 1.28 (m, 3H). **^{13}C NMR** (101 MHz, $CDCl_3$) δ 167.8, 149.4, 148.2, 138.2, 134.9, 132.5, 119.2, 117.6, 111.2, 51.7, 45.2, 41.9, 41.0, 40.8, 38.7, 36.8, 32.9, 28.7, 22.8. **IR** (KBr, cm^{-1}) 2949, 2868, 1716, 1601, 1304, 1168, 837. **HRMS** (ESI) m/z: $[M+Na]^+$ Calcd for $C_{20}H_{27}NO_2Na$: 336.1939; Found: 336.1935.

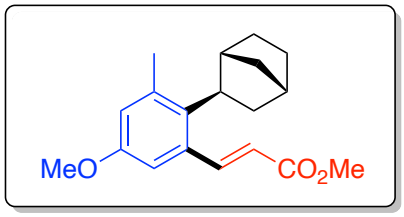

methyl (*E*)-3-(2-(bicyclo[2.2.1]heptan-2-yl)-5-methoxy-3-methylphenyl)acrylate (4l): Synthesized from **1l**, **2a**, and **3a** according to the general procedure. 0.2 mmol scale: 62% yield (38.9 mg). Yellow oil. R_f = 0.65 (hexane/EtOAc = 9:1). **^{1}H NMR** (400 MHz, Chloroform-*d*) δ 8.42 (d, *J* = 15.5 Hz, 1H), 6.75 (d, *J* = 2.9 Hz, 1H), 6.72 (d, *J* = 2.9 Hz, 1H), 6.11 (d, *J* = 15.6 Hz, 1H), 3.81 (s, 3H), 3.78 (s, 3H), 2.97 (t, *J* = 8.4 Hz, 1H), 2.58 – 2.53 (m, 1H), 2.38 (s, 3H), 2.36 (d, *J* = 5.4 Hz, 1H), 1.90 – 1.79 (m, 2H), 1.61 (dq, *J* = 5.9, 3.4 Hz, 2H), 1.54 (dddd, *J* = 11.8, 7.6, 3.8, 2.3 Hz, 1H), 1.40 (ddq, *J* = 10.0, 2.9, 1.5 Hz, 1H), 1.32 (dq, *J* = 9.2, 2.1 Hz, 2H). **^{13}C NMR** (101 MHz, $CDCl_3$) δ 167.6, 156.8, 148.2, 139.0, 136.5, 135.2, 119.7, 118.8,

111.5, 55.3, 51.8, 45.5, 41.8, 40.9, 38.8, 36.7, 32.9, 28.6, 22.6. **IR** (KBr, cm^{-1}) 2951, 2869, 2091, 1716, 1630, 1600, 1471, 1435, 1169, 1069, 859. **HRMS** (ESI) m/z: $[M+H]^+$ Calcd for $C_{19}H_{24}O_3H$: 301.1804; Found: 301.1803.

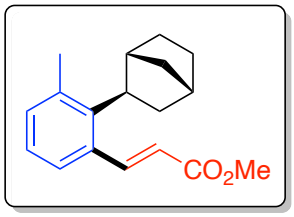

methyl (*E*)-3-(2-(bicyclo[2.2.1]heptan-2-yl)-3-methylphenyl)acrylate (4m): Synthesized from **1m**, **2a**, and **3a** according to the general procedure. 0.2 mmol scale: 43% yield (23.3 mg). Colorless oil. R_f = 0.31 (hexane/EtOAc = 19:1). **^{1}H NMR** (400 MHz, Chloroform-*d*) δ 8.44 (d, *J* = 15.6 Hz, 1H), 7.18 (ddd, *J* = 11.6, 7.8, 4.1 Hz, 2H), 7.06 (t, *J* = 7.5 Hz, 1H), 6.10 (d, *J* = 15.5 Hz, 1H), 3.81 (s, 3H), 3.04 (t, *J* = 8.4 Hz, 1H), 2.61 (d, *J* = 2.7 Hz, 1H), 2.41 (s, 3H), 2.37 (s, 1H), 1.93 – 1.81 (m, 3H), 1.69 – 1.58 (m, 3H), 1.37 – 1.29 (m, 3H). **^{13}C NMR** (101 MHz, $CDCl_3$) δ 167.7, 148.3, 143.9, 137.4, 134.3, 132.7, 127.4, 125.8, 119.6, 51.8, 46.3, 41.7, 40.7, 38.9, 36.7, 32.9, 28.7, 22.3. **IR** (KBr, cm^{-1}) 2950, 2869, 1719, 1629, 1163, 792. **HRMS** (ESI) m/z: $[M+H]^+$ Calcd for $C_{18}H_{22}O_2H$: 271.1698; Found: 271.1693.

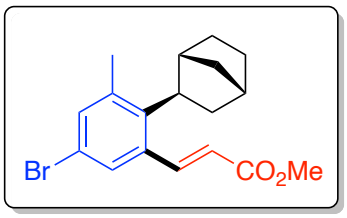

methyl (*E*)-3-(2-(bicyclo[2.2.1]heptan-2-yl)-5-bromo-3-methylphenyl)acrylate (4n): Synthesized from **1n**, **2a**, and **3a** according to the general procedure. 0.2 mmol scale: 61% yield (42.6 mg). Pale-yellow oil. R_f = 0.63 (hexane/EtOAc = 19:1). **^{1}H NMR** (400 MHz, Chloroform-*d*) δ 8.33 (d, *J* = 15.5 Hz, 1H), 7.30 (d, *J* = 2.3 Hz, 1H), 7.28 (d, *J* = 2.4 Hz, 1H), 6.09 (d, *J* = 15.5 Hz, 1H), 3.81 (s, 3H), 2.95 (t, *J* = 8.4 Hz, 1H), 2.60 –

2.55 (m, 1H), 2.37 (s, 3H), 2.36 (d, J = 3.0 Hz, 1H), 1.92 – 1.82 (m, 1H), 1.78 (dp, J = 10.0, 1.9 Hz, 1H), 1.68 – 1.59 (m, 2H), 1.50 (dddd, J = 11.7, 7.5, 3.8, 2.3 Hz, 1H), 1.41 (ddt, J = 10.0, 4.0, 1.5 Hz, 1H), 1.31 (dt, J = 8.8, 2.6 Hz, 2H). **^{13}C NMR** (101 MHz, $CDCl_3$) δ 167.7, 148.3, 143.9, 137.4, 134.3, 132.7, 127.4, 125.8, 119.6, 51.8, 46.3, 41.7, 40.7, 38.9, 36.7, 32.9, 28.7, 22.3. **IR** (KBr, cm^{-1}) 2951, 2870, 1721, 1632, 1309, 1170. **HRMS** (ESI) m/z: $[M+H]^+$ Calcd for $C_{18}H_{21}BrO_2H$: 349.0803; Found: 349.0797.

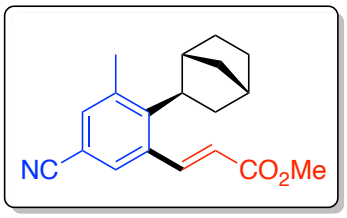

methyl (*E*)-3-(2-(bicyclo[2.2.1]heptan-2-yl)-5-cyano-3-methylphenyl)acrylate (4o): Synthesized from **1o**, **2a**, and **3a** according to the general procedure. 0.2 mmol scale: 45% yield (26.6 mg). Yellow oil. R_f = 0.46 (hexane/EtOAc = 10:1). **^{1}H NMR** (400 MHz, Chloroform-*d*) δ 8.33 (d, J = 15.6 Hz, 1H), 7.43 (d, J = 2.0 Hz, 1H), 7.41 (d, J = 2.0 Hz, 1H), 6.10 (d, J = 15.6 Hz, 1H), 3.82 (s, 3H), 3.03 (t, J = 8.4 Hz, 1H), 2.43 (s, 3H), 2.39 (d, J = 4.2 Hz, 1H), 1.92 (ddd, J = 11.9, 9.1, 2.3 Hz, 1H), 1.76 (dp, J = 10.3, 2.0 Hz, 1H), 1.70 – 1.61 (m, 2H), 1.54 – 1.48 (m, 1H), 1.47 – 1.42 (m, 2H), 1.36 – 1.29 (m, 2H). **^{13}C NMR** (101 MHz, $CDCl_3$) δ 167.7, 148.3, 143.9, 137.4, 134.3, 132.7, 127.4, 125.8, 119.6, 51.8, 46.3, 41.7, 40.7, 38.9, 36.7, 32.9, 28.7, 22.3. **IR** (KBr, cm^{-1}) 2959, 2870, 2228, 1719, 1636, 1320, 1261, 1031, 800. **HRMS** (ESI) m/z: $[M+H]^+$ Calcd for $C_{19}H_{21}NO_2H$: 296.1651; Found: 296.1649.

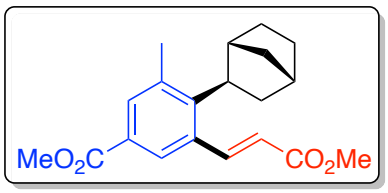

methyl (*E*)-4-(bicyclo[2.2.1]heptan-2-yl)-3-(3-methoxy-3-oxoprop-1-en-1-yl)-5-methylbenzo-ate (4p): Synthesized from **1p**, **2a**, and **3a** according to the

general procedure. 0.2 mmol scale: 28% yield (18.5 mg). Yellow oil. R_f = 0.46 (hexane/EtOAc = 10:1). **^{1}H NMR** (400 MHz, Chloroform-*d*) δ 8.40 (d, *J* = 15.6 Hz, 1H), 7.84 (d, *J* = 2.0 Hz, 1H), 7.80 (d, *J* = 2.0 Hz, 1H), 6.18 (d, *J* = 15.6 Hz, 1H), 3.90 (s, 3H), 3.82 (s, 3H), 3.06 (t, *J* = 8.4 Hz, 1H), 2.64 (s, 1H), 2.45 (s, 3H), 2.38 (s, 1H), 1.92 (ddd, *J* = 11.8, 8.8, 2.1 Hz, 1H), 1.81 (dt, *J* = 10.1, 2.0 Hz, 1H), 1.64 (dq, *J* = 8.5, 3.4 Hz, 2H), 1.55 – 1.49 (m, 1H), 1.48 – 1.41 (m, 1H), 1.34 (dt, *J* = 8.6, 2.5 Hz, 2H). ^{13}C NMR (101 MHz, $CDCl_3$) δ 167.7, 148.3, 143.9, 137.4, 134.3, 132.7, 127.4, 125.8, 119.6, 51.8, 46.3, 41.7, 40.7, 38.9, 36.7, 32.9, 28.7, 22.3. **IR** (KBr, cm^{-1}) 2954, 2360, 2342, 1720, 1261, 1034. **HRMS** (ESI) m/z: $[M+H]^+$ Calcd for $C_{20}H_{24}O_4H$: 329.1753; Found: 329.1750.

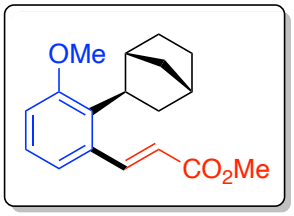

methyl (*E*)-3-(2-(bicyclo[2.2.1]heptan-2-yl)-3-methoxyphenyl)acrylate (4q): Synthesized from **1q**, **2a**, and **3a** according to the general procedure. 0.2 mmol scale: 37% yield (21.4 mg). Yellow oil. R_f = 0.35 (hexane/EtOAc = 10:1). **^{1}H NMR** (400 MHz, Chloroform-*d*) δ 8.17 (d, *J* = 15.7 Hz, 1H), 7.14 (t, *J* = 7.9 Hz, 1H), 7.02 (dd, *J* = 7.8, 1.3 Hz, 1H), 6.89 (dd, *J* = 8.2, 1.3 Hz, 1H), 6.20 (d, *J* = 15.7 Hz, 1H), 3.81 (s, 3H), 3.78 (s, 3H), 2.95 (t, *J* = 8.2 Hz, 1H), 2.49 (dt, *J* = 3.4, 1.6 Hz, 1H), 2.31 (d, *J* = 4.2 Hz, 1H), 1.99 (dt, *J* = 9.4, 2.0 Hz, 1H), 1.85 – 1.77 (m, 1H), 1.71 (ddd, *J* = 13.3, 8.8, 2.2 Hz, 1H), 1.62 – 1.59 (m, 1H), 1.57 – 1.52 (m, 1H), 1.31 (dddd, *J* = 13.0, 8.7, 5.0, 2.0 Hz, 2H), 1.24 (dt, *J* = 8.9, 1.7 Hz, 1H). **^{13}C NMR** (101 MHz, $CDCl_3$) δ 167.7, 148.3, 143.9, 137.4, 134.3, 132.7, 127.4, 125.8, 119.6, 51.8, 46.3, 41.7, 40.7, 38.9, 36.7, 32.9, 28.7, 22.3. **IR** (KBr, cm^{-1}) 2949, 2869, 1719, 1469, 1256, 1166, 794. **HRMS** (ESI) m/z: $[M+H]^+$ Calcd for $C_{18}H_{22}O_3H$: 287.1647; Found: 287.1645.

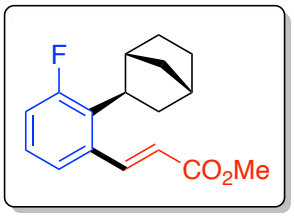

methyl (*E*)-3-(2-(bicyclo[2.2.1]heptan-2-yl)-3-fluorophenyl)acrylate (4r): Synthesized from **1r**, **2a**, and **3a** according to the general procedure. 0.2 mmol scale: 30% yield (1:1.3 **4r:4ra**; 19.4 mg total). Yellow oil. R_f = 0.62 (hexane/EtOAc = 10:1). Note: Products **4r** and **4ra** could not be separated by silica gel chromatography and were found to be unstable under preparatory TLC conditions. Therefore, the purity is limited and ^{13}C NMR spectra could not be obtained. **^{1}H NMR** (400 MHz, Chloroform-*d*) δ 8.06 (d, *J* = 15.7 Hz, 1H), 7.23 (s, 1H), 7.12 (tt, *J* = 8.2, 4.0 Hz, 1H), 7.00 (dd, *J* = 12.5, 7.9 Hz, 1H), 6.26 (d, *J* = 15.7 Hz, 1H), 3.82 (s, 3H), 2.97 – 2.90 (m, 1H), 2.61 (s, 1H), 2.34 (s, 2H), 1.80 (q, *J* = 14.1, 13.4 Hz, 3H), 1.73 – 1.58 (m, 8H), 1.35 – 1.29 (m, 6H). **^{19}F NMR** (376 MHz, Chloroform-*d*) δ -111.54 (d, *J* = 12.5 Hz). **IR** (KBr, cm^{-1}) 2951, 2870, 1722, 1636, 1464, 1314, 1231 1172, 982, 796. **HRMS** (ESI) m/z: $[M+H]^+$ Calcd for $C_{17}H_{19}FO_2H$: 275.1447; Found: 275.1445.

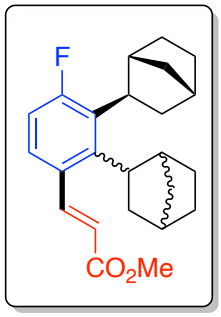

methyl (*E*)-3-(2,3-di(bicyclo[2.2.1]heptan-2-yl)-4-fluorophenyl)acrylate (4ra): Synthesized from **1r**, **2a**, and **3a** according to the general procedure. 0.2 mmol scale: 30% yield (1:1.3 **4r:4ra**; 19.4 mg total). Yellow oil. R_f = 0.62 (hexane/EtOAc = 10:1). Note: Products **4r** and **4ra** could not be separated by silica gel chromatography and were found to be unstable under preparatory TLC conditions. Therefore, the purity is limited and ^{13}C NMR spectra could not

be obtained. **^{1}H NMR** (400 MHz, Chloroform-*d*) δ 8.46 – 8.30 (m, 1H), 7.17 – 7.05 (m, 1H), 6.83 (td, *J* = 10.6, 9.6, 5.2 Hz, 1H), 6.02 (dd, *J* = 15.9, 2.9 Hz, 1H), 3.80 (d, *J* = 3.2 Hz, 3H), 3.16 (s, 1H), 3.05 (s, 2H), 2.40 (t, *J* = 23.9 Hz, 6H), 2.06 – 1.86 (m, 3H), 1.78 (s, 2H), 1.73 – 1.59 (m, 2H), 1.47 – 1.29 (m, 4H). **^{19}F NMR** (376 MHz, Chloroform-*d*) δ -105.84. **IR** (KBr, cm^{-1}) 2950, 2869, 1721, 1631, 1257, 1164, 1071, 814. **HRMS** (ESI) m/z: $[M+H]^+$ Calcd for $C_{24}H_{29}FO_2H$: 369.2230; Found: 369.2228.

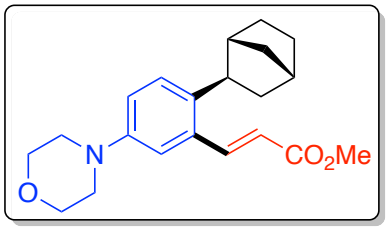

methyl (*E*)-3-(2-(bicyclo[2.2.1]heptan-2-yl)-5-morpholinophenyl)acrylate (4s): Synthesized from **1s**, **2a**, and **3a** according to the general procedure. 0.2 mmol scale: 32% yield (22.1 mg, 9:1 *E:Z*). Yellow oil. R_f = 0.36 (hexane/EtOAc = 4:1). Note: data shown for *Z* isomer. **^{1}H NMR** (400 MHz, Chloroform-*d*) δ 7.23 – 7.15 (m, 2H), 6.90 (d, *J* = 2.7 Hz, 1H), 6.83 (dd, *J* = 8.6, 2.8 Hz, 1H), 6.00 (d, *J* = 12.2 Hz, 1H), 3.88 – 3.81 (m, 4H), 3.62 (s, 3H), 3.16 – 3.12 (m, 1H), 3.15 – 3.07 (m, 4H), 2.69 (dd, *J* = 9.1, 5.5 Hz, 1H), 2.37 – 2.29 (m, 2H), 1.69 (ddd, *J* = 11.6, 8.9, 2.3 Hz, 1H), 1.61 – 1.56 (m, 2H), 1.54 – 1.49 (m, 2H), 1.35 – 1.26 (m, 3H). **^{13}C NMR** (101 MHz, $CDCl_3$) δ 167.7, 148.3, 143.9, 137.4, 134.3, 132.7, 127.4, 125.8, 119.6, 51.8, 46.3, 41.7, 40.7, 38.9, 36.7, 32.9, 28.7, 22.3. Mixture: **IR** (KBr, cm^{-1}) 2952, 2868, 1729, 1606, 1450, 1236, 1122, 818. **HRMS** (ESI) m/z: $[M+Na]^+$ Calcd for $C_{21}H_{27}NO_3Na$: 364.1889; Found: 364.1884.

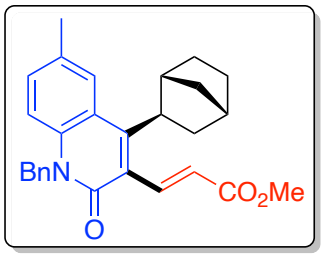

methyl (*E*)-3-(1-benzyl-4-(bicyclo[2.2.1]heptan-2-yl)-6-methyl-2-oxo-1,2-dihydroquinolin-3-yl)acrylate (4t): Synthesized from **1t**, **2a**, and **3a** according to the general procedure. 0.2 mmol scale: 59% yield (50.0 mg). Yellow solid. Melting point: 74 – 77 °C. R_f = 0.2 (hexane/EtOAc = 4:1). **^{1}H NMR** (400 MHz, Chloroform-*d*) δ 8.16 (d, *J* = 16.0 Hz, 1H), 7.79 (s, 1H), 7.32 – 7.27 (m, 1H), 7.25 – 7.12 (m, 6H), 6.81 (d, *J* = 15.9 Hz, 1H), 5.54 (br s, 2H), 3.80 (s, 3H), 3.35 (dd, *J* = 9.5, 7.6 Hz, 1H), 2.87 (s, 1H), 2.42 (s, 1H), 2.40 (s, 3H), 2.04 (t, *J* = 10.8 Hz, 1H), 1.88 (d, *J* = 9.9 Hz, 1H), 1.72 (d, *J* = 9.5 Hz, 3H), 1.52 (d, *J* = 10.6 Hz, 1H), 1.44 (d, *J* = 2.4 Hz, 1H), 1.42 (s, 1H). **^{13}C NMR** (101 MHz, $CDCl_3$) δ 167.7, 148.3, 143.9, 137.4, 134.3, 132.7, 127.4, 125.8, 119.6, 51.8, 46.3, 41.7, 40.7, 38.9, 36.7, 32.9, 28.7, 22.3. **IR** (KBr, cm^{-1}) 2951, 2870, 1719, 1647, 1497, 1437, 1299, 1271, 1169, 807, 728. **HRMS** (ESI) m/z: $[M+Na]^+$ Calcd for $C_{28}H_{29}NO_3Na$: 450.2045; Found: 450.2043.

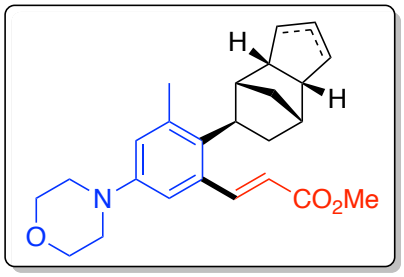

Methyl (*E*)-3-(2-(3a,4,5,6,7,7a-hexahydro-1*H*-4,7-methanoinden-5/6-yl)-3-methyl-5-morph-olinophenyl)acryl-ate (4u): Synthesized from **1a**, **2a**, and **3u** according to the general procedure. 0.2 mmol scale: 77% yield (60.3 mg, *r.r.* = 1:1). Yellow oil. R_f = 0.37 (hexane/EtOAc = 4:1). **^{1}H NMR** (400 MHz, Chloroform-*d*) δ 8.40 (m, 1H), 6.75 (m, 1H), 6.69 (m, 1H), 6.08 (m, 1H), 5.85 – 5.74 (m, 1H), 5.74 – 5.62 (m, 1H), 3.87 – 3.82

(m, 4H), 3.81 (s, 3H), 3.25 – 3.17 (m, 2H), 3.14 – 3.07 (m, 4H), 3.09 – 3.04 (m, 1H), 2.99 (t, J = 8.6 Hz, 0.5H), 2.63 (m, 1H), 2.53 (m, 1H), 2.44 – 2.35 (m, 1H), 2.33 (m, 3H), 2.30 – 2.22 (m, 2H), 2.00 (m, 1H), 1.93 – 1.83 (m, 1H), 1.64 (s, 0.5H), 1.61 (s, 0.5H), 1.56 (q, J = 3.0, 2.3 Hz, 0.5H). **^{13}C NMR** (101 MHz, $CDCl_3$) δ 167.7, 148.3, 143.9, 137.4, 134.3, 132.7, 127.4, 125.8, 119.6, 51.8, 46.3, 41.7, 40.7, 38.9, 36.7, 32.9, 28.7, 22.3. **IR** (KBr, cm^{-1}) 2949, 2851, 1718, 1597, 1168, 1122. **HRMS** (ESI) m/z: $[M+Na]^+$ Calcd for $C_{25}H_{31}NO_3Na$: 416.2202; Found: 416.2201.

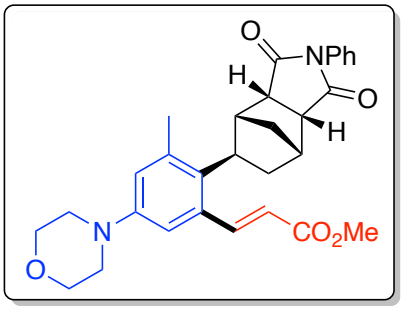

methyl (*E*)-3-(2-*endo*-(1,3-dioxo-2-phenyloctahydro-1*H*-4,7-methanoisoindol-5-yl)-3-methyl-5-morpholinophenyl)acrylate (4v): Synthesized from **1t**, **2a**, and **3a** according to the general procedure. 0.2 mmol scale: 68% yield (67.8 mg). Orange solid. Melting point: 112 – 115 °C. R_f = 0.11 (hexane/EtOAc = 4:1). **^{1}H NMR** (400 MHz, Chloroform-*d*) δ 8.30 (d, J = 15.4 Hz, 1H), 7.53 – 7.46 (m, 2H), 7.45 – 7.38 (m, 1H), 7.34 – 7.29 (m, 2H), 6.75 (d, J = 2.8 Hz, 1H), 6.63 (d, J = 2.8 Hz, 1H), 6.08 (d, J = 15.5 Hz, 1H), 3.88 – 3.81 (m, 4H), 3.79 (s, 3H), 3.43 – 3.30 (m, 2H), 3.23 (dd, J = 16.3, 6.5 Hz, 2H), 3.15 – 3.09 (m, 4H), 2.99 (s, 1H), 2.31 (s, 3H), 2.22 – 2.09 (m, 2H), 1.94 – 1.80 (m, 2H). **^{13}C NMR** (101 MHz, $CDCl_3$) δ 177.2, 177.1, 167.2, 149.1, 148.5, 138.7, 134.9, 132.8, 132.0, 129.4, 128.9, 126.7, 120.9, 120.2, 114.8, 51.9, 49.8, 49.1, 48.8, 45.1, 42.2, 41.1, 39.7, 35.4, 22.9. **IR** (KBr, cm^{-1}) 2957, 2852, 1711, 1628, 1598, 1251, 1160, 1122. **HRMS** (ESI) m/z: $[M+H]^+$ Calcd for $C_{30}H_{32}N_2O_5H$: 501.2389; Found: 501.2388.

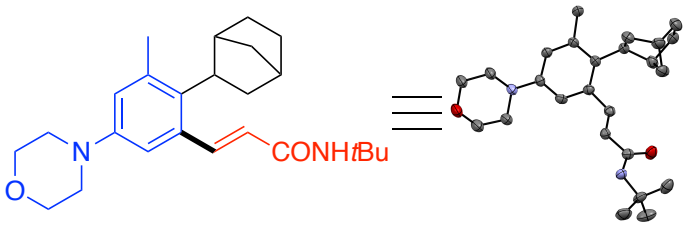

The enantiomer on the norbornyl ring and hydrogen atoms were omitted for clarity; thermal ellipsoids drawn at 50% probability.

Identification code	**4d** (CCDC# 1990447)
Empirical formula	$C_{25}H_{36}N_2O_2$
Formula weight	396.56
Temperature/K	100(2)
Crystal system	hexagonal
Space group	$P6_5$
a/Å	13.2389(8)
b/Å	13.2389(8)
c/Å	22.8347(14)
α/°	90
β/°	90
γ/°	120
Volume/Å^3	3466.0(5)
Z	6
ρ_{calc}g/cm^3	1.140

μ/mm^{-1}	0.072
F(000)	1296.0
Crystal size/mm^3	0.317 × 0.192 × 0.126
Radiation	MoKα (λ = 0.71073)
2Θ range for data collection/°	5.036 to 50.786
Index ranges	-15 ≤ h ≤ 15, -15 ≤ k ≤ 15, -27 ≤ l ≤ 27
Reflections collected	79372
Independent reflections	4236 [R_{int} = 0.1095, R_{sigma} = 0.0492]
Data/restraints/parameters	4236/267/312
Goodness-of-fit on F^2	1.034
Final R indexes [I>=2σ (I)]	R_1 = 0.0510, wR_2 = 0.1027
Final R indexes [all data]	R_1 = 0.0872, wR_2 = 0.1169
Largest diff. peak/hole / e $Å^{-3}$	0.23/-0.19
Flack parameter	-0.8(6)

4.5. ^{1}H-NMR, ^{2}H-NMR, ^{13}C-NMR, and ^{19}F-NMR Spectra

Figure 4.3. ^{1}H NMR Spectrum of **2a-d$_3$**

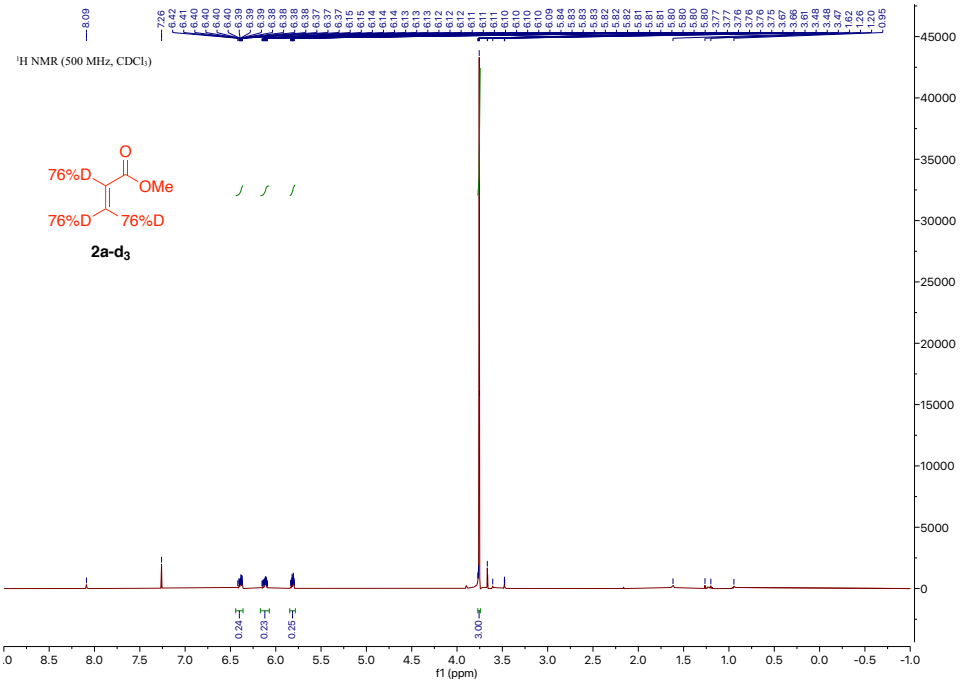

Figure 4.4. ^{2}H NMR Spectrum of **2a-d$_3$**

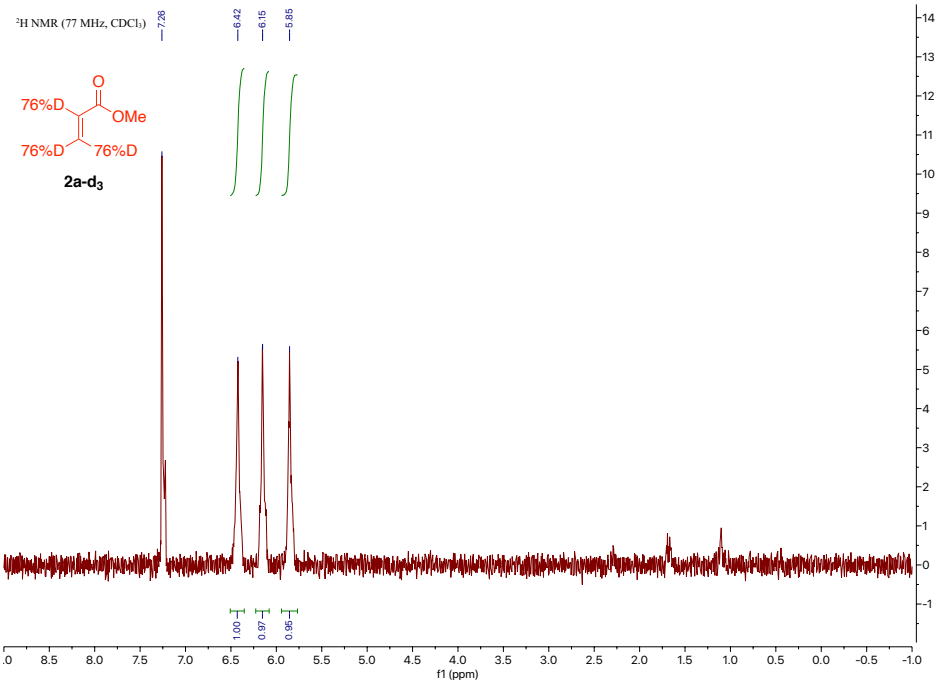

Figure 4.5. ^{2}H NMR Spectrum of **1i-d$_7$**

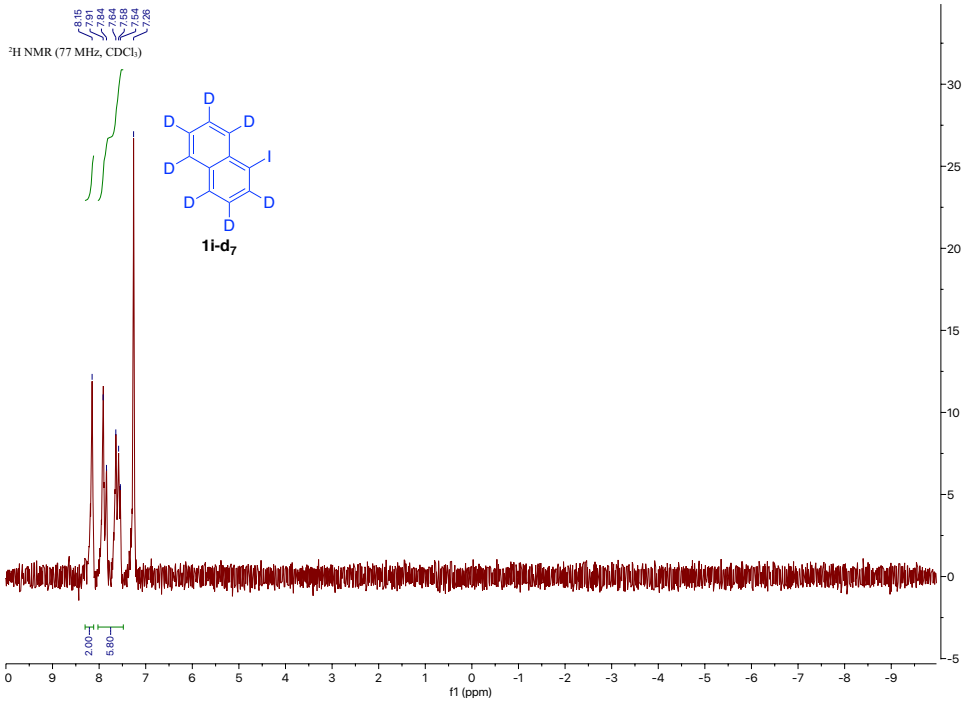

Figure 4.6. ^{13}C NMR Spectrum of **1i-d$_7$**

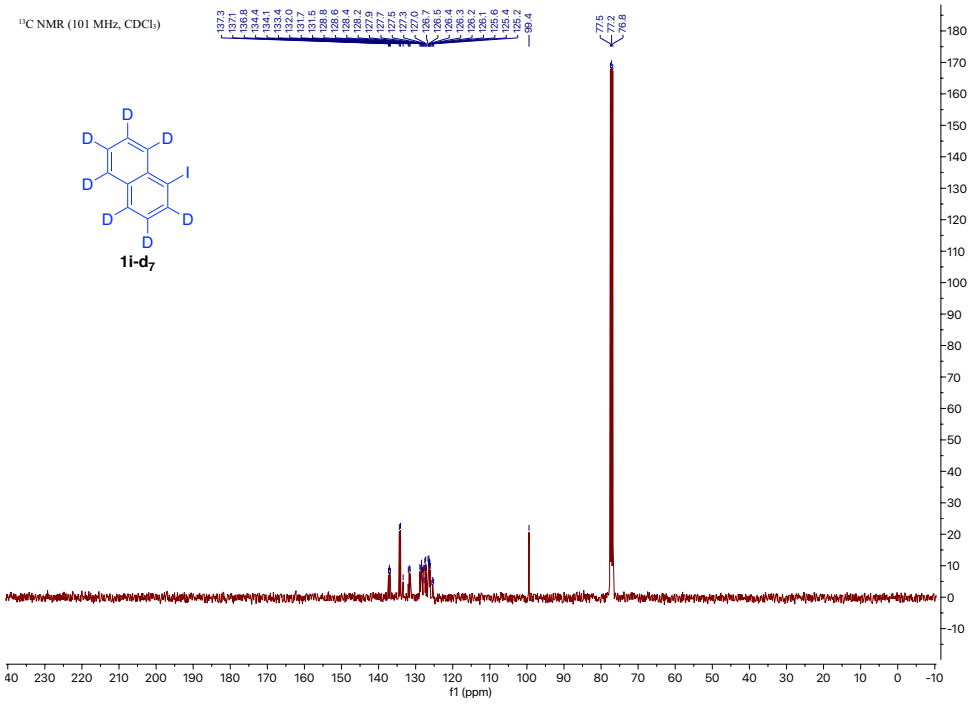

Figure 4.7. ^{1}H NMR Spectrum of **4a**

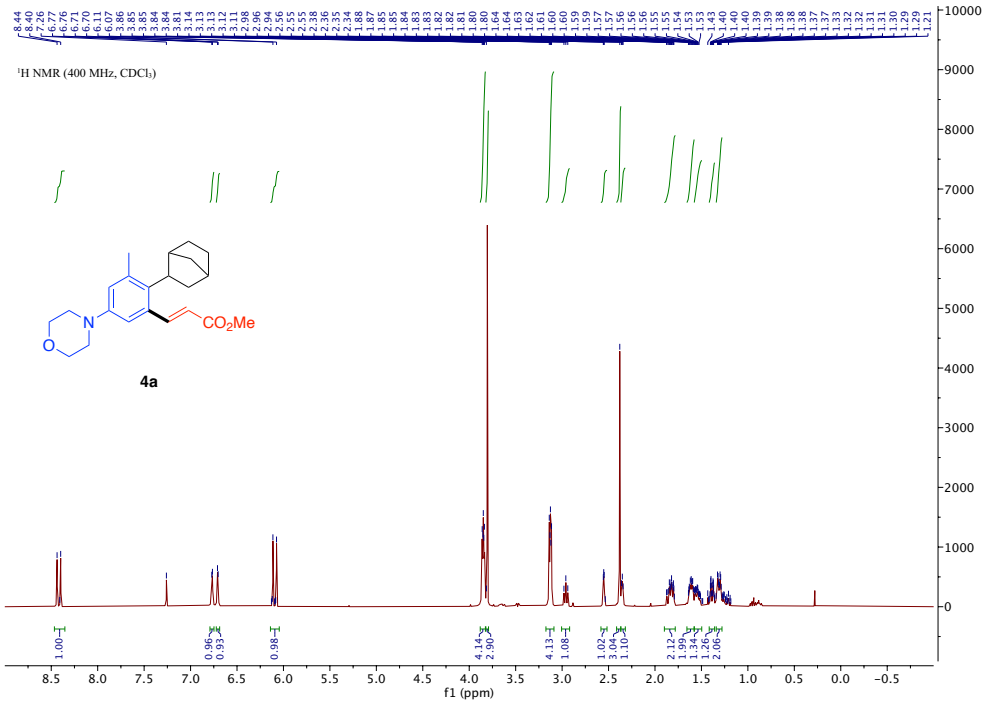

Figure 4.8. ^{13}C NMR Spectrum of **4a**

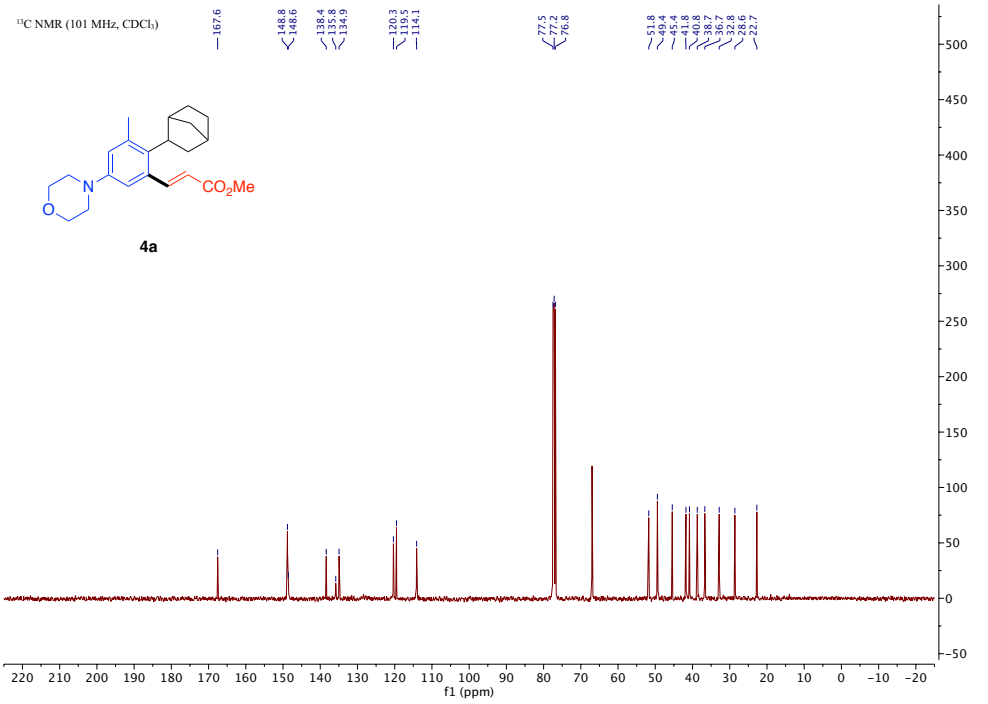

Figure 4.9. ^{1}H NMR Spectrum of **4aa**

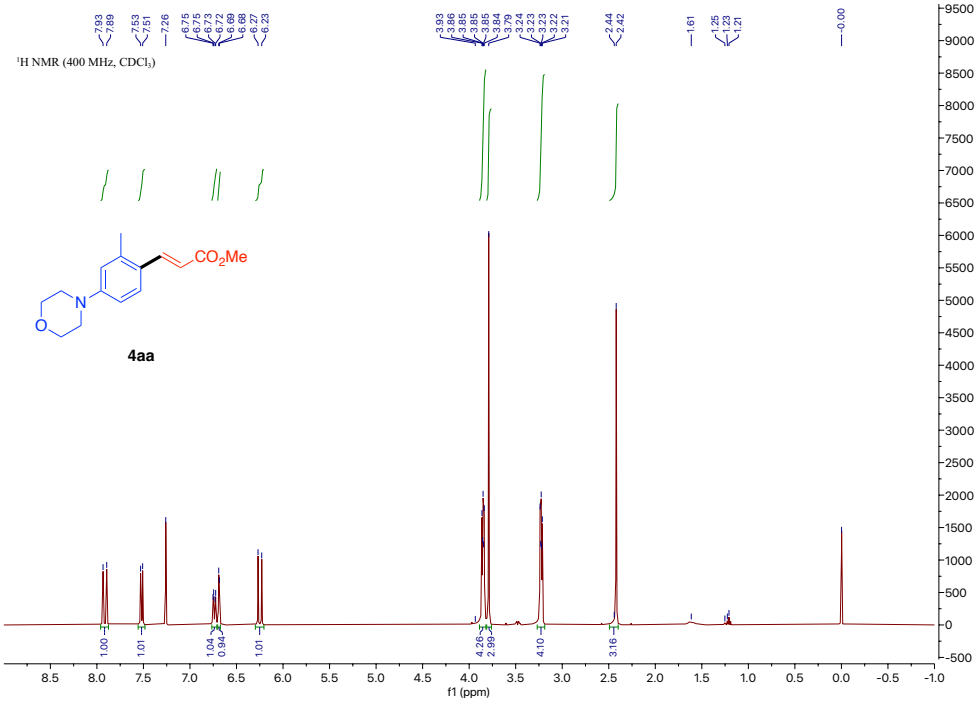

Figure 4.10. ^{13}C NMR Spectrum of **4aa**

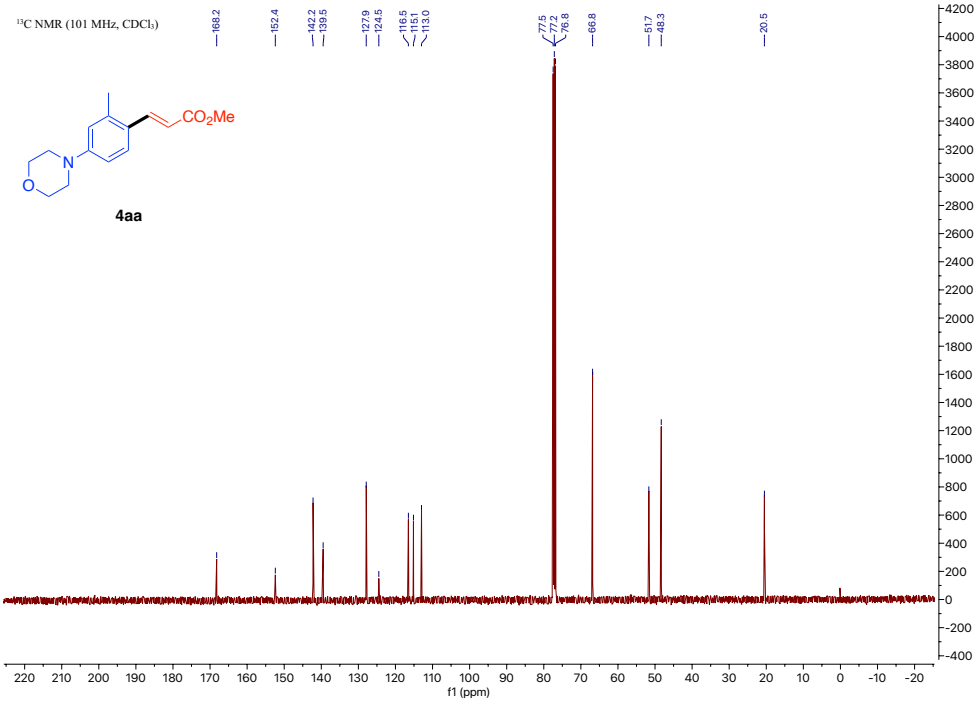

Figure 4.11. ^{1}H NMR Spectrum of **4ab**

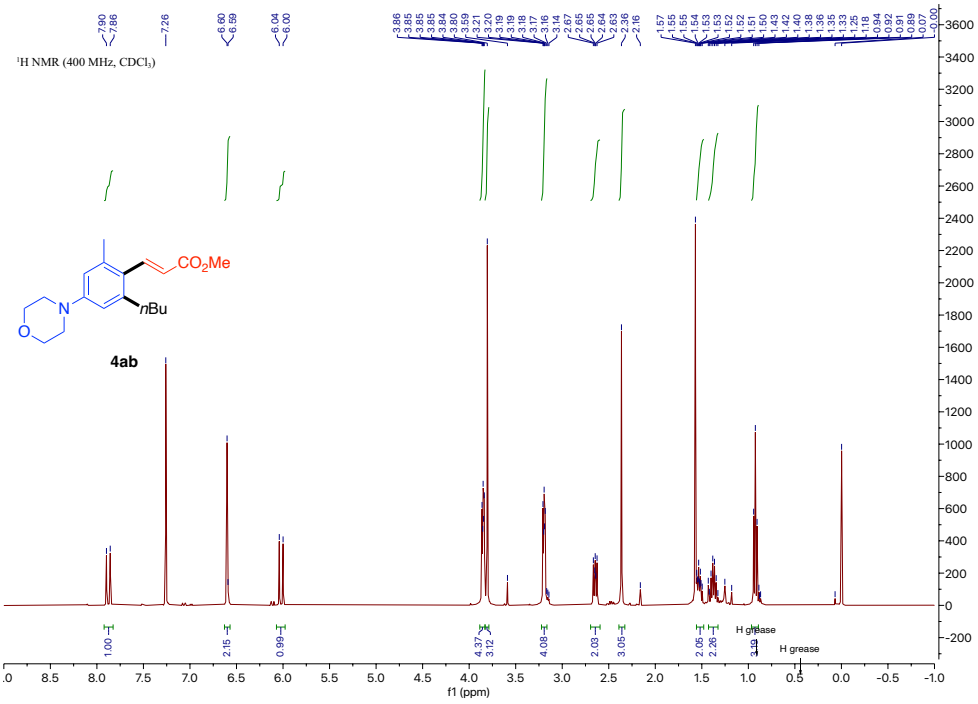

Figure 4.12. ^{13}C NMR Spectrum of **4ab**

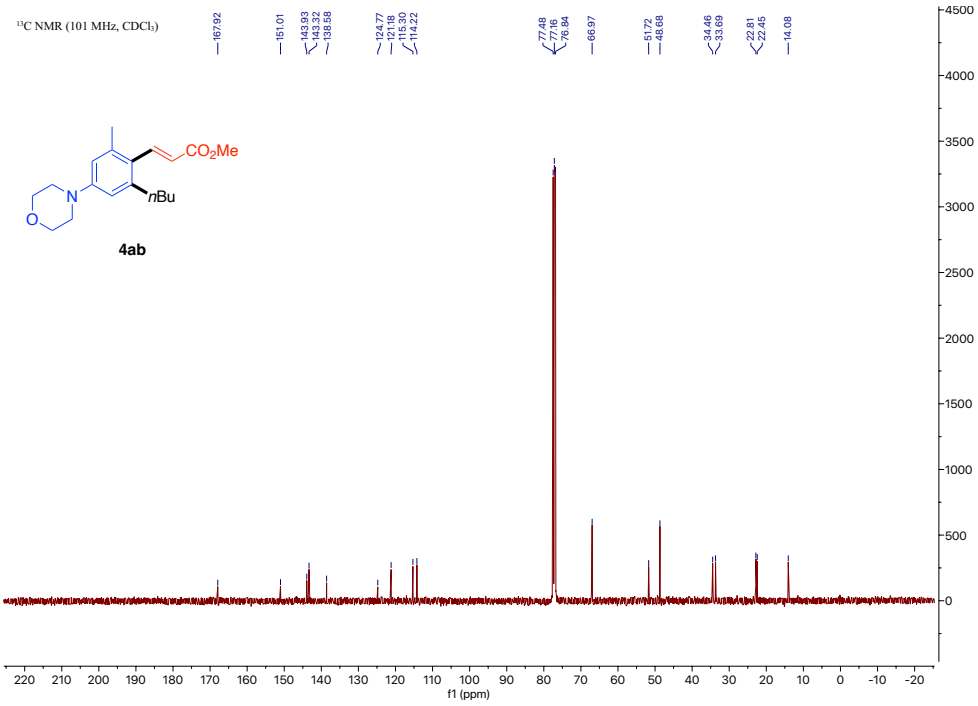

Figure 4.13. ^{1}H NMR Spectrum of **4i**

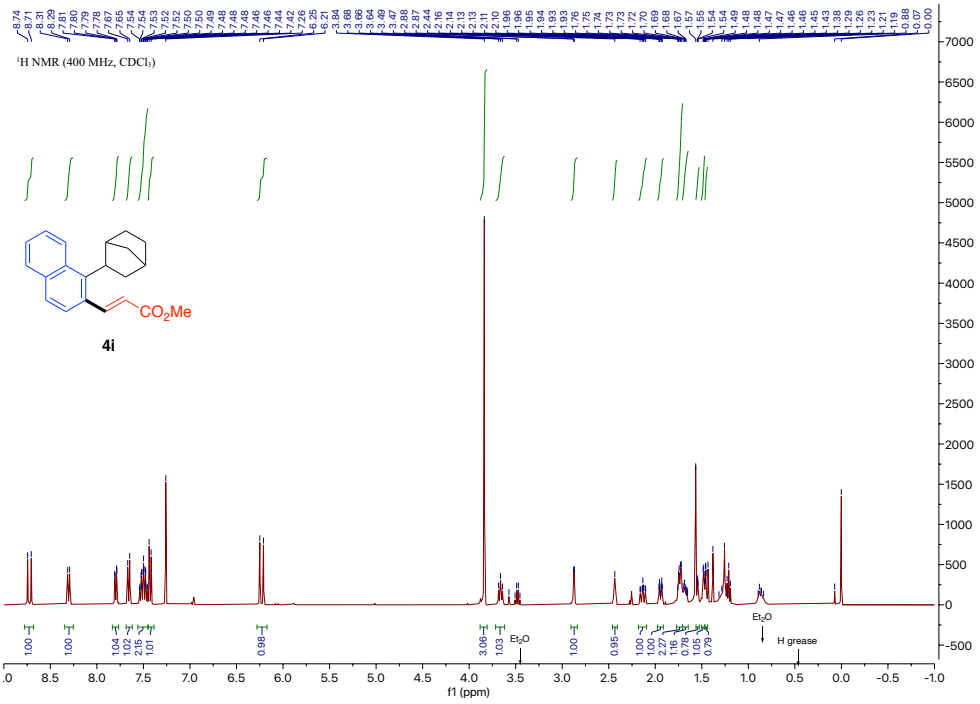

Figure 4.14. ^{13}C NMR Spectrum of **4i**

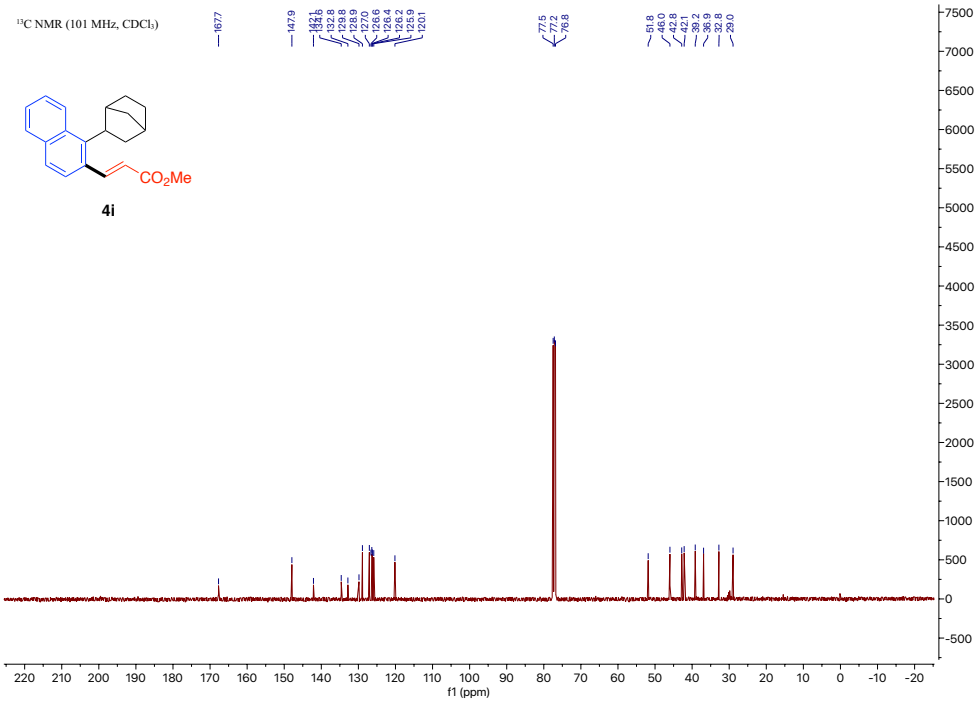

Figure 4.15. HSQC 2D NMR Spectrum of **4i**

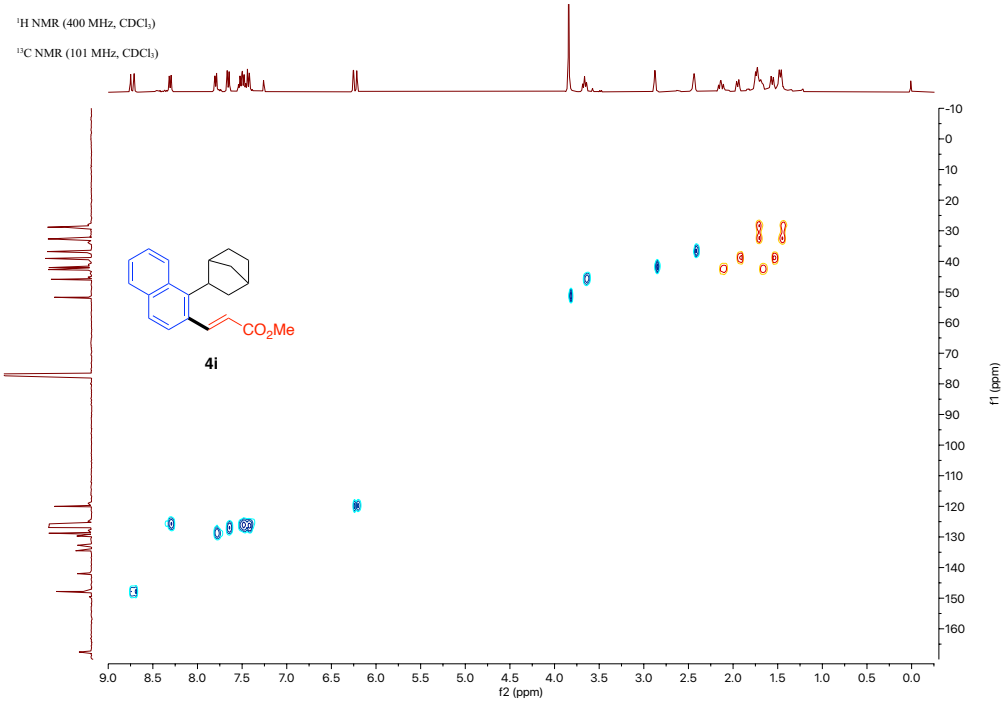

Figure 4.16. COSY 2D NMR Spectrum of **4i**

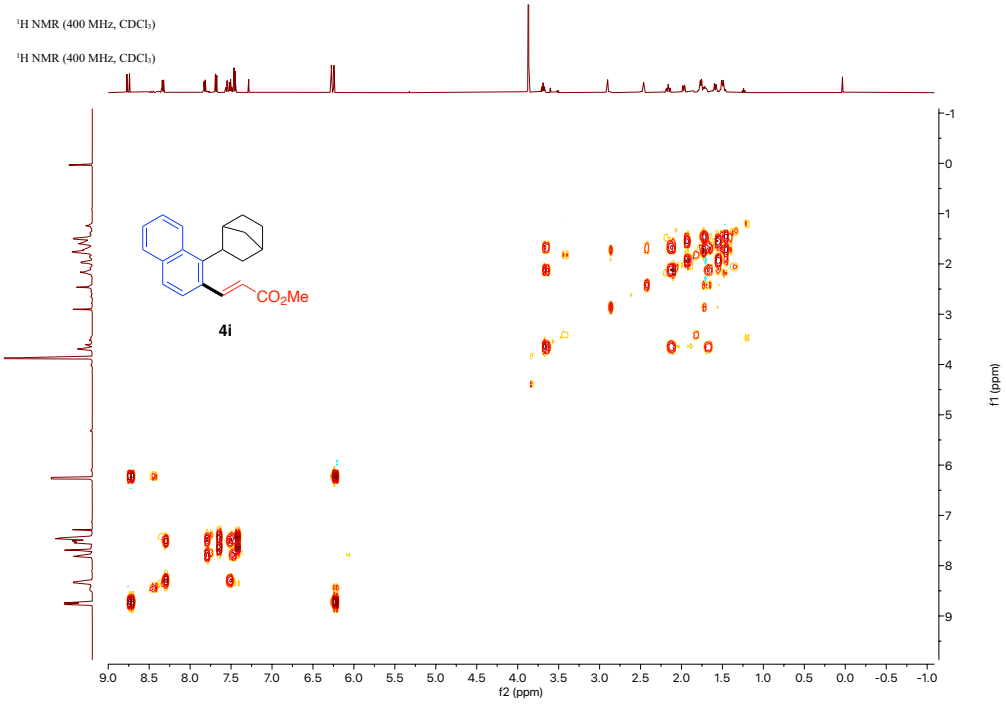

Figure 4.17. NOESY 2D NMR Spectrum of **4i** (alkyl region)

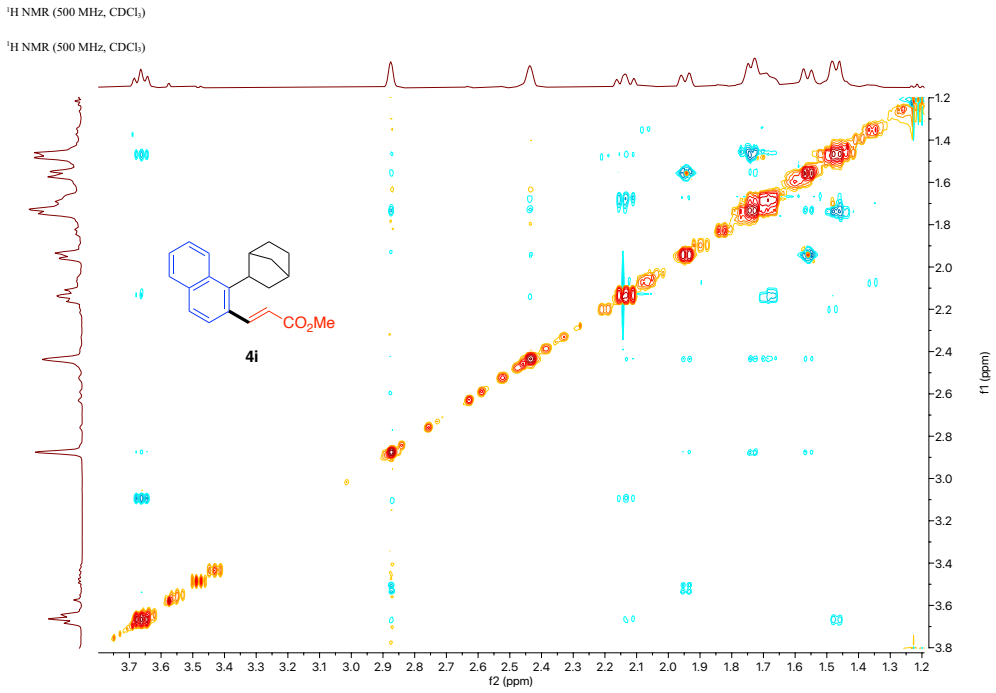

Figure 4.18. Assigned ^{1}H NMR signals (increasing as signal is more downfield)

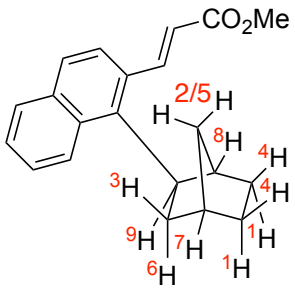

Figure 4.19. ^{1}H NMR Spectrum of **4i-d$_2$**

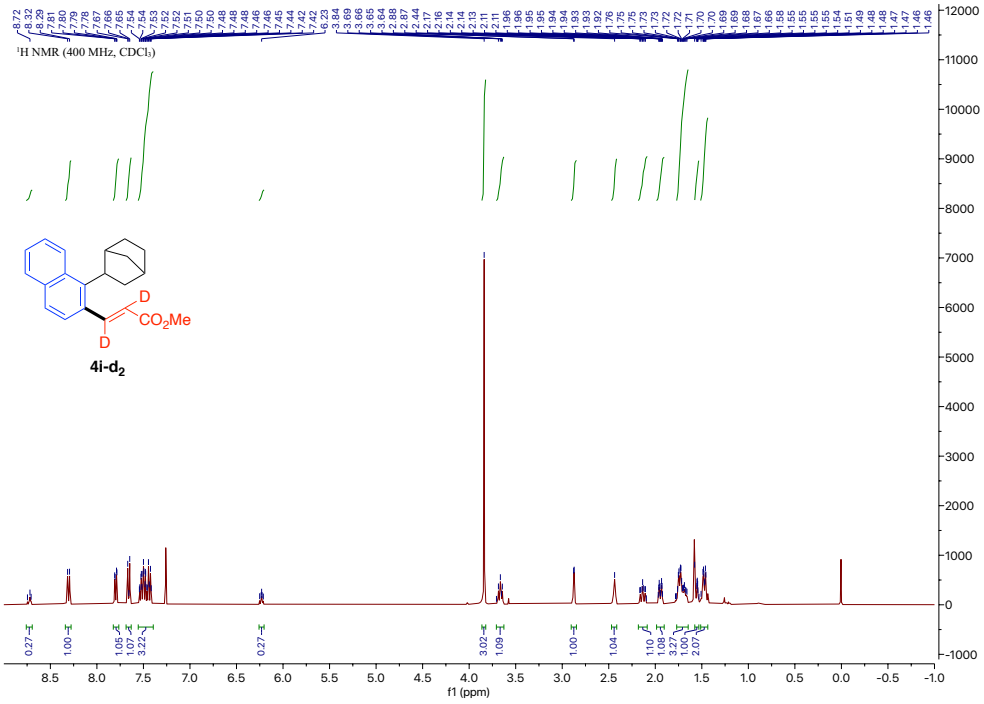

Figure 4.20. ^{2}H NMR Spectrum of **4i-d$_2$**

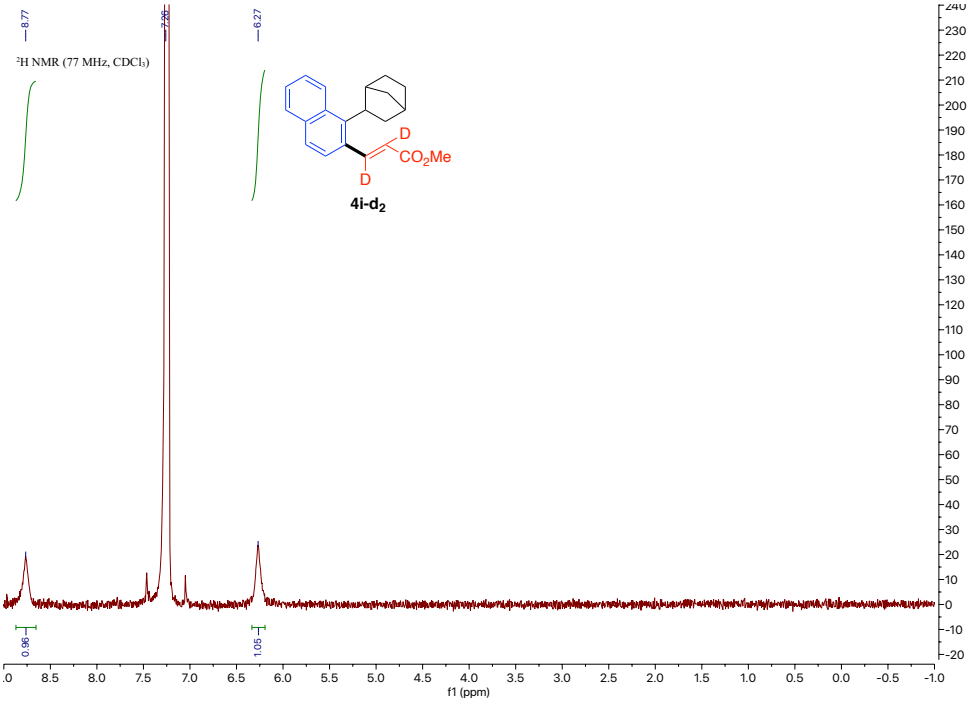

Figure 4.21. ^{1}H NMR Spectrum of **4i-d$_7$**

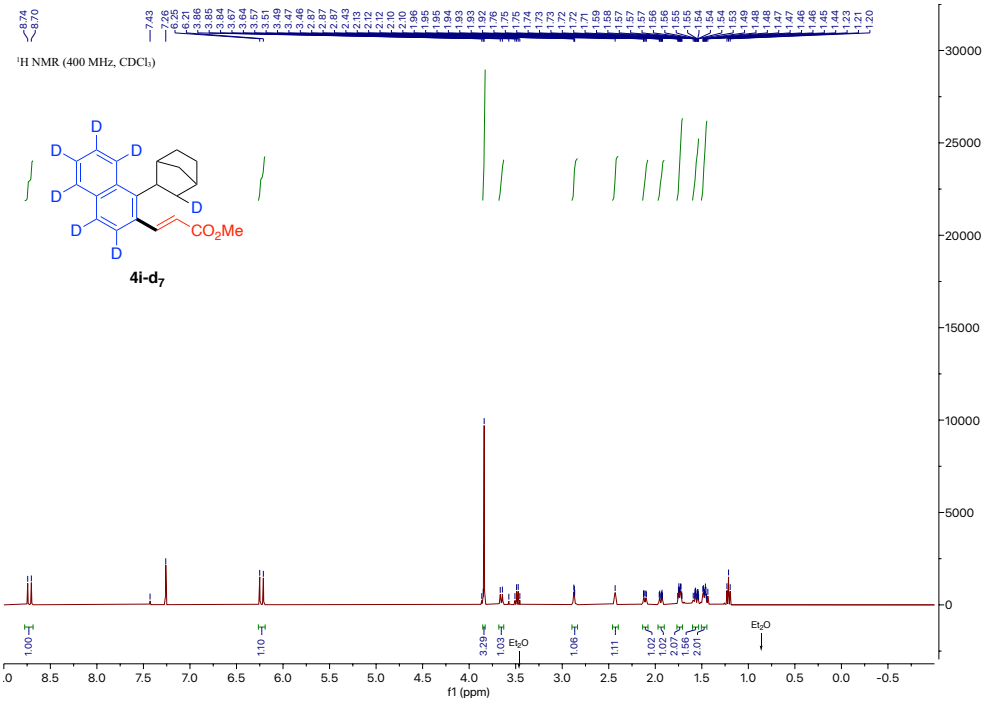

Figure 4.22. ^{2}H NMR Spectrum of **4i-d$_7$**

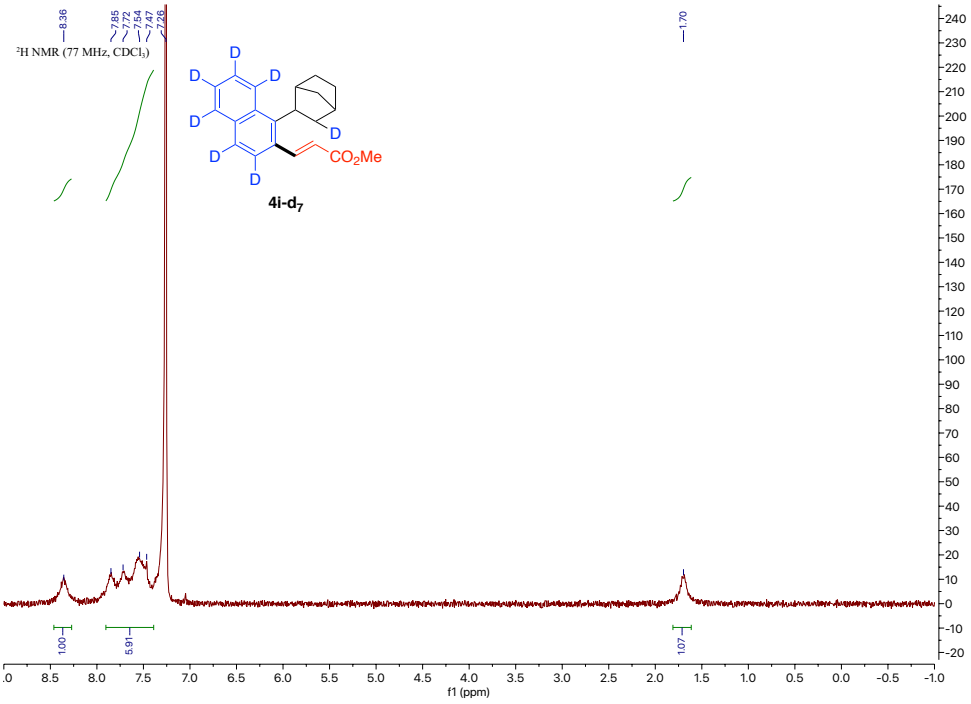

Figure 4.23. ^{1}H NMR Spectrum of **4b**

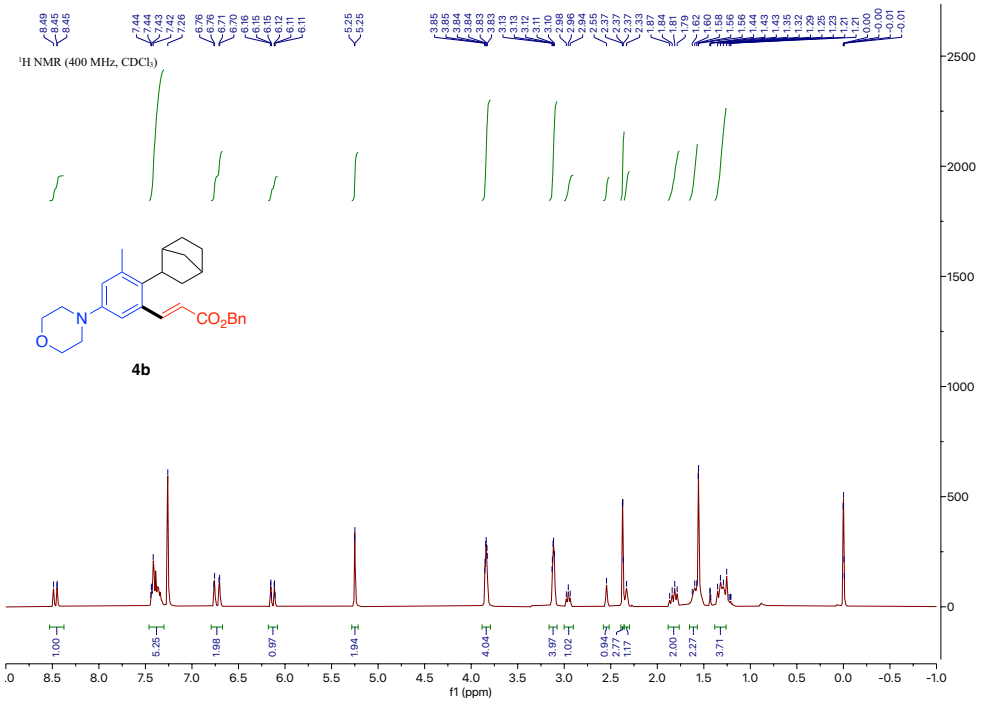

Figure 4.24. ^{13}C NMR Spectrum of **4b**

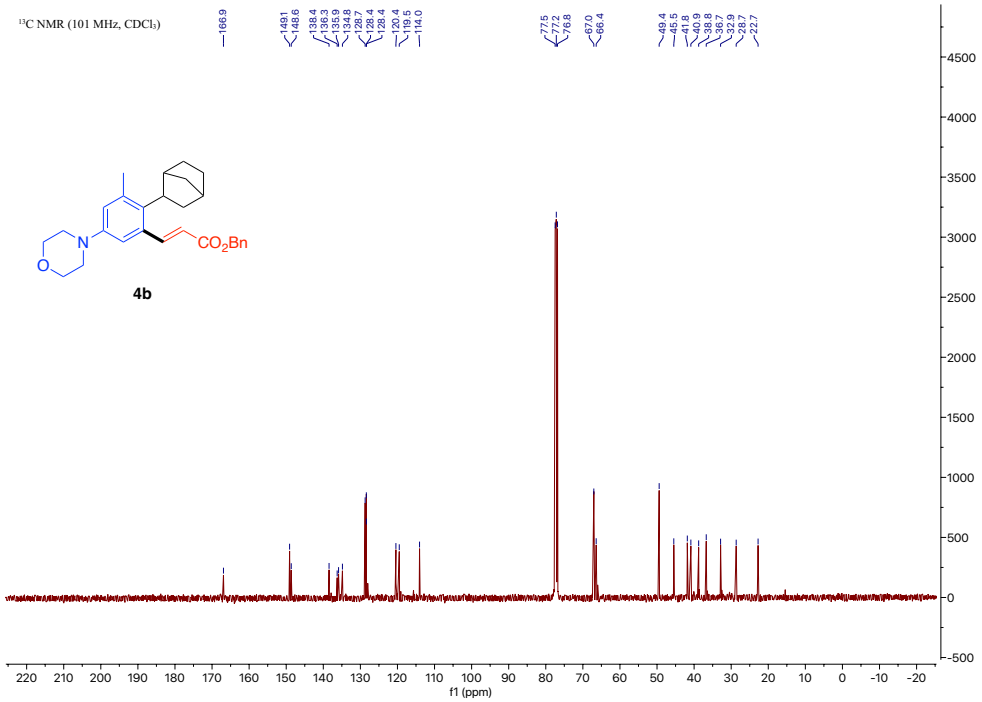

Figure 4.25. ^{1}H NMR Spectrum of **4c**

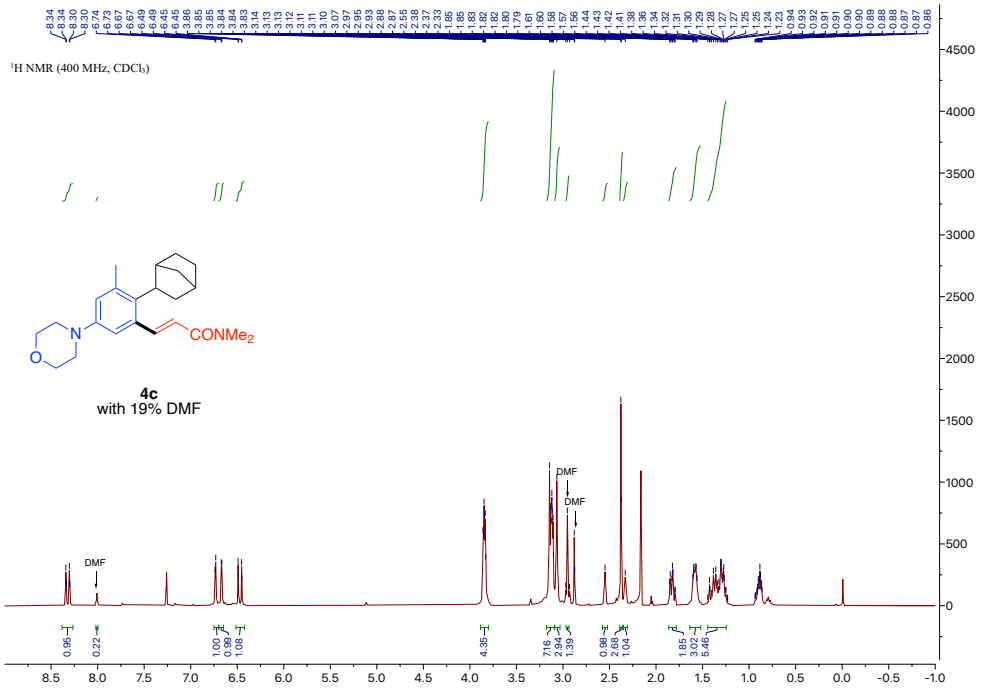

Figure 4.26. ^{13}C NMR Spectrum of **4c**

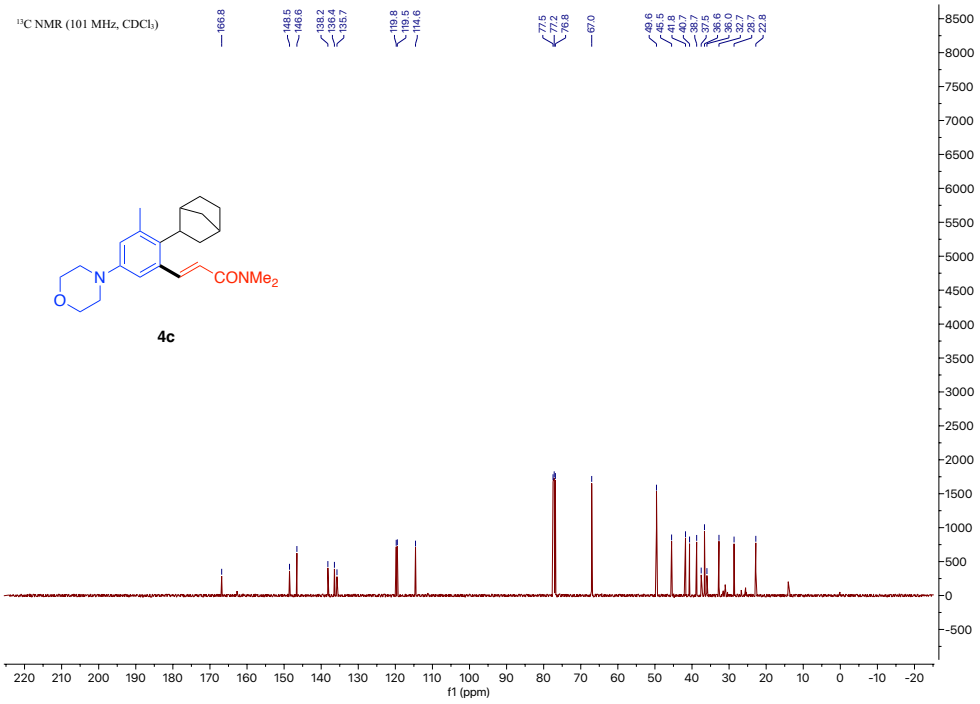

Figure 4.27. ^{1}H NMR Spectrum of **4d**

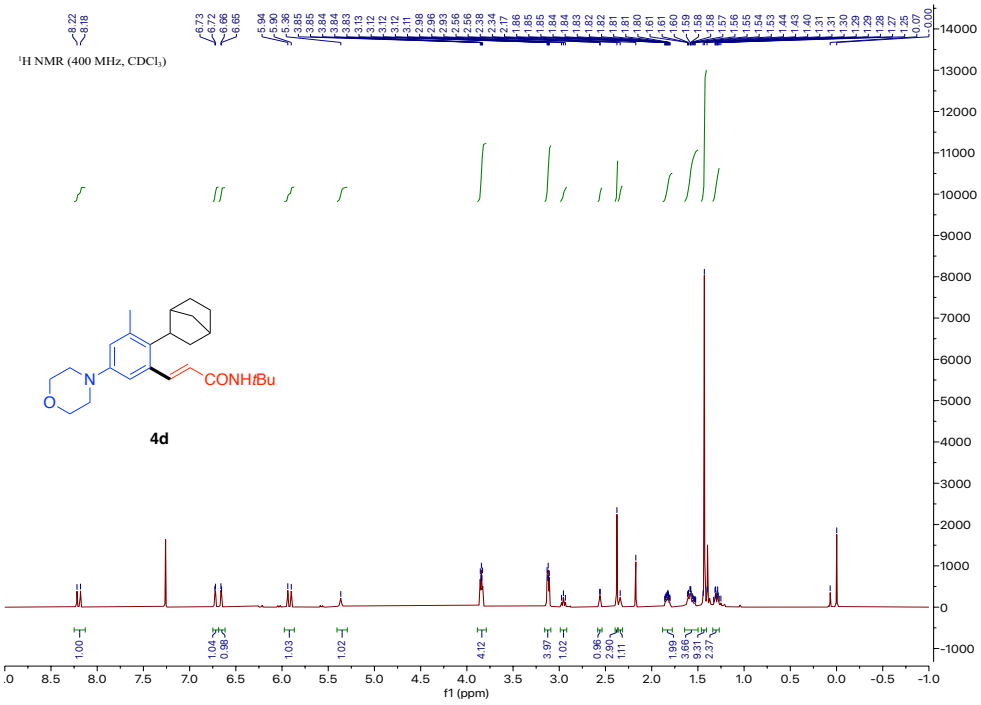

Figure 4.28. ^{13}C NMR Spectrum of **4d**

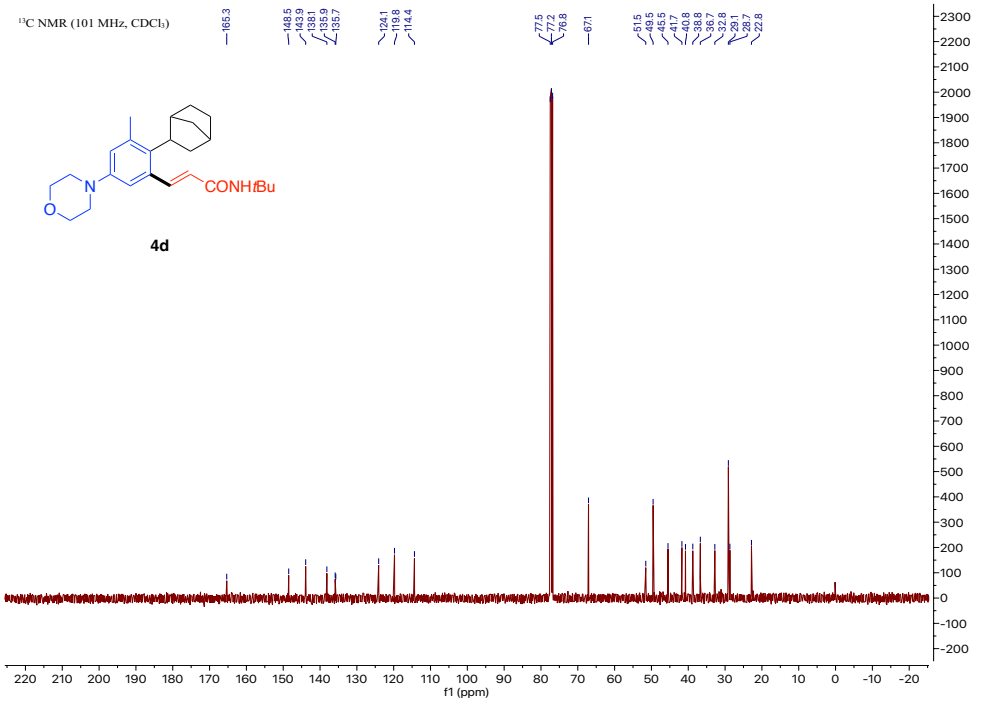

Figure 4.29. ^{1}H NMR Spectrum of **4e**

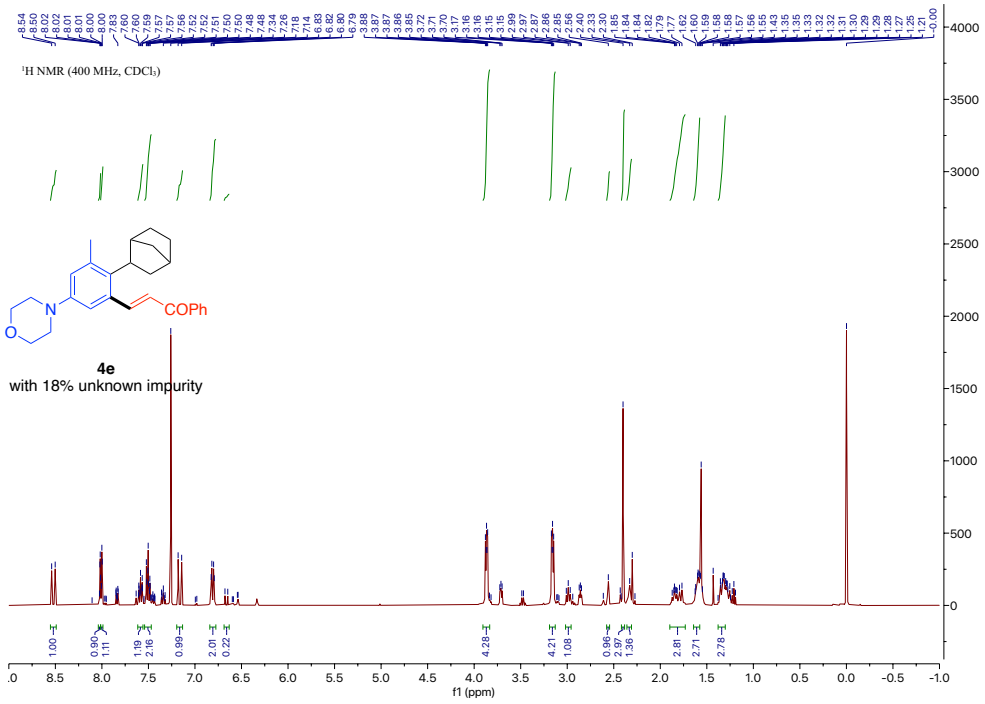

Figure 4.30. ^{13}C NMR Spectrum of **4e**

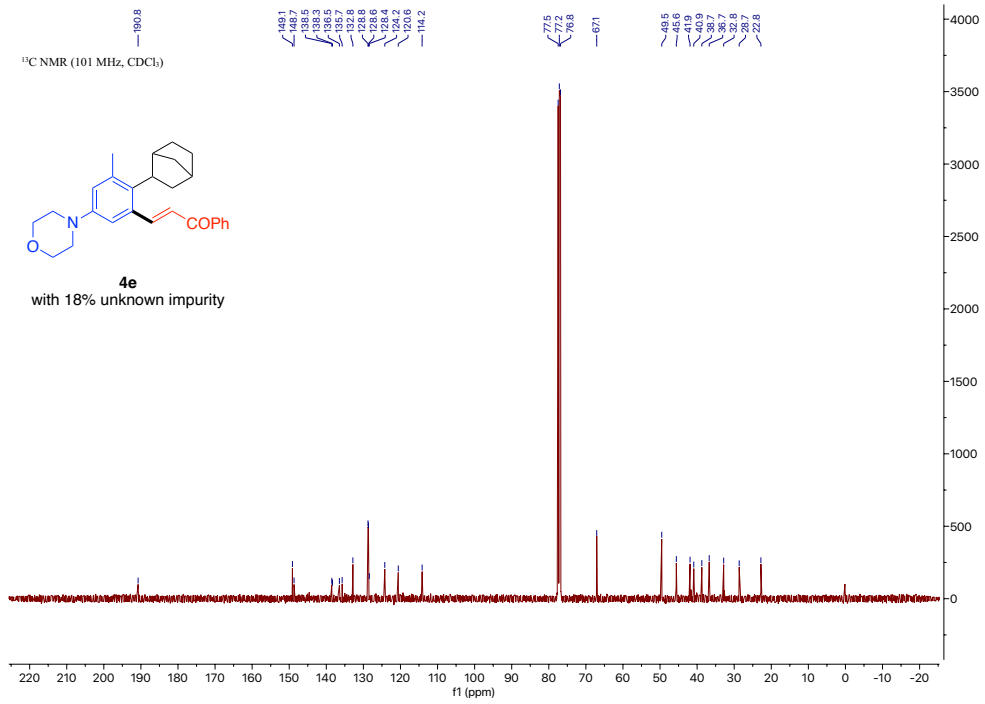

Figure 4.31. ^{1}H NMR Spectrum of **4f**

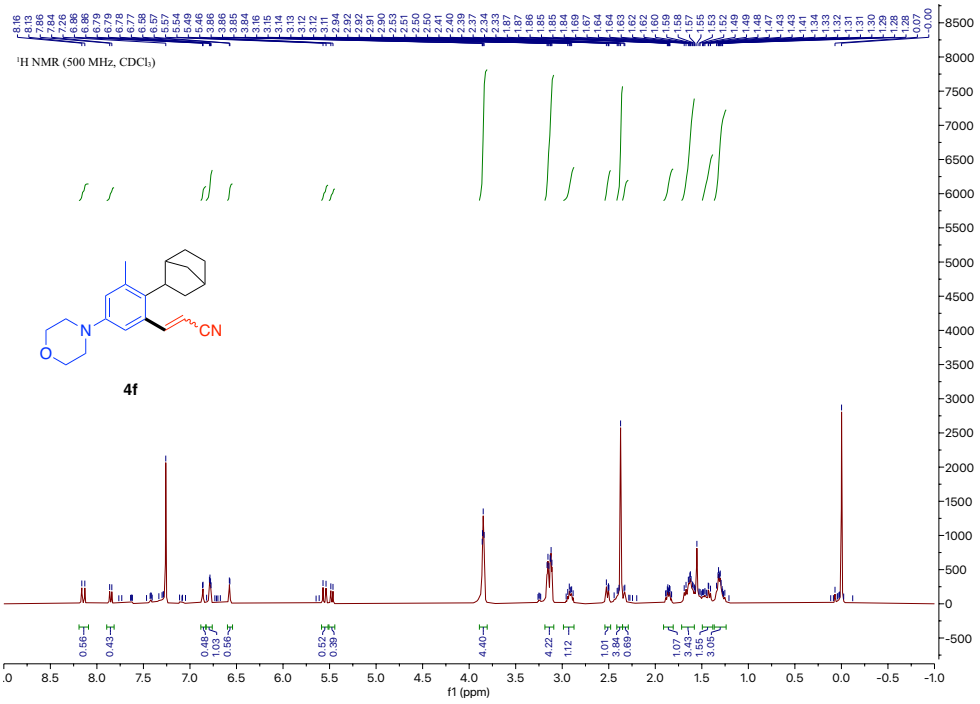

Figure 4.32. ^{13}C NMR Spectrum of **4f**

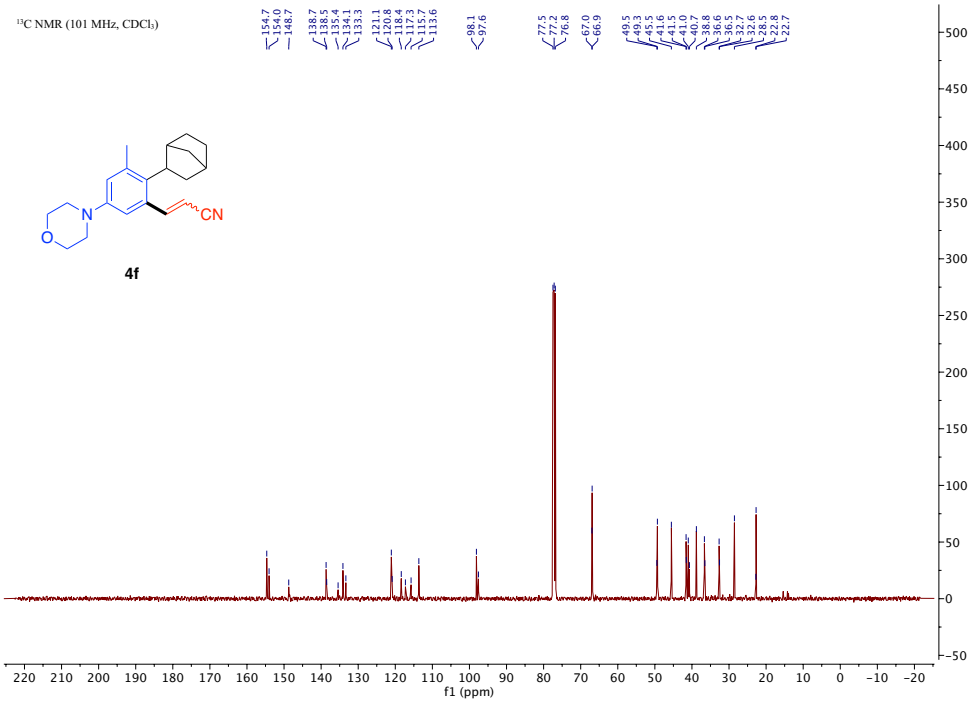

Figure 4.33. ^{1}H NMR Spectrum of **4g**

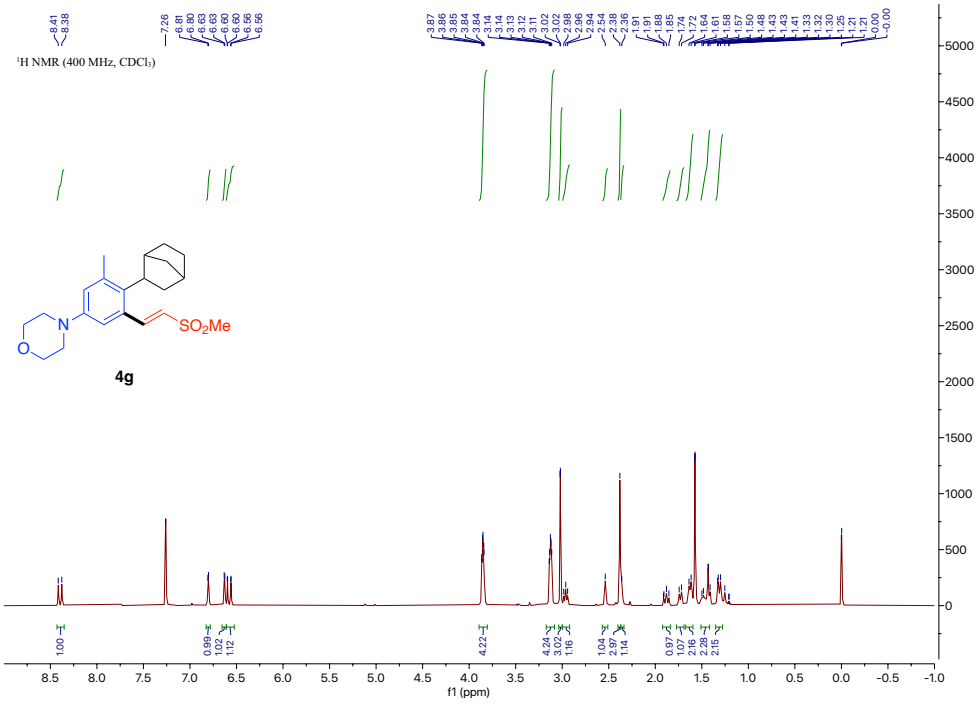

Figure 4.34. ^{13}C NMR Spectrum of **4g**

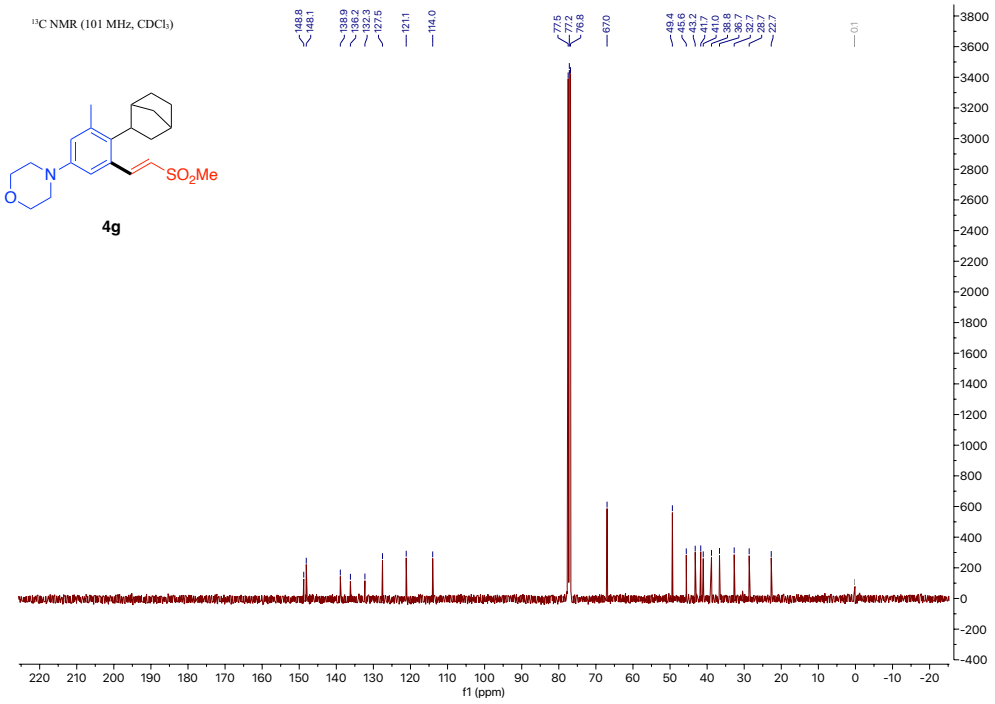

Figure 4.35. ^{1}H NMR Spectrum of **4h**

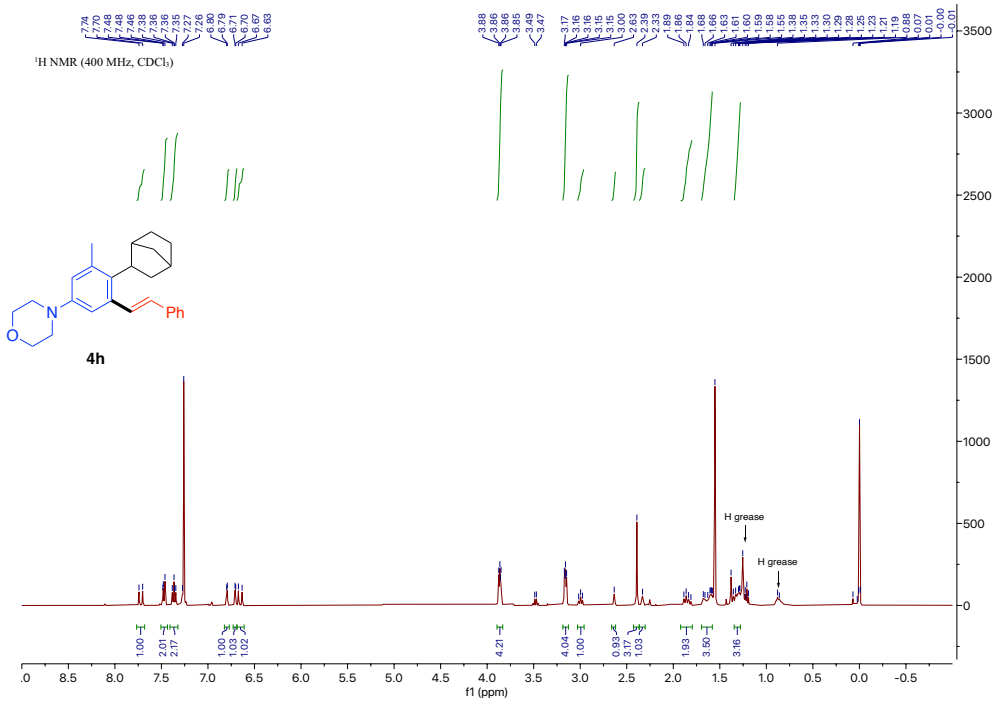

Figure 4.36. ^{13}C NMR Spectrum of **4h**

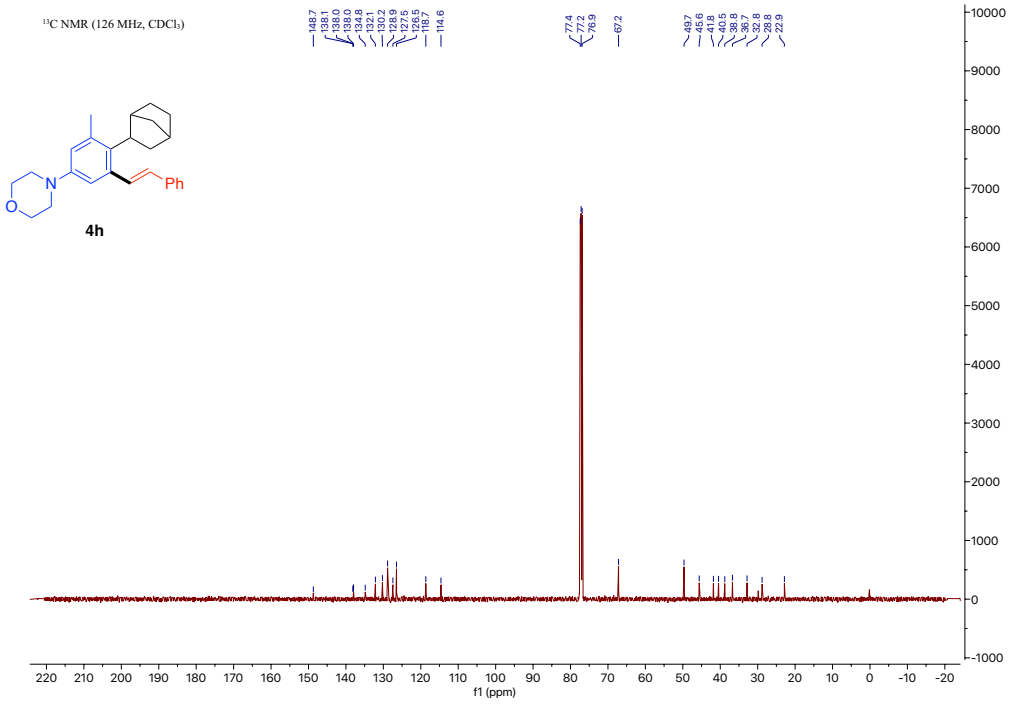

Figure 4.37 ^{1}H NMR Spectrum of **4j**

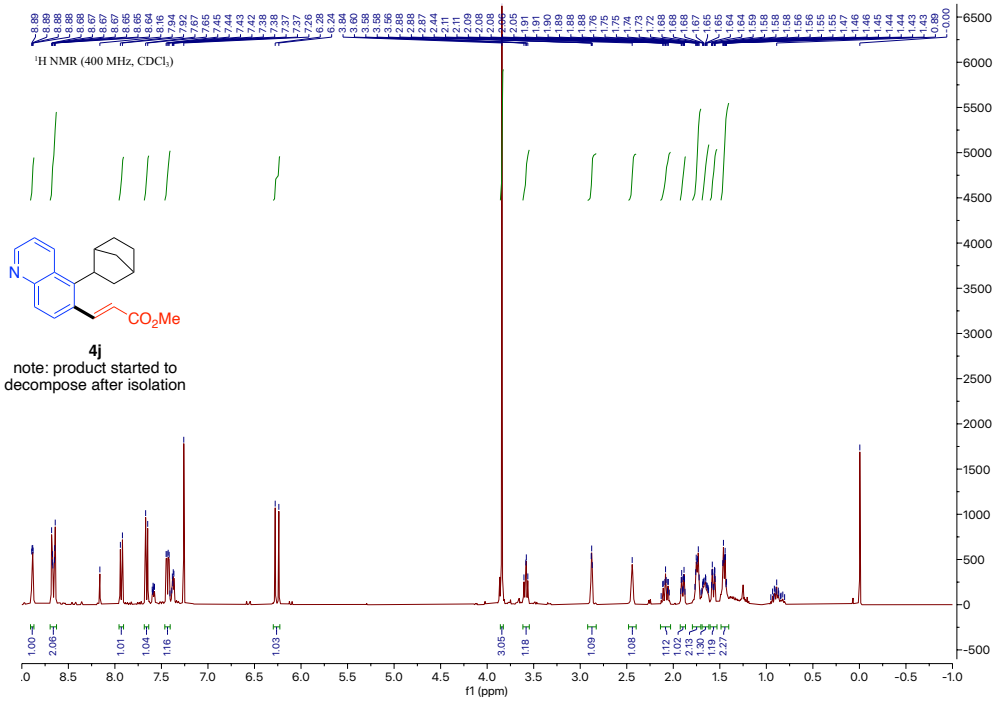

Figure 4.38. ^{13}C NMR Spectrum of **4j**

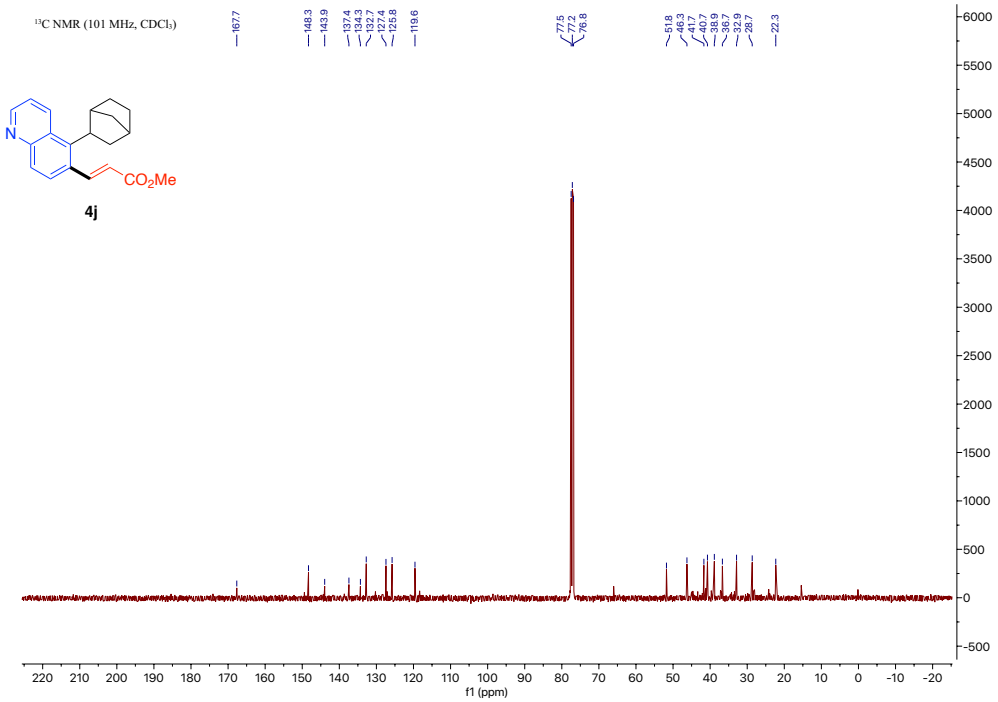

Figure 4.39. ^{1}H NMR Spectrum of **4k**

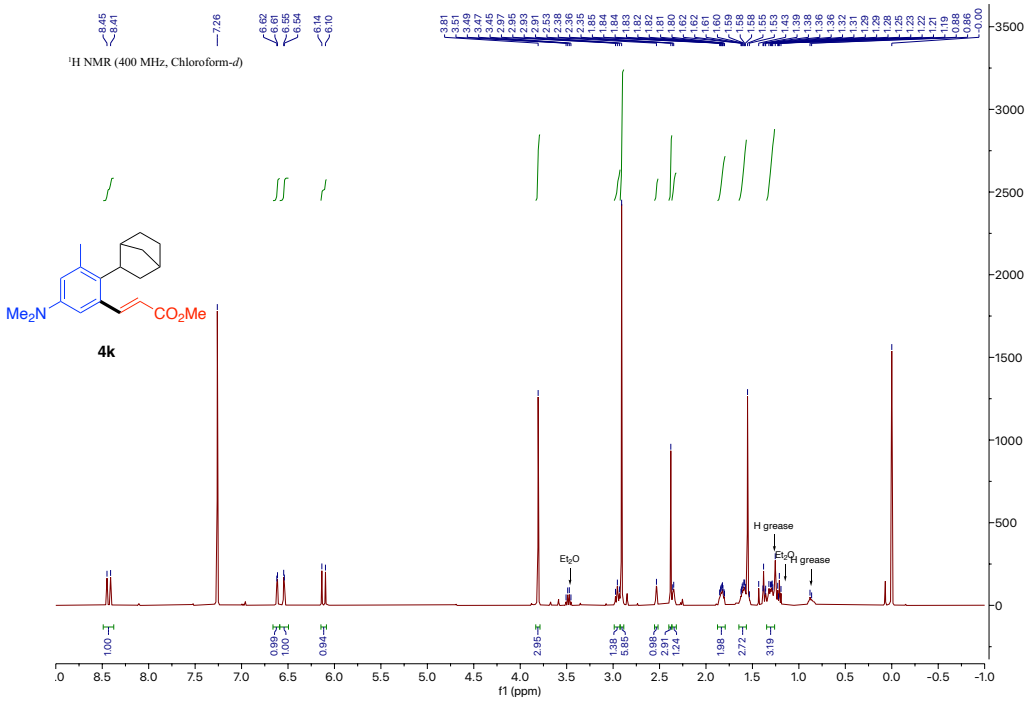

Figure 4.40. ^{13}C NMR Spectrum of **4k**

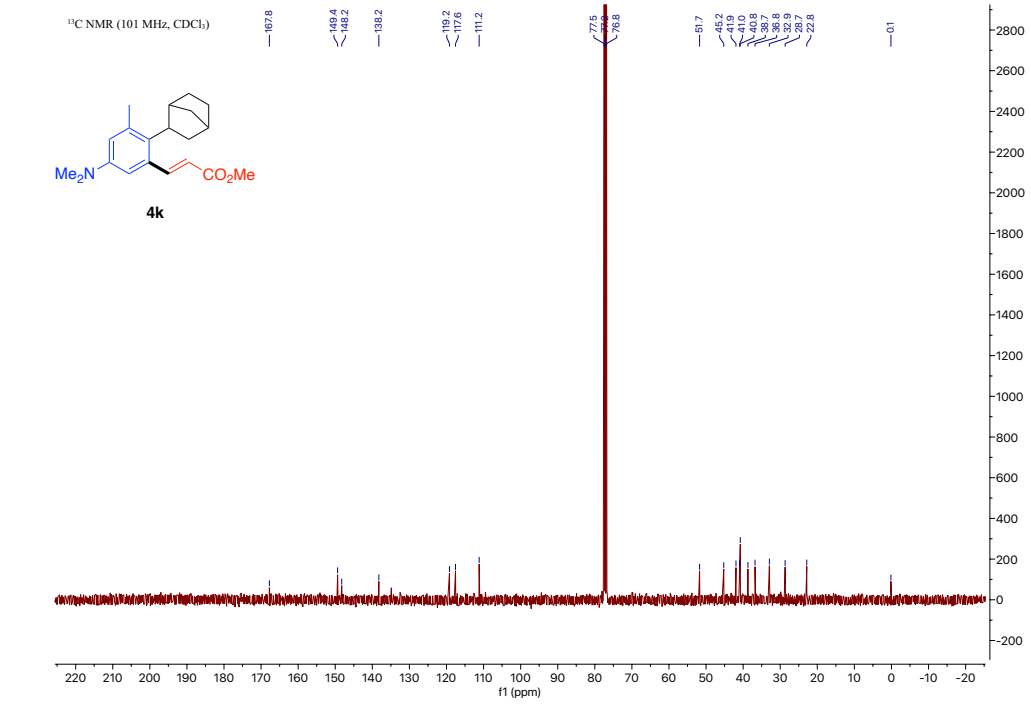

Figure 4.41. ^{1}H NMR Spectrum of **4l**

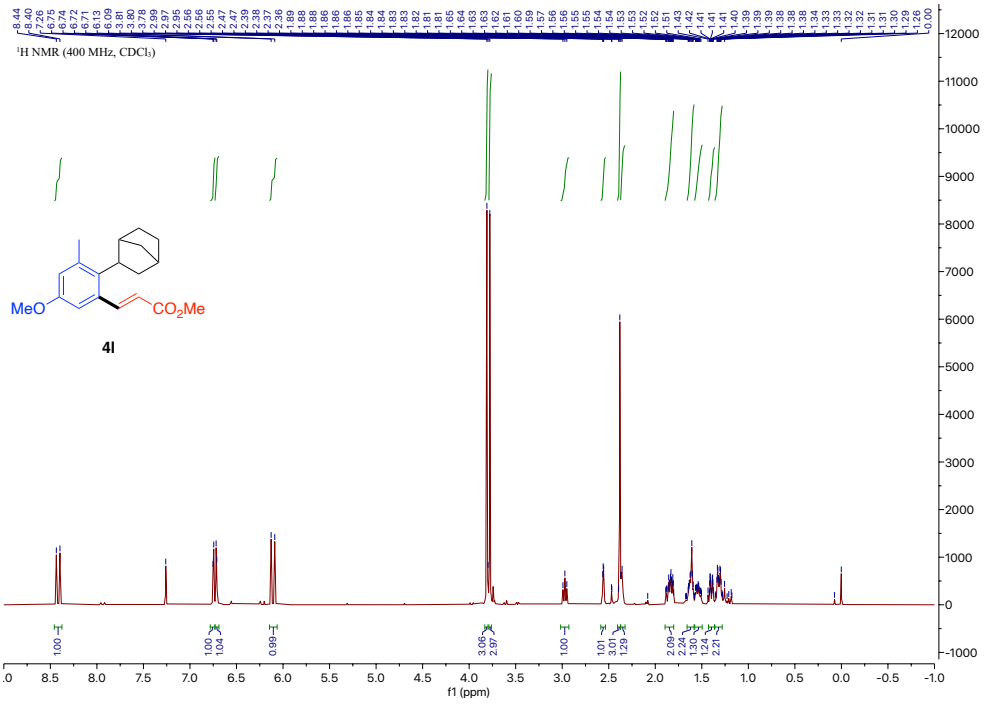

Figure 4.42. ^{13}C NMR Spectrum of **4l**

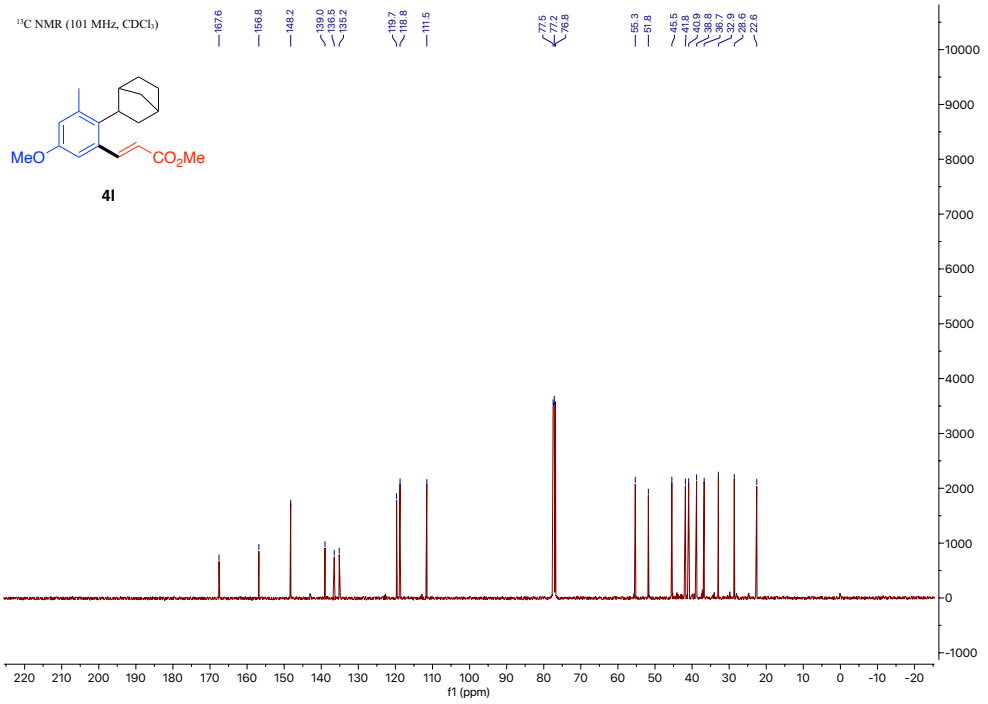

Figure 4.43. ^{1}H NMR Spectrum of **4m**

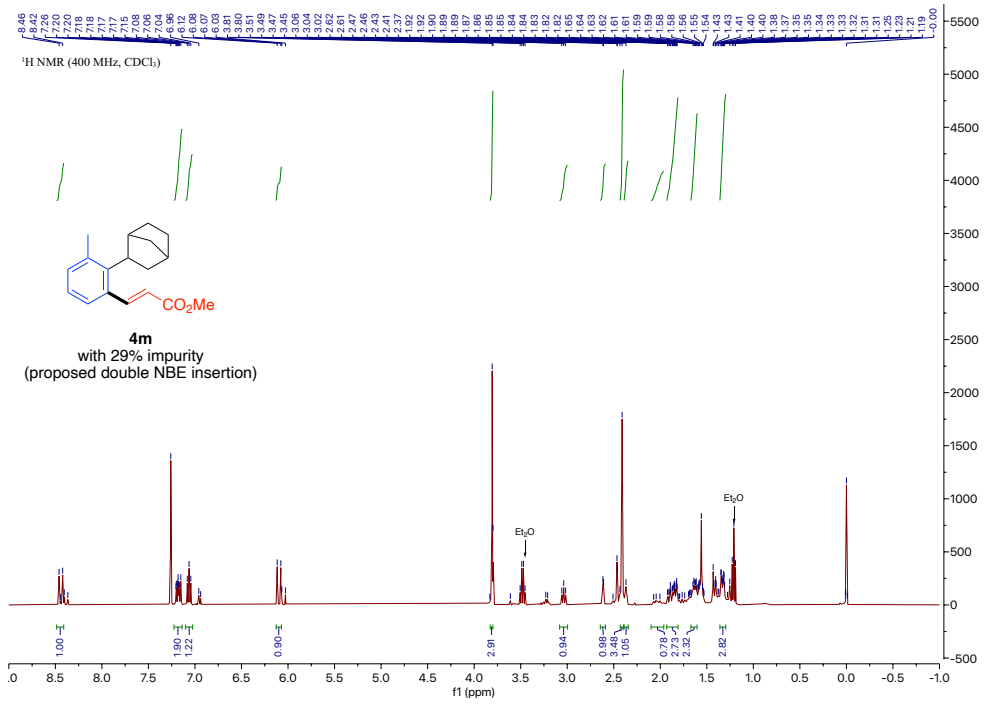

Figure 4.44. ^{13}C NMR Spectrum of **4m**

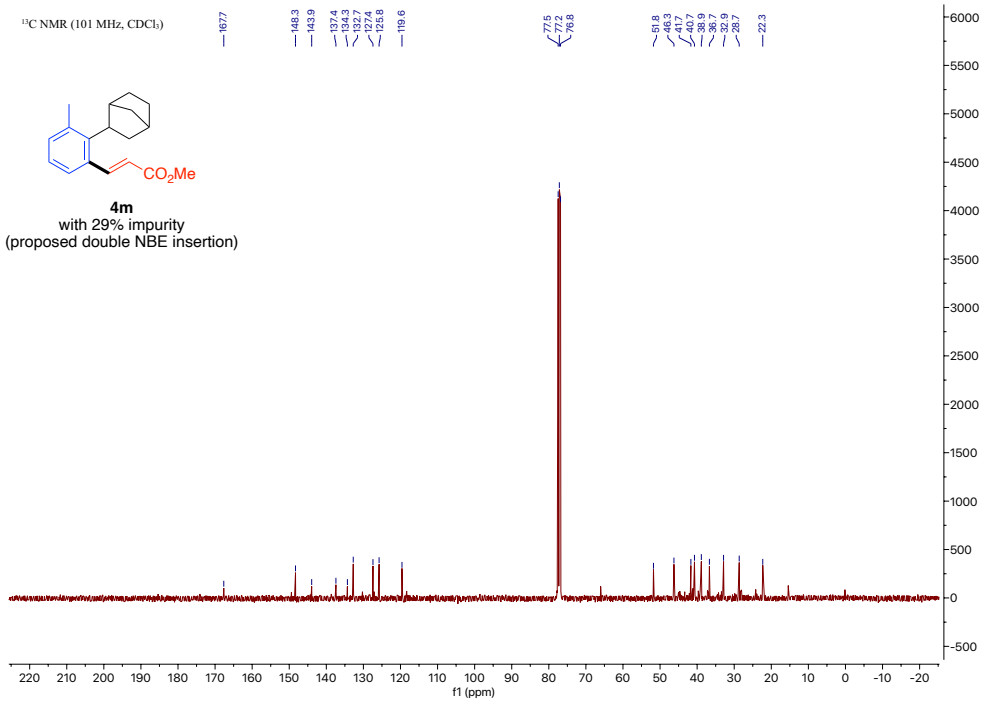

Figure 4.45. ^{1}H NMR Spectrum of **4n**

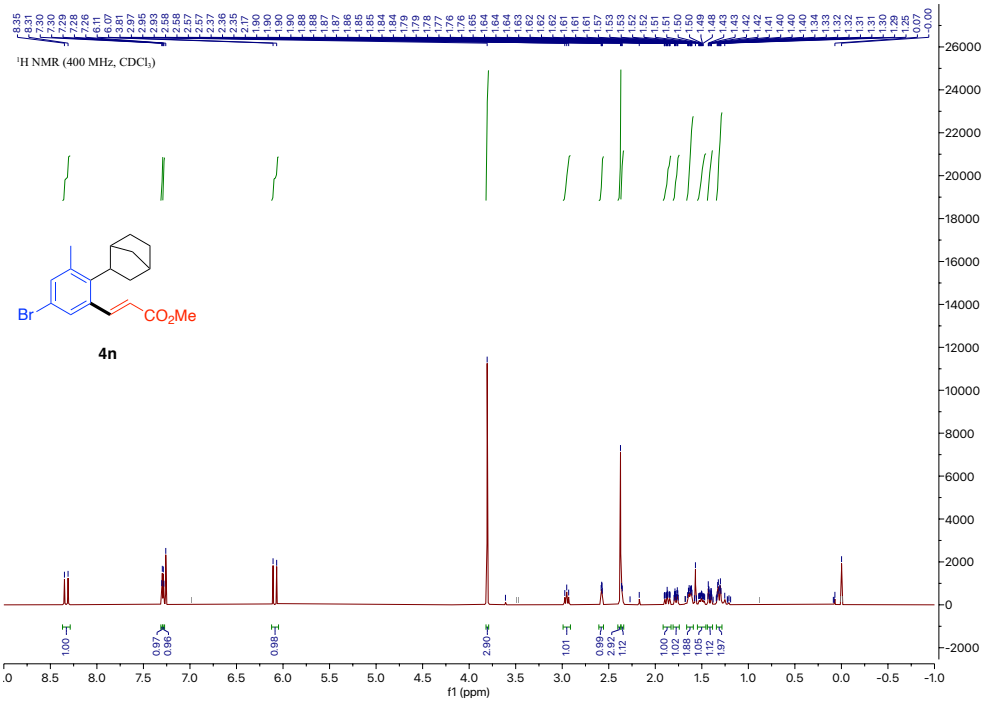

Figure 4.46. ^{13}C NMR Spectrum of **4n**

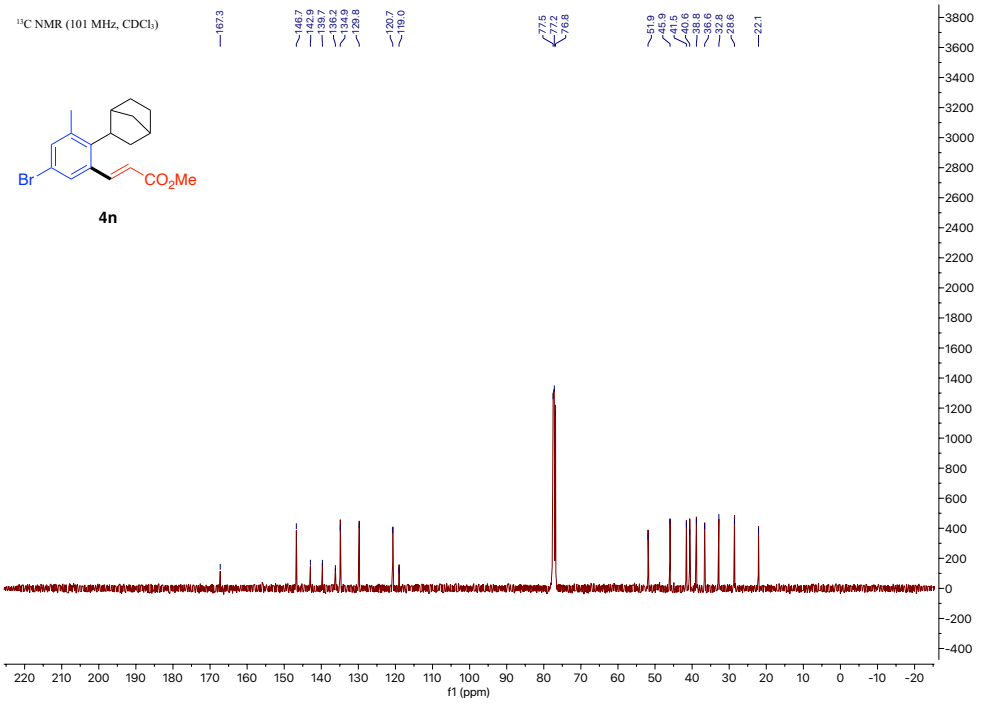

Figure 4.47. ^{1}H NMR Spectrum of **4o**

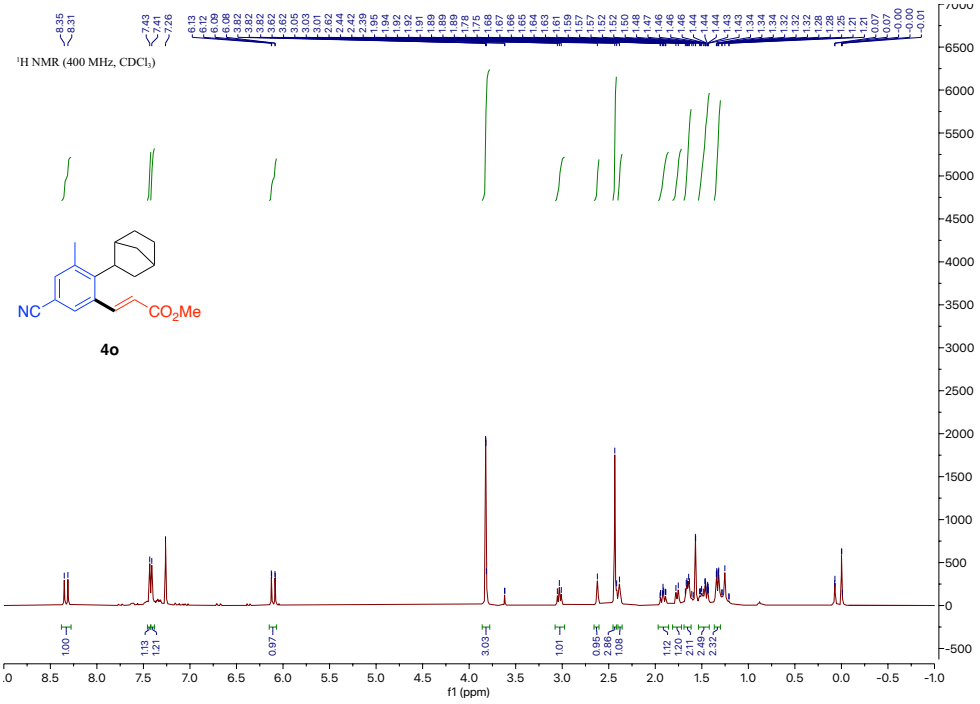

Figure 4.48. ^{13}C NMR Spectrum of **4o**

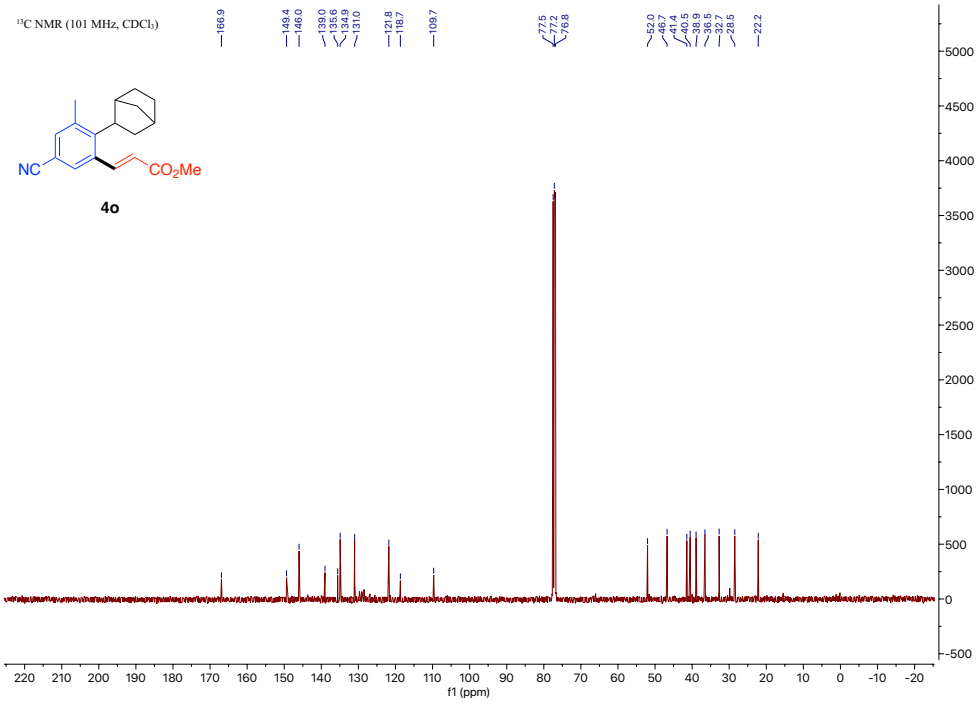

Figure 4.49. ^{1}H NMR Spectrum of **4p**

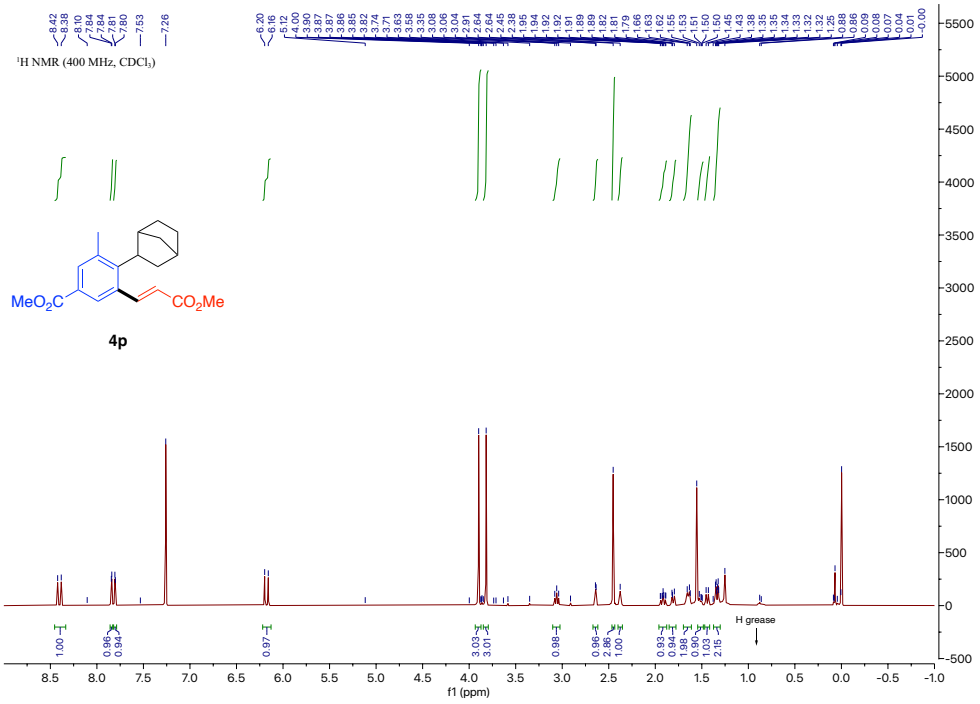

Figure 4.50. ^{13}C NMR Spectrum of **4p**

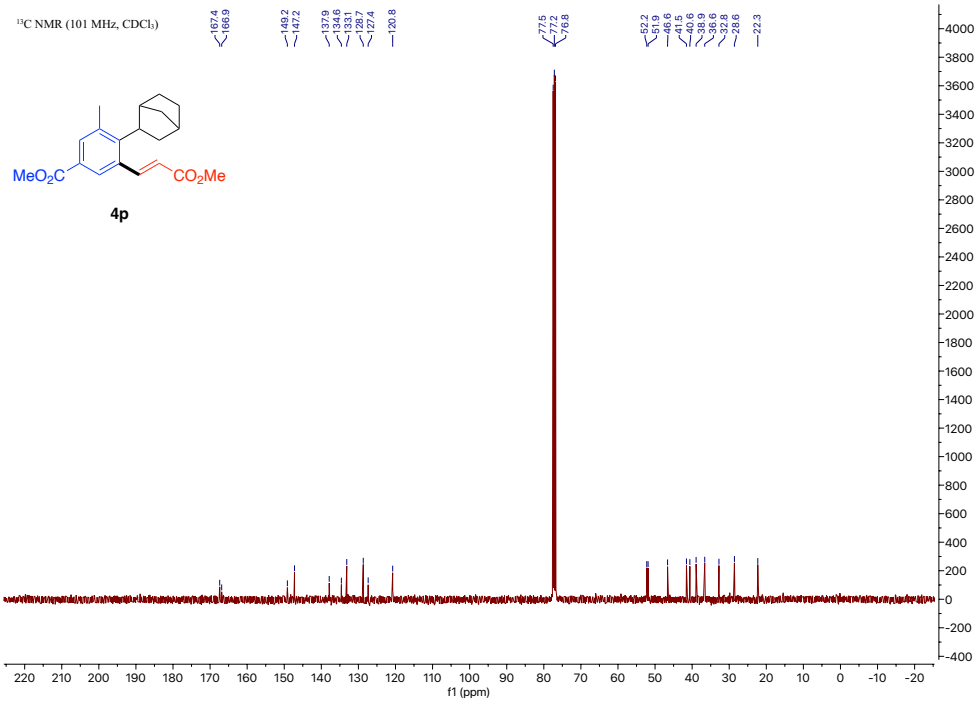

Figure 4.51. ^{1}H NMR Spectrum of **4q**

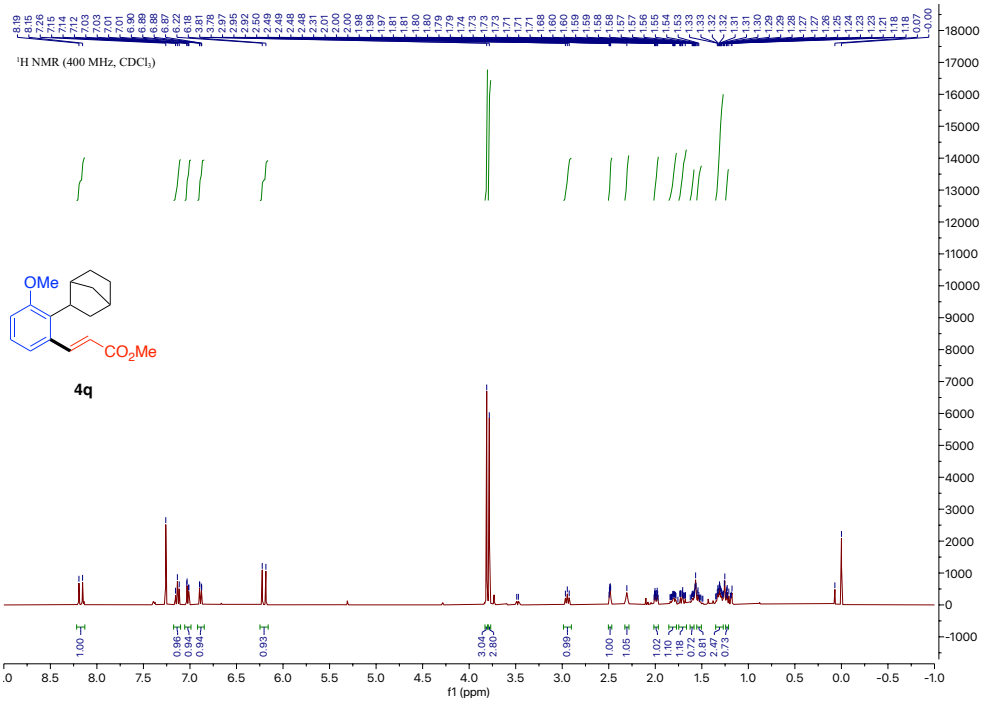

Figure 4.52. ^{13}C NMR Spectrum of **4q**

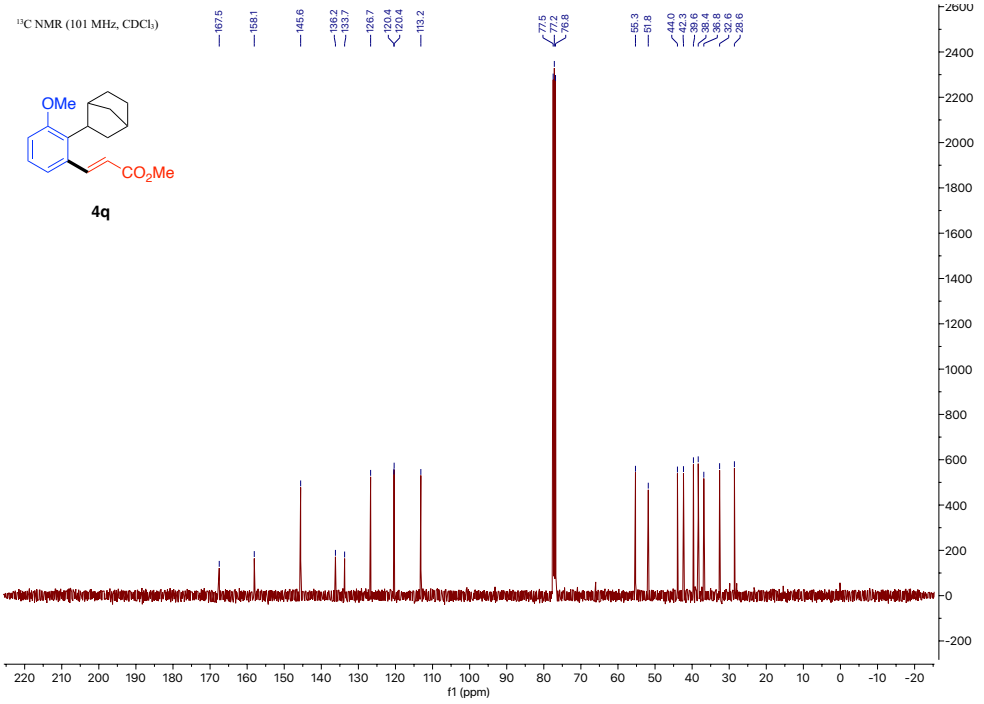

Figure 4.53. ^{1}H NMR Spectrum of **4r**

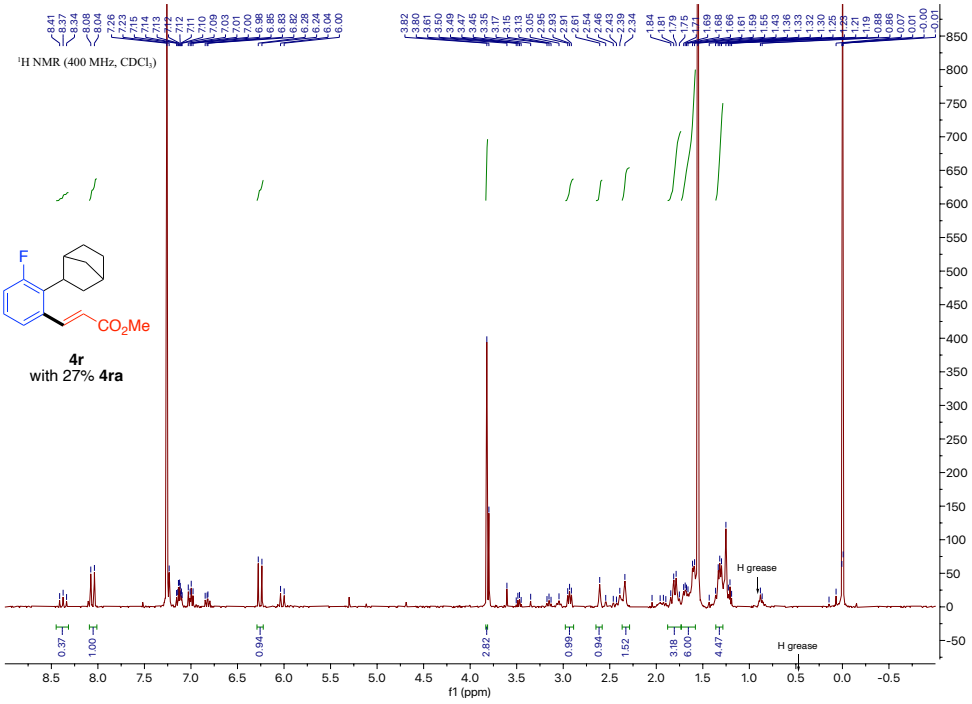

Figure 4.54. ^{19}F NMR Spectrum of **4r**

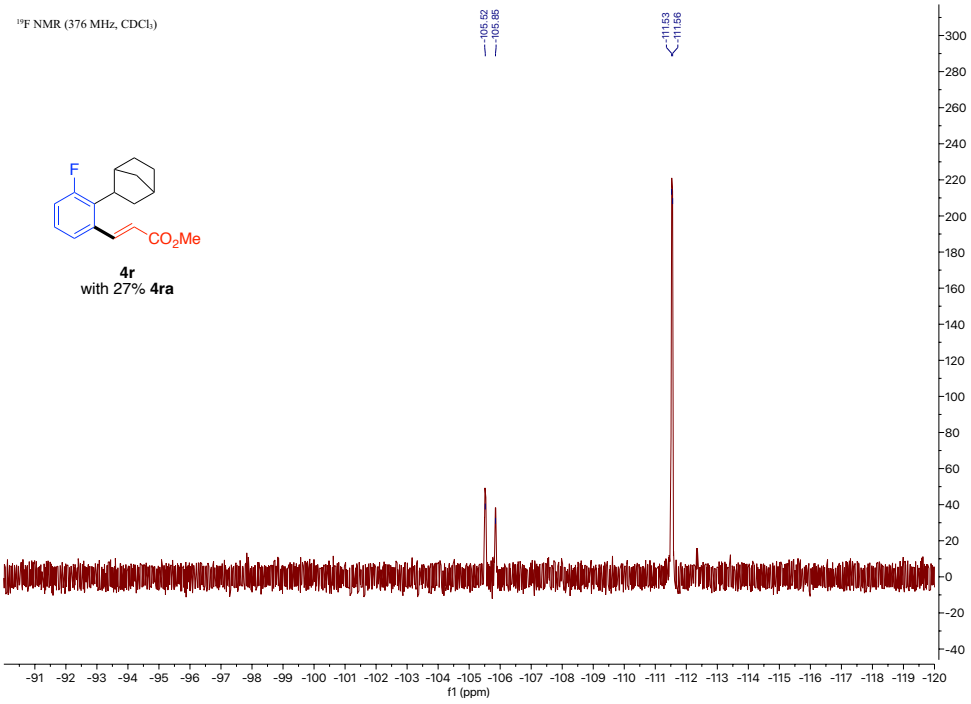

Figure 4.55 ^{1}H NMR Spectrum of **4ra**

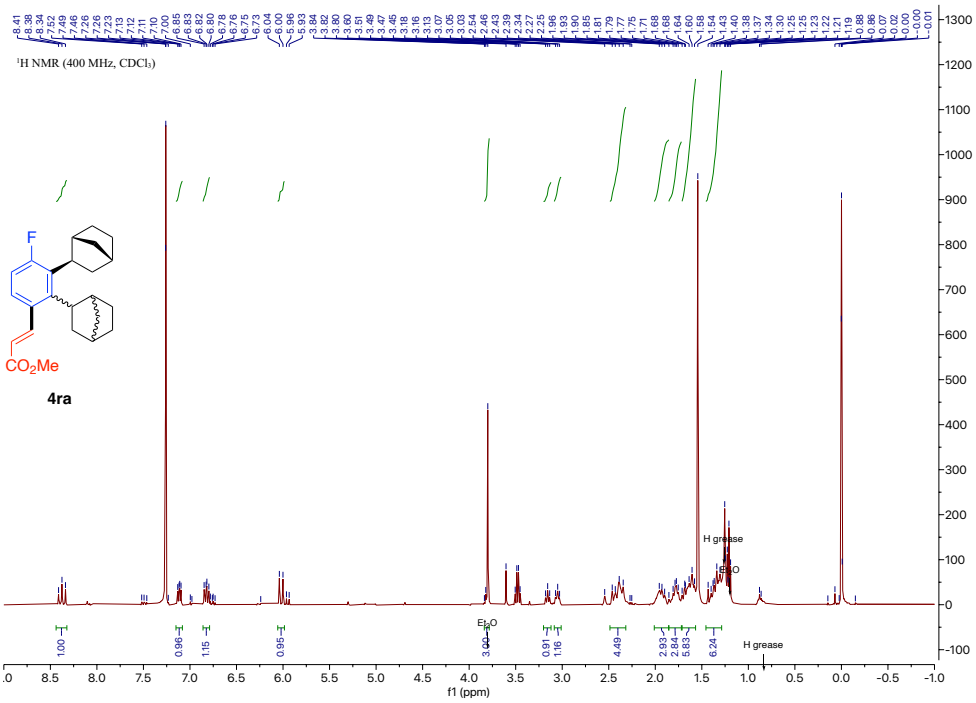

Figure 4.56. ^{19}F NMR Spectrum of **4ra**

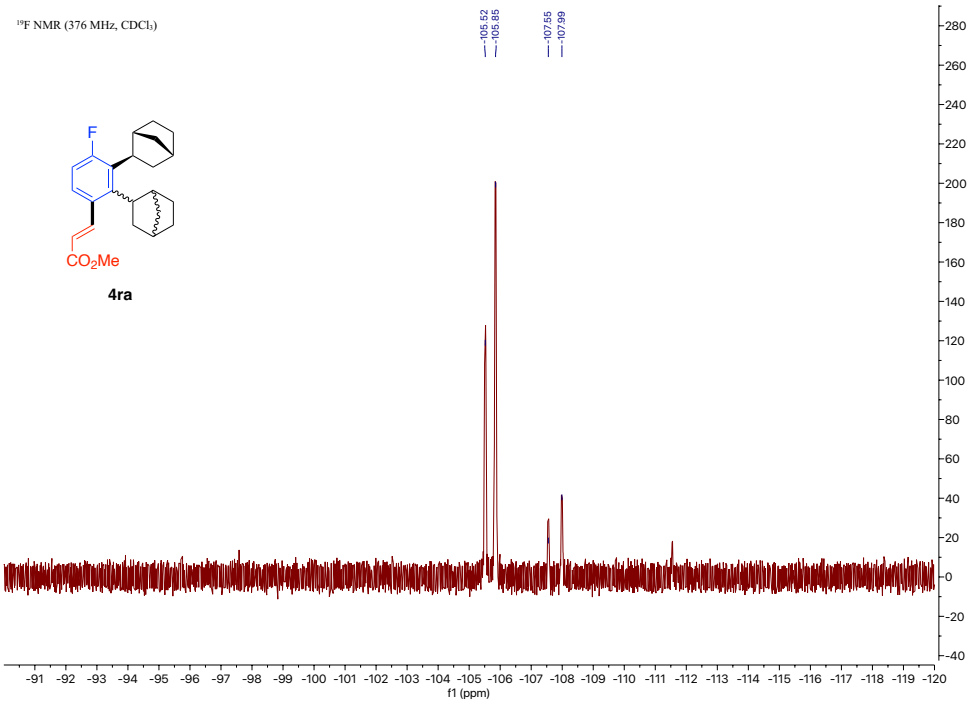

Figure 4.57. ^{1}H NMR Spectrum of **4s**

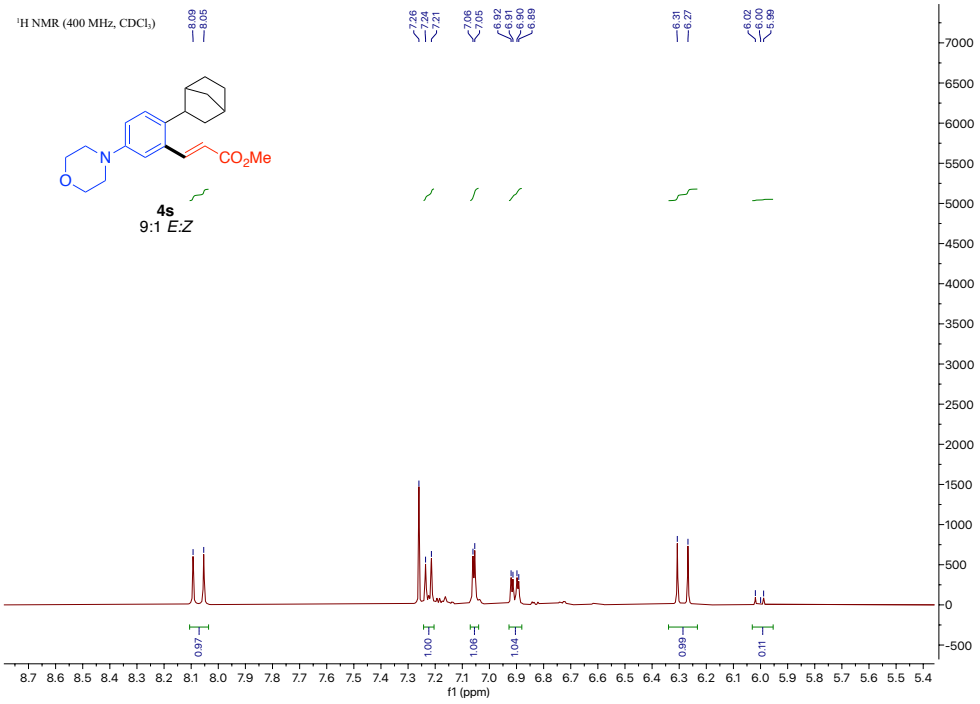

Figure 4.58 ^{1}H NMR Spectrum of **4s (*Z*)**

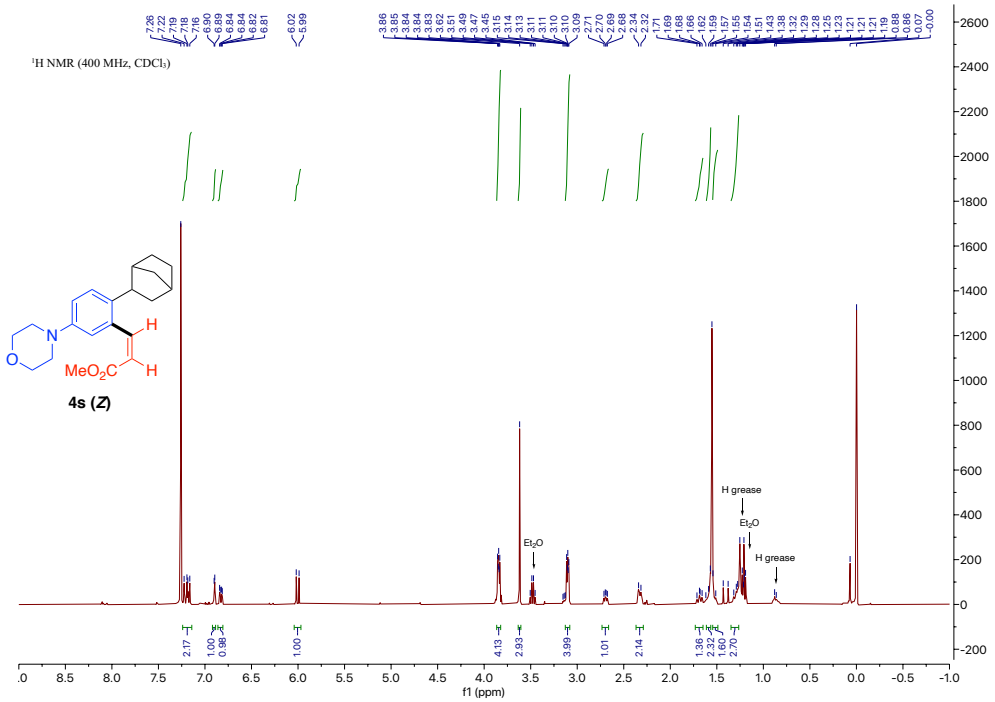

Figure 4.59. ^{13}C NMR Spectrum of **4s (*Z*)**

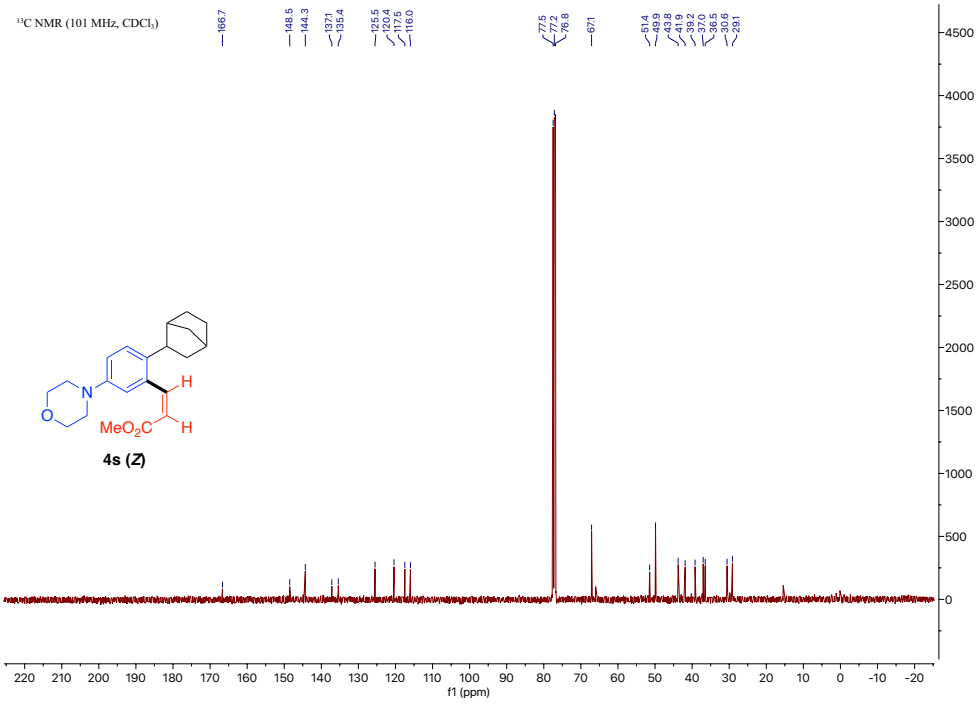

Figure 4.60. ^{1}H NMR Spectrum of **4t**

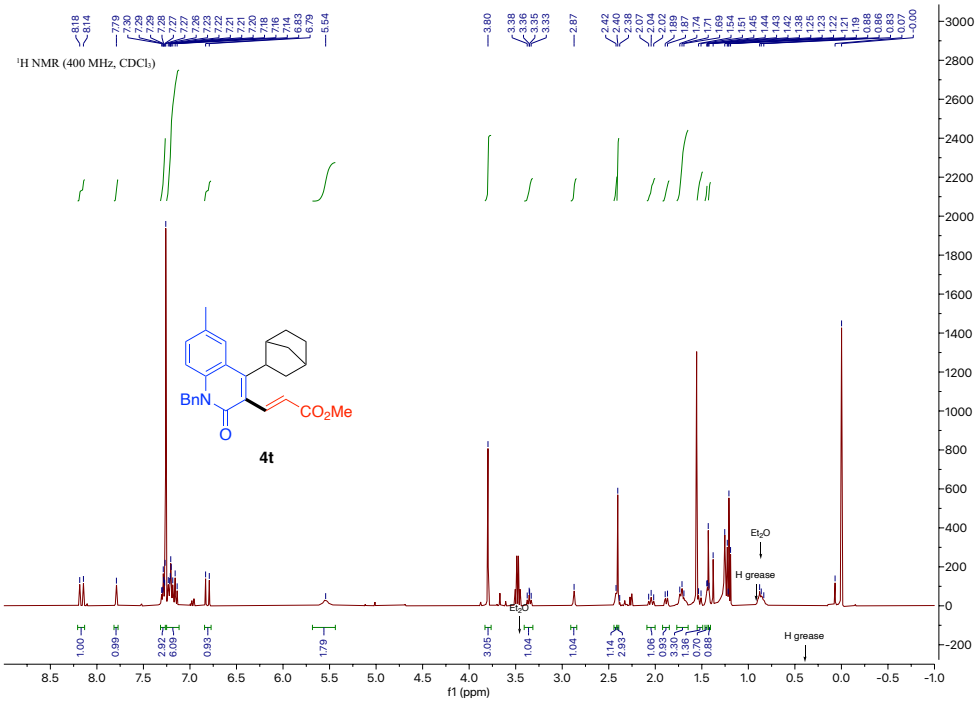

Figure 4.61. ^{13}C NMR Spectrum of **4t**

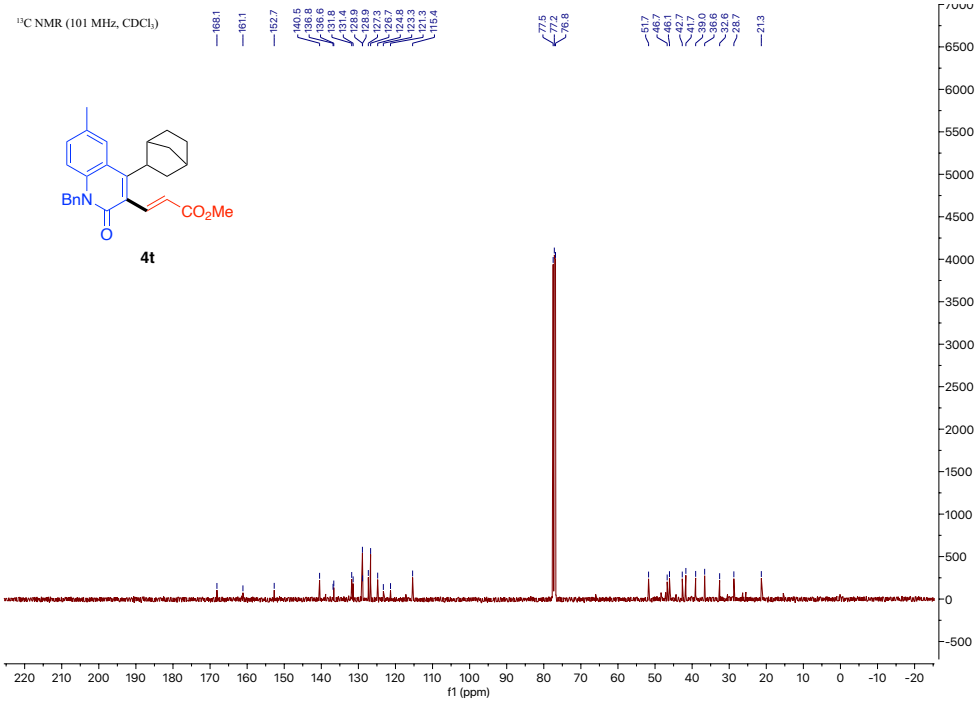

Figure 4.62. ^{1}H NMR Spectrum of **4u**

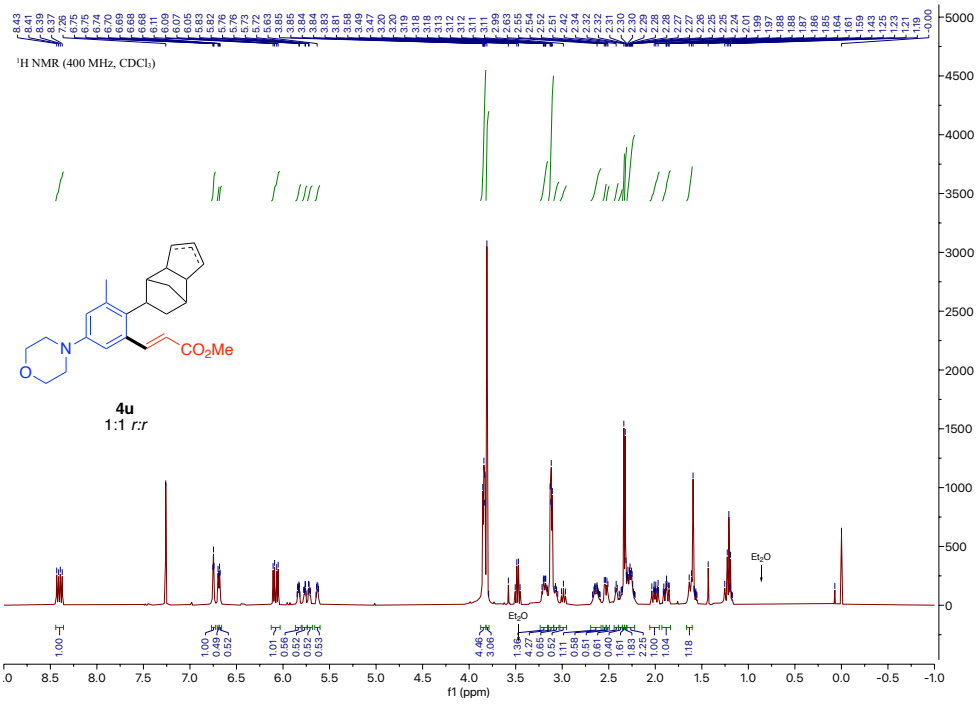

Figure 4.63. ^{13}C NMR Spectrum of **4u**

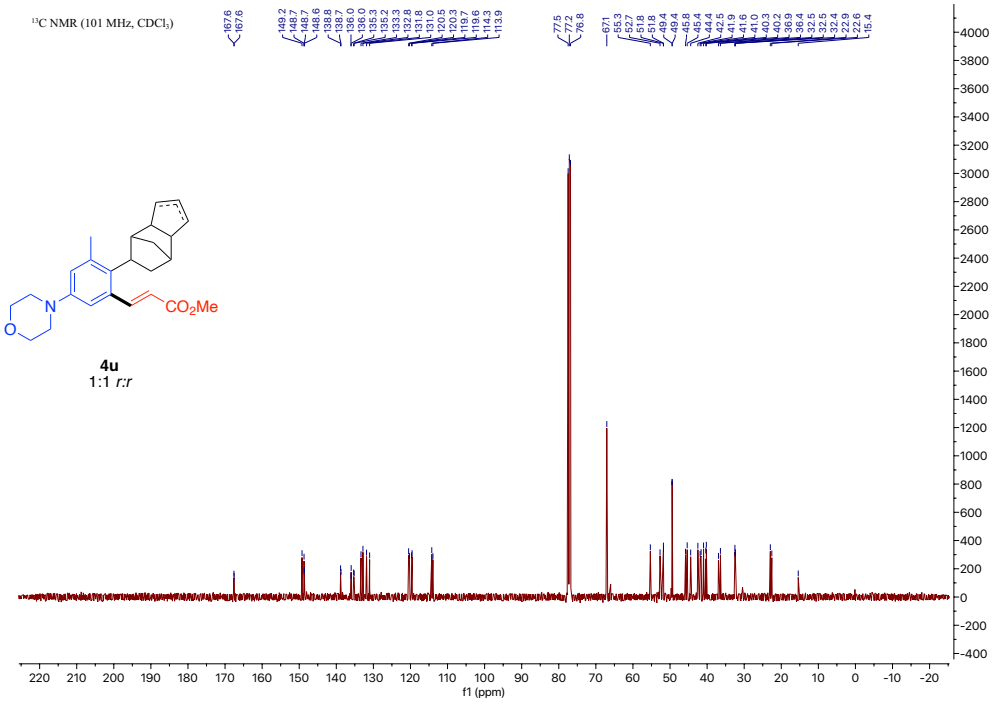

Figure 4.64. ^{1}H NMR Spectrum of **4v**

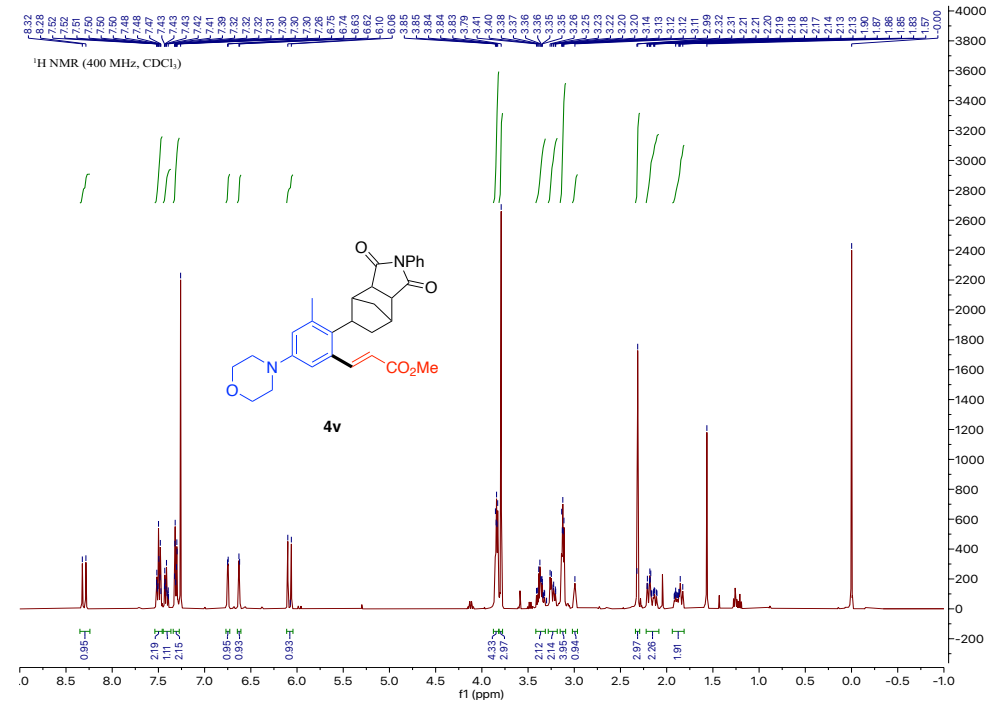

Figure 4.65. ^{13}C NMR Spectrum of **4v**

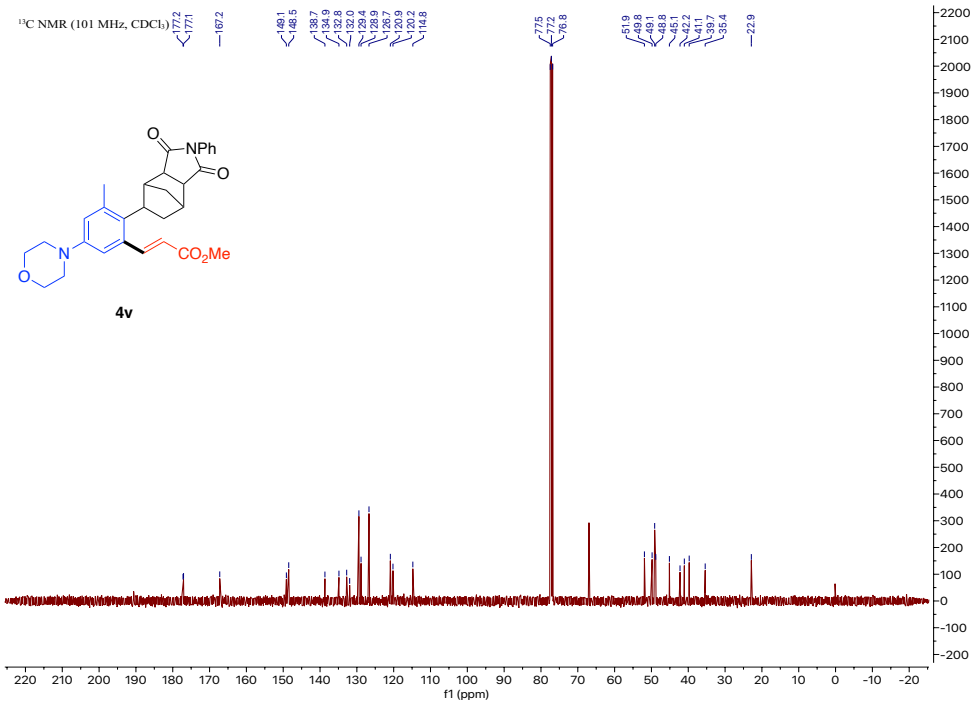

4.6. References

1. Ye, J.; Lautens, M. *Nat. Chem.* **2015**, *7*, 863–870.
2. Della, Ca',N.; Fontana, M.: Motti, E.; Catellani, M. *Acc. Chem. Res.* **2016**, *49*, 1389-1400.
3. Zhao, K.; Ding, L.; Gu, Z. *Synlett* **2019**, *30*, 129-140.
4. Wegmann, M.; Henkel, M.; Bach, T. *Org. Biomol. Chem.* **2018**, *16*, 5736-5385.
5. Cheng, H.-G.; Chen, S.; Chen, R.; Zhou, Q. *Angew. Chem., Int. Ed.* **2019**, *58*, 5832–5844.
6. Wang, J.; Dong, G. *Chem. Rev.* **2019**, *119*, 7478-7528.
7. Catellani, M.; Frignani, F.; Rangoni, A. *Angew. Chem., Int. Ed.* **1997**, *36*, 119-122.
8. Catellani, M.; Cugini, F. *Tetrahedron* **1999**, *55*, 6595-6602.
9. Lautens, M.; Paquin, J.-F.; Piguel, S. *J. Org. Chem.* **2002**, *67*, 3972-3974.
10. Wilhelm, T.; Lautens, M. *Org. Lett.* **2005**, *7*, 4053-4056.
11. Mariampillai, B.; Alliot, J.; Li, M.; Lautens, M. *J. Am. Chem. Soc.* **2007**, *129*, 15372.

12. Li, R,; Dong, G. *Angew. Chem., Int. Ed.* **2018**, *57*, 1697-1701.

13. Dong, Z.; Dong, G. *J. Am. Chem. Soc.* **2013**, *135*, 18350-18353.

14. Shi, H.; Babinski, D. J.; Ritter, T. *J. Am. Chem. Soc.* **2015**, *137*, 3775-3778.

15. Zhou, P.-X.; Ye, Y.-Y.; Liu, C.; Zhao, L.-B.; Hou, J.-Y.; Chen, D.-Q.; Tang, Q.; Wang, A.-Q.; Zhang, J.-Y.; Huang, Q.-X.; Xu, P.-F.; Liang, Y.-M. *ACS Catal.* **2015,** *5*, 4927-4931.

16. Huang, Y.; Zhu, R.; Zhao, K.; Gu, Z. *Angew. Chem. Int. Ed.* **2015,** *54*, 12669-12672.

17. Dong, Z.; Wang, J.; Ren, Z.; Dong, G. *Angew. Chem., Int. Ed.* **2015**, *54*, 12664-12668.

18. Wang, J.; Zhang, L.; Dong, Z.; Dong, G. *Chem.* **2016**, *1*, 581.

19. Cai, W.; Gu, Z. *Org. Lett.* **2019**, *21*, 3204-3209.

20. Li, R.; Zhou, Y.; Yoon, K.-Y.; Dong, Z.; Dong, G. *Nat. Comm.* **2019**, *10*, 3555-3563.

21. Shen, P.-X.; Wang, X.-C.; Wang, P.; Zhu, R.-Y.; Yu, J.-Q. *J. Am. Chem. Soc.* **2015**, *137*, 11574-11577.

22. Dong, Z.; Wang, J.; Dong, G. *J. Am. Chem. Soc.* **2015**, *137*, 5887-5890.

23. Motti, E.; Catellani. M. *Adv. Synth. Catal.* **2008**, *350*, 565-569.

24. Dong, Z.; Lu, G.; Wang, J.; Liu, P.; Dong, G. *J. Am. Chem. Soc.* **2018**, *140*, 8551-8562.

25. Lv, W.; Yu, J.; Ge, B.; Wen, S.; Cheng, G. *J. Org. Chem.* **2018**, *83*, 12683-12693.

26. Yang, S.-Y.; Han, W.-Y.; He, C.; Cui, B.-D.; Wan, N.-W.; Chen, Y.-Z. *Org. Lett.* **2019**, *21*, 8857-8860.

27. Similar *ortho*-Heck products have also been observed in small quantities during optimization of other Pd/NBE transformations in our group.

28. Catellani, M.; Chiusoli, G. P. *J. Organomet. Chem.* **1988**, *346*, C27-C30.

29. Catellani, M.; Mann, B. E. *J. Organomet. Chem.* **1990**, *390*, 251-255.

30. Ma, S.; Gu, Z. *Angew. Chem., Int. Ed.* **2005**, *44*, 7512-7517.

31. Rahim, A.; Feng, J.; Gu, Z. *Chin. J. Chem.* **2019**, *37*, 929-945.

32. Bechtoldt, A.; Ackermann, L. *ChemCatChem* **2019**, *11*, 435-438.

33. Huang, Q.; Fazio, A.; Dai, G.; Campo, M. A.; Larock, R. C. *J. Am. Chem. Soc.* **2004**, *126*, 7460-7461.

34. Piou, T.; Bunescu, A.; Wang, Q.; Neuville, L. *Angew. Chem., Int. Ed.* **2013**, *52*, 12385-12389.

35. Gao, A.; Liu, X.-Y.; Li, H.; Ding, C.-H.; Hou, X.-L. *J. Org. Chem.* **2017**, *82*, 9988-9994.

36. The exact mechanism for the 1,4-palladium migration is not entirely clear. Either a σ-bond metathesis or oxidative addition into the sp^2 C−H bond is possible. For related DFT studies, see: Mota, A. J.; Dedieu, A. *J. Org. Chem.* **2007**, *72*, 9669-9678.

37. Yu, Y.; Chakraborty, P.; Song, J.; Zhu, L.; Li, C.; Huang, X. *Nat. Comm.* **2019**, *11*, 461-469.

38. An aryl bromide was shown to produce the desired product in 10% yield.

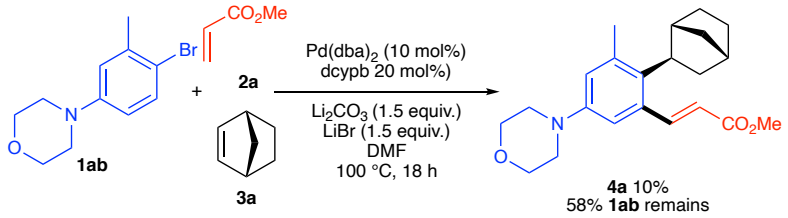

39. Oguma, K.; Miura, M.; Satoh, T.; Nomura, M. *J. Am. Chem. Soc.* **2000**, *122*, 10464-10465.

40. Chen, X; Engle, K. M.; Wang, D.-H.; Yu, J.-Q. *Angew. Chem., Int. Ed.* **2009**, *48*, 5094-5115.

41. He, J.; Wasa, M.; Chan, K. S. L.; Shao, Q.; Yu, J.-Q. *Chem. Rev.* **2017**, *117*, 8754-8786.

42. Dong, Z.; Wang, J.; Ren, Z.; Dong, G. *Angew. Chem. Int. Ed.* **2015**, *54*, 12664-12668.

43. Wu, T. Y.-H.; Li, Y.; Cortez, A.; Zou,m Y.; Mishra, P.; Zhang, X.; Skibinski, D.; Singh, M.; Valiante, N. U.S. Patent WO 2009-US35563, February 27, 2009.

44. Lu, Z.; Twieg, R. J.; Huang, S. D. *Tetrahedron Lett.* **2003**, *44*, 6289-6292.

45. Chen, Z.; Hu, L.; Zeng, F.; Zhu, R.; Zheng, S.; Yu, Q.; Huang, J. *Chem. Commun.* **2017**, *30*, 4258-4261.

46. Hell, S. M.; Meyer, C. F.; Laudadio, G.; Misale, A.; Willis, M. C.; Noël, T.; Trabanco, A. A.; Gouverneur, V. *J. Am. Chem. Soc.* **2020**, *142*, 720-725.

47. Chen, Z.; Hu, L.; Zeng, F.; Zhu, R.; Zheng, S.; Yu, Q.; Huang, J. *Chem. Commun.* **2017**, *30*, 4258-4261.

48. Lautens, M.; Paquin, J.-F.; Piguel, S. *J. Org. Chem.* **2002**, *67*, 3972-3974.

49. Della Ca', N.; Maestri, G.; Malacria, M.; Derat, E.; Catellani, M. *Angew. Chem., Int. Ed.* **2011**, *50*, 12257-12261.

50. Dostas, I. D.; Andreadaki, F. J.; Medlycott, E. A.; Hanan, G. S.; Monflier, E. *Tetrahedron Lett.* **2009**, *50*, 1851-1854.

51. Mo, F.; Yan, J. M.; Qiu, D.; Li, F.; Zhang, Y.; Wang, J. *Angew. Chem., Int. Ed.* **2010**, *49*, 2028-2032.

52. Bonvallet, P. A.; Breitkreuz, C. J.; Kim, Y. S.; Todd, E. M.; Traynor, K.; Fry, C. G.; Ediger, M. D.; McMahon, R. J. *J. Org. Chem.* **2007**, *72*, 10051-10057.

53. Catellani, M.; Cugini, F. *Tetrahedron* **1999**, *55*, 6595-6602.

(Portions of this chapter have previously been published in *Organic Letters*: Rago, A. J.; Dong, G. *Org. Lett.* **2020**, *22*, 3770-3774.)